Nico D. Fessner, MSci

Bioprospecting for novel fungal heme-dependent monooxygenases expressed in yeast

DOCTORAL THESIS

to achieve the university degree of

Doktor der Naturwissenschaften

submitted to

Graz University of Technology

Supervisor

Ao.Univ.-Prof. Mag.rer.nat. Dr.rer.nat. Anton Glieder

Institute of Molecular Biotechnology

Graz, October 2020

AFFIDAVIT

I declare that I have authored this thesis independently, that I have not used other than the declared sources/resources, and that I have explicitly indicated all material which has been quoted either literally or by content from the sources used. The text document uploaded to TUGRAZonline is identical to the present doctoral thesis.

15. October 2020 

Date, Signature

Abstract

Cytochrome P450 enzymes (P450s) are the most versatile enzymes in nature catalysing a range of different types of reactions such as hydroxylation *via* the activation of inert sp^3-hybridised C-H bonds. The ability to operate in a synthetic late-stage fashion of complex molecular scaffolds inspired the application of these monooxygenases in the diversification of natural products for drug discovery purposes.
In particular the principal human drug-metabolising P450 enzyme 3A4 was found to be proficient in this task with the natural steroid testosterone when applied as a whole-cell biocatalyst at high expression levels in *P. pastoris*. A bioreactor experiment served as the proof-of-principle that such biocatalytic system can be used for natural product diversification to generate preparative-scale quantities, and to demonstrate scalability for possible implementations of such biooxidations in industry.
Similar to CYP3A4 in human liver, numerous detoxification enzymes with multifunctional activities await recovery from the enzymatic repertoire of wood-degrading fungi. Their natural functional diversity makes them particularly interesting for modifying natural products. In this thesis a multifunctional P450 with activities towards several different natural product classes was identified from the white-rot fungus *Polyporus arcularius*.
This thesis advances the technologies and opportunities for the implementation of P450-catalysed natural product diversification into the environment of synthetic chemistry, highlights the importance of profound enzyme expression for efficient biocatalysis and showcases the potential of bioprospecting for novel eukaryotic P450s.

Keywords:
Cytochrome P450 enzymes — *Pichia pastoris* — Bioprospecting — Natural products — Late-stage diversification

Kurzfassung

Cytochrom P450-Enzyme (P450s) sind die vielseitigsten Enzyme der Natur, weil sie mehrere verschiedene Reaktionen katalysieren, wie etwa die Hydroxylierung mittels einer Aktivierung von inerten sp^3-hybridisierten C-H-Bindungen. Ihre Fähigkeit im Spätstadium einer Synthese zu agieren, inspirierte die Anwendung solcher Monooxygenasen für die Diversifizierung von Naturstoffen in der Pharmaforschung.
Besonders das P450-Cytochrom 3A4 —Hauptenzym des Menschen zum Abbau von Medikamenten— stellte sich als hervorragend geeignet für die Diversifizierung des natürlichen Steroids Testosteron heraus, wenn es als Ganzzell-Biokatalysator in *Pichia pastoris* bei hohen Expressionsleveln benutzt wurde. Ein Bioreaktorexperiment fungierte als „Proof of Principle", dass ein solch biokatalytisches System angewendet werden kann, um Naturstoffdiversifizierung im präparativen Maßstab auszuführen, und damit die Skalierbarkeit für eine mögliche Implementierung derartiger Biooxidationen in der Industrie zu demonstrieren.
Ähnlich wie CYP3A4 in der menschlichen Leber gibt es sehr viele Entgiftungsenzyme mit einer multifunktionalen Aktivität im enzymatischen Repertoire von Pilzen, die Holzfäule verursachen. Deren natürliche Funktionsvielfalt macht sie besonders interessant für die Modifizierung von Naturstoffen. In dieser Dissertation wurde ein solch multifunktionales P450-Enzym, das viele verschiedene Naturstoffklassen umsetzen kann, in dem Weißfäule verursachenden Pilz *Polyporus arcularius* identifiziert.
Somit entwickelt diese Thesis die Technologie der P450-katalysierten Naturstoffdiversifizierung weiter und zeigt deren Potential im Bereich der synthetischen Chemie, verdeutlicht die Wichtigkeit von effizienter Proteinexpression für die Biokatalyse und präsentiert die Möglichkeiten der Bioprospektion neuer eukaryotischer P450-Enzyme.

Keywords:
Cytochrome P450-Enzyme — *Pichia pastoris* — Bioprospektion — Naturstoffe — Diversifikation im Spätstadium

Acknowledgement

It is an extraordinary achievement when succeeding in your Ph.D. studies because it is the fundamental proof of your audacity to tackle the unknown, persistently solve problems, overcome challenges and be creative in project planning and managing, while working long hours in the laboratory. Ultimately, one needs the ability to never give up. Therefore, mental health issues of Ph.D. students are generally increasing.
Hence, I wish to express my gratitude to all the people who supported me during my three years as a doctoral student.

First of all I would like to thank my supervisor Prof. Anton Glieder for giving me the opportunity to work in a scientific field new to me, his guidance in the project and especially the freedom to pursue my own ideas.
As ESR5 of the OXYtrain project I was in a privileged position and am grateful to the European Union for financially supporting this training network as well as to Prof. Marco Fraaije as the project coordinator. Thank you to all partner OXYtrain beneficiaries and my OXYtrain fellows for the great times during project meetings and secondments. I acknowledge especially the close collaboration and friendship with Matic Srdič. Thanks also to Dr. Brenda Bley Folly for the support while she was part of OXYtrain.

Many thanks also to all people that are or were members of the Glieder group or of *bisy* for making work more joyful and supporting me during my project. I am glad to have found new friends among you so quickly when I newly moved to Graz. I am especially indebted to Christian Schmid for sharing with me his seemingly endless knowledge with me plus the great conversations and fun we had outside the lab, and to Anna Hatzl for her helpful advice and outstanding judgement on any issue I might have had on scientific or any other topic. You both kept me going in difficult times and not lose my mind.

Big thanks to Lukas Rieder for welcoming me in Graz and helping me to settle down, Astrid Weninger for patiently introducing me to the laboratory and essential techniques in Biotechnology, Stefan Ertl for the great lunch conversations and fantastic climbing trips, Bianca Huber for the funny running gags and efficient help in- and outside the lab, Katherina Eber for the laughter and competent scientific support, Christoph Reisinger for both the jokes and exotic work-related methods that all seemed to work, Prof. Margit Winkler, Melissa Horvat and Daniel Schwendenwein for patiently helping me with the HPLC instuments, Jasmin Fischer and Veronika Schusterbauer for helping me with the knockout and computational work, respectively, Carsten Pichler for the nice conversations and trying to replace Christian and Kirill Smirnov for the running gag of taking up my space, Kay Novak for an exquisite experience, Carla Aguilar and Rosa Peces for your Spanish, Pierre Reinprecht, Tobias Baumgartner, Lukas Pfeifenberger, Florian Weiss, Stephen Kennedy and Lisa Wasserer for cool stories, jokes and happy faces.

Thank you to my loving partner Silvia for accompanying the final stage of my Ph.D. studies, patiently tolerating and understanding all the unpredictability and tension that comes with it.

Finally, above all and again, I am extremely grateful to my family for their unconditional love, compassion and support that provide me with a basis I can fall back on whenever I need to. I am extremely grateful to my father in particular for his relentless support and dedicative advice to any matter I might have during my Ph.D. studies.

This PhD thesis was the ESR5 project of the OXYtrain MSCA-ITN programme (http://www.oxytrain.eu).

This project received funding from the European Union's Horizon 2020 research and innovation programme, OXYtrain MSCA-ITN, under grant agreement No. 722390.

Table of Contents

Dissemination

Posters and oral presentations

1. J.I. Murray, N.J. Flodén, A. Bauer, N.D. Fessner, D.L. Dunklemann, O. Bob-Egbe, H.S. Rzepa, T. Bürgi, J. Richardson and A.C. Spivey, *Asymmetric synthesis of phosphorothioate-nucleosides via atropisomeric pyridine-N-oxide catalysis*, **Biotransformations 2017**, Hannover, Germany, July 2017

2. N.D. Fessner, A. Weninger and A. Glieder, *Development of a highly efficient HTS method for the discovery of novel Cytochrome P450 enzymes from eukaryotic cDNA*, **Biocatalysis as a Key Enabling Technology**, Siena, Italy, October 2017

3. N.D. Fessner, A. Weninger and A. Glieder, *Development of a highly efficient HTS method for the discovery of novel P450 enzymes from eukaryotic cDNA*, **European Summit of Industrial Biotechnology** & **OXYtrain training school** (SC1 & TSC1), Graz, Austria, November 2017

4. N.D. Fessner and A. Glieder, *Bioprospecting for novel fungal and plant heme-dependent monooxygenases, expressed in yeasts*, **OXYtrain training school** (SC2 & TSC2), Aachen, Germany, April 2018

5. N.D. Fessner and A. Glieder, *Bioprospecting for novel fungal and plant heme-dependent monooxygenases, expressed in yeasts*, **Process development for biooxidations**, Copenhagen, Denmark, April, 2018

6. M. Srdič, L. Wasserer, N.D. Fessner and A. Glieder, *Investigating the structure-function relationship of human CYP3A4 towards testosterone*, **Novel Enzymes 2018**, Darmstadt, Germany, October 2018

7. N.D. Fessner and A. Glieder, *Bioprospecting for novel fungal and plant heme-dependent monooxygenases, expressed in yeasts*, **OXYtrain training school** (SC3), Oslo, Norway, November 2018

8. M. Srdič, L. Wasserer, N.D. Fessner and A. Glieder, *Investigating the structure-function relationship of human CYP3A4 towards testosterone*, **ScienceConnect**, Graz, Austria, November 2018

9. N.D. Fessner and A. Glieder, *Bioprospecting for novel fungal and plant heme-dependent monooxygenases, expressed in yeasts*, **OXYtrain training school** (SC4 & TSC3), Delft, Netherlands, April 2019

10. N.D. Fessner, M. Srdič, C. Schmid and A. Glieder, *Preparative synthesis of testosterone metabolites using human liver P450 3A4*, **BioTrans 2019**, Groningen, Netherlands, July 2019

11. N.D. Fessner, M. Srdič, H. Weber, C. Schmid and A. Glieder, *Preparative-scale production of testosterone metabolites by human liver cytochrome P450 enzyme 3A4*, **Graz Molecular Biosciences Doctoral Day** — Graz, Austria, February 2020

12. N.D. Fessner, Srdič, H. Weber, C. Schmid and A. Glieder, *Preparative-scale production of testosterone metabolites by human liver P450 3A4*, **Applied late-stage functionalisation: where chemistry meets biology**, Manchester, February 2020

Published papers with peer-review

1. P450 Monooxygenases Enable Rapid Late-Stage Diversification of Natural Products via C-H Bond Activation
   Nico D. Fessner, *ChemCatChem*, **2019**, *11*, 2226-2242

2. Preparative-Scale Production of Testosterone Metabolites by Human Liver Cytochrome P450 Enzyme 3A4
   Nico D. Fessner, Matic Srdič, Hansjörg Weber, Christian Schmid, David Schönauer, Ulrich Schwaneberg and Anton Glieder, *Adv. Synth. Catal.*, **2020**, *362*, 2725-2738

Publications submitted

3. Evolution and Enrichment of CYP5035 and CYP5136 in *Polyporales*: Functionality of an understudied P450 family
   Nico D. Fessner, David R. Nelson and Anton Glieder, submitted to *Appl. Microbiol. Biotechnol.*

Publications in preparation

4. Regioselective Hydroxylation of Stilbenes by P450s of the White-Rot Fungus *Polyporus Arcularius* Enables Preparative-Scale Synthesis of Stilbenoids
   Nico D. Fessner *et al.*

5. Regioselective Hydroxylation of Monoterpenes by Detoxifying CYP5035S7 Monooxygenase of the White-Rot Fungus *Polyporus Arcularius*
   Nico D. Fessner *et al.*

6. Late-stage Functionalisation of Polycyclic Aromatic Hydrocarbons by Detoxifying CYP5035S7 Monooxygenase of the White-Rot Fungus *Polyporus Arcularius*
   Nico D. Fessner *et al.*

7. Oxidative Natural Product Diversification by One-Pot-One-Enzyme Biocatalysis using Human P450 3A4
   Nico D. Fessner *et al.*

8. Bioprospecting for Cytochrome P450 Enzymes of White- and Brown-Rot Fungi as Biocatalysts for the Late-Stage Functionalisation of Natural Products
   Nico D. Fessner *et al.*

Introduction

In light of sustainability needs, the principles of *Green Chemistry* were established to guide the efforts in chemical research and production towards the energy-efficient, waste-free and environmentally friendly manufacture of chemical products in order to face up-coming global challenges (Figure 1, Sustainability).[1] These guidelines are especially relevant for industry because the impact is greatest in large-scale processes.[2] Therefore, efforts in synthetic chemistry drive the development of more and more innovative catalysts and elegant methods such as the activation of sp^3-hybridised C-H bonds.[3,4] Especially when occurring at a late stage of a synthesis of highly functionalised molecules, selective C-H activation adds considerable flexibility to a synthetic strategy. Cutting down the number of synthetic steps, this powerful technique also significantly improves the economy of the overall synthesis in alignment with the mentioned principles. In the last decade it entered the toolbox of medicinal chemistry[5–7] and simplified the total synthesis[8–11] or diversification[12–17] of natural products.
In modern synthetic chemistry, usually noble or late transition metal catalysis is inevitable for the activation of unreactive chemical bonds in the presence of reactive ones. They have thus been dominating the field of homologous catalysis up to now.[18] However, the toxicity, high price and low abundance of transition metal catalysts outweigh such methodological advantage resulting in an overall disagreement with desired sustainable catalysis.[19]

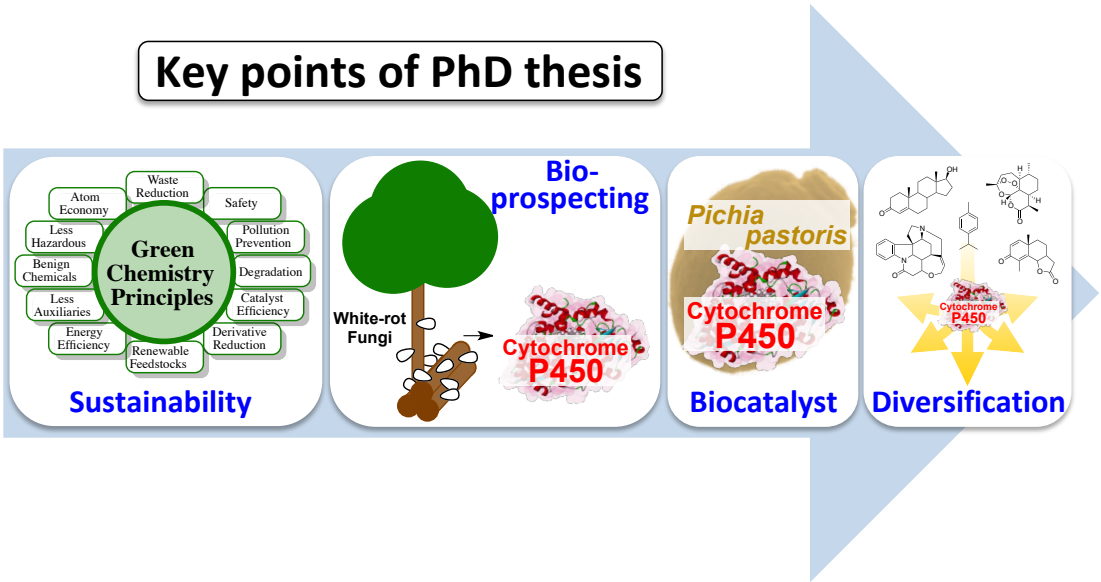

Figure 1: The key points of this PhD thesis are depicted here. **Sustainability**: Biocatalysis is a promising technology to satisfy the need for sustainability driven by the Green Chemistry principles to face global challenges. **Bioprospecting**: White-rot fungi represent a rich source of innovative P450s for the manipulation of natural products and were the target organisms for bioprospecting in this thesis. **Biocatalyst**: The fungal yeast *Pichia pastoris* was chosen here as the protein production host and its whole-cell P450s proved to be very efficient biocatalysts. **Diversification**: In this thesis the concept of natural product diversification for drug discovery was introduced using human P450 3A4 and CYP5035S7 of *Polyporus arcularius* as examples of biocatalysts to demonstrate its power.

This controversy can be successfully tackled by biocatalysis because enzymes are able to somewhat bend the rules by circumventing the general requirement of polar functionality to guide reactivity, while working in benign conditions — water at ambient temperature.[2,20–22] The call for the integration of enzymes into the synthetic toolbox

thus revolutionised the omnipresent retrosynthetic approach in Chemistry and resulted in the concept of "Biocatalytic retrosynthesis" as a novel strategy.[23–26]
Among other enzymes, particularly cytochrome P450 enzymes (P450s, CYPs) are able to modify inert sp^3-hybridised C–H bonds of with high selectivity.[27,28] In fact, especially these enzymes' exquisite ability to selectively oxidise even highly functionalised molecules at a late stage of their synthesis makes cytochrome P450 enzymes (P450s) so valuable (Figure 2). All kingdoms of life are employing P450s in the biosynthesis or detoxification of complex and diverse natural products,[29] which inspired the application of such monooxygenases in the chemoenzymatic total synthesis of high-value natural products, considerably simplifying them.[30–34]
Natural products represent the origin of medicine itself since humans learned to apply medicinal herbs to treat diseases for the first time,[35] and they are still exerting substantial influence on modern drugs in form of complementary medicines such as traditional Chinese medicine[36] or as inspiration for Western lead drug development.[37] Indeed, in the last few years the field of drug discovery considerably re-emphasised natural products due to their immense existing chemical space unmatched by artificial synthetic compound libraries.[37–39] Many natural products are considered pharmaceutically active compounds, however, require improvement of their drug quality to be considered as suitable lead drugs for safe oral application in humans.[40–42] Effective late-stage functionalisation enables the adjustment of properties like solubility by derivatisation of the molecular scaffold. Therefore, **Chapter 1** examines the potential of P450-catalysed late-stage diversification of natural products for drug discovery (Figure 1, Diversification).[43]

Notably, examples of P450-catalysed reactions reviewed in recent studies[30–34,43–45] or much earlier articles[46–48] almost exclusively used bacterial or human P450s such as the prominent CYP102 (BM3) and the most important human liver enzyme P450 3A4, respectively. These enzymes are dominating the research of P450-applied biocatalysis for apparent reasons: The former P450s are soluble, self-sufficient, stable and can be tuned to catalyse even unnatural reactions *via* proficient enzyme engineering;[49] the latter have obvious pharmaceutical relevance as they metabolically clear the human body of about 75% of all commercial drugs.[50] However, bacterial P450s are often limited by narrow substrate scopes and require extensive directed evolution efforts to achieve the desired activity, and human monooxygenases have symptomatically low catalytic turnover numbers and stability.[45] Indeed, almost all eukaryotic P450s necessitate an independent reductase protein just for the electron transfer from the NAD(P)H co-factor to the heme-domain in order to reduce the iron ion at the active site and start off the catalytic cycle. As there is a high diversity of reductase proteins, a suitable partner matching the P450 heme-domain is also essential.[51,52] In addition, both these proteins are membrane-bound in eukaryotic P450 systems. Consequently, when using eukaryotic P450s the coupling efficiency of both P450 domains represents a major limitation to consider.[53] Hence, efficient recombinant co-expression of the two P450 domains is clearly key for a synthetic application[54] and such complicated enzymes encourage the use of whole-cell systems.[55]
Developing versatile expression host platforms is a major area of research in Biotechnology.[56] Native organisms are generally less suitable for the production of the desired native protein because the genetic manipulation especially of higher eukaryotes is a very challenging endeavour.[57,58] Therefore, several expression systems were established, of which the bacterial and yeast host organisms *Escherichia coli* and *Saccharomyces cerevisiae*, respectively, are the most famous and best developed. For the

heterologous expression of single genes, however, the non-conventional yeast *Komagataella phaffii* (*Pichia pastoris*) was ranked on the second place as the most frequently used host organism in 2014.[59] In early days of *Pichia* research and application this statistic was owed primarily to the growth at high cell density upon cultivation in cheap medium,[60] which supports the use of whole-cell systems. Combined with strongly regulated promoters for individual carbon sources (glucose and methanol),[61,62] a high biomass of *P. pastoris* provides excellent means for high-level protein production and high space-time yields for whole-cell biocatalyst production. Great tolerance for membrane-bound proteins[63,64] and native-like post-translational modifications[65] further promote the use of *P. pastoris* as a proficient eukaryotic P450 production host.
These theoretical characteristics were finally manifested in the study of Geier *et al.* in 2012,[66] who compared the expression levels for a human P450 in different standard host organisms and concluded *P. pastoris* as the superior expression host for this purpose. **Chapter 2** builds up on this result and showcases *P. pastoris* as a suitable eukaryotic P450 production host for the preparative-scale synthesis of human testosterone metabolites in the pharmaceutical industry. Using a commercial *P. pastoris* strain expressing human P450 3A4, a more refined metabolic fate of testosterone in the human body was verified and the major testosterone metabolites synthesised at a 100 mg-scale by using a bioreactor. With the help of high expression levels, P450 3A4 diversified the natural product testosterone more than previously thought also forming dihydroxylated testosterone compounds (Figure 1, Biocatalyst).

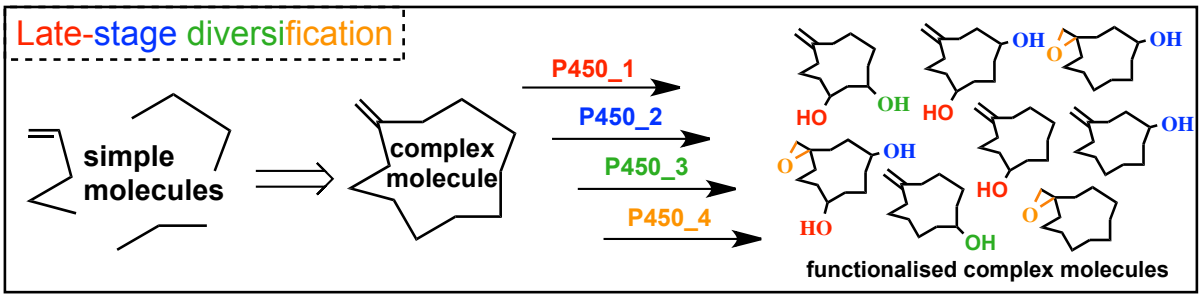

Figure 2: Illustrated is the concept of late-stage diversification catalysed by four different P450s. The individual P450s specifically functionalise a complex molecule post-synthetically to form analogues.

Chapter 2 emphasised that bacterial and human enzymes dominate the research and synthetic application of P450s. Though the P450 universe is vast, full of extremely versatile attractive alternatives currently underrepresented in synthetic applications. Accordingly, the aim of this thesis was to find eukaryotic alternatives to the established bacterial equivalents. Interestingly, when looking more closely at the dominant bacterial and human P450s CYP102 (BM3) and CYP3A4, respectively, both enzymes are involved in the detoxification of xenobiotics. P450s of this type are extremely unselective, yet possess a broad substrate scope in order to functionalise endogenous substances for increased hydrophilicity and rid them of the organism. Clearly, this represents a complementary potential for broad synthetic applications, particularly late-stage functionalisation.
In the context of xenobiotic degradation, white-rot (WR) fungi are particularly relevant organisms. Colonising and feeding on wood, these fungi are able to completely mineralise wood to CO_2 and H_2O by breaking down lignin and (hemi-)cellulose *via* enzymatic oxidation reactions.[67,68] Consequently, they are key players in the carbon recycling of the ecosystem. These fungi are also renowned for their bioremediation

potential of industrial persistant organic pollutants in soil or waste water.[69] Genetically, their evolution indicates the triumphal procession into new ecological niches of harsh conditions.[70,71] Hence, all these characteristics clearly necessitated WR fungi to establish an extraordinarily diverse and efficient enzymatic repertoire for the detoxification of xenobiotics from the environment or the plant defence system.[71–73]
The interest in the enzymes that enable such lifestyle and depolymerise recalcitrant macromolecules was accordingly high. Especially fungal laccases,[74–78] peroxidases[79–81] and peroxygenases[82–85] have already found their way into synthetic research and development, mainly in the hope to utilise lignin industrially as a source of fine chemicals. However, unspecific fungal peroxygenases are also receiving increasing attention as the next generation of hybrid P450s for oxidation reactions due to several biocatalytic advantages such as membrane-free enzyme solubility, self-sufficiency and enhanced stability.[82]
P450s of WR fungi, on the other hand, were sparingly characterised considering the long history of P450 enzymes,[86,87] although the P450ome of WR fungi possesses the highest genome density determined so far in nature[70] and reveals substantial sequence diversification.[87,88] Considering that an organism's P450ome is a measure for metabolic diversity and evolutionary adaptability,[70] such fungal features promise a rich source of versatile enzymes with novel activity for lignin valorisation.
There are several P450 families enriched within the WR fungal genomes, however, some are still lacking comprehensive functional profiling, or were never analysed at all.[71] In fact, information on them are still severely limited considering the small number of species analysed yet, the large amount of genes of each family within the P450ome and few P450s actually expressed and functionally characterised, although multifunctional P450s with activities across different classes of natural products had been discovered *via* functional profiling.[71,89,98–104,90–97] Recently, fungal metagenomics programmes such as the 1000 Fungal Genome project sequenced dozens of WR fungal genomes and revealed numerous P450 sequences that are freely accessible from databases.[105]
Bioprospecting for such novel P450s from fungal detoxification is therefore holding a lot of potential and embodies the subject of **Chapter 3** (Figure 1, Bioprospecting).(manuscript submitted) It showcases an example how easy multifunctional P450s converting several different natural product classes can be identified by *in silico* enzyme discovery for the conversion of several different natural product classes and highlights the need for more comprehensive studies.
Targeting the identification of new P450 enzymes for de-methylation, de-ethylation or selective functionalisation of heterocycles, protein sequences of a small P450 library consisting of nine CYP5035 from the WR fungus *Polyporus arcularius* were expressed in *P. pastoris* and screened for activity using the 7-methoxy-4-(trifluoromethyl)coumarin (MFC) de-methylation assay.[106] Previous efforts to generate enhanced *P. pastoris* platform strains for this fluorescent assay had failed using CRISPR/Cas9 technology (data not shown), which had been established in our laboratory for this host organism[107] and recently won the Nobel prize in chemistry.[108]
Though only Enzyme CYP5035S7 was active in the fluorescent assay employing substrate MFC for activity screening anyway. Hence, functional screening of all nine CYP5035 towards various substrate classes was continued using HPLC. Particularly interesting was a mutual activity towards known fungicidal agents or their derivatives indicating that the hardly explored CYP5035 family[71] can be categorised as member of the fungus' detoxification machinery, which is also supported by the –omics studies of Miyauchi et al.[109] With the help of phylogenetic analysis of the P450omes of *P. arcularius* as well as related species *Polyporus brumalis*, *Lentinus tigrinus* and *Polyporus*

squamosus, the unusually high enrichment of CYP5035 in these species could be traced back to the *Ganoderma* macrofungus as the potential evolutionary origin. Aligning CYP5035S7 to 102,000 putative P450 sequences of 36 fungal species from JGI-provided genomes located hundreds of further CYP5035 family members, which subfamilies were classified if possible.
These results provide a valuable starting point for future bioprospecting for detoxifying eukaryotic P450s with the ability to modify plant compounds similar or complementary to *P. arcularius*.

[1] R. A. Sheldon, *Green Chem.* **2017**, *19*, 1–320.
[2] R. A. Sheldon, J. M. Woodley, *Chem. Rev.* **2018**, *118*, 801–838.
[3] D. C. Blakemore, L. Castro, I. Churcher, D. C. Rees, A. W. Thomas, D. M. Wilson, A. Wood, *Nat. Chem.* **2018**, *10*, 383–394.
[4] H. M. L. Davies, D. Morton, *ACS Cent. Sci.* **2017**, *3*, 936–943.
[5] J. Boström, D. G. Brown, R. J. Young, G. M. Keserü, *Nat. Rev. Drug Discov.* **2018**, DOI 10.1038/nrd.2018.116.
[6] I. B. Campbell, S. J. F. Macdonald, P. A. Procopiou, *Drug Discov. Today* **2018**, *23*, 219–234.
[7] T. Cernak, K. D. Dykstra, S. Tyagarajan, P. Vachal, S. W. Krska, *Chem. Soc. Rev.* **2016**, *45*, 546–576.
[8] J. Yamaguchi, A. D. Yamaguchi, K. Itami, *Angew. Chemie - Int. Ed.* **2012**, *51*, 8960–9009.
[9] L. McMurray, F. O'Hara, M. J. Gaunt, *Chem. Soc. Rev.* **2011**, *40*, 1885–1898.
[10] D. Y. K. Chen, S. W. Youn, *Chem. - A Eur. J.* **2012**, *18*, 9452–9474.
[11] Y. Qiu, S. Gao, *Nat. Prod. Rep.* **2016**, *33*, 562–581.
[12] B. Hong, T. Luo, X. Lei, *ACS Cent. Sci.* **2020**, *6*, 622–635.
[13] R. R. Karimov, J. F. Hartwig, *Angew. Chemie - Int. Ed.* **2018**, *57*, 4234–4241.
[14] X. Zhang, S. Li, *Nat. Prod. Rep.* **2017**, *34*, 1061–1089.
[15] C. R. Shugrue, S. J. Miller, *Chem. Rev.* **2017**, *117*, 11894–11951.
[16] O. Robles, D. Romo, *Nat. Prod. Rep.* **2014**, *31*, 318–334.
[17] K. C. Morrison, P. J. Hergenrother, *Nat. Prod. Rep.* **2014**, *31*, 6–14.
[18] B. Su, Z. C. Cao, Z. J. Shi, *Acc. Chem. Res.* **2015**, *48*, 886–896.
[19] A. Fürstner, *ACS Cent. Sci.* **2016**, *2*, 778–789.
[20] F. Rudroff, M. D. Mihovilovic, H. Gröger, R. Snajdrova, H. Iding, U. T. Bornscheuer, *Nat. Catal.* **2018**, *1*, 12–22.
[21] A. Wells, H.-P. Meyer, *ChemCatChem* **2014**, *6*, 918–920.
[22] N. Ran, L. Zhao, Z. Chen, J. Tao, *Green Chem.* **2008**, *10*, 361–372.
[23] N. J. Turner, E. O'Reilly, *Nat. Chem. Biol.* **2013**, *9*, 285–288.
[24] N. Turner, L. Humphreys, *Biocatalysis in Organic Synthesis: The Retrosynthesis Approach*, Royal Society Of Chemistry, **2018**.
[25] R. O. M. A. de Souza, L. S. M. Miranda, U. T. Bornscheuer, *Chem. - A Eur. J.* **2017**, *23*, 12040–12063.
[26] A. P. Green, N. J. Turner, *Perspect. Sci.* **2016**, *9*, 42–48.
[27] P. Ortiz de Montellano, *Cytochrome P450*, Springer International Publishing, Cham, **2015**.
[28] S. Shaik, S. Cohen, Y. Wang, H. Chen, D. Kumar, W. Thiel, *Chem. Rev.* **2010**, *110*, 949–1017.
[29] D. R. Nelson, *Biochim. Biophys. Acta - Proteins Proteomics* **2018**, *1866*, 141–154.
[30] E. King-Smith, C. R. Zwick, H. Renata, *Biochemistry* **2018**, *57*, 403–412.
[31] M. Winkler, M. Geier, S. P. Hanlon, B. Nidetzky, A. Glieder, *Angew. Chemie Int. Ed.*

2018, *57*, 13406–13423.
[32] F. Li, X. Zhang, H. Renata, *Curr. Opin. Chem. Biol.* **2019**, *49*, 25–32.
[33] M. T. Lundemo, J. M. Woodley, *Appl. Microbiol. Biotechnol.* **2015**, *99*, 2465–2483.
[34] Y. Wei, E. L. Ang, H. Zhao, *Curr. Opin. Chem. Biol.* **2018**, *43*, 1–7.
[35] B. David, J.-L. Wolfender, D. A. Dias, *Phytochem. Rev.* **2015**, *14*, 299–315.
[36] H. Yuan, Q. Ma, L. Ye, G. Piao, *Molecules* **2016**, *21*, 559.
[37] D. J. Newman, G. M. Cragg, *J. Nat. Prod.* **2020**, *83*, 770–803.
[38] T. Rodrigues, D. Reker, P. Schneider, G. Schneider, *Nat. Chem.* **2016**, *8*, 531–541.
[39] A. L. Harvey, R. Edrada-Ebel, R. J. Quinn, *Nat. Rev. Drug Discov.* **2015**, *14*, 111–129.
[40] G. Li, H.-X. Lou, *Med. Res. Rev.* **2018**, *38*, 1255–1294.
[41] A. M. Ehrenworth, P. Peralta-Yahya, *Nat. Chem. Biol.* **2017**, *13*, 249–258.
[42] J. Chen, W. Li, H. Yao, J. Xu, *Fitoterapia* **2015**, *103*, 231–241.
[43] N. D. Fessner, *ChemCatChem* **2019**, *11*, 2226–2242.
[44] G. Di Nardo, G. Gilardi, *Trends Biochem. Sci.* **2020**, *45*, 511–525.
[45] V. B. Urlacher, M. Girhard, *Trends Biotechnol.* **2019**, *37*, 882–897.
[46] F. P. Guengerich, *Nat. Rev. Drug Discov.* **2002**, *1*, 359–366.
[47] V. B. Urlacher, M. Girhard, *Trends Biotechnol.* **2012**, *30*, 26–36.
[48] J. M. Caswell, M. O'Neill, S. J. C. Taylor, T. S. Moody, *Curr. Opin. Chem. Biol.* **2013**, *17*, 271–275.
[49] C. J. C. Whitehouse, S. G. Bell, L.-L. Wong, *Chem. Soc. Rev.* **2012**, *41*, 1218–1260.
[50] S. Rendic, F. P. Guengerich, *Chem. Res. Toxicol.* **2015**, *28*, 38–42.
[51] L. Lah, N. Kraševec, P. Trontelj, R. Komel, *Fungal Genet. Biol.* **2008**, *45*, 446–458.
[52] D. Ohta, *Front. Biosci.* **2004**, *9*, 1587.
[53] E. O'Reilly, V. Köhler, S. L. Flitsch, N. J. Turner, *Chem. Commun.* **2011**, *47*, 2490–2501.
[54] A. Mitrovic, A. Glieder, in *Fungal Biomol. Sources, Appl. Recent Dev.* (Eds.: V.K. Gupta, R.L. Mach, S. Sreenivasaprasad), John Wiley & Sons, Ltd, Chichester, UK, **2015**, pp. 51–62.
[55] M. T. Lundemo, J. M. Woodley, *Appl. Microbiol. Biotechnol.* **2015**, *99*, 2465–2483.
[56] T. Vogl, T. Kickenweiz, J. Pitzer, L. Sturmberger, A. Weninger, B. W. Biggs, E.-M. Köhler, A. Baumschlager, J. E. Fischer, P. Hyden, et al., *Nat. Commun.* **2018**, *9*, 3589.
[57] A. Lichius, D. M. Ruiz, S. Zeilinger, in *Gd. Challenges Fungal Biotechnol. Gd. Challenges Biol. Biotechnol.* (Ed.: H. Nevalainen), Springer Nature Switzerland, Cham, **2020**, pp. 123–164.
[58] M. J. B. Burnett, A. C. Burnett, *PLANTS, PEOPLE, PLANET* **2020**, *2*, 121–132.
[59] R. M. Bill, *Front. Microbiol.* **2014**, *5*, 1–5.
[60] G. P. L. Cereghino, J. L. Cereghino, C. Ilgen, J. M. Cregg, *Curr. Opin. Biotechnol.* **2002**, *13*, 329–332.
[61] V. Juturu, J. C. Wu, *ChemBioChem* **2018**, *19*, 7–21.
[62] M. Ahmad, M. Hirz, H. Pichler, H. Schwab, *Appl. Microbiol. Biotechnol.* **2014**, *98*, 5301–5317.
[63] A. Emmerstorfer, T. Wriessnegger, M. Hirz, H. Pichler, *Appl. Microbiol. Biotechnol.* **2014**, *98*, 7671–7698.
[64] B. Byrne, *Curr. Opin. Struct. Biol.* **2015**, *32*, 9–17.
[65] V. Puxbaum, D. Mattanovich, B. Gasser, *Appl. Microbiol. Biotechnol.* **2015**, *99*, 2925–2938.
[66] M. Geier, A. Braun, A. Emmerstorfer, H. Pichler, A. Glieder, *Biotechnol. J.* **2012**, *7*, 1346–1358.
[67] J. C. Chan, M. Paice, X. Zhang, *ChemCatChem* **2020**, *12*, 401–425.
[68] G. Janusz, A. Pawlik, J. Sulej, U. Świderska-Burek, A. Jarosz-Wilkołazka, A.

Paszczyński, *FEMS Microbiol. Rev.* **2017**, *41*, 941–962.
[69] U. Kües, *Curr. Opin. Biotechnol.* **2015**, *33*, 268–278.
[70] W. Chen, M.-K. Lee, C. Jefcoate, S.-C. Kim, F. Chen, J.-H. Yu, *Genome Biol. Evol.* **2014**, *6*, 1620–1634.
[71] K. Syed, K. Shale, N. S. Pagadala, J. Tuszynski, *PLoS One* **2014**, *9*, e86683.
[72] M. Sahebi, M. M. Hanafi, A. J. van Wijnen, A. S. N. Akmar, P. Azizi, A. S. Idris, S. Taheri, M. Foroughi, *Int. Biodeterior. Biodegradation* **2017**, *122*, 151–164.
[73] T. Pusztahelyi, I. J. Holb, I. Pócsi, *Front. Plant Sci.* **2015**, *6*, 1–23.
[74] A. D. Moreno, D. Ibarra, M. E. Eugenio, E. Tomás-Pejó, *J. Chem. Technol. Biotechnol.* **2020**, *95*, 481–494.
[75] C. Romero-Guido, A. Baez, E. Torres, *Catalysts* **2018**, *8*, 223.
[76] M. D. Cannatelli, A. J. Ragauskas, *Chem. Rec.* **2017**, *17*, 122–140.
[77] T. Kudanga, B. Nemadziva, M. Le Roes-Hill, *Appl. Microbiol. Biotechnol.* **2017**, *101*, 13–33.
[78] D. M. Mate, M. Alcalde, *Microb. Biotechnol.* **2016**, *10*, 1457–1467.
[79] J. D. C. Medina, A. L. Woiciechowski, L. R. C. Guimarães, S. G. Karp, C. R. Soccol, in *Curr. Dev. Biotechnol. Bioeng. Prod. Isol. Purif. Ind. Prod.* (Eds.: A. Pandey, S. Negi, C.R. Soccol), Elsevier, Amsterdam, **2017**, pp. 217–232.
[80] A. O. Falade, U. U. Nwodo, B. C. Iweriebor, E. Green, L. V. Mabinya, A. I. Okoh, *Microbiologyopen* **2017**, *6*, e00394.
[81] L. Casella, E. Monzani, S. Nicolis, in *Biocatal. Based Heme Peroxidases Peroxidases as Potential Ind. Biocatal.* (Eds.: E. Torres, M. Ayala), Springer, Heidelberg, **2010**, pp. 111–153.
[82] Y. Wang, D. Lan, R. Durrani, F. Hollmann, *Curr. Opin. Chem. Biol.* **2017**, *37*, 1–9.
[83] M. Hofrichter, H. Kellner, M. J. Pecyna, U. René, in *Monooxygenase, Peroxidase Peroxygenase Prop. Mech. Cytochrome P450* (Eds.: E.G. Hrycay, S.M. Bandiera), Springer, Cham, **2015**, pp. 341–368.
[84] S. Bormann, A. Gomez Baraibar, Y. Ni, D. Holtmann, F. Hollmann, *Catal. Sci. Technol.* **2015**, *5*, 2038–2052.
[85] M. Hofrichter, R. Ullrich, *Curr. Opin. Chem. Biol.* **2014**, *19*, 116–125.
[86] C. Schmidt-Dannert, *Curr. Opin. Chem. Biol.* **2016**, *31*, 40–49.
[87] P. Durairaj, J.-S. Hur, H. Yun, *Microb. Cell Fact.* **2016**, *15*, 125.
[88] B. Črešnar, Š. Petrič, *Biochim. Biophys. Acta - Proteins Proteomics* **2011**, *1814*, 29–35.
[89] J. Wang, H. Ohno, Y. Ide, H. Ichinose, T. Mori, H. Kawagishi, H. Hirai, *J. Hazard. Mater.* **2019**, *371*, 494–498.
[90] H. Ichinose, T. Kitaoka, *Microb. Biotechnol.* **2018**, *11*, 952–965.
[91] K. Sakai, F. Matsuzaki, L. Wise, Y. Sakai, S. Jindou, H. Ichinose, N. Takaya, M. Kato, H. Wariishi, M. Shimizu, *Appl. Environ. Microbiol.* **2018**, *84*, 1–15.
[92] C. Yang, W. Li, C. Li, Z. Zhou, Y. Xiao, X. Yan, *Phytochemistry* **2018**, *155*, 83–92.
[93] M. Hatakeyama, T. Kitaoka, H. Ichinose, *Enzyme Microb. Technol.* **2016**, *89*, 7–14.
[94] K. Syed, A. Porollo, Y. W. Lam, P. E. Grimmett, J. S. Yadav, *Appl. Environ. Microbiol.* **2013**, *79*, 2692–2702.
[95] K. Syed, A. Porollo, D. Miller, J. S. Yadav, *Protein Eng. Des. Sel.* **2013**, *26*, 553–557.
[96] M. Ide, H. Ichinose, H. Wariishi, *Arch. Microbiol.* **2012**, *194*, 243–253.
[97] H. Ichinose, H. Wariishi, *Arch. Biochem. Biophys.* **2012**, *518*, 8–15.
[98] S. Hirosue, M. Tazaki, N. Hiratsuka, S. Yanai, H. Kabumoto, R. Shinkyo, A. Arisawa, T. Sakaki, H. Tsunekawa, O. Johdo, et al., *Biochem. Biophys. Res. Commun.* **2011**, *407*, 118–123.
[99] K. Syed, A. Porollo, Y. W. Lam, J. S. Yadav, *PLoS One* **2011**, *6*, e28286.

[100] K. Syed, H. Doddapaneni, V. Subramanian, Y. W. Lam, J. S. Yadav, *Biochem. Biophys. Res. Commun.* **2010**, *399*, 492–497.
[101] N. Kasai, S. Ikushiro, S. Hirosue, A. Arisawa, H. Ichinose, Y. Uchida, H. Wariishi, M. Ohta, T. Sakaki, *J. Biochem.* **2010**, *147*, 117–125.
[102] N. Kasai, S. Ikushiro, R. Shinkyo, K. Yasuda, S. Hirosue, A. Arisawa, H. Ichinose, H. Wariishi, T. Sakaki, *Appl. Microbiol. Biotechnol.* **2010**, *86*, 773–780.
[103] N. L. Chigu, S. Hirosue, C. Nakamura, H. Teramoto, H. Ichinose, H. Wariishi, *Appl. Microbiol. Biotechnol.* **2010**, *87*, 1907–1916.
[104] N. Kasai, S. Ikushiro, S. Hirosue, A. Arisawa, H. Ichinose, H. Wariishi, M. Ohta, T. Sakaki, *Biochem. Biophys. Res. Commun.* **2009**, *387*, 103–108.
[105] I. V. Grigoriev, R. Nikitin, S. Haridas, A. Kuo, R. Ohm, R. Otillar, R. Riley, A. Salamov, X. Zhao, F. Korzeniewski, et al., *Nucleic Acids Res.* **2014**, *42*, 699–704.
[106] M. T. Donato, N. Jiménez, J. V. Castell, M. J. Gómez-Lechón, *Drug Metab. Dispos.* **2004**, *32*, 699–706.
[107] A. Weninger, A. M. Hatzl, C. Schmid, T. Vogl, A. Glieder, *J. Biotechnol.* **2016**, *235*, 139–149.
[108] "The Nobel Prize in Chemistry 2020. NobelPrize.org. Nobel Media AB 2020. Sat. 7 Oct 2020," DOI https://www.nobelprize.org/prizes/chemistry/2020/summary/, **n.d.**
[109] S. Miyauchi, H. Hage, E. Drula, L. Lesage-Meessen, J.-G. Berrin, D. Navarro, A. Favel, D. Chaduli, S. Grisel, M. Haon, et al., *DNA Res.* **2020**, *27*, 1–14.

ChemPubSoc Europe
DOI: 10.1002/cctc.201801829
CHEMCATCHEM Reviews

P450 Monooxygenases Enable Rapid Late-Stage Diversification of Natural Products *via* C–H Bond Activation

Nico D. Fessner*[a]

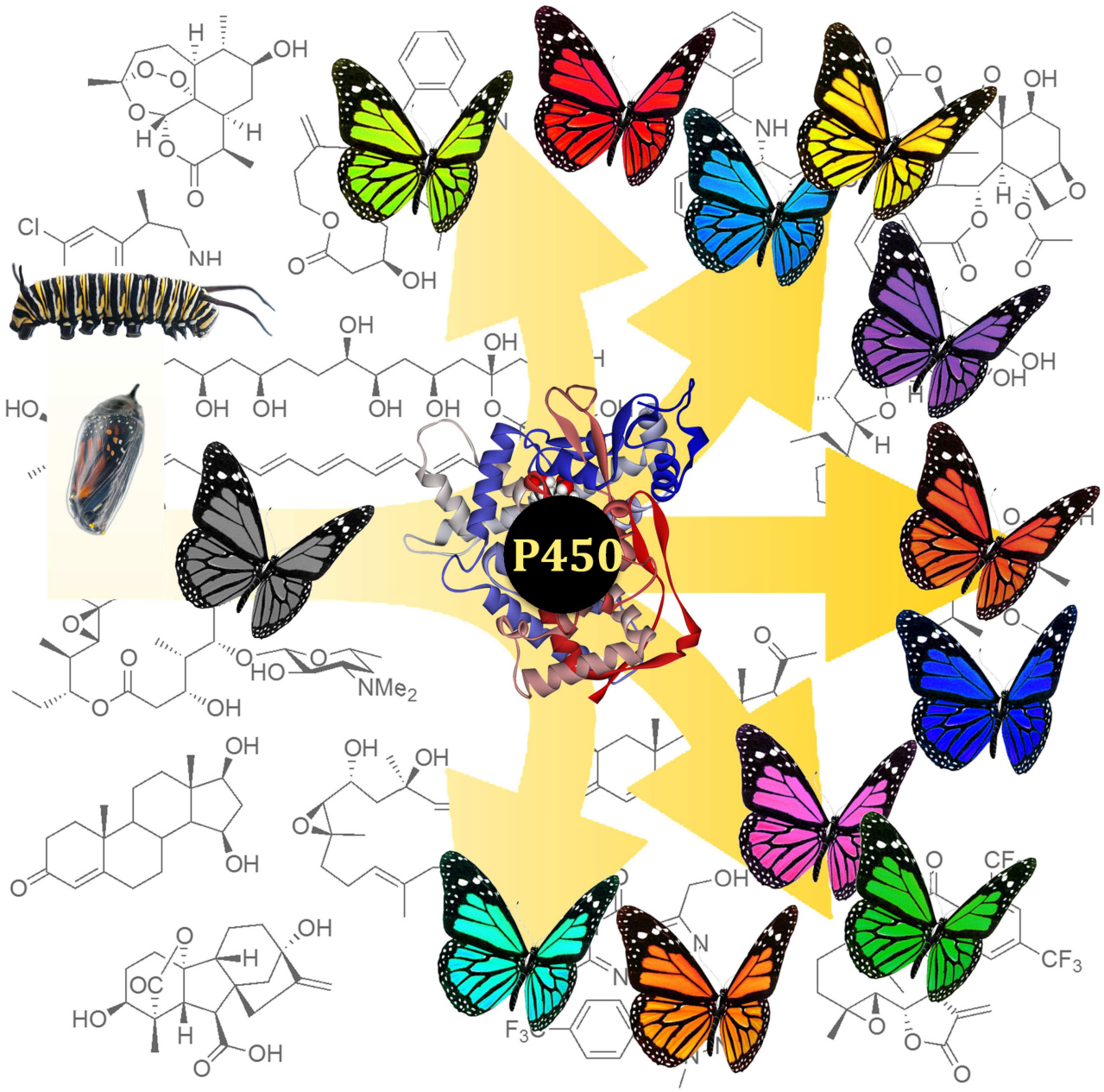

The biological potency of natural products has been exploited for decades. Their inherent structural complexity and natural diversity might hold the key to efficiently address the urgent need for the development of novel pharmaceuticals. At the same time, it is that very complexity, which impedes necessary chemical modifications such as structural diversification, to improve the effectiveness of the drug. For this purpose, Cytochrome P450 enzymes, which possess unique abilities to activate inert sp^3-hybridised C–H bonds in a late-stage fashion, offer an attractive synthetic tool. In this review the potential of cytochrome P450 enzymes in chemoenzymatic lead diversification is illustrated discussing studies reporting late-stage functionalisations of natural products and other high-value compounds. These enzymes were proven to extend the synthetic toolbox significantly by adding to the flexibility and efficacy of synthetic strategies of natural product chemists, and scientists of other related disciplines.

1. Introduction

Natural products such as taxol, artemisinin, monensin, amphotericin – to name but a few – belong to the group of molecules that changed the world as we know it, and will continue to do so.[1] Their structural complexity and diversity are unmatched, and arise from a constant evolutionary refinement by host organisms.[2,3] Similarly, efficient natural product diversification is essential in the field of drug discovery, in order to meet the demand for novel drugs and drug analogues with improved specificity, or to test their metabolism in the body.[4] This occurs preferably using chemical late-stage modifications.[5–7] However, due to natural products' inherent complexity, such task is difficult to accomplish in a selective fashion. Often, chemically highly similar derivatives require independent synthetic access,[8] violating the desired time and material efficiency.[9]

Bond polarity dictates the type of reactivity; the polarity profile inherent in a molecule regulates how to install functional groups (FGs). The insertion of FGs at a late stage of the synthesis, however, is difficult due to the inertness of sp^3-hybridised C–H bonds within the carbon backbone. In an attempt to avoid problems and foresee solutions to the installation of FGs, the retrosynthetic approach consolidated in the chemical community.[10–13] In contrast, nature developed its enzymatic machinery providing elegant tools to somewhat bend these rules. Among other enzymes, particularly cytochrome P450 enzymes (P450s) stand out with their ability to activate sp^3-hybridised C–H bonds for oxygen functionalisation. Moreover, this even happens with outstanding chemo-, regio- and stereo-selectivities, thereby oxidising substrates more inert than their own surrounding protein framework.[14–16]

The increasing need for sustainability is changing the rules of synthetic chemistry considerably, driving the application of Green Chemistry principles,[17–19] the current trend toward protecting-group-free syntheses[20] and the continuous interest in the total synthesis of natural products in more elegant ways.[21] This calls for the integration of enzymes into the synthetic toolbox, supported by the discovery of a broad diversity of novel enzymes (e.g. by metagenomics) and the recent success in tuning enzymes in vitro to process requirements by rational engineering and directed enzyme evolution.[22–28] As a consequence, the term "Biocatalytic retrosynthesis" was introduced in 2013, which revitalised the attention given to the use of enzymes for upgrading synthetic routes to complex targets, implementing an effective tool to achieve FG installation in a highly selective fashion under mild reaction conditions.[29–33]

Natural products form the basis of drugs targeting a range of severe diseases, like cancer or malaria, and can serve as an inspiration in drug discovery. Between 1940s to the end of 2014, every second small molecule drug approved was either a natural product or a direct derivative of it[34,35] despite the fundamental shift in the drug industry towards synthetic small molecule libraries driven by combinatorial chemistry.[36] Generally, the generation of a diverse compounds library to cover a diverse chemical space increases the chances to identify or improve a promising lead compound, while the occupation of a focused chemical space is sufficient for fine-tuning.[37,38] When dealing with complex molecules like natural products, late-stage functionalisation offers an effective starting point for further diversification (Figure 1). This strategy has become popular only very recently and is about to enter the toolbox of medicinal chemistry.[5,7] Enzymes such as P450s are well known for their ability to install oxygenated FGs into primary and secondary metabolites, often operating at a later stage of the biosynthesis.[15] Thus, in combination with the broad range of available P450s and their diversified reaction scope, functional-

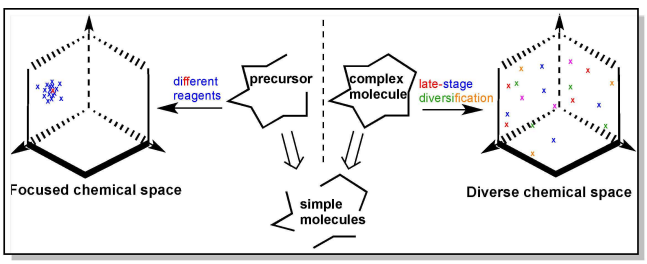

Figure 1. Focused and diverse chemical space covered by compound libraries of complex molecules. The two different libraries are generated either by using different reagents to synthesise similar final products from precursor, or by applying late-stage diversification to an already synthesised complex molecule, respectively.

[a] *N. D. Fessner*
Institute of Molecular Biotechnology
Graz University of Technology, NAWI Graz
Petersgasse 14, 8010 Graz, Austria
E-mail: nfessner@tugraz.at

isation *via* C–H activation embodies a method of immense potential for easy and rapid diversification of complex natural products.

This review will highlight the power of using cytochrome P450 enzymes for the concept of biocatalytic late-stage diversification by demonstrating the current progress in this field with recent examples. The importance of natural products will be introduced, and the elegancy of late-stage Csp^3-H bond activation to achieve efficient natural product diversification outlined. First reports proved the efficient use of cytochrome P450 enzymes in total synthesis of natural products.[39–41] Complementary to a recent summary focusing on the applications of oxygenases for total syntheses,[42] this review will prioritise P450-catalysed late-stage diversification of natural products for drug discovery.

1.1. Cytochrome P450 Enzymes

The more "noble and late" transition metal catalysts (Pd, Rh, Pt, Au, etc.) have proven very effective in activating unreactive chemical bonds over other more reactive ones. They dominated the field of homogeneous catalysis (e.g. Pd-catalysed cross-coupling reactions) up to now.[43] However, their toxicity, low abundance and high price have often outweighed their advantages, and are no more in agreement with the need for a sustainable catalyst.[44] The focus of recent research has thus increasingly shifted towards coinage metals such as Co-, Ni- and particularly Fe-based catalysts, albeit their benignity should be used as a "selling point" with care.[45] Iron is the most abundant transition metal on earth and plays an important role in nature. Providing some interesting all-round characteristics for catalysis, a lot of progress has been made on its use for the activation of C–H bonds.[44] Nonetheless, this stands in no comparison whatsoever to the capabilities that biological "Fe-catalysts" exhibit in nature in the form of cytochrome P450 enzymes.

The energy required for breaking the inert C–H bond is partially compensated with forming a strong O–H bond (Scheme 1).[46] The binding of the substrate results in a spin shift (low to high spin state) of the Fe-complex, allowing Fe(III) to Fe (II) reduction by a corresponding reductase as the redox partner. Subsequently, a ferryl oxo porphyrin radical cation species (compound I) is formed, which abstracts the hydrogen atom of the substrate radically.[47,48] The strength of the FeO–H bond is the driving force controlling the hydrogen transfer to yield compound II.[14] Product formation then occurs *via* a radical rebound mechanism.[48]

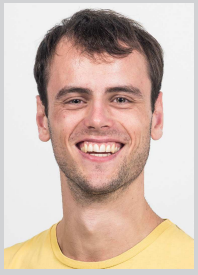

Nico D. Fessner obtained his MSci in Chemistry and was the recipient of the Joachim Steinke Prize for Excellence in Organic Chemistry at Imperial College London, where he graduated in the group of Prof. Alan Spivey. After working on a project in neuroscience in the group of Dr. Matthieu Louis in Barcelona, he started his PhD under the supervision of Prof. Anton Glieder at the Graz University of Technology as part of the European H2020 MSCA-ITN project OXYtrain (No.722390).

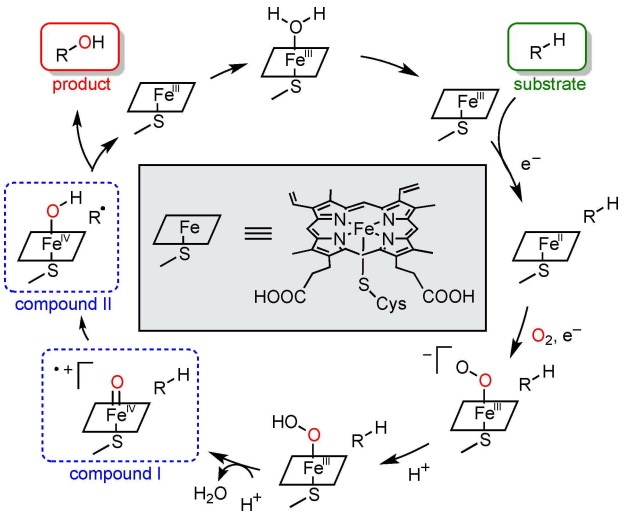

Scheme 1. The P450 reaction mechanism catalysing the hydroxylation of a C–H bond. Marked in blue are the hydrogen abstraction step by compound I and the subsequent radical rebound with compound II to form the hydroxylated product.[47,48]

Of course, the large protein framework, the exact geometry of the active-site and the heme-ligand surrounding the iron ion are of high importance.[14,49]

However, essential for the P450's ability to activate the inert C–H bonds is the directly coordinated cysteine thiolate.[46,48,50,51] Chemically, a strong electron donor like thiolate seems counter-intuitive for the design of a strong oxidant. In actual fact, the electron "push" to the iron centre generates the necessary "pull" for the C–H abstraction (Scheme 2).[14] This happens by increasing the basicity sufficiently, while sacrificing some of its redox potential.[50] This helps to effectively balance side reactions like uncoupling,[51] which is the undesired production of H_2O_2 as a by-product releasing reactive oxygen species that can deactivate the P450 enzyme itself.[52]

The majority of P450s exist as a pair of individual heme and reductase proteins since the terminal monooxygenase is no electron-transfer domain itself. The electrons required to reduce the P450 iron centre are provided by NAD(P)H and transferred *via* a FAD-containing reductase and a ferredoxin unit. Only a few P450s have their corresponding redox partners integrated

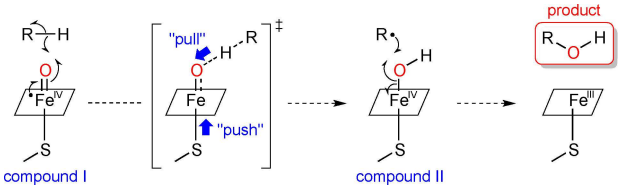

Scheme 2. The "push" effect of the electron-rich thiolate in compound I to enable a stronger "pull" and abstract the hydrogen from the C–H bond.[14] The formed compound II leads to product formation *via* radical rebound.

within the same polypeptide and are therefore self-sufficient.[53] The dependence on an efficient electron-transfer by different cofactors often makes the reduction of P450s the rate-limiting factor. As eukaryotic P450s are additionally membrane-bound while their bacterial equivalents are soluble, self-sufficient fusion systems like the bacterial BM3 (CYP102 A1) are usually more inviting for application.[54]

1.2. Natural Diversity of Natural Products

Natural selection is the key mechanism of evolution that enables *'nature to live on the edge'* meaning the constant development and improvement towards the status quo in order to replicate, adapt and survive.[55] One way to get a potential advantage over competitors is the generation of unique natural products. However, useful, potent biological activity was a rare feature among them. Therefore a larger number of natural products synthesised increased the probability of obtaining a "*lucky hit*"[56–58] that would enhance the fitness of the organism.

In this fashion, natural product diversification served as a natural screening platform for further structural exploration (cf. diversity-oriented synthesis).

Firn and Jones[56] nicely illustrated the origin for chemical diversity of natural products with the help of a matrix grid (Figure 2) stating that it is mainly the result of the broad

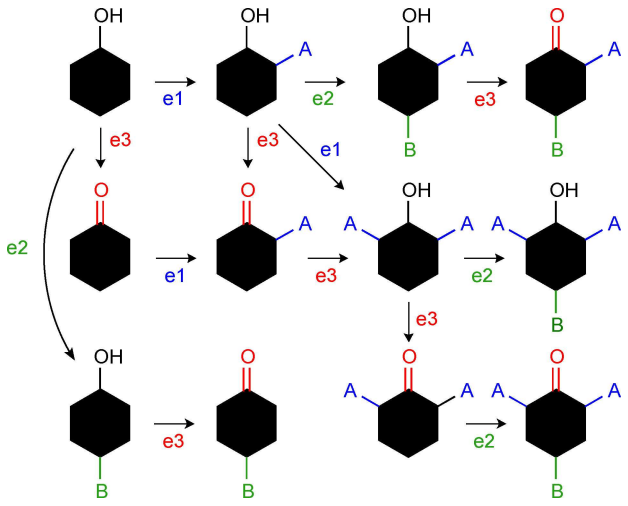

Figure 2. Matrix grid to illustrate chemical diversity from broad substrate tolerance of enzymes e1, e2 and e3.[56]

substrate tolerance of some enzymes involved in the biosynthesis. Thus, a combination of only three enzymes can generate eleven different product molecules if they also tolerate derivatives of the starting material as substrates.

Cytochrome P450 enzymes are well known for catalysing a wide range of distinct reaction types counting 20 already in 1996 and the number is still growing.[59] When possessing a relaxed specificity, these enzymes can drive diversification as shown in the example of the Gibberellin biosynthetic

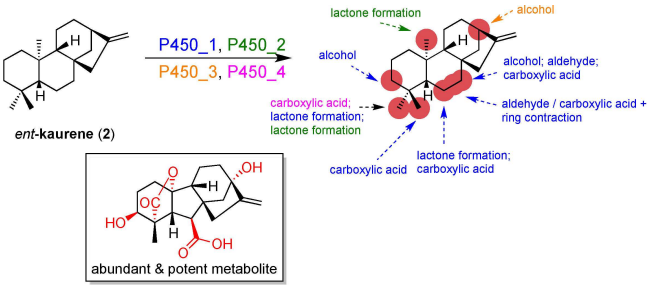

Scheme 3. The diversification of *ent*-kaurene (**2**) by four P450 enzymes occurring in the Gibberellin biosynthetic pathway.[60,61] The positions accessible by different P450s are marked in red and the enzymes with their corresponding reactions are colour-coded. One of the most abundant metabolites with known potency is shown in the box with the introduced functional groups coloured in red.

pathway.[60] The refinement of the *ent*-kaurene intermediate results in more than 136 distinct products using practically only four different P450 enzymes (Scheme 3). The oxidations happen in a combinatorial pattern similar to the matrix grid shown in Figure 2, thus increasing the diversity polynomially. Remarkably, in this pathway the alkene – the only chemically reactive functional group present – is left intact, although two of the P450s involved in oxidative modifications are multifunctional.[61] Every manipulation in this diversification process involves a C–H activation, yet many complex natural products like the one shown in the box with variable functionality are formed seemingly easily using only four enzymes.

At the same time the lack of selectivity hampers the probability for synthesising a particularly attractive product in useful quantities. This may represent a major challenge in the preparative applications of P450s *in vitro*.

1.3. Drug Discovery – Need for Diversification Tools

Some natural products are considered active compounds due to their excellent pharmacological profiles, thus lending themselves as attractive starting points in drug discovery. However, their diversity and complexity are a gift and a curse at the same time. Their quality as lead molecules is likely to be suitable, but effective diversification is essential in order to improve their drug quality.[4] The latter often proves to be challenging. Natural products are inadequate for modern high-throughput screening (HTS) with biochemical assays in the pharmaceutical industry,[62] they often fail to comply with the desired physiochemical properties (e.g. Lipinski's Rule of Five)[34,63,64] and difficulties are faced in accessing sufficient amounts of the target natural product.[34,65,66] Supply by extraction from natural resources by fermentation using metabolically engineered organisms or total synthesis can be cost intensive,[67] incompatible[68] or tedious,[8] respectively. Nonetheless, in recent years the focus in drug discovery is increasingly shifting back towards natural product scaffolds.[34,36,69] They received more attention in the light of (i) the misjudgement regarding the success of the discovery of

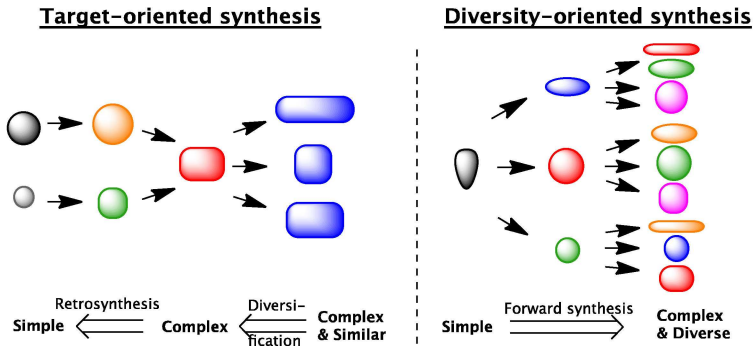

Figure 3. Concept of target- and diversity-oriented synthesis illustrated with colour and shape to code for diversity and complexity, respectively.[77]

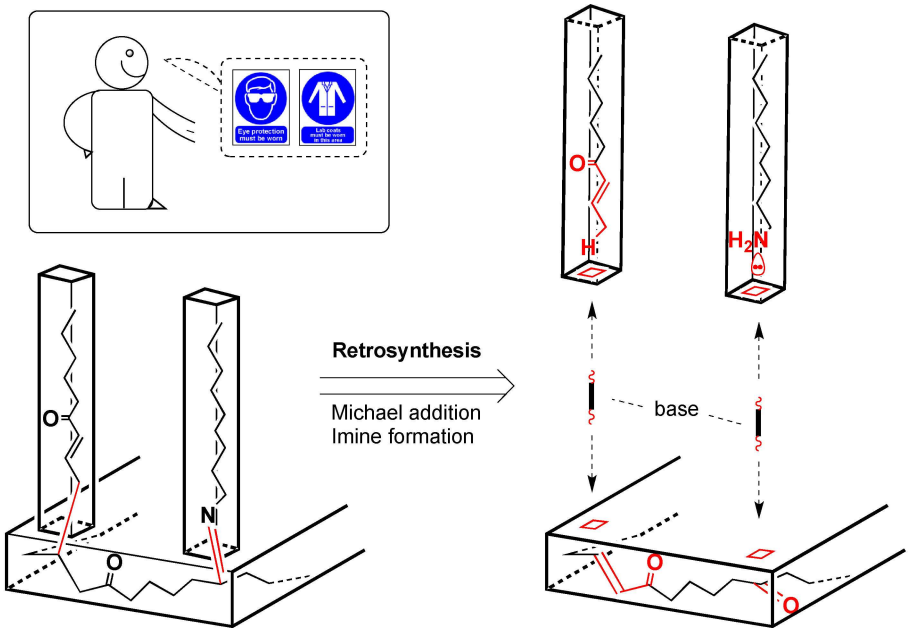

Figure 4. Symbolic illustration of the retrosynthetic approach applied to both molecules and do-it-yourself furniture assembly.

small, synthetic lead compounds by HTS methods,[36,64,69] (ii) the growing antibiotic resistance[70] and need for new antibiotics,[71,72] (iii) the change of strategy from a conventional target-oriented to a modern diversity-oriented synthesis (DOS)[73–75] and (iv) the shortcomings in the productivity in combination with expenses for clinical trials.[76]

Traditionally, a target-oriented strategy was used in drug discovery to find the best-fitting drug molecule for a predefined protein target in need of modulation. However, the success rate of the molecule's actual target-modulating abilities was unpredictable due to the biological complexity of living systems.[73,77] By leaving unknown both the target within a certain pathway as well as the compound expected to modulate it, modern DOS allows a certain degree of freedom for the final lead structure. This strategy aims to divergently synthesise a collection of compounds to cover a large chemical space around a specific template (Figure 3).[73,77]

Synthetic strategies are planned using the retrosynthetic approach,[78,79] which is based upon the step-wise detachment of the product molecule with maximum efficiency until its origin is found in commercially available starting materials. Often, for highly similar derivatives of the desired product completely new pathways must be developed because the synthesis of complex molecules requires reactive sites of suitable polarity placed at the correct positions.[8] The deliberate choice of methods for carbon backbone construction with the help of appropriate polar functional groups is therefore an important factor in the retrosynthetic strategy.[80] Common synthetic strategies include the *umpolung* process, FG interconversion or use of protecting groups.[12]

Similarly, in a manner resembling the do-it-yourself furniture assembly, where the item is built up from small pieces following step-by-step assembly instructions, this synthetic approach also had to be devised in the reverse direction beforehand (Figure 4).

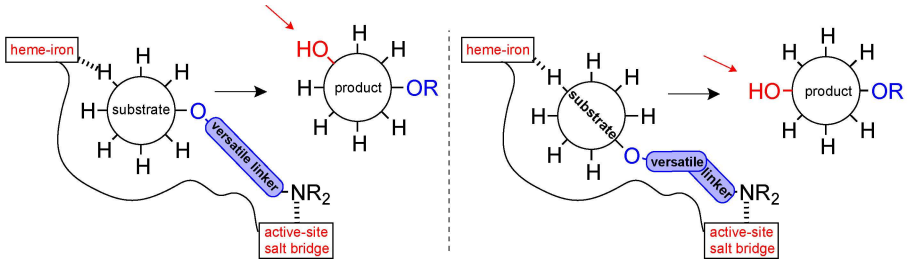

Scheme 4. The structure of the anchoring group for PikC substrate recognition can be changed for controlling the regioselectivity of the enzymatic hydroxylation.[102]

Analogously to the demand for specific local functionalisation in the construction of complex molecular scaffolds, if assembly holes are missing on the furniture material or wrong screws have been used, it will be impossible to construct the desired product as planned. Sheer force or the help of tools such as a drilling machine would be required. This is very similar in synthetic chemistry; to modify or functionalise the target molecule by activating an sp^3-hybridised C–H bond (i.e. "drill a hole") extreme conditions like high temperatures or toxic metal catalysts are required.[81–85]

This comparison nicely illustrates the obstacles that need to be overcome when attempting a late-stage modification of a complex molecular scaffold possessing various other reactive groups. The number of publications on C–H activation and their application in the synthesis of pharmaceuticals are steadily increasing, reflecting the ongoing chemical research on this topic.[86]

Such late-stage refinement adds a great deal of flexibility to synthetic strategies and diversification purposes in the drug discovery industry making it such an attractive and powerful tool.

Excellent reviews have summarised approaches like C–H activation used in the synthesis[86–89] or diversification of natural products.[4,90–94] In the following chapter, the application of P450 enzymes in diversity-oriented syntheses is illustrated with some recent examples.

2. Examples

2.1. Macrocycle Synthesis and Diversification

Macrocycles hold great therapeutic capacities because their ring structure is conformationally defined, often resulting in high affinity and selectivity for protein targets.[95] Several natural products that have been exploited successfully as powerful therapeutics possess a macrocyclic skeleton.[96]

The recent example of Gilbert *et al.* therefore represents an appealing template for macrocycle functionalisation using P450s.[97] The P450 enzyme of choice was the bacterial PikC from the pikromycin pathway, which had been characterised by the Sherman group,[98] then engineered to make it self-sufficient by fusion to the known RhFRED reductase domain.[99] The enzyme's natural anchoring mechanism involves a salt bridge and hydrogen bonding network to the desosamine sugar functionality of glycosylated macrolactone substrates.[100,101] This mechanism enables substrate specificity for the macrolide antibiotics in the pikromycin and methymycin pathways.[99] In a recent study, the Sherman group took advantage of this mechanism by replacing the desosamine sugar with a synthetic anchoring group.[102] The possibility to add or remove the anchoring group, and the relationship between its size and rigidity and the regioselectivity of the enzymatic hydroxylation makes this a highly versatile strategy in synthetic chemistry (Scheme 4).

A nice demonstration was thus given at the end of last year with the diversification of macrocycles **4**–**6**.[97] From the common intermediate **3**, 12- and 11-membered products **4** and *S*,*S*-**5**, as well as the latter's diastereomeric equivalent *R*,*R*-**6**, were formed by endo- and exocyclisation, respectively. Diversification could then be further driven by the attachment of different linker groups **a**–**e** (Scheme 5). These were synthesised *via* azide-alkyne click chemistry, thus improving once more the substrate engineering method by allowing access to high-throughput linker synthesis. The linkers differed in length and shape i.e. *ortho*-, *meta*- and *para*-substituted benzene or absence of phenyl group.

In substrate **4** longer linkers, i.e. **a** and **b** provided regiochemical access to C–H bonds distal of the linker, while shorter ones (**c** and **d**) oxidised C–H bonds proximal to the directing group. In contrast, for diastereomer *R*,*R*-**6** linkers **a** and **b** led to distal oxidation like **c** and **d**, similar to **4** where the shortest linker **e** oxidised the proximal allylic proton.

Neither epoxidation, nor amine linker oxidation was observed, although linker **e** had intentionally been designed as the diethylamine to avoid N-demethylation observed in some cases. To test orthogonal chemoselectivity for C–H oxidation, **5** was oxidised to its epoxide **12** and PikC then oxidised it to **13a**. Noteworthy, albeit left unmentioned by the authors, the presence of the epoxide changed the selectivity towards a distal position compared to product **9a**, due to the missing allylic activation. Proximal allylic oxidation also occurred in substrate **6**, albeit with very low selectivity, and some unidentified minor products were formed from **4** and **5**, which was not discussed in the paper. More diverse linker modifications are yet to be explored.

No total turnover numbers (TTN) were provided – the maximum number of chemical conversions of substrate mole-

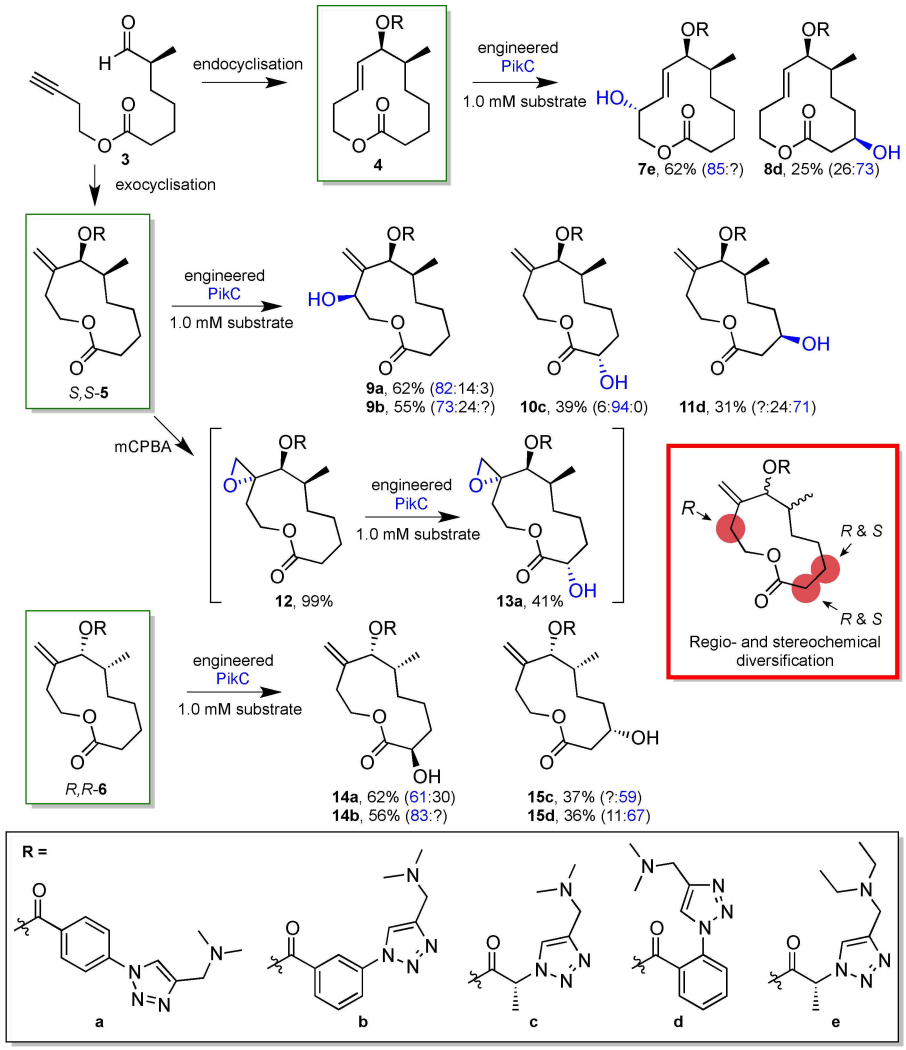

Scheme 5. Late-stage diversification of macrocycles **4**, *S,S*-**5** and *R,R*-**6** (green boxes) with only a single P450 (PikC) directed by the different linkers **a** – **e** (black box).[97] The product ratio is given in brackets highlighting the product with blue colour. Question marks indicate unknown fraction of corresponding regioisomers. Yields of preparative reactions ranged between 25% and 62%. In the red box the regio- and stereoselectivity profile of the exocyclisation products of **12** is summarised.

cules per enzyme molecule over the catalyst's lifetime. However, preparative experiments were conducted on a 30–60 mg scale.

The combination of esterification and click reactions enables access to a range of different products with regio- and stereoselectivity, where the linker length and geometry is the decisive diversification factor. The full extent of this method's potential has certainly not materialised so far, and more is yet to come in the use of directing groups in combination with enzyme catalysis. However, the above mentioned study has demonstrated that a single enzyme can selectively functionalise macrocycles bearing so many C–H bonds in a controllable manner with the help of linkers.

2.2. Simulation-Guided Mutagenesis of P450 for Selectivity Prediction

Using directed evolution of an enzyme for tuning it towards desired selectivities requires extensive time and effort due to the need for screening all of the generated variants.[16,23] This can be minimised by deriving the most beneficial mutations, generating smaller libraries with site-specific mutagenesis and verifying mutations experimentally.[103] The semi-rational approach is made increasingly efficient combining structural and biochemical data with computational data. Rather than generating a maximum diversity of active site geometries,[22,104,105] more focused libraries can thereby be generated like this.

Cytochrome P450 enzymes,[50,106–108] particularly BM3,[109,110] have been the subject of intense research computationally.. With macrocycles as the substrate, the study of Urlacher *et al.* in 2018 demonstrated the power of *in silico* engineering to impose

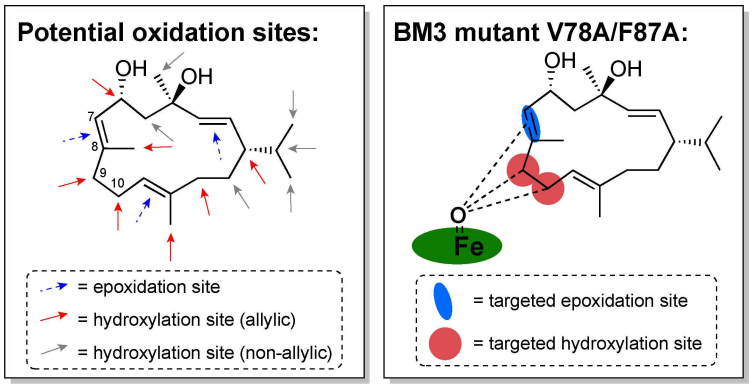

Figure 5. The potential oxidation sites of β-cembrenediol on the left, and the three positions unselectively targeted by BM3 mutant V78A/F87A on the right.[111]

control on the selectivity of P450 enzyme BM3 on the diterpenoid β-cembrenediol.[111] In a previous study the Urlacher group had already investigated the BM3 on the β-cembrenediol.[112,113] The carbon backbone of this macrocycle of neuroprotective function has 16 possible oxidation sites, and three of them are accessible with the wild-type enzyme (Figure 5). Using first-sphere active site mutagenesis, a small library of mutants was generated, of which two showed excellent regioselectivity either for positions C9 (product **18**) or C10 (product **19**), and quite good stereoselectivity in each case. Another mutant, BM3V78A/F87A, was unselective, though in addition to **18** and **19** the epoxide product **17** was yielded as well.

Using the mutant V78A/F87A as the starting template, a subsequent study computationally investigated what active site residue would significantly influence the enzyme's selectivity for **16** upon mutation.[111] The strategy was based on the premise that the substrate's binding mode within the active site determines the selectivity of reaction. Given multiple conformational modes possible for a large molecule like a macrocycle, careful conformational analysis and substrate docking simulations were necessary to obtain possible enzyme-substrate complexes. However, with those in hand the binding density surface (BDS, i.e. the 2D surface of two probability density functions) could be mapped for different positions of **16** keeping in mind the reaction mechanisms and optimal distance for the reaction to occur. The BDS of the chemo- and regioselectivity of BM3V78A/F87A catalysing the oxidation of **16** is shown in Scheme 6. The major hotspot shown in red indicates that the hydroxylation reactions are favoured over the epoxidation towards product **17**, supporting the experimental data. Further BDS graphs were modelled giving valuable information about the regioselectivity between the hydroxylation products **18** and **19** and their stereoselectivities, or that of the epoxidation reaction.

In combination with modelled protein-substrate orientations, the binding free energies of individual active site residues could be calculated, indicating whether this amino acid would stabilise or destabilise the substrate position and thus the corresponding product formation.

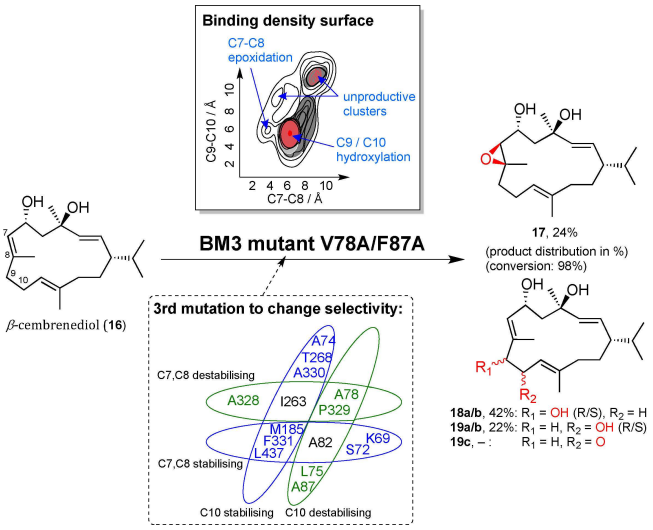

Scheme 6. β-cembrenediol (**16**) is converted to epoxide **17** and hydroxylation products **18** and **19** by the BM3 mutant V78A/F87A.[111] The percentage refers to the product distribution. The mapped binding density surface indicates a preference for products **18** and **19**. Binding free energy of different active site residues suggested additional mutations and predicted a potential selectivity outcome by stabilising the corresponding binding mode.

An *in silico* mutation simulation then identified the most favourable triple mutants. Experiments were performed to test the suggested mutations and it was found that six out of ten caused an increase in desired product by at least 2-fold. In one case both products **17** and **18** were eliminated completely, and production of **19** was increased more than 5-fold.

The objective to construct a computational methodology of enzyme engineering to predict a shift in enzyme selectivity was well accomplished, albeit enzyme activity itself was not included in the calculations as noted by the authors: It was observed that four of ten triple mutants showed significantly lower conversion than the imperfect template. Computational predictions can provide essential information for application in enzyme engineering for diversification This presents a signifi-

cant paradigm on how to generate and control the distribution of products.

2.3. Facile Transformation of an Antibiotic Macrolide to other Members of its Class *via* Late-Stage Diversification using Natural P450 Enzymes

The availability of novel antimicrobial drugs is severely limited urgently demanding solutions when considering the mounting crisis of antibiotic resistance and the simultaneous lack of economic incentive for antibiotic drug discovery.[70] Natural products present a renewed hope especially for the resolution of this crisis because they had once paved the way for the Golden age of antibiotic discovery.[71,72] Novel chemical structures may prove to be the key against evolving pathogens. Macrolides are an important class of antibiotics, but do not always comply with the desired characteristics for pharmaceutical use.[114] Chemical modifications of these naturally occurring therapeutics is thus essential and tools for their derivatisation desirable. In fact, derivatives of the same bioactive chemical scaffold represent the main source of "novel" antibiotics.[115]

The Sherman group had already studied several biocatalytic syntheses of macrolactone glycosides in the past.[116] Recently, they examined the interconnection of pharmaceutically valued macrolides within this compound family *via* P450 diversification, thus giving an example of the application of this enzyme class in actual drug discovery.[117] Following up on its first biocatalytic total synthesis, antibiotic M-4365 G_1 (**20**) was successively functionalised to a set of juvenimicin and rosamicin macrolides possessing the same core structure. The executing tools were three P450s TylI, JuvD and MycCl, all part of the biosynthesis of closely related compounds: macrolactone glycosides tylosin, juvenimicin and mycinamicin, respectively (Scheme 7). Using self-sufficient P450-RhFRED fusion proteins, several mg of product per 1 L overexpression culture could be obtained in preparative-scale reactions.

The concept of interconnecting different antibiotic families from a common scaffold *via* late-stage adjustments with the best-fitting P450s of biosynthesis of this compound family worked out well. Barely functionalised compound **20** offered itself as a good starting point to be oxidised twice up to the aldehyde **22** by P450 TylI. From each of the compounds **20**–**22** either an epoxide at positions C12 and C13 or a hydroxyl group at position C23 could be introduced with P450s JuvD or MycCl, respectively.

The authors reasoned their P450 enzyme selection as follows: (i) Epoxidation of **22** leads to rosamicin **25**. Logically, first choice were thus P450s JuvC and JuvD due to their high sequence similarity to the established P450 enzymes RosC (87%) and RosD (84%) of the rosamicin biosynthesis.[118] (ii) However, since JuvC's activity on **20** was disappointing, the job was allocated to TylI. (iii) MycCl was employed due to its characterised task to hydroxylate this position in the Mycinamicin biosynthetic pathway, and its unusual substrate flexibility.[119]

Unfortunately, the sequential application of P450s JuvD and MycCl on either one of compounds **20**–**22** was not reported, and neither was that of TylI on any of compounds **23**, **24**, **26** and **27**. Therefore, a complete assessment of the ease of transformation from one antibiotic to another by P450 enzymes can therefore not be made. Furthermore, while the performance of TylI in first oxidation to **21** was satisfactory (61% isolated yield), the low yield obtained in the second oxidation step (~10%) forced the authors to prepare **22** with the help of chemical methods by using a copper(I)/TEMPO catalyst system.

Nevertheless, given the number of studies that have explored the derivatisation of known antibiotics, the biocatalytic component in this study makes it stand out. It highlights the capacity of P450s in the application to the drug discovery process, allowing facile access of a variety of chemical derivatives. Two different functional groups at three individual positions could be selectively introduced to pharmaceutically active natural products. The fact that this can be achieved post-synthetically at a late-stage fashion to a complex macrolide heralds both the establishment of P450 enzymes into drug discovery, as well as the benefit of recourse to natural products.

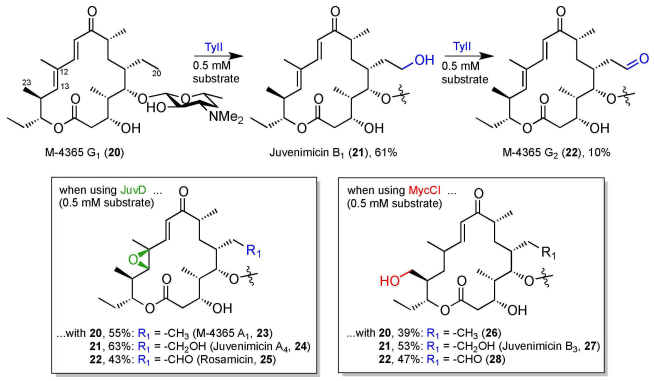

Scheme 7. Late-stage diversification of natural product M-4365 G_1 (**20**) with three natural P450s to obtain the improved antibiotic forms (**21**–**28**).[117] The functional groups introduced bare the same colour to the respectively catalysing P450 enzyme.

2.4. Artemisinin Functionalisation with Absolute Regio- and Stereoselectivities using Active-Site Fingerprinted and Engineered BM3 Variants

As an alternative to performing exhaustive computational simulations on the active site of BM3 towards the designed generation of substrate diversity, the Fasan group developed a 'fingerprinting method' to map the binding pocket of cytochrome P450 enzyme BM3 variants in order to predict the regioselectivity exhibited towards terpenes.[120]

The workflow is illustrated in Scheme 8A. Five different molecules were selected as substrate probes covering a range of different molecular scaffolds present in many terpenes of pharmaceutical value. The template BM3 mutant FL#62 exhibited high activity on all of these probes and was thus chosen as the template for mutagenesis. A mutant library was generated by using site-saturation mutagenesis on six positions

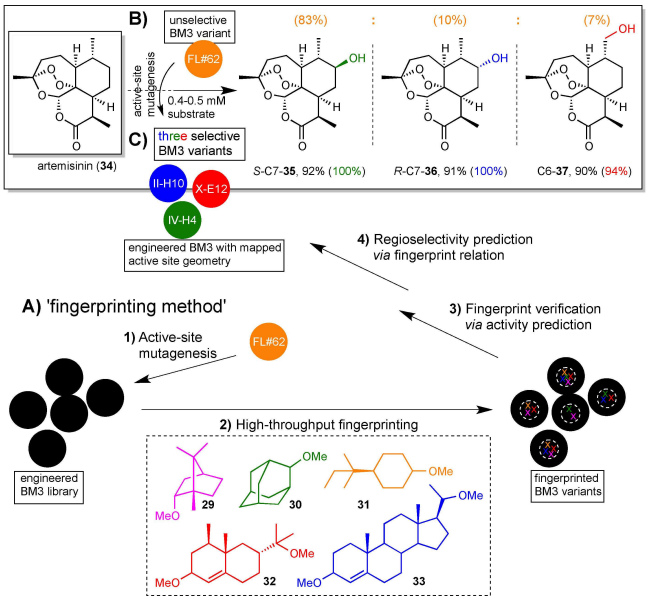

Scheme 8. Late-stage functionalisation of artemisinin (**34**) with BM3 variants after active-site geometry fingerprinting and active site mutagenesis.[121] The percentage yield is indicated, and in brackets the product distribution is shown in the same colour as the corresponding BM3 mutant. **A)** The application of a developed high-throughput fingerprinting method[120] on FL#62, a known variant of BM3 is illustrated. Active-site mutagenesis on FL#62 afforded a library of mutants, which active-site geometries were mapped to identify three BM3 variants appropriate for the substrate of choice. **B)** FL#62 itself catalysed the transformation of artemisinin (**30**) yielding an improvable product distribution of 83:10:7 for **35**, **36**, **37**, respectively, with a TTN of 340. **C)** The three identified BM3 variants of FL#62 hydroxylated **30** at two different positions, IV-H4 (362 TTN) and II-H10 (270 TTN) with absolute (100%) regio- and *R*- and *S*-stereoselectivity, and the X-E12 (113 TTN) with high regioselectivity (94%).[121]

within the FL#62's active site that were known to have an impact directly on the enzyme's binding pocket. With the help of high-throughput screening the activity of the variants towards the five molecular skeletons gave an indication on the size and geometry of the active site. This in turn was used to predict the activity of a given variant for substrates of similar molecular structure, thus verifying the fingerprint. In 87–97% of times the predictions were found to be correct. Interestingly, most enzymes (5/6) having different fingerprints also displayed diverse regioselectivity, which again was verified experimentally.

Conclusively, this 'fingerprinting method' of mapping the active site geometry yielded BM3 variants of diversified regioselectivity that are able to target positions across the whole molecular scaffold of terpenes.

Yet, would this method also be transferable to other substrates? This question was answered with a second paper from the group, applying the method to the popular example of the anti-malarial drug artemisinin (**43**).[121] P450 enzymes are involved in artemisinin's biosynthesis and thus semi-synthetic supply is applicable,[122,123] which is managed through methods of metabolic engineering and synthetic biology.[124,125] Late-stage diversification of the drug can be achieved through synthetic chemistry tools used to synthesise new analogues or metabolic products,[93,126] often with aid of organometallic catalysis.[127,128]

The authors aimed at obtaining P450 enzymes that would catalyse the late-stage functionalisation of artemisinin with high regio- and stereoselectivity.[121] Their strategy was the application of the described 'fingerprinting method'. They thus started off with the same BM3 mutant FL#62, which had proven to possess a broad substrate scope including multiple ring scaffolds. FL#62 was indeed accepting **34** as a substrate with 340 total turnovers to yield **35**–**37** (83:10:7) with an unselective product distribution (Scheme 8B). A small library of mutants was yielded by rational driven site-saturation mutagenesis of the active site, regiochemically diverse variants predicted by P450 fingerprinting, verified experimentally and the three most promising mutants (II-H10, X-E12 and IV-H4) identified (Scheme 8B). These catalysed the formation of S–C7-35, R–C7-36 and C6-37 with 100, 100 and 94% selectivity (Scheme 8C).

The success of the developed 'fingerprinting method' on a complex, yet fragile compound of high pharmaceutical interest like artemisinin speaks for itself. Vital for the positive result was the large and unselective binding pocket of the starting template BM3 FL#62 that could be fine-tuned towards the target substrate. Given an effective high-throughput screening method, the method's ease of execution makes the extremely high selectivities obtained even more remarkable.

2.5. Late-Stage Functionalisation of Steroidal Scaffolds with Engineered P450 Variants

One major challenge of mutagenesis is to find an adequate balance between the enzyme's selectivity and specific activity,[129] since improving one usually diminishes the other.[120] Therefore alternatives to mutagenesis have been explored[130,131] including the use of directing groups such as those in section 2.1. to determine the selectivity and substrate tolerance[102] or in section 2.3. for substrate recognition by the enzymes.[101,119] While clearly very compelling, such alternatives to improve the selectivity are likely to suffer from a lack of wide-ranging applicability.

Example A)

Already back in 2011, the Reetz group published an example of P450 mutagenesis for hydroxylating the complex steroidal scaffold with near complete regioselectivity.[132] Their approach followed a typical 'evolve-and-screen' strategy of a BM3 variant, however, combinatorial active site saturation test (CAST) coupled with rational design reduced the amount of screening – bottleneck of directed evolution[133] – immensely. CAST efficiently generates focused libraries by mutating all relevant residues in proximity to the active site[134] and had originally been developed within the Reetz group, to broaden the substrate tolerance.[135] The BM3(F87A) variant chosen for their study already unselectively catalysed the transformation of testosterone (**37**) to a mixture of the 2β- and 15β-alcohols. The F87A mutation of the template BM3 has long been known to change the substrate orientation and thus the regioselectivity,[136] and has been widely used.[137]

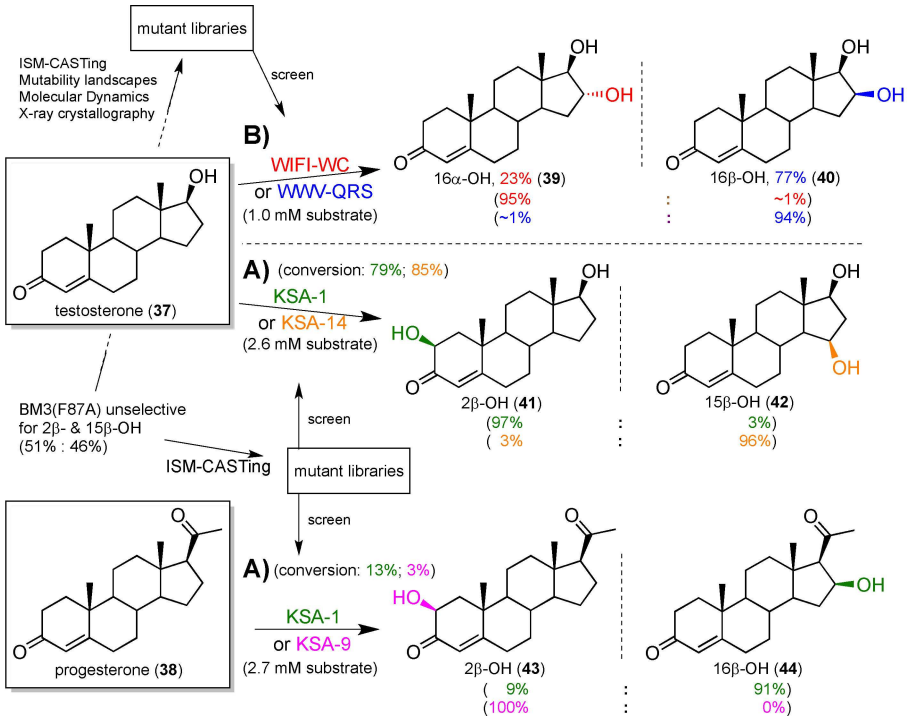

Scheme 9. Three different studies showed a proof-of-concept late-stage functionalisation of testosterone (**37**) and/or progesterone (**38**) with excellent regio- and/or stereoselectivities using engineered P450 mutants. The product distributions are given in brackets and coloured according to the respective enzyme variant that catalysed the reaction. **A)** Using iterative saturation mutagenesis (ISM) the lack of selectivity of $P450_{BM3}$ variant F87A for positions 2β and 15β (1:1 mixture) was shifted almost completely towards either one to afford **41** and **42** with 97% and 96% selectively over the other.[132] **B)** With the help of molecular dynamic simulations, X-ray data and an explored mutability landscape, ISM-CASTing was performed on the residues lining the binding pocket of the same BM3 variant F87 A to change the regioselectivity to position C16 with stereoselectivities of 95% and 94% ee for both enantiomers **39** and **40**, respectively.[129] Percentage yield is given for an up-scaling transformation carried out with the respective best mutant.

Favourable residues were selected with the help of mechanistic and structural data, which were grouped and filtered to render cooperative effects more likely, and the amino-acid alphabet was partly reduced: Having focused at first on only three sites, the same number of combinatorial libraries was generated and the screening thus reduced to 8,700 transformants.[132] These included two mutants, KSA-1 and KSA-14, which catalysed the hydroxylation of testosterone at positions C2, **41**, and C15, **42**, with 97% and 96% regioselectivity, respectively, and complete stereoselectivity for the β-H (Scheme 9A). As another example, progesterone was tested as a substrate. Products 2β-OH, **43**, and 16β-OH, **44**, were formed with 100% and 91% selectivity using mutants KSA-9 and again KSA-1, respectively. According to computational calculations, the extremely high regioselectivity is due to the restriction of **37** and **38** to two defined orientations within the enzyme's binding pocket.

Example B)

In a follow-up study, the Reetz group extended the scope of their BM3 variants to the C16 position of testosterone, setting target to both 16α and 16β stereoisomers.[129] Synthetically, C–H activation at this position in steroids is of high interest because it allows easier access to biologically active glucocorticoids. Rather than using a mutant that had already shown some C16 hydroxylation, here the authors started with the same BM3 (F87 A) mutant as before. To guide mutagenesis identifying the appropriate amino acid residues, even more trust was put into rational design and molecular dynamics computations were carried out supportively. The main rational element was a protein mutability landscape (Figure 6), which is the systematic analysis of the effect any amino acid at a particular position has on the enzyme's performance.[138,139]

Such a map of the sequence-function relationship was generated for the F87A template enzyme by analysing previous data from Commandeur *et al.*,[140–142] Payne *et al.*,[143] and their own lab,[144] and by screening mutants available from a previous study.[145] For example the group of Commandeur had identified residue 72 to be important for substrate orientation, and showed that it was completely inverting the stereoselectivity of C16 hydroxylation.[141] The analysis was directed towards four aims: (i) conversion of testosterone, a C16 hydroxylation considering both (ii) α- and (iii) β-protons, in contrast to the previously observed (iv) 15β-product.

With the mutability landscape at hand, the residues were filtered, grouped and five of them selected each for libraries A and B. Three cycles of iterative saturation mutagenesis (ISM) was performed: The method CAST was first applied to library A (950 mutants screened). Then the mutant with the best selectivity for each 16α- and 16β-OH products was used as the template to generate one library B in each case (2×950 mutants screened). Again, the best mutant of every library B was optimised into four further enzyme variants with the help of

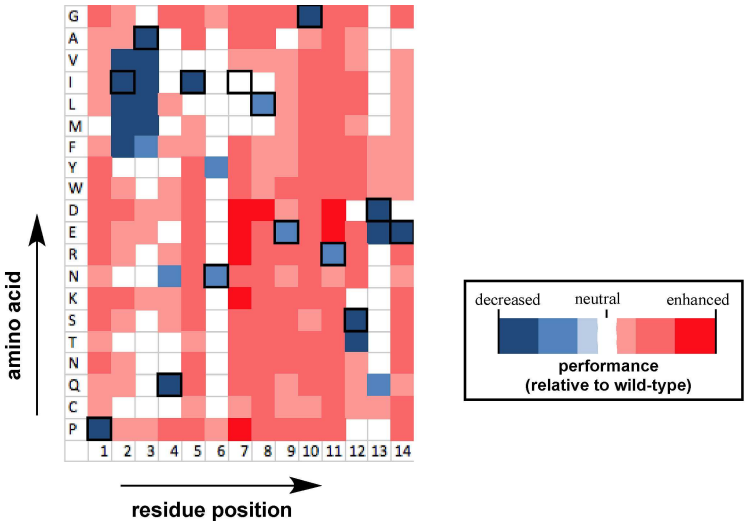

Figure 6. Example of a mutability landscape in the form of a heat map for different amino acids at 14 residue positions within an enzyme.[138]

MD simulations (2×5 mutants screened). Even after the third ISM cycle and the computationally guided third step, the 16β-OH selective mutant had to be fine-tuned further because a strong trade-off between activity and selectivity was observed. This strategy resulted in mutant WIFI-WC catalysing the hydroxylation of **37** to afford 16α-**39** with 96% selectivity, 95% conversion and 8660 TTN, and mutant WWV-QRS with 92% selectivity for 16β-**40**, 92% conversion and 9044 TTN (Scheme 9B). Furthermore, the best mutants found also catalysed the C16 hydroxylations of four other steroids, namely androstenedione, nandrolone, boldenone and norethindrone, with exquisite selectivity and activity.

While Reetz *et al.* had already achieved significant improvements in selectivity and relative rate profiles with ITM and CAST approaches in 2011 (Scheme 9A),[132] they criticised the trade-off in activity and the amount of screening (2×9000 mutants screened) themselves later. In comparison, in the study from 2018[129] activities close to the one exhibited by the BM3 wild type towards fatty acids with far less screening effort (3×950+X mutants screened) could be obtained. Of course, other factors like enzyme stability have not been considered here, but still this proof-of-principle study awakens hope for a greater involvement of such enzymes in industry, and elegantly demonstrates the potential of a well thought-through semi-rational directed evolution approach.

2.6. Late-Stage Diversification of Lead Compounds with Liver Microsomes

The synthesis of drug metabolites represents an integral part of every drug discovery programme in order to predict the half-time of a drug or to test the toxicity of its metabolic products. Obviously, human liver P450s are in the focus of research in drug discovery because they are responsible for the degradation of drugs and xenobiotics in the body.[15] With their broad substrate tolerance these liver P450s are attractive tools for predicting *in vivo* drug interactions *via in vitro* reactions[146–148] or drug metabolite synthesis *via* late-stage modifications.[149,150]

Often, preclinical drug screening involves the use of liver models to understand the downstream process of the drug in a natural environment simulation.

Since the human liver cannot be used for this purpose, animal livers and liver microsomes – vesicles of fragmented endoplasmic reticulum containing P450s – are employed as models[151] and even BM3 variants instead.[152,153] Many metabolites can be formed from the corresponding drug precursor as shown in Scheme 10 with the example of the lorcaserin metabolism by human liver microsomes.[153] Structural derivatisation in a late-stage fashion is therefore preferred for the chemical metabolite synthesis, and liver microsomes are a practical tool to use.[154]

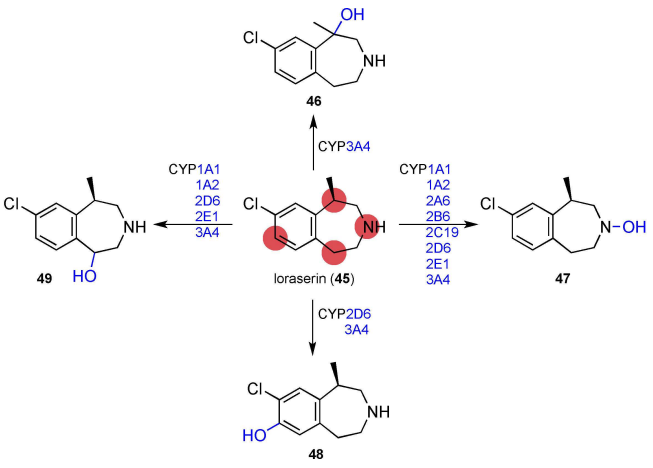

Scheme 10. Metabolism of the 5-hydroxytryptamine 2 C agonist lorcaserin by P450s of human liver microsomes.[153]

In two very recent studies, Obach *et al.* searched for new inhibitors targeting the human phosphodiesterase-2 (PDE2),[155,156] which is one of a group of enzymes that hydrolyse the phosphodiester bond within second messenger molecules cyclic adenosine monophosphate and cyclic guanosine monophosphate. PDE2s are thus important for the human physiology, for example cardiac and vascular processes. Consequently, PDE2 inhibitors are of high clinical relevance for treatment of stroke or heart rate regulation.[157] In the first study, Obach and co-workers improved a lead candidate for PDE2 inhibition by hydroxylation using monkey liver microsomes. The newly generated candidate had more favourable physiochemical properties while retaining the parent potency.[155]

The research group then extended their work to the transformation of nine lead compounds applying liver microsomes of eight different species each case.[156] Their aim was to obtain a better structure-activity understanding for PDE2s in order to enable improvement of target potency, metabolic lability and membrane permeability. The nine leads were incubated with the liver microsomes and the metabolic product profile analysed by HPLC to identify the most promising of the applied species. The product of scale-up experiments was fractionated by HPLC, isolated and checked for purity by UHPLC-UV-MS and its structure determined by quantitative NMR. The latter technique had been established in a previous study as a handy tool to allow for structure and concentration determination of the metabolites.[158] This way 36 new analogues were generated, which were tested for PDE2 inhibition, drug clearance and membrane permeability. Up to seven derivatives of the parent lead compound were generated.

A better potency was observed for some of the metabolites. In the case of compound **51 c** the demethylation of parent lead **50** carried out by hamster microsomes increased the potency by 10-times (Scheme 11). Analogue **51 c** also had a greater metabolic stability, but at the cost of a slightly diminished membrane permeability. Following an N-demethylation to compound **51 a** decreased the potency slightly, albeit still better than lead **50**. However, the 10-fold decrease in permeability makes **51 a** unsuitable. In total, most derivatives showed a mild to significant decrease in potency and often lost out in at least one more of the other two features in comparison to its parent lead compound. At most, the same quality could be maintained.

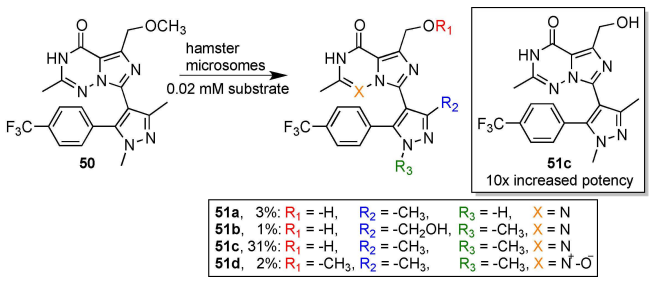

Scheme 11. Late-stage diversification of human phosphodiesterase-2 (PDE2) inhibitor **50** using liver microsomes of different animals. The analogue **51 c** was observed to have a 10-fold increased potency, an increased metabolic stability and a slightly decreased membrane permeability relative to the parent lead compound **50**.[156]

The analytical analysis came with the handy feature that only less than a micromole of the lead compound is required for this process. Furthermore, reactions are carried out under mild conditions in aqueous solutions of known concentrations. This clearly represents a great time-saver compared to chemical reactions of milligram scale at harsher conditions. Notwithstanding, the authors admitted that some screening effort is required to identify the liver microsomes of the best-fitting species and good fortune to be able to produce a favourable structure-activity relationship.

This study illustrates nicely the applicability of liver microsomes for late-stage diversification purposes of lead drug compounds. In hindsight, the authors did not discover a novel improved drug because compound **51 c** was already the figurehead of the previous publications described before,[155] despite their extension of diversity *via* more substrates and other species' liver microsomes. This indicates the limitation and requirement of the aforementioned luck factor. However, in view of late-stage diversification this work is a convincing example of achieving this within a few simple working steps. Process development for the synthesis of larger quantities will certainly remain a significant challenge.

2.7. Late-Stage Functionalisation of the Antileukemic Agent Parthenolide with Engineered BM3 Variants to Improve its Potency

Another example of the Fasan group, who again applied their active-site geometry 'fingerprinting' method in combination with active site mutagenesis,[120] gives an idea of how newly generated functionalisation can be used for further diversification. Kolev *et al.* studied the emerging natural product parthenolide as substrate due to its extraordinary properties against various diseases,[159] particularly its anticancer activity.[160,161] However, its low solubility in water and stability at various conditions necessitates the synthesis of derivatives, and thus attracted a lot of attention from research. The reactive position C13 and the C1–C10 double bond have been accessed chemically, however, only the C-13 analogue DMAPT was convincing enough to enter clinical trials.[162]

In 2014, Fasan *et al.* therefore devised cytochrome P450 enzymes to access positions C9 and C14.[159] Indeed, their previously engineered $P450_{BM3}$ variant FL#62 catalysed the hydroxylation of parthenolide (**52**) to afford the epoxide **53**, C9-**54** and C14-**55** in a product ratio of 77:13:10 and >1000 total turnovers. Their 'fingerprinting' method resulted in mutant enzymes III-D4 (4980 TTN), XII-F12 (1310 TTN) and XII–D8 (60 TTN) having 90, 80 and 95% selectivity for the products, respectively (Scheme 12). These alcohols were then further diversified by chemical benzoylation using acid chloride reactants carrying aromatic substituents to furnish derivatives that had a greater potency against primary acute myelogenous leukaemia (AML) cells (e.g. **56** and **57**) than **52**. In addition, Fasan showed a greater selectivity against malignant over

healthy Bone Marrow (BM) cells motivating the authors to classify positions C9 and C14 as 'hot-spots'.

The Fasan group were able to further improve their enzymatic synthesis in 2016 and designed new analogues by extending the diversification scope.[163] In addition to acylation and alkylation reactions, carbene insertion were applied as alternative O–H functionalisations. At the same time, the new compounds avoided the potentially labile ester linkage to hydrolysis, and few showed even better potency. Carbamate analogues were also added to the diversification spectrum.[164] A diverse library of parthenolide derivatives was generated, tested against a range of different malignant cell lines and compared *via* a heat map. This provided the authors with a tumour-cell specific anticancer activity profile of various molecular scaffolds. In the end, compounds bearing high cytotoxicity against every malignant cell type with up to 14-fold increased activity compared to **52** were identified.

These studies nicely demonstrate the power of P450 enzymes for late-stage functionalisation as an entry to the diversification of parthenolide alcohols by different chemical reactions.[159,163,164] The latter has set the fundament for tailoring a library of different analogues to successfully improve the potency and selectivity to malignant cells in comparison to parthenolide itself. Noteworthy is that the authors included healthy cell lines as controls in order to analyse the selectivity of the compounds towards malignant cells over healthy cells. This was a point of appropriate criticism for many studies that did not assess the cytotoxicity on healthy cells, thus creating the illusion that parthenolide was only toxic to tumour cells. However, similar to many other studies, Fasan *et al.* did not reveal the water solubility and thus bioavailability of their lead compounds, which remains the greatest obstacle for entering clinical application.[162]

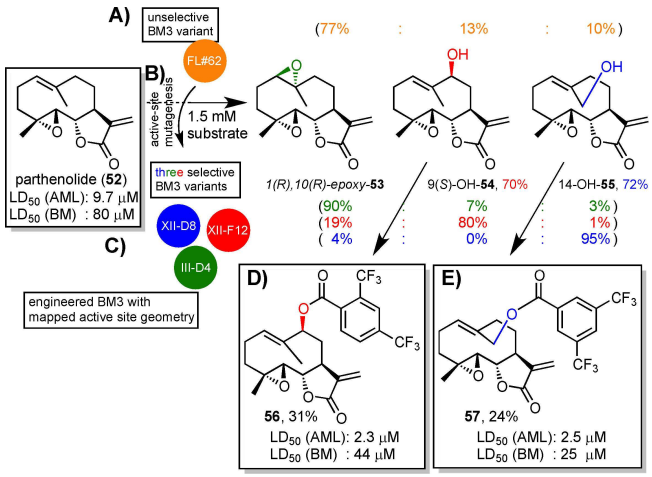

Scheme 12. Late-stage functionalisation of parthenolide (**52**) with $P450_{BM3}$ variants after active-site geometry fingerprinting[120] and active site mutagenesis.[159] The percentage yield of a preparative scale synthesis is indicated in the colour of the respective best mutant that catalysed it. Product distributions are shown in brackets and coloured according to the respective enzyme variant that catalysed the reaction. **A)** FL#62 catalysed the transformation of parthenolide yielding an improvable product distribution of 77:13:10 for **53**, **54** and **55**, respectively. **B)** Active-site mutagenesis on FL#62 was used just like in Scheme 9 to identify three selective BM3 mutants: III-D4 (4980 TTN), XII-F12 (1310 TTN) and XII-D8 (60 TTN). **C)** Parthenolide was hydroxylated at three different positions to form an epoxide 1(R),10(R)-epoxy-**53**, 9(S)-OH-**54** and 14-OH-**55** with absolute stereo- and excellent regioselectivities (90%, 80% and 95%, respectively). **D)** Further derivatisation was carried out with the hydroxylated products and compounds **56** and **57** were found to have better LD50 values for primary acute myelogenous leukaemia and normal bone marrow cells compared to **52**.

3. Conclusion

Natural products will exert a substantial influence on drug discovery in the future. This is not only reflected by their increasing re-emphasis, but also by the immense existing chemical space of natural products that has yet to be fully explored. Clearly, the vast diversity and complexity of natural products is currently unmatched by man-made synthetic compound libraries. Statistics show that the discovery rate of structurally unique scaffolds of natural products remains stable despite the ever-increasing number of known structures.[75]

The use of sp^3-hybridised C–H bond activation has advanced considerably in the last decade and has proven very useful in many natural product total syntheses.[165] The convincing atom and step economies of C–H functionalisation as well as the possibility of powerful manipulations in a late-stage fashion add significant benefits and flexibility to the synthetic strategies. However, the activation of unreactive carbon centres usually requires metal catalysts, which are unsustainable and in many cases lack selectivity.[5,7,165–167] Cytochrome P450 enzymes thus offer an attractive, albeit complex alternative that is in line with environmentally friendly research. The promise to exploit their unique benefits for synthetic application led to extensive effort in protein engineering and many promising studies, which demonstrate its potential for expansion of the chemical toolbox (Figure 7).[168,169]

Therefore, this review attempted to illustrate the potential of P450s in lead diversification from the perspective of drug discovery. This was done by presenting novel studies reporting late-stage functionalisation of natural products and other high-value compounds, and by complementing the recent review of Renata *et al.*[42] who looked at the first endeavours to introduce P450 enzymes in total syntheses of natural products.

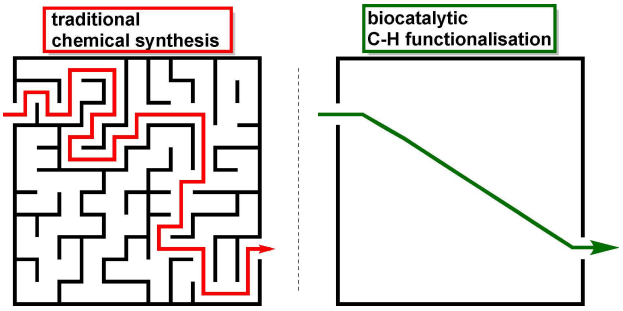

Figure 7. Comparison of functional group installation en route *via* traditional chemical synthesis versus late-stage biocatalytic C–H functionalization.

As seen in the examples presented above, P450s work beautifully for the diversification of complex scaffolds post-synthetically by providing nucleophilic or electrophilic handles that allow further attachment of different building blocks. In this late-stage manner, novel therapeutic analogues could therefore be generated with synthetic ease resulting in derivatives of improved potency and physiochemical properties.

It is worth noting that self-sufficient P450 enzymes work best because their natural fusion to redox partners permits easier handling and accounts for the observed highest turnover numbers and coupling efficiencies.[170] It is thus not astonishing that BM3 is such a prominent P450 candidate and used in the majority of the examples shown here. However, artificial fusion to redox partners may be used to increase efficiency of other P450s and interestingly, a variation in redox partners also offers an opportunity to change the enzyme's selectivity.[171]

Although substrates of P450s often include high value molecules like fine chemicals and pharmaceuticals, the application of P450s in industrial processes is still limited due to several issues such as instability, poor solvent tolerance and low substrate solubility, or cofactor dependence. In general, these issues can be successfully addressed by immobilisation and use of whole-cell catalysts, bi-phasic reaction systems and a cofactor regeneration system, respectively.[25,31,54,172,173] Moreover, P450s sometimes also possess an unfavourable (regio-)selectivity or are too specific. The range of creative strategies to tackle this problem as seen above *via* anchoring groups, computational modelling, a 'fingerprinting method' or simple directed evolution not only paints a promising picture, but also gives an idea of methods yet to be invented to address other P450 drawbacks. While use of cytochrome P450 enzymes in synthesis and in industry seems still in its infancy, it clearly holds an immense potential,[168,171] as demonstrated by studies to evolve P450s even into catalysing reactions totally unknown to nature.[22,94,174–176] Eventually, the elegancy and success in protein engineering will be the determining factor, as underlined by the recent Nobel prize in chemistry, awarded to Frances H. Arnold for developing and furnishing the technique of directed evolution of enzymes to a wider audience.[177]

Biocatalysis on a whole is on the rise. Its 'fourth wave'[178] or 'golden age'[179] of biocatalysis is approaching rapidly, as indicated by an increasing frequency of innovative discoveries, the sprouting influential ideas and the joining of forces among chemists, biologists and engineers. It can be anticipated that advanced computational approaches and laboratory automation will further accelerate the transition of conventional organic synthesis[180,181] and scaffold diversification,[182,183] towards a modern productive science that uses all kinds of sustainable chemical and enzymatic technologies on an equal footing.[184,185]

Acknowledgements

This project received funding from the European Union's Horizon 2020 research and innovation programme, OXYtrain MSCA-ITN, under grant agreement No. 722390. I would like to thank my academic mentor Prof. A. Glieder for suggesting to write this review. I am grateful to Dr. S. Schmidt for critical reading the manuscript and for fruitful discussions. I would also like to thank Anna Hatzl for proofreading and helpful comments.

Conflict of Interest

The authors declare no conflict of interest.

Keywords: chemoenzymatic synthesis · cytochrome P450 enzymes · drug discovery · late-stage diversification · natural products

[1] K. C. Nicolau, T. Montagnon, *Molecules That Changed the World*, Wiley-VCH, **2008**.
[2] A. Osbourn, R. Ross, G. Carter, *No Natural Products: Discourse, Diversity, and Design*, Wiley & Sons Inc., **2014**.
[3] A. -u. Rahman, *Studies in Natural Products Chemistry Vol. 59*, Elsevier Inc., **2018**.
[4] G. Li, H.-X. Lou, *Med. Res. Rev.* **2018**, *38*, 1255–1294.
[5] T. Cernak, K. D. Dykstra, S. Tyagarajan, P. Vachal, S. W. Krska, *Chem. Soc. Rev.* **2016**, *45*, 453–754.
[6] J. Wencel-Delord, F. Glorius, *Nat. Chem.* **2013**, *5*, 369–375.
[7] D. C. Blakemore, L. Castro, I. Churcher, D. C. Rees, A. W. Thomas, D. M. Wilson, A. Wood, *Nat. Chem.* **2018**, *10*, 383–394.
[8] J. Piel, *Natural Products via Enzymatic Reactions*, Springer-Verlag Heidelberg, **2010**.
[9] B. Trost, *J. Org. Chem.* **2014**, *79*, 9913–9913.
[10] M. Harmata, *Stategies and Tactics in Organic Synthesis Vol. 8*, Elsevier Ltd., Amsterdam, **2012**.
[11] S. Warren, P. Wyatt, *Organic Synthesis The Disconnection Approach 2nd Ed.*, Wiley & Sons Inc., Chichester, **2008**.
[12] J. Clayden, N. Greeves, S. Warren, *Organic Chemistry 2nd Ed.*, Oxford University Press, **2013**.
[13] V. Šunjić, V. Petrović Peroković, *Organic Chemistry from Retrosynthesis to Asymmetric Synthesis*, Springer International Publishing, New York, **2016**.
[14] J. T. Groves, *Nat. Chem.* **2014**, *6*, 89–91.
[15] P. Ortiz de Montellano, *Cytochrome P450: Structure, Mechanism, and Biochemistry*, Springer Science & Business Media, **2015**.
[16] V. B. Urlacher, M. Girhard, *Trends Biotechnol.* **2012**, *30*, 26–36.
[17] R. A. Sheldon, *Green Chem.* **2017**, *19*, 1–320.
[18] F. Hollmann, I. W. C. E. Arends, K. Buehler, A. Schallmey, B. Bühler, *Green Chem.* **2011**, *13*, 226–265.
[19] J. M. Woodley, *Trends Biotechnol.* **2008**, *26*, 321–327.
[20] I. S. Young, P. S. Baran, *Nat. Chem.* **2009**, *1*, 193–205.
[21] P. S. Baran, *J. Am. Chem. Soc.* **2018**, *140*, 4751–4755.
[22] F. H. Arnold, *Angew. Chem. Int. Ed.* **2018**, *57*, 4143–4148; *Angew. Chem.* **2018**, *130*, 4212–4218.
[23] J. bo Wang, G. Li, M. T. Reetz, *Chem. Commun.* **2017**, *53*, 3916–3928.
[24] F. Cheng, L. Zhu, U. Schwaneberg, *Chem. Commun.* **2015**, *51*, 9760–9772.
[25] J. B. Y. H. Behrendorff, W. Huang, E. M. J. Gillam, *Biochem. J.* **2015**, *467*, 1–15.
[26] G. D. Roiban, M. T. Reetz, *Chem. Commun.* **2015**, *51*, 2208–2224.
[27] J. A. McIntosh, C. C. Farwell, F. H. Arnold, *Curr. Opin. Chem. Biol.* **2014**, *19*, 126–134.
[28] M. T. Reetz, *Tetrahedron* **2012**, *68*, 7530–7548.
[29] N. Turner, L. Humphreys, *Biocatalysis in Organic Synthesis: The Retrosynthesis Approach*, Royal Society Of Chemistry, **2018**.
[30] M. Hönig, P. Sondermann, N. J. Turner, E. M. Carreira, *Angew. Chem. Int. Ed.* **2017**, *56*, 8942–8973; *Angew. Chem.* **2017**, *129*, 9068–9100.
[31] R. O. M. A. de Souza, L. S. M. Miranda, U. T. Bornscheuer, *Chem. Eur. J.* **2017**, *23*, 12040–12063.
[32] A. P. Green, N. J. Turner, *Perspect. Sci.* **2016**, *9*, 42–48.
[33] N. J. Turner, E. O'reilly, *Nat. Chem. Biol.* **2013**, *9*, 285–288.
[34] D. J. Newman, G. M. Cragg, *J. Nat. Prod.* **2016**, *79*, 629–661.

[35] E. Patridge, P. Gareiss, M. S. Kinch, D. Hoyer, *Drug Discovery Today* **2016**, *21*, 204–207.
[36] A. L. Harvey, R. Edrada-Ebel, R. J. Quinn, *Nat. Rev. Drug Discovery* **2015**, *14*, 111–129.
[37] M. E. Welsch, S. A. Snyder, B. R. Stockwell, *Curr. Opin. Chem. Biol.* **2010**, *14*, 347–361.
[38] E. C. Barnes, R. Kumar, R. A. Davis, *Nat. Prod. Rep.* **2016**, *33*, 372–381.
[39] S. A. Loskot, D. K. Romney, F. H. Arnold, B. M. Stoltz, *J. Am. Chem. Soc.* **2017**, *139*, 10196–10199.
[40] M. Werneburg, C. Hertweck, *ChemBioChem* **2008**, *9*, 2064–2066.
[41] M. Henrot, M. E. A. Richter, J. Maddaluno, C. Hertweck, M. De Paolis, *Angew. Chem. Int. Ed.* **2012**, *51*, 9587–9591; *Angew. Chem.* **2012**, *124*, 9725–9729.
[42] E. King-Smith, C. R. Zwick, H. Renata, *Biochemistry* **2017**, *57*, 403–412.
[43] B. Su, Z. C. Cao, Z. J. Shi, *Acc. Chem. Res.* **2015**, *48*, 886–896.
[44] A. Fürstner, *ACS Cent. Sci.* **2016**, *2*, 778–789.
[45] K. S. Egorova, V. P. Ananikov, *Angew. Chem. Int. Ed.* **2016**, *55*, 12150–12162; *Angew. Chem.* **2016**, *128*, 12334–12347.
[46] S. J. Benkovic, S. Hammes-Schiffer, *Science (80-.).* **2003**, *301*, 1196–1202.
[47] F. P. Guengerich, *ACS Catal.* **2018**, *8*, 10964–10976.
[48] A. W. Munro, H. M. Girvan, A. E. Mason, A. J. Dunford, K. J. McLean, *Trends Biochem. Sci.* **2013**, *38*, 140–150.
[49] P. Schyman, W. Lai, H. Chen, Y. Wang, S. Shaik, *J. Am. Chem. Soc.* **2011**, *133*, 7977–7984.
[50] S. Shaik, S. Cohen, Y. Wang, H. Chen, D. Kumar, W. Thiel, *Chem. Rev.* **2010**, *110*, 949–1017.
[51] T. H. Yosca, T. H. Yosca, J. Rittle, C. M. Krest, E. L. Onderko, A. Silakov, J. C. Calixto, R. K. Behan, M. T. Green, *Science (80-.).* **2013**, *342*, 825–829.
[52] M. E. Albertolle, F. Peter Guengerich, *J. Inorg. Biochem.* **2018**, *186*, 228–234.
[53] F. Hannemann, A. Bichet, K. M. Ewen, R. Bernhardt, *Biochim. Biophys. Acta Gen. Subj.* **2007**, *1770*, 330–344.
[54] M. T. Lundemo, J. M. Woodley, *Appl. Microbiol. Biotechnol.* **2015**, *99*, 2465–2483.
[55] A. Long, G. Liti, A. Luptak, O. Tenaillon, *Nat. Rev. Genet.* **2015**, *16*, 567–582.
[56] R. D. Firn, C. G. Jones, *Nat. Prod. Rep.* **2003**, *20*, 382–391.
[57] R. D. Firn, C. G. Jones, *Mol. Microbiol.* **2000**, *37*, 989–994.
[58] M. Radman, *Nature* **1999**, *401*, 866–867.
[59] R. Bernhardt, *J. Biotechnol.* **2006**, *124*, 128–145.
[60] M. A. Fischbach, J. Clardy, *Nat. Chem. Biol.* **2007**, *3*, 353–355.
[61] B. Tudzynski, *Appl. Microbiol. Biotechnol.* **2005**, *66*, 597–611.
[62] G. M. Rishton, *Am. J. Cardiol.* **2008**, *101*, 43–49.
[63] F. E. Koehn, *MedChemComm* **2012**, *3*, 854–865.
[64] I. B. Campbell, S. J. F. Macdonald, P. A. Procopiou, *Drug Discovery Today* **2018**, *23*, 219–234.
[65] B. David, J.-L. Wolfender, D. A. Dias, *Phytochem. Rev.* **2015**, *14*, 299–315.
[66] D. J. Newman, *Pharmacol. Ther.* **2016**, *162*, 1–9.
[67] F. Chemat, M. A. Vian, G. Cravotto, *Int. J. Mol. Sci.* **2012**, *13*, 8615–8627.
[68] A. Krivoruchko, J. Nielsen, *Curr. Opin. Biotechnol.* **2015**, *35*, 7–15.
[69] T. Rodrigues, D. Reker, P. Schneider, G. Schneider, *Nat. Chem.* **2016**, *8*, 531–541.
[70] C. L. Ventola, *P T* **2015**, *40*, 277–83.
[71] G. D. Wright, *Nat. Prod. Rep.* **2017**, *34*, 694–701.
[72] M. G. Moloney, *Trends Pharmacol. Sci.* **2016**, *37*, 689–701.
[73] S. L. Schreiber, *Science (80-.).* **2000**, *287*, 1964–1969.
[74] M. W. P. Bebbington, *Chem. Soc. Rev.* **2017**, *46*, 5059–5109.
[75] C. R. Pye, M. J. Bertin, R. S. Lokey, W. H. Gerwick, R. G. Linington, *Proc. Mont. Acad. Sci.* **2017**, *114*, 5601–5606.
[76] M. Hay, D. W. Thomas, J. L. Craighead, C. Economides, J. Rosenthal, *Nat. Biotechnol.* **2014**, *32*, 40–51.
[77] M. D. Burke, S. L. Schreiber, *Angew. Chem. Int. Ed.* **2004**, *43*, 46–58; *Angew. Chem.* **2004**, *116*, 48–60.
[78] E. J. Corey, X.-M. Cheng, *Logic of Chemical Synthesis*, Wiley-VCH Verlag GmBH & Co. KGaA, New York, **1995**.
[79] E. J. Corey, *Angew. Chem. Int. Ed.* **1991**, *30*, 455–465; *Angew. Chem.* **1991**, *103*, 469–479.
[80] T. Newhouse, P. S. Baran, R. W. Hoffmann, *Chem. Soc. Rev.* **2009**, *38*, 3010–3021.
[81] J.-Q. Yu, *Catalytic Transformations via C–H Activation Vol. 1 & 2*, Georg Thieme Verlag KG, **2016**.
[82] P. Pérez, *Alkane C–H Activation by Single-Site Metal Catalysis*, Springer Science & Business Media, **2016**.
[83] G. Dyker, *Handbook of C–H Transformations: Applications in Organic Synthesis*, Wiley-VCH Verlag GmBH & Co. KGaA, **2008**.
[84] R. Mas-Ballesté, L. Que, *Science (80-.).* **2006**, *312*, 1885–1886.
[85] J. A. Labinger, J. E. Bercaw, *Nature* **2002**, *417*, 507–514.
[86] J. Yamaguchi, A. D. Yamaguchi, K. Itami, *Angew. Chem. Int. Ed.* **2012**, *51*, 8960–9009; *Angew. Chem.* **2012**, *124*, 9092–9142.
[87] L. McMurray, F. O'Hara, M. J. Gaunt, *Chem. Soc. Rev.* **2011**, *40*, 1885–1898.
[88] D. Y. K. Chen, S. W. Youn, *Chem. Eur. J.* **2012**, *18*, 9452–9474.
[89] Y. Qiu, S. Gao, *Nat. Prod. Rep.* **2016**, *33*, 562–581.
[90] C. R. Shugrue, S. J. Miller, *Chem. Rev.* **2017**, *117*, 11894–11951.
[91] O. Robles, D. Romo, *Nat. Prod. Rep.* **2014**, *31*, 318–334.
[92] K. C. Morrison, P. J. Hergenrother, *Nat. Prod. Rep.* **2014**, *31*, 6–14.
[93] R. R. Karimov, J. F. Hartwig, *Angew. Chem. Int. Ed.* **2018**, *57*, 4234–4241; *Angew. Chem.* **2018**, *130*, 4309–4317.
[94] X. Zhang, S. Li, *Nat. Prod. Rep.* **2017**, *34*, 1061–1089.
[95] E. M. Driggers, S. P. Hale, J. Lee, N. K. Terrett, *Nat. Rev. Drug Discovery* **2008**, *7*, 608–624.
[96] X. Yu, D. Sun, *Molecules* **2013**, *18*, 6230–6268.
[97] M. M. Gilbert, M. D. DeMars, S. Yang, J. M. Grandner, S. Wang, H. Wang, A. R. H. Narayan, D. H. Sherman, K. N. Houk, J. Montgomery, *ACS Cent. Sci.* **2017**, *3*, 1304–1310.
[98] Y. Xue, D. Wilson, L. Zhao, H. W. Liu, D. H. Sherman, *Chem. Biol.* **1998**, *5*, 661–667.
[99] S. Li, L. M. Podust, D. H. Sherman, *J. Am. Chem. Soc.* **2007**, *129*, 12940–12941.
[100] D. H. Sherman, S. Li, L. V. Yermalitskaya, Y. Kim, J. A. Smith, M. R. Waterman, L. M. Podust, *J. Biol. Chem.* **2006**, *281*, 26289–26297.
[101] S. Li, M. R. Chaulagain, A. R. Knauff, L. M. Podust, J. Montgomery, D. H. Sherman, *Proc. Natl. Acad. Sci. USA* **2009**, *106*, 18463–8.
[102] S. Negretti, A. R. H. Narayan, K. C. Chiou, P. M. Kells, J. L. Stachowski, D. A. Hansen, L. M. Podust, J. Montgomery, D. H. Sherman, *J. Am. Chem. Soc.* **2014**, *136*, 4901–4904.
[103] K. Steiner, H. Schwab, *Comput. Struct. Biotechnol. J.* **2012**, *2*, e201209010.
[104] M. D. Toscano, K. J. Woycechowsky, D. Hilvert, *Angew. Chem. Int. Ed.* **2007**, *46*, 3212–3236; *Angew. Chem.* **2007**, *119*, 3274–3300.
[105] A. J. Ruff, A. Dennig, U. Schwaneberg, *FEBS J.* **2013**, *280*, 2961–2978.
[106] P. C. Nair, R. A. McKinnon, J. O. Miners, *Drug Metab. Rev.* **2016**, *48*, 434–452.
[107] E. Stjernschantz, N. P. E. Vermeulen, C. Oostenbrink, *Expert Opin. Drug Metab. Toxicol.* **2008**, *4*, 513–527.
[108] S. Shaik, S. De Visser, in *Cytochrome P450* (Ed.: P. Ortiz de Montellano), Springer Science & Business Media, **2005**.
[109] D. Roccatano, *J. Phys. Condens. Matter* **2015**, *27*, 273102.
[110] L. Tian, R. A. Friesner, *J. Chem. Theory Comput.* **2009**, *5*, 1421–1431.
[111] D. Petrović, A. Bokel, M. Allan, V. B. Urlacher, B. Strodel, *J. Chem. Inf. Model.* **2018**, *58*, 848–858.
[112] P. Le-Huu, T. Heidt, B. Claasen, S. Laschat, V. B. Urlacher, *ACS Catal.* **2015**, *5*, 1772–1780.
[113] P. Le-Huu, D. Petrović, B. Strodel, V. B. Urlacher, *ChemCatChem* **2016**, *8*, 3755–3761.
[114] S. Omura, *Macrolide Antibiotics: Chemistry, Biology, and Practice*, Academic Press, **2002**.
[115] M. A. Fischbach, C. T. Walsh, *Science (80-.).* **2009**, *325*, 1089–1094.
[116] D. A. Hansen, C. M. Rath, E. B. Eisman, A. R. H. Narayan, J. D. Kittendorf, J. D. Mortison, Y. J. Yoon, D. H. Sherman, *J. Am. Chem. Soc.* **2013**, *135*, 11232–11238.
[117] A. N. Lowell, M. D. DeMars, S. T. Slocum, F. Yu, K. Anand, J. A. Chemler, N. Korakavi, J. K. Priessnitz, S. R. Park, A. A. Koch, *J. Am. Chem. Soc.* **2017**, *139*, 7913–7920.
[118] Y. Iizaka, N. Higashi, M. Ishida, R. Oiwa, Y. Ichikawa, M. Takeda, Y. Anzai, F. Kato, *Antimicrob. Agents Chemother.* **2013**, *57*, 1529–1531.
[119] M. D. DeMars, F. Sheng, S. R. Park, A. N. Lowell, L. M. Podust, D. H. Sherman, *ACS Chem. Biol.* **2016**, *11*, 2642–2654.
[120] K. Zhang, S. El Damaty, R. Fasan, *J. Am. Chem. Soc.* **2011**, *133*, 3242–3245.
[121] K. Zhang, B. M. Shafer, M. D. DeMars, H. A. Stern, R. Fasan, *J. Am. Chem. Soc.* **2012**, *134*, 18695–18704.
[122] H. Renault, J. E. Bassard, B. Hamberger, D. Werck-Reichhart, *Curr. Opin. Plant Biol.* **2014**, *19*, 27–34.
[123] D. Y. Xie, D.-M. Ma, R. Judd, A. L. Jones, *Phytochem. Rev.* **2016**, *15*, 1093–1114.
[124] S. H. Kung, S. Lund, A. Murarka, D. McPhee, C. J. Paddon, *Front. Plant Sci.* **2018**, *87*, 1–7.

[125] C. J. Paddon, J. D. Keasling, *Nat. Rev. Microbiol.* **2014**, *12*, 355–367.
[126] D. Chaturvedi, A. Goswami, P. P. Saikia, N. C. Barua, P. G. Rao, *Chem. Soc. Rev.* **2010**, *39*, 435–454.
[127] X. Huang, T. M. Bergsten, J. T. Groves, *J. Am. Chem. Soc.* **2015**, *137*, 5300–5303.
[128] P. E. Gormisky, M. C. White, *J. Am. Chem. Soc.* **2013**, *135*, 14052–14055.
[129] C. G. Acevedo-Rocha, C. G. Gamble, R. Lonsdale, A. Li, N. Nett, S. Hoebenreich, J. B. Lingnau, C. Wirtz, C. Fares, H. Hinrichs, *ACS Catal.* **2018**, *8*, 3395–3410.
[130] V. Polic, K. Auclair, *Bioorg. Med. Chem.* **2014**, *22*, 5547–5554.
[131] K. Auclair, V. Polic, in *Monooxygenase, Peroxidase Peroxygenase Prop. Mech. Cytochrome P450. Adv. Exp. Med. Biol.* (Eds.: E. Hrycay, S. Badiera), Springer Science & Business Media, **2015**.
[132] S. Kille, F. E. Zilly, J. P. Acevedo, M. T. Reetz, *Nat. Chem.* **2011**, *3*, 738–743.
[133] S. Lutz, U. Bornscheuer, *Protein Engineering Handbook Vol. 1–2*, Wiley-VCH, **2009**.
[134] M. T. Reetz, *Angew. Chem. Int. Ed.* **2011**, *50*, 138–174; *Angew. Chem.* **2011**, *123*, 144–182.
[135] M. T. Reetz, M. Bocola, J. D. Carballeira, D. Zha, A. Vogel, *Angew. Chem. Int. Ed.* **2005**, *117*, 4264–4268.
[136] C. F. Oliver, S. Modi, M. J. Sutcliffe, W. U. Primrose, L. Y. Lian, G. C. K. Roberts, *Biochemistry* **1997**, *36*, 1567–1572.
[137] C. J. C. Whitehouse, S. G. Bell, L.-L. Wong, *Chem. Soc. Rev.* **2012**, *41*, 1218–1260.
[138] J. Y. van der Meer, L. Biewenga, G. J. Poelarends, *ChemBioChem* **2016**, *17*, 1792–1799.
[139] C. Acevedo-Rocha, M. Ferla, M. Reetz, in *Protein Eng. Methods Mol. Biol.* (Eds.: U. Bornscheuer, M. Höhne), Humana Press, **2018**.
[140] V. Rea, A. J. Kolkman, E. Vottero, E. J. Stronks, K. A. M. Ampt, M. Honing, N. P. E. Vermeulen, S. S. Wijmenga, J. N. M. Commandeur, *Biochemistry* **2012**, *51*, 750–760.
[141] H. Venkataraman, S. B. A. de Beer, L. A. H. van Bergen, N. van Essen, D. P. Geerke, N. P. E. Vermeulen, J. N. M. Commandeur, *ChemBioChem* **2012**, *13*, 520–523.
[142] E. Vottero, V. Rea, J. Lastdrager, M. Honing, N. P. E. Vermeulen, J. N. M. Commandeur, *J. Biol. Inorg. Chem.* **2011**, *16*, 899–912.
[143] I. Geronimo, C. A. Denning, W. E. Rogers, T. Othman, T. Huxford, D. K. Heidary, E. C. Glazer, C. M. Payne, *Biochemistry* **2016**, *55*, 3594–3606.
[144] S. Hoebenreich, F. E. Zilly, C. G. Acevedo-Rocha, M. Zilly, M. T. Reetz, *ACS Synth. Biol.* **2015**, *4*, 317–331.
[145] Y. Khatri, I. K. Jóźwik, M. Ringle, I. A. Ionescu, M. Litzenburger, M. C. Hutter, A. M. W. H. Thunnissen, R. Bernhardt, *ACS Chem. Biol.* **2018**, *13*, 1021–1028.
[146] L. C. Wienkers, T. G. Heath, *Nat. Rev. Drug Discovery* **2005**, *4*, 825–833.
[147] J. Kirchmair, A. H. Göller, D. Lang, J. Kunze, B. Testa, I. D. Wilson, R. C. Glen, G. Schneider, *Nat. Rev. Drug Discovery* **2015**, *14*, 387–404.
[148] J. D. Tyzack, P. A. Hunt, M. D. Segall, *J. Chem. Inf. Model.* **2016**, *56*, 2180–2193.
[149] F. P. Guengerich, *Nat. Rev. Drug Discovery* **2002**, *1*, 359–366.
[150] M. Winkler, M. Geier, S. P. Hanlon, B. Nidetzky, A. Glieder, *Angew. Chem. Int. Ed.* **2018**, 10.1002/anie.201800678.
[151] S. Asha, M. Vidyavathi, *Appl. Biochem. Biotechnol.* **2010**, *160*, 1699–1722.
[152] A. M. Sawayama, M. M. Y. Chen, P. Kulanthaivel, M. S. Kuo, H. Hemmerle, F. H. Arnold, *Chem. Eur. J.* **2009**, *15*, 11723–11729.
[153] K. A. Usmani, W. G. Chen, A. J. M. Sadeque, *Drug Metab. Dispos.* **2012**, *40*, 761–771.
[154] K. P. Cusack, H. F. Koolman, U. E. W. Lange, H. M. Peltier, I. Piel, A. Vasudevan, *Bioorg. Med. Chem. Lett.* **2013**, *23*, 5471–5483.
[155] A. F. Stepan, T. P. Tran, C. J. Helal, M. S. Brown, C. Chang, R. E. O'Connor, M. De Vivo, S. D. Doran, E. L. Fisher, S. Jenkinson, *ACS Med. Chem. Lett.* **2018**, *9*, 68–72.
[156] R. S. Obach, G. S. Walker, R. Sharma, S. Jenkinson, T. P. Tran, A. F. Stepan, *J. Med. Chem.* **2018**, *61*, 3626–3640.
[157] R. Shafiee-Nick, A. R. Afshari, S. H. Mousavi, A. Rafighdoust, V. R. Askari, H. Mollazadeh, S. Fanoudi, E. Mohtashami, V. B. Rahimi, M. Mohebbi, *Biomed. Pharmacother.* **2017**, *94*, 541–556.
[158] G. S. Walker, J. N. Bauman, T. F. Ryder, E. B. Smith, D. K. Spracklin, R. S. Obach, *Drug Metab. Dispos.* **2014**, *42*, 1627–1639.
[159] J. N. Kolev, K. M. O'Dwyer, C. T. Jordan, R. Fasan, *ACS Chem. Biol.* **2014**, *9*, 164–173.
[160] G. Babaei, A. Aliarab, S. Abroon, Y. Rasmi, S. G. G. Aziz, *Biomed. Pharmacother.* **2018**, *106*, 239–246.
[161] K. Gach, A. Długosz, A. Janecka, *Naunyn-Schmiedeberg's Arch. Pharmacol.* **2015**, *388*, 477–486.
[162] A. Seca, A. Silva, D. Pinto, in *Stud. Nat. Prod. Chem.* (Ed.: A. Rahman), Elsevier, **2017**.
[163] V. Tyagi, H. Alwaseem, K. M. O'Dwyer, J. Ponder, Q. Y. Li, C. T. Jordan, R. Fasan, *Bioorg. Med. Chem.* **2016**, *24*, 3876–3886.
[164] H. Alwaseem, B. J. Frisch, R. Fasan, *Bioorg. Med. Chem.* **2018**, *26*, 1365–1373.
[165] K. Chen, X. Lei, *Curr. Opin. Green Sustain. Chem.* **2018**, *11*, 9–14.
[166] M. C. White, J. Zhao, *J. Am. Chem. Soc.* **2018**, jacs.8b05195.
[167] H. M. L. Davies, D. Morton, *ACS Cent. Sci.* **2017**, *3*, 936–943.
[168] F. Li, X. Zhang, H. Renata, *Curr. Opin. Chem. Biol.* **2019**, *49*, 25–32.
[169] J. Boström, D. G. Brown, R. J. Young, G. M. Keserü, *Nat. Rev. Drug Discovery* **2018**, DOI 10.1038/nrd.2018.116.
[170] A. Ciaramella, D. Minerdi, G. Gilardi, *Rend. Lincei* **2017**, *28*, 169–181.
[171] Y. Wei, E. L. Ang, H. Zhao, *Curr. Opin. Chem. Biol.* **2018**, *43*, 1–7.
[172] L. Hammerer, C. K. Winkler, W. Kroutil, *Catal. Lett.* **2018**, *148*, 787–812.
[173] R. A. Sheldon, J. M. Woodley, *Chem. Rev.* **2018**, *118*, 801–838.
[174] O. F. Brandenberg, R. Fasan, F. H. Arnold, *Curr. Opin. Biotechnol.* **2017**, *47*, 102–111.
[175] S. C. Hammer, A. M. Knight, F. H. Arnold, *Curr. Opin. Green Sustain. Chem.* **2017**, *7*, 23–30.
[176] H. Davis, A. Plowright, E. Valeur, *Nat. Rev. Drug Discovery* **2017**, *16*, 681–698.
[177] "The Nobel Prize in Chemistry 2018. NobelPrize.org. Nobel Media AB 2018. Sat. 10 Nov 2018," can be found under https://www.nobelprize.org/prizes/chemistry/2018/summary/, **2018**.
[178] U. T. Bornscheuer, *Philos. Trans. R. Soc. A Math. Phys. Eng. Sci.* **2018**, *376*, 1–7.
[179] N. J. Turner, R. Kumar, *Curr. Opin. Chem. Biol.* **2018**, *43*, A1–A3.
[180] C. W. Coley, L. Rogers, W. H. Green, K. F. Jensen, *ACS Cent. Sci.* **2017**, *3*, 1237–1245.
[181] S. V. Ley, D. E. Fitzpatrick, R. J. Ingham, R. M. Myers, *Angew. Chem. Int. Ed.* **2015**, *54*, 3449–3464; *Angew. Chem.* **2015**, *127*, 3514–3530.
[182] J. Li, S. G. Ballmer, E. P. Gillis, S. Fujii, M. J. Schmidt, A. M. E. Palazzolo, J. W. Lehmann, G. F. Morehouse, M. D. Burke, *Science (80-.).* **2015**, *347*, 1221–1226.
[183] T. Klucznik, B. Mikulak-Klucznik, M. P. McCormack, H. Lima, S. Szymkuć, M. Bhowmick, K. Molga, Y. Zhou, L. Rickershauser, E. P. Gajewska, *Chem* **2018**, *4*, 522–532.
[184] B. H. Lipshutz, *Curr. Opin. Green Sustain. Chem.* **2018**, *11*, 1–8.
[185] D. K. Romney, F. H. Arnold, B. H. Lipshutz, C. J. Li, *J. Org. Chem.* **2018**, *83*, 7319–7322.

Manuscript received: November 10, 2018
Revised manuscript received: January 7, 2019
Accepted manuscript online: January 22, 2019
Version of record online: February 15, 2019

FULL PAPER DOI: 10.1002/adsc.202000251

Preparative-Scale Production of Testosterone Metabolites by Human Liver Cytochrome P450 Enzyme 3A4

Nico D. Fessner,[a] Matic Srdič,[b, c] Hansjörg Weber,[d] Christian Schmid,[a, e] David Schönauer,[b] Ulrich Schwaneberg,[f] and Anton Glieder[a,*]

[a] Institute of Molecular Biotechnology, Graz University of Technology, NAWI Graz, Petersgasse 14/3, Austria
Fax: (+43)-316-873-9302
phone: (+43)-316-873-4074
E-mail: a.glieder@tugraz.at
[b] SeSaM-Biotech GmbH, Aachen, Germany
[c] Bisy GmbH, Hofstaetten, Austria
[d] Institute of Organic Chemistry, Graz University of Technology, NAWI Graz, Austria
[e] Austrian Centre of Industrial Biotechnology (ACIB), Graz, Austria
[f] Institute of Biotechnology, RWTH Aachen University, Aachen, Germany

Manuscript received: February 21, 2020; Revised manuscript received: April 9, 2020;
Version of record online: May 29, 2020

Supporting information for this article is available on the WWW under https://doi.org/10.1002/adsc.202000251

Abstract: Just like the drugs themselves, their metabolites have to be evaluated to succeed in a drug development and approval process. It is therefore essential to be able to predict drug metabolism and to synthesise sufficient metabolite quantities for further pharmacological testing. This study evaluates the possibility of using *in vitro* biotransformations to solve both these challenges in the case of testosterone as a representative component for steroids. The application of cells of *Pichia pastoris* with expressed membrane-associated human liver cytochrome P450 enzyme (P450) 3A4 in two cycles of a preparative-scale bioreactor experiment enabled the isolation of the common metabolites 6β-hydroxytestosterone and 6β-hydroxyandrostenedione on a 100 mg scale. Side-product formation caused by enzymes intrinsic to *P. pastoris* was reduced. In addition more polar testosterone metabolites formed by a P450 3A4-catalysed bioconversion, than the known mono-hydroxylated ones, are reported and 6-dehydro-15β-hydroxytestosterone as well as the di-hydroxylated steroids 6β,16β-dihydroxytestosterone, 6β,17β-dihydroxy-4-androstene-3,16-dione and 6β,12β-dihydroxyandrostenedione were isolated and verified by NMR analysis. Their respective biological significance remains to be investigated. Whole-cell P450 catalysts expressed in *P. pastoris* qualify as a tool for the preparative-scale synthesis of human metabolites. Biotransformation processes in combination with standard chemical procedures allow the isolation and characterisation even of minor drug metabolite products.

Keywords: human drug metabolites; cytochrome P450 3A4; Preparative-scale synthesis; steroids; whole cell biotransformation

Introduction

Poor pharmacokinetics or toxicity caused a major percentage of drugs to fail approval at a late stage of drug development processes,[1] although clinical trials are extremely costly and time-consuming.[2] Recently, the FDA acknowledged that individual drug metabolites might have a different pharmacological or chemical activity compared to the parent drug, and each must now be investigated separately to assess a drug's safety.[3] Consequently, an efficient, quick and authentic identification as well as preparative production of metabolites is highly important to the pharmaceutical industry.[4]

Traditional methods to elaborate a drug's metabolic profile include animal models,[5–7] liver microsomes[8,9] – vesicles of fragmented endoplasmic reticulum containing cytochrome P450 monooxygenases (P450s) – or computational predictions,[10,11] and there are also novel concepts emerging such as "organs-on-chips".[12] However, none of these approaches can provide sufficient metabolite quantities. While conventional methods of chemical synthesis could produce the required amounts of such materials, it is often difficult and time-demanding to functionalise structurally complex drugs with specific regioselectivity. For these reasons the potential of biocatalysis, operating in a synthetic late-stage fashion,[13] was investigated by many studies for the preparative-scale production of human metabolites. There are several examples of successful applications of recombinant human P450s,[14–16] and for some specific products also microbial P450s were deemed successful at providing typical human drug metabolites at such a scale.[17–25] However, in many cases microbial P450s resulted in different product profiles and desired metabolites were only obtained after time intensive enzyme engineering.

The body's mechanism for clearance of chemicals like drugs, typically consists of two enzymatic phases with different significance.[26,27] In phase I the compound is made more polar *via* hydrolytic conversions or oxidative functionalisation, while phase II consists of a conjugation step attaching polar units like peptides, acids or sugar moieties to the newly installed or liberated functional group. More than 90% of the phase I enzymatic drug degradation reactions are caused by human liver P450s.[28] Among those, P450 3A4 is the key player in human xenobiotic clearance. It is the most abundant enzyme in this group,[29,30] and, due to its versatility, responsible for the degradation of more than 50% of approved drugs including testosterone (Scheme 1A).[28,31] Therefore, P450 3A4 in particular offers itself as a representative and meaningful model and tool for the study of enzymatic drug metabolism by P450 enzymes. The goal was to employ the hepatic function of this key enzyme for the preparative synthesis and identification of the respective metabolites to generate new data for future drug evaluations and models for drug metabolite predictions.

Liver P450 3A4 expressed in recombinant *E. coli* was described to hydroxylate testosterone (**1**) at four different positions, namely 6β, 2β, 1β and 15β in descending order of rates.[32] Thus, 6β-hydroxytestosterone (**2**) is typically used as the determinant of the overall testosterone bioconversion efficiency (Scheme 2A).[33] However, oxidation of **1** at positions 2α, 6α, 7α, 11β, 16α and 17 (forming the ketone androstenedione (**3**)) was also observed when using isolated human liver microsomes.[32,34] In fact, upon applying **1** to hepatic rat microsomes Pfeiffer and

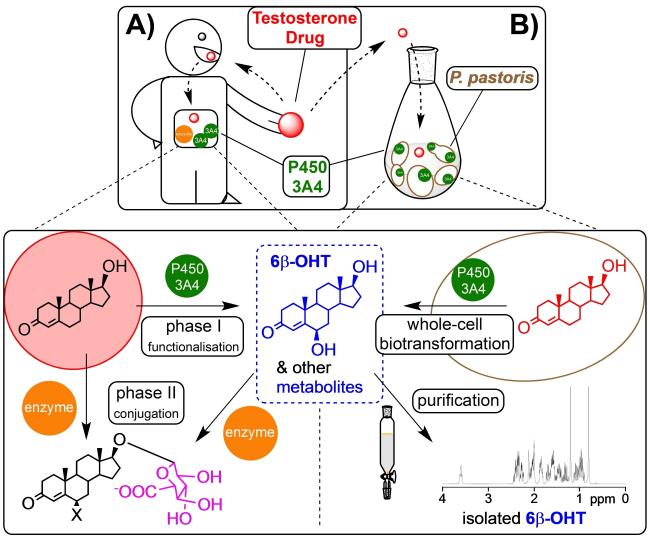

Scheme 1. Major routes of *in vivo* human drug metabolism are compared to an *in vitro* imitation approach. **A)** Administered testosterone drug (red) is metabolised in the liver by P450 3A4 (green) and conjugation enzymes (orange) in two phases to yield an *O*-glucuronide (pink) derivative for excretion. **B)** The same testosterone drug is added to cells of *P. pastoris* expressing recombinant P450 3A4 to simulate human phase I metabolism *in vitro*, and allow isolation of metabolites.

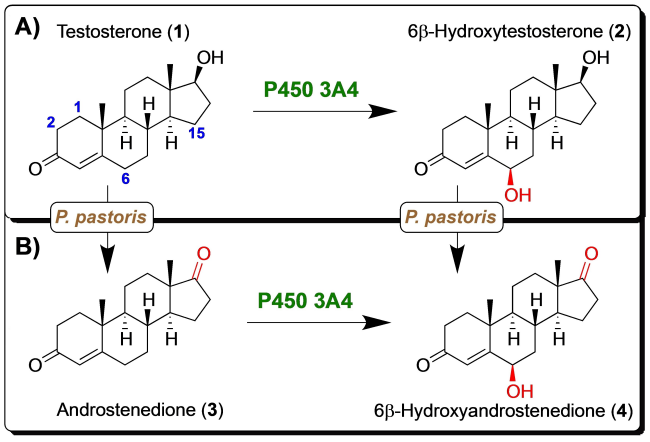

Scheme 2. Illustration of the major reactions observed in this study employing whole-cell catalysts. **A)** Cytochrome P450 3A4 catalysed the conversion of testosterone (**1**) to 6β-hydroxytestosterone (**2**); minor hydroxylation positions of **1** reported in the literature for this enzyme are indicated in blue. **B)** Competing redox enzymes intrinsic to *P. pastoris* can oxidise **1** to furnish 4-androstene-3,17-dione (**3**); Overexpressed P450 3A4 also accepted the latter as a substrate to yield the corresponding 6β-hydroxyandrostenedione **4**, confirming observations of previous studies.[31]

Metzler could detect at least 17 metabolites by HPLC analysis, some of which included di-hydroxylated derivatives of **1** and **3**.[35] Although rats are not a reliable model to predict drug metabolism in

humans,[36,37] it was still hypothesised that the conversion of **1** in the human liver may produce a similarly high number of metabolic products. Many enzymes can produce metabolites; the related human liver P450 2D6 for example also converts steroids, albeit poorly.[38] Still, in that case a further presumption was that P450 3A4 itself could be mainly responsible for such a large metabolic product spectrum due to its prevalence in the testosterone metabolism and its extraordinary active site promiscuity,[39,40] cooperativity[41] and multiple substrate binding sites.[42,43]

In this study cells of *Komagataella phaffii (Pichia pastoris*) containing the main wild-type P450 3A4 at high expression level were used to simulate the human metabolism of testosterone and to synthesise its well-characterised metabolites such as 6β-hydroxytestosterone at a 100 mg scale (Scheme 1B).[44]

P. pastoris was the host organism of choice because of the observed advantages in a comparative expression study for human liver P450 2D6/CPR catalysts in different standard expression hosts. *P. pastoris* was identified to be superior to *Escherichia coli*, *Saccharomyces cerevisiae* and *Yarrowia lipolytica*.[45] Furthermore, also compared to other yeasts convincing characteristics of *P. pastoris* are high cell density achievable in a cheap growth medium,[46] excellent capacity for native-like post-translational modifications of eukaryotic proteins,[47] tolerance for membrane protein production such as for P450 3A4,[48,49] and strongly regulated promoters that enable controlled growth on two individual carbon sources (glycerol/glucose and methanol).[50,51] These features allow a highly productive cell cultivation and efficient bioconversion under controlled conditions in a bioreactor.[46,49] First successful expression of active human P450 3A4 was reported in 2013.[52] Here we demonstrated the almost complete conversion of about one gram of testosterone in a 1.3 litre bioreactor system, validating the potential of this system for further up-scaling.

Results and Discussion

The analysis of steroids is symptomatically challenging because of the small polarity changes induced upon functionalisation of the large hydrophobic scaffolds.[53] The development of a high-resolution separation method was therefore key to the successful analysis and isolation of steroidal metabolites, which is why the proven HPLC conditions of Pfeiffer and Metzler[35] were adapted. Commercial human P450 3A4/hCPR expressing *P. pastoris* cells (stored as frozen cells at −80 °C) were diluted to obtain standardised whole-cell catalyst stock solutions of a cell concentration of $OD_{600} = 200$, which was used for all experiments. Figure 1 displays the metabolite profile obtained from

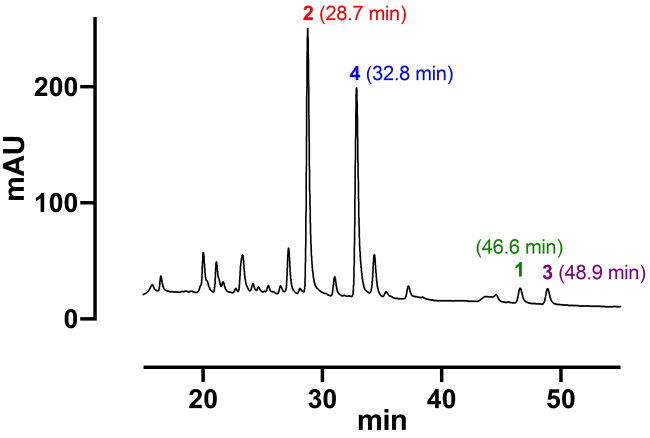

Figure 1. The HPLC analysis of metabolites of **1** obtained by the bioconversion of **1** with P450 3A4 (2 mM **1**, 1 mL total volume, cell concentration = 200 OD600, 225 rpm, 22 h, 30 °C).

a 1 mL-scale test experiment using 2.0 mM **1** after a 22 hours biotransformation. The high number of peaks with a wide R_f spread suggested the formation of various products with rather different polarity. Peaks eluting at 46.5, 28.7 and 48.8 min could be assigned to compounds **1**, **2** and **3**, respectively, with the aid of authentic reference materials. The peak of compound **4** was deduced from corresponding results shown in Figure 3. The other peaks around **2** and **4** could only partly be assigned during the course of this study.

Formation of ketones **3** and **4** occurred, although P450 3A4 is not known to oxidise **1** at position 17. In fact, this oxidation happened regardless of the presence of the expressed P450 as shown by the corresponding negative control experiment using wild-type *P. pastoris* cells, indicating the existence of an intrinsic oxidase or dehydrogenase in P. pastoris, competing with P450 3A4 for the substrate. After 24 hours more than 50% of **1** had been converted to **3** (Figure 2). This side reaction was noticed to be reversible by subjecting **3** as the sole substrate, which yielded an equilibrium between the two components as a consequence of the redox state of the host cells (Figure S1). The prevalence of low amounts of these additional oxidation products compared to the control reaction employing cells expressing no P450 3A4 indicated high efficiency of the expressed human P450 enzyme.

Furthermore, these results suggested the responsibility of a dehydrogenase for this reaction rather than an oxidase. The same effect had been noticed in the related yeasts *S. cerevisiae* and *Schizosaccharomyces pombe* (*S. pombe*)[54] and the intrinsic glucose-6-phosphate dehydrogenase was suggested as a possible candidate for steroid interconversion in S. cerevisiae.[55] In *P. pastoris* related intrinsic alcohol dehydrogenases (ADHs) might be responsible for the oxidation of **1** to **3** over time. However, many

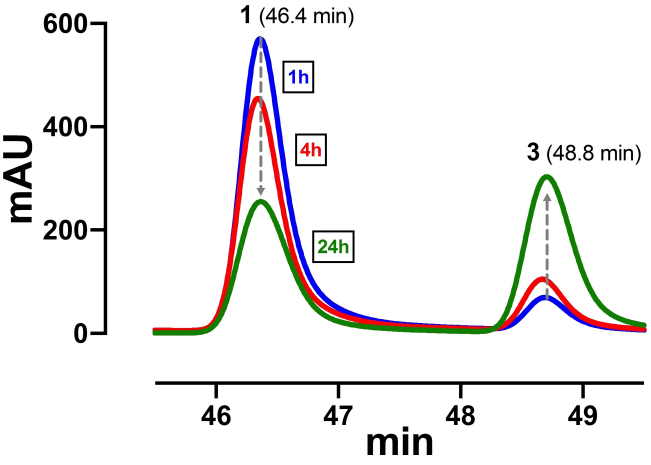

Figure 2. HPLC monitoring of a bioconversion of **1** using the empty vector control strain lacking P450 3A4 expression, which shows oxidation to **3** by *P. pastoris'* intrinsic enzymes (2.5 mM **1**, 30 mL, $OD_{600}=200$, 130 rpm, 24 h, 28 °C). After 24 h, the concentration of ketone **3** exceeded that of substrate **1**.

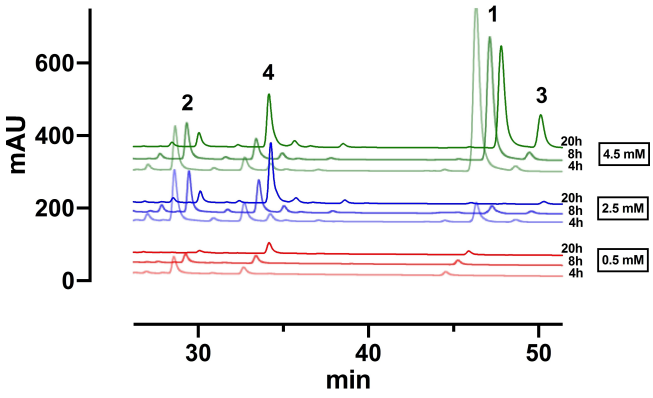

Figure 3. HPLC traces of the bioconversion of **1** at different concentrations (0.5, 2.5 and 4.5 mM shown in red, blue and green, respectively) by P450 3A4 in shake flasks (30 mL, 130 rpm, 24 h, 28 °C, $OD_{600}=200$). Samples of each biotransformation were taken at three different time points in between 4 and 20 hours.

dehydrogenases can be found in the organism's genome as dehydrogenases play a role in different biochemical pathways.[56] For example, three ADHs of *P. pastoris* that catalyse the reversible oxidation of alcohols with simultaneous reduction of the cofactor $NAD(P)^+$ to NAD(P)H had been described in more detail.[57] The identification of the one(s) specifically accounting for the observed steroid conversion remains to be investigated.

Yet, due to efficient overexpression of the recombinant enzyme, the presented yeast model does not lead to an unrealistic metabolite profile for human testosterone metabolism in the liver as ketone formation also happens when using human liver microsomes as mentioned before.[34] However, the side-product formation negatively affected the preparative-scale metabolite synthesis, as the yield of individual components was reduced, and their subsequent separation became more complicated. Since **3** is likewise accepted by P450 3A4 as a substrate (Scheme 2B),[31] this leads to a much more complex product mixture, essentially composed of duplicate sets of complementary metabolites when all derivatives of **1** were produced in the equivalent ketone form.

Controlling the reaction progress thus became crucial to maximise product yield by anticipating the time, at which the rate of oxidation of **2** to **4** was higher than the rate of its formation, in order to stop the conversion beforehand. As indicated best in Figure 3 (upper traces, 4.5 mM **1**), concentrations of **1** decreased over time while those of **3** increased, and likewise the peaks of the desired product **2** diminished, while those of **4** rose correspondingly. Because peaks of **2** at 8 hours reaction time were slightly lower than at 4 hours both for runs with 2.5 and 4.5 mM **1**, the optimum point in time had already passed in between. With 0.5 mM of **1**, one hour was sufficient to fully exhaust the substrate (data not shown). In comparison, a concentration of 4.5 mM **1** was too high for the biocatalyst to be fully used-up within 20 hours, indicating decay in enzyme activity over time or potential substrate/product inhibition at higher concentrations. Consequently, for subsequent biotransformations 2.5 mM of substrate **1** was chosen.

Having established the optimal reaction time, it was attempted to further minimise the side-product formation by either changing the availability of the ADHs or their co-factors within the cells. The former can be achieved by addressing the ADH expression levels, which depend on the cell's metabolic state. Usually strains of *P. pastoris* are grown on glucose or glycerol as carbon source, and the recombinant expression of the desired protein is subsequently induced by the addition of methanol in Mut^S-type strains (Methanol utilisation Slow), only then activating the responsible, tightly regulated promoter.[58] A change in metabolism will also trigger or suppress the expression of ADHs.[59] Following methanol induction, cells were thus again exposed to either glucose or glycerol for 3 hours before the biotransformation. In another attempt to enhance the availability of reduced cofactors, methanol was added to the biotransformation not only to limit the availability of NAD(P)+, but also to supply a substrate competing with **1** for the ADH active site. In addition, high NAD(P)H concentrations supply sufficient electrons to P450 3A4 *via* the reductase, which often represents the rate-limiting step.[60] Because high methanol concentrations are rather lethal to *P. pastoris*,[61] three different concentrations from 0.5 to 3% were tested. The results of both these strategies are presented in Figure 4.

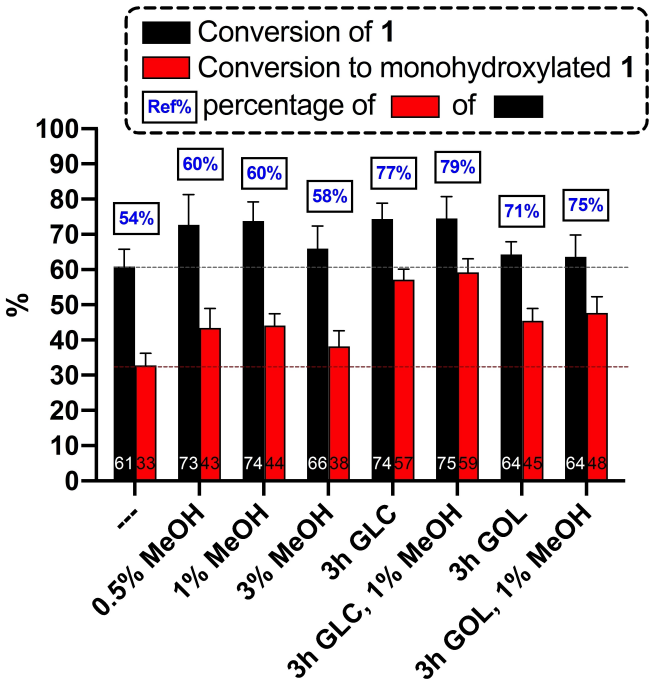

Figure 4. Conversion of **1** (black) to the respective fraction of mono-hydroxylated derivatives of **1** (red) are shown for biotransformations with cells in microwell plates under standard conditions (2.5 mM testosterone, 0.4 mL, 310 rpm, 17 h, 28 °C, OD_{600} = 200) without (–) and with the addition of methanol (0.5, 1 and 3% MeOH), or with cells pre-treated by 3 hours cultivation in glycerol (3 h GOL) or glucose (3 h GLC) and a combination of cultivation and methanol addition (3 h GOL, 1% MeOH; 3 h GLC, 1% MeOH). For a comparison, the calculated Ref% indicates the percentage of formed conversion to mono-hydroxylated products relative to the total uptake of **1**.

All biotransformations were intentionally incubated for 17 hours, i.e. beyond the optimal reaction time, to intensify a potential reduction effect on the 17-ketone formation. "Ref%" was calculated for better quantification and facilitated comparison of the individual approaches. For the total conversion of **1** (black bars) all cumulated conversions caused by P450 3A4 were considered, while disregarding ADH involvement; thus **4** was included since hydroxylation must have preceded the oxidation, but not **3**. The total conversion data also acknowledge only three mono-hydroxylated derivatives of **1** leaving many extra peaks unaccounted (Figure S2). A significant difference could be observed across the different approaches relative to untreated cells. Addition of methanol alone increased the total conversion of **1** and the fraction of mono-hydroxylated products as seen by a slight increase in Ref%. Upon pre-incubation with glucose, the conversion increased to a similar level as for methanol addition, while glycerol pre-treatment had almost no effect. Interestingly though, less oxidation to ketones occurred in both cases as represented by significantly higher Ref% values suggesting that the ADHs present in *P. pastoris* cells that were tuned to carbon source metabolism cause less steroid oxidation. In combination with methanol addition both cases generally experienced a slight further boost. Therefore, it seems like both strategies for increasing product selectivity were successful individually as well as in combination, and suppression of ADH oxidation could enhance selectivity from 54% for untreated conditions to a peak value of 79% (glucose and methanol). A study demonstrated how the co-expression of the human 17β-hydroxysteroid dehydrogenase type 3 could further suppress the side-product formation in *P. pastoris*.[55] Another option would be the generation of knock-out strains lacking ADH genes *via* knock-out, eg. using recently established CRISPR/Cas9 technology.[62]

With reaction conditions optimised, a scale-up biotransformation (BT1) from a several 10 mL scale in 2.5 L cultivation flasks to 1.3 litres in a bioreactor under controlled conditions was performed next (Figure 5). Almost 1 gram of **1** was used with implementation of 1% methanol addition.

After 8 hours (black trace) a conversion of 85% and a mono-hydroxylation selectivity factor of 62% had been achieved, similar to the results in shake flasks (Figure 3), but significantly better than by 96-well plate cultivation (Figure 4). Enzyme stability and oxygen-transfer rates were considered to be some of the major limitations of P450s. Quite likely, the oxygen requirements of P450s had been met more accurately by the greater oxygen supply in the bioreactor.[63] A high cell density needs careful adaptation to match the enzyme's oxygen demand, and thus the full potential of a cell density at OD_{600} = 200 might not have been fully exploited.[64] On the other hand, the known rather poor stability of P450 3A4[30] may account for the observed shrinking in conversion rate from 21% (Ref

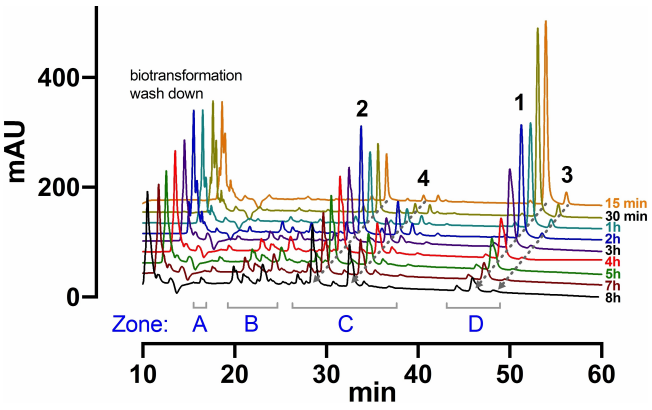

Figure 5. HPLC monitoring of the scale-up biotransformation (BT1) in a bioreactor under controlled conditions is shown (2.5 mM of **1** = 959 mg, 1.3 L, 400 rpm, 8 h, 28 °C, OD_{600} = 200, pH 7.0, air flow = 5.0 L/min).

%=87%) during the first 15 minutes (15 min, orange) to 45% (81%) after one hour (1 h, turquoise) and 73% (70%) after five hours (5 h, green) of reaction time despite the application of whole-cell biocatalysts, which supports membrane-bound enzymes with the supply of cofactors and electrons.[60,65]

The recovered cells from the first batch were used for a second cycle of biotransformation (BT2) in the bioreactor under identical conditions in order to test the durability of the catalyst system and the amount of testosterone substrate that can be metabolised. In fact, within 9 hours (9 h, blue) of the second cycle another 66% of 1 gram of the substrate was converted (Figure 6) with a Ref% of 58% that dramatically dropped afterwards. This is an extraordinary performance of a human P450 considering their poor stability and short lifetime usually described in literature.[66]

Between 17 (not shown) and 37 hours the peaks of compounds **1** and **2** had vanished completely. Nevertheless, the biotransformation was continued for a total of 105 hours to ensure all derivatives of **1** had been dehydrogenated to their respective ketone equivalents. The reduced number of peaks simplified the HPLC analysis and revealed only those peaks belonging to derivatives of **3**. The controlled reactor conditions, efficient performance of the biocatalyst, large amount of substrate and frequent sampling provided a more comprehensive picture about the kinetics of substrate consumption and sequence of metabolite formation. Apparently, all metabolite peaks in Figures 5 and 6 clustered into four distinct zones A to D according to their polarity and their elution times (marked in blue). Because zone D comprises the untreated, non-hydroxylated substrates **1** and **3** and zone C the mono-hydroxylated metabolites **2** and **4**, it seemed logical to assume di-hydroxylated metabolites in zone B and even tri-hydroxylated ones in zone A. The extent the regiochemistry of hydroxylation affects the polarity of the molecule decreases with rising degree of hydroxylation matching the smaller zone widths towards shorter elution times. Analysis of the same HPLC samples by mass detector indeed strongly supported such hypothesis (Figure S3). This experiment also indicated the presence of five, not just four mono-hydroxylated derivatives of **1**.

A zoomed-in perspective of zones A and B from Figure 6 was not sufficient to analyse the different compounds in detail (Figure S4). Another HPLC method was developed specifically for compounds eluting in zones A and B and revealed a complex picture of more than ten different peaks as displayed in Figure 7.

For isolation and product characterisation, the extracted metabolite mixtures from runs BT1 and BT2 were separately pre-purified by manual column chromatography in order to simplify the product isolation by preparative HPLC. However, further HPLC purification was obsolete because clean fraction of **2** and **4** could be collected, which furnished 108 mg of **2** from the mixture of the first bioreactor cycle (yield = 11.3%, productivity[67] [g/g] using dry cell weight = 0.16%) and 87 mg of **4** from the second (9.1%, 0.13%). Higher masses were reported for human metabolites of other drugs,[68] but to the best of the author's knowledge the quantities isolated here represent the highest reported in literature for these particular metabolites in comparison to other preparative studies.[16,69,70] Additionally, a refinement or repetition of the purification procedure holds the potential of increasing the yield further.

From both mixtures of the two cycles of biotransformations executed in the bioreactor, two sets of two samples of about 10 mg each could also be isolated by

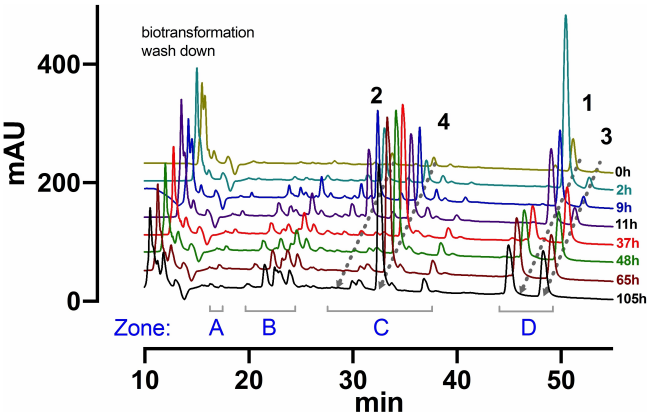

Figure 6. HPLC monitoring for the second cycle of the scale-up biotransformation (BT2) in a bioreactor under controlled conditions (2.5 mM of **1** = 959 mg, 1.3 L, 400 rpm, 8 h, 28 °C, OD_{600} = 200, pH 7.0, air flow = 5.0 L/min) is shown.

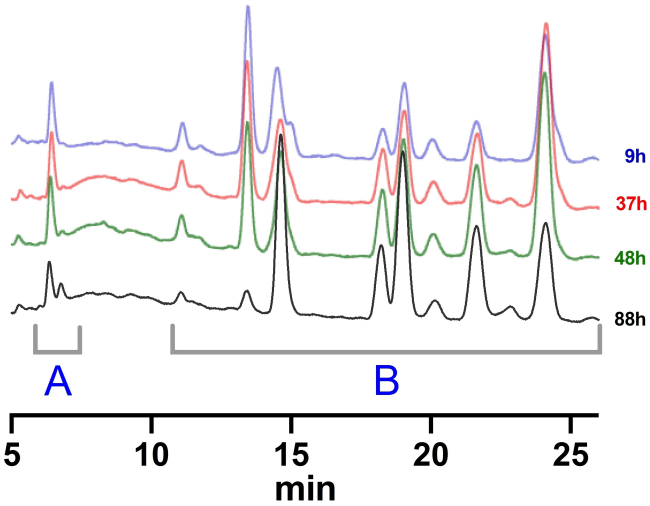

Figure 7. An illustration of the HPLC traces of zones A and B of BT2. A new HPLC method was used for better separation of the more polar metabolites.

column chromatography. They contained more polar compounds than **2** or **4** seemingly pure as determined by TLC analysis. NMR and HPLC analysis, however, clearly indicated the need for further purification, which was done by collecting the fractions manually using an analytical HPLC instrument as illustrated in Figure S5. At a wavelength of 270 nm the metabolites had only about 10% absorbance enabling a more precise isolation of specific peaks than a preparative HPLC would have achieved (Figures S6–S9). Compounds 1β- (**5**) and 15β-hydroxytestosterone (**6**) could be isolated from BT1,[71,72] which confirmed the results published by Guengerich *et al.*[32] In addition, 6-dehydro-15β-hydroxytestosterone (**7**) could be uncovered as the minor component of a mixture with **6**. More polar compounds of BT1 were only present as mixtures and with quantities of less than 1 mg each, making an identification by NMR spectroscopy impossible. The same was true with many of the isolated fractions of samples of BT2. However, for the first time the NMR spectra of four isolated peaks confirmed the formation of the di-hydroxylated compounds 6β,16β-dihydroxytestosterone (**8**) 6β,17β-dihydroxy-4-androstene-3,16-dione (**9**) and 6β,12β-dihydroxyandrostenedione (**10**). Compounds **7**, **8** and **10** were also confirmed by high-resolution mass spectrometry, while the spectrum for **9** was inconclusive due to the presence of several other compounds. Their elution times and their structures are displayed in Figure 8. Compound **5** eluted between the peaks of **2** and **4**. Most likely, the peak eluting just after 4 is 2β-hydroxytestosterone, which was not isolated in this study. Consequently, the rate of formation of the mono-hydroxylated metabolites reported by Guengerich *et al.*[32] could not be confirmed here, but looks rather like $6\beta > 15\beta \approx 2\beta > 1\beta$.

Although the discovered metabolites **7**–**10** occupy a noteworthy area of the HPLC profile at least in this study, their existence remained unknown until now. Having found evidence for the presence of di-hydroxylated metabolites of P450 3A4, the peaks around those of **8** and **10** will likely be either of the same sort or of other oxidised species like **9** or **7**. Given the fact that many NMR spectra indicated the presence of compound mixtures, although some of these were derived from just one HPLC peak, there must be even a larger amount of individual di-hydroxylated compounds formed than represented by the number of peaks.

Remarkably, poly-hydroxylated testosterone products have barely been considered in combination with microsomal liver enzymes. Database searches yielded only few articles that suggested the presence of poly-hydroxylated testosterone metabolites since 1968.[35,73,74] Perhaps this might be due to the chronically bad stabilities and thus short lifetimes of recombinant human P450s causing a rapid decline in

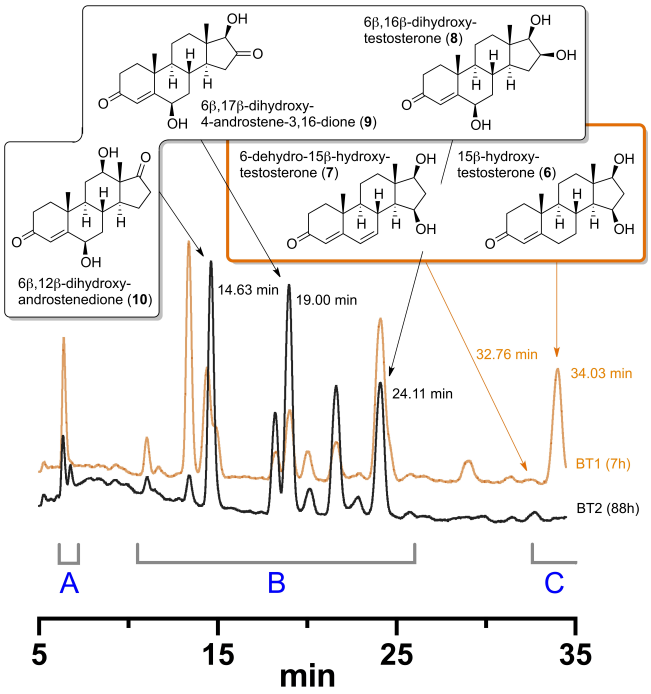

Figure 8. Display of the elution times of the newly discovered metabolites 6-dehydro-15β-hydroxytestosterone (**7**), 6β,16β-dihydroxytestosterone (**8**), 6β,17β-dihydroxy-4-androstene-3,16-dione (**9**) and 6β,12β-dihydroxyandrostenedione (**10**) relative to the already known 15β-hydroxytestosterone (**6**).

enzyme activity after a few hours in the most commonly used microbial host organisms.[45]

Providing more stable catalysts in combination with highly efficient (co-)expression levels of these enzymes could therefore generate a different metabolic profile. Here, high stability was achieved in form of whole-cell biocatalysts using robust yeast chassis, which also allows cost effective scale up and independence of NADPH addition or regeneration. Alternatively ancestral sequence reconstruction of the P450 3 family was also found to enhance stability of the enzyme itself without a loss in activity, albeit slightly changing its regioselectivity.[75]

Another reason might be that such profile is beyond the normal expectations. Not realising the complexity of the human liver P450s and their metabolic spectrum generated, which is still not completely understood nowadays,[31] many studies focused on the major metabolite **2**, which is accessed most easily and promises good results more quickly. Furthermore, the hydroxylation of **1** is not a prerequisite for entering phase II metabolism because the molecule already has an alcohol functional group attached (Scheme 1). The majority of phase I steps rather involve 17-oxidation, reductions of the A ring or the 3-position making consecutive hydroxylation steps less predictable.[76] Nevertheless, just like compound **5** was discovered in

2004 as a novel metabolite[32] and *in-vitro* experiments pointed towards some physiological potential,[77] the existence of such poly-hydroxylated products might as well have pharmacological relevance, which is yet to be investigated.

Hydroxylated testosterone products may be already minor metabolites in the human liver,[76] though it is still desirable and necessary to identify and synthesise such minor metabolites in sufficient quantities.[78] Clearly, efficient biocatalysis enables access to them.[79] Owed to its high cell density, *P. pastoris* is frequently advertised by literature as excellently suitable for its application in large-scale bioreactor experiments.[49,80–83] Human P450 3A4 enzyme catalyst preparations based on *P. pastoris*[84–86] are commercially available from several companies, claiming also multiple cycles of biotransformation.[70] However, no peer-reviewed example of the bioreactor-scale application of human P450 enzymes produced by *P. pastoris* followed by several cycles of whole-cell biotransformations and description of experimental procedure for such scalable human P450-catalysed biotransformations had been published so far.

Reliable expression levels are difficult to obtain for membrane-bound proteins and hardly give representable information about the catalytic efficiency of an enzyme that is so dependent on the electron-transfer from the reductase to the heme domain.[60,87,88] The volumes used for cultivation and the subsequent biotransformation outcome provide better comparability: While in a bioreactor experiment using whole-cell *E. coli*[16] human P450 3A4 catalysts, Vail *et al.* needed more than 3 L of the *E. coli* culture to perform their conversion of **1** and to isolate 59 mg of **2** in 20.5% yield, this study employed less than 0,5 L of the yeast culture broth to obtain 108 mg of the same metabolite (Table 1). In addition, due to their size *P. pastoris* cells are easy to remove from the reaction broth. Yields of other metabolites than **2** were not discussed in the *E. coli* based biotransformation. Furthermore, confirmation of the identity of their product was only provided using LC-MS.

Table 1. Comparison of the cultivation and biotransformation parameters between this study and a previous publication of Vail *et al.*[16]

	Vail *et al.*[16]	BT1, this study
Cultivation Volume	10 L	5 L
Wet cell wt. produced	~300 g	~2000 g
Wet cell wt. used	100 g	200 g
Substrate **1** used	288 mg (25 mL, 40 mM)	959 mg (3.33 mL, 1 M)
Product **2** isolated	59 mg	108 mg
Yield of **2** (%)	20.5%	11.3%
Productivity[67]	*n.d. (no dry cell wt. data available)*	0.16%

While P450 3A4 was also successfully expressed in other yeasts,[89,90] no preparative biotransformation with testosterone was performed with those catalysts. On the other hand, using *S. pombe* excellent human P450 expression and biocatalysis was exemplified by Drăgan *et al.*, but no direct comparison is possible as a different human P450 converting another drug was reported for their preparative synthesis.[68]

Alternatively, *E. coli* expressing microbial monooxygenases was used to make some individual metabolites of testosterone with excellent yields.[21,79,91,92] Those enzymes are soluble, can be easily tuned *via* directed evolution, are often self-sufficient with high coupling efficiencies and turnover numbers, and have a more narrow substrate tolerance than the human liver P450s. However, often non-human metabolites are formed as main products and long lasting enzyme engineering was necessary to change the substrate and product selectivity, making it inconvenient human drug metabolites of new drug candidates.

Incubation of **2** with the empty plasmid cells as the negative control showed no conversion, other than the alcohol oxidation ruling out an influence of the yeast's ADHs. Therefore it seems like **2** and **4** are also acceptable substrates of P450 3A4 as already implied by the study of Pfeiffer and Metzler, who identified their di-hydroxylated metabolites by adding mono-hydroxylated ones to the liver microsomes.[35] The presence of a 6β-hydroxyl seems to change the enzyme's hydroxylation regioselectivity relative to **1** because positions 16 and 12 were observed as the second hydroxylation site. These results are in line with those by Guengerich *et al.*,[35] whose results suggested a major selectivity difference of P450 3A4 upon the small change in the substrate structure **1** to dihydrotestosterone with a reduced $\Delta^{4,5}$-bond. However, the here discovered α,β,γ,δ-unsaturated compound **7** was formed either after sequential or stepwise hydroxylation i.e. $\Delta^{6,7}$-elimination after the first or second hydroxylation at positions 6 and 15. This means that position 15 is either a conserved target of P450 3A4 with **2** as the substrate or the regioselectivity was not affected by the structural changes of double unsaturation. It seems also plausible that just like the 17β- and 16β-hydroxyl oxidation, the $\Delta^{4,5}$-bond reduction was caused by the ADHs, and compounds **7**, **9** and **10** are therefore no natural metabolites generated by P450 3A4 biocatalysis alone. But it seems reasonable to assume that the 17β-alcohol equivalent of compound **10** will be such metabolite. Interestingly, P450 3A4 seems to have a stereoselective preference for the β-face of the steroidal scaffold in agreement with the observations of Guengerich *et al.*[93] Not only all mono-, but also the newly identified di-hydroxylations of **1** occurred on the β-face.

Conclusion

Human liver enzyme P450 3A4 apparently diversifies the steroidal scaffold of **1** in a late-stage fashion to a larger extent than previously thought.[32] Not only four mono-hydroxylated derivatives at positions 1β, 2β, 6β and 15β are formed,[13] but also several di-hydroxylated and perhaps even at least one tri-hydroxylated metabolite. In this work so far the positions 16β and 12β could be clearly identified as accessible sites for a second hydroxylation by P450 3A4. However, the data presented suggest the presence of a vast number of additional poly-hydroxylated steroids opening up the opportunity for many interesting future discoveries with the help of an improved HPLC separation method combined with highly advanced analytical instrumentation used by Guengerich *et al.*[32]

This study displays how enzymatic metabolite production can balance the industrial production requirements of time, quantity and profile authenticity.[63] The constraints of efficiency, stability and scalability of recombinant human P450s often reported in literature[14,66] could be successfully bypassed using *P. pastoris*-based whole-cell biocatalysts at efficient expression levels. Such robust tool enabled the synthesis of new human metabolites at a preparative scale for the first time. The yeast's protein production features allow for easy transferability of the results to further scale-up strategies and potential industrial application[80] because the optimal conditions (pH, oxygen content, temperature, nutrient supply) for biomass growth, P450 enzyme expression and substrate conversion can differ dramatically among individual hosts and chemical reactions.[4,63] Hence, easy adaption to a bioreactor is just as important as strategies for optimisation strategies.[66] Moreover, the application of surprisingly simple standard chemical procedures for reaction work-up, product purification and analytical identification should make the implementation of this approach worthwhile for chemists and industry alike.

Experimental Section

All solvents and chemicals were purchased from Sigma-Aldrich/Merck (Steinheim/Darmstadt, Germany), VWR International (Fontenay-sous-Bois, France), Carl Roth GmbH (Karlsruhe, Germany) or Fisher Scientific (Loughborough, UK) in best available purity and were used as received without further purification. HPLC tubes were bought from Macherey-Nagel (Düren, Germany) and the corresponding caps and inserts from Bruckner Analysentechnik (Linz, Austria). In experiments (A) and (B) an Agilent Technologies 1100 Series HPLC was used, for experiments (C) and (D) an Agilent Technologies 1200 Series HPLC system coupled with a G1956B mass selective detector (MSD) and an Agilent Technologies 1100 Series HPLC system (D) were employed, respectively. The bioreactor Biostat C_{plus} from Sartorius BBI Systems was used for experiment (D). The cells of *P. pastoris* with expressed P450 3A4 were obtained from Bisy GmbH (Hofstaetten, Austria). They had been cultivated, then stored as frozen pellets at −80 °C. OD measurements were executed with an Eppendorf BioPhotometer *plus*. NMR spectra were recorded with a Varian/Agilent Inova 500 MHz NMR spectrometer equipped with an indirect detection probe 5 mm.

(A) Reaction Tube Biotransformation: HPLC Profile Analysis (Figure 1)

Test tubes with screw caps (20×150 mm) were used. A cell concentration OD_{600} of 200 was generated by resuspending cells in 100 mM phosphate buffer (pH 7.4). The biotransformation was started by adding 25 µL of 100 mM testosterone in DMSO to 975 µL of the cell solution and the reaction mixture was incubated at 28 °C and 225 rpm. The biotransformation was stopped after 22 hours by adding 1 mL of a 1:1 mixture (v/v) of acetonitrile/methanol. The resulting mixture was vortexed, centrifuged at top speed and the supernatant taken for HPLC analysis. Compounds were separated *via* a reverse-phase column Zorbax SB-C18 (21.2 mm i.d. ×25 cm) at a flow rate of 4 mL/min. Water containing 0.1% acetic acid (A) and acetonitrile (B) were used for elution at 25 °C in the following ratios: 0 min: A/B 75/25; 50 min: A/B 0/100; 52 min: A/B 75/25; 60 min: A/B 75/25.

(B) 2.5 L Shake Flask Biotransformations: Kinetic Study (Figures 2 and 3)

Cells were resuspended in 30 mL of phosphate buffer until an OD_{600} of 200 was obtained and the broth was filled into a sterile 2.5 L shake flask, 0.5, 2.5 or 4.5 mM of 100 mM testosterone in DMSO or 2.5 mM of 100 mM androstenedione in DMSO was added. For the negative control, wild-type cells of P. pastoris were handled as the other samples with a 2.5 mM testosterone end concentration. The flasks were shaken at 130 rpm for 24 hours. Samples (1 mL) were taken after 4, 8, 20 and 24 hours, and treated as well as analysed as described above.

(C) 96-Well Plate Biotransformations: Change in Metabolism (Figure 4)

Cells were resuspended in 40 mL of 100 mM phosphate buffer (pH 7.4) until an OD_{600} of 200 was obtained and the broth was filled into a sterile 250 mL shake flask. Then 1030 µL of 20% glucose, 340 µL of 60% glycerol were added to obtain a final concentration of 0.5%. Control cells were left untreated. The cells were shaken for 3 hours at 140 rpm before they were used for biotransformation. The cell broth was added into a 96-deep-well-plate (390 µL each) and the reaction was started with the addition of 10 µL of 100 mM testosterone in DMSO. Methanol was added into the respective wells to obtain a final methanol concentration of 0.5, 1 or 3%. For each variation of the cell conditions, 14 repeats were tested. The plates were incubated at 28 °C at a speed of 320 rpm in a tilted orientation on the shaker to ensure maximal oxygen availability. The addition of 1 mL of a 1:1 mixture (v/v) of acetonitrile/methanol stopped the reaction. The plate was then centrifuged at 16,100 g for 10 min

and the supernatant was transferred into 96-well GreinerV plates for HPLC analysis. Separation was carried out *via* a Kinetex C18 (100 Å; 50×4.6 mm; 2.6 µm) reverse-phase column at a flow rate of 1 mL/min. A positive electrospray ionisation mode was selected for the mass spectrometer. Water containing 0.1% acetic acid (A) and acetonitrile (B) were used for elution at 25 °C in the following ratios: 0 min: A/B 80/20; 1 min: A/B 80/20; 3 min: A/B 0/100; 5 min: A/B 0/100; 5.01 min: A/B 80/20; 6 min: A/B 80/20.

(D) Preparative-Scale Biotransformation in a Bioreactor (Figures 5, 6, 7 and 8)

The obtained cells (ca. 200 g wet corresponding to 68 g dry cell weight) were resuspended in 100 mM phosphate buffer (pH 7.4) and filled up to 1.3 L to obtain an OD_{600} of 200. The cell broth was filled into the previously sterilised bioreactor, stirred at 400 rpm and kept at pH 7.4 with 1 M solutions of potassium hydroxide and phosphorous acid. The biotransformation was started with the addition of 13.3 mL of methanol and 3330 µL of a 1 M solution of testosterone (959 mg) in DMSO. Samples were taken regularly during the course of the reaction and simultaneously analysed using HPLC for end point determination. The biotransformation was stopped after 8 hours by centrifugation of the collected reaction broth and washing the cells twice with phosphate buffer. After the final centrifugation the cell pellet was suspended again in 1.3 L of phosphate buffer, filled into the same bioreactor and the second cycle of biotransformation was carried out analogously to the first one. Samples were taken with increasing time intervals and the biotransformation was stopped after 105 hours as before. Both aqueous reaction broths were worked up individually by liquid-liquid extraction washing the aqueous phase several times with ethyl acetate (3×150 mL). The resulting organic layer was dried over $MgSO_4$, concentrated by rotary evaporation and loaded onto the column for chromatographic purification (50% EtOAc in hexane). 6β-hydroxytestosterone (108 mg, 11.3% yield, 0.16% productivity[67] [g/g] using dry cell weight for the catalyst) was isolated as a white crystalline solid, and 6β-hydroxyandrostenedione (87 mg, 9.1%, 0.13%) as an off-white solid. Mixtures of other mono- or dihydroxylated metabolites were also collected with masses up to 10 mg. These mixtures were further purified with the help of an Agilent Technologies 1100 Series HPLC system adapted for manual preparative collection. Separation was carried out *via* a reverse-phase Purospher Star RP-18e (5.0 µm; 250 × 4 mm) column at 35 °C and a flow rate of 1 mL/min, and water containing 0.1% acetic acid (A) and acetonitrile (B) were used as the eluents in a steadily increasing gradient. Then methanol (C) was mixed in to wash the column thoroughly. Mono-hydroxylated metabolites were purified using the following method with the ratios: 0 min: A/B 80/20; 31 min: A/B 75/25; 31.01 min: B/C: 60/40; 34.00 min: B/C 60/40; 34.01 min: A/B 80/20; 36 min: A/B 80/20. Di-hydroxylated metabolites were purified using the method with the ratios: 0 min: A/B 85/15; 33.50 min: A/B 80/20; 33.51 min: B/C: 60/40; 36.00 min: B/C 60/40; 36.01 min: A/B 85/15; 38 min: A/B 85/15. The aqueous HPLC solvents were removed under a stream of nitrogen. The compounds 1β- (**5**) and 15β-hydroxytestosterone (**6**), 6-dehydro-15β-hydroxytestosterone (**7**) and, 6β,16β-dihydroxytestosterone (**8**), 6β,17β-dihydroxy-4-androstene-3,16-dione (**9**) and 6β,12β-dihydroxyandrostenedione (**10**) could be identified. Compounds **5**, **6**, **7** and **8** were obtained as white/off-white solids, the appearance of **9** and **10** was hardly definable because of too little quantities. For the same reason other isolated compounds, which were also present as mixtures, could not be elucidated.

6β-Hydroxytestosterone (**2**, $C_{19}H_{28}O_3$, white crystalline solid, 108 mg, 11%): ^{1}H NMR (300 MHz, $CDCl_3$): δ = 5.80 (1H, s, 4-H), 4.34 (1H, m, 6α-H), 3.65 (1H, dd, J = 10.3, 8.1 Hz, 17α-H), 2.50 (1H, ddd, J = 14.9, 4.5, 2.0 Hz, 2β-H), 2.40 (1H, ddd, J = 15.6, 4.3, 2.2, 2α-H), 2.02 (4H, m, 16α-H, 1α-H, 7β-H, 8-H), 1.88 (1H, ddd, J = 12.2, 4.1, 3.0 Hz, 12β-H), 1.70 (1H, dd, J = 14.2, 4.2 Hz, 1β-H), 1.61 (1H, m, 15α-H), 1.57 (1H, m, 11α-H), 1.49 (1H, m, 11β-H), 1.45 (1H, m, 16β-H), 1.40 (1H, m, 15β-H), 1.38 (3H, s, 19-CH_3), 1.21 (1H, m, 7α-H), 1.09 (1H, dd, J = 12.8, 4.3 Hz, 12α-H), 0.98 (1H, m, 14-H), 0.90 (1H, m, 9-H), 0.81 (3H, s, 18-CH_3). ^{13}C NMR (75 MHz, CDCl3): δ = 200.5 (C-3), 168.5 (C-5), 126.5 (C-4), 81.8 (C-17), 73.1 (C-6), 53.9 (C-9), 50.6 (C-14), 43.1 (C-13), 41.1 (C-10), 38.2 (C-7), 37.3 (C-1), 36.6 (C-12), 34.4 (C-2), 30.6 (C-16), 29.9 (C-8), 23.4 (C-15), 20.7 (C-11), 19.7 (C-19), 11.2 (C-18).

6β-Hydroxyandrostenedione (**4**, $C_{19}H_{26}O_3$, off-white solid, 87 mg, 9%): ^{1}H NMR (300 MHz, $CDCl_3$): δ = 5.77 (1H, s, 4-H), 4.35 (1H, s, 6α-H), 2.49–2.36 (3H, m, 2α-H, 2β-H, 16β-H), 2.16–1.96 (5H, m, 1β-H, 7β-H, 8-H, 15α-H, 16α-H), 1.84 (1H, ddd, J = 12.4, 3.7, 2.7 Hz, 12β-H), 1.71–1.59 (3H, m, 1α-H, 11α-H, 15β-H), 1.51 (2H, ddd, J = 14.04, 13.3, 3.5 Hz, 11β-H), 1.36 (3H, s, 19-CH_3), 1.29–1.19 (3H, m, 7α-H, 12α-H, 14-H), 1.01–0.95 (1H, m, 9-H), 0.90 (3H, s, 18-CH_3). ^{13}C NMR (75 MHz, CDCl3): δ = 220.1 (C-17), 200.5 (C-3), 168.3 (C-5), 126.4 (C-4), 72.6 (C-6), 53.7 (C-9), 50.9 (C-14), 47.7 (C-13), 38.1 (C-10), 37.3 (C-7), 37.1 (C-1), 35.8 (C-12), 34.2 (C-2), 31.3 (C-16), 29.5 (C-8), 21.8 (C-15), 20.3 (C-11), 19.6 (C-19), 13.8 (C-18)

1β-Hydroxytestosterone (**5**, $C_{19}H_{28}O_3$, white crystalline solid, 1 mg, 0.1%): ^{1}H NMR (500 MHz, $CDCl_3$): δ = 5.79 (1H, s, 4-H), 4.04 (1H, dd, J = 7.6, 7.0 Hz, 1α-H), 3.67–3.62 (1H, m, 17-H), 2.54 (2H, d, J = 7.8 Hz, 2α-, 2β-H), 2.49 (1H, dddd, J = 14.8, 13.8, 5.3, 1.3 Hz, 6β-H), 2.33 (1H, dddd, 14.2, 4.4, 2.6, 0.4 Hz, 6α-H), 2.11–2.03 (1H, m, 11α-H), 2.02–1.97 (1H, m, 16α-H), 1.91–1.85 (2H, m, 7β-, 12β-H), 1.69–1.57 (3H, m, 8-, 11β-, 15α-H), 1.49–1.41 (2H, m, 16β-H, 1β-OH), 1.33–1.29 (1H, m, 15β-H), 1.25 (3H, s, 19-H), 1.16–1.08 (2H, m, 9-, 12α-H), 1.06–0.94 (2H, m, 7α-, 14-H), 0.80 (3H, s, 18-H).

In the COSY spectrum the carbinol proton (δ 4.04 ppm) of interest was found to couple with protons in the region of 2.54 ppm corresponding to those of positions 2 or 6, and with a proton of the doublet at 1.46 ppm, which should correspond to the newly introduced hydroxyl group. No coupling to 8-H at δ 1.69 ppm was observed as previously described by Guengerich *et al.*[80,81] Additionally, the HSQC spectrum revealed the carbinol proton (δ 4.02 ppm) to be attached to the carbon at 74.0 (C-1) ppm. With the carbon shifts in hand, the HMBC spectrum confirmed the hydroxylation at C-1 due to the coupling of the 18-Hs to C-10, −9, −5 and the carbinol carbon −1. The NOESY spectrum indicated interactions between the carbinol proton and protons at 2.53 (2α- and 2β-H), 1.69 ppm (11β-H), 1.47 (1β-OH) and 1.11 (9-H). The correlation with

11β-H and the lack of it with the H-19 protons proved the hydroxylation having occurred at 1β.

15β-Hydroxytestosterone (**6**, $C_{19}H_{28}O_3$, white solid, 1 mg, 0.1%): ^{1}H NMR (500 MHz, $CDCl_3$): δ = 5.75 (1H, s, 4-H), 4.24–4.20 (1H, m, 15α-H), 3.59 (1H, dd, J = 14.0, 8.7 Hz, 17α-H), 2.66–2.60 (1H, m, 16α-H), 2.47 (1H, ddd, J = 15.6, 15.3, 5.0 Hz, 6β-H), 2.43 (1H, dd, J = 14.1, 5.0 Hz, 2β-H), 2.37–2.28 (2H, m, 2α-, 6α-H), 2.13–2.08 (1H, m, 7β-H), 2.07–2.03 (1H, m, 1β-H), 2.00 (1H, ddd, J = 11.4, 10.8, 2.95, 8-H), 1.87–1.83 (1H, m, 12β-H), 1.72 (1H, ddd, J = 14.2, 14.1, 4.3 Hz, 1α-H), 1.63–1.57 (2H, m, 11α-, 16β-H), 1.47 (1H, ddd, J = 13.2, 13.1, 3.9 Hz, 11β-H), 1.35 (1H, d, 15β-OH), 1.24 (3H, s, 19-H), 1.16–1.04 (2H, m, 7α-, 12α-H), 1.07 (3H, s, 18-H), 1.00 (1H, ddd, J = 12.3, 11.3, 4.0, Hz, 9-H), 0.85 (1H, dd, J = 11.3, 5.6 Hz, 14-H). ^{13}C NMR (75 MHz, CDCl3): δ = 199.8 (C-3), 171.3 (C-5), 124.0 (C-4), 81.2 (C-17), 69.2 (C-15), 55.3 (C-14), 54.4 (C-9), 42.4 (C-13), 38.9 (C-10), 38.0 (C-12), 35.9 (C-1), 34.0 (C-2), 32.8 (C-6), 31.6 (C-8), 31.2 (C-7), 20.7 (C-11), 17.5 (C-19), 13.9 (C-18).

6-Dehydro-15β-hydroxytestosterone (**7**, $C_{19}H_{26}O_3$, white solid, 3 mg, 0.3%): ^{1}H NMR (500 MHz, $CDCl_3$): δ = 6.30 (1H, d, J = 9.86 Hz, 7-H), 6.16 (1H, dd, J = 9.86, 2.72 Hz, 6-H), 5.69 (1H, s, 3-H), 4.41–4.37 (1H, m, 15α-H), 3.65–3.60 (1H, m, 17-H), 2.70–2.66 (1H, m, 16α-H), 2.56 (1H, dd, J = 14.23, 5.41 Hz, 2β-H), 2.51 (1H, dd, J = 5.34, 1.53 Hz, 2α-H), 1.17 (3H, s, 19-C), 1.12 (3H, s, 18-H). HRMS (TOF-EI+) m/z: calcd. for $C_{19}H_{28}O_4$ 302.1882, found 302.1864.

This compound was isolated as the minor component in a mixture with 15β-hydroxytestosterone as reflected by HPLC, NMR and HRMS analysis. The peaks at 6.30 and 6.16 ppm implied the presence of another alkene group and the roof effect observed between two shifts indicates a strong second-order coupling effect. This was supported by their strong correlation in the NOESY spectrum. In the HMBC spectrum the 18-Hs at 1.13 ppm coupled with carbons at 80.9 (C-17), 52.8 (C-14), 43.8 (C-13) and 37.7 (C-12) ppm, and the 19-Hs at 1.19 ppm with carbons at 163.4 (C-5), 51.1 (C-9), 36.8 (C-10) and 32.6 (C-1) ppm ruling out the known α,β-unsaturated compound 1-dehydrotestosterone. The interaction of the proton at 6.16 ppm with the H-4 (5.69 ppm) in the NOESY spectrum therefore revealed the alkene to be between positions 6 and 7. Here, a correlation between the other alkene proton (6.30 ppm) and the carbinol proton (4.39 ppm) also strongly pointed towards the hydroxylation to have occurred at position 15, on the β-face of the steroid due to the lack of a coupling to 18-H. Indeed, the carbinol proton (4.40 ppm) was attached to a carbon with a shift of 69.0 ppm in the HSQC spectrum, comparing well with the shifts of position 15 of 15β-hydroxytestosterone. Additionally, the carbinol proton (4.40 ppm) coupled to a proton at 2.69 ppm in the COSY spectrum, which in turn was found to correlate with 17-H (3.62 ppm), fitting well to 15α-H and 16α-H, respectively.

6β,16β-Dihydroxytestosterone (**8**, $C_{19}H_{28}O_4$, off-white solid, 1 mg, 0.1%): ^{1}H NMR (500 MHz, $CDCl_3$): δ = 5.82 (1H, s, 4-H), 4.36 (1H, br, 6α-H), 4.22–4.17 (1H, m, 16α-H), 3.40 (1H, dd, J = 8.86, 7.98 Hz, 17-H), 1.40 (3H, s, 19-H), 0.94 (1H, ddd, J = 11.8, 11.2, 3.9 Hz, 9-H), 0.90 (3H, s, 18-H), 0.83 (1H, ddd, J = 13.2, 10.7, 7.1, 14-H). HRMS (TOF-EI+) m/z: calcd. for $C_{19}H_{28}O_4$ 320.1988, found 320.1975.

The first carbinol proton at 4.36 ppm was attached to a carbon at 73.0 ppm as determined by HSQC. Therefore it did not only have the same proton and carbon shifts as the 6α-H of **2**, but was also found to couple with protons of peaks at 2.04 (7β-H) and 1.23 (7α-H) ppm in the COSY spectrum. A slight coupling to a proton at 1.58 ppm was also visible in the COSY spectrum, which is likely the 6β-OH as it showed no other coupling and appeared as a broad singlet in the proton spectrum. In addition, the first carbinol proton (4.36 ppm) showed a clear correlation to 4-H in the HMBC and NOESY spectrum. The latter spectrum also revealed hydroxylation to have occurred at the β-face of testosterone by the lack of any correlation with the protons at position 19. The second carbinol proton at 4.19 ppm was attached to a carbon at 69.9 ppm as determined by HSQC. A strong correlation with 17-H in the COSY spectrum clearly indicated the other hydroxylation to have occurred at C-16. The presence of the same interaction in the NOESY spectrum in combination with the lack of a correlation with the C-18 methyl group suggested the hydroxyl group being in the equatorial position.

6β,17β-Dihydroxy-4-androstene-3,16-dione (**9**, $C_{19}H_{26}O_4$, < 1 mg, < 0.1%): 5.85 (1H, s, 4-H), 4.40 (1H, br, 6α-H), 3.78 (1H, br, 17α-H), 2.62 (1H, d, J = 3.22 Hz, 17β-OH), 2.58–2.51 (1H, m, 2β-H), 2.45–2.36 (2H, m, 2α-, 15β-H), 1.62 (1H, br, 6β-OH), 1.42 (3H, s, 19-H), 1.15–1.10 (1H, m, 9-H), 0.81 (3H, s, 18-H)

The interaction between the first carbinol proton at 4.39 ppm and H-4 (5.96 ppm) in the NOESY spectrum pointed towards the hydroxylation to have occurred at position 6. In the HSQC spectrum the carbinol proton is attached to a carbon with a shift of 72.3 ppm fitting the usual 6α-proton shifts. It was also found to couple with protons at 1.98 (7α-H) and 1.36 (7β-H) ppm as well as to one proton at 1.62 ppm likely to be the 6β-OH in the COSY spectrum. The latter coupling is visible with the same shift and peak shape as in the proton spectra of 6β,16β-dihydroxytestosterone and 6β,12β-dihydroxyandrostenedione. In the HMBC spectrum a proton at 1.95 ppm was found to interact with a carbon at 215.0 ppm indicating the presence of a second ketone like in derivatives of androstenedione. However, the 18-Hs showed coupling to C-17 at 85.5 ppm as well as to other carbons in a range from 35 to 45 ppm. Consequently, the ketone had to be at a different position than 17. The 19-Hs coupled to C-5 at 158.7 ppm and to other carbons in a range from 30 to 53 ppm. The shifts of the A-ring in general were the same as for 6β-hydroxytestosterone. The peak shape of 9-H is quite distinct and could be identified easily in the proton spectrum. The proton interacted with carbons below 60 ppm. Therefore only positions 15 and 16 qualified having the ketone functional group attached. In the COSY 17α-H correlated with a proton at 2.58 ppm, however, quite likely this is 17β-OH as it appears as a high doublet signal in the ^{1}H spectrum integrating to only 0.6 protons. In contrast to the first carbinol proton H-6α of this compound or 17α-H of any other testosterone derivative determined here, no evidence for any other interaction of 17α-H was noticeable in the COSY spectrum. The same was observed in the NOESY spectrum, where 17α-H only coupled with two protons at 2.09 (12α-H) and 1.54 (14-H). The lack of coupling to neighbouring protons at position 16 strongly pointed towards their absence. In addition, C-17 (85.5 ppm) must have experienced a deshielding effect compared to its usual shift of about

81 ppm supporting the presence of a vicinal ketone functional group at position 16.

6β,12β-Dihydroxyandrostenedione (**10**, $C_{19}H_{26}O_4$, <1 mg, $<0.1\%$): ^{1}H NMR (500 MHz, $CDCl_3$): $\delta = 5.85$ (1H, s, 4-H), 4.42–4.40 (1H, m, 6α-H), 3.80 (1H, dd, J = 11.5, 4.6 Hz, 12α-H), 3.50–3.48 (1H, m, 17-H), 1.63 (1H, br, 6β-OH), 1.42 (3H, s, 19-H), 1.08 (1H, ddd, J = 12.5, 11.5, 3.9 Hz, 9-H), 1.03 (3H, s, 18-H). HRMS (TOF-EI+) m/z: calcd. for $C_{19}H_{26}O_4$ 318.1831, found 318.1828.

In the proton spectrum two carbinol protons were found at 4.41 and 3.80 ppm, which are attached to carbons at 72.7 and 72.4 ppm, respectively. For this compound the HMBC spectrum was very informative. The coupling of the 18-Hs to a carbon at 222 ppm indicated that this compound had to be an androstenedione derivative with a ketone functional group at C-17. In addition to this interaction, the 18-Hs (1.05 ppm) couple with three other carbons at 48.7, 51.5 and 72.3 ppm corresponding to C-13, −14, and −12, respectively. Therefore, one of the hydroxylations occurred at C-12. The NOESY spectrum revealed that this carbinol proton at C-12 should be in the axial position because a correlations to 9-H (1.08 ppm), 14-H (1.27 ppm) and 11α-H (1.81 ppm) was visible. The other hydroxylation pattern (4.41, 72.7 ppm) compared well with the shifts of 6β-hydroxyandrostenedione. In the NOESY spectrum a strong interaction to the 4-H proton (5.85 ppm) was the most convincing. Two interactions with other protons at 2.15 and 1.29 ppm (7α-H and 7β-H), as well as one to a proton at 1.63 ppm in both the NOESY and COSY spectra left no room for doubt. The latter shift was assigned to the 6β-OH as it is a broad singlet in the proton spectrum with no other interactions in the COSY, just as for 6β,16β-dihydroxytestosterone and 6β,17β-dihydroxy-4-androstene-3,16-dione.

Author contributions

N.D.F., M.S. and A.G. devised the study concept. N.D.F. conducted all experiments. M.S. and C.S. provided material. N.D.F. and M.S. developed methods. N.D.F. and H.W. performed data acquisition and analysis. C.S., D.S., U.S and A.G. jointly supervised. N.D.F. wrote the original manuscript. N.D.F. and A.G. reviewed and edited the manuscript. A.G. administrated the project. D.S., U.S. and A.G. acquired the funding. All authors critically reviewed and approved the manuscript.

Acknowledgements

This project has received funding from the European Union's Horizon 2020 research and innovation programme, OXYtrain MSCA-ITN, under grant agreement No 722390. The authors would like to thank Prof. Breinbauer for access to his chemistry facilities and material. The authors are also grateful to Dr. G. Strohmeier and Prof. M. Winkler for their support with the HPLC instruments.

References

[1] H. van de Waterbeemd, E. Gifford, *Nat. Rev. Drug Discovery* **2003**, *2*, 192–204.
[2] S. Piantadosi, *Clinical Trials: A Methodologic Perspective*, Wiley & Sons Inc., Hoboken, **2017**.
[3] FDA, *Guidance for Industry: Safety Testing of Drug Metabolites*, U. S. Department Of Health and Human Services, Food and Drug Administration, Center For Drug Evaluation and Research (CDER), **2016**.
[4] C. Martinez, S. Rupashinghe, *Curr. Top. Med. Chem.* **2013**, *13*, 1470–1490.
[5] D. S. Wishart, *Drugs R&D* **2008**, *9*, 307–322.
[6] L. F. Shyur, N. S. Yang, *Curr. Opin. Chem. Biol.* **2008**, *12*, 66–71.
[7] O. Fiehn, D. Robertson, J. Griffin, M. van der Werf, B. Nikolau, N. Morrison, L. W. Sumner, R. Goodacre, N. W. Hardy, C. Taylor, J. Fostel, B. Kristal, R. Kaddurah-Daouk, P. Mendes, B. van Ommen, J. C. Lindon, S. A. Sansone, *Metabolomics* **2007**, *3*, 175–178.
[8] L. Di, E. H. Kerns, *Curr. Opin. Chem. Biol.* **2003**, *7*, 402–408.
[9] S. Asha, M. Vidyavathi, *Appl. Biochem. Biotechnol.* **2010**, *160*, 1699–1722.
[10] S. R. Kazmi, R. Jun, M. S. Yu, C. Jung, D. Na, *Comput. Biol. Med.* **2019**, *106*, 54–64.
[11] J. Kirchmair, A. H. Göller, D. Lang, J. Kunze, B. Testa, I. D. Wilson, R. C. Glen, G. Schneider, *Nat. Rev. Drug Discovery* **2015**, *14*, 387–404.
[12] E. W. Esch, A. Bahinski, D. Huh, *Nat. Rev. Drug Discovery* **2015**, *14*, 248–260.
[13] N. D. Fessner, *ChemCatChem* **2019**, *11*, 2226–2242.
[14] M. Winkler, M. Geier, S. P. Hanlon, B. Nidetzky, A. Glieder, *Angew. Chem. Int. Ed.* **2018**, *57*, 13406–13423.
[15] K. Schroer, M. Kittelmann, S. Lütz, *Biotechnol. Bioeng.* **2010**, *106*, 699–706.
[16] R. B. Vail, M. J. Homann, I. Hanna, A. Zaks, *J. Ind. Microbiol. Biotechnol.* **2005**, *32*, 67–74.
[17] J. M. Caswell, M. O'Neill, S. J. C. Taylor, T. S. Moody, *Curr. Opin. Chem. Biol.* **2013**, *17*, 271–275.
[18] H. M. Girvan, A. W. Munro, *Curr. Opin. Chem. Biol.* **2016**, *31*, 136–145.
[19] A. Worsch, F. K. Eggimann, M. Girhard, C. J. von Bühler, F. Tieves, R. Czaja, A. Vogel, C. Grumaz, K. Sohn, S. Lütz, M. Kittelmann, V. B. Urlacher, *Biotechnol. Bioeng.* **2018**, *115*, 2156–2166.
[20] D. Schmitz, S. Janocha, F. M. Kiss, R. Bernhardt, *Biochim. Biophys. Acta Proteins Proteomics* **2018**, *1866*, 11–22.
[21] X. Ren, J. A. Yorke, E. Taylor, T. Zhang, W. Zhou, L. L. Wong, *Chem. Eur. J.* **2015**, *21*, 15039–15047.
[22] G. Di Nardo, G. Gilardi, *Int. J. Mol. Sci.* **2012**, *13*, 15901–15924.
[23] M. Poraj-Kobielska, M. Kinne, R. Ullrich, K. Scheibner, G. Kayser, K. E. Hammel, M. Hofrichter, *Biochem. Pharmacol.* **2011**, *82*, 789–796.
[24] C. D. Murphy, *Biotechnol. Lett.* **2015**, *37*, 19–28.

[25] R. Weis, M. Winkler, M. Schittmayer, S. Kambourakis, M. Vink, J. David Rozzell, A. Glieder, *Adv. Synth. Catal.* **2009**, *351*, 2140–2146.
[26] O. Ghisalba, M. Kittelmann, in: *Mod. Biooxidation Enzym. React. Appl.* (Eds.: R. D. Schmid, V. Urlacher), Wiley-VCH, Weinheim, **2007**, pp. 211–232.
[27] T. Testa, in: *Pract. Med. Chem.* (Ed.: C. G. Wermuth), Elsevier Ltd, Amsterdam, **2008**, pp. 655–673.
[28] S. Rendic, F. P. Guengerich, *Chem. Res. Toxicol.* **2015**, *28*, 38–42.
[29] M. Miyazaki, K. Nakamura, Y. Fujita, F. P. Guengerich, R. Horiuchi, K. Yamamoto, *Drug Metab. Dispos.* **2008**, *36*, 2287–2291.
[30] P. Anzenbacher, E. Anzenbacherová, *Cell. Mol. Life Sci.* **2001**, *58*, 737–747.
[31] F. P. Guengerich, *Chem. Res. Toxicol.* **2017**, *30*, 2–12.
[32] J. A. Krauser, M. Voehler, L.-H. Tseng, A.-B. Schefer, M. Godejohann, F. P. Guengerich, *Eur. J. Biochem.* **2004**, *271*, 3962–3969.
[33] J. A. Krauser, F. P. Guengerich, *J. Biol. Chem.* **2005**, *280*, 19496–19506.
[34] H. C. Man, P. L. Skipper, J. S. Wishnok, S. R. Tannenbaum, *Drug Metab. Dispos.* **2005**, *33*, 714–718.
[35] E. Pfeiffer, M. Metzler, *Arch. Toxicol.* **2004**, *78*, 369–377.
[36] X. Cao, S. T. Gibbs, L. Fang, H. A. Miller, C. P. Landowski, H. C. Shin, H. Lennernas, Y. Zhong, G. L. Amidon, L. X. Yu, D. Sun, *Pharm. Res.* **2006**, *23*, 1675–1686.
[37] R. Zuber, E. Anzenbacherová, P. Anzenbacher, *J. Cell. Mol. Med.* **2002**, *6*, 189–198.
[38] M. Geier, A. Braun, P. Fladischer, P. Stepniak, F. Rudroff, C. Hametner, M. D. Mihovilovic, A. Glieder, *FEBS J.* **2013**, *280*, 3094–3108.
[39] M. Paloncýová, V. Navrátilová, K. Berka, A. Laio, M. Otyep, *J. Chem. Theory Comput.* **2016**, *12*, 2101–2109.
[40] M. Ekroos, T. Sjögren, *Proc. Natl. Acad. Sci. USA* **2006**, *103*, 13682–13687.
[41] J. C. Hackett, *J. Biol. Chem.* **2018**, *293*, 4037–4046.
[42] Y. Kapelyukh, M. J. I. Paine, J. D. Maréchal, M. J. Sutcliffe, C. R. Wolf, G. C. K. Roberts, *Drug Metab. Dispos.* **2008**, *36*, 2136–2144.
[43] I. G. Denisov, P. J. Mak, Y. V. Grinkova, D. Bastien, G. Bérubé, S. G. Sligar, J. R. Kincaid, *J. Inorg. Biochem.* **2016**, *158*, 77–85.
[44] L. C. Wienkers, T. G. Heath, *Nat. Rev. Drug Discovery* **2005**, *4*, 825–833.
[45] M. Geier, A. Braun, A. Emmerstorfer, H. Pichler, A. Glieder, *Biotechnol. J.* **2012**, *7*, 1346–1358.
[46] G. P. L. Cereghino, J. L. Cereghino, C. Ilgen, J. M. Cregg, *Curr. Opin. Biotechnol.* **2002**, *13*, 329–332.
[47] V. Puxbaum, D. Mattanovich, B. Gasser, *Appl. Microbiol. Biotechnol.* **2015**, *99*, 2925–2938.
[48] A. Emmerstorfer, T. Wriessnegger, M. Hirz, H. Pichler, *Appl. Microbiol. Biotechnol.* **2014**, *98*, 7671–7698.
[49] B. Byrne, *Curr. Opin. Struct. Biol.* **2015**, *32*, 9–17.
[50] V. Juturu, J. C. Wu, *ChemBioChem* **2018**, *19*, 7–21.
[51] M. Ahmad, M. Hirz, H. Pichler, H. Schwab, *Appl. Microbiol. Biotechnol.* **2014**, *98*, 5301–5317.
[52] M. Geier, C. Schmid, A. Glieder, *Chim. Oggi* **2013**, *31*, 24–27.
[53] H. L. J. Makin, J. W. Honour, C. H. L. Shackleton, W. J. Griffith, in: *Steroid Anal.* (Eds.: H. L. J. Makin, D. B. Gower), Springer Science & Business Media, Dordrecht, **2010**, pp. 163–784.
[54] T. Pajič, M. Vitas, D. Žigon, A. Pavko, S. L. Kelly, R. Komel, *Yeast* **1999**, *15*, 639–645.
[55] M. Shao, X. Zhang, Z. Rao, M. Xu, T. Yang, H. Li, Z. Xu, S. Yang, *Green Chem.* **2016**, *18*, 1774–1784.
[56] R. A. Canuto, *Dehydrogenases*, InTech, London, **2012**.
[57] H. Zhang, Q. Li, L. Wang, Y. Chen, *Biochim. Biophys. Acta Gen. Subj.* **2018**, *1862*, 1199–1208.
[58] F. W. Krainer, C. Dietzsch, T. Hajek, C. Herwig, O. Spadiut, A. Glieder, *Microb. Cell Fact.* **2012**, *22*, 1–14.
[59] T. Vogl, L. Sturmberger, T. Kickenweiz, R. Wasmayer, C. Schmid, A. M. Hatzl, M. A. Gerstmann, J. Pitzer, M. Wagner, G. G. Thallinger, et al., *ACS Synth. Biol.* **2016**, *5*, 172–186.
[60] E. O'Reilly, V. Köhler, S. L. Flitsch, N. J. Turner, *Chem. Commun.* **2011**, *47*, 2490–2501.
[61] W. Zhang, M. A. Bevins, B. A. Plantz, L. A. Smith, M. M. Meagher, *Biotechnol. Bioeng.* **2000**, *70*, 1–8.
[62] A. Weninger, A. M. Hatzl, C. Schmid, T. Vogl, A. Glieder, *J. Biotechnol.* **2016**, *235*, 139–149.
[63] M. T. Lundemo, J. M. Woodley, *Appl. Microbiol. Biotechnol.* **2015**, *99*, 2465–2483.
[64] W. A. Duetz, J. B. Van Beilen, B. Witholt, *Curr. Opin. Biotechnol.* **2001**, *12*, 419–425.
[65] R. A. Sheldon, D. Brady, *Chem. Commun.* **2018**, *54*, 6088–6104.
[66] V. B. Urlacher, M. Girhard, *Trends Biotechnol.* **2019**, *37*, 882–897.
[67] R. Kratzer, J. M. Woodley, B. Nidetzky, *Biotechnol. Adv.* **2015**, *33*, 1641–1652.
[68] C. A. Dra˘gan, F. T. Peters, P. Bour, A. E. Schwaninger, S. M. Schaan, I. Neunzig, M. Widjaja, J. Zapp, T. Kraemer, H. H. Maurer, M. Bureik, *Appl. Biochem. Biotechnol.* **2011**, *163*, 965–980.
[69] Y. Kanamori, K. Fujita, K. Nakayama, T. Kamataki, H. Kawai, *Drug Metab. Pharmacokinet.* **2003**, *18*, 42–47.
[70] M. Subramanian, S. Das, E. Martinez, D. Callewaert, in *Rapid Identif. Prod. Metab. Using CypExpressTM 2D6, 3A4, 2C9*, 19th Annual Meeting Of The International Society For The Study Of Xenobiotics, San Francisco, **2014**.
[71] D. N. Kirk, H. C. Toms, C. Douglas, K. A. White, K. E. Smith, S. Latif, R. W. P. Hubbard, *J. Chem. Soc. Perkin Trans. 2* **1990**, *2*, 1567–1594.
[72] I. Černý, J. Fajkoš, V. Pouzar, *Steroids* **1996**, *61*, 58–64.
[73] J. J. Sheets, R. W. Estabrook, *Biochemistry* **1985**, *24*, 6591–6597.
[74] B. P. Lisboa, J.-A. Gustafsson, J. Sjövall, *Eur. J. Biochem.* **1968**, *4*, 496–505.
[75] Y. Gumulya, J.-M. Baek, S.-J. Wun, R. E. S. Thomson, K. L. Harris, D. J. B. Hunter, J. B. Y. H. Behrendorff, J.

Kulig, S. Zheng, X. Wu, J. E. Stok, J. J. De Voss, G. Schenk, U. Jurva, S. Andersson, E. M. Isin, M. Bodén, L. Guddat, E. M. J. Gillam, *Nat. Can.* **2018**, *1*, 878–888.
[76] O. J. Pozo, J. Marcos, R. Ventura, A. Fabregat, J. Segura, *Anal. Bioanal. Chem.* **2010**, *398*, 1759–1770.
[77] C. Jo Corbin, S. M. Mapes, J. Marcos, C. H. Shackleton, D. Morrow, S. Safe, T. Wise, J. Joe Ford, A. J. Conley, *Endocrinology* **2004**, *145*, 2157–2164.
[78] D. J. B. Hunter, J. B. Y. H. Behrendorff, W. A. Johnston, P. Y. Hayes, W. Huang, B. Bonn, M. A. Hayes, J. J. De Voss, E. M. J. Gillam, *Metab. Eng.* **2011**, *13*, 682–693.
[79] S. Kille, F. E. Zilly, J. P. Acevedo, M. T. Reetz, *Nat. Chem.* **2011**, *3*, 738–743.
[80] V. Looser, B. Bruhlmann, F. Bumbak, C. Stenger, M. Costa, A. Camattari, D. Fotiadis, K. Kovar, *Biotechnol. Adv.* **2015**, *33*, 1177–1193.
[81] Z. Yang, Z. Zhang, *Biotechnol. Adv.* **2018**, *36*, 182–195.
[82] A. Schmideder, S. Hensler, M. Lang, A. Stratmann, U. Giesecke, D. Weuster-Botz, *Process Biochem.* **2016**, *51*, 177–184.
[83] C. W. Theron, J. Berrios, F. Delvigne, P. Fickers, *Appl. Microbiol. Biotechnol.* **2018**, *102*, 63–80.
[84] BioVision, "EZCyp," can be found under https://www.biovision.com/ezcyptm-active-human-cytochrome-p450-3a4.html, **2020**.
[85] S. Aldrich, "CYPExpress," can be found under https://www.sigmaaldrich.com/catalog/product/sigma/mtox-ce3a4?lang=de&region=AT, **2020**.
[86] Bisy, "Biocatalysts," can be found under https://www.bisy.at, **2020**.
[87] Y. Farooq, G. C. K. Roberts, *Biochem. J.* **2010**, *432*, 485–493.
[88] V. R. Dodhia, C. Sassone, A. Fantuzzi, G. Di Nardo, S. J. Sadeghi, G. Gilardi, *Electrochem. Commun.* **2008**, *10*, 1744–1747.
[89] A. Braun, M. Geier, B. Bühler, A. Schmid, S. Mauersberger, A. Glieder, *Microb. Cell Fact.* **2012**, *11*, 106.
[90] B. Palabiyik, S. Karaer, N. Arda, S. Erturk Toker, G. Temizkan, S. Kelly, A. Topal Sarikaya, *Biologia* **2008**, *63*, 450–454.
[91] H. Venkataraman, S. B. A. de Beer, L. A. H. van Bergen, N. van Essen, D. P. Geerke, N. P. E. Vermeulen, J. N. M. Commandeur, *ChemBioChem* **2012**, *13*, 520–523.
[92] D. Zehentgruber, F. Hannemann, S. Bleif, R. Bernhardt, S. Lütz, *ChemBioChem* **2010**, *11*, 713–721.
[93] Q. Cheng, C. D. Sohl, F. K. Yoshimoto, F. P. Guengerich, *J. Biol. Chem.* **2012**, *287*, 29554–29567.

Supporting Information

Preparative-Scale Production of Testosterone Metabolites by Recombinant Human Liver Cytochrome P450 Enzyme 3A4

Nico D. Fessner, Matic Srdič, Hansjörg Weber, Christian Schmid, David Schönauer, Ulrich Schwaneberg, and Anton Glieder*

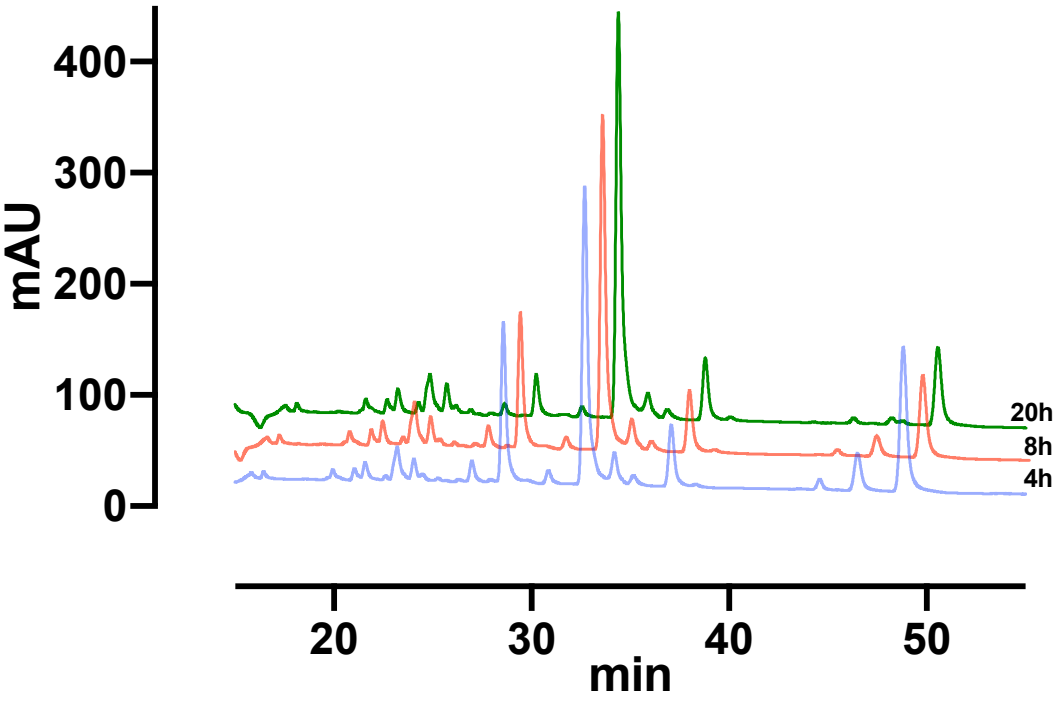

Figure S1: HPLC traces of the bioconversion of **3** as the substrate at three different time points (4, 8 and 20 hours) by P450 3A4 (30 mL, 130 rpm, 24h, 28 °C, 200 OD600).

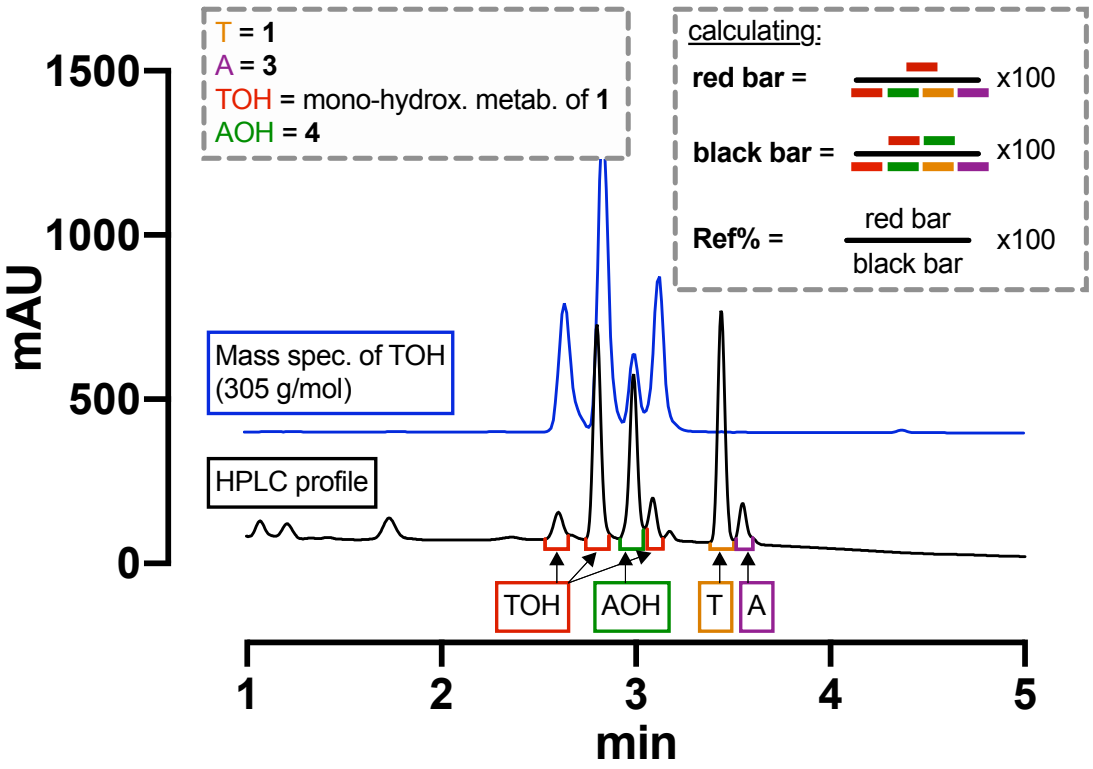

Figure S2: Shown are the HPLC traces of the elution profile as well as that given by the mass detector when tuned to mono-hydroxylation products of **1** (305 g/mol). Four of these compounds have

been detected, however, the peak of **4** covers the peak of the third one in the UV spectrum. The integration of the peaks and the calculations used to generate Figure 4 is shown in different colours.

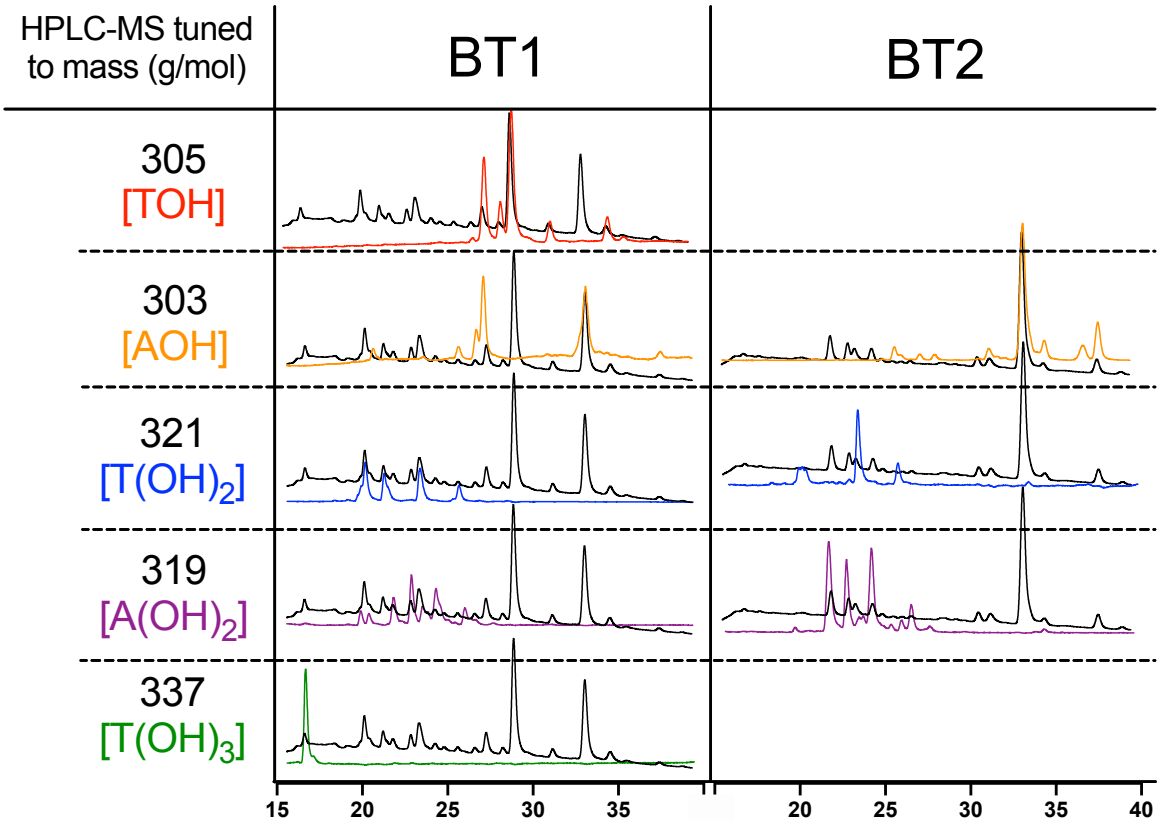

Figure S3: Display of the HPLC profiles of BT1 and BT2 compared to their profiles generated by the mass spectrometer tuned to the following masses: 305 g/mol = mono-hydroxylated derivatives of **1** (red), 303 g/mol = mono-hydroxylated derivatives of **3** (orange), 321 g/mol = di-hydroxylated derivatives of **1** (blue), 319 g/mol = mono-hydroxylated derivatives of **3** (violet), 337 g/mol = tri-hydroxylated derivatives of **1** (green).

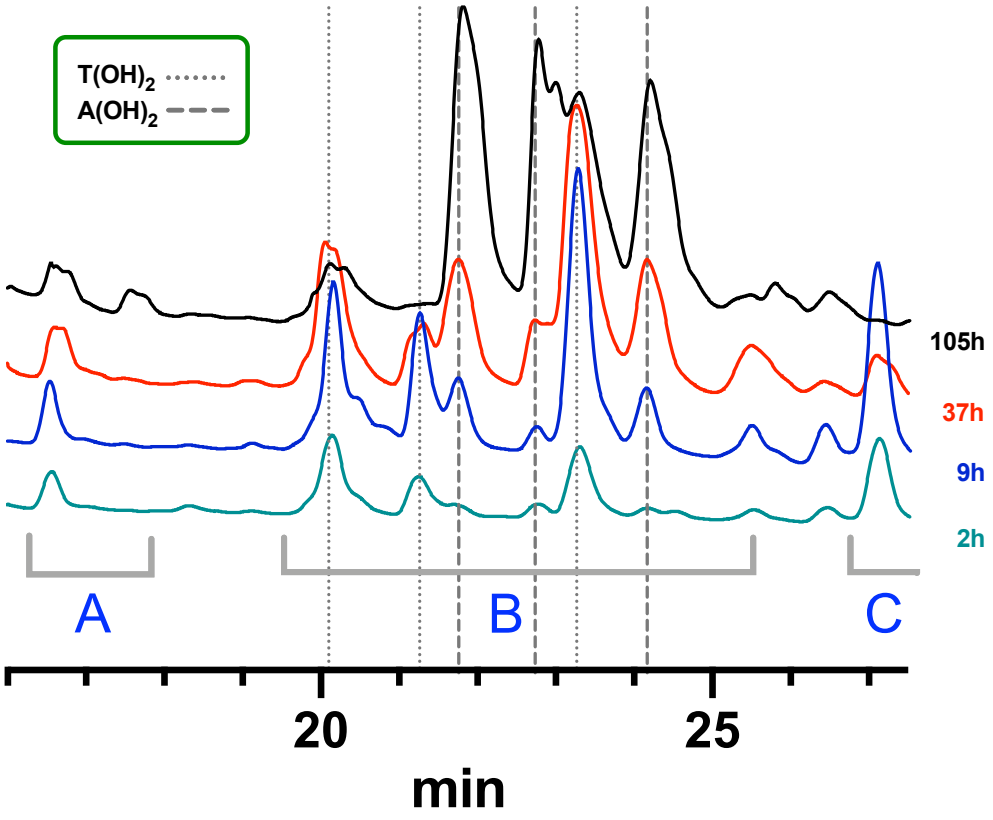

Figure S4: Zoomed-in perspective of zones A and B for selected HPLC traces from the profiles shown in **Figure 6**. Two sets of three peaks each are marked, namely those appearing early (2h, turquoise) and growing rapidly (9h, blue) with dotted lines, and those taking over in size later (37h, red) and not decaying until the end (105h, black) with dashed lines.

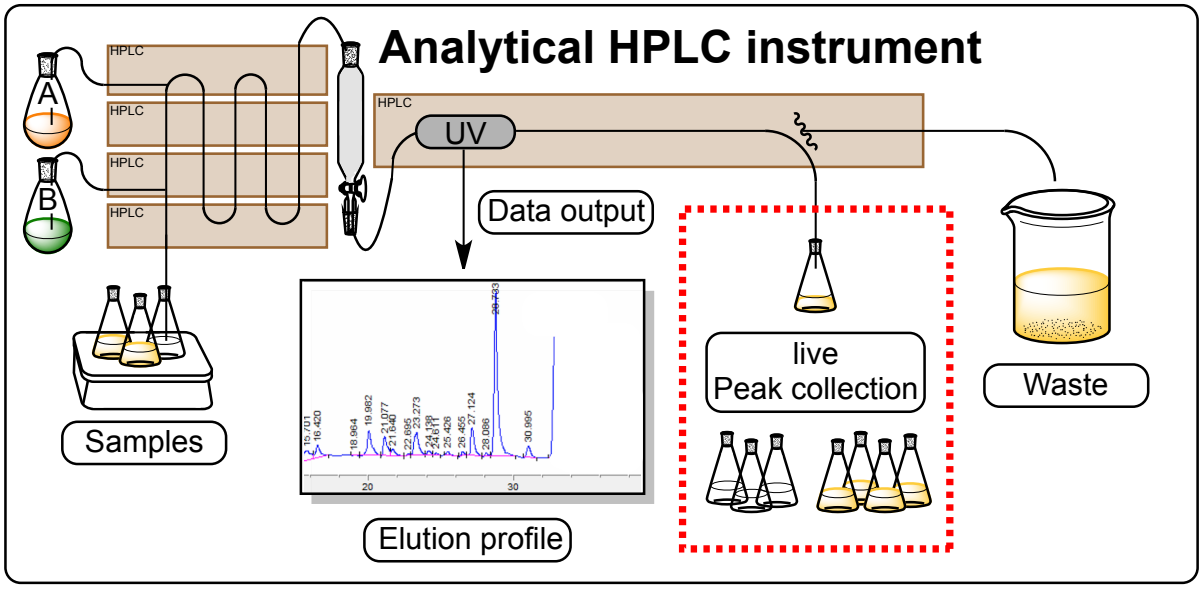

Figure S5: Display of the experimental set-up used to isolate those metabolites of BT1 and BT2 that were more polar than 6β-hydroxytestosterone and 6β-hydroxyandorstenedione, respectively. Two sets of two samples of each about 10 mg had been obtained by column chromatography separation, but showed up as a compound mixture by NMR and HPLC analysis. Their peaks were isolated by live collection of the HPLC flow-through simultaneously to the UV spectrum being drawn. These preparative profiles were measured at 270 nm because metabolites were found to have an

absorbance of only about 10% at this wavelength avoiding a saturation of the UV signal received. This way a more precise isolation of specific peaks was possible. Analytical profiles were measured using a wavelength of 240 nm.

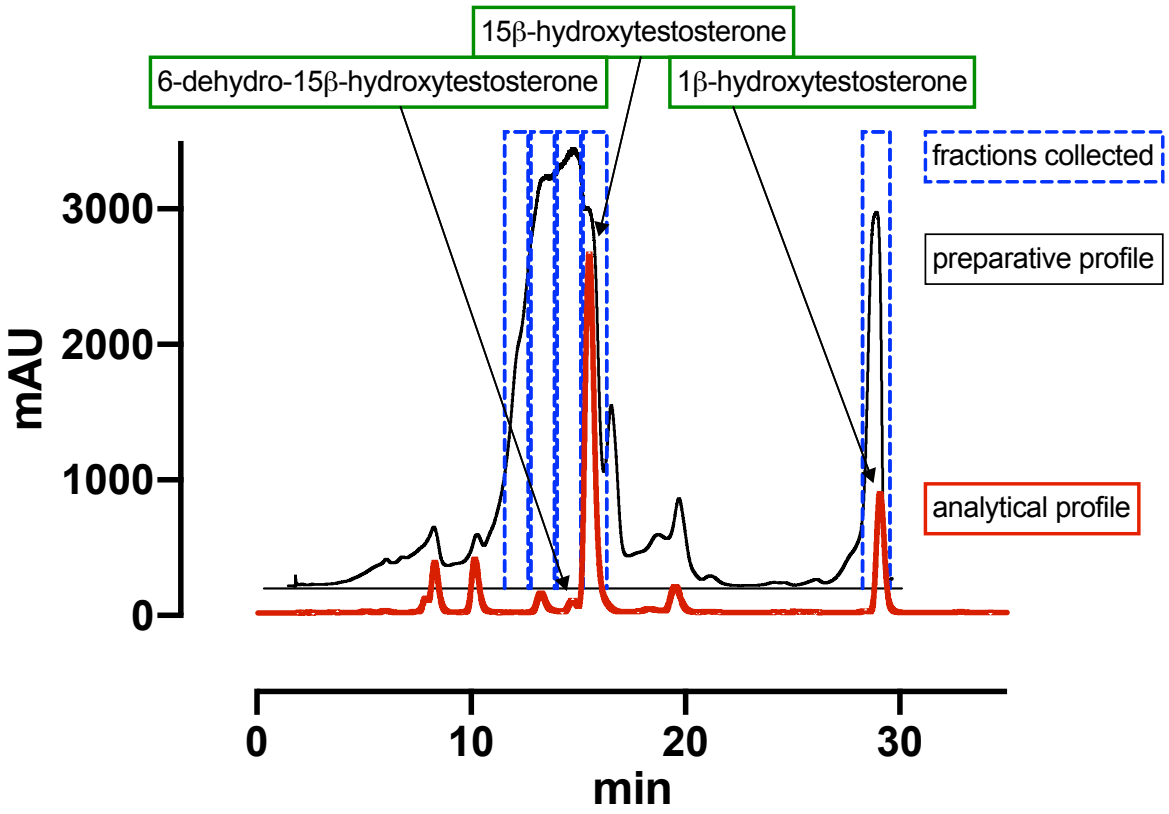

Figure S6: Display of the analytical (240 nm, red) and preparative (270 nm, black) HPLC profiles used to isolate the mono-hydroxylated testosterone metabolites 1β- and 15β-hydroxytestosterone as well as 6-dehydro-15β-hydroxytestosterone from BT1. For this isolation a separate HPLC method was developed.

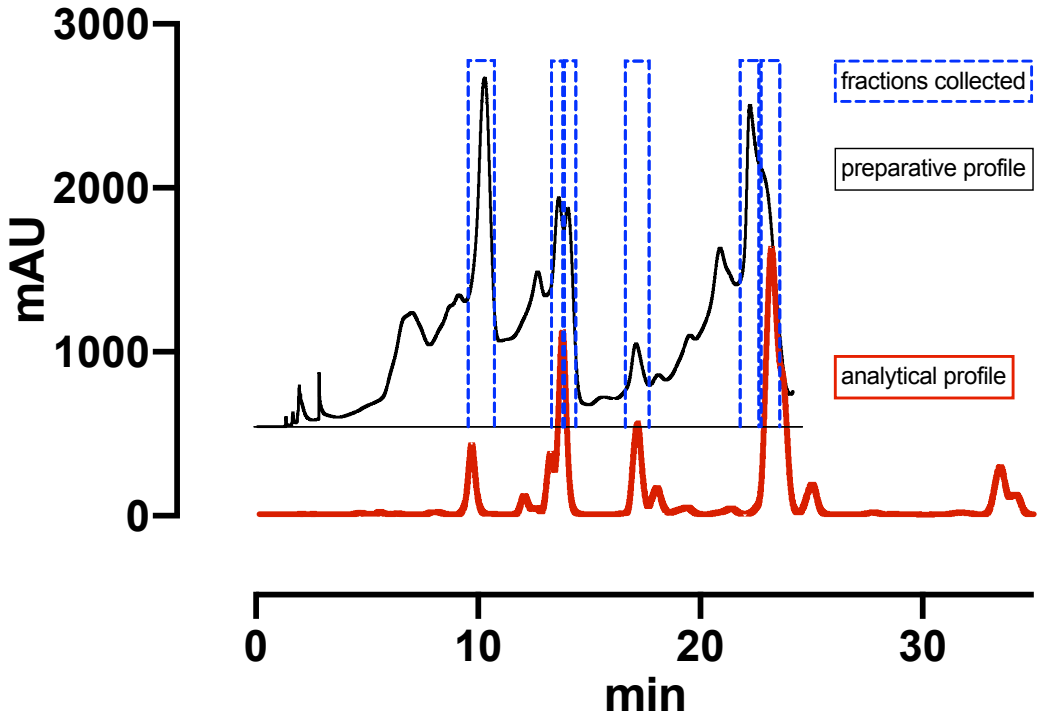

Figure S7: Display of the analytical (240 nm, red) and preparative (270 nm, black) HPLC profiles used in the attempt to isolate di-hydroxylated testosterone metabolites from BT1. Samples only included mixtures of different metabolites in small concentrations making identification impossible. For this isolation the same HPLC method was applied as used in Figures 7 and 8.

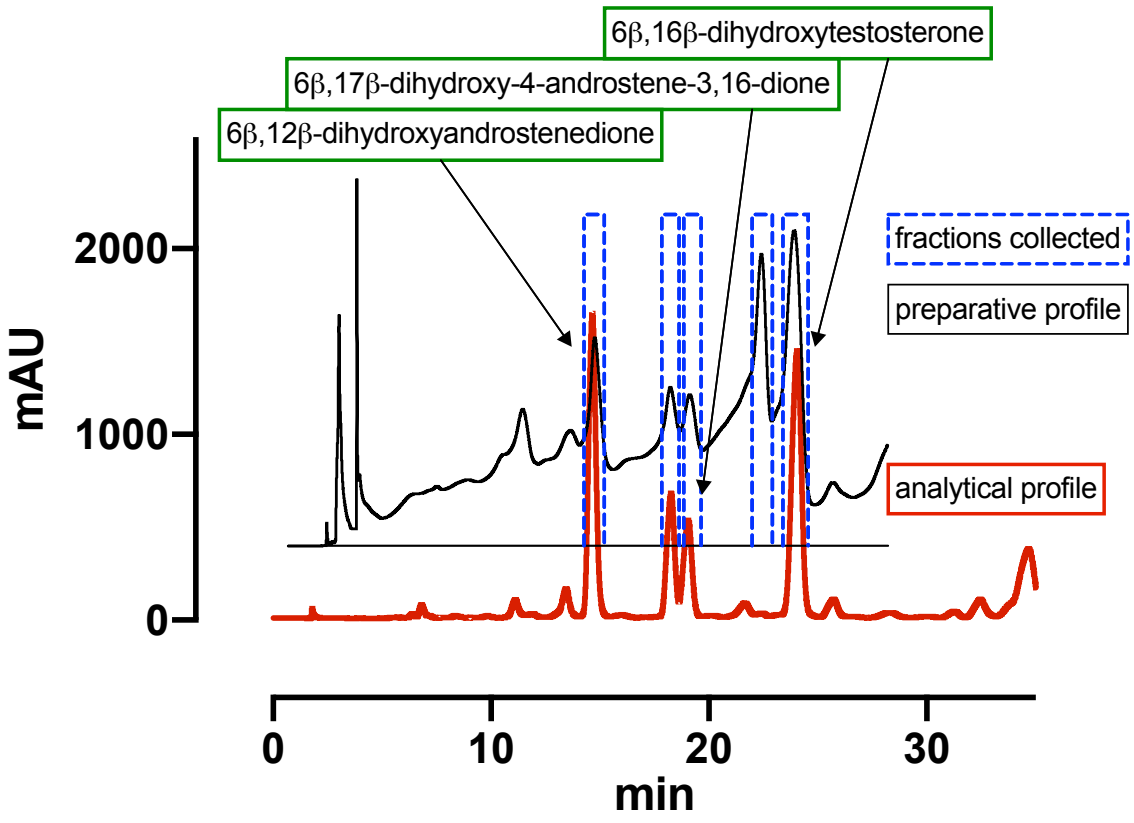

Figure S8: Display of the analytical (240 nm, red) and preparative (270 nm, black) HPLC profiles

used to isolate the di-hydroxylated testosterone metabolites 6β,16β-dihydroxytestosterone and 6β,12β-dihydroxyandrostenedione from BT2. For this isolation the same HPLC method was applied as used in Figures 7 and 8.

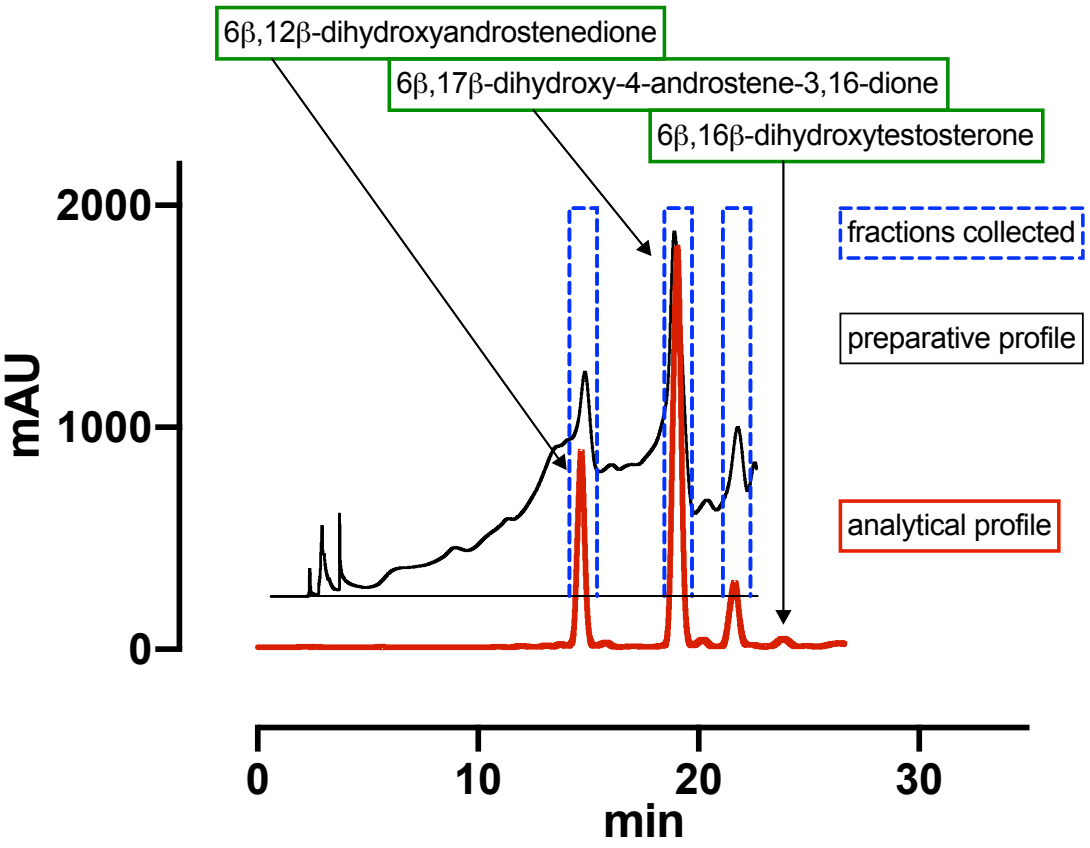

Figure S9: Display of the analytical (240 nm, red) and preparative (270 nm, black) HPLC profiles used in the attempt to isolate di-hydroxylated testosterone metabolites from BT2. Samples only included mixtures of different metabolites in small concentrations making identification impossible. For this isolation the same HPLC method was applied as used in Figures 7 and 8.

High-resolution mass spectrum of 6-dehydro-15β-hydroxytestosterone (**7**, $C_{19}H_{26}O_3$)

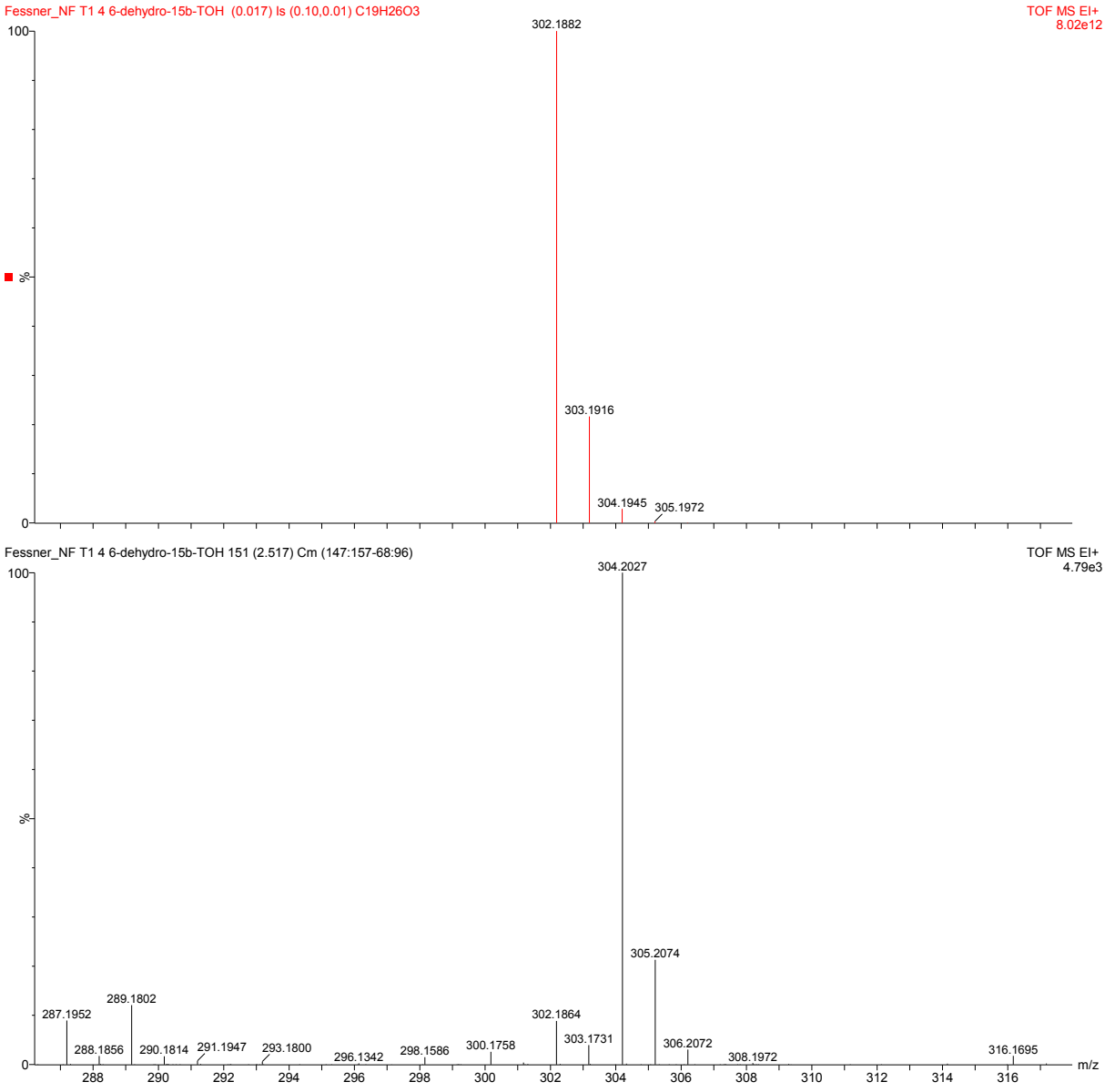

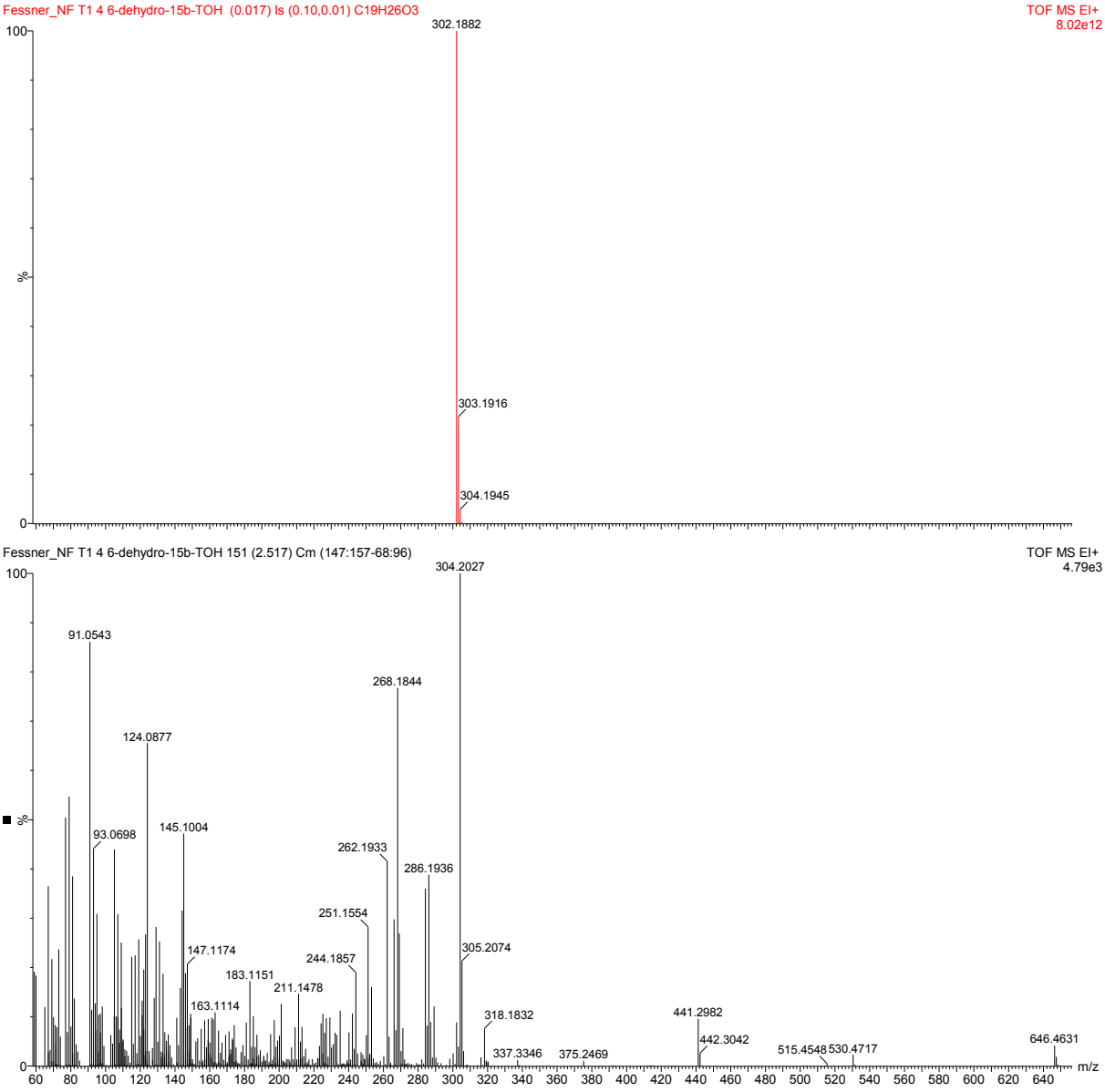
Fessner_NF T1 4 6-dehydro-15b-TOH (0.017) Is (0.10,0.01) C19H26O3
TOF MS EI+
8.02e12
100
%
0
302.1882
303.1916
304.1945
Fessner_NF T1 4 6-dehydro-15b-TOH 151 (2.517) Cm (147:157-68:96)
TOF MS EI+
4.79e3
304.2027
91.0543
268.1844
124.0877
145.1004
93.0698
262.1933
286.1936
251.1554
147.1174
244.1857
305.2074
183.1151
211.1478
163.1114
318.1832
441.2982
442.3042
337.3346
375.2469
515.4548
530.4717
646.4631
m/z
60 80 100 120 140 160 180 200 220 240 260 280 300 320 340 360 380 400 420 440 460 480 500 520 540 560 580 600 620 640

High-resolution mass spectrum of 6β,16β-dihydroxytestosterone (**8**, $C_{19}H_{28}O_4$)

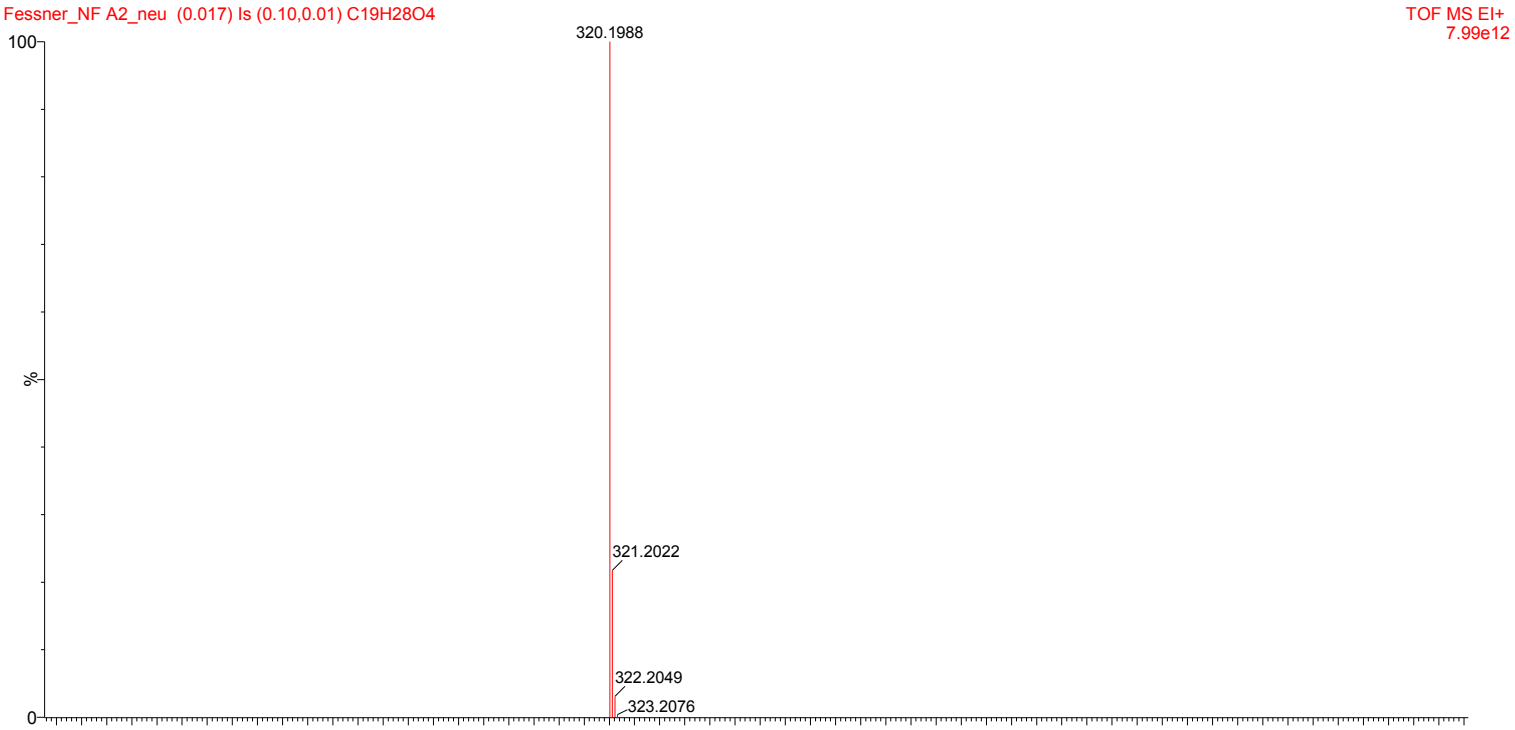

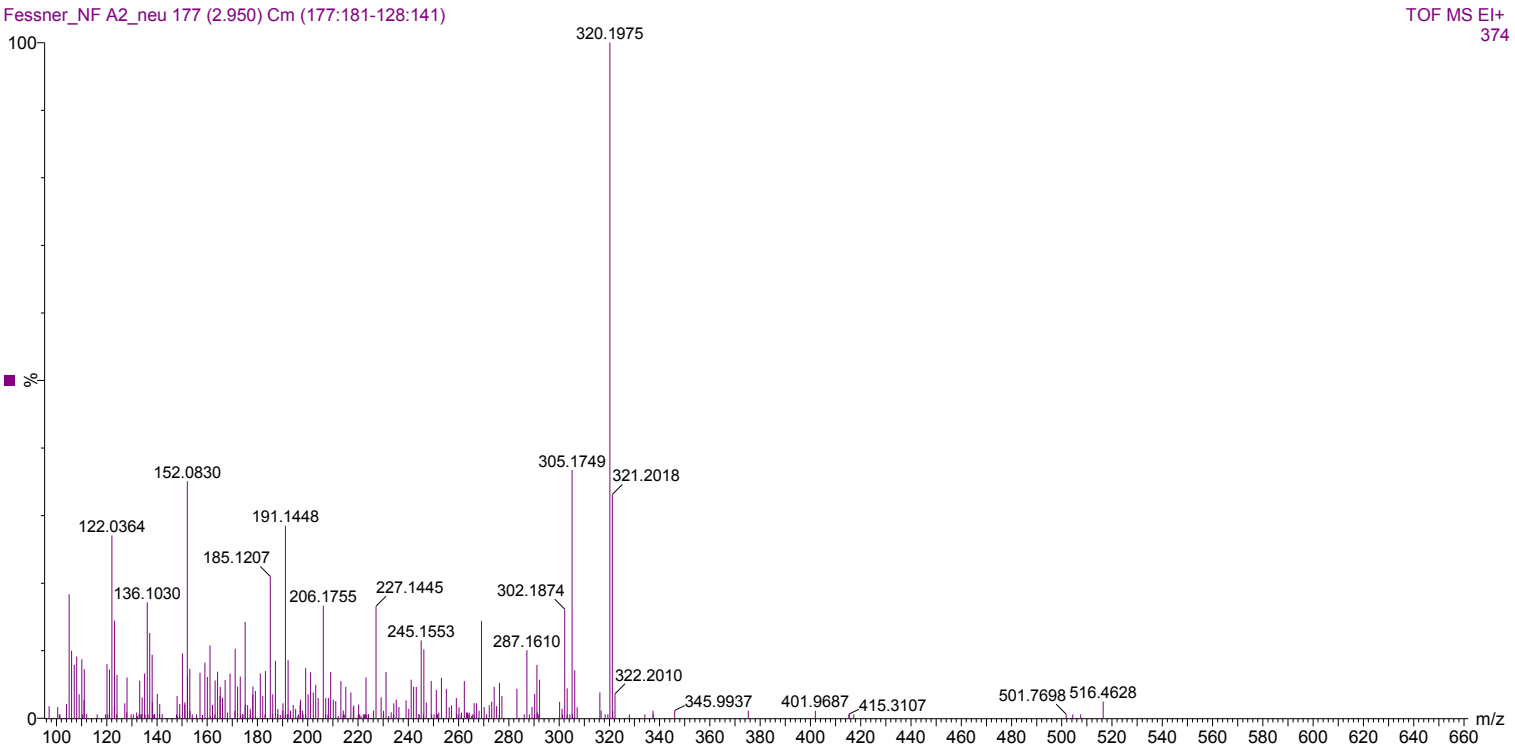

High-resolution mass spectrum of 6β,17β-dihydroxy-4-androstene-3,16-dione (**9**, $C_{19}H_{26}O_4$)

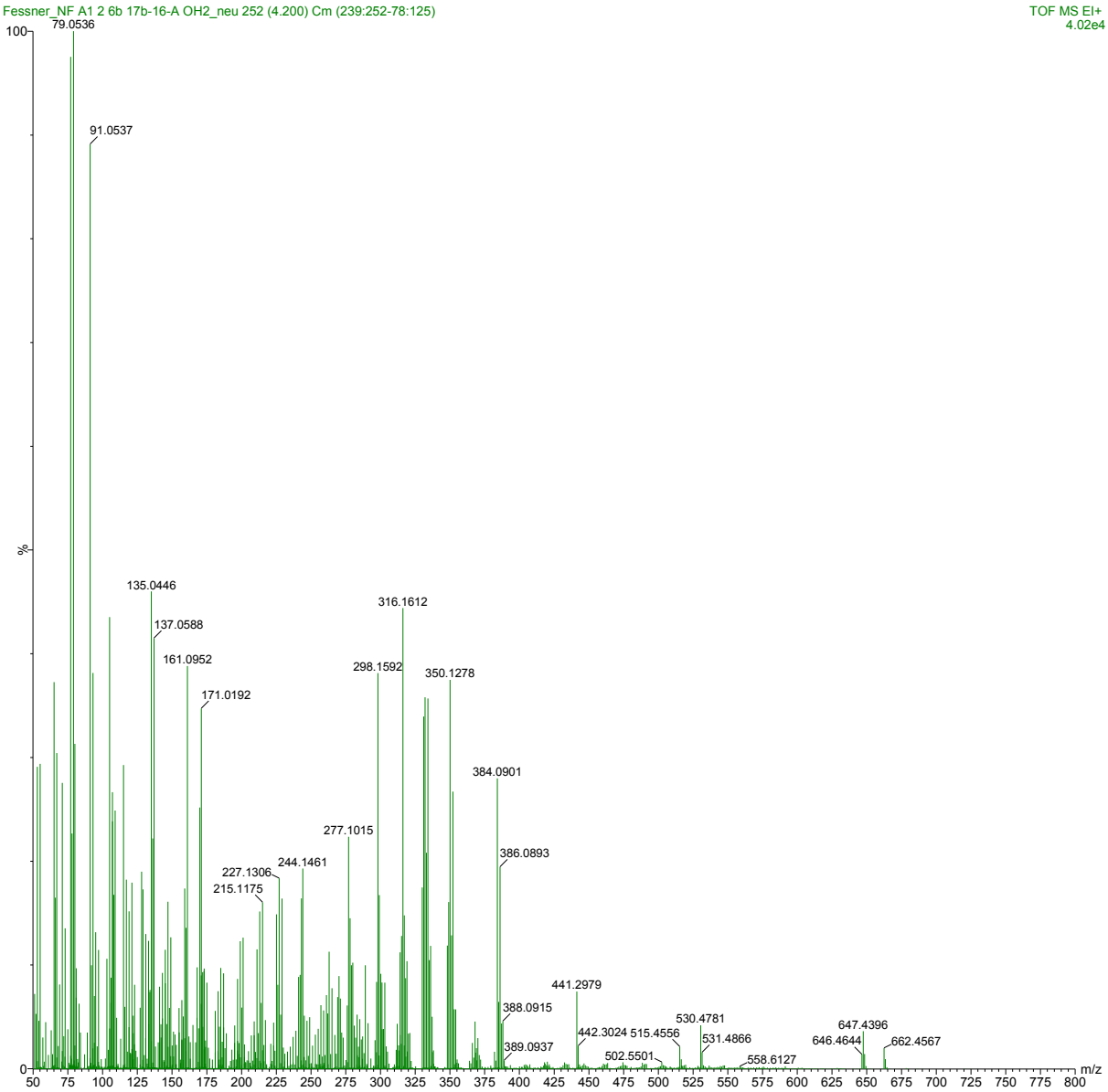

High-resolution mass spectrum of 6β,12β-dihydroxyandrostenedione (**10**, $C_{19}H_{26}O_4$)

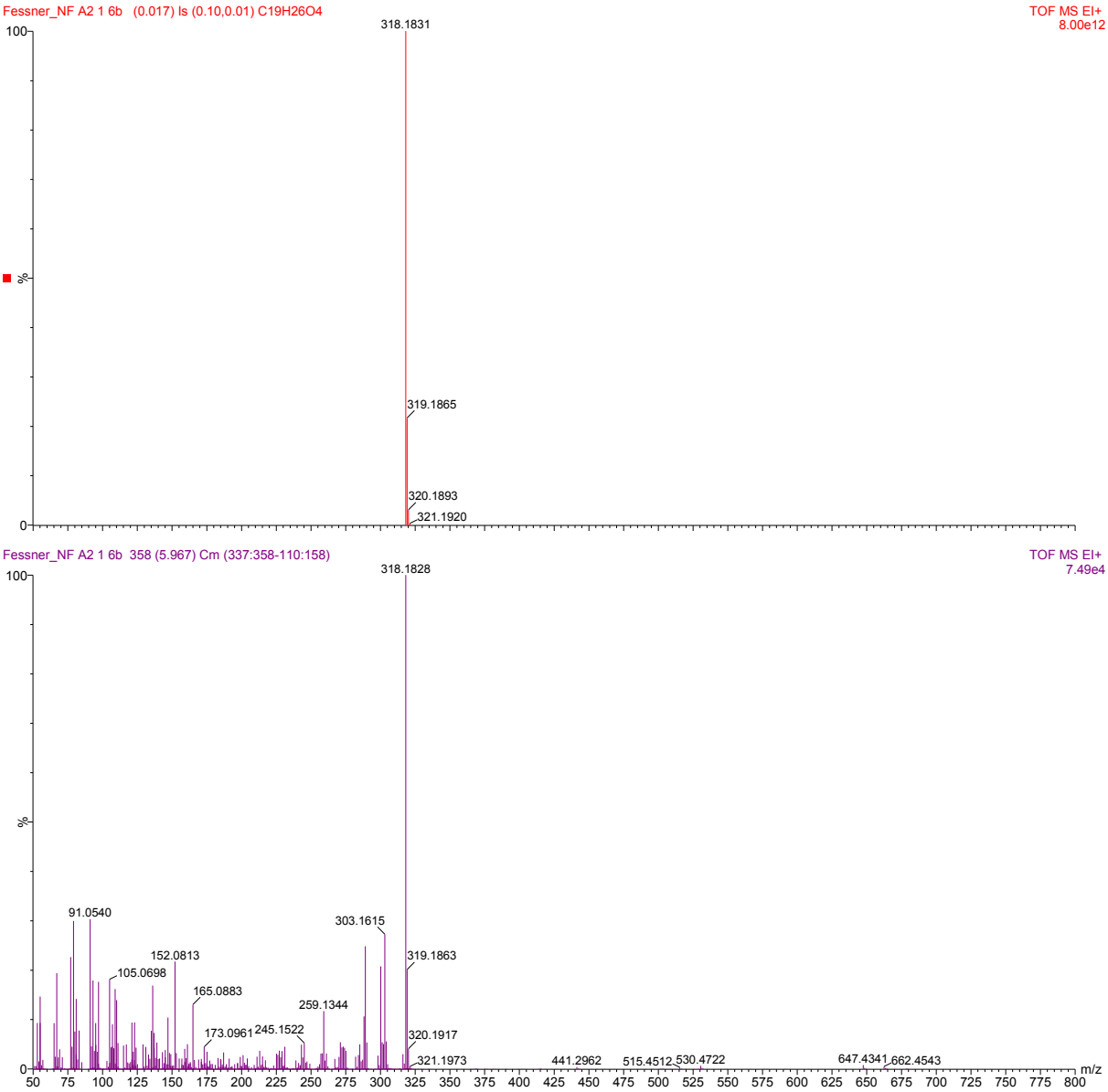

NMR spectra

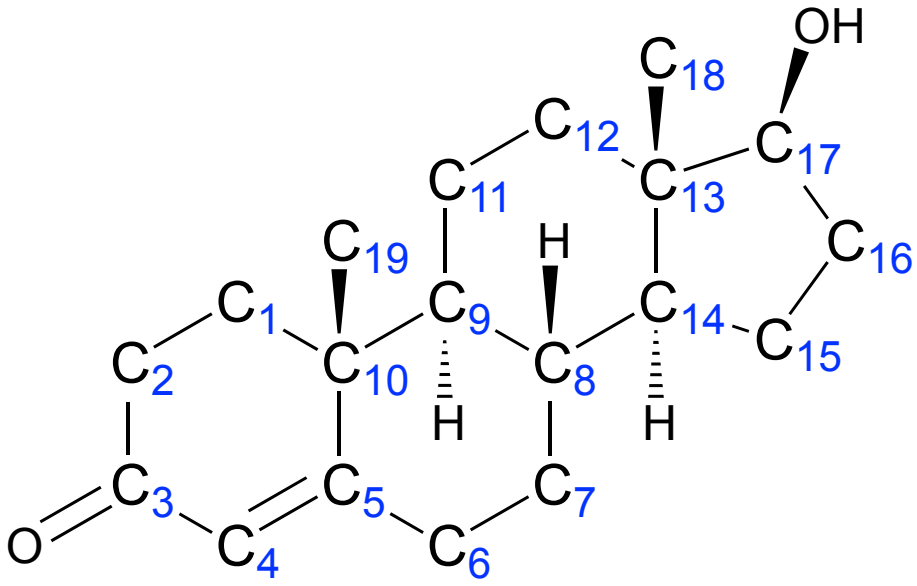

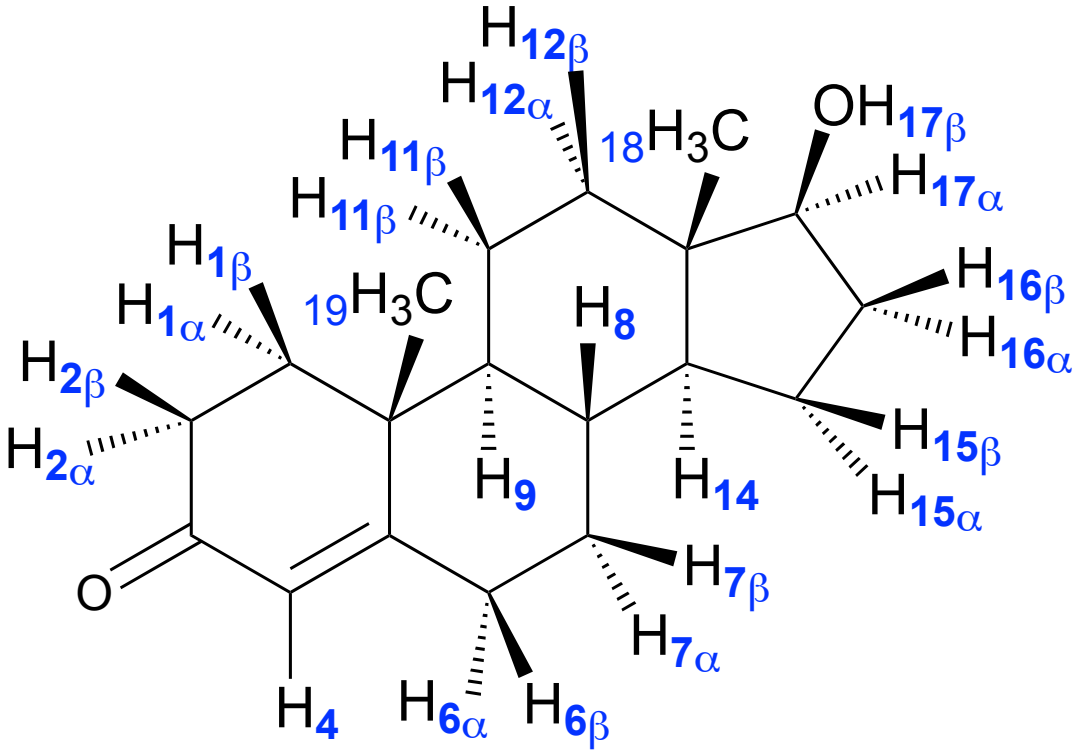

Carbon numbering Testosterone Proton numbering

6β-Hydroxytestosterone (**2**)

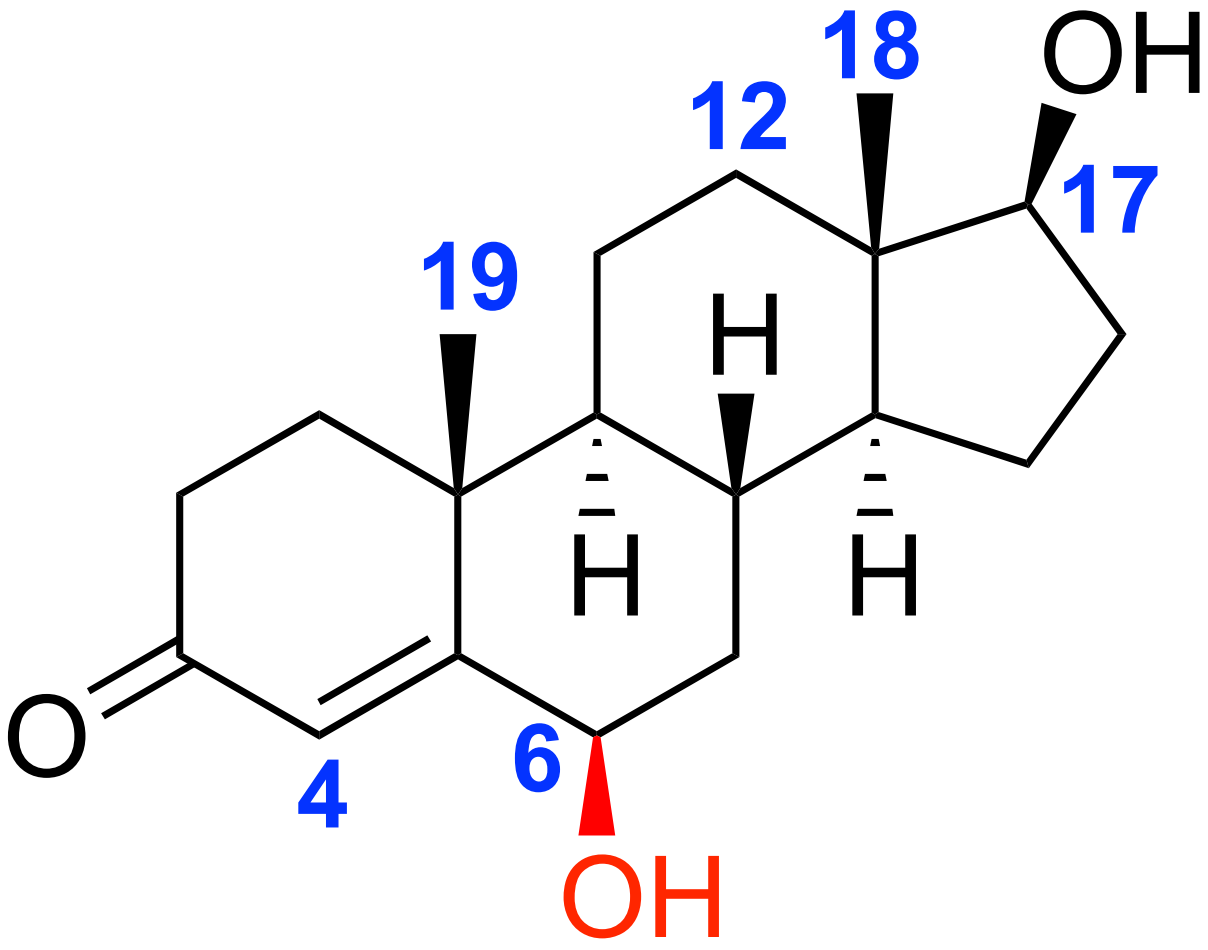

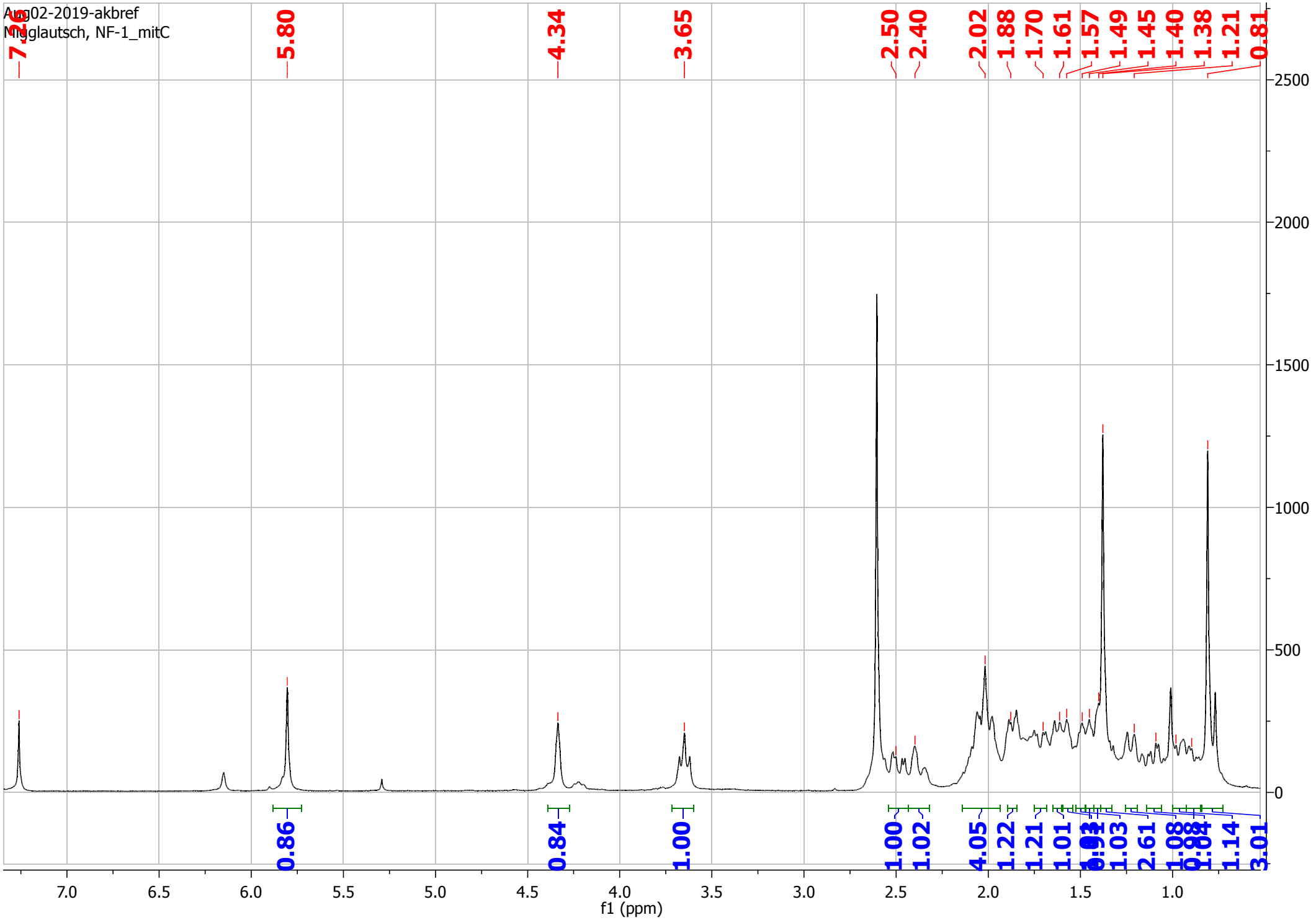
Aug02-2019-akbref
Nigglautsch, NF-1_mitC
7.26
5.80
4.34
3.65
2.50
2.40
2.02
1.88
1.70
1.61
1.57
1.49
1.45
1.40
1.38
1.21
0.81
0.86
0.84
1.00
1.00
1.02
4.05
1.22
1.21
1.01
1.03
2.61
1.08
1.14
3.01
f1 (ppm)

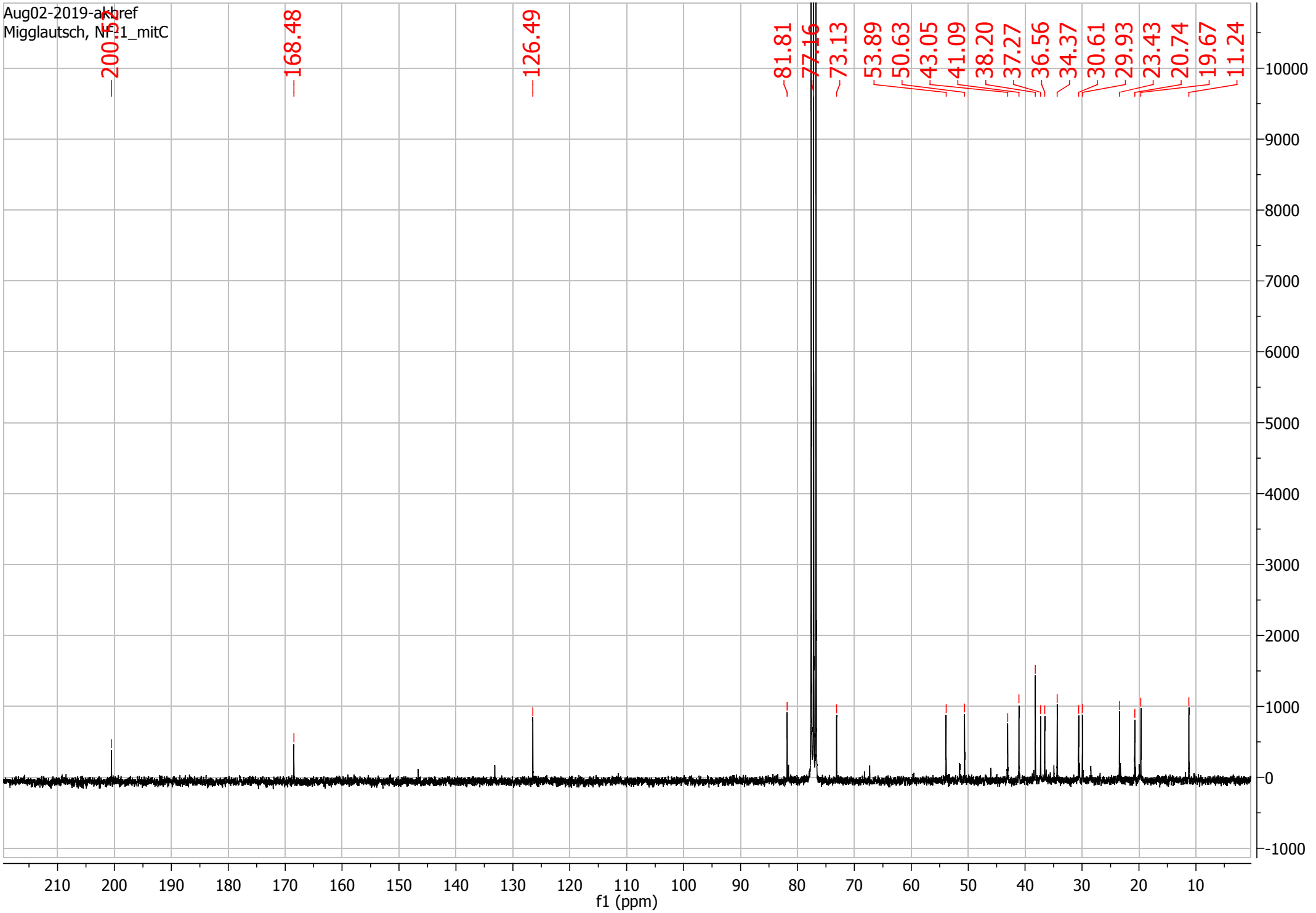
Aug02-2019-akkref
Migglautsch, NF-1_mitC
200.55
168.48
126.49
81.81
77.16
73.13
53.89
50.63
43.05
41.09
38.20
37.27
36.56
34.37
30.61
29.93
23.43
20.74
19.67
11.24
10000
9000
8000
7000
6000
5000
4000
3000
2000
1000
0
-1000
210
200
190
180
170
160
150
140
130
120
110
100
90
80
70
60
50
40
30
20
10
f1 (ppm)

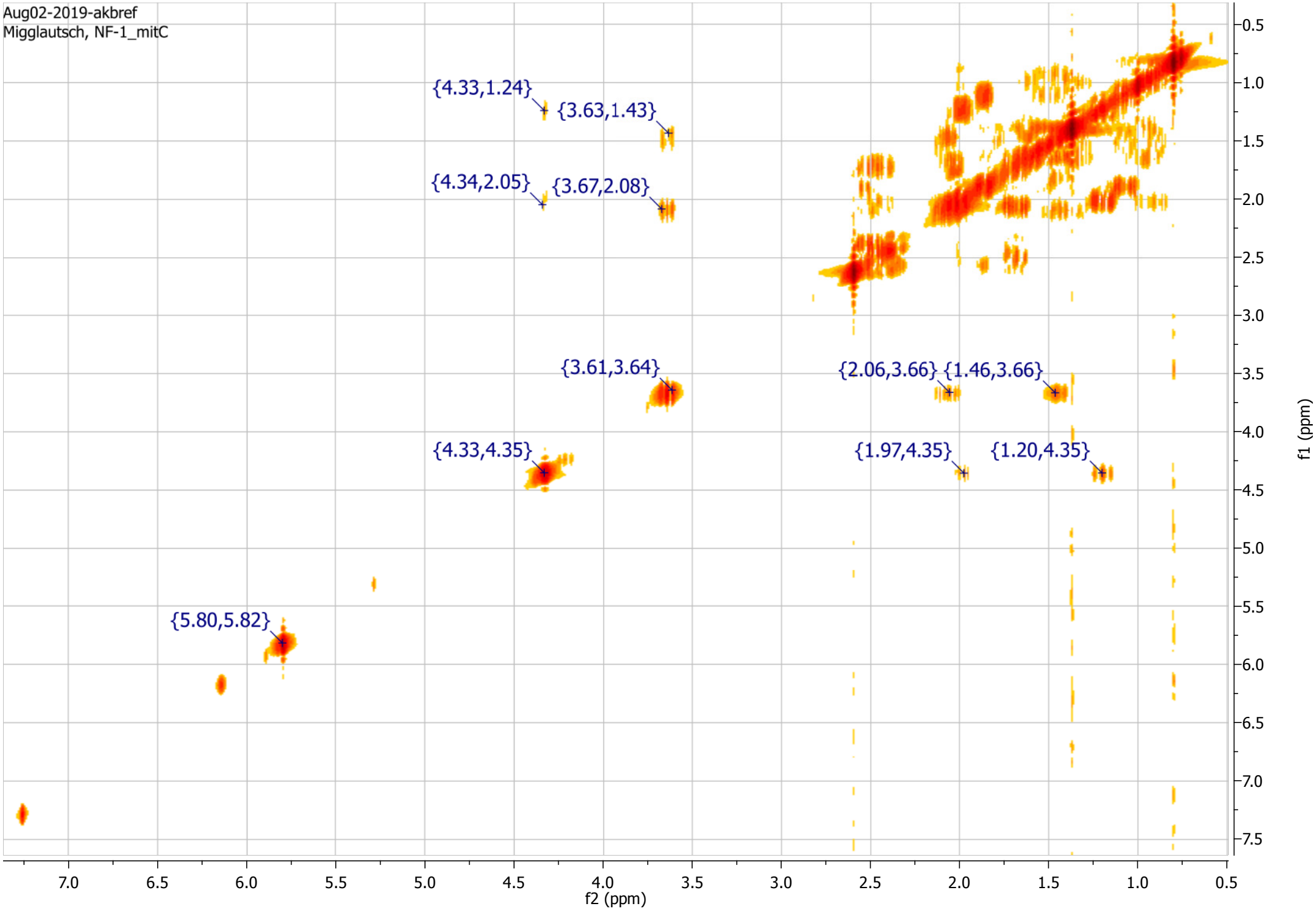
Aug02-2019-akbref
Migglautsch, NF-1_mitC
{4.33,1.24}
{3.63,1.43}
{4.34,2.05}
{3.67,2.08}
{3.61,3.64}
{2.06,3.66}
{1.46,3.66}
{4.33,4.35}
{1.97,4.35}
{1.20,4.35}
{5.80,5.82}
f2 (ppm)
f1 (ppm)

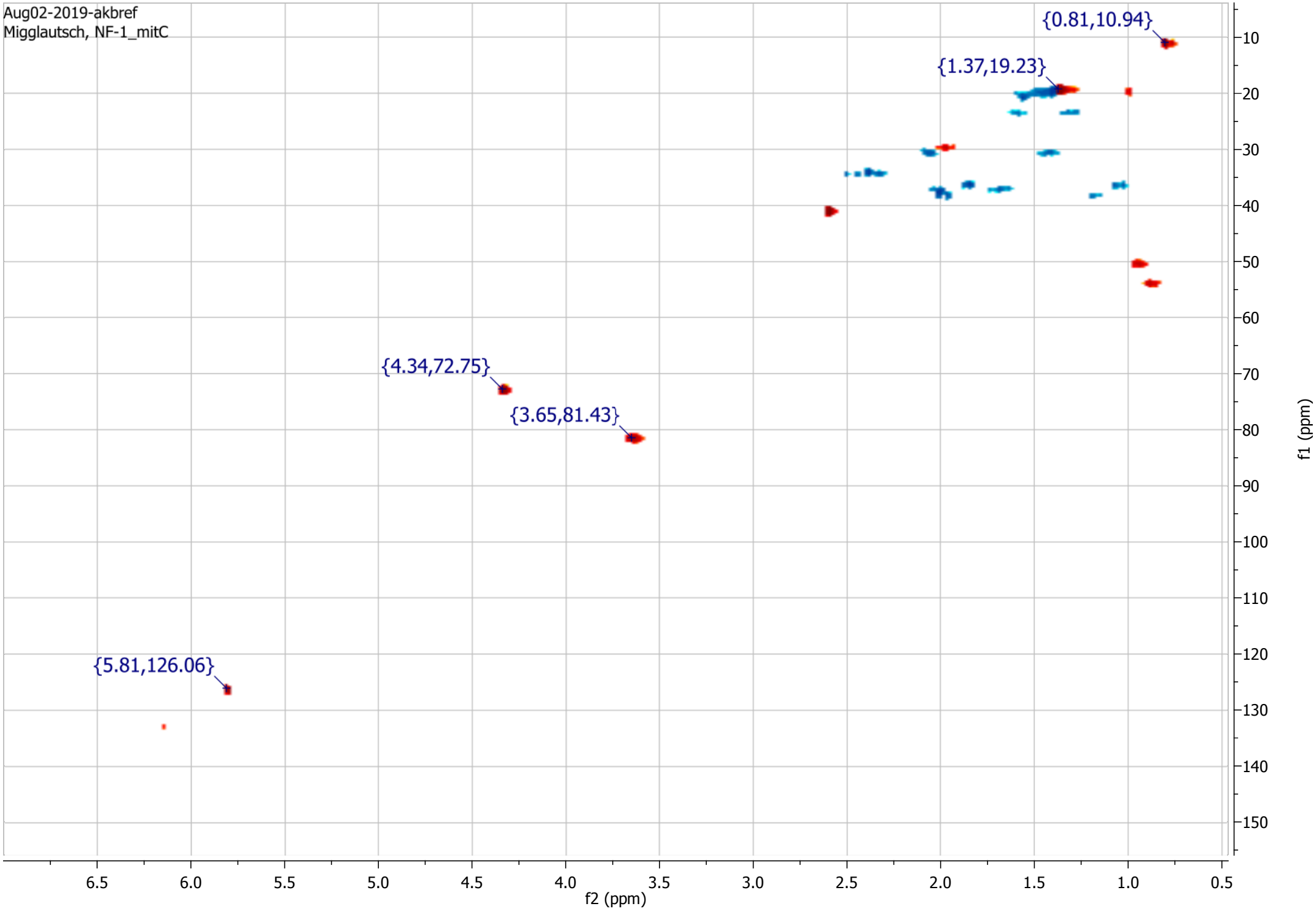
Aug02-2019-akbref
Migglautsch, NF-1_mitC
{0.81,10.94}
{1.37,19.23}
{4.34,72.75}
{3.65,81.43}
{5.81,126.06}
f2 (ppm)
f1 (ppm)

6β-Hydroxyandrostenedione (**4**)

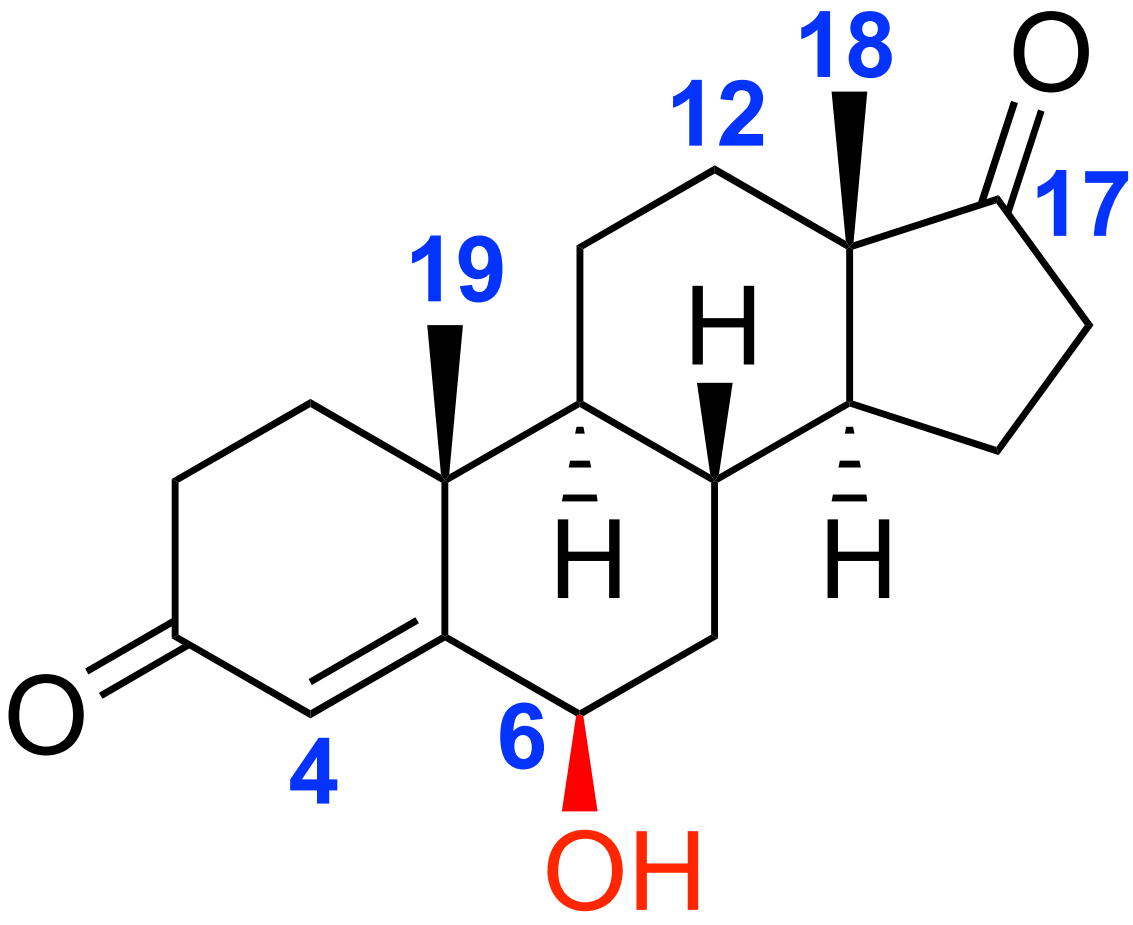

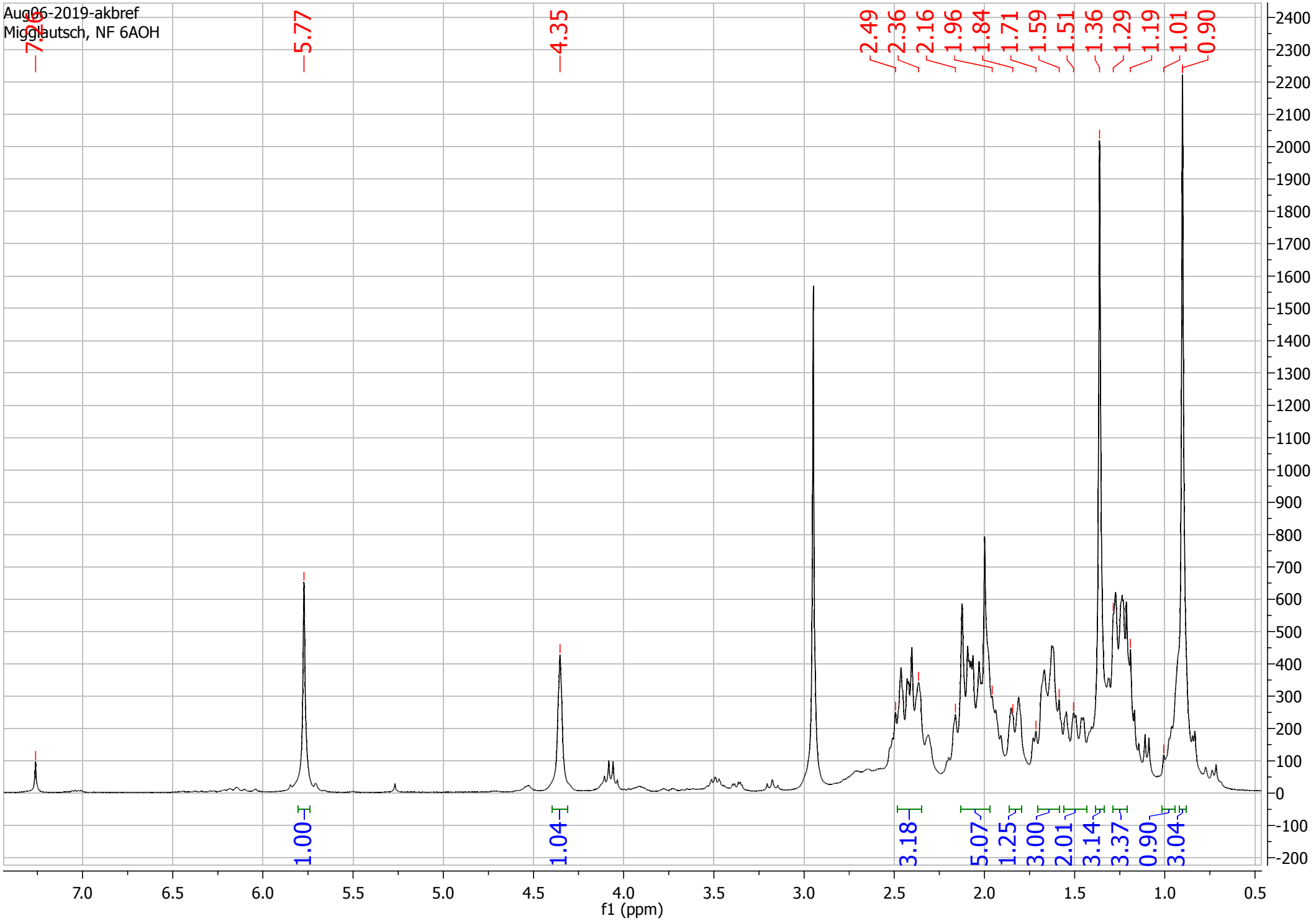
Aug06-2019-akbref
Migglautsch, NF 6AOH
7.26
5.77
4.35
2.49
2.36
2.16
1.96
1.84
1.71
1.59
1.51
1.36
1.29
1.19
1.01
0.90
1.00
1.04
3.18
5.07
1.25
3.00
2.01
3.14
3.37
0.90
3.04
f1 (ppm)

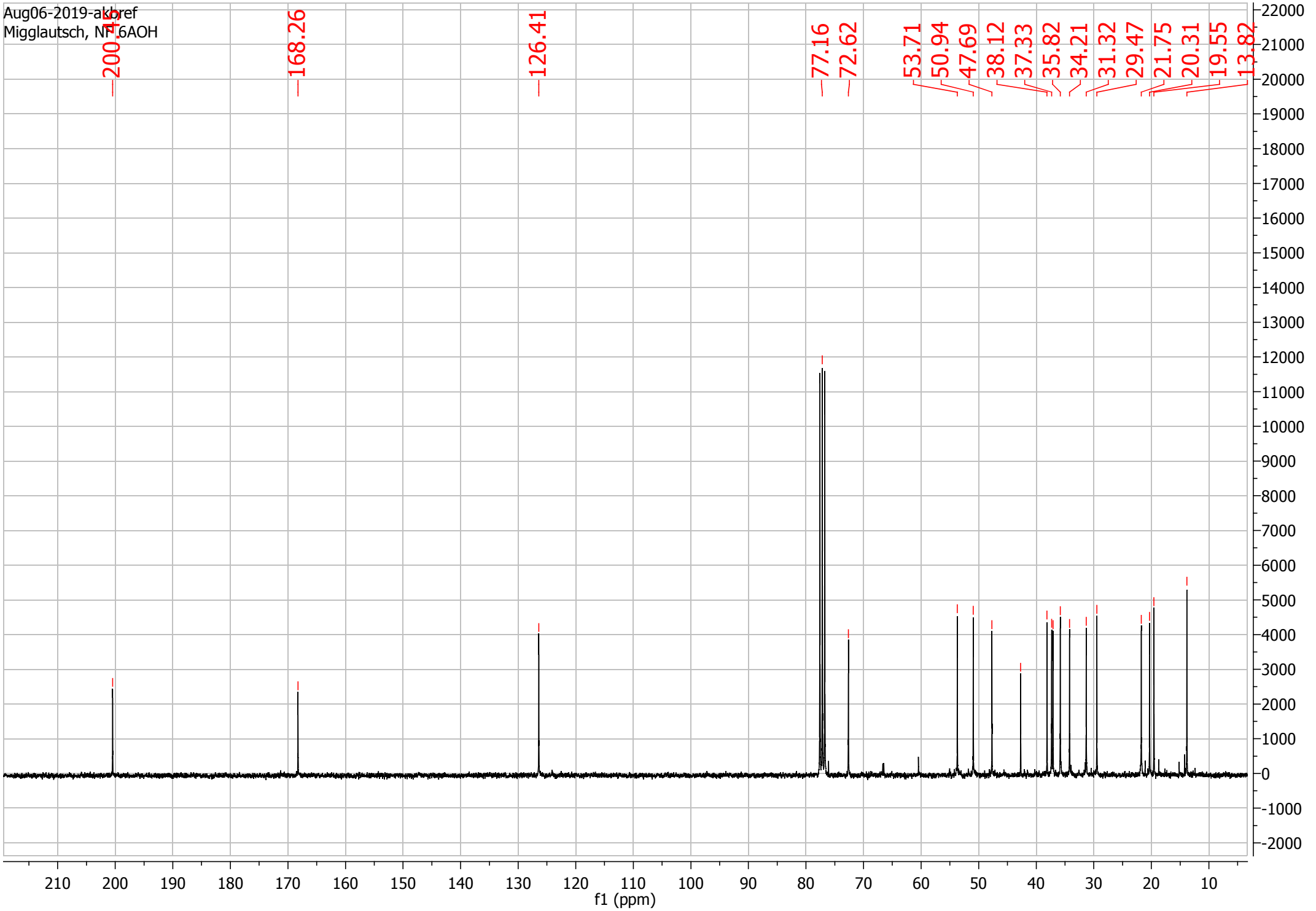
Aug06-2019-akbref
Migglautsch, NF 6AOH
200.41
168.26
126.41
77.16
72.62
53.71
50.94
47.69
38.12
37.33
35.82
34.21
31.32
29.47
21.75
20.31
19.55
13.82
f1 (ppm)

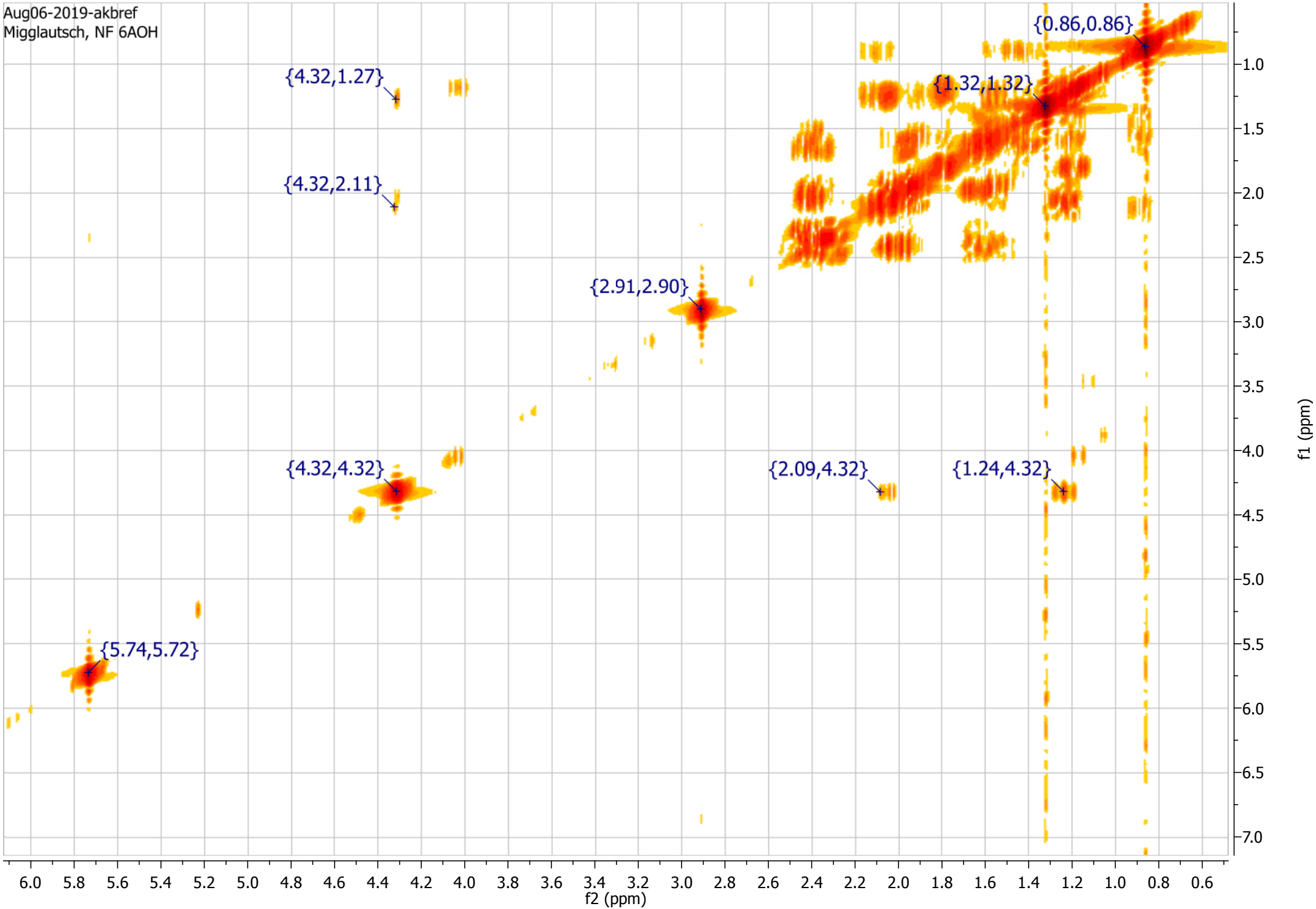
Aug06-2019-akbref
Migglautsch, NF 6AOH
{0.86,0.86}
{1.32,1.32}
{4.32,1.27}
{4.32,2.11}
{2.91,2.90}
{4.32,4.32}
{2.09,4.32}
{1.24,4.32}
{5.74,5.72}
f2 (ppm)
f1 (ppm)

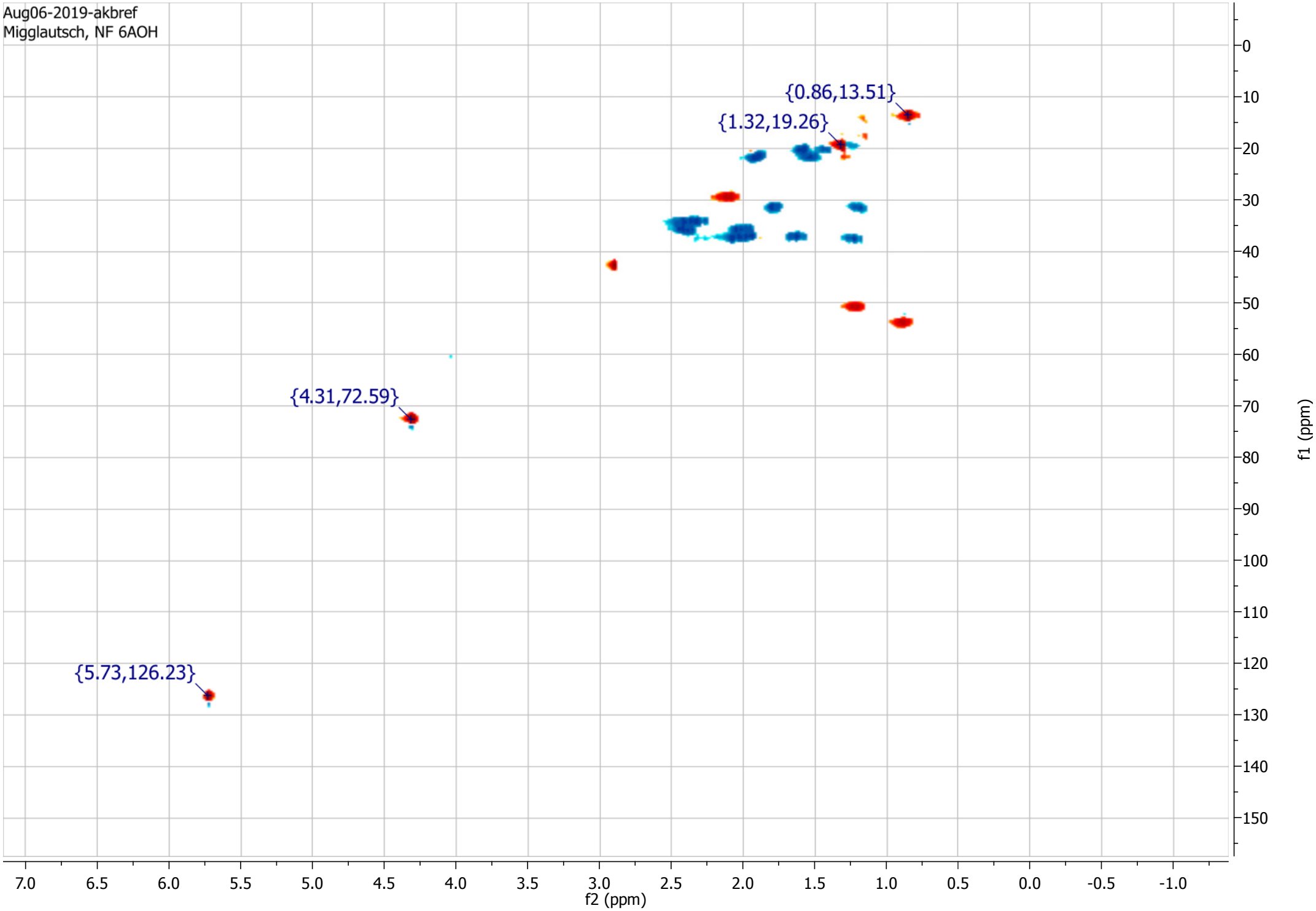
Aug06-2019-akbref
Migglautsch, NF 6AOH
{0.86,13.51}
{1.32,19.26}
{4.31,72.59}
{5.73,126.23}
f2 (ppm)
f1 (ppm)

1β-hydroxytestosterone (**5**)

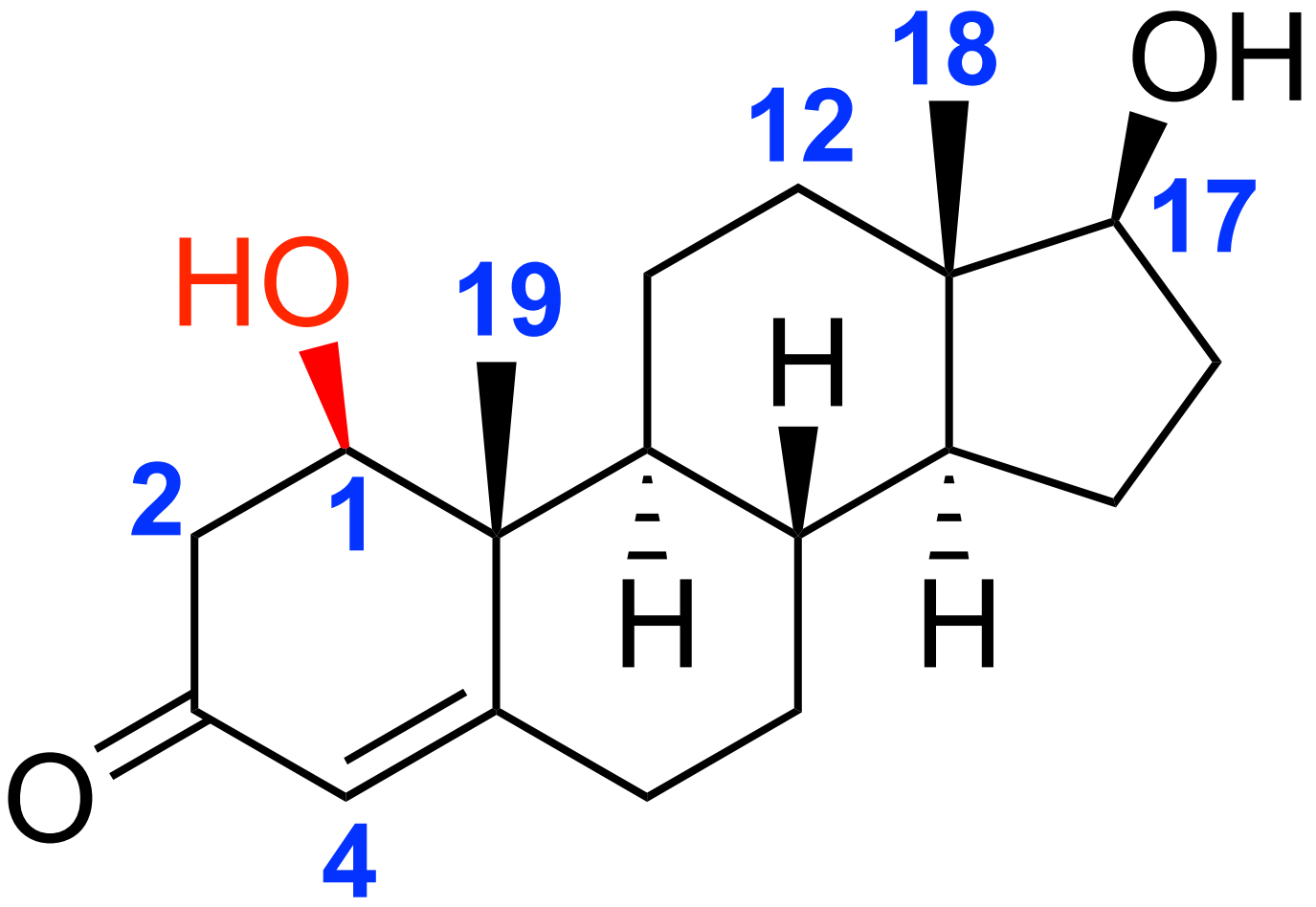

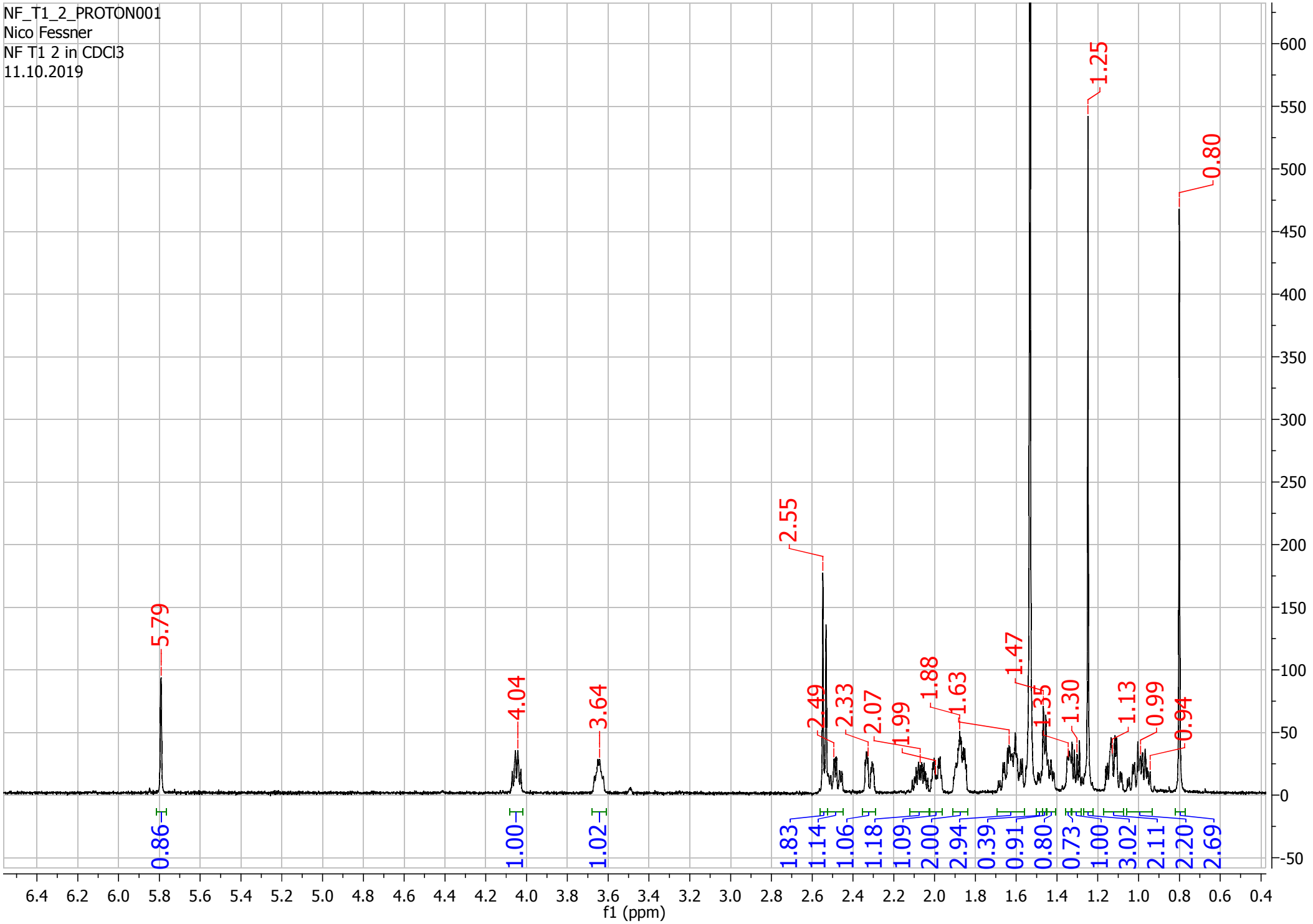
NF_T1_2_PROTON001
Nico Fessner
NF T1 2 in CDCl3
11.10.2019
5.79
4.04
3.64
2.55
2.49
2.33
2.07
1.99
1.88
1.63
1.47
1.35
1.30
1.25
1.13
0.99
0.94
0.80
0.86
1.00
1.02
1.83
1.14
1.06
1.18
1.09
2.00
2.94
0.39
0.91
0.80
0.73
1.00
3.02
2.11
2.20
2.69
f1 (ppm)

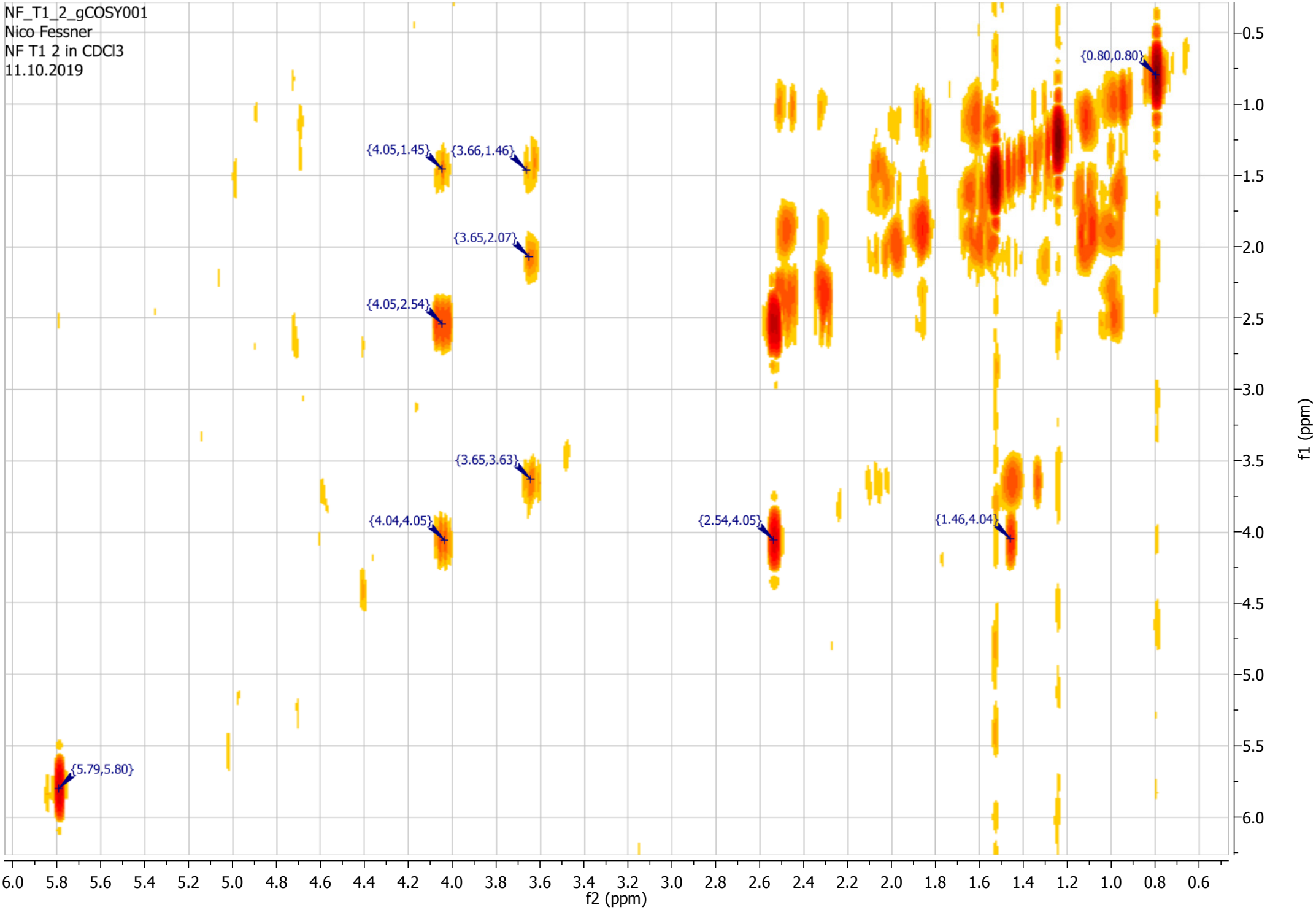
NF_T1_2_gCOSY001
Nico Fessner
NF T1 2 in CDCl3
11.10.2019
{0.80,0.80}
{4.05,1.45}
{3.66,1.46}
{3.65,2.07}
{4.05,2.54}
{3.65,3.63}
{4.04,4.05}
{2.54,4.05}
{1.46,4.04}
{5.79,5.80}
f2 (ppm)
f1 (ppm)

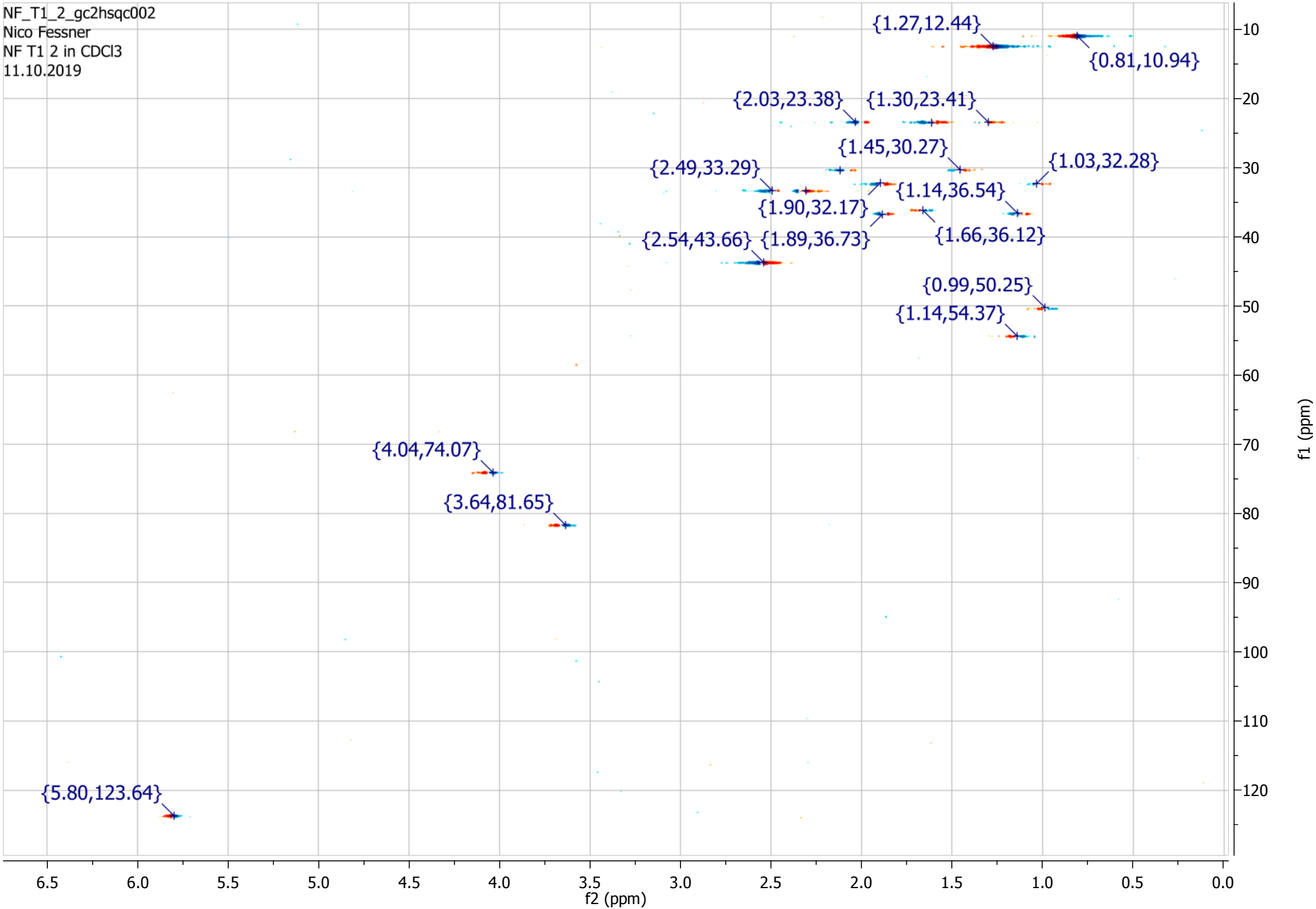
NF_T1_2_gc2hsqc002
Nico Fessner
NF T1 2 in CDCl3
11.10.2019
{1.27,12.44}
{0.81,10.94}
{2.03,23.38}
{1.30,23.41}
{1.45,30.27}
{2.49,33.29}
{1.03,32.28}
{1.14,36.54}
{1.90,32.17}
{2.54,43.66}
{1.89,36.73}
{1.66,36.12}
{0.99,50.25}
{1.14,54.37}
{4.04,74.07}
{3.64,81.65}
{5.80,123.64}
f2 (ppm)
f1 (ppm)

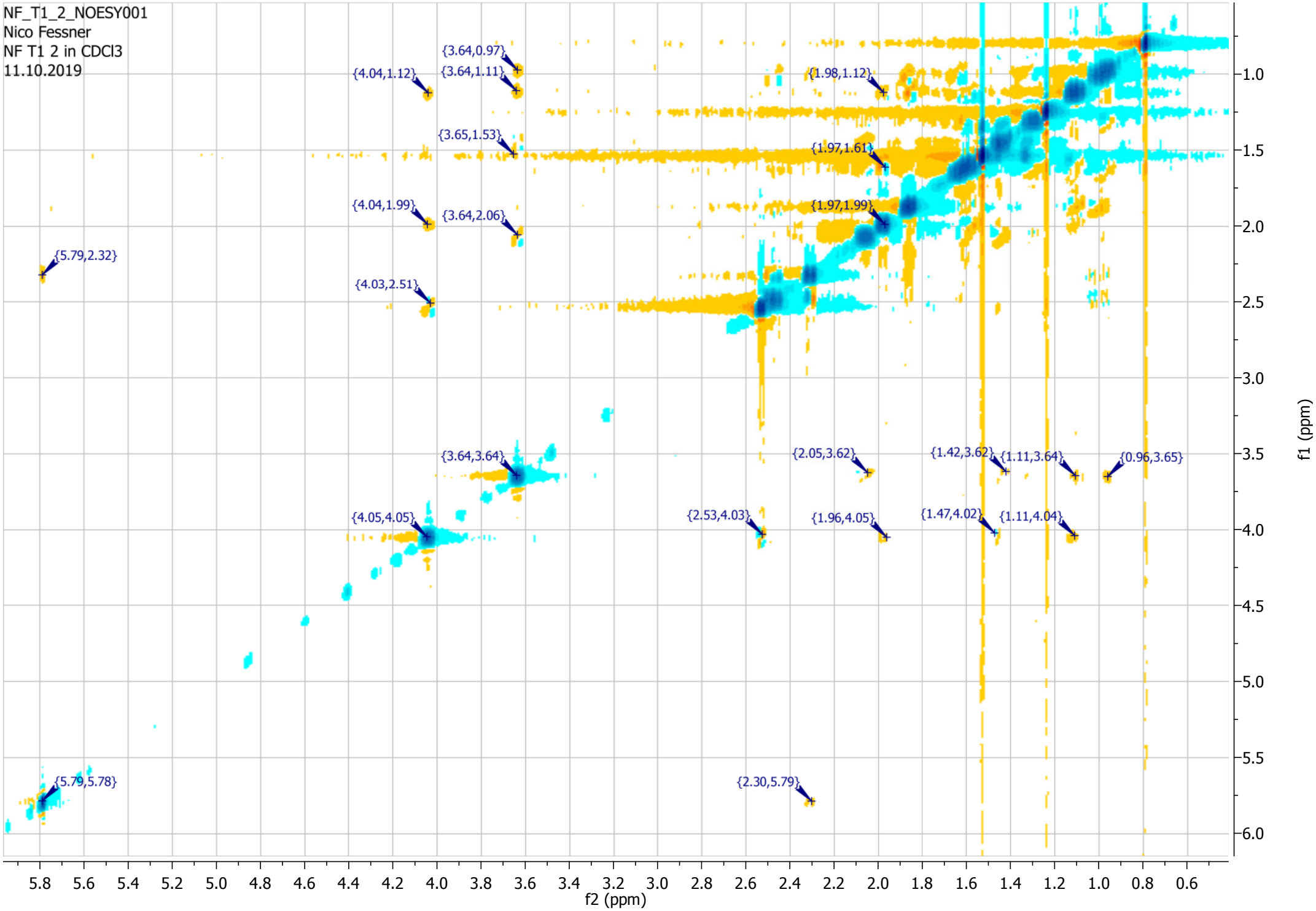
NF_T1_2_NOESY001
Nico Fessner
NF T1 2 in CDCl3
11.10.2019
{3.64,0.97}
{4.04,1.12}
{3.64,1.11}
{1.98,1.12}
{3.65,1.53}
{1.97,1.61}
{4.04,1.99}
{3.64,2.06}
{1.97,1.99}
{5.79,2.32}
{4.03,2.51}
{3.64,3.64}
{2.05,3.62}
{1.42,3.62}
{1.11,3.64}
{0.96,3.65}
{4.05,4.05}
{2.53,4.03}
{1.96,4.05}
{1.47,4.02}
{1.11,4.04}
{5.79,5.78}
{2.30,5.79}
f2 (ppm)
f1 (ppm)


NF_T1_2_gc2hmbc001
Nico Fessner
NF T1 2 in CDCl3
11.10.2019
{5.81,33.54}
{5.81,44.83}
{5.81,43.63}
{2.55,44.88}
{0.81,36.59}
{1.27,44.89}
{1.27,54.40}
{2.55,74.05}
{1.27,74.06}
{0.81,81.64}
{1.27,169.98}
{2.56,197.97}
f2 (ppm)
f1 (ppm)

15β-hydroxytestosterone (**6**)

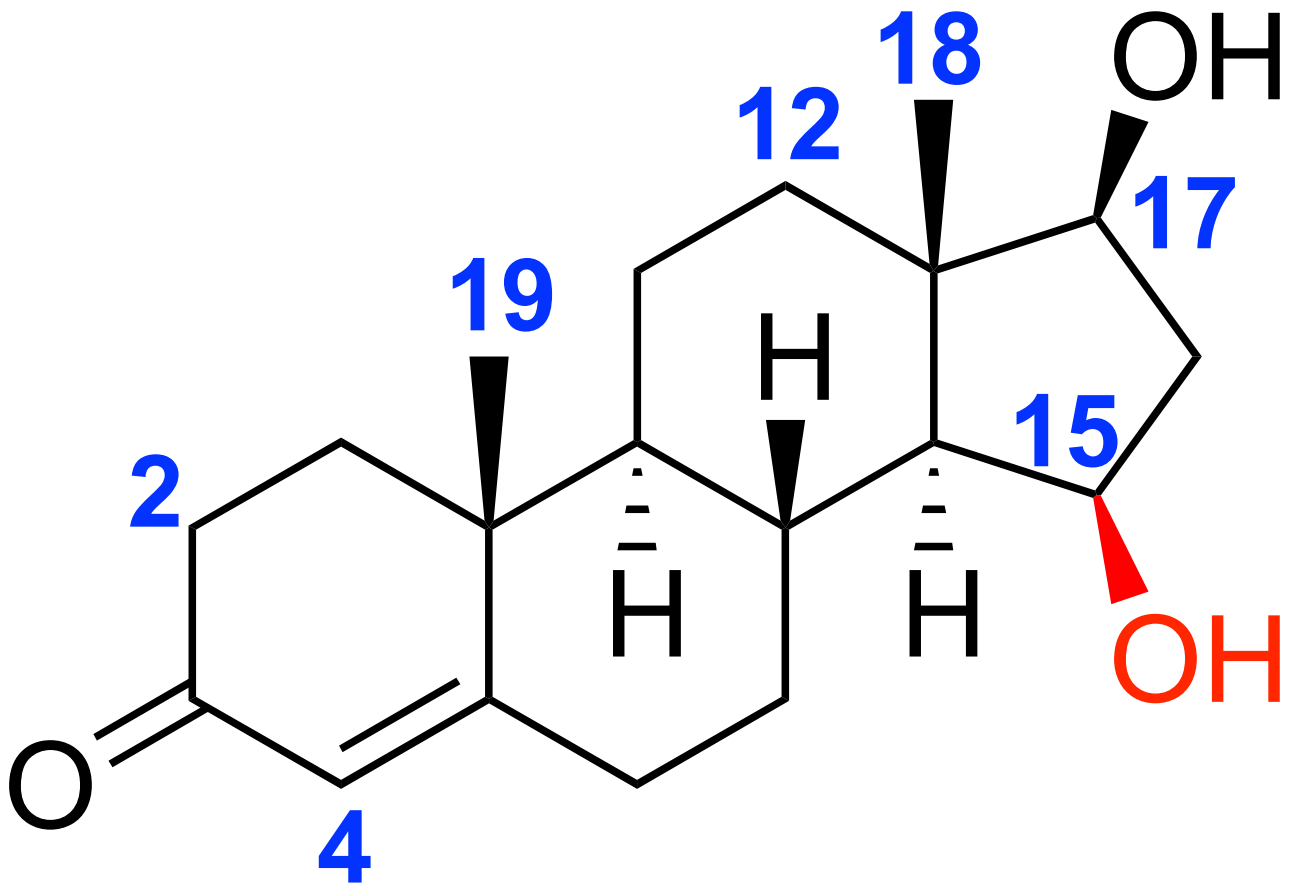

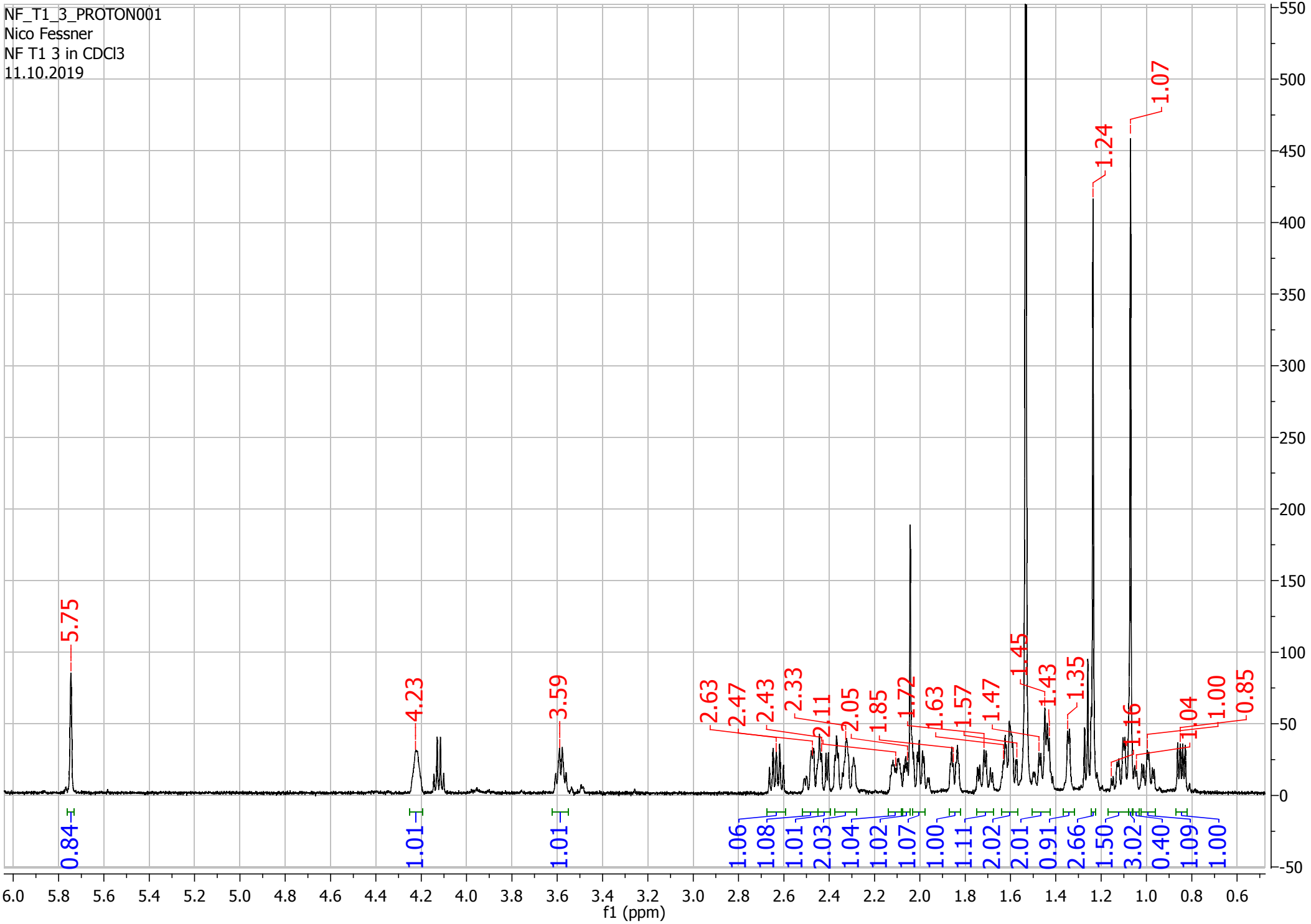
NF_T1_3_PROTON001
Nico Fessner
NF T1 3 in CDCl3
11.10.2019
5.75
4.23
3.59
2.63
2.47
2.43
2.33
2.11
2.05
1.85
1.72
1.63
1.57
1.47
1.45
1.43
1.35
1.24
1.16
1.07
1.04
1.00
0.85
0.84
1.01
1.01
1.06
1.08
1.01
2.03
1.04
1.02
1.07
1.00
1.11
2.02
2.01
0.91
2.66
1.50
3.02
0.40
1.09
1.00
f1 (ppm)

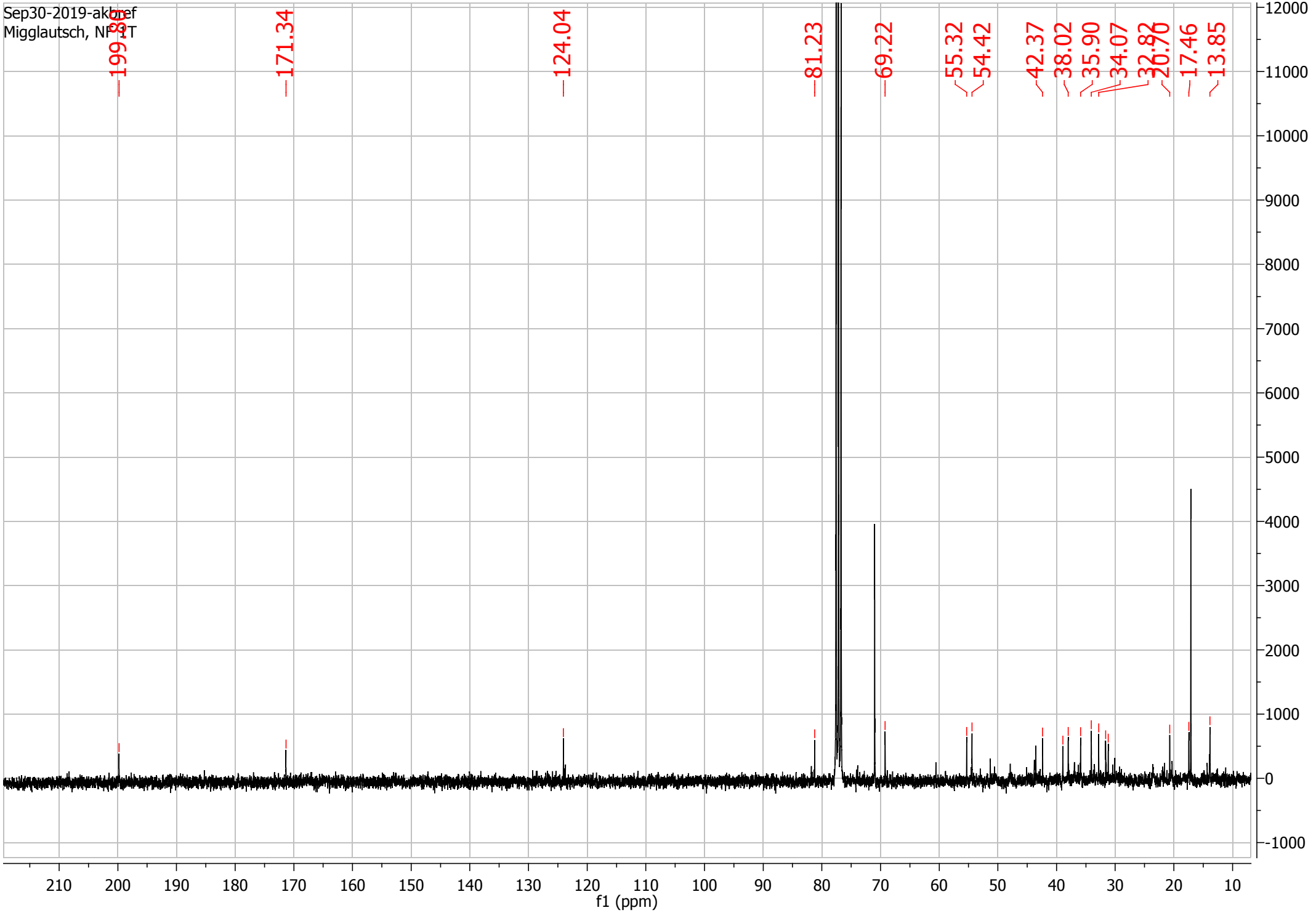
Sep30-2019-akbref
Migglautsch, NF 1T
199.80
171.34
124.04
81.23
69.22
55.32
54.42
42.37
38.02
35.90
34.07
32.82
30.70
17.46
13.85
f1 (ppm)

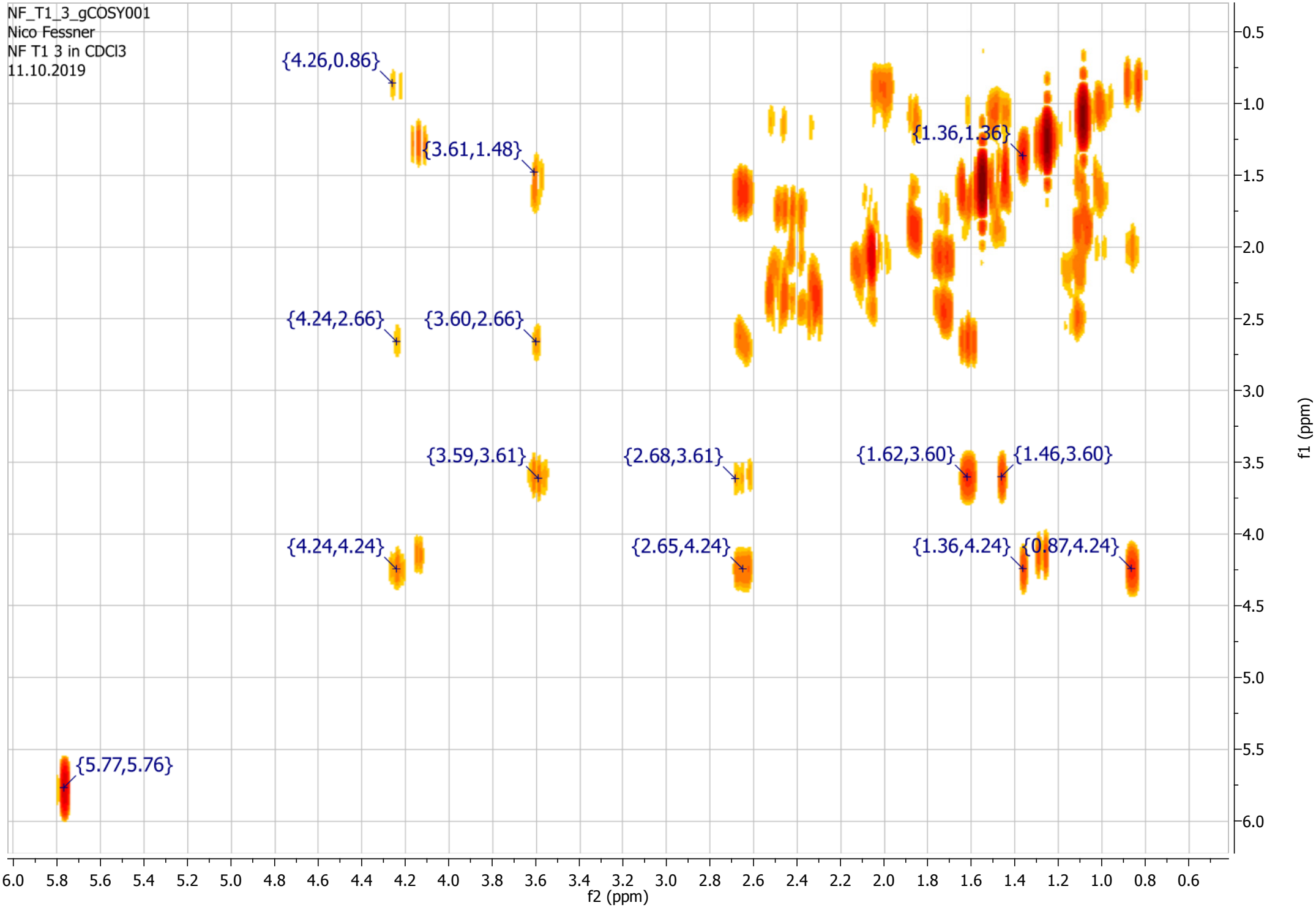
NF_T1_3_gCOSY001
Nico Fessner
NF T1 3 in CDCl3
11.10.2019
{4.26,0.86}
{3.61,1.48}
{1.36,1.36}
{4.24,2.66}
{3.60,2.66}
{3.59,3.61}
{2.68,3.61}
{1.62,3.60}
{1.46,3.60}
{4.24,4.24}
{2.65,4.24}
{1.36,4.24}
{0.87,4.24}
{5.77,5.76}
f2 (ppm)
f1 (ppm)

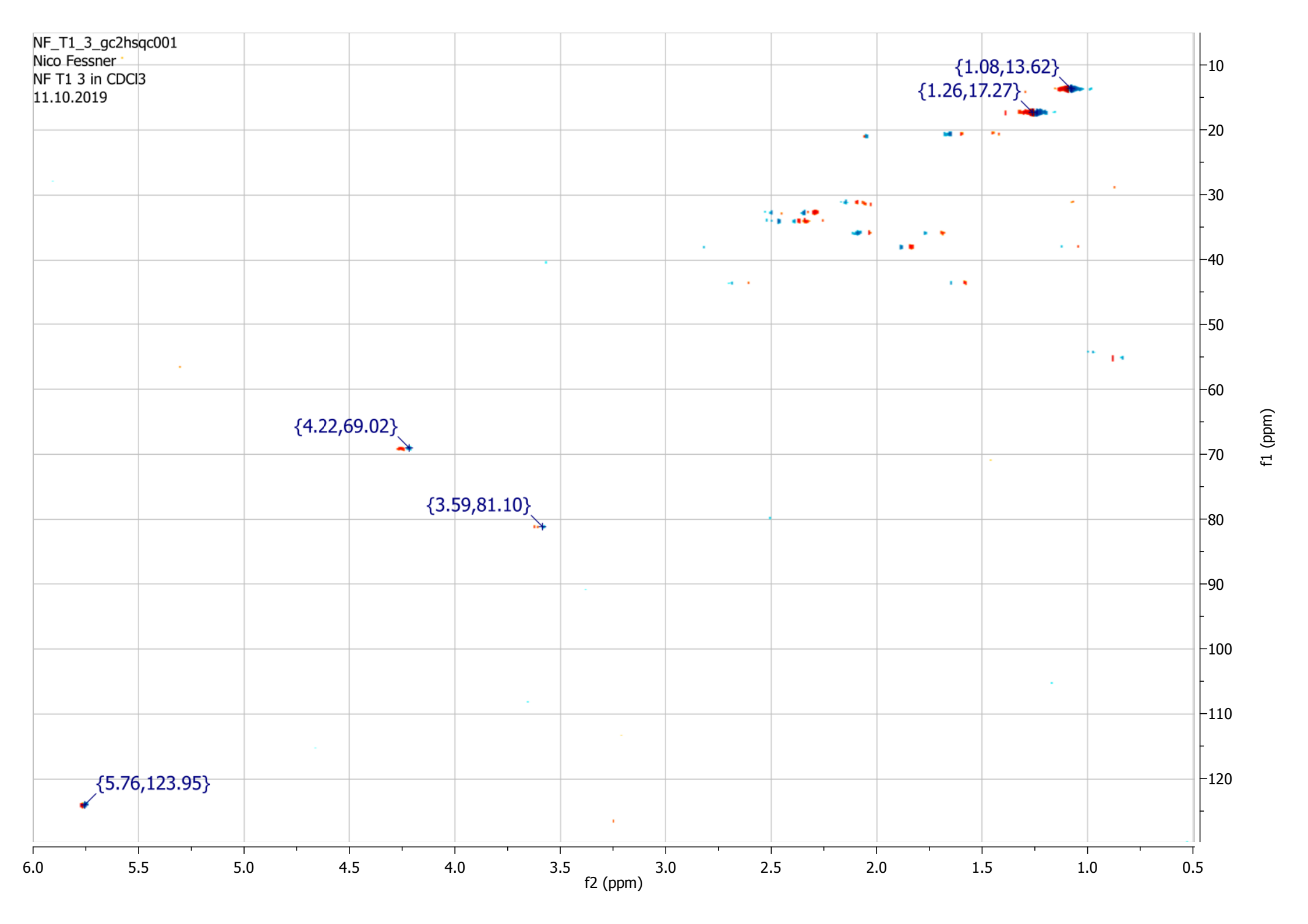
NF_T1_3_gc2hsqc001
Nico Fessner
NF T1 3 in CDCl3
11.10.2019
{1.08,13.62}
{1.26,17.27}
{4.22,69.02}
{3.59,81.10}
{5.76,123.95}
f2 (ppm)
f1 (ppm)

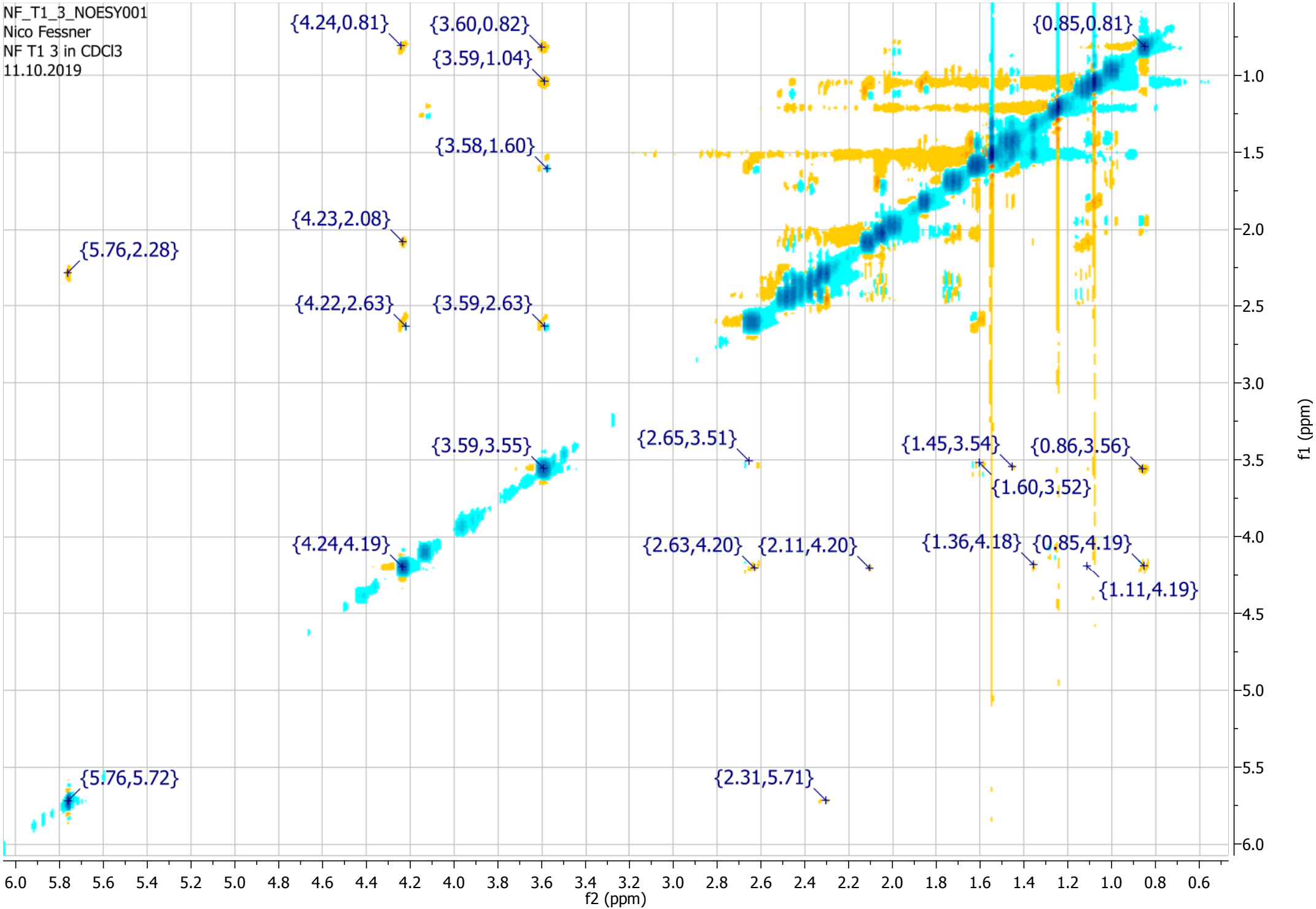
NF_T1_3_NOESY001
Nico Fessner
NF T1 3 in CDCl3
11.10.2019
{4.24,0.81}
{3.60,0.82}
{3.59,1.04}
{0.85,0.81}
{3.58,1.60}
{4.23,2.08}
{5.76,2.28}
{4.22,2.63}
{3.59,2.63}
{3.59,3.55}
{2.65,3.51}
{1.45,3.54}
{0.86,3.56}
{1.60,3.52}
{4.24,4.19}
{2.63,4.20}
{2.11,4.20}
{1.36,4.18}
{0.85,4.19}
{1.11,4.19}
{5.76,5.72}
{2.31,5.71}
f2 (ppm)
f1 (ppm)

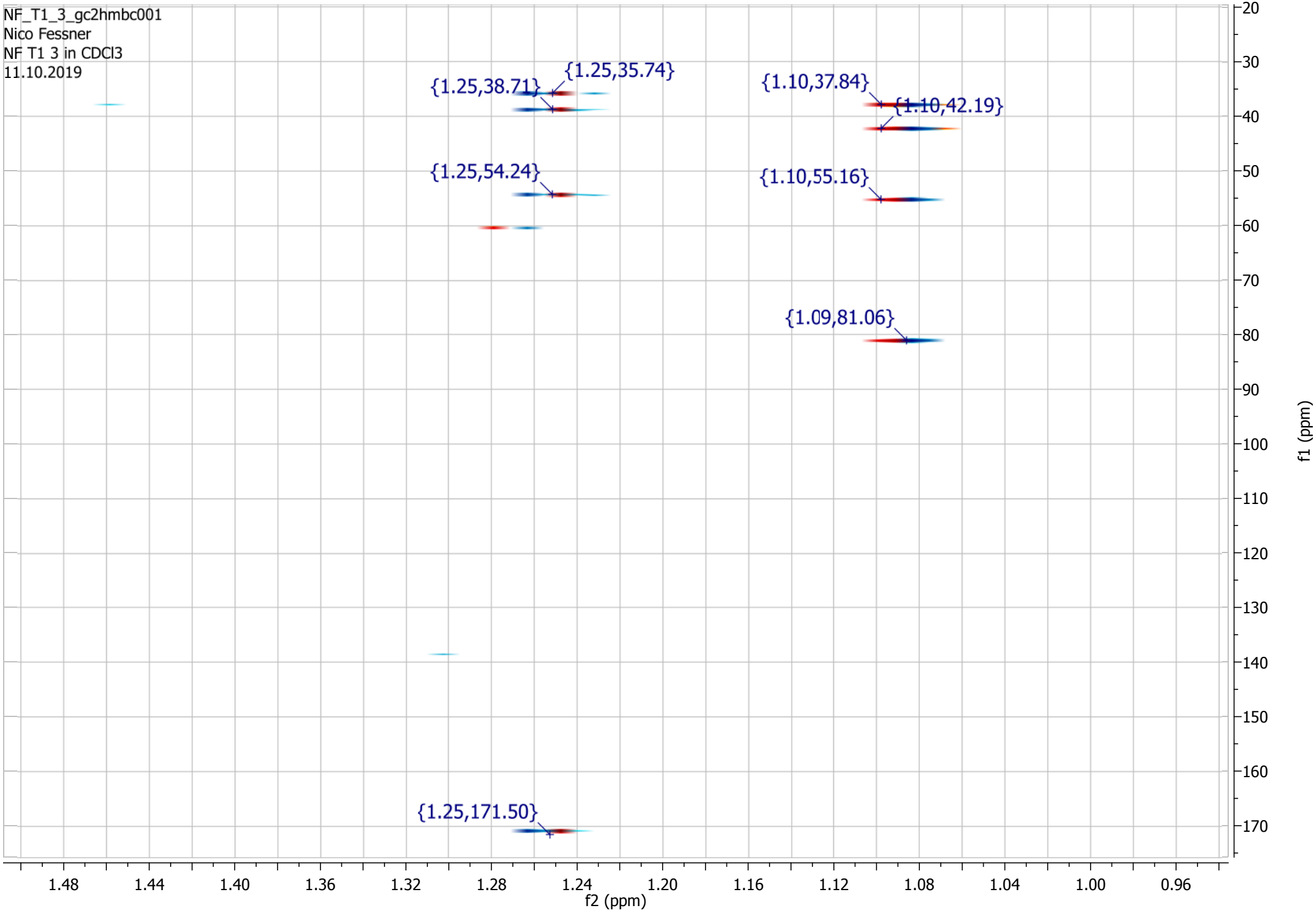
NF_T1_3_gc2hmbc001
Nico Fessner
NF T1 3 in CDCl3
11.10.2019
{1.25,35.74}
{1.25,38.71}
{1.10,37.84}
{1.10,42.19}
{1.25,54.24}
{1.10,55.16}
{1.09,81.06}
{1.25,171.50}
f2 (ppm)
f1 (ppm)

6-dehydro-15β-hydroxytestosterone (**7**)

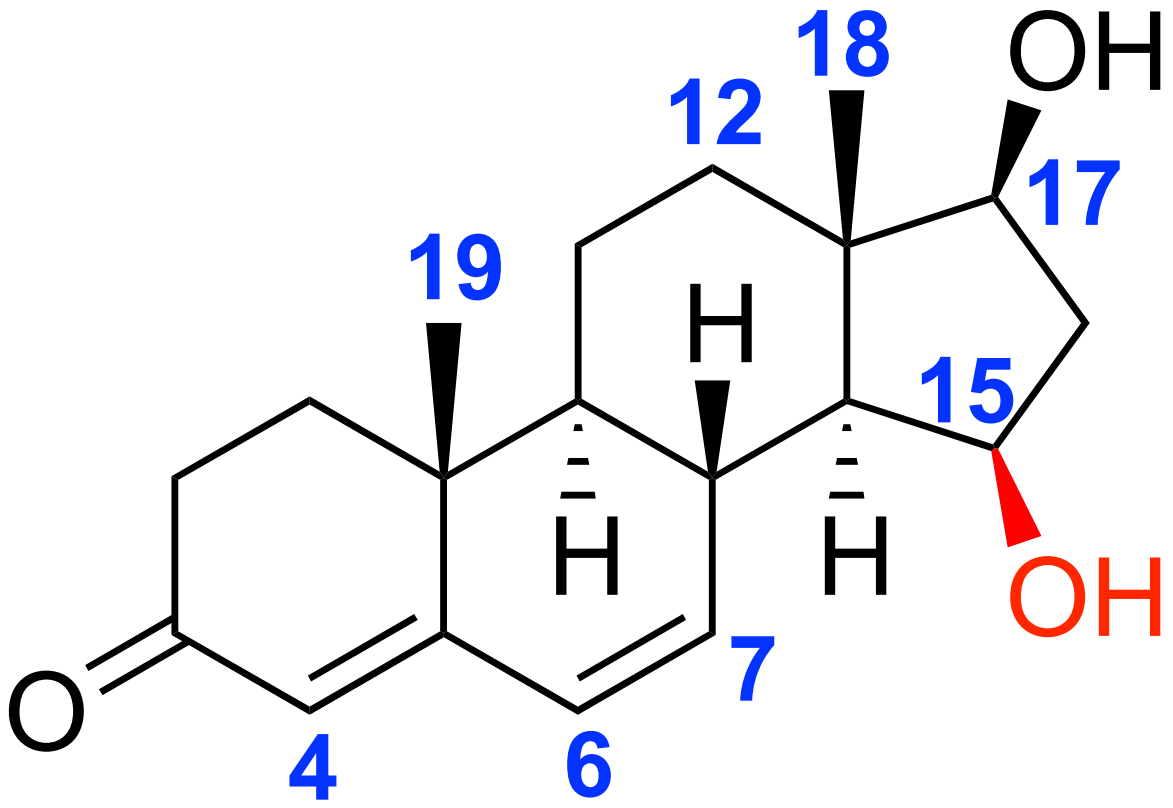

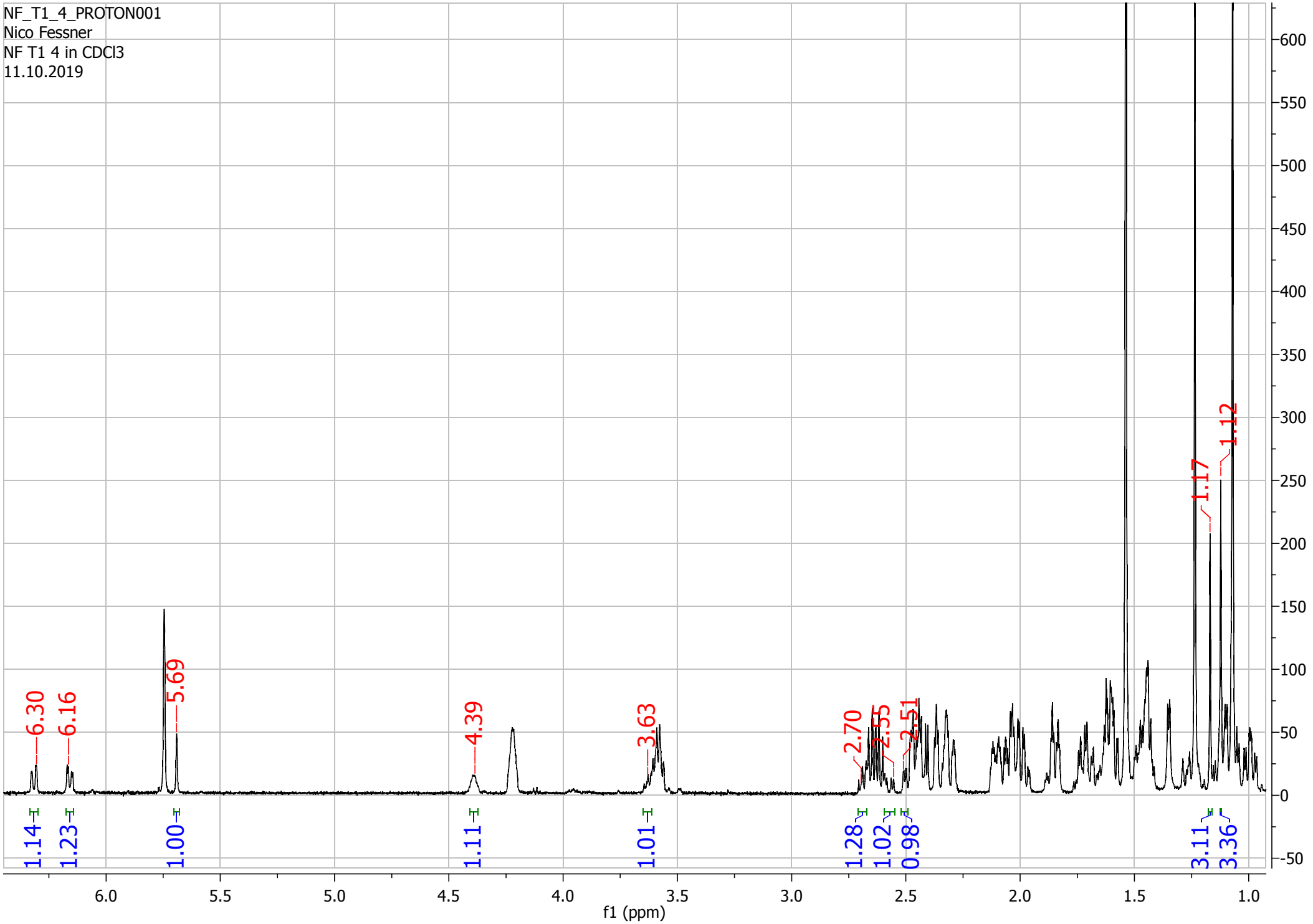
NF_T1_4_PROTON001
Nico Fessner
NF T1 4 in CDCl3
11.10.2019
6.30
6.16
5.69
4.39
3.63
2.70
2.55
2.51
1.17
1.12
1.14
1.23
1.00
1.11
1.01
1.28
1.02
0.98
3.11
3.36
f1 (ppm)

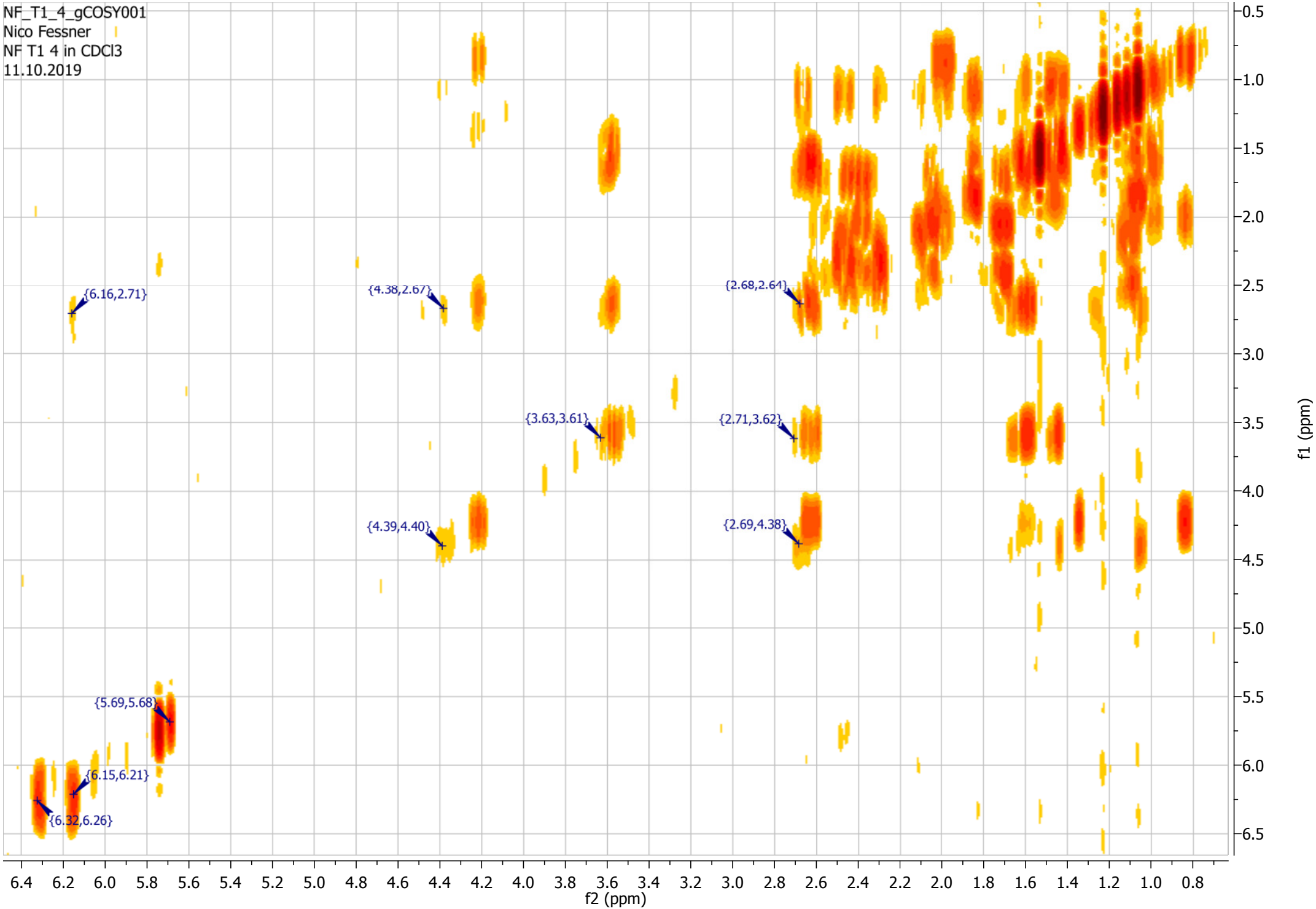
NF_T1_4_gCOSY001
Nico Fessner
NF T1 4 in CDCl3
11.10.2019
{6.16,2.71}
{4.38,2.67}
{2.68,2.64}
{3.63,3.61}
{2.71,3.62}
{4.39,4.40}
{2.69,4.38}
{5.69,5.68}
{6.15,6.21}
{6.32,6.26}
f2 (ppm)
f1 (ppm)

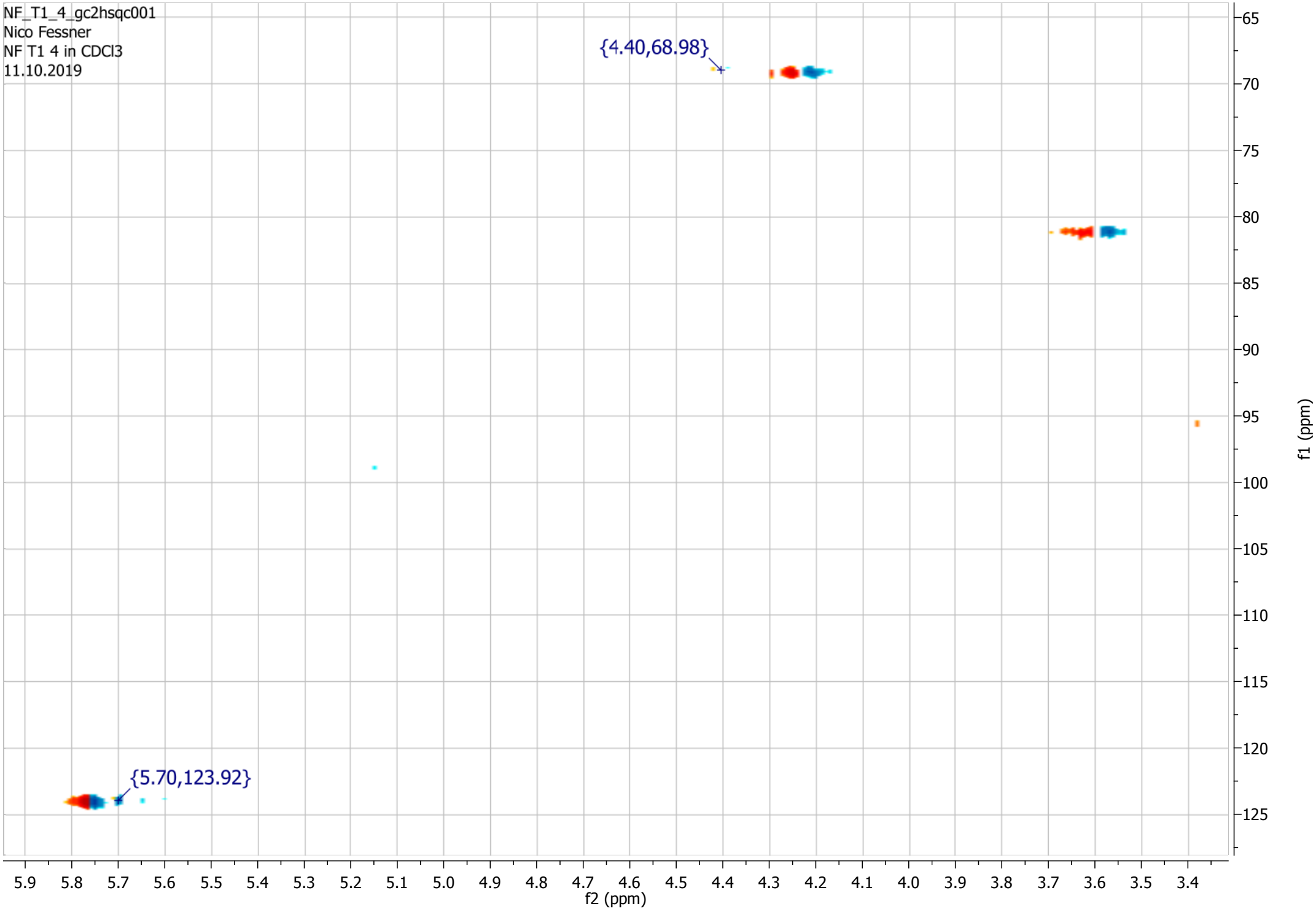
NF_T1_4_gc2hsqc001
Nico Fessner
NF T1 4 in CDCl3
11.10.2019
{4.40,68.98}
{5.70,123.92}
f2 (ppm)
f1 (ppm)

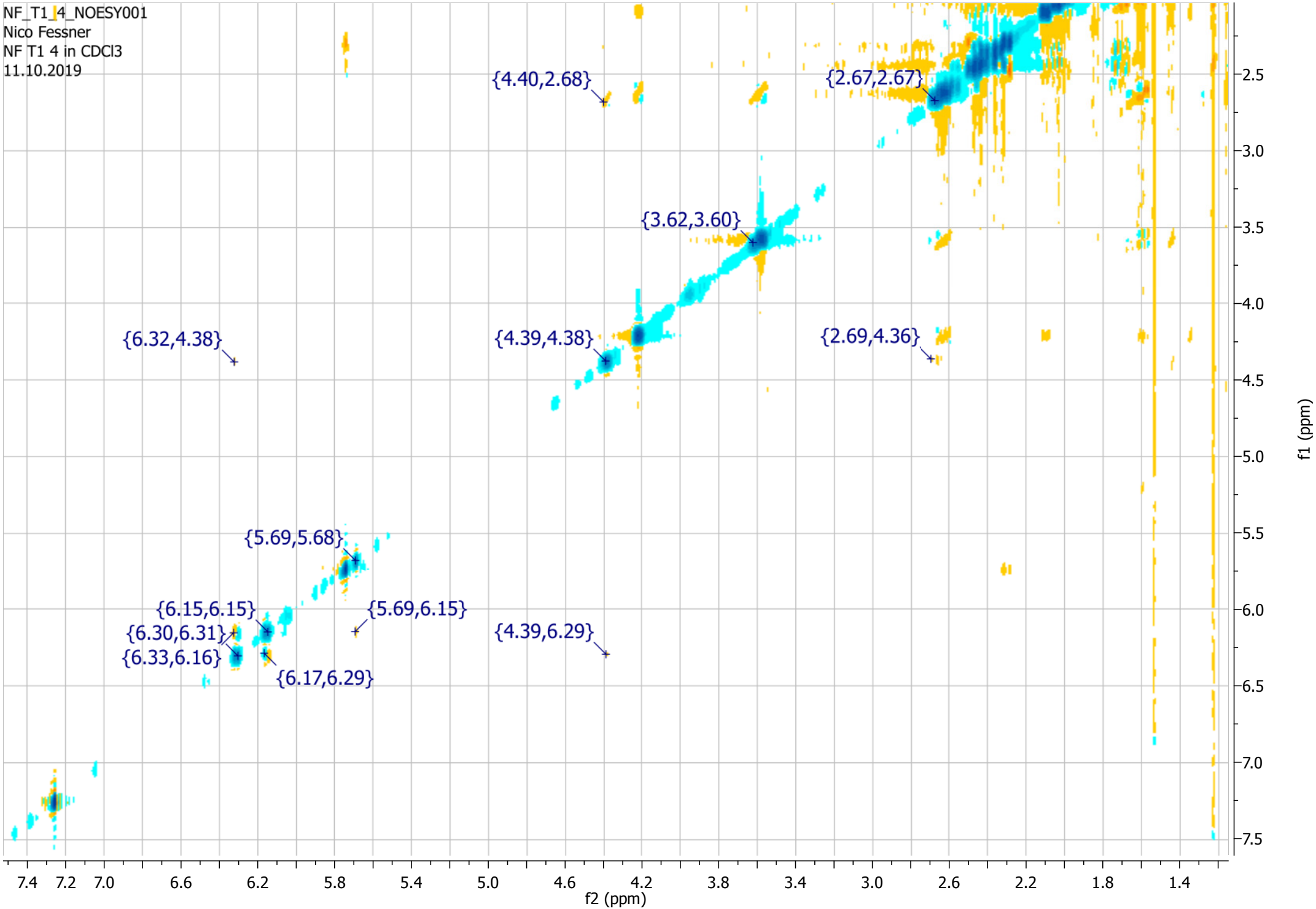
NF_T1_4_NOESY001
Nico Fessner
NF T1 4 in CDCl3
11.10.2019
{4.40,2.68}
{2.67,2.67}
{3.62,3.60}
{6.32,4.38}
{4.39,4.38}
{2.69,4.36}
{5.69,5.68}
{6.15,6.15}
{5.69,6.15}
{6.30,6.31}
{4.39,6.29}
{6.33,6.16}
{6.17,6.29}
f2 (ppm)
f1 (ppm)

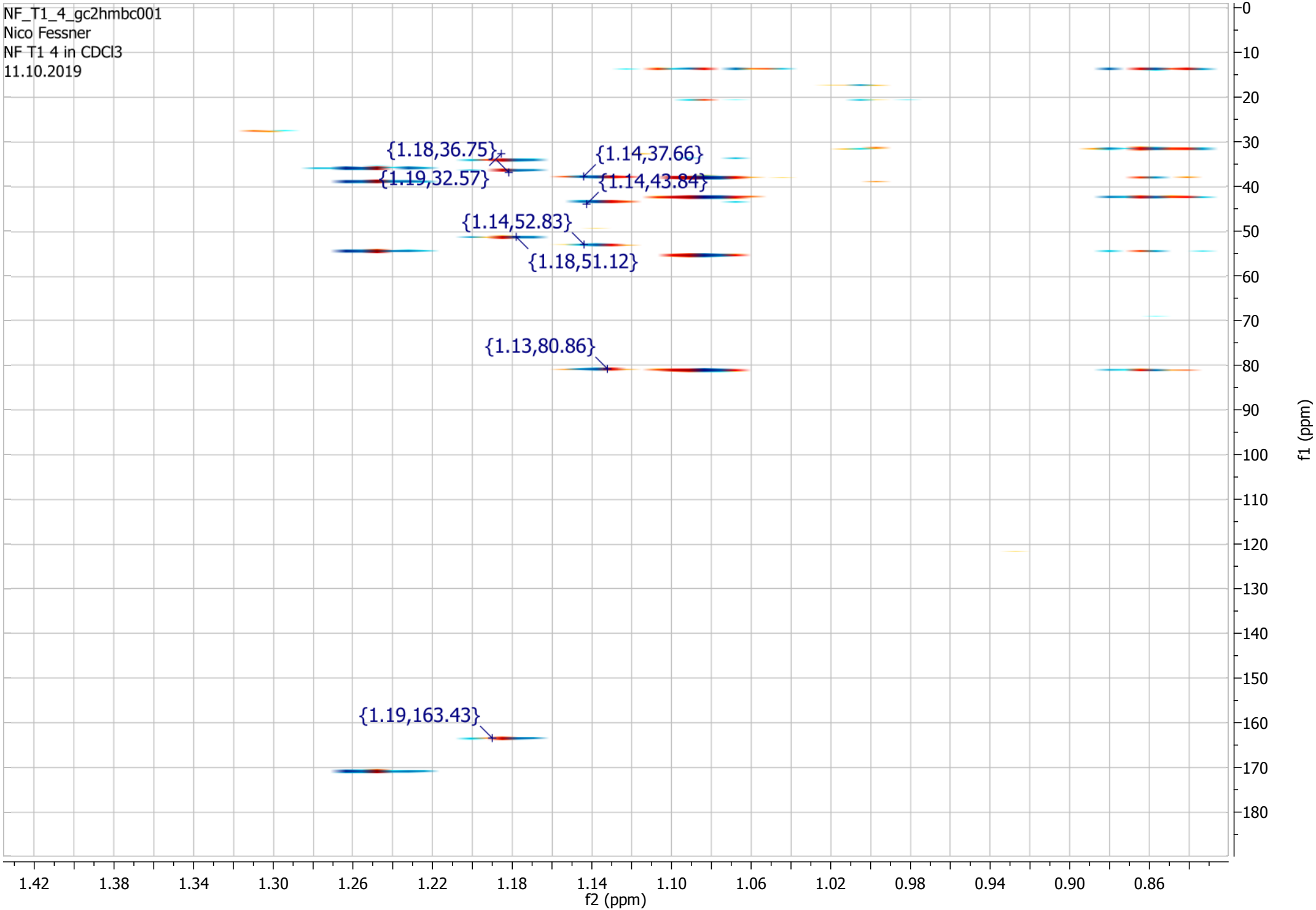
NF_T1_4_gc2hmbc001
Nico Fessner
NF T1 4 in CDCl3
11.10.2019
{1.18,36.75}
{1.19,32.57}
{1.14,37.66}
{1.14,43.84}
{1.14,52.83}
{1.18,51.12}
{1.13,80.86}
{1.19,163.43}
f2 (ppm)
f1 (ppm)

6β,16β-dihydroxytestosterone (**8**)

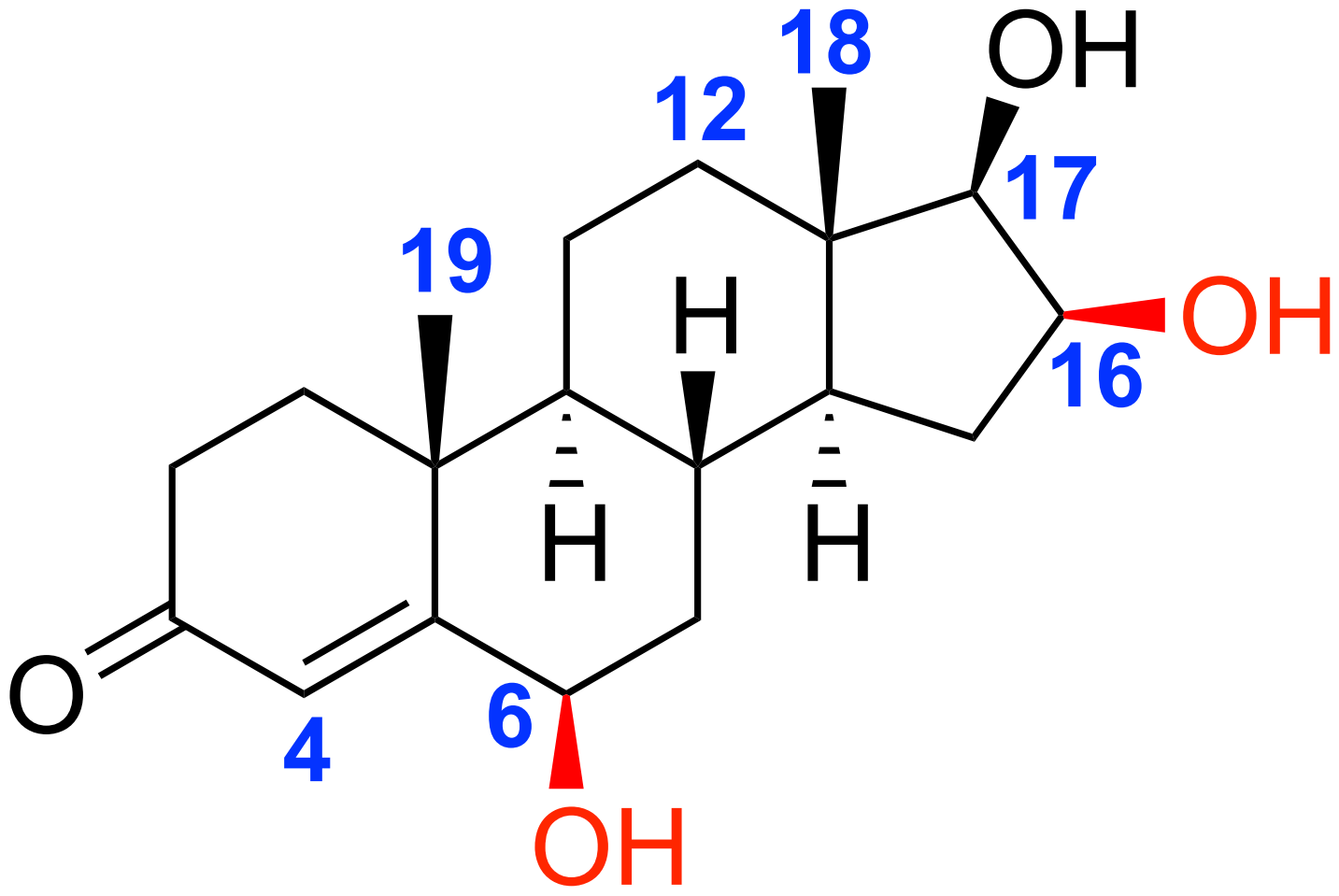

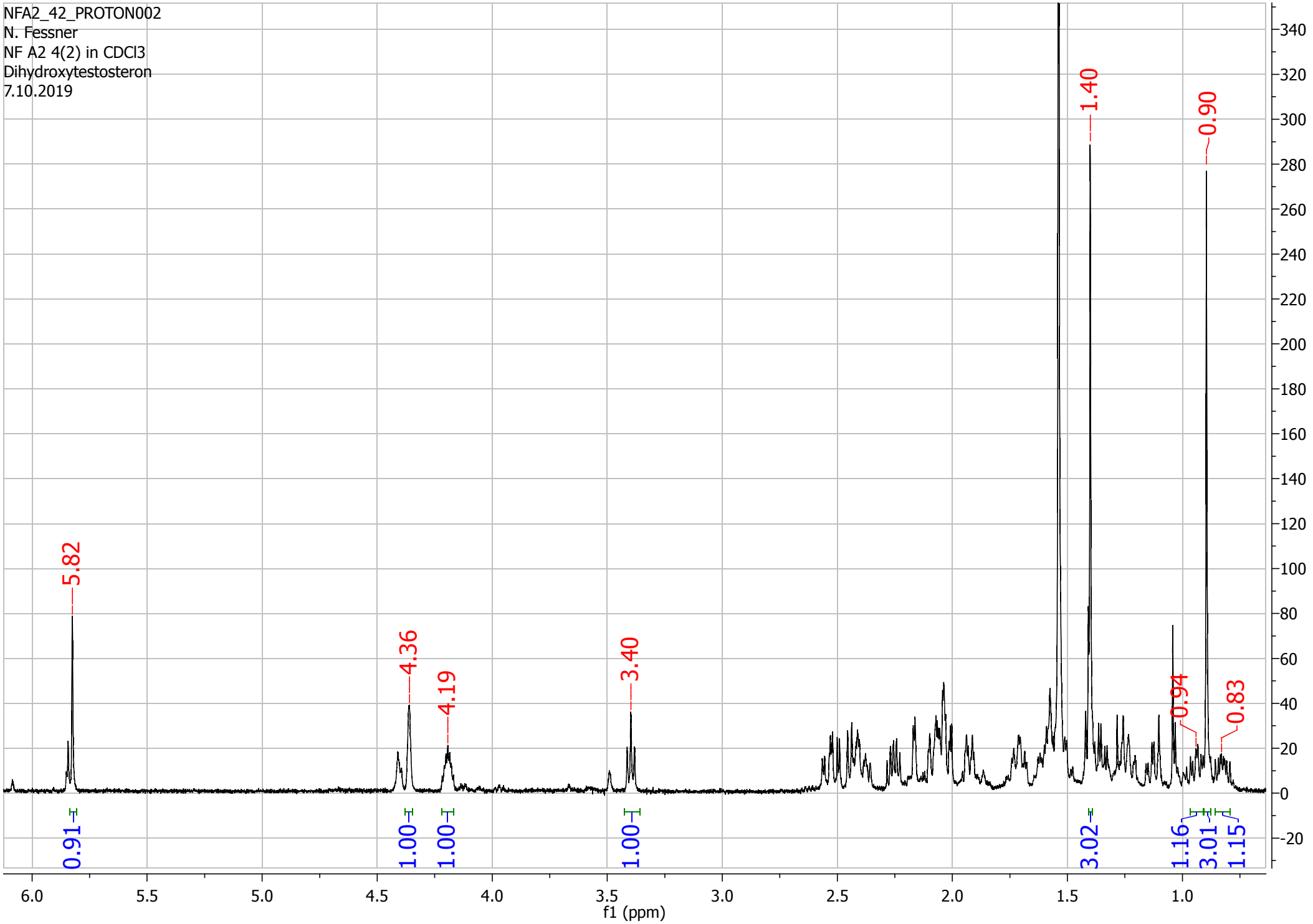
NFA2_42_PROTON002
N. Fessner
NF A2 4(2) in CDCl3
Dihydroxytestosteron
7.10.2019
5.82
4.36
4.19
3.40
1.40
0.94
0.90
0.83
0.91
1.00
1.00
1.00
3.02
1.16
3.01
1.15
f1 (ppm)

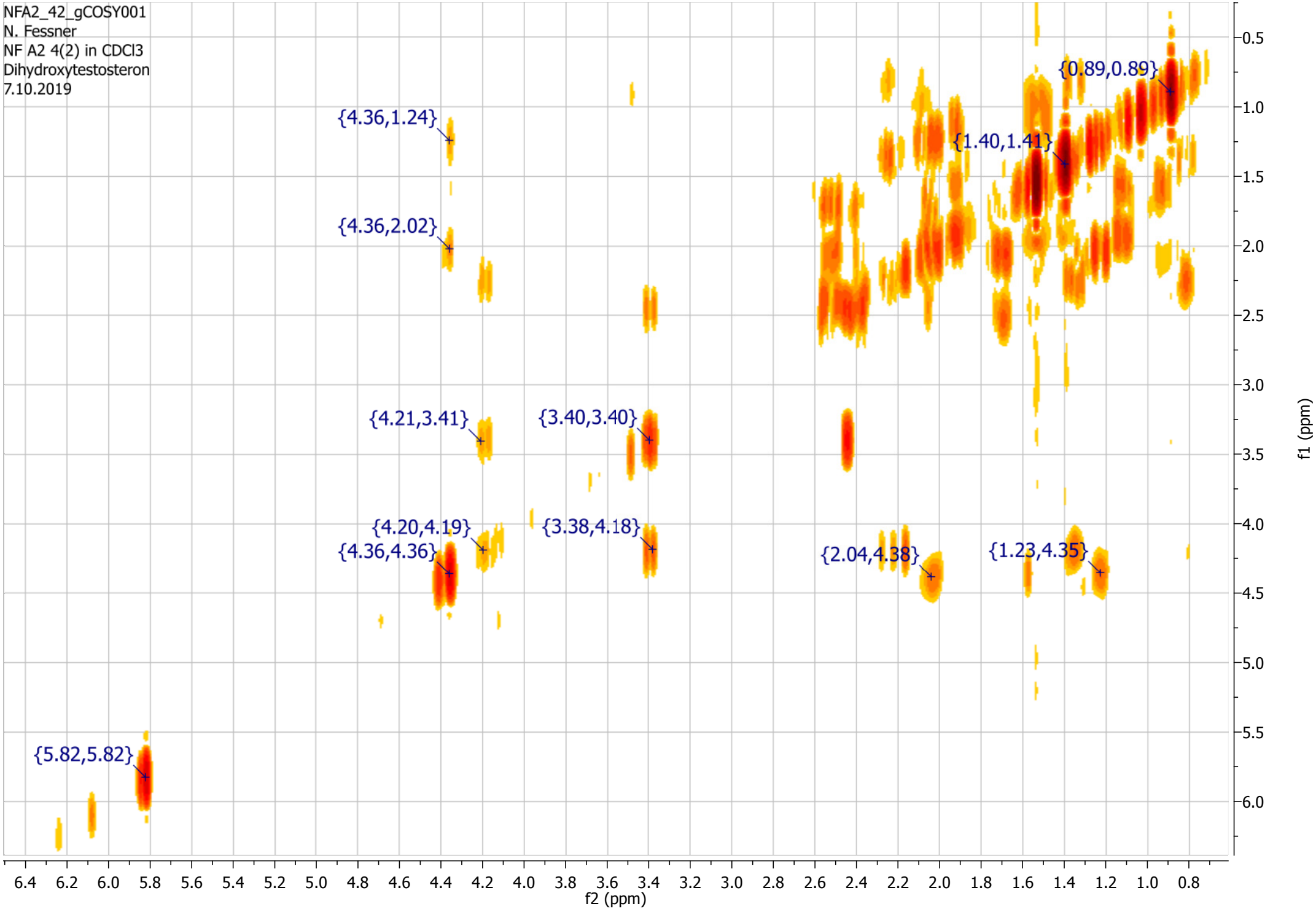
NFA2_42_gCOSY001
N. Fessner
NF A2 4(2) in CDCl3
Dihydroxytestosteron
7.10.2019
{0.89,0.89}
{1.40,1.41}
{4.36,1.24}
{4.36,2.02}
{4.21,3.41}
{3.40,3.40}
{4.20,4.19}
{3.38,4.18}
{4.36,4.36}
{2.04,4.38}
{1.23,4.35}
{5.82,5.82}
f2 (ppm)
f1 (ppm)

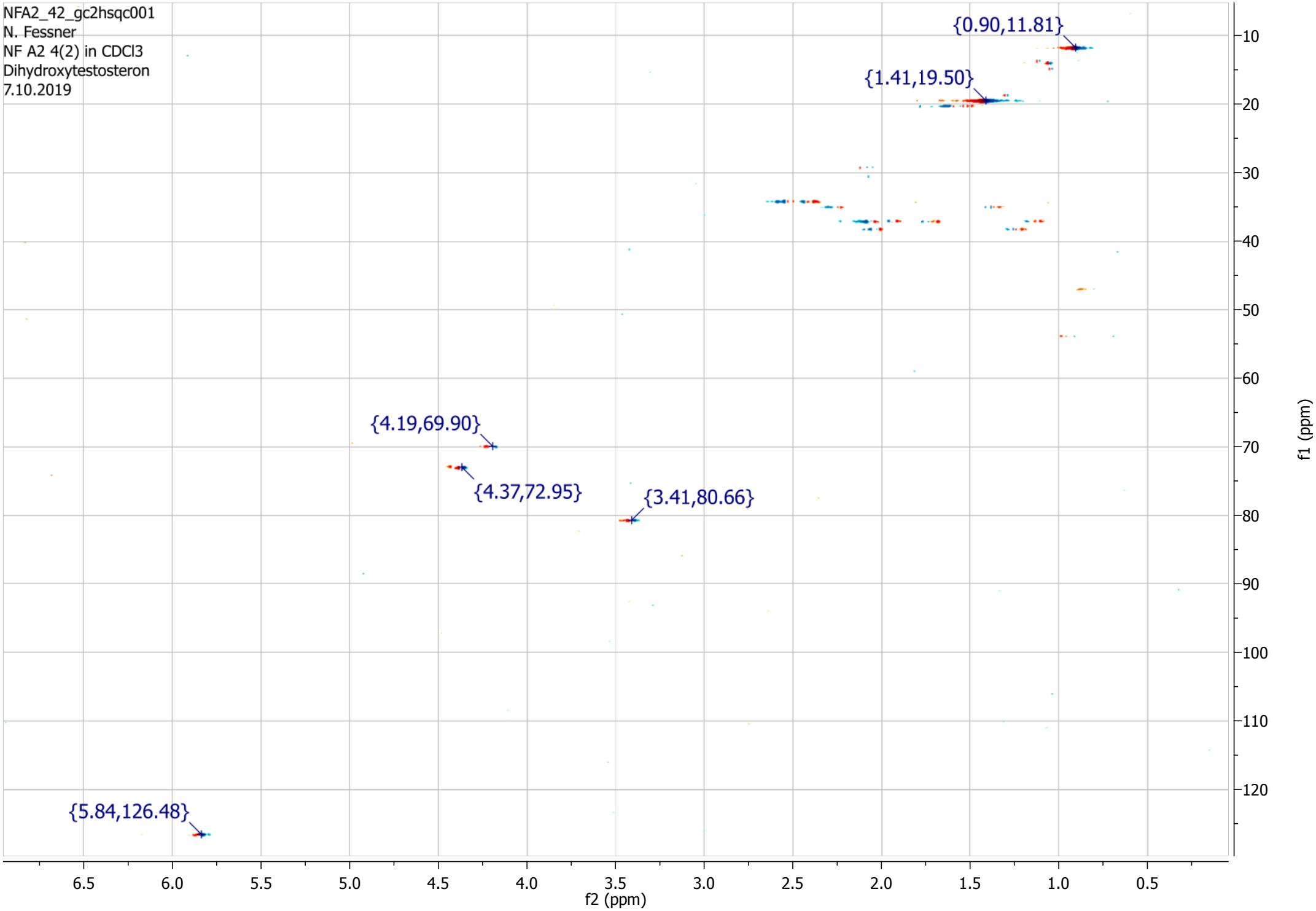
NFA2_42_gc2hsqc001
N. Fessner
NF A2 4(2) in CDCl3
Dihydroxytestosteron
7.10.2019
{0.90,11.81}
{1.41,19.50}
{4.19,69.90}
{4.37,72.95}
{3.41,80.66}
{5.84,126.48}
f2 (ppm)
f1 (ppm)

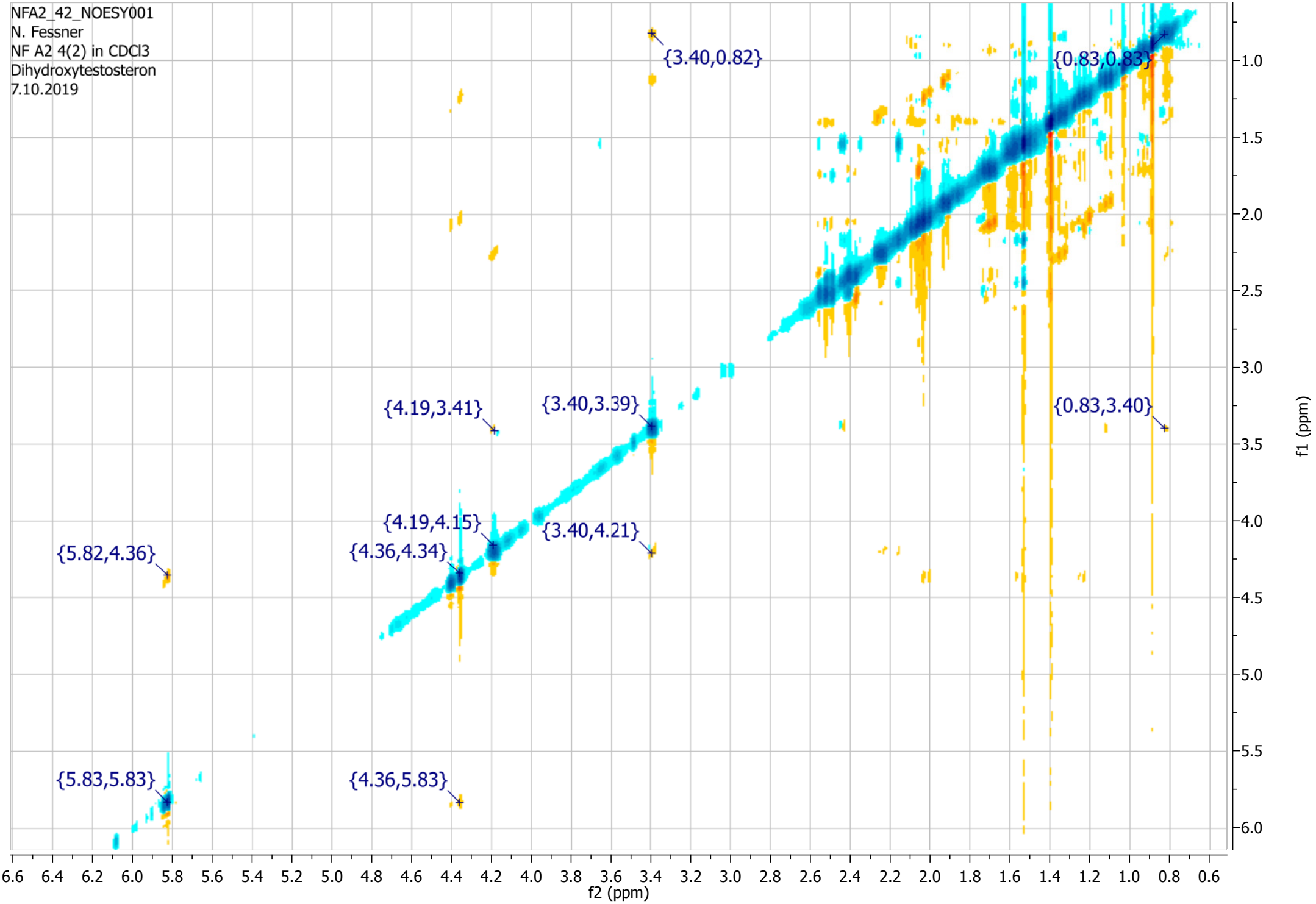
NFA2_42_NOESY001
N. Fessner
NF A2 4(2) in CDCl3
Dihydroxytestosteron
7.10.2019
{3.40,0.82}
{0.83,0.83}
{4.19,3.41}
{3.40,3.39}
{0.83,3.40}
{4.19,4.15}
{3.40,4.21}
{4.36,4.34}
{5.82,4.36}
{5.83,5.83}
{4.36,5.83}
f2 (ppm)
f1 (ppm)

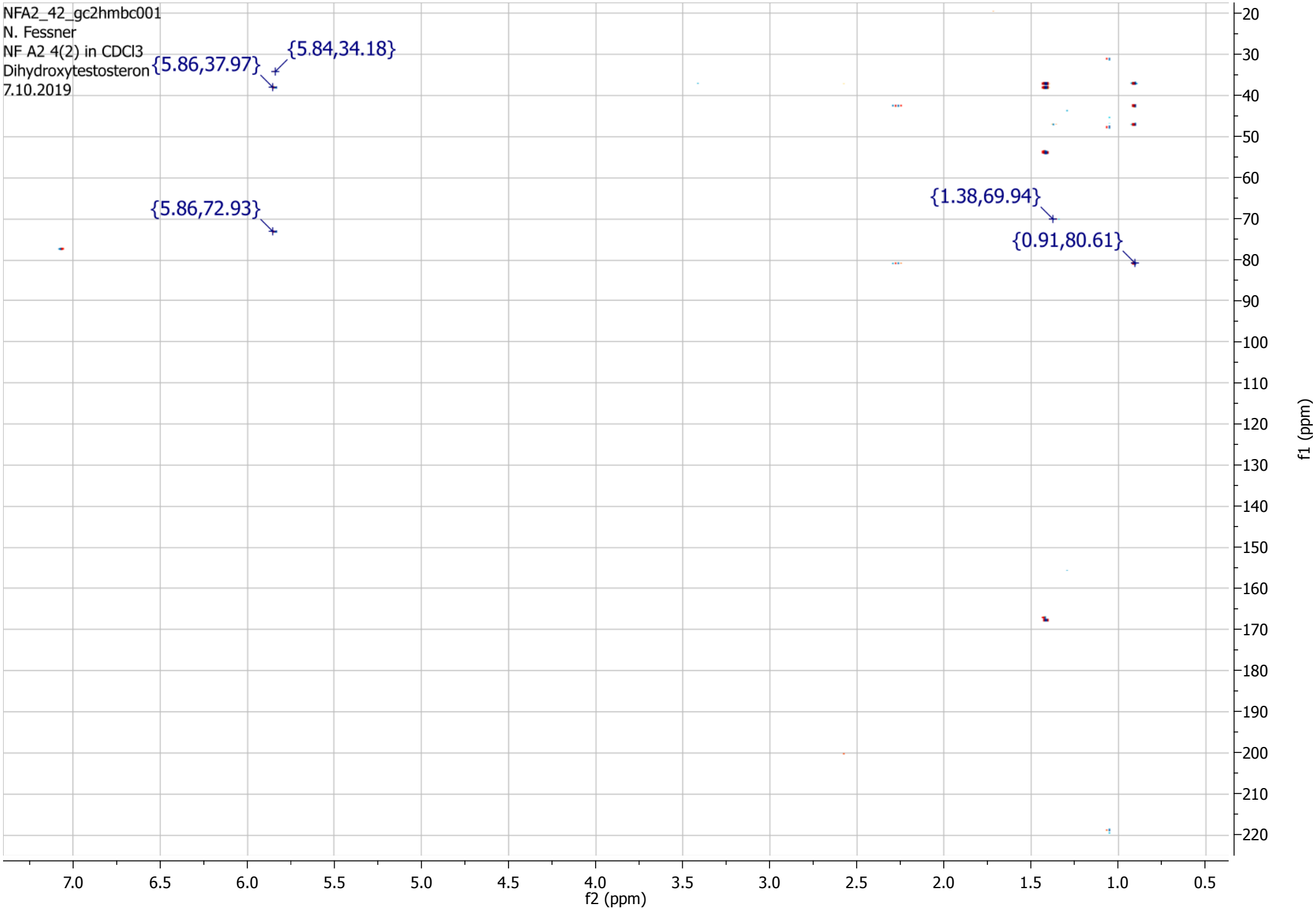
NFA2_42_gc2hmbc001
N. Fessner
NF A2 4(2) in CDCl3
Dihydroxytestosteron
7.10.2019
{5.84,34.18}
{5.86,37.97}
{5.86,72.93}
{1.38,69.94}
{0.91,80.61}
f2 (ppm)
f1 (ppm)

6β,17β-dihydroxy-4-androstene-3,16-dione (**9**)

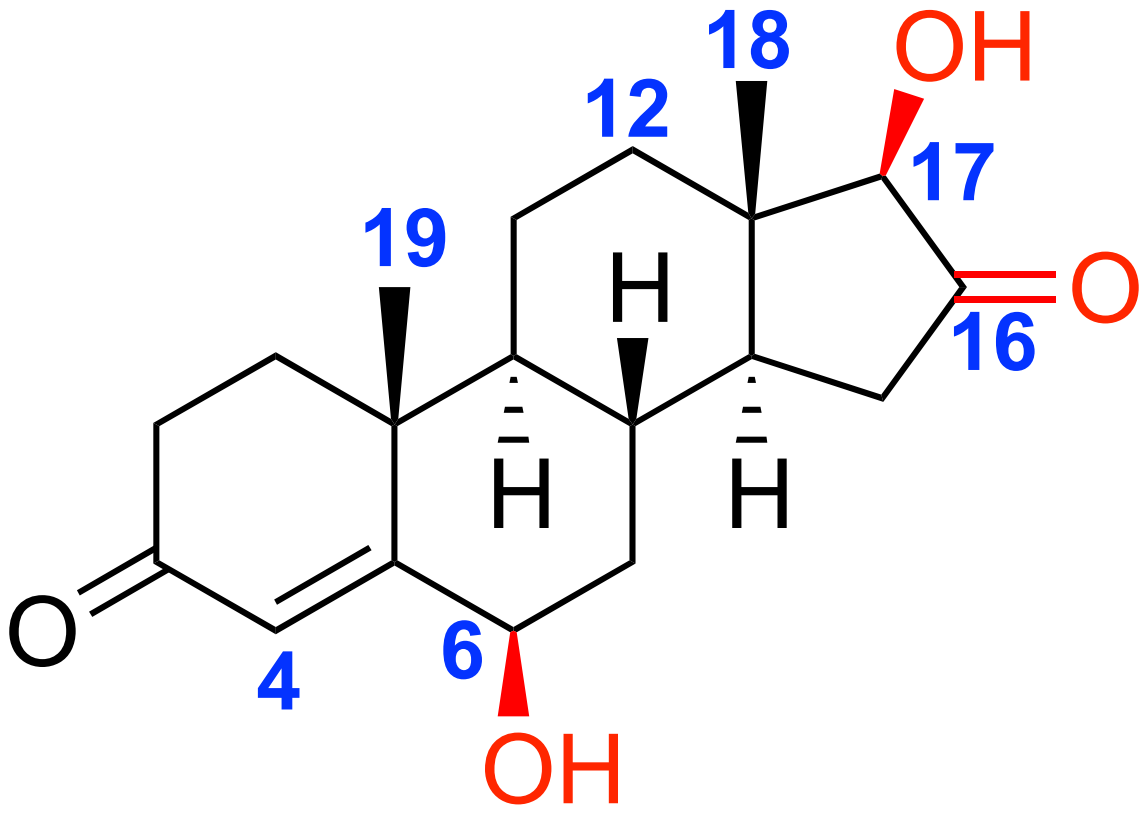

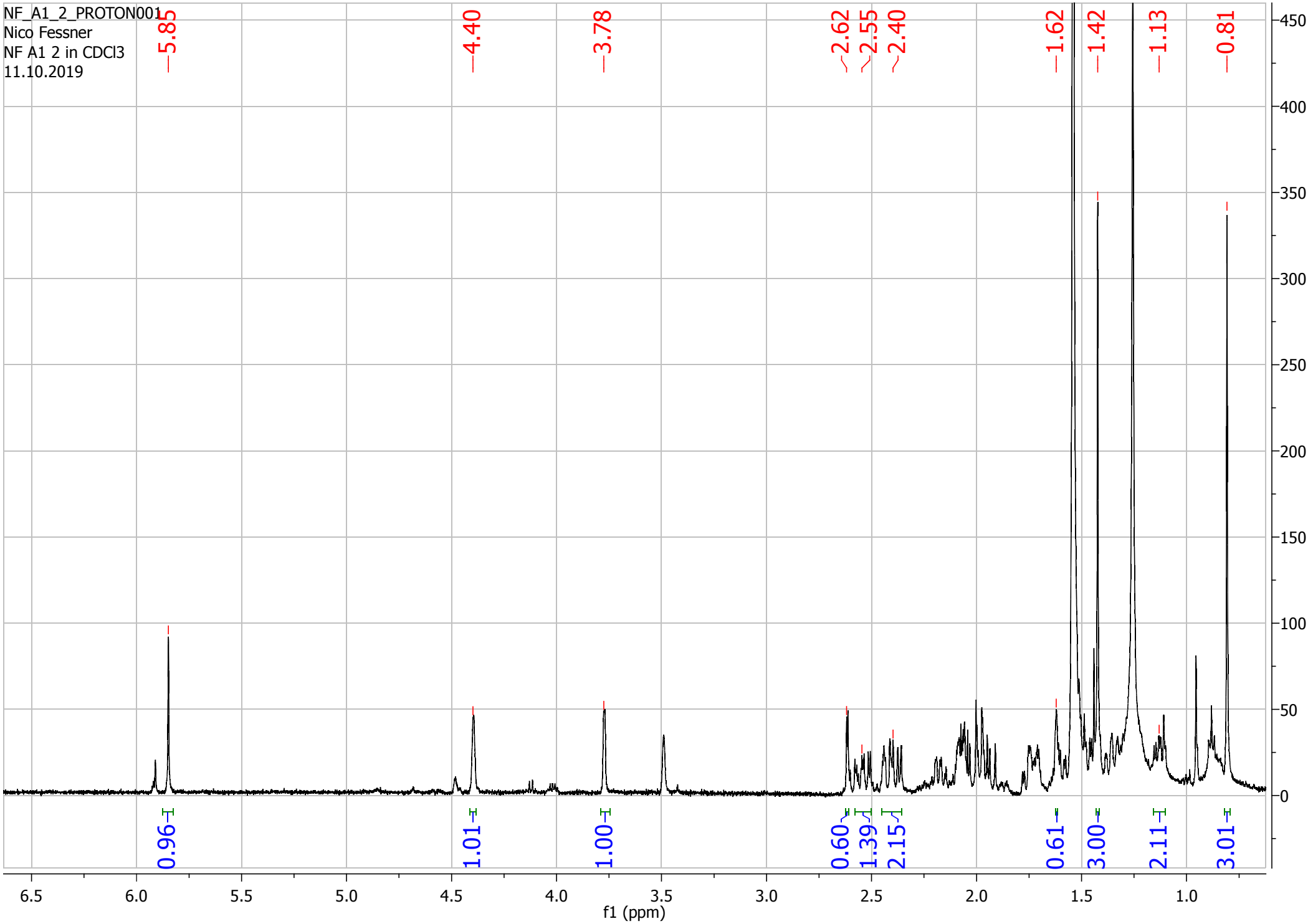
NF_A1_2_PROTON001
Nico Fessner
NF A1 2 in CDCl3
11.10.2019
5.85
4.40
3.78
2.62
2.55
2.40
1.62
1.42
1.13
0.81
0.96
1.01
1.00
0.60
1.39
2.15
0.61
3.00
2.11
3.01
f1 (ppm)

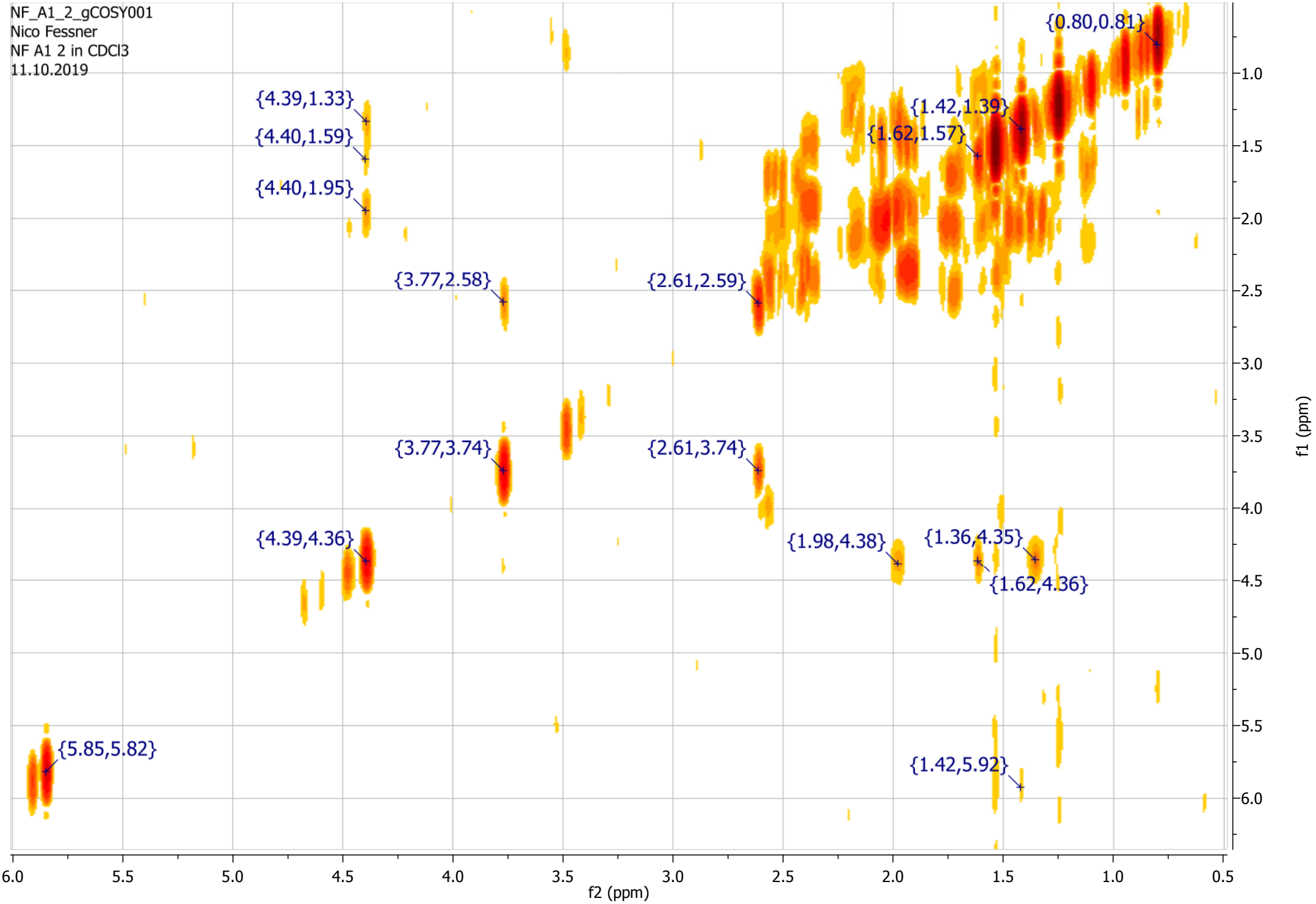
NF_A1_2_gCOSY001
Nico Fessner
NF A1 2 in CDCl3
11.10.2019
{0.80,0.81}
{4.39,1.33}
{4.40,1.59}
{4.40,1.95}
{1.42,1.39}
{1.62,1.57}
{3.77,2.58}
{2.61,2.59}
{3.77,3.74}
{2.61,3.74}
{4.39,4.36}
{1.98,4.38}
{1.36,4.35}
{1.62,4.36}
{5.85,5.82}
{1.42,5.92}
f2 (ppm)
f1 (ppm)

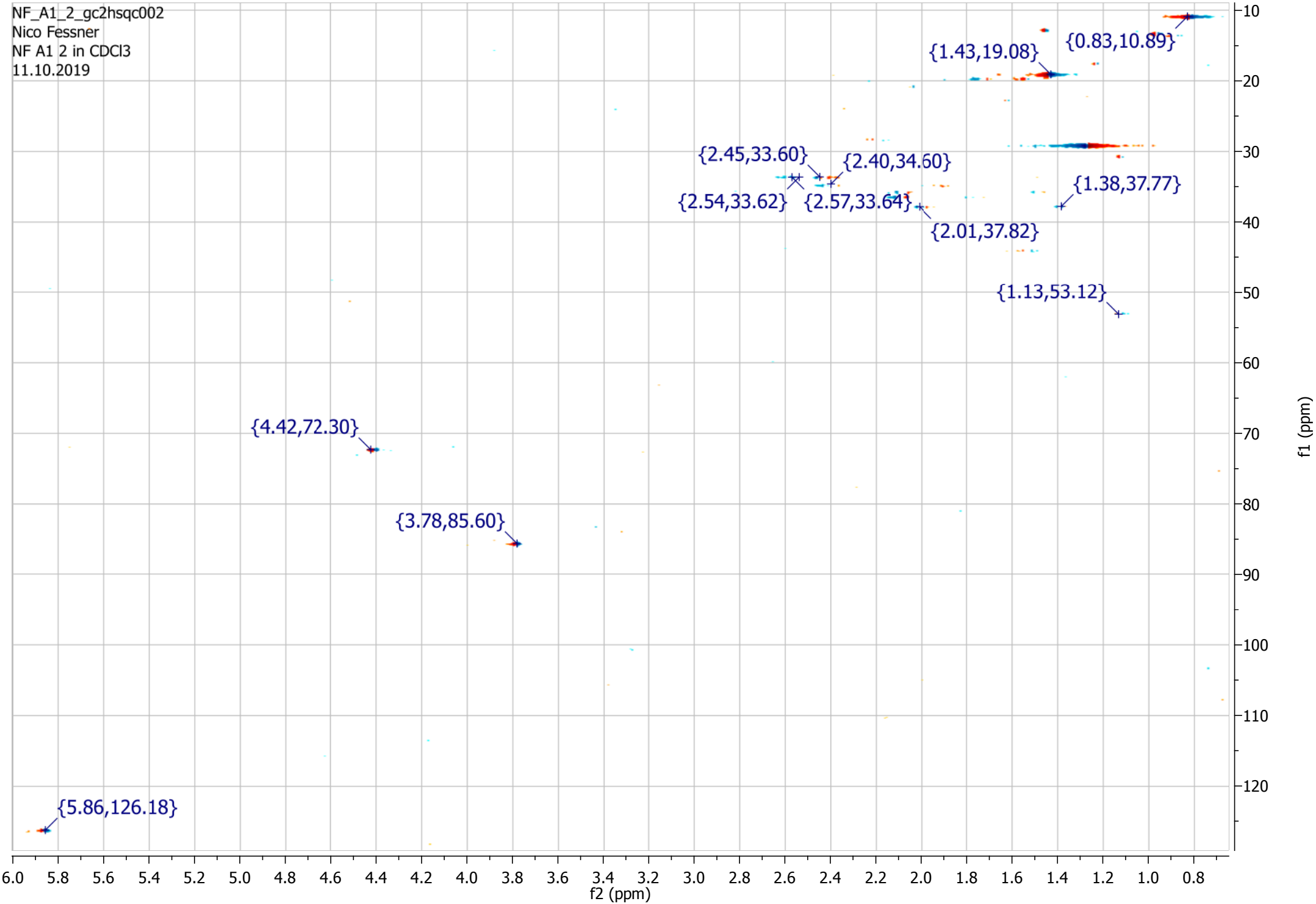
NF_A1_2_gc2hsqc002
Nico Fessner
NF A1 2 in CDCl3
11.10.2019
{0.83,10.89}
{1.43,19.08}
{2.45,33.60}
{2.40,34.60}
{2.54,33.62}
{2.57,33.64}
{1.38,37.77}
{2.01,37.82}
{1.13,53.12}
{4.42,72.30}
{3.78,85.60}
{5.86,126.18}
f2 (ppm)
f1 (ppm)

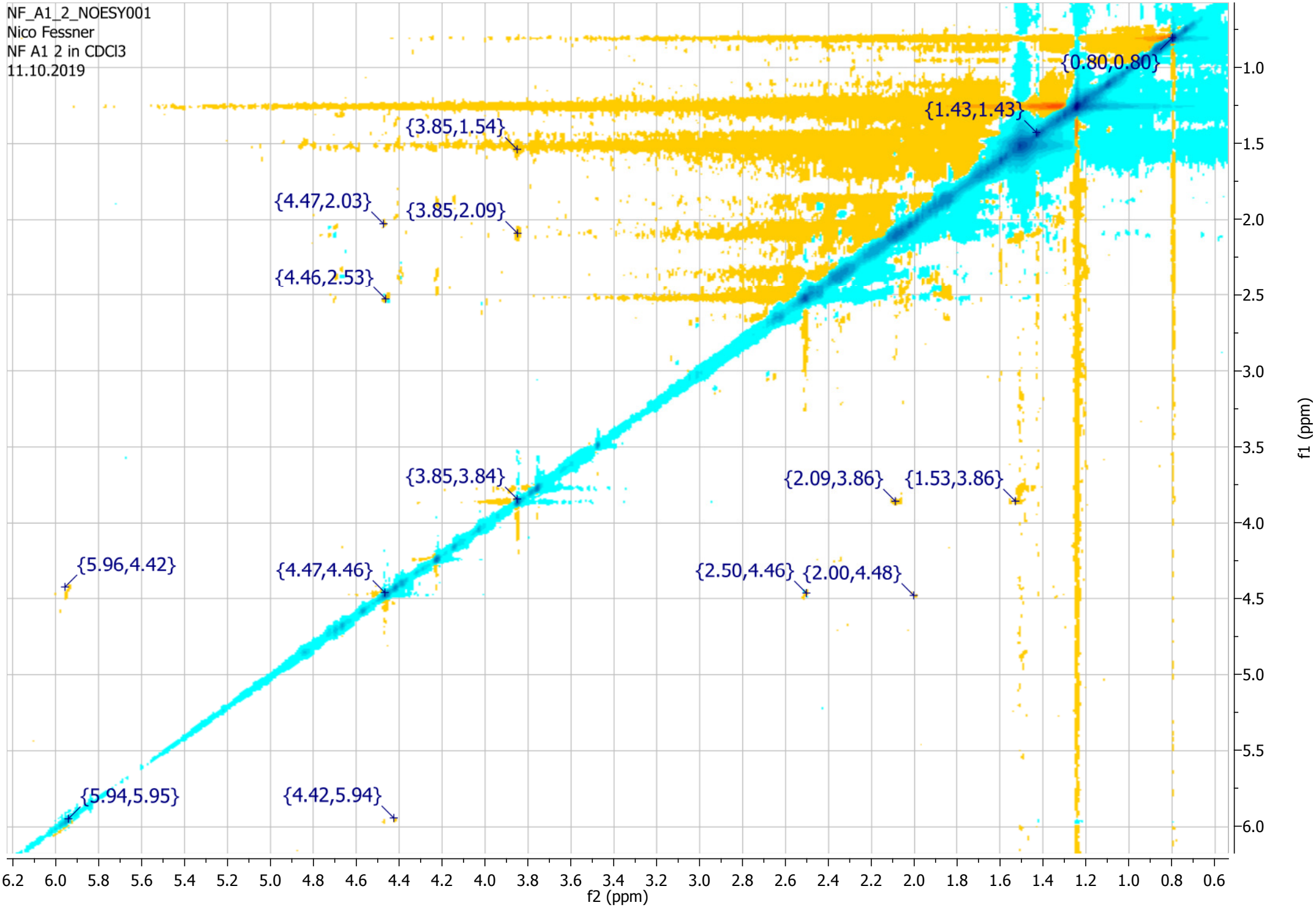
NF_A1_2_NOESY001
Nico Fessner
NF A1 2 in CDCl3
11.10.2019
{0.80,0.80}
{1.43,1.43}
{3.85,1.54}
{4.47,2.03}
{3.85,2.09}
{4.46,2.53}
{3.85,3.84}
{2.09,3.86}
{1.53,3.86}
{5.96,4.42}
{4.47,4.46}
{2.50,4.46}
{2.00,4.48}
{5.94,5.95}
{4.42,5.94}
f2 (ppm)
f1 (ppm)

Nico Fessner
NF A1 2 in CDCl3
11.10.2019

Sample Name:
NF_A1_2
Data Collected on:
fochpc35-inova500
Archive directory:
/home/weber_j/vnmrsys/data/i500_Oct11
Sample directory:
NF_A1_201
FidFile: NF_A1_2_gc2hmbc001

Pulse Sequence: gc2hmbc
Solvent: cdcl3
Data collected on: Oct 18 2019

Temp. 30.0 C / 303.1 K
Operator: weber_j

Relax. delay 1.000 sec
Acq. time 0.150 sec
Width 7997.6 Hz
2D Width 30165.9 Hz
64 repetitions
2 x 512 increments
OBSERVE H1, 499.8397616 MHz
DATA PROCESSING
Sq. sine bell 0.064 sec
F1 DATA PROCESSING
Gauss apodization 0.008 sec
FT size 2048 x 4096
Total time 23 hr, 11 min

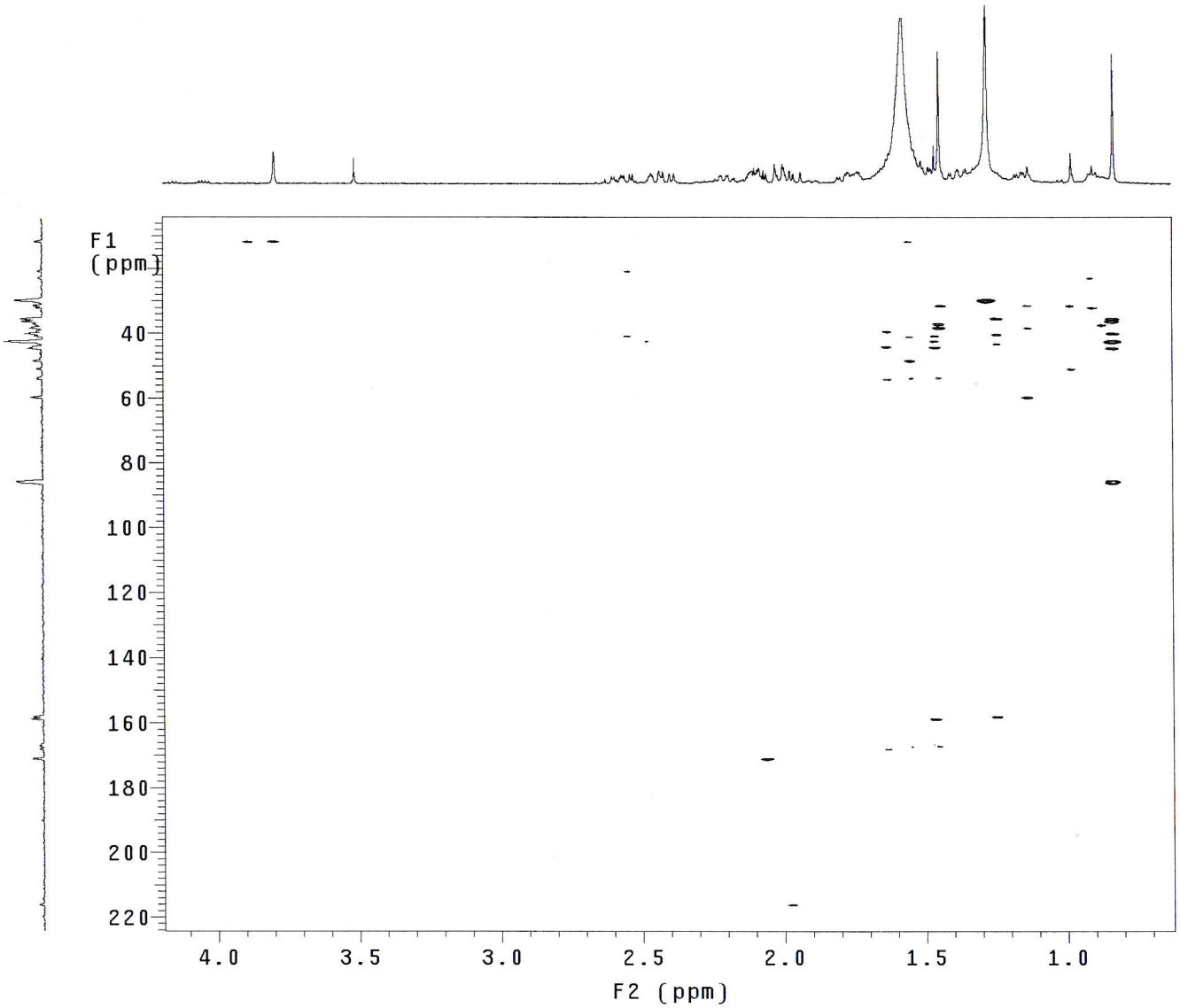

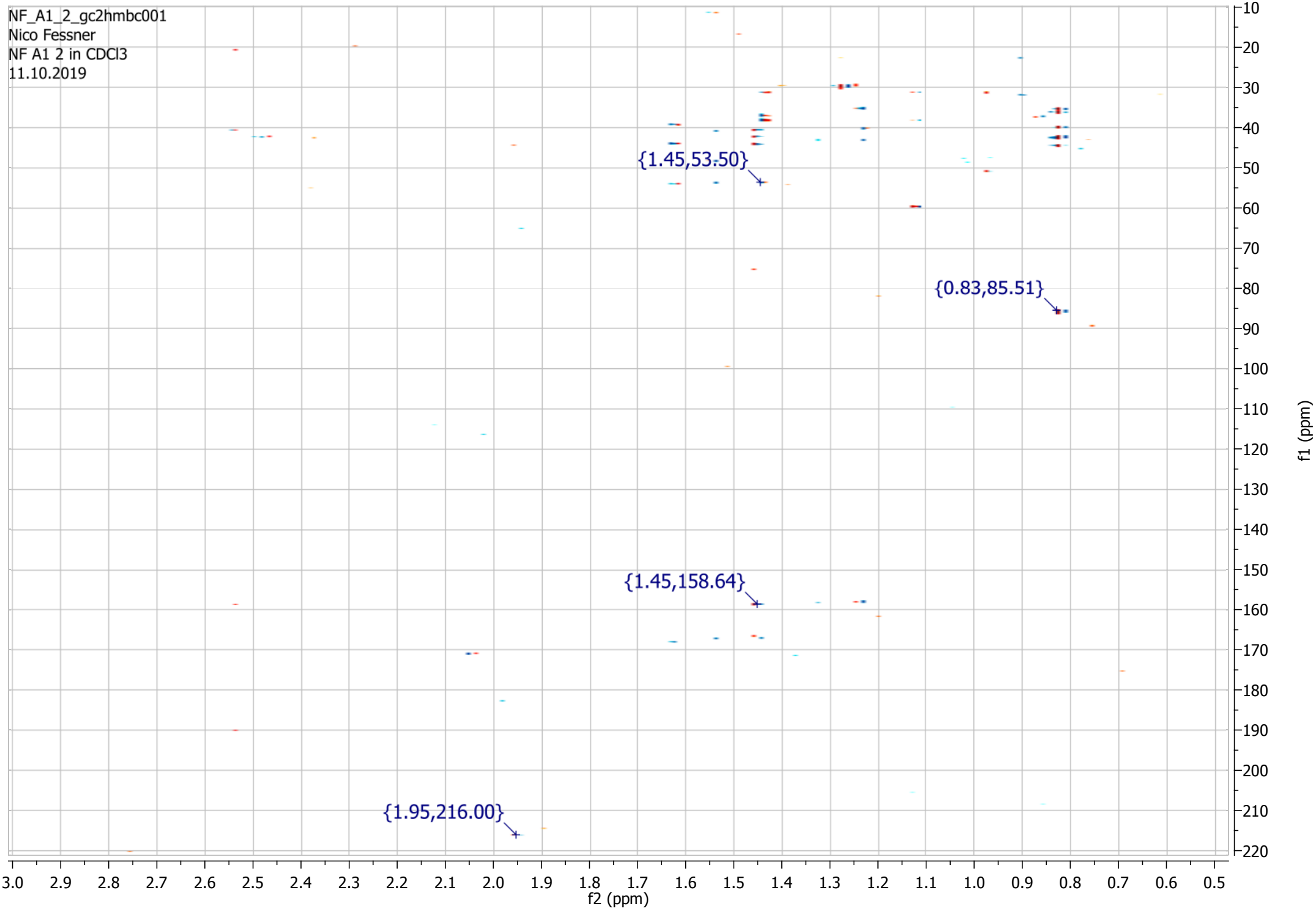
NF_A1_2_gc2hmbc001
Nico Fessner
NF A1 2 in CDCl3
11.10.2019
{1.45,53.50}
{0.83,85.51}
{1.45,158.64}
{1.95,216.00}
f2 (ppm)
f1 (ppm)

Nico Fessner
NF A1 2 in CDCl3
11.10.2019

Sample Name:
NF_A1_2
Data Collected on:
fochpc35-inova500
Archive directory:
/home/weber_j/vnmrsys/data/i500_Oct11
Sample directory:
NF_A1_201
FidFile: NF_A1_2_gc2hmbc001

Pulse Sequence: gc2hmbc
Solvent: cdcl3
Data collected on: Oct 18 2019

Temp. 30.0 C / 303.1 K
Operator: weber_j

Relax. delay 1.000 sec
Acq. time 0.150 sec
Width 7997.6 Hz
2D Width 30165.9 Hz
64 repetitions
2 x 512 increments
OBSERVE H1, 499.8397616 MHz
DATA PROCESSING
Sq. sine bell 0.064 sec
F1 DATA PROCESSING
Gauss apodization 0.008 sec
FT size 2048 x 4096
Total time 23 hr, 11 min

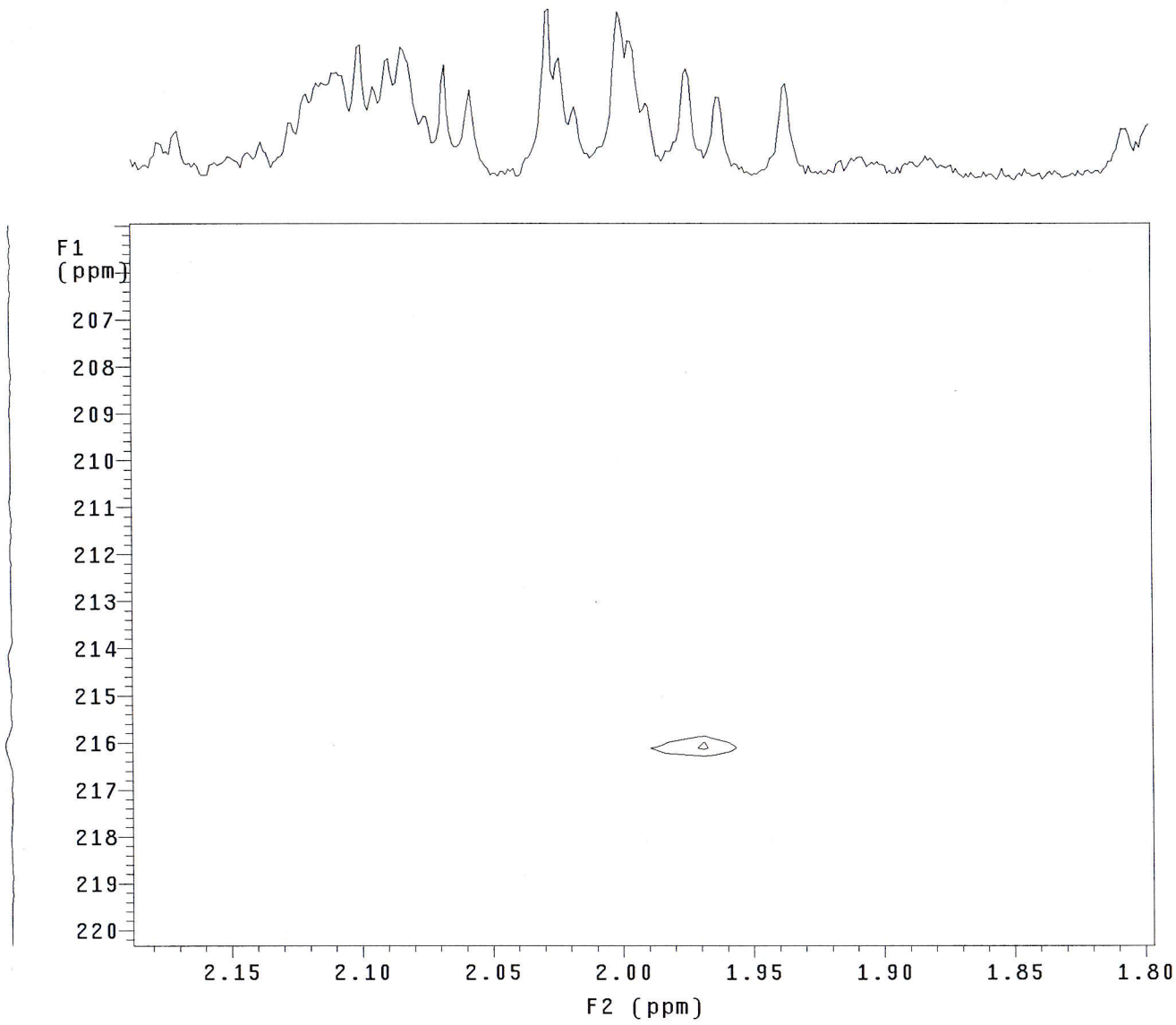

6β,12β-dihydroxyandrostenedione (**10**)

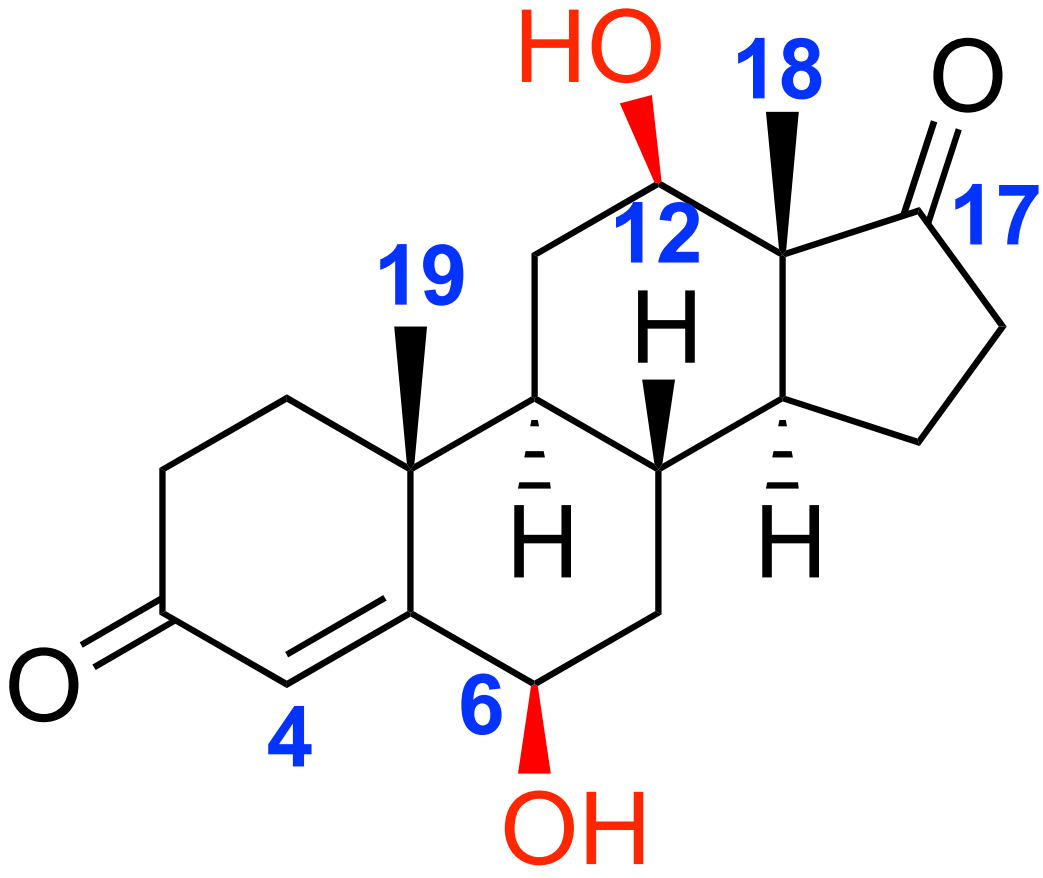

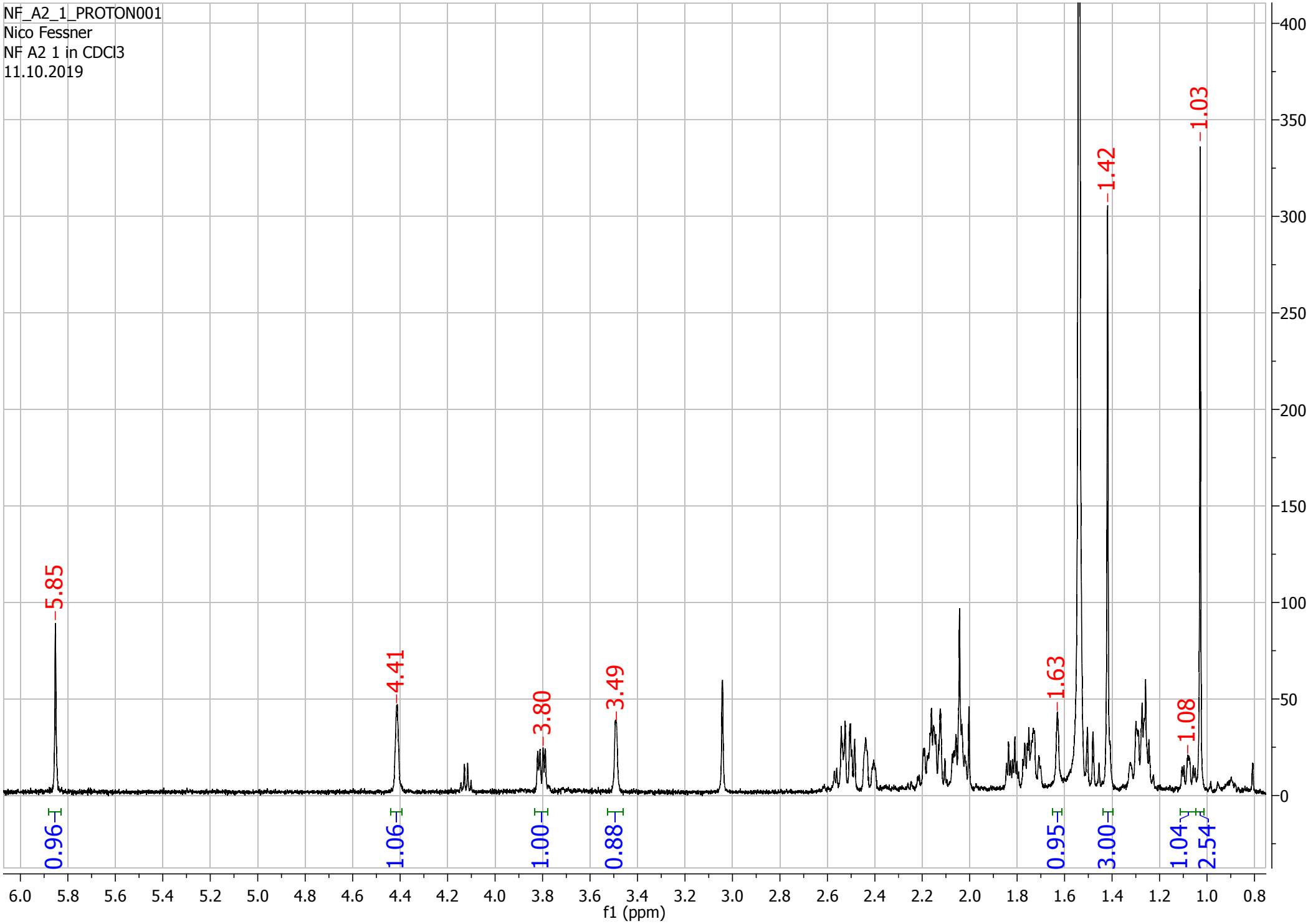
NF_A2_1_PROTON001
Nico Fessner
NF A2 1 in CDCl3
11.10.2019
5.85
4.41
3.80
3.49
1.63
1.42
1.08
1.03
0.96
1.06
1.00
0.88
0.95
3.00
1.04
2.54
f1 (ppm)

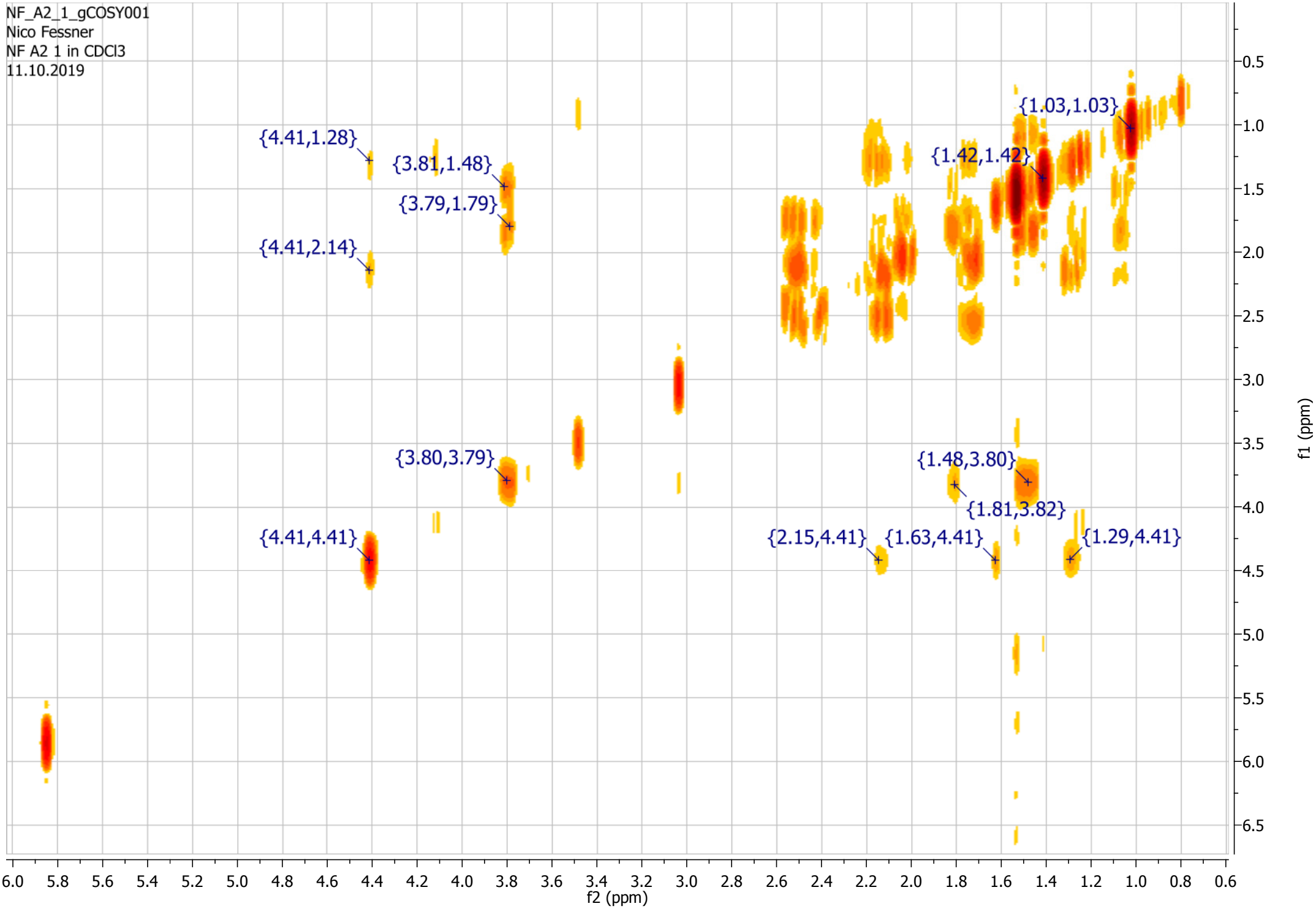
NF_A2_1_gCOSY001
Nico Fessner
NF A2 1 in CDCl3
11.10.2019
{4.41,1.28}
{3.81,1.48}
{3.79,1.79}
{4.41,2.14}
{3.80,3.79}
{4.41,4.41}
{1.03,1.03}
{1.42,1.42}
{1.48,3.80}
{1.81,3.82}
{2.15,4.41}
{1.63,4.41}
{1.29,4.41}
f2 (ppm)
f1 (ppm)

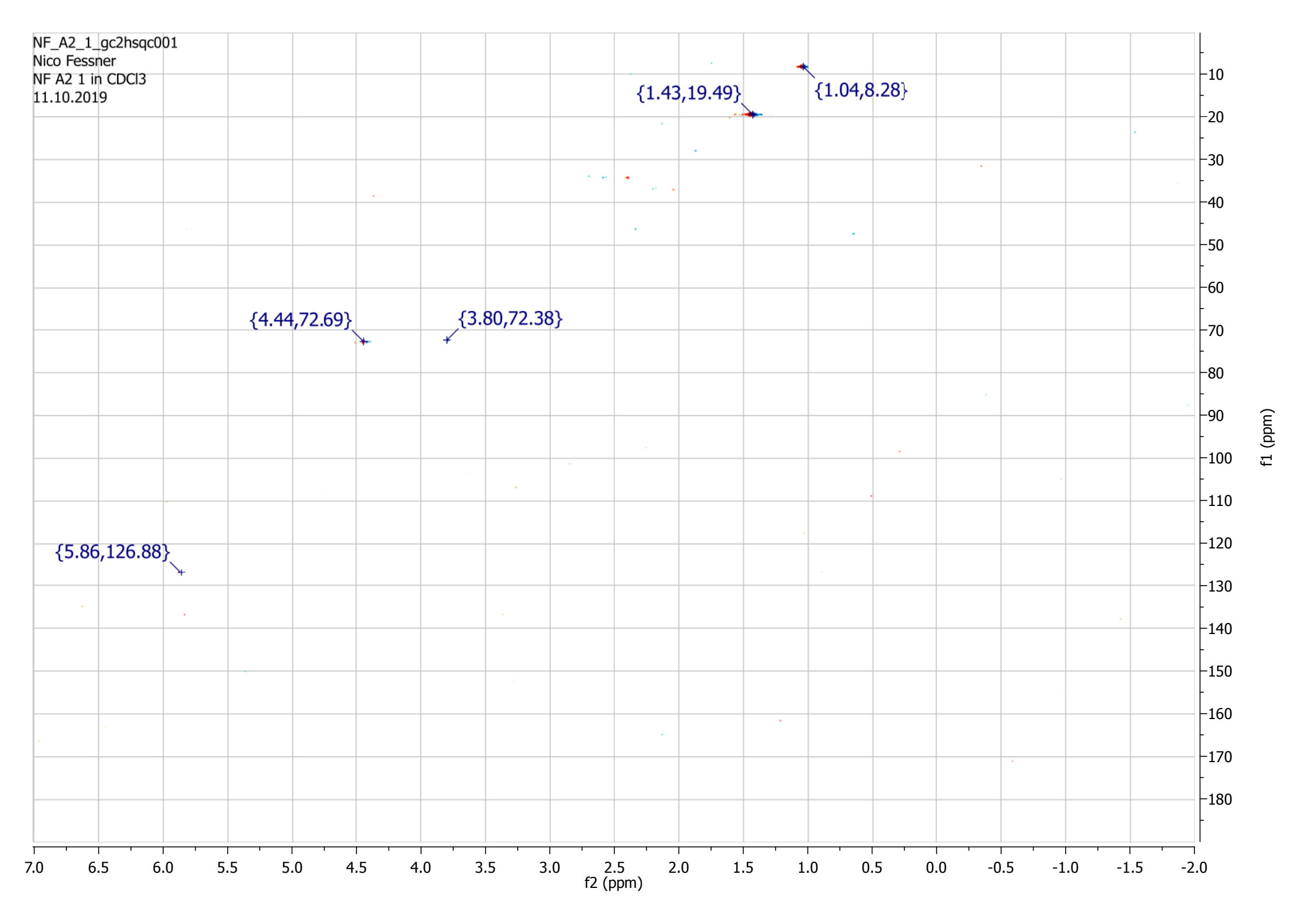
NF_A2_1_gc2hsqc001
Nico Fessner
NF A2 1 in CDCl3
11.10.2019
{1.43,19.49}
{1.04,8.28}
{4.44,72.69}
{3.80,72.38}
{5.86,126.88}
f2 (ppm)
f1 (ppm)

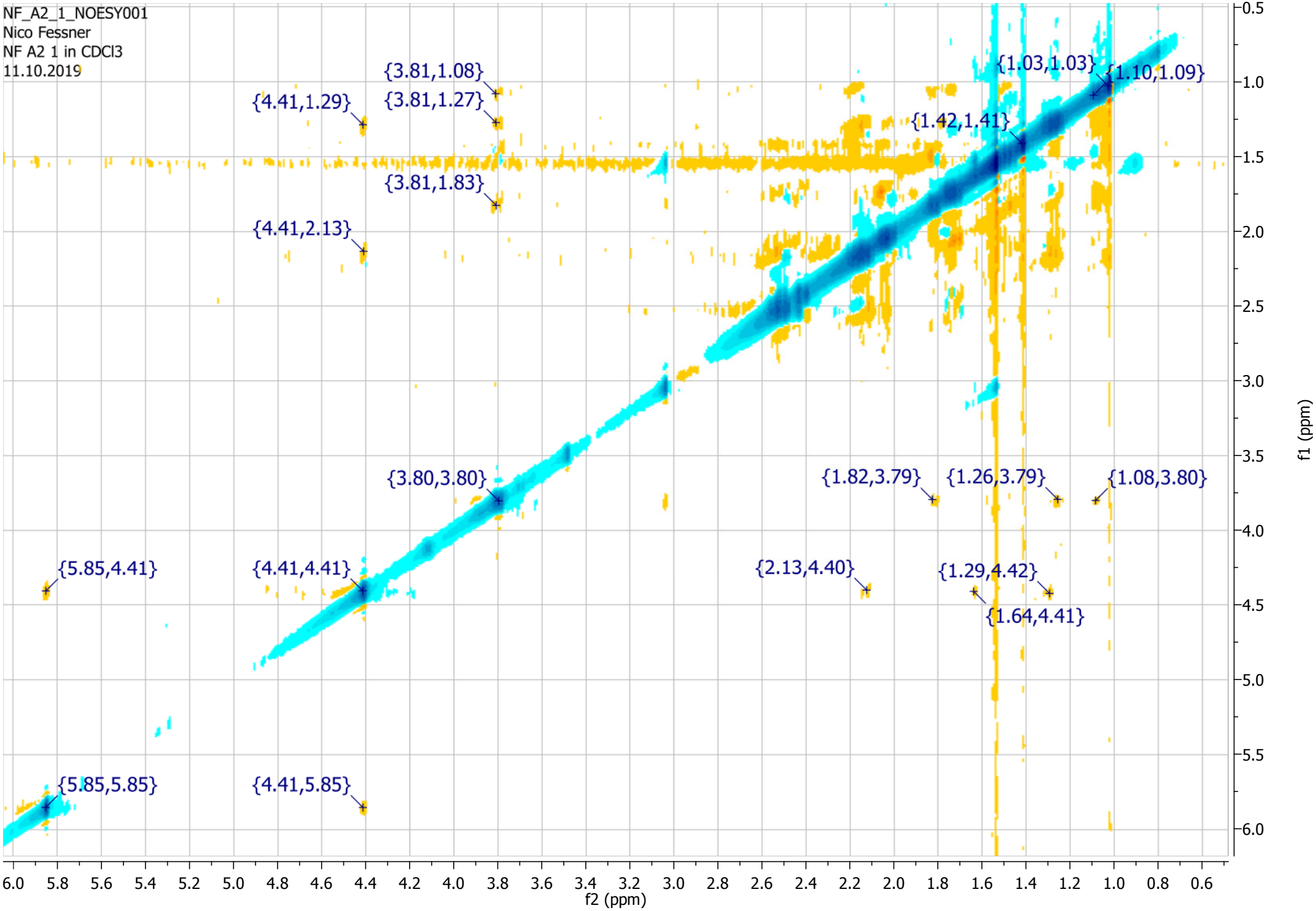
NF_A2_1_NOESY001
Nico Fessner
NF A2 1 in CDCl3
11.10.2019
{3.81,1.08}
{4.41,1.29}
{3.81,1.27}
{1.03,1.03}
{1.10,1.09}
{1.42,1.41}
{3.81,1.83}
{4.41,2.13}
{3.80,3.80}
{1.82,3.79}
{1.26,3.79}
{1.08,3.80}
{5.85,4.41}
{4.41,4.41}
{2.13,4.40}
{1.29,4.42}
{1.64,4.41}
{5.85,5.85}
{4.41,5.85}
f2 (ppm)
f1 (ppm)

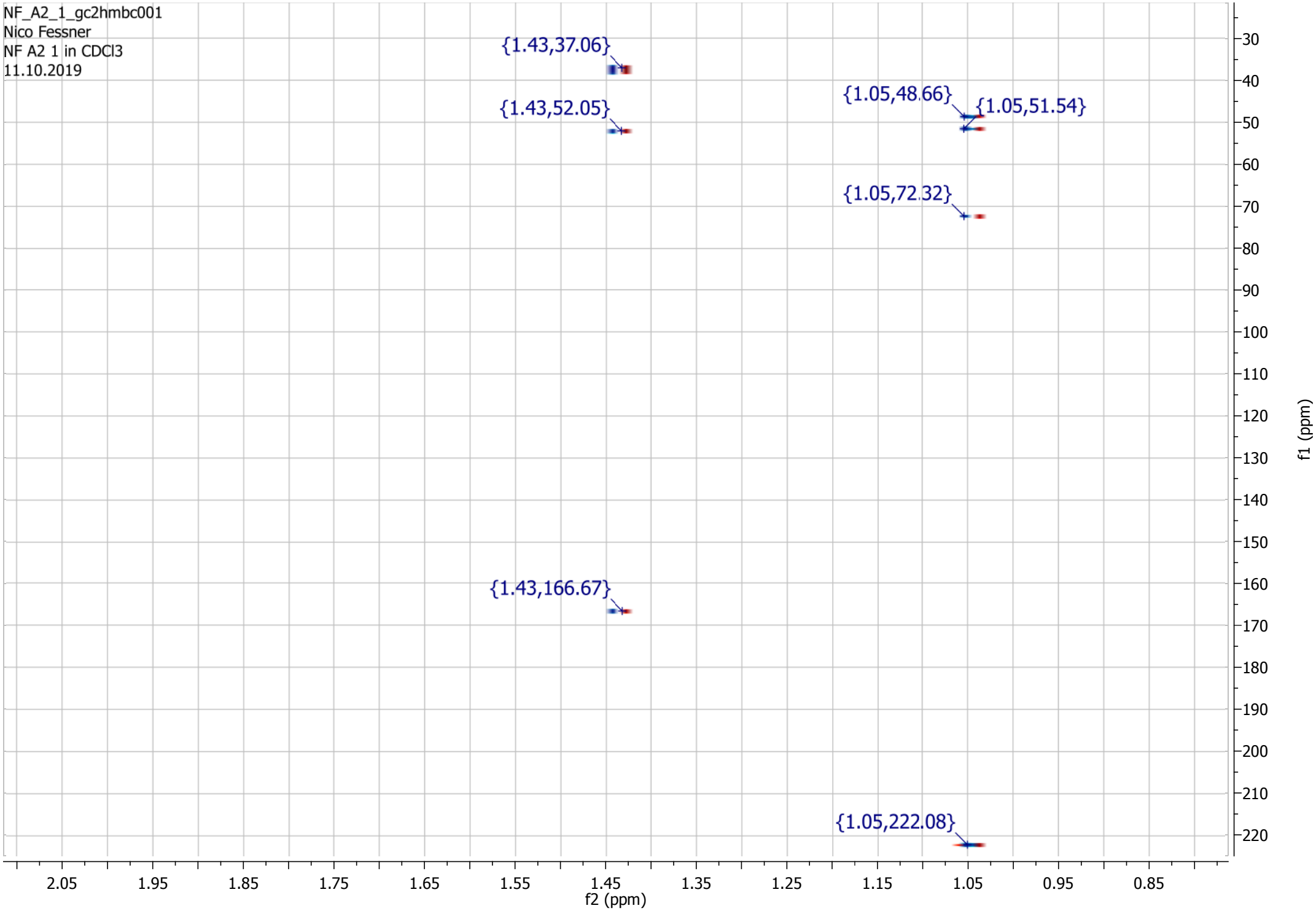
NF_A2_1_gc2hmbc001
Nico Fessner
NF A2 1 in CDCl3
11.10.2019
{1.43,37.06}
{1.43,52.05}
{1.05,48.66}
{1.05,51.54}
{1.05,72.32}
{1.43,166.67}
{1.05,222.08}
2.05
1.95
1.85
1.75
1.65
1.55
1.45
1.35
1.25
1.15
1.05
0.95
0.85
f2 (ppm)
30
40
50
60
70
80
90
100
110
120
130
140
150
160
170
180
190
200
210
220
f1 (ppm)

Evolution and Enrichment of CYP5035 and CYP5136 in *Polyporales*: Functionality of an understudied P450 family

Nico D. Fessner,[1] David R. Nelson[2] and Anton Glieder[1,*]

1 Institute of Molecular Biotechnology, Graz University of Technology, NAWI Graz, Petersgasse 14/3, Austria
2 Department of Microbiology, Immunology and Biochemistry, University of Tennessee Health Science Center, Memphis, TN 38163, USA
* corresponding author: Anton Glieder; email: a.glieder@tugraz.at
ORCID numbers: 0000-0001-8247-1356 (Nico D. Fessner), 0000-0003-0583-5421 (David R. Nelson), 0000-0002-5986-9689 (Anton Glieder)

Abstract

Bioprospecting for innovative basidiomycete cytochrome P450 enzymes (P450s) is highly desirable due to the fungi's enormous enzymatic repertoire and outstanding ability to degrade lignin and detoxify various xenobiotics. While fungal metagenomics is progressing rapidly, the biocatalytic potential of the majority of thus annotated P450 sequences usually remains concealed, although functional profiling identified several P450 families with versatile substrate scopes towards various natural products. Functional knowledge about the CYP5035 family, for example, is largely insufficient. In this study the families of the putative P450 sequences of the four white-rot fungi *Polyporus arcularius*, *Polyporus brumalis*, *Polyporus squamosus* and *Lentinus tigrinus* were assigned and the CYPomes revealed an unusual enrichment of CYP5035 and CYP5136. By computational analysis of the phylogeny of these P450 families, the evolution of their enrichment could be traced back to the *Ganoderma* macrofungus indicating their evolutionary benefit. In order to address the knowledge gap on CYP5035 functionality, a representative subgroup of this P450 family of *P. arcularius* was expressed and screened against a test set of substrates. Thereby, the multifunctional enzyme CYP5035S7 converting several plant natural product classes was discovered. Aligning CYP5035S7 to 102,000 putative P450 sequences of 36 fungal species from JGI-provided genomes located hundreds of further CYP5035 family members, which subfamilies were classified if possible. Exemplified by these specific enzyme analyses, this study gives valuable hints for future bioprospecting of such xenobiotic-detoxifying P450s.

Key points

The P450 families CYP5035 and CYP5136 are unusually enriched in P. arcularius.
Phylogenetic analysis of CYP5035 traces their evolution back to Ganoderma species.
Functional screening shows CYP5035 capability to assist in the fungal detoxification machinery.
CYP5035S7 is a promiscuous P450 converting several natural product classes.
Some Polyporales encompass an unusually large repertoire of detoxification P450s.

Keywords Enzyme discovery CYPome CYP5035 Biotransformation

Introduction

White-rot Basidiomycota possess the highest percentage of CYPome in their genome of all organisms (Chen et al. 2014). Such high density of cytochrome P450 enzymes (P450s/CYPs) helps these fungi to fully degrade the most recalcitrant aromatic polymer lignin or its low molecular weight degradation products (Peralta et al. 2017), and to survive in harsh conditions by detoxifying a vast variety of plant-based xenobiotics and other environmental hazards (Kües 2015). In order to investigate these fascinating features for their application in bioenergy processing or bioremediation (Yadav et al. 2019; Mäkelä et al. 2020), programmes such as the 1000 Fungal Genome project were initiated and already sequenced numerous genomes of white-rot fungi (Grigoriev et al. 2011; Grigoriev et al. 2014), providing free access to an incredible amount of P450 sequences.

Computational efforts were mobilised to annotate such enzyme sequences with unknown function (Gerlt et al. 2011; McKay et al. 2015). Starting with the model white-rot fungus *Phanerochaete chrysosporium*, the P450s of several other wood-degrading basidiomycetes were previously analysed computationally (Suzuki et al. 2012; Syed et al. 2013a; Syed et al. 2014; Hori et al. 2014; Kües et al. 2015; Zhu et al. 2015; Mgbeahuruike et al. 2017) and grouped into (sub-)families according to the 40% (family) and 55% (subfamily) sequence identity rules of the International P450 Nomenclature Committee (Nelson 2006). Yet, such low sequence identity and a scarce number of functionally characterised basidiomycete P450s render simulated predictions of biochemical capacities extremely difficult (Ichinose 2013). Even the closest homologs may have divergent reactivity (Gerlt 2007). Therefore, some studies attempted to express and functionally analyse the entire CYPome of *P. chrysosporium* and model brown-rot fungus *Postia placenta* (Hirosue et al. 2011; Ide et al. 2012; Ichinose 2013). A few individual P450s with interesting activities were also looked at more closely (Kasai et al. 2009; Syed et al. 2010; Kasai et al. 2010a; Kasai et al. 2010b; Chigu et al. 2010; Syed et al. 2011; Ichinose and Wariishi 2012; Syed et al. 2013b; Syed et al. 2013c; Hatakeyama et al. 2016; Sakai et al. 2018; Yang et al. 2018; Wang et al. 2019). However, the research of fungal P450s is still in its early stages and often shares ideas and limited information, rather than comprehensive details on the P450 function. Generally, the biocatalytic repertoire of basidiomycetes as a whole remains greatly understudied (Schmidt-Dannert 2016). One reason for this might be the more challenging recombinant expression and availability of isolated enzymes compared to bacterial P450 enzymes.

Comparison of the CYPomes of six model wood-degrading fungi revealed that 11 out of 68 P450 families were enriched, including CYP5035, CYP5136 and CYP5150 (Syed et al. 2014). While a few studies analysed enzymes of the latter two families (Syed et al. 2011; Ichinose and Wariishi 2012; Syed et al. 2013c; Hatakeyama et al. 2016), the function of CYP5035 is still inconclusive (Syed et al. 2014). Four members of its subfamilies A and B from *P. chrysosporium* accepted naproxen, flavone or dehydroabietic acid to form yet unresolved products (Hirosue et al. 2011). However, no activity could be observed for the 13 other expressed CYP5035 enzymes of subfamilies A – E from the same fungus (Hirosue et al. 2011), or of subfamily F of *P. placenta* (Supplementary Table S1) (Ide et al. 2012). Hence, the knowledge about this enriched P450 family is largely insufficient and calls for further investigation.

In this study, putative P450 sequences from publicly available genomes of closely related white-rot fungi *Polyporus arcularius*, *Polyporus brumalis*, *Polyporus squamosus* and *Lentinus tigrinus* were extracted and their P450 families assigned. Thereby, it was noticed that the CYP5035 and CYP5136 families were enhanced even more than in any of the model white-rot fungi already analysed in literature, except in *Ganoderma* species. By sketching their phylogeny in contrast to *P. chrysosporium* and other model basidiomycetes, the evolution of these enzyme families was studied in the systematic order of *polyporales*. To fill part of the described functional gap, a representative group of nine CYP5035 sequences dispersed over the available CYP5035 subfamilies in *P. arcularius* were heterologously expressed in *Komagataella phaffii* (*Pichia pastoris*) and screened for activity towards a test set of structurally diverse substrates representing several different natural product classes. Thereby, a promiscuous CYP5035 was discovered.

Materials and Methods

All solvents and chemicals were purchased from Sigma-Aldrich/Merck (Steinheim/Darmstadt, Germany), VWR International (Fontenay-sous-Bois, France), Carl Roth GmbH (Karlsruhe, Germany) or Fisher Scientific (Loughborough, UK) in best available purity and were used as received without further purification. HPLC tubes were bought from Macherey-Nagel (Düren, Germany) and the corresponding caps and inserts from Bruckner Analysentechnik (Linz, Austria). An Agilent Technologies 1100 Series executed the HPLC analysis, and a Shimadzu GCMS-QP2010 SE instrument equipped with an AOC-20i/s auto sampler and injector unit together with a Zebron ZB-5MSi capillary column (30 m x 0.25 mm x 0.25 µm, Phenomenex) performed the GC-MS measurements. OD values were determined with an Eppendorf BioPhotometer *plus*. The CYP5035 coding regions, identified from the publicly available databases were ordered as double-stranded DNA fragments from TWIST Bioscience. Cells of *P. pastoris* with expressed and versatile P450 3A4 were obtained from bisy GmbH (Hofstaetten, Austria) and used as positive control for biotransformations. These Pichia cells had been cultivated, then stored as frozen pellets at -80 °C. Figures were generated in the programmes GraphPad Prism 8 and CS ChemDraw Ultra.

Fungal CYPome determination

Publicly available protein sequences of the genomes of the following species were downloaded from the JGI Genome Portal website (https://genome.jgi.doe.gov/portal/) of the US-DOE (Grigoriev et al. 2014):

- *Polyporus arcularius* (Varga et al. 2019) HHB13444 v1.0: Project: 1006899 (https://mycocosm.jgi.doe.gov/Polar1/Polar1.home.html);
- *Polyporus brumalis* (Miyauchi et al. 2018) BRFM 1820 v1.0: Project: 1051563 (https://mycocosm.jgi.doe.gov/Polbr1/Polbr1.home.html);
- *Polyporus squamosus* CCBS676 v1.0: Project 1108915 (https://genome.jgi.doe.gov/portal/Polsqu1/Polsqu1.download.html);
- *Lentinus tigrinus* (Wu et al. 2018) ALCF2SS1-6 v1.0: Project 1020066 (https://genome.jgi.doe.gov/portal/Lenti6_1/Lenti6_1.download.html).

In each case, the Files -> Annotation -> Filtered Models ("best") -> Proteins -> '*Species*'_GeneCatalog_proteins.aa.fasta.gz files were used.

Additionally, the necessary genome P450s sequences (Martinez et al. 2004; Martinez et al. 2009; Eastwood et al. 2011; Suzuki et al. 2012; Floudas et al. 2012; Morin et al. 2012; Binder et al. 2013) or CYPome statistics of the fungi *Phanerochaete chrysosporium* (Syed and Yadav 2012; Syed et al. 2014), *Phanerochaete carnosa* (Suzuki et al. 2012; Syed et al. 2014), *Agaricus bisporus* (Syed et al. 2014), *Postia placenta* (Ide et al. 2012; Syed et al. 2014), *Ganoderma* sp. (Syed et al. 2013a; Syed et al. 2014; Kües et al. 2015), *Serpula lacrymans* (Syed et al. 2014), *Trametes versicolor* (Syed and Mashele 2014), *Bjerkandera adusta* (Syed et al. 2013a), *Phlebia brevispora* (Syed et al. 2013a), *Heterobasidion irregulare* (Mgbeahuruike et al. 2017), *Phlebiopsis gigantea* (Hori et al. 2014), *Lignosus rhinoceritis* (Yap et al. 2014), *Ganoderma lucidum* (Chen et al. 2012; Kües et al. 2015) and *Ganoderma sinense* (Zhu et al. 2015) were obtained from the cited literature or accessed according to their instructions (Online Resource 1).

The CYPomes of *P. arcularius*, *P. brumalis*, *P. squamosus* and *L. tigrinus* (Online Resource 2) were determined according to the P450 identification and annotation strategy described by Syed *et al.* (Syed and Mashele 2014) with a slight adjustment as the old BLAST server on the Cytochrome P450 Homepage (Nelson 2009) did not work and the new P450 BLAST page (http://www.p450.unizulu.ac.za/?page_id=21) had not been installed at the time:

1. Superfamily annotation of the protein sequences by the Batch CD-Search Tool of the NCBI (https://www.ncbi.nlm.nih.gov/Structure/bwrpsb/bwrpsb.cgi).
2. Verification of the P450 signature motifs "E-x-x-R" and "C-x-G" in the putative P450 sequences using the ScanProsite tool (https://prosite.expasy.org/scanprosite/).
3. P450 family assignment by applying the FCPB BLAST Search of the verified P450 protein sequence (http://p450.riceblast.snu.ac.kr/blast.php) (Moktali et al. 2012).
4. Verification of the P450 family assignment by alignment against already assigned P450 sequences of previous publications using the Protein BLAST option of the NCBI. P450 families were verified according to the 40% (family) and 55% (subfamily) sequence identity rules of the International P450 Nomenclature Committee (Nelson 2006).

Step [4] was of utter importance to assign less common P450 families correctly because the FCPB did not consider enzyme families of the *Ganoderma* macrofungus. P450 sequences that did not get a good match were left unassigned.

Evolutionary P450 sequence analysis

Following the same strategy as Syed *et al.* (Syed et al. 2014), evolutionary analyses of the desired P450 protein sequences were conducted in MEGA X (Kumar et al. 2018; Stecher et al. 2020). The evolutionary history was inferred using the minimum evolution method (Rzhetsky and Nei 1992). The evolutionary distances were computed using the Poisson correction method (Zuckerhandl and Pauling 1965) and are in the units of the number of amino acid substitutions per site. The minimum evolution tree was searched using the close-neighbour-interchange algorithm (Nei and Kumar 2000) at a search level of 1. The neighbour-joining algorithm (Saitou and Nei 1987) was used to generate the initial tree. All ambiguous positions were removed for each sequence pair (pairwise deletion option).

CYP5035 enzyme expression in *Pichia pastoris*

Nine CYP5035 sequences of *P arcularius* were ordered as synthetic double-stranded DNA fragments from TWIST Bioscience, amplified, cloned into the expression vector (Supplementary Fig. S15) equipped with Zeocin resistance and a bidirectional promoter for co-expression of the *P. pastoris*' CPR (Pp-CPR) gene by Gibson assembly. The *P. pastoris* strain BSYBG11 (*aox1*Δ, MUT^S), which originates from strain BG08 of BioGrammatics Inc. (Carlsbad, USA) (Sturmberger et al. 2016), was transformed with the resulting linearised plasmids for genomic integration of the expression cassettes. Small-scale cultivations were done for the MFC demethylation assay and carried out following the deep-well plate (DWP) and induction protocols reported previously (Weis et al. 2004). For the substrate screening, cultivations were scaled up to 250 mL shake-flasks inoculating 45 mL BMD1 (pH 7.4), adding of 5 mL BMM10 (pH 7.4) after 60 hours (Weis et al. 2004) and three times further feeding with 0.5 mL methanol every 12 hours. Having harvested and washed cells twice in 50 mM potassium phosphate buffer (pH 7.4), cells were resuspended in the same phosphate buffer until an OD_{600} of 100 was obtained. A cell broth volume of 400 µL was filled into each well of a DWP and 4 µL of the 100 mM compound added to get a final substrate concentration of 1 mM. The biotransformation was carried out for 17 hours at 28 °C, 80% humidity and 320 rpm in a tilted orientation on the shaker to ensure maximal oxygen availability. After stopping the reaction with the addition of 300 µL of an acetonitrile/methanol (1:1; v/v) solution, the resulting mixture was vortexed, centrifuged and 200 µL of supernatant of each well

was transferred into 96-well GreinerV plates for HPLC analysis. Separation was carried out *via* a Kinetex C18 (100 Å; 50 x 4.6 mm; 2.6 µm) reverse-phase column. Water containing 0.1% acetic acid (A) and acetonitrile (B) were used for elution at 25 °C in the following ratios: 0 min: A/B 80/20; 1 min: A/B 80/20; 1.01 min: A/B 50/50; 4 min: A/B 0/100; 5.50 min: A/B 0/100; 5.51 min: A/B 80/20; 6.50 min: A/B 80/20. For GC-MS analysis, equal volumes of dichloromethane containing 0.01% undecane were added to the biotransformations and after phase separation the organic layer was dried with anhydrous Na_2SO_4. The following method (Linear velocity of 39.5 cm sec^{-1} using He carrier gas; total and column flow of 15.2 mL min^{-1} and 1.21 mL min^{-1}, respectively; injection temperature of 250 °C; split ratio of 9.1) was applied: 35 °C for 5 min, 20 °C min^{-1} to 300 °C and 300 °C for 5 min in a total run time of 23.25 min.

Results

Using the publicly available genome protein sequences from the JGI Genome Portal website (Grigoriev et al. 2014), a genome-wide search for putative P450s in *P. arcularius* (Supplementary Fig. S1) was carried out following the identification and annotation strategy of Syed *et al.* (Syed and Mashele 2014) (Online Resource 2) with a few adjustments as outlined in the Materials and Methods section. The CYPome of *P. arcularius* showed a similar collection of P450s to that of *Ganoderma* sp. primarily owing to the presence of numerous CYP5359 and a few CYP5144 (Online Resource 1). Likewise, a CYPome comparison between *P. arcularius* and well-known model white- (eg. *P. chrysosporium*) and brown-rot (eg. *P. placenta*) fungi analysed extensively by Syed et al. (Syed et al. 2013a; Syed et al. 2014; Syed and Mashele 2014) revealed an unusually large number of CYP5035 (23) and CYP5136 (12) in this fungus: approximately 2-fold more (13; 5) than in *P. chrysosporium* (Fig. 1). In fact, even when extending the comparison to a total of 17 wood-degrading fungi, *P. arcularius* had the highest percentages of these two P450 families in its genome (Supplementary Figs. S3 and S5). Only the absolute number of CYP5035 and CYP5136 was surpassed slightly by *Ganoderma sinense* and *P. brumalis*, respectively (Supplementary Figs. S2 and S4) (Zhu et al. 2015). Additionally, CYP5150 sequences were frequent in the genome (Supplementary Fig. S6), with the percentage of this family in the genome higher in *Ganoderma* species and *Trametes versicolor* (Supplementary Fig. S7).

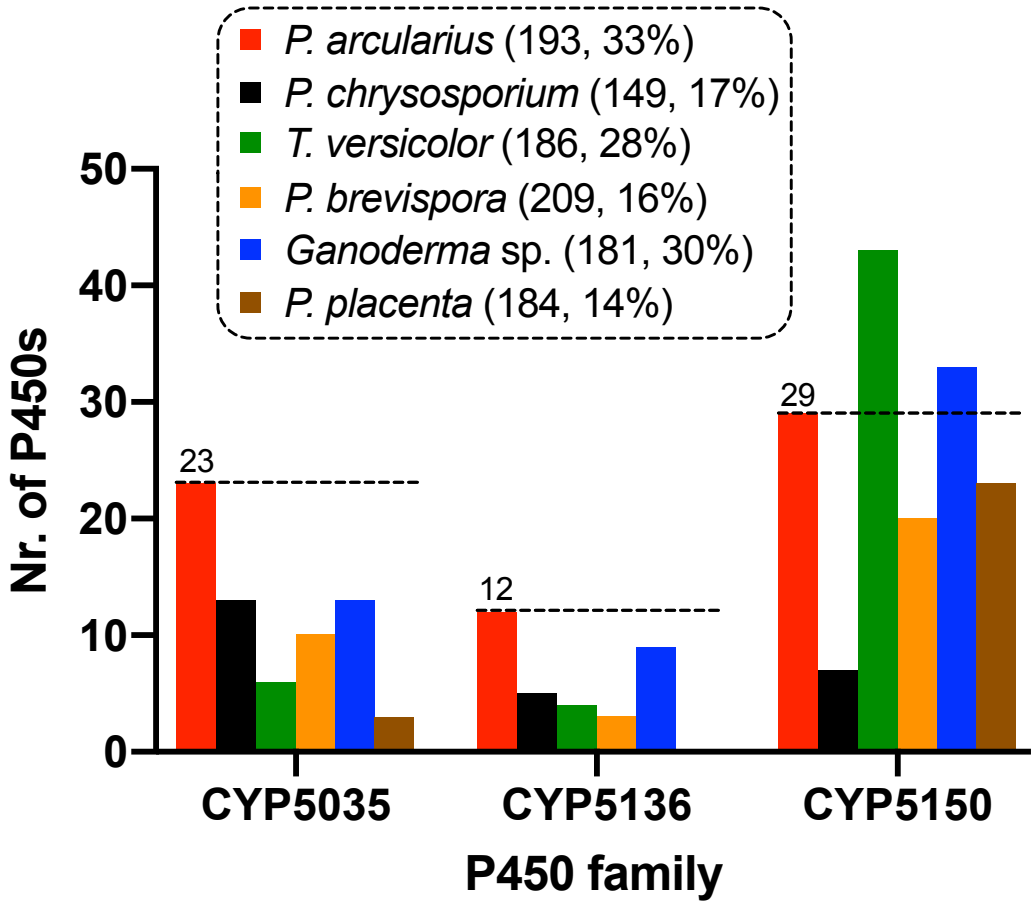

Fig. 1: A comparison of the number of P450s in the families CYP5035, 5136 and 5150 identified in the genome of *P. arcularius* (Parc) with several model white- (*P. chrysosporium*, *T. versicolor*, *Phlebia brevispora*, *Ganoderma* sp.) and brown-rot fungi (*P. placenta*, *Ppla*) is shown. The total number of P450s and the percentage of these three families in comparison to all P450s in the genome of each species are given in parenthesis. A more detailed CYPome comparison is provided in Online Resource 1.

When examining the phylogeny of the white-rot fungal species to the previously analysed species in literature (Justo and Hibbett 2011; Floudas et al. 2012; Binder et al. 2013), the *Ganoderma* macrofungus indeed turned out to be the fungus most closely related to *P. arcularius* (Supplementary Fig. S8). Perhaps the evolution of the enrichment of CYP5035 and CYP5136 had its origin at approximately this branching point in fungal diversification and continued downstream to *P. arcularius*? In order to answer this hypothesis the CYPomes of *P. squamosus* (Supplementary Fig. S9), *L. tigrinus* (Supplementary Fig. S10) (Wu et al. 2018) and *P. brumalis* (Supplementary Fig. S11) (Miyauchi et al. 2018) were determined according to the aforementioned genome-wide P450 identification strategy. The selected fungal genomes unveiled a similarly high number of CYP5035 and CYP5136 (Online Resource 1). The computation of minimum evolution trees of both P450 families shown in Figs. 2 and 3, respectively, further supported the proposed evolutionary theory. Due to its close phylogeny to *P. arcularius* (Supplementary Fig. S12), *P. brumalis* was only included together with further white- and brown-rot fungi in extended phylogenetic trees (Supplementary Figs. S13 and S14), which contributed towards the same conclusions.

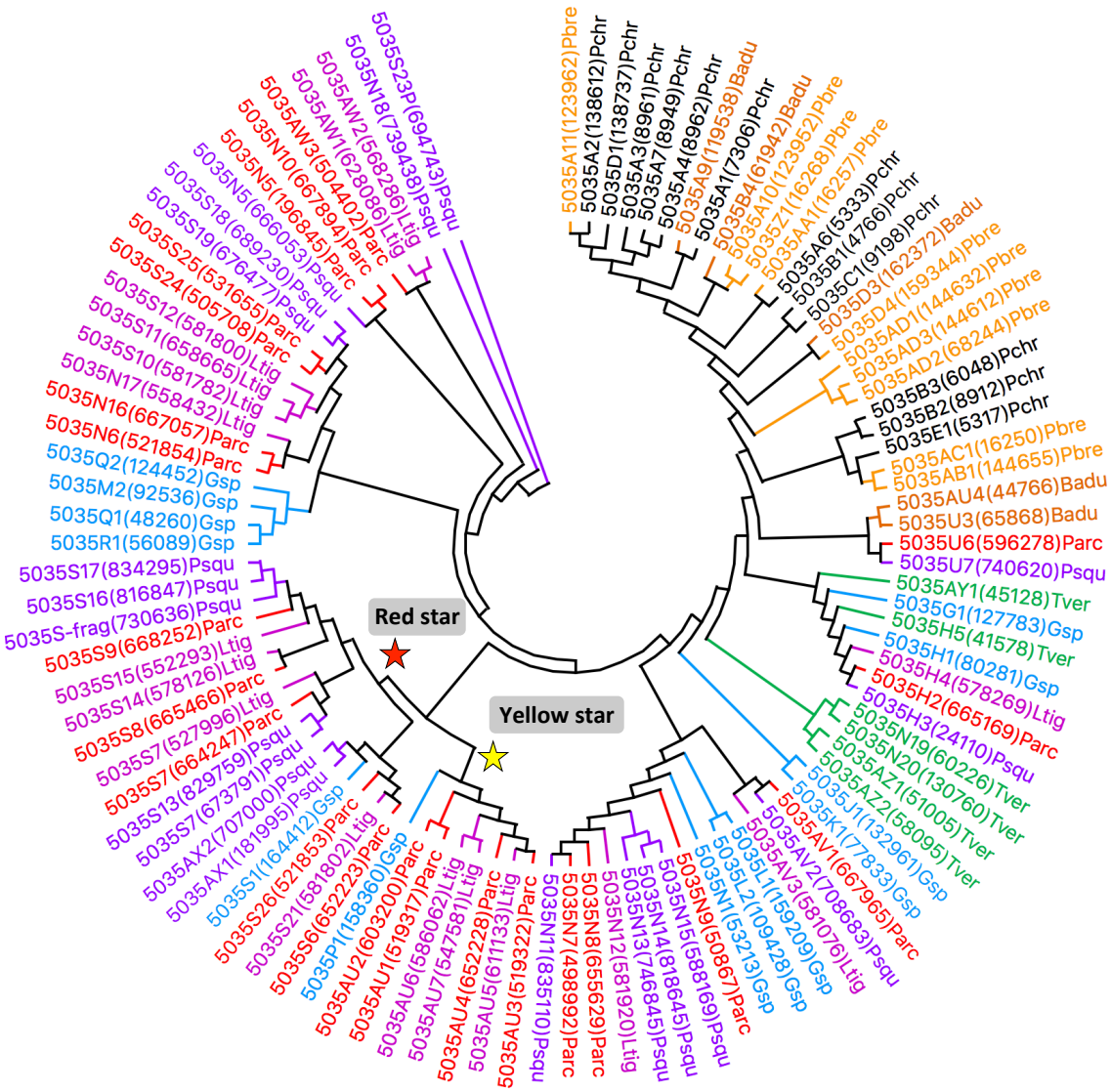

Fig. 2: A minimum evolution tree of the CYP5035 family involving 103 amino acid sequences from eight different organisms. The phylogeny of CYP5035 enzymes of the fungus *P. arcularius* (Parc; red) compared to related species *L. tigrinus* (Ltig; violet) and *P. squamosus* (Psqu; purple), and the other model white-rot fungi *Ganoderma* sp. (Gsp; blue), *T. versicolor* (Tver; green), *P. chrysosporium* (Pchr; black), *B. adusta* (Badu; dark orange) and *P. brevispora* (Pbre; orange) in order to get an insight into the evolution of this P450 family. The yellow or red stars indicate a diversification process and new branch of the P450 families compared to *Ganoderma* sp., respectively. The tree was constructed using the close-neighbour-interchange algorithm in MEGA X. An extended tree can be found in Supplementary Fig. S13.

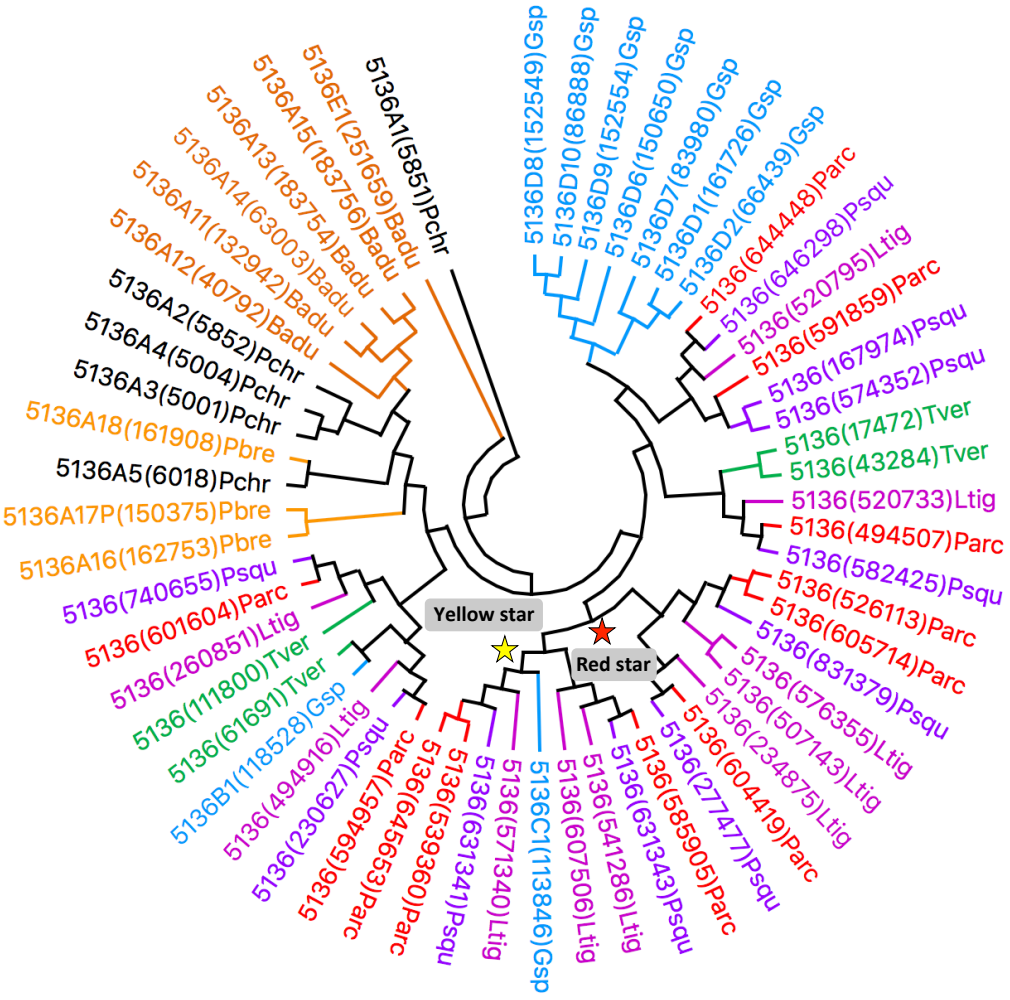

Figure 3: Displayed is a minimum evolution tree of the CYP5136 family involving 58 amino acid sequences from eight different organisms. Phylogeny of CYP5136 enzymes of fungus *P. arcularius* (Parc; red) compared to related species *L. tigrinus* (Ltig; violet) and *P. squamosus* (Psqu; purple), and the other model white-rot fungi *Ganoderma* sp. (Gsp; blue), *T. versicolor* (Tver; green), *P. chrysosporium* (Pchr; black), *B. adusta* (Badu; dark orange) and *P. brevispora* (Pbre; orange) in order to get an insight into the evolution of this P450 family. The yellow or red stars indicate a diversification process and new branch of the P450 families compared to *Ganoderma* sp., respectively. The tree was constructed using the close-neighbour-interchange algorithm in MEGA X. An extended tree can be found in Supplementary Fig. S14.

The presence of the large number of CYP5035 sequences in the genome of *P. arcularius* awoke our interest in studying this P450 family in more detail. It was thus decided to pick a small, representative selection of nine CYP5035 sequences of *P. arcularius* distributed among the available subfamilies (Supplementary Table S1, Online Resource 2), to express them in *Pichia pastoris* and to test their activities and substrate scope. These nine CYP5035 were cloned into bidirectional co-expression plasmids together with *P. pastoris*' native P450 reductase (Supplementary Figure S15). Fourteen transformants of each CYP5035 variant were screened for activity using the 7-methoxy-4-(trifluoromethyl)coumarin (MFC) de-methylation assay (Donato et al. 2004) to select the best clonal variants. However, only CYP5035S7 was active employing MFC. Due to the absence of demethylation activity on this fluorescent substrate, individual transformants for each of the other enzymes were selected randomly for further biotransformationtests using alternative substrates, followed by chromatographic analysis. For this substrate specificity screening, the selected CYP5035-expressing

strains were cultivated and applied in whole-cell biotransformations of over 40 structurally diverse and complementary compounds of eight different natural product classes (terpenes, steroids, alkaloids, stilbenoid- and flavonoid-backbones, phenylpropanoids, fatty acid derivative and coumarins) and also pharmaceuticals, (nitrogen-containing) polycyclic aromatic hydrocarbons ((N)PAHs) and other chemicals (Fig. 4). Due to its known broad substrate acceptance, the human P450 3A4 co-expressed with its human CPR in *P. pastoris* was used as a positive control for all biotransformations (Fessner et al. 2020).

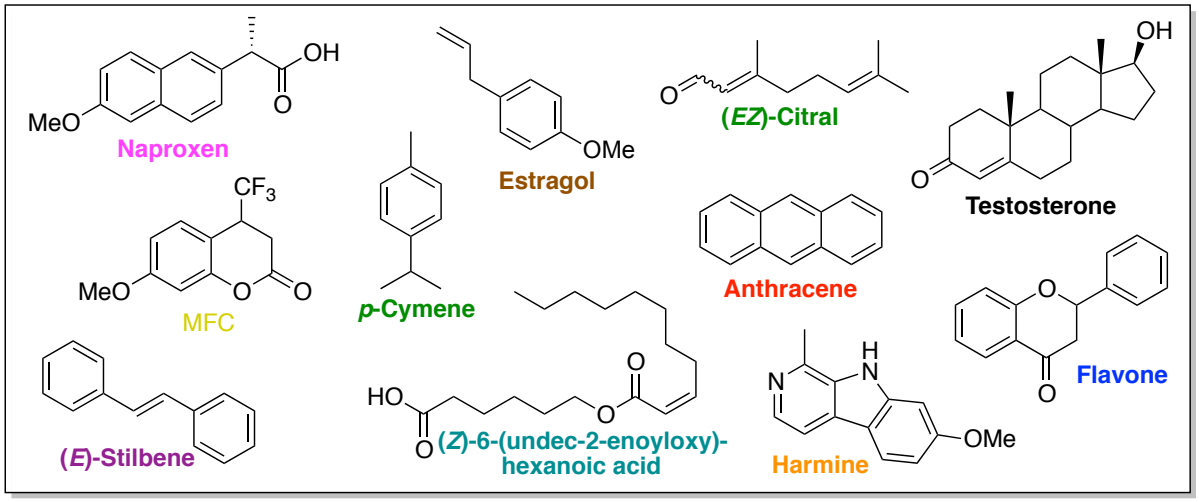

Fig. 4: Examples of the diverse compounds used for screening to establish the substrate scope of the nine CYP5035 enzymes of *P. arcularius*: MFC (yellow), terpenes (green), pharmaceutical (pink), steroid (black), polycyclic aromatic hydrocarbon (red), phenylpropanoid (brown), stilbenoid- (purple) and flavonoid-backbones (blue), alkaloid (orange), and fatty acid dimer (teal)

The heat map in Fig. 5 illustrates the activity pattern that was obtained from the HPLC or GC analysis. Notably, the observed activities imply different substrate scopes even among P450s of the same subfamily CYP5035S. While the three enzymes CYP5035H2, -S6, and -S9 only converted at least one of (*E*)-stilbene, (*EZ*)-citral, *p*-cymene and indole, the fourth variant CYP5035S7 demonstrated a much larger substrate scope being active especially on PAHs and terpenes, but also across other natural product classes like the phenylpropanoid estragol and the stilbenoid-backbone (*E*)-stilbene. In contrast, cells with expression constructs for CYP5035S8 as well as four other individual CYP5035 genes did not show any activity whatsoever.

Having identified such promiscuous enzyme, a BLAST search for hits to CYP5035S7 against the personal P450 collection of Dr. Nelson encompassing 102,000 sequences from JGI was performed to locate orthologous CYP5035 or similar sequences in other fungi (Online Resource 3). A total of 314 sequences in 36 different fungal species were longer than 450 amino acids and aligned with >40% identity indicating an allocation to the same CYP5035 family, though only sequences of fungi used in this study were found to belong to the same subfamily with >55% identity. Hence, better allocation was achieved by blasting the 314 sequences each against all CYP5035 sequences named so far (Online Resource 3). The results were sorted by subfamily, percentage identity and species.

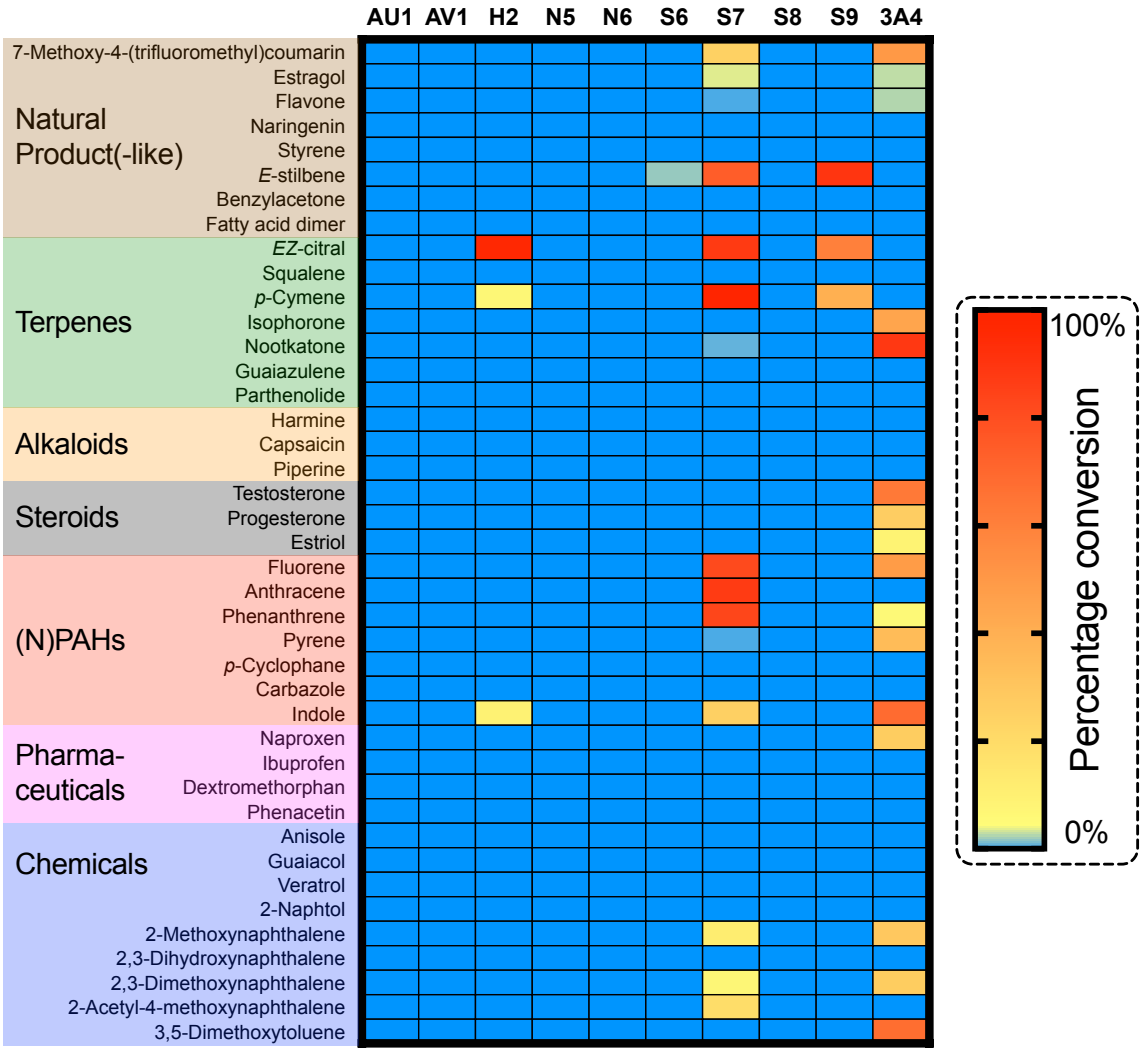

Fig. 5: This heat map illustrates the result of the activity screening of nine CYP5035 enzymes of *P. arcularius* and the positive control P450 3A4. The percentage conversions were calculated from peak integration in HPLC and GC profiles. Reaction conditions were as follows: OD600 of 100, 28 °C, 320 rpm, 1 mM substrate concentration

Discussion

P. arcularius was selected for this work because in 2019 a study took the fungus into closer consideration as one of the candidates with high potential for organic pollutant degradation (Dao et al. 2019), and in the same year its genome was sequenced (Varga et al. 2019). By assigning the P450 families to the CYPomes of *P. arcularius*, *P. brumalis*, *P. squamosus* and *L. tigrinus*, a much larger enrichment of CYP5035 and CYP5136 compared to other model white- and brown-rot fungi, except for *Ganoderma* species, and high amounts of CYP5150 were noticed. Therefore, these listed white-rot *polyporales* seemed to have more diverse P450s than other white-rot fungi. Most likely such enrichments happened in order to adapt to harsher conditions in new ecological niches and to detoxify the high diversity of degradation products in such world of different available carbon sources. The increase in functional P450s of these two families must have secured some evolutionary advantage (Syed et al. 2014; Kües et al. 2015). Former studies had clearly classified CYP5136 and CYP5150 as enzymes participating in the fungal defence mechanism and metabolic diversity degrading both

plant material and xenobiotics. Equipped with broad substrate scopes, members of these P450 families were able to oxidise hydrocarbons, plant chemicals, steroids and pharmaceuticals (Kasai et al. 2010a; Syed et al. 2011; Ichinose and Wariishi 2012; Syed et al. 2013c; Syed et al. 2014; Hatakeyama et al. 2016; Lu et al. 2019). The facts that non-wood-degrading basidiomycetes conversely only possessed a few P450 genes and these three enriched P450 families were completely absent in their genomes, strengthened their results (Syed et al. 2014). On the other hand, CYP5150L8 was recently found to execute steps of the biosynthesis of ganoderic acid in *G. lucidum* (Wang et al. 2018). Therefore, the observed diversity of P450s in these studied organisms also might suggest essential roles in the synthesis of natural products.

However, the functional examination of CYP5035 has been rather neglected in literature because it appeared to be only a mildly enriched family (Syed et al. 2014), which showed limited activity converting only plant products flavone and abietic acid and the pharmaceutical naproxen (Hirosue et al. 2011; Ichinose 2013). Hence, in the history of recent literature the expression of only 17 CYP5035s had ever been attempted, of which only four enzymes showed activities accepting one or two of the named chemicals (Supplementary Table S1) (Hirosue et al. 2011; Ide et al. 2012). Clearly, this did not ignite immediate interest in the few studies that were researching novel wood-degrading fungal P450s and the function of CYP5035 was left unassigned.

The presence of so many more CYP5035 sequences thus awoke new curiosity for this P450 family. Therefore, this study aimed at investigating the functional potential of CYP5035 that might harbour an evolutionary advantage for some fungal species, keeping in mind the possibility of successful bioprospecting for innovative P450 enzymes useful for synthetic and industrial purposes.

For efficient heterologous expression the yeast *P. pastoris* was used as the host organism due to strong promoters and expression strategies established in our laboratory (Vogl and Glieder 2013; Vogl et al. 2014; Weninger et al. 2015; Vogl et al. 2016; Vogl et al. 2018) and the advantage of the presence of an intrinsic, fungal P450 reductase (CPR) at low abundance of intracellular P450s. This CPR can be co-expressed additionally for better quantity. Based on literature results undertaking CYPome functionality studies, the native CPR of the yeast *Saccharomyces cerevisiae* generally seemed to couple well with basidiomycete P450s across different families (Hirosue et al. 2011; Nazir et al. 2011; Ide et al. 2012). It was thus presumed that the same would apply to the closely related yeast *Pichia pastoris*, which had proven to be an excellent host for P450 expression with the potential for industrial up-scaling in a bioreactor (Martinez and Rupashinghe 2013; Byrne 2015; Fessner et al. 2020).

Only a small library of nine CYP5035 monooxygenases of *P. arcularius* was picked in order to balance efforts to cover the high enzymatic diversity representatively on the one hand, and the immense screening efforts faced for the many substrates per enzyme planned on the other. In the end, this limited CYP5035 selection was sufficient to give a representative idea of the enzyme family's capabilities, although only CYP5035S7 was active in the fluorescence assay employing substrate MFC for activity screening. In light of missing demethylation activity, transformants of the other tested CYP5035 expression strains were picked randomly. Ultimately, authentic activity information as well as the efficient bioprospecting for fungal enzymes towards industrial application relies on efficient heterologous expression (Mitrovic and Glieder 2015). This subset of nine new and different P450 genes was expected to provide also some information about which fraction of new fungal P450 genes can be functionally expressed at all. Previous published studies demonstrated that functional expression of basidiomycete P450s is commonly based on trial and error (Schmidt-Dannert 2016).

In the substrate screening, especially CYP5035S7 showed a broad substrate scope encompassing PAHs and several natural product classes offering itself as an attractive P450 for natural product modification. The high conversion of PAHs is in line with several articles that identified white-rot fungal P450s of different families with remarkable PAH conversion abilities towards various ring sizes (Syed et al. 2010; Syed et al. 2011; Syed et al. 2013b). Particularly striking was the mutual conversion of *p*-cymene, *E*-stilbene and *EZ*-citral by three different CYP5035 enzymes each because carvacrol and resveratrol, which are derivatives of the former two compounds, as well as *EZ*-citral itself are known fungicidal agents (Yoneyama and Natsume 2010; Jian et al. 2016). Interestingly, none of the active enzymes tested here accepted any of the tested active pharmaceutical ingredients (APIs), although three of four active CYP5035 of *P. chrysosporium* converted naproxen in a previous study (Hirosue et al. 2011). These observations highlight the deviating nature of P450s of phylogenetically similar species or even the same subfamily with sequence identities of >60% but different chemoselectivity. At the same time, candidates of CYP5035 have now been shown to be multifunctional with a diverse catalytic activity oxidising PAHs, pharmaceuticals and various plant materials encompassing fungicidal agents, which strongly suggests that CYP5035 are part of the fungal detoxification mechanism just like CYP5136 and CYP5150.

In addition to the other two enriched families CYP5136 and CYP5150 mentioned earlier, this further increases the percentage of those enriched P450s with a detoxifying function to a third of the CYPome in the genome of *P. arcularius* (Supplementary Fig. S16). Apparently, *P. arcularius* and other species following the phylogenetic ladder up to the *Ganoderma* complex have an extensive repertoire of such xenobiotic-biodegrading P450s. As shown in Fig. 6 this phenomenon is preserved even when including P450 families CYP512 and CYP5141, which have also been flagged with xenobiotic-degrading functions (Syed et al. 2014). Interestingly, *T. versicolor* as the phylogenetic parent of the *Ganoderma* macrofungus also possesses an enhanced collection of such P450s in its genome compared to the other white-rot fungi. However, this is mainly due to the unmatched number of CYP5150 (Figs. 1, Supplementary Figs. S6 and S7).

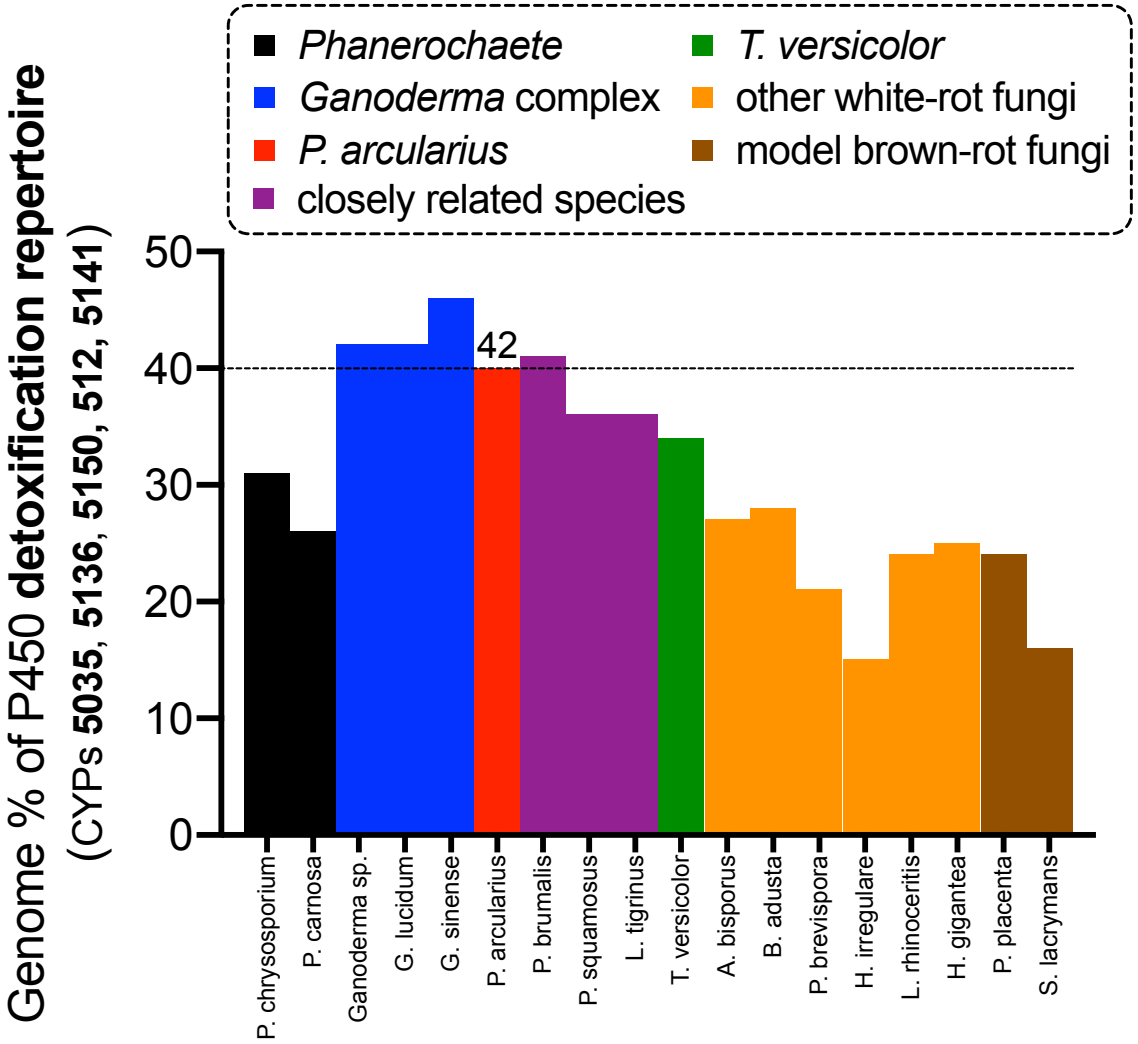

Fig. 6: A comparison of the P450s considered to be part of the detoxification repertoire of various white-rot fungi (CYP5035, CYP5136, CYP5150, CYP512 and CYP5141) as a percentage of the total number P450s in the fungus's genome.

Computing the phylogeny of both P450 families with minimum evolution trees made it possible to follow the evolutionary tree of this enrichment up to the *Ganoderma* complex, where the diversification of CYP5035 members might have branched off. The CYP5136 family expansion was found to have occurred separately for *Ganoderma* species and was intensified later. These conclusions were drawn due to the following observations: (1) The closer phylogenetic relation within the group of *P. arcularius*, *P. squamosus* and *L. tigrinus* to *Ganoderma* sp. than to white-rot fungi *P. chrysosporium*, *P. brevispora*, *T. versicolor* or *Bjerkandera adusta* became clearly visible. (2) An intensified diversification process of the P450 families can be noticed especially in Fig. 2 for CYP5035 in parallel to almost all of *Ganoderma* sp.'s enzymes, often yielding higher numbers of homologous P450s (examples marked by yellow stars). (3) Additionally, from some common nodes new branches diverged, which do not contain an enzyme member of *Ganoderma* sp. (examples marked by red stars). (4) Therefore, CYP5035 family expansion likely happened before speciation with *Ganoderma* as the starting point and continued further downstream. (5) In contrast, diversification of CYP5136

occurred separately in the case of *Ganoderma* as indicated by the lack of ortholog pairs, and started only later in time.

It remains unclear whether the *Ganoderma* macrofungus itself really is the starting point or merely one of the species in the row of the evolution of CYP5035 enrichment. However, the range of 13 – 26 members of CYP5035 and 7 – 9 members of CYP5136 within *Ganoderma* sp., *G. sinense* and *Ganoderma lucidum* is one argument for the former. The starting point of the diversification of CYP5136 is also unknown. Syed *et al.* suggested P450 gene duplication due to environmental adaptation as the origin for such family expansions (Syed et al. 2014). For example, the ortholog P450 of CYP5035C1 of *P. chrysosporium* was duplicated several times in *P. carnosa*, indicating some evolutionary advantage.

The sequence alignment search of CYP5035S7 against 102,000 P450 sequences from JGI only revealed orthologous enzymes (>80%) within the fungal species used in this study and generally indicated relatively small amounts of CYP5035 in each of the >30 other fungal species (Online Resource 3). Only *Dichomitus squalens* and *Earliella scabrosa* possessed a considerable number of CYP5035 sequences, suggesting that large numbers of this P450 family are rather rare. In addition, 38 of the 314 blasted sequences had <55% identity and will belong to yet undefined CYP5035 subfamilies.

In combination with the observed reasonable success rate for functional recombinant expression and the phylogenetic analysis of CYP5035 and CYP5136, this BLAST result provides a valuable starting point for future bioprospecting for xenobiotic-degrading P450s with activity towards plant compounds similar or complementary to *P. arcularius*. The large repertoire of such detoxification monooxygenases within the white-rot fungal genomes shown in Figure 6 incites further interest because it may provide a versatile toolbox of white-rot fungal P450 enzymes for natural product modification. Information about the activities of only three subfamilies were uncovered to date, although already >50 different CYP5035 subfamilies were categorised and will increase further. Hence, despite the efforts of this study, there remains a large functional gap and an unhidden catalytic potential for CYP5035.

Despite their biosynthetic potential (Fessner 2019), the majority of P450s remain so-called functionally uncharacterised 'orphan P450s' (Kelly and Kelly 2013) due to the shortage of studies investigating them (Durairaj et al. 2016), the expression difficulties (Schmidt-Dannert 2016) also observed in this study and the sheer amount of sequences available in the sequenced genomes (Ferrer et al. 2016). Therefore, this study aimed at and substantially helped to obtain more information about the function of the hardly studied CYP5035. Additionally, the multifunctional enzyme CYP5035S7 was identified in *P. arcularius* holding a versatile synthetic potential that remains to be investigated further in lab- and pilot-scale experiments.

Acknowledgement

The authors thank Prof. Margit Winkler and Prof. Harald Pichler, Prof. Rolf Breinbauer and Prof. Wolfgang Kroutil for providing substrates for the screening. The authors also acknowledge the JGI Mycocosm Fungal Genomics Resource database for the publicly accessible genomes. The authors are grateful to Prof. Francis Martin and the CSP 1974 '1KFG: Deep sequencing of ecologically-relevant Dikaria' consortium for access to the unpublished genome data of *P. squamosus*. The genome sequence data were produced by the US Department of Energy Joint Genome Institute in collaboration with the user community.

Declarations

Funding
This project has received funding from the European Union's Horizon 2020 research and innovation programme, OXYtrain MSCA-ITN, under grant agreement No 722390.

Conflict of interest
The authors declare that they have no competing interests.

Ethics approval
This article does not contain any studies with human participants or animals performed by any of the authors.

Consent to participate
This article does not contain any studies with human participants.

Consent for publication
The authors give formal consent for the publication of this study.

Availability of data and material
The data supporting the findings of this study are available within this article and the supplementary materials. The fungal genome data, on which this study is based, are publicly available online as outlined in the Material and Methods section.

Code availability
Any software used in this study for genomic data processing is publicly available online *via* the links provided in the Material and Methods section.

Author Contributions
N.D.F. and A.G. conceived of and designed research. N.D.F. conducted experiments, analysed data and wrote the original manuscript. D.R.N. annotated the P450s and performed the alignment search. N.D.F. and A.G. jointly reviewed and edited manuscript. A.G. supervised and managed scientific and financial project reporting. All authors read and approved the manuscript.

Binder M, Justo A, Riley R, Salamov A, Lopez-Giraldez F, Sjökvist E, Copeland A, Foster B, Sun H, Larsson E, Larsson K-H, Townsend J, Grigoriev I V., Hibbett DS (2013) Phylogenetic and phylogenomic overview of the Polyporales. Mycologia 105:1350–1373 . https://doi.org/10.3852/13-003

Byrne B (2015) Pichia pastoris as an expression host for membrane protein structural biology. Curr Opin Struct Biol 32:9–17 . https://doi.org/10.1016/j.sbi.2015.01.005

Chen S, Xu J, Liu C, Zhu Y, Nelson DR, Zhou S, Li C, Wang L, Guo X, Sun Y, Luo H, Li Y, Song J, Henrissat B, Levasseur A, Qian J, Li J, Luo X, Shi L, He L, Xiang L, Xu X, Niu Y, Li Q, Han M V., Yan H, Zhang J, Chen H, Lv A, Wang Z, Liu M, Schwartz DC, Sun C (2012) Genome sequence of the model medicinal mushroom Ganoderma lucidum. Nat Commun 3:913 . https://doi.org/10.1038/ncomms1923

Chen W, Lee M-K, Jefcoate C, Kim S-C, Chen F, Yu J-H (2014) Fungal Cytochrome P450 Monooxygenases: Their Distribution, Structure, Functions, Family Expansion, and Evolutionary Origin. Genome Biol Evol 6:1620–1634 . https://doi.org/10.1093/gbe/evu132

Chigu NL, Hirosue S, Nakamura C, Teramoto H, Ichinose H, Wariishi H (2010)

Cytochrome P450 monooxygenases involved in anthracene metabolism by the white-rot basidiomycete Phanerochaete chrysosporium. Appl Microbiol Biotechnol 87:1907–1916 . https://doi.org/10.1007/s00253-010-2616-1

Dao ATN, Vonck J, Janssens TKS, Dang HTC, Brouwer A, de Boer TE (2019) Screening white-rot fungi for bioremediation potential of 2,3,7,8-tetrachlorodibenzo-p-dioxin. Ind Crops Prod 128:153–161 . https://doi.org/10.1016/j.indcrop.2018.10.059

Donato MT, Jiménez N, Castell J V., Gómez-Lechón MJ (2004) FLUORESCENCE-BASED ASSAYS FOR SCREENING NINE CYTOCHROME P450 (P450) ACTIVITIES IN INTACT CELLS EXPRESSING INDIVIDUAL HUMAN P450 ENZYMES. Drug Metab Dispos 32:699–706 . https://doi.org/10.1124/dmd.32.7.699

Durairaj P, Hur J-S, Yun H (2016) Versatile biocatalysis of fungal cytochrome P450 monooxygenases. Microb Cell Fact 15:125 . https://doi.org/10.1186/s12934-016-0523-6

Eastwood DC, Floudas D, Binder M, Majcherczyk A, Schneider P, Aerts A, Asiegbu FO, Baker SE, Barry K, Bendiksby M, Blumentritt M, Coutinho PM, Cullen D, de Vries RP, Gathman A, Goodell B, Henrissat B, Ihrmark K, Kauserud H, Kohler A, LaButti K, Lapidus A, Lavin JL, Lee Y-H, Lindquist E, Lilly W, Lucas S, Morin E, Murat C, Oguiza JA, Park J, Pisabarro AG, Riley R, Rosling A, Salamov A, Schmidt O, Schmutz J, Skrede I, Stenlid J, Wiebenga A, Xie X, Kues U, Hibbett DS, Hoffmeister D, Hogberg N, Martin F, Grigoriev I V., Watkinson SC (2011) The Plant Cell Wall-Decomposing Machinery Underlies the Functional Diversity of Forest Fungi. Science (80-) 333:762–765 . https://doi.org/10.1126/science.1205411

Ferrer M, Martínez-Martínez M, Bargiela R, Streit WR, Golyshina O V., Golyshin PN (2016) Estimating the success of enzyme bioprospecting through metagenomics: current status and future trends. Microb Biotechnol 9:22–34 . https://doi.org/10.1111/1751-7915.12309

Fessner ND (2019) P450 Monooxygenases Enable Rapid Late-Stage Diversification of Natural Products via C−H Bond Activation. ChemCatChem 11:2226–2242 . https://doi.org/10.1002/cctc.201801829

Fessner ND, Srdic M, Weber H, Schmid C, Schoenauer D, Schwaneberg U, Glieder A (2020) Preparative-Scale Production of Testosterone Metabolites by Human Liver Cytochrome P450 3A4. Adv Synth Catal 362:adsc.202000251 . https://doi.org/10.1002/adsc.202000251

Floudas D, Binder M, Riley R, Barry K, Blanchette RA, Henrissat B, Martínez AT, Otillar R, Spatafora JW, Yadav JS, Aerts A, Benoit I, Boyd A, Carlson A, Copeland A, Coutinho PM, de Vries RP, Ferreira P, Findley K, Foster B, Gaskell J, Glotzer D, Górecki P, Heitman J, Hesse C, Hori C, Igarashi K, Jurgens JA, Kallen N, Kersten P, Kohler A, Kües U, Kumar TKA, Kuo A, LaButti K, Larrondo LF, Lindquist E, Ling A, Lombard V, Lucas S, Lundell T, Martin R, McLaughlin DJ, Morgenstern I, Morin E, Murat C, Nagy LG, Nolan M, Ohm RA, Patyshakuliyeva A, Rokas A, Ruiz-Dueñas FJ, Sabat G, Salamov A, Samejima M, Schmutz J, Slot JC, St. John F, Stenlid J, Sun H, Sun S, Syed K, Tsang A, Wiebenga A, Young D, Pisabarro A, Eastwood DC, Martin F, Cullen D, Grigoriev I V., Hibbett DS (2012) The Paleozoic Origin of Enzymatic Lignin Decomposition Reconstructed from 31 Fungal Genomes. Science (80-) 336:1715–1719 . https://doi.org/10.1126/science.1221748

Gerlt JA (2007) A Protein Structure (or Function ?) Initiative. Structure 15:1353–1356 . https://doi.org/10.1016/j.str.2007.10.003

Gerlt JA, Allen KN, Almo SC, Armstrong RN, Babbitt PC, Cronan JE, Dunaway-Mariano D, Imker HJ, Jacobson MP, Minor W, Poulter CD, Raushel FM, Sali A, Shoichet BK, Sweedler J V. (2011) The Enzyme Function Initiative. Biochemistry 50:9950–9962 .

608 https://doi.org/10.1021/bi201312u
609 Grigoriev I V., Cullen D, Goodwin SB, Hibbett D, Jeffries TW, Kubicek CP, Kuske C,
610 Magnuson JK, Martin F, Spatafora JW, Tsang A, Baker SE (2011) Fueling the future
611 with fungal genomics. Mycology 2:192–209 .
612 https://doi.org/10.1080/21501203.2011.584577
613 Grigoriev I V., Nikitin R, Haridas S, Kuo A, Ohm R, Otillar R, Riley R, Salamov A, Zhao X,
614 Korzeniewski F, Smirnova T, Nordberg H, Dubchak I, Shabalov I (2014) MycoCosm
615 portal: Gearing up for 1000 fungal genomes. Nucleic Acids Res 42:699–704 .
616 https://doi.org/10.1093/nar/gkt1183
617 Hatakeyama M, Kitaoka T, Ichinose H (2016) Heterologous expression of fungal
618 cytochromes P450 (CYP5136A1 and CYP5136A3) from the white-rot basidiomycete
619 Phanerochaete chrysosporium: Functionalization with cytochrome b5 in
620 Escherichia coli. Enzyme Microb Technol 89:7–14 .
621 https://doi.org/10.1016/j.enzmictec.2016.03.004
622 Hirosue S, Tazaki M, Hiratsuka N, Yanai S, Kabumoto H, Shinkyo R, Arisawa A, Sakaki T,
623 Tsunekawa H, Johdo O, Ichinose H, Wariishi H (2011) Insight into functional
624 diversity of cytochrome P450 in the white-rot basidiomycete Phanerochaete
625 chrysosporium: Involvement of versatile monooxygenase. Biochem Biophys Res
626 Commun 407:118–123 . https://doi.org/10.1016/j.bbrc.2011.02.121
627 Hori C, Ishida T, Igarashi K, Samejima M, Suzuki H, Master E, Ferreira P, Ruiz-Dueñas FJ,
628 Held B, Canessa P, Larrondo LF, Schmoll M, Druzhinina IS, Kubicek CP, Gaskell JA,
629 Kersten P, St. John F, Glasner J, Sabat G, Splinter BonDurant S, Syed K, Yadav J,
630 Mgbeahuruike AC, Kovalchuk A, Asiegbu FO, Lackner G, Hoffmeister D, Rencoret J,
631 Gutiérrez A, Sun H, Lindquist E, Barry K, Riley R, Grigoriev I V., Henrissat B, Kües U,
632 Berka RM, Martínez AT, Covert SF, Blanchette RA, Cullen D (2014) Analysis of the
633 Phlebiopsis gigantea Genome, Transcriptome and Secretome Provides Insight into
634 Its Pioneer Colonization Strategies of Wood. PLoS Genet 10:e1004759 .
635 https://doi.org/10.1371/journal.pgen.1004759
636 Ichinose H (2013) Cytochrome P450 of wood-rotting basidiomycetes and
637 biotechnological applications. Biotechnol Appl Biochem 60:71–81 .
638 https://doi.org/10.1002/bab.1061
639 Ichinose H, Wariishi H (2012) Heterologous expression and mechanistic investigation of
640 a fungal cytochrome P450 (CYP5150A2): Involvement of alternative redox
641 partners. Arch Biochem Biophys 518:8–15 .
642 https://doi.org/10.1016/j.abb.2011.12.010
643 Ide M, Ichinose H, Wariishi H (2012) Molecular identification and functional
644 characterization of cytochrome P450 monooxygenases from the brown-rot
645 basidiomycete Postia placenta. Arch Microbiol 194:243–253 .
646 https://doi.org/10.1007/s00203-011-0753-2
647 Jian W, He D, Song S (2016) Synthesis, Biological Evaluation and Molecular Modeling
648 Studies of New Oxadiazole-Stilbene Hybrids against Phytopathogenic Fungi. Sci Rep
649 6:31045 . https://doi.org/10.1038/srep31045
650 Justo A, Hibbett DS (2011) Phylogenetic classification of Trametes (Basidiomycota,
651 Polyporales) based on a five-marker dataset. Taxon 60:1567–1583 .
652 https://doi.org/10.1002/tax.606003
653 Kasai N, Ikushiro S, Hirosue S, Arisawa A, Ichinose H, Uchida Y, Wariishi H, Ohta M,
654 Sakaki T (2010a) Atypical kinetics of cytochromes P450 catalysing 3'-hydroxylation
655 of flavone from the white-rot fungus Phanerochaete chrysosporium. J Biochem
656 147:117–125 . https://doi.org/10.1093/jb/mvp155
657 Kasai N, Ikushiro S, Hirosue S, Arisawa A, Ichinose H, Wariishi H, Ohta M, Sakaki T

(2009) Enzymatic properties of cytochrome P450 catalyzing 3′-hydroxylation of naringenin from the white-rot fungus Phanerochaete chrysosporium. Biochem Biophys Res Commun 387:103–108 . https://doi.org/10.1016/j.bbrc.2009.06.134
Kasai N, Ikushiro S, Shinkyo R, Yasuda K, Hirosue S, Arisawa A, Ichinose H, Wariishi H, Sakaki T (2010b) Metabolism of mono- and dichloro-dibenzo-p-dioxins by Phanerochaete chrysosporium cytochromes P450. Appl Microbiol Biotechnol 86:773–780 . https://doi.org/10.1007/s00253-009-2413-x
Kelly SL, Kelly DE (2013) Microbial cytochromes P450: biodiversity and biotechnology. Where do cytochromes P450 come from, what do they do and what can they do for us? Philos Trans R Soc B Biol Sci 368:20120476 . https://doi.org/10.1098/rstb.2012.0476
Kües U (2015) Fungal enzymes for environmental management. Curr Opin Biotechnol 33:268–278 . https://doi.org/10.1016/j.copbio.2015.03.006
Kües U, Nelson DR, Liu C, Yu G-J, Zhang J, Li J, Wang X-C, Sun H (2015) Genome analysis of medicinal Ganoderma spp. with plant-pathogenic and saprotrophic life-styles. Phytochemistry 114:18–37 . https://doi.org/10.1016/j.phytochem.2014.11.019
Kumar S, Stecher G, Li M, Knyaz C, Tamura K (2018) MEGA X: Molecular Evolutionary Genetics Analysis across Computing Platforms. Mol Biol Evol 35:1547–1549 . https://doi.org/10.1093/molbev/msy096
Lu W, Feng J, Chen X, Bao Y-J, Wang Y, Wu Q, Ma Y, Zhu D (2019) Distinct Regioselectivity of Fungal P450 Enzymes for Steroidal Hydroxylation. Appl Environ Microbiol 85:1–13 . https://doi.org/10.1128/AEM.01182-19
Mäkelä MR, Hildén K, Kowalczyk JE, Hatakka A (2020) Progress and Research Needs of Plant Biomass Degradation by Basidiomycete Fungi. In: Nevalainen H (ed) Grand Challenges in Fungal Biotechnology. Grand Challenges in Biology and Biotechnology. Springer Nature Switzerland, Cham, pp 405–438
Martinez C, Rupashinghe S (2013) Cytochrome P450 Bioreactors in the Pharmaceutical Industry: Challenges and Opportunities. Curr Top Med Chem 13:1470–1490 . https://doi.org/10.2174/15680266113139990111
Martinez D, Challacombe J, Morgenstern I, Hibbett D, Schmoll M, Kubicek CP, Ferreira P, Ruiz-Duenas FJ, Martinez AT, Kersten P, Hammel KE, Vanden Wymelenberg A, Gaskell J, Lindquist E, Sabat G, Splinter BonDurant S, Larrondo LF, Canessa P, Vicuna R, Yadav J, Doddapaneni H, Subramanian V, Pisabarro AG, Lavín JL, Oguiza JA, Master E, Henrissat B, Coutinho PM, Harris P, Magnuson JK, Baker SE, Bruno K, Kenealy W, Hoegger PJ, Kües U, Ramaiya P, Lucas S, Salamov A, Shapiro H, Tu H, Chee CL, Misra M, Xie G, Teter S, Yaver D, James T, Mokrejs M, Pospisek M, Grigoriev I V., Brettin T, Rokhsar D, Berka R, Cullen D (2009) Genome, transcriptome, and secretome analysis of wood decay fungus Postia placenta supports unique mechanisms of lignocellulose conversion. Proc Natl Acad Sci 106:1954–1959 . https://doi.org/10.1073/pnas.0809575106
Martinez D, Larrondo LF, Putnam N, Gelpke MDS, Huang K, Chapman J, Helfenbein KG, Ramaiya P, Detter JC, Larimer F, Coutinho PM, Henrissat B, Berka R, Cullen D, Rokhsar D (2004) Genome sequence of the lignocellulose degrading fungus Phanerochaete chrysosporium strain RP78. Nat Biotechnol 22:695–700 . https://doi.org/10.1038/nbt967
McKay T, Hart K, Horn A, Kessler H, Dodge G, Bardhi K, Bardhi K, Mills JL, Bernstein HJ, Craig PA (2015) Annotation of proteins of unknown function: initial enzyme results. J Struct Funct Genomics 16:43–54 . https://doi.org/10.1007/s10969-015-9194-5
Mgbeahuruike AC, Kovalchuk A, Ubhayasekera W, Nelson DR, Yadav JS (2017) CYPome of the conifer pathogen Heterobasidion irregulare: Inventory, phylogeny, and

transcriptional analysis of the response to biocontrol. Fungal Biol 121:158–171 . https://doi.org/10.1016/j.funbio.2016.11.006
Mitrovic A, Glieder A (2015) Discovery of fungal enzymes and pathways. In: Gupta VK, Mach RL, Sreenivasaprasad S (eds) Fungal Biomolecules: Sources, Applications and Recent Developments. John Wiley & Sons, Ltd, Chichester, UK, pp 51–62
Miyauchi S, Rancon A, Drula E, Hage H, Chaduli D, Favel A, Grisel S, Henrissat B, Herpoël-Gimbert I, Ruiz-Dueñas FJ, Chevret D, Hainaut M, Lin J, Wang M, Pangilinan J, Lipzen A, Lesage-Meessen L, Navarro D, Riley R, Grigoriev I V., Zhou S, Raouche S, Rosso M-N (2018) Integrative visual omics of the white-rot fungus Polyporus brumalis exposes the biotechnological potential of its oxidative enzymes for delignifying raw plant biomass. Biotechnol Biofuels 11:201 . https://doi.org/10.1186/s13068-018-1198-5
Moktali V, Park J, Fedorova-Abrams ND, Park B, Choi J, Lee Y-H, Kang S (2012) Systematic and searchable classification of cytochrome P450 proteins encoded by fungal and oomycete genomes. BMC Genomics 13:1–13 . https://doi.org/10.1186/1471-2164-13-525
Morin E, Kohler A, Baker AR, Foulongne-Oriol M, Lombard V, Nagye LG, Ohm RA, Patyshakuliyeva A, Brun A, Aerts AL, Bailey AM, Billette C, Coutinho PM, Deakin G, Doddapaneni H, Floudas D, Grimwood J, Hilden K, Kues U, LaButti KM, Lapidus A, Lindquist EA, Lucas SM, Murat C, Riley RW, Salamov AA, Schmutz J, Subramanian V, Wosten HAB, Xu J, Eastwood DC, Foster GD, Sonnenberg ASM, Cullen D, de Vries RP, Lundell T, Hibbett DS, Henrissat B, Burton KS, Kerrigan RW, Challen MP, Grigoriev I V., Martin F (2012) Genome sequence of the button mushroom Agaricus bisporus reveals mechanisms governing adaptation to a humic-rich ecological niche. Proc Natl Acad Sci 109:17501–17506 . https://doi.org/10.1073/pnas.1206847109
Nazir KHMNH, Ichinose H, Wariishi H (2011) Construction and Application of a Functional Library of Cytochrome P450 Monooxygenases from the Filamentous Fungus Aspergillus oryzae. Appl Environ Microbiol 77:3147–3150 . https://doi.org/10.1128/AEM.02491-10
Nei M, Kumar S (2000) Molecular Evolution and Phylogenetics. Oxford University Press, New York
Nelson DR (2006) Cytochrome P450 Nomenclature, 2004. In: Philips IR, Shephard EA (eds) Cytochrome P450 Protocols. Humana Press, New Jersey, pp 1–10
Nelson DR (2009) The Cytochrome P450 Homepage. Hum Genomics 4:59 . https://doi.org/10.1186/1479-7364-4-1-59
Peralta RM, da Silva BP, Gomes Côrrea RC, Kato CG, Vicente Seixas FA, Bracht A (2017) Enzymes from Basidiomycetes—Peculiar and Efficient Tools for Biotechnology. In: Brahmachari G (ed) Biotechnology of Microbial Enzymes. Elsevier Inc., pp 119–149
Rzhetsky A, Nei M (1992) A Simple Method for Estimating and Testing Minimum-Evolution Trees. Mol Biol Evol 9:945–967 . https://doi.org/10.1093/oxfordjournals.molbev.a040771
Saitou N, Nei M (1987) The neighbor-joining method: a new method for reconstructing phylogenetic trees. Mol Biol Evol 4:406–425 . https://doi.org/10.1093/oxfordjournals.molbev.a040454
Sakai K, Matsuzaki F, Wise L, Sakai Y, Jindou S, Ichinose H, Takaya N, Kato M, Wariishi H, Shimizu M (2018) Biochemical Characterization of CYP505D6, a Self-Sufficient Cytochrome P450 from the White-Rot Fungus Phanerochaete chrysosporium. Appl Environ Microbiol 84:1–15 . https://doi.org/10.1128/AEM.01091-18
Schmidt-Dannert C (2016) Biocatalytic portfolio of Basidiomycota. Curr Opin Chem Biol 31:40–49 . https://doi.org/10.1016/j.cbpa.2016.01.002

758 Stecher G, Tamura K, Kumar S (2020) Molecular Evolutionary Genetics Analysis (MEGA)
759 for macOS. Mol Biol Evol 37:1237–1239 . https://doi.org/10.1093/molbev/msz312
760 Sturmberger L, Chappell T, Geier M, Krainer F, Day KJ, Vide U, Trstenjak S, Schiefer A,
761 Richardson T, Soriaga L, Darnhofer B, Birner-Gruenberger R, Glick BS, Tolstorukov
762 I, Cregg J, Madden K, Glieder A (2016) Refined Pichia pastoris reference genome
763 sequence. J Biotechnol 235:121–131 .
764 https://doi.org/10.1016/j.jbiotec.2016.04.023
765 Suzuki H, MacDonald J, Syed K, Salamov A, Hori C, Aerts A, Henrissat B, Wiebenga A,
766 VanKuyk PA, Barry K, Lindquist E, LaButti K, Lapidus A, Lucas S, Coutinho P, Gong Y,
767 Samejima M, Mahadevan R, Abou-Zaid M, de Vries RP, Igarashi K, Yadav JS,
768 Grigoriev I V., Master ER (2012) Comparative genomics of the white-rot fungi,
769 Phanerochaete carnosa and P. chrysosporium, to elucidate the genetic basis of the
770 distinct wood types they colonize. BMC Genomics 13:444 .
771 https://doi.org/10.1186/1471-2164-13-444
772 Syed K, Doddapaneni H, Subramanian V, Lam YW, Yadav JS (2010) Genome-to-function
773 characterization of novel fungal P450 monooxygenases oxidizing polycyclic
774 aromatic hydrocarbons (PAHs). Biochem Biophys Res Commun 399:492–497 .
775 https://doi.org/10.1016/j.bbrc.2010.07.094
776 Syed K, Mashele SS (2014) Comparative Analysis of P450 Signature Motifs EXXR and
777 CXG in the Large and Diverse Kingdom of Fungi: Identification of Evolutionarily
778 Conserved Amino Acid Patterns Characteristic of P450 Family. PLoS One 9:e95616 .
779 https://doi.org/10.1371/journal.pone.0095616
780 Syed K, Nelson DR, Riley R, Yadav JS (2013a) Genomewide annotation and comparative
781 genomics of cytochrome P450 monooxygenases (P450s) in the polypore species
782 Bjerkandera adusta , Ganoderma sp. and Phlebia brevispora. Mycologia 105:1445–
783 1455 . https://doi.org/10.3852/13-002
784 Syed K, Porollo A, Lam YW, Grimmett PE, Yadav JS (2013b) CYP63A2, a Catalytically
785 Versatile Fungal P450 Monooxygenase Capable of Oxidizing Higher-Molecular-
786 Weight Polycyclic Aromatic Hydrocarbons, Alkylphenols, and Alkanes. Appl Environ
787 Microbiol 79:2692–2702 . https://doi.org/10.1128/AEM.03767-12
788 Syed K, Porollo A, Lam YW, Yadav JS (2011) A Fungal P450 (CYP5136A3) Capable of
789 Oxidizing Polycyclic Aromatic Hydrocarbons and Endocrine Disrupting
790 Alkylphenols: Role of Trp129 and Leu324. PLoS One 6:e28286 .
791 https://doi.org/10.1371/journal.pone.0028286
792 Syed K, Porollo A, Miller D, Yadav JS (2013c) Rational engineering of the fungal P450
793 monooxygenase CYP5136A3 to improve its oxidizing activity toward polycyclic
794 aromatic hydrocarbons. Protein Eng Des Sel 26:553–557 .
795 https://doi.org/10.1093/protein/gzt036
796 Syed K, Shale K, Pagadala NS, Tuszynski J (2014) Systematic Identification and
797 Evolutionary Analysis of Catalytically Versatile Cytochrome P450 Monooxygenase
798 Families Enriched in Model Basidiomycete Fungi. PLoS One 9:e86683 .
799 https://doi.org/10.1371/journal.pone.0086683
800 Syed K, Yadav JS (2012) P450 monooxygenases (P450ome) of the model white rot
801 fungus Phanerochaete chrysosporium. Crit Rev Microbiol 38:339–363 .
802 https://doi.org/10.3109/1040841X.2012.682050
803 Varga T, Krizsán K, Földi C, Dima B, Sánchez-García M, Sánchez-Ramírez S, Szöllősi GJ,
804 Szarkándi JG, Papp V, Albert L, Andreopoulos W, Angelini C, Antonín V, Barry KW,
805 Bougher NL, Buchanan P, Buyck B, Bense V, Catcheside P, Chovatia M, Cooper J,
806 Dämon W, Desjardin D, Finy P, Geml J, Haridas S, Hughes K, Justo A, Karasiński D,
807 Kautmanova I, Kiss B, Kocsubé S, Kotiranta H, LaButti KM, Lechner BE, Liimatainen

808 K, Lipzen A, Lukács Z, Mihaltcheva S, Morgado LN, Niskanen T, Noordeloos ME, Ohm
809 RA, Ortiz-Santana B, Ovrebo C, Rácz N, Riley R, Savchenko A, Shiryaev A, Soop K,
810 Spirin V, Szebenyi C, Tomšovský M, Tulloss RE, Uehling J, Grigoriev I V., Vágvölgyi C,
811 Papp T, Martin FM, Miettinen O, Hibbett DS, Nagy LG (2019) Megaphylogeny
812 resolves global patterns of mushroom evolution. Nat Ecol Evol 3:668–678 .
813 https://doi.org/10.1038/s41559-019-0834-1
814 Vogl T, Glieder A (2013) Regulation of Pichia pastoris promoters and its consequences
815 for protein production. N Biotechnol 30:385–404 .
816 https://doi.org/10.1016/j.nbt.2012.11.010
817 Vogl T, Kickenweiz T, Pitzer J, Sturmberger L, Weninger A, Biggs BW, Köhler E-M,
818 Baumschlager A, Fischer JE, Hyden P, Wagner M, Baumann M, Borth N, Geier M,
819 Ajikumar PK, Glieder A (2018) Engineered bidirectional promoters enable rapid
820 multi-gene co-expression optimization. Nat Commun 9:3589 .
821 https://doi.org/10.1038/s41467-018-05915-w
822 Vogl T, Ruth C, Pitzer J, Kickenweiz T, Glieder A (2014) Synthetic Core Promoters for
823 Pichia pastoris. ACS Synth Biol 3:188–191 . https://doi.org/10.1021/sb400091p
824 Vogl T, Sturmberger L, Kickenweiz T, Wasmayer R, Schmid C, Hatzl AM, Gerstmann MA,
825 Pitzer J, Wagner M, Thallinger GG, Geier M, Glieder A (2016) A Toolbox of Diverse
826 Promoters Related to Methanol Utilization: Functionally Verified Parts for
827 Heterologous Pathway Expression in Pichia pastoris. ACS Synth Biol 5:172–186 .
828 https://doi.org/10.1021/acssynbio.5b00199
829 Wang J, Ohno H, Ide Y, Ichinose H, Mori T, Kawagishi H, Hirai H (2019) Identification of
830 the cytochrome P450 involved in the degradation of neonicotinoid insecticide
831 acetamiprid in Phanerochaete chrysosporium. J Hazard Mater 371:494–498 .
832 https://doi.org/10.1016/j.jhazmat.2019.03.042
833 Wang W-F, Xiao H, Zhong J-J (2018) Biosynthesis of a ganoderic acid in Saccharomyces
834 cerevisiae by expressing a cytochrome P450 gene from Ganoderma lucidum.
835 Biotechnol Bioeng 115:1842–1854 . https://doi.org/10.1002/bit.26583
836 Weis R, Luiten R, Skranc W, Schwab H, Wubbolts M, Glieder A (2004) Reliable high-
837 throughput screening with by limiting yeast cell death phenomena. FEMS Yeast Res
838 5:179–189 . https://doi.org/10.1016/j.femsyr.2004.06.016
839 Weninger A, Glieder A, Vogl T (2015) A toolbox of endogenous and heterologous nuclear
840 localization sequences for the methylotrophic yeastpichia pastoris. FEMS Yeast Res
841 15:fov082 . https://doi.org/10.1093/femsyr/fov082
842 Wu B, Xu Z, Knudson A, Carlson A, Chen N, Kovaka S, LaButti K, Lipzen A, Pennachio C,
843 Riley R, Schakwitz W, Umezawa K, Ohm RA, Grigoriev I V., Nagy LG, Gibbons J,
844 Hibbett D (2018) Genomics and Development of Lentinus tigrinus : A White-Rot
845 Wood-Decaying Mushroom with Dimorphic Fruiting Bodies. Genome Biol Evol
846 10:3250–3261 . https://doi.org/10.1093/gbe/evy246
847 Yadav AN, Gupta A, Mishra S, Singh S (2019) Recent Advancement in White
848 Biotechnology Through Fungi. Springer International Publishing, Cham
849 Yang C, Li W, Li C, Zhou Z, Xiao Y, Yan X (2018) Metabolism of ganoderic acids by a
850 Ganoderma lucidum cytochrome P450 and the 3-keto sterol reductase ERG27 from
851 yeast. Phytochemistry 155:83–92 .
852 https://doi.org/10.1016/j.phytochem.2018.07.009
853 Yap H-YY, Chooi Y-H, Firdaus-Raih M, Fung S-Y, Ng S-T, Tan C-S, Tan N-H (2014) The
854 genome of the Tiger Milk mushroom, Lignosus rhinocerotis, provides insights into
855 the genetic basis of its medicinal properties. BMC Genomics 15:635 .
856 https://doi.org/10.1186/1471-2164-15-635
857 Yoneyama K, Natsume M (2010) Allelochemicals for Plant–Plant and Plant–Microbe

Interactions. In: Liu H-W, Mander L (eds) Comprehensive natural products II: Chemistry and Biology, vol. 4. Elsevier Ltd., Amsterdam, pp 539–561

Zhu Y, Xu J, Sun C, Zhou S, Xu H, Nelson DR, Qian J, Song J, Luo H, Xiang L, Li Y, Xu Z, Ji A, Wang L, Lu S, Hayward A, Sun W, Li X, Schwartz DC, Wang Y, Chen S (2015) Chromosome-level genome map provides insights into diverse defense mechanisms in the medicinal fungus Ganoderma sinense. Sci Rep 5:11087 . https://doi.org/10.1038/srep11087

Zuckerhandl E, Pauling L (1965) Evolutionary divergence and convergence in proteins. In: Bryson V, Vogel HJ (eds) Evolving Genes and Proteins. Academic Press, New York, pp 97–166

Supporting Information

Evolution and Enrichment of CYP5035 and CYP5136 in *Polyporales*: Functionality of an understudied P450 family

Nico D. Fessner, David R. Nelson and Anton Glieder*

Table S1: Displayed are all CYP5035 expressed here and in prior literature so far together with their tested substrate tolerance, host fungus and corresponding reference.

Reference	Fungus	**CYP5035…**	**Sequence ID**	**Substrate**
10.1016/j.bbrc.2011.02.121	*Phanerochaete chrysosporium*	A1	7306	naproxen
		A2	138612	naproxen
		A3	8961	?
		A4	8962	?
		A5	138737	flavone
		A6	5333	?
		A7	8949	?
		B1	–	?
		B2	8912	naproxen & abietic acid
		B3	6048	?
		C1	9198	?
		D1	–	?
		E1	5317	?
10.1007/s00203-011-0753-2	*Postia placenta*	F1	112190	?
		F2	129155	?
		F3v1	89499	?
		F3v2	89499	?
This study	*Polyporus arcularius*	H2	665169	(*EZ*)-citral, *p*-cymene, indole
		N5	196845	?
		N6	521854	?
		S6	652223	(*E*)-stilbene
		S7	664247	**multi-functional**
		S8	665466	?
		S9	668252	(*E*)-stilbene, (*EZ)*-citral, *p*-cymene
		AU1	519317	?
		AV1	667965	?

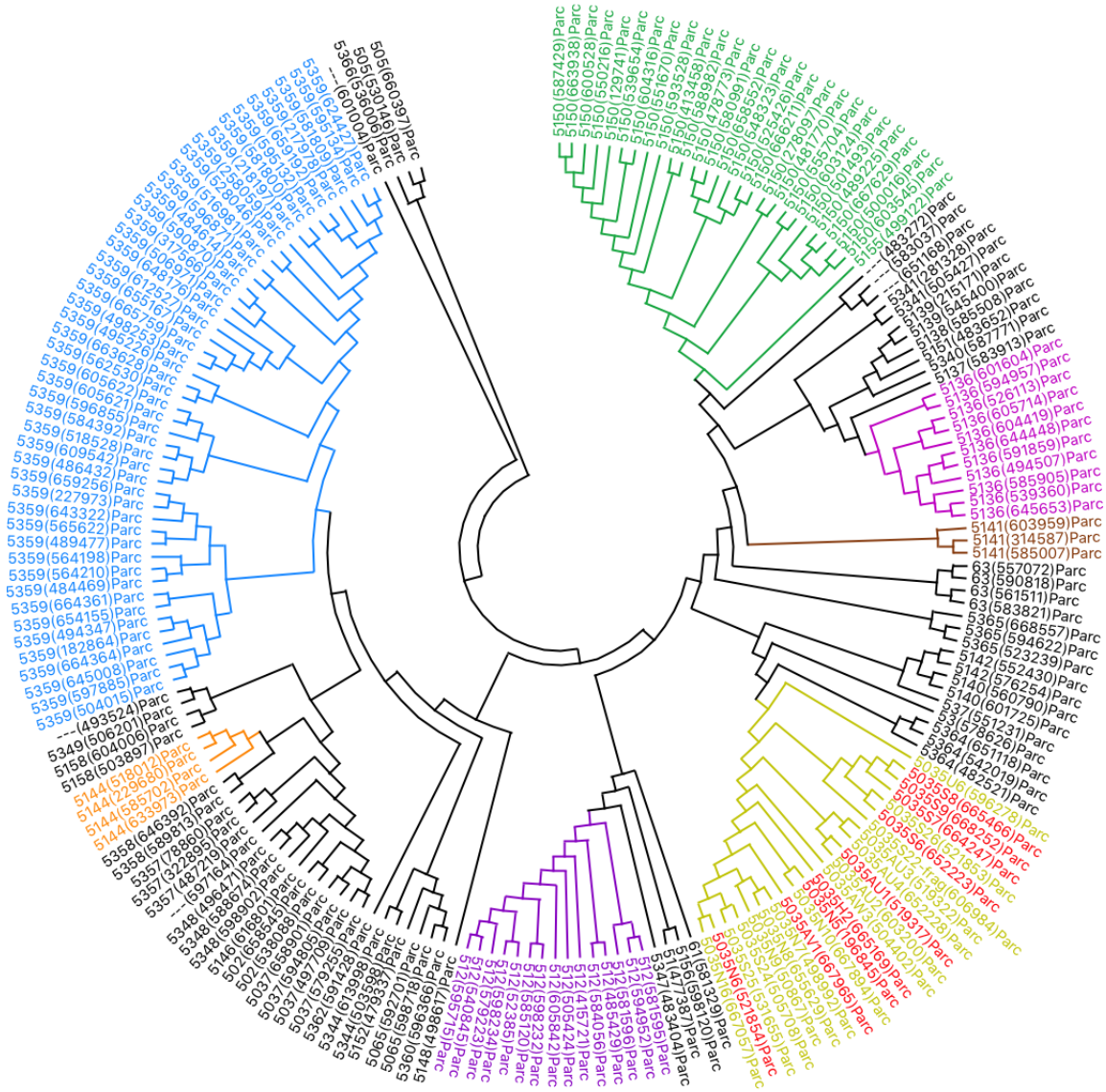

Fig. S1: A minimum evolution tree of the P450ome of *P. arcularius* involving 193 amino acid sequences. CYP512 (purple), CYP5035 (dark yellow), CYP5136 (violet), CYP5141 (brown), CYP5144 (orange), CYP5150 (green) and CYP5359 (blue) have been coloured. The P450 nomenclature of the CYP5035 selected and expressed for a functional screening is shown in red. The tree was constructed using the close-neighbour-interchange algorithm in MEGA X.

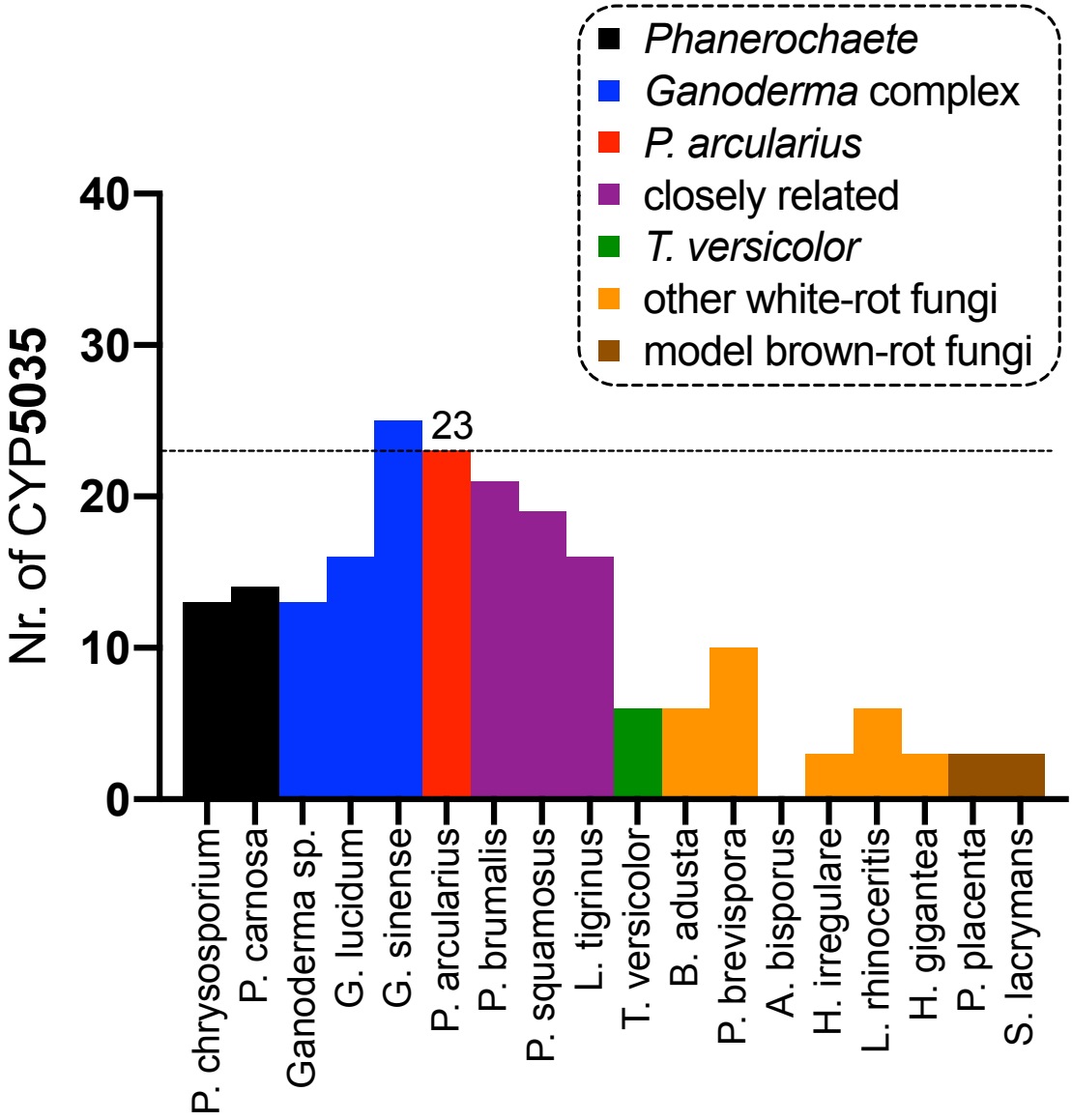

Fig. S2: Comparison of the number of CYP5035 in the genome of *P. arcularius* versus a variety of white- and brown-rot fungi.

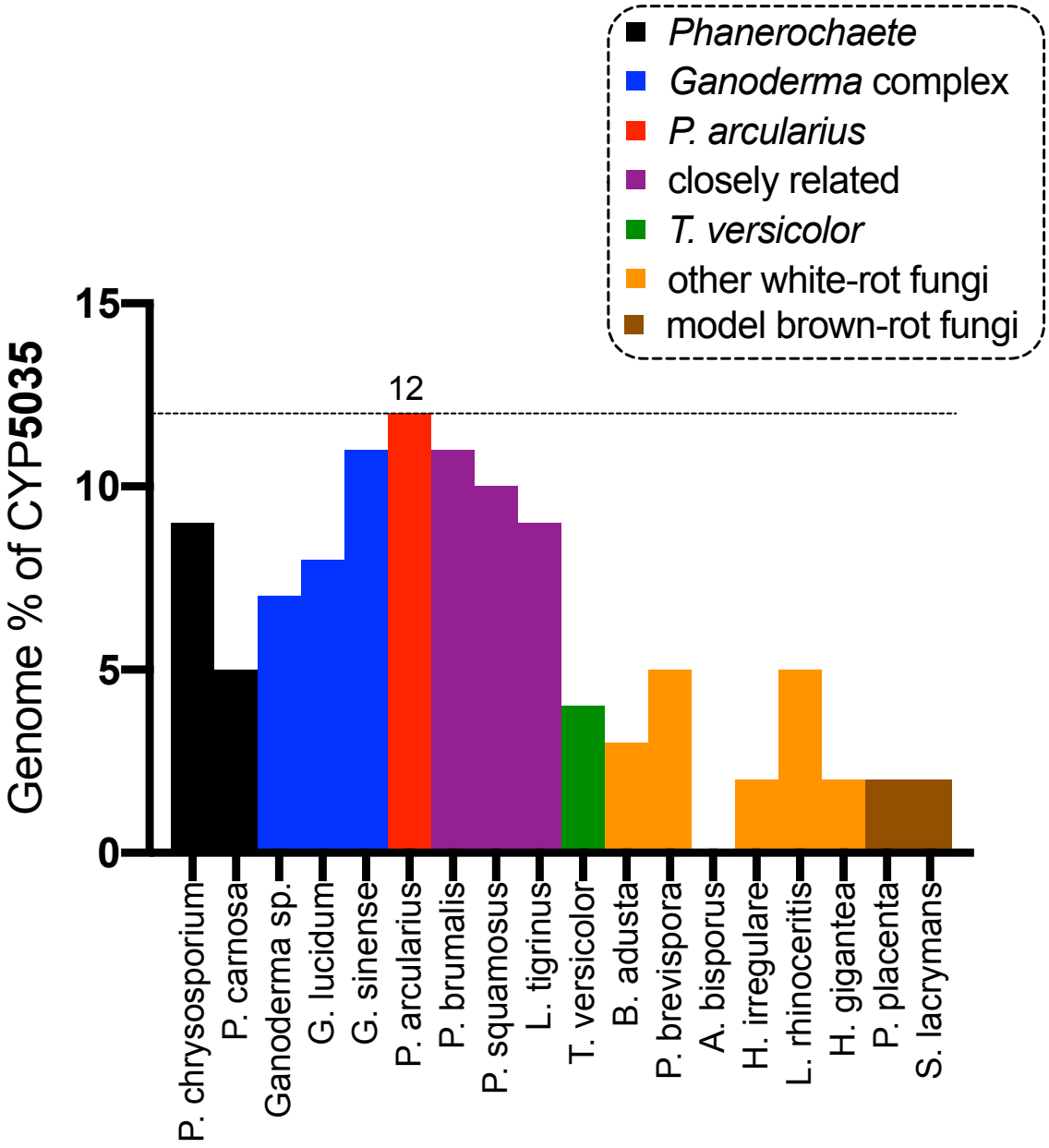

Fig. S3: Comparison of the percentage of CYP5035s in the genome of *P. arcularius* versus a variety of white- and brown-rot fungi.

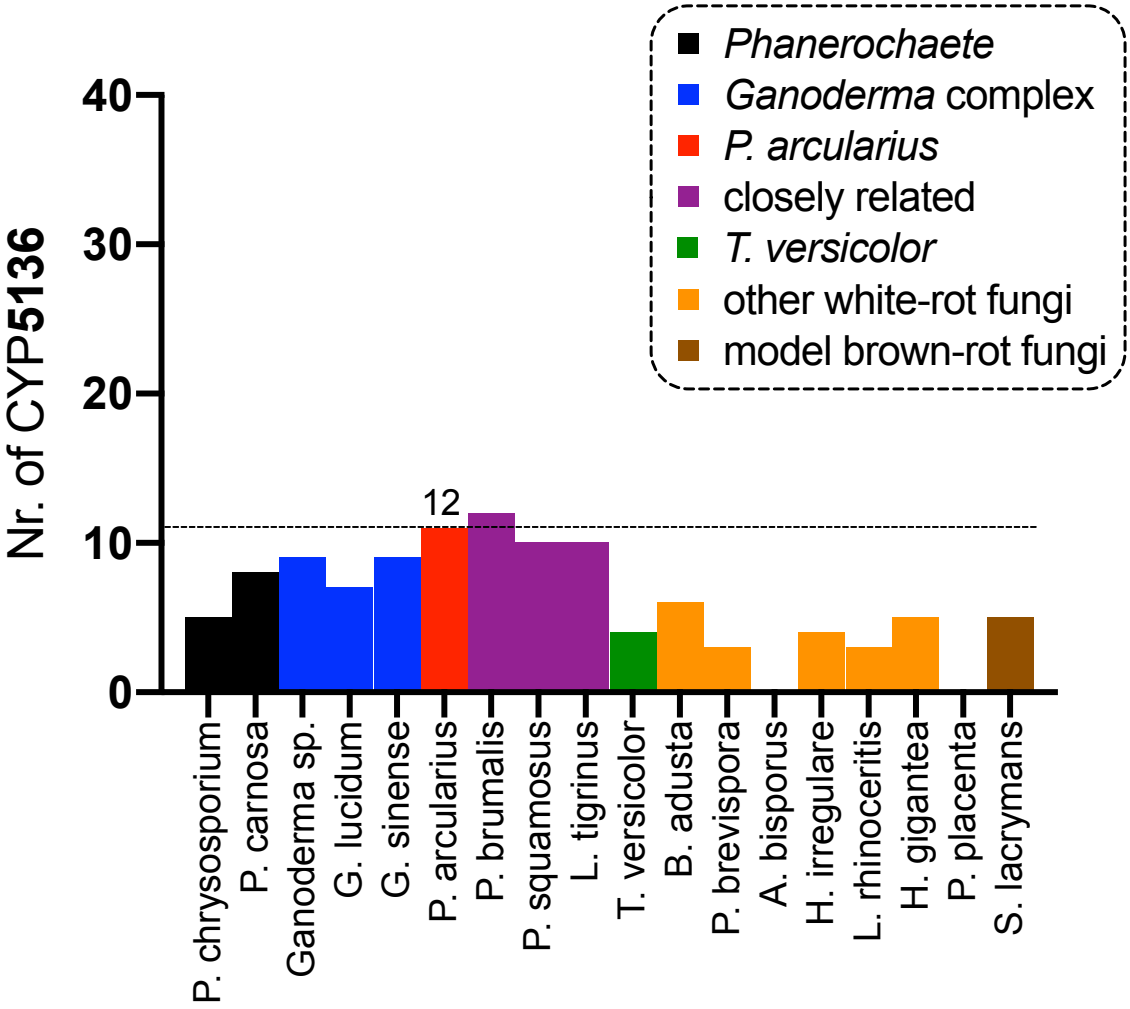

Fig. S4: Comparison of the number of CYP5136 in the genome of *P. arcularius* versus a variety of white- and brown-rot fungi.

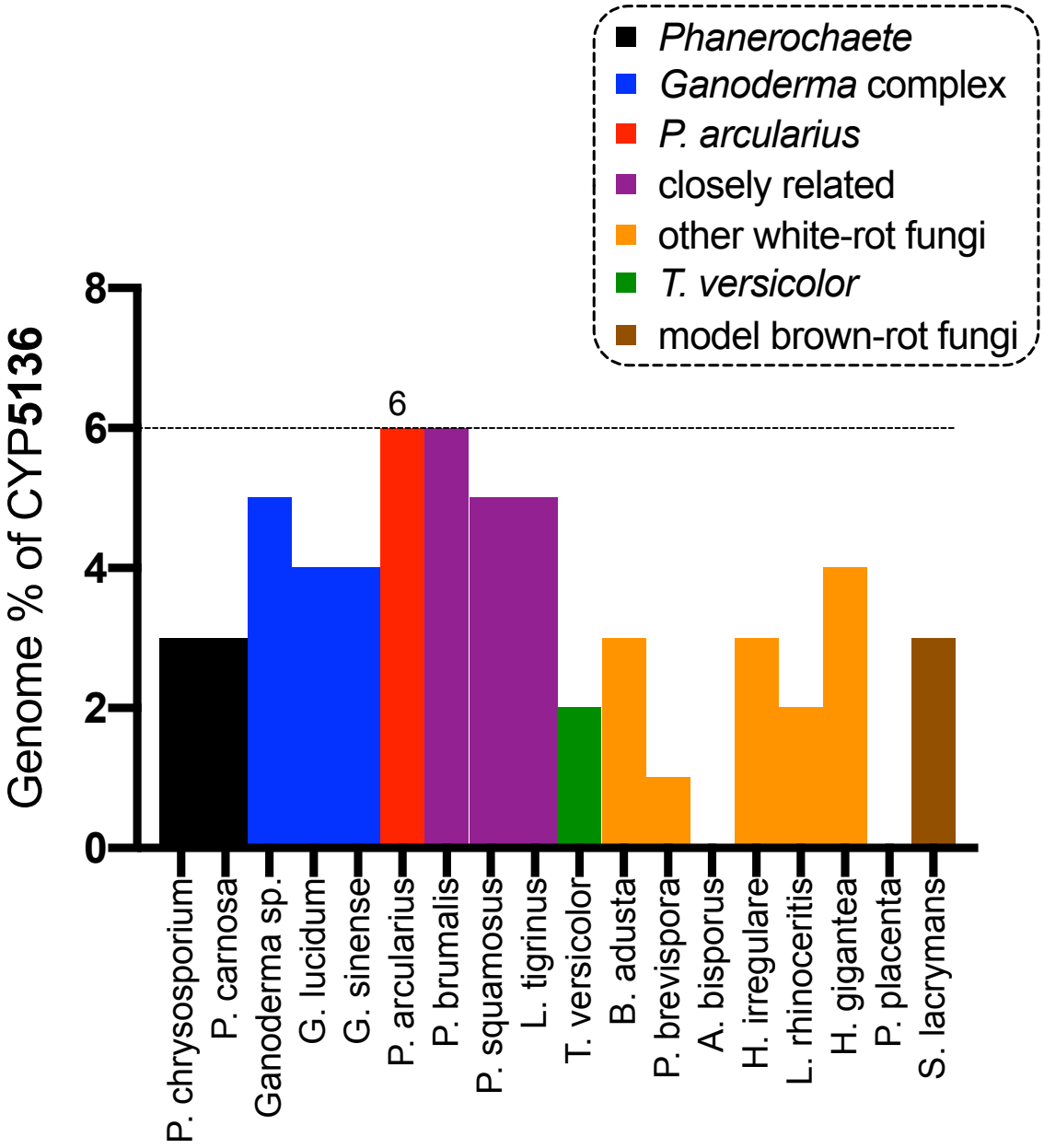

Fig. S5: Comparison of the percentage of CYP5136s in the genome of *P. arcularius* versus a variety of white- and brown-rot fungi.

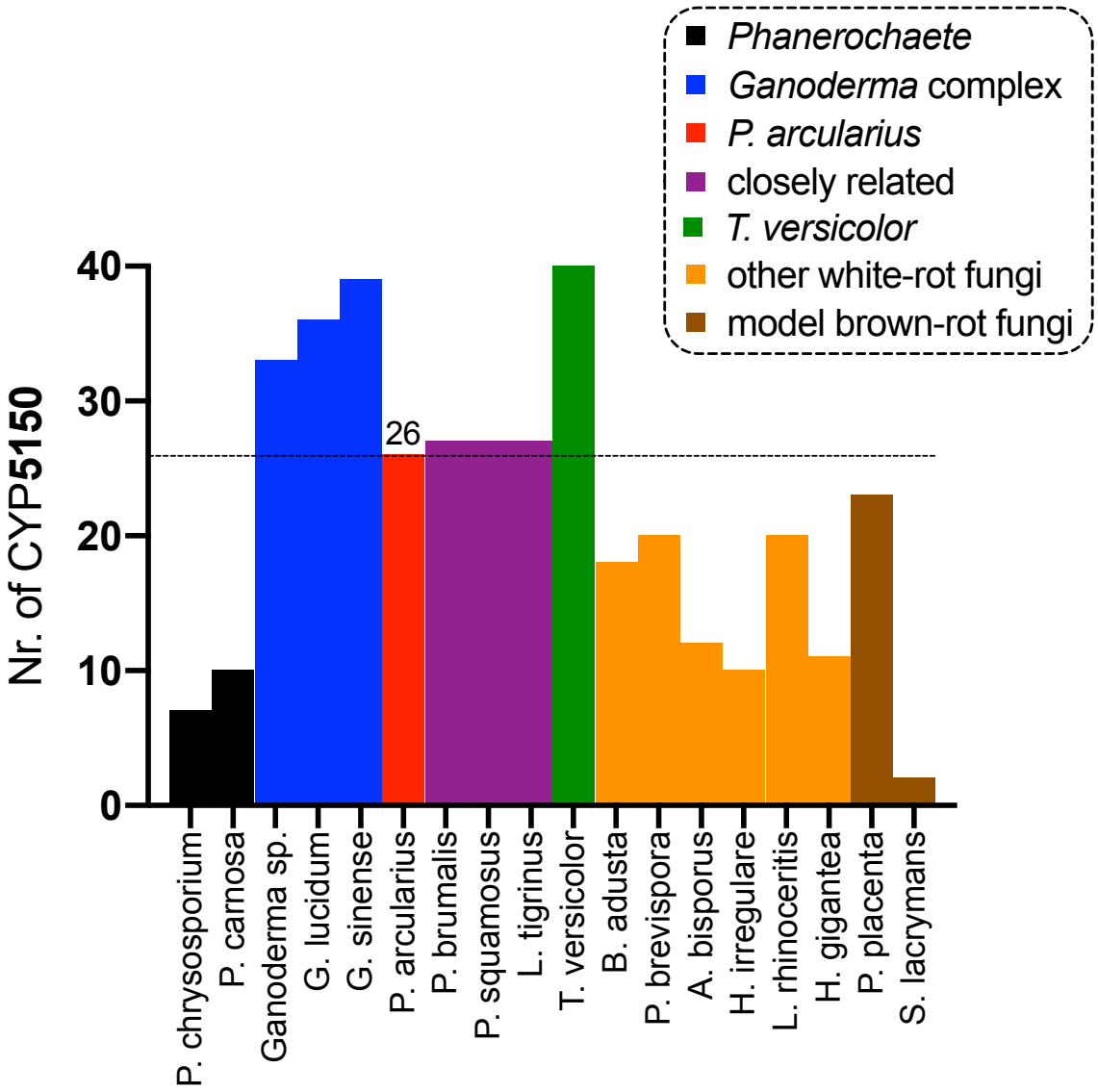

Fig. S6: Comparison of the number of CYP5150 in the genome of *P. arcularius* versus a variety of white- and brown-rot fungi.

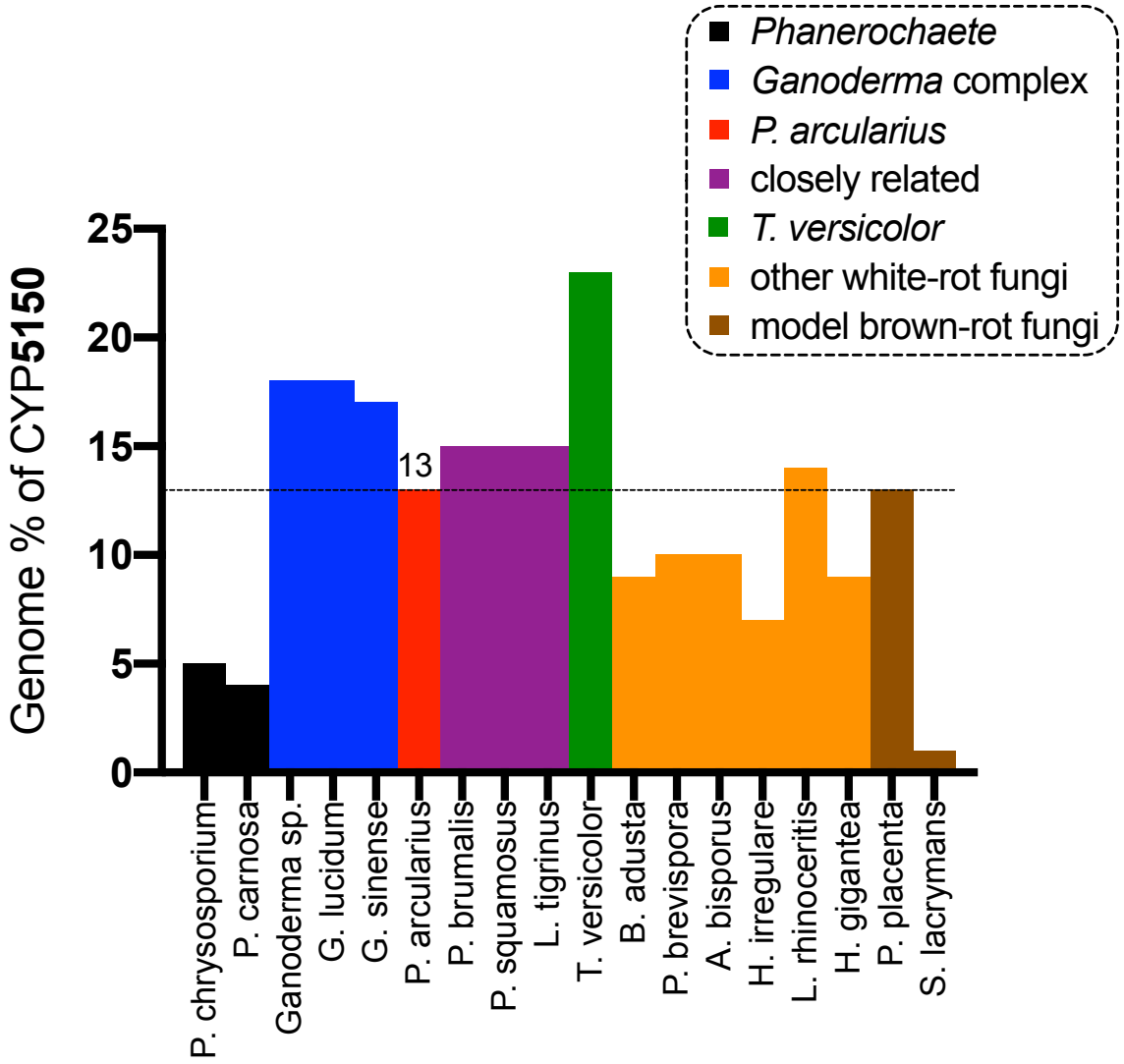

Fig. S7: Comparison of the percentage of CYP5150s in the genome of *P. arcularius* versus a variety of white- and brown-rot fungi.

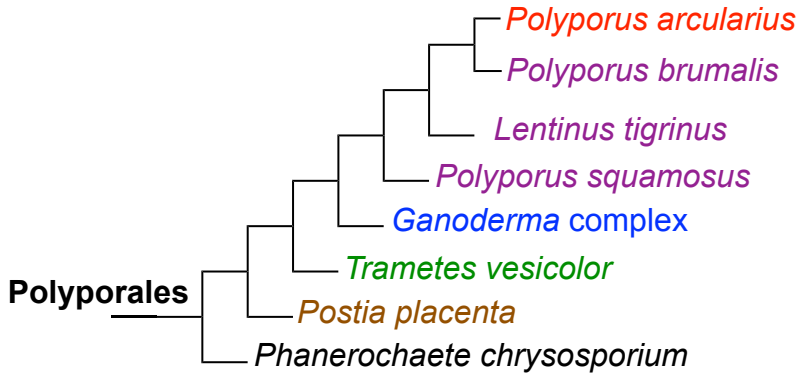

Fig. S8: Rough re-make of the phylogenetic trees drawn in previous studies illustrating the evolutionary distances of different model wood-degrading polypore fungi, and white-rot fungi selected and analysed in this study (Justo and Hibbett 2011; Floudas et al. 2012; Binder et al. 2013).

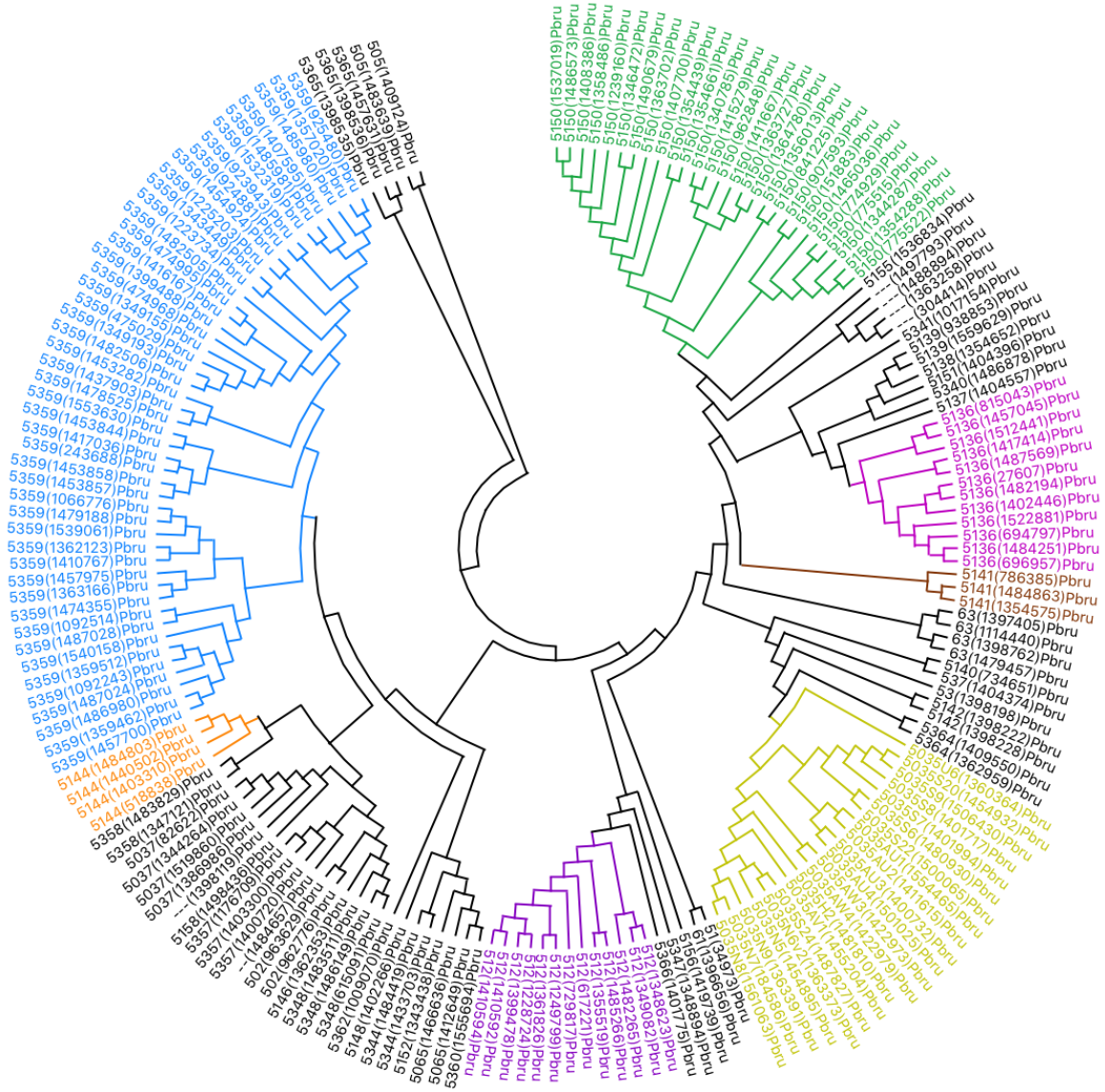

Fig. S9: A minimum evolution tree of the P450ome of *P. brumalis* involving 186 amino acid sequences. CYP512 (purple), CYP5035 (dark yellow), CYP5136 (violet), CYP5141 (brown), CYP5144 (orange), CYP5150 (green) and CYP5359 (blue) have been coloured. The tree was constructed using the close-neighbour-interchange algorithm in MEGA X.

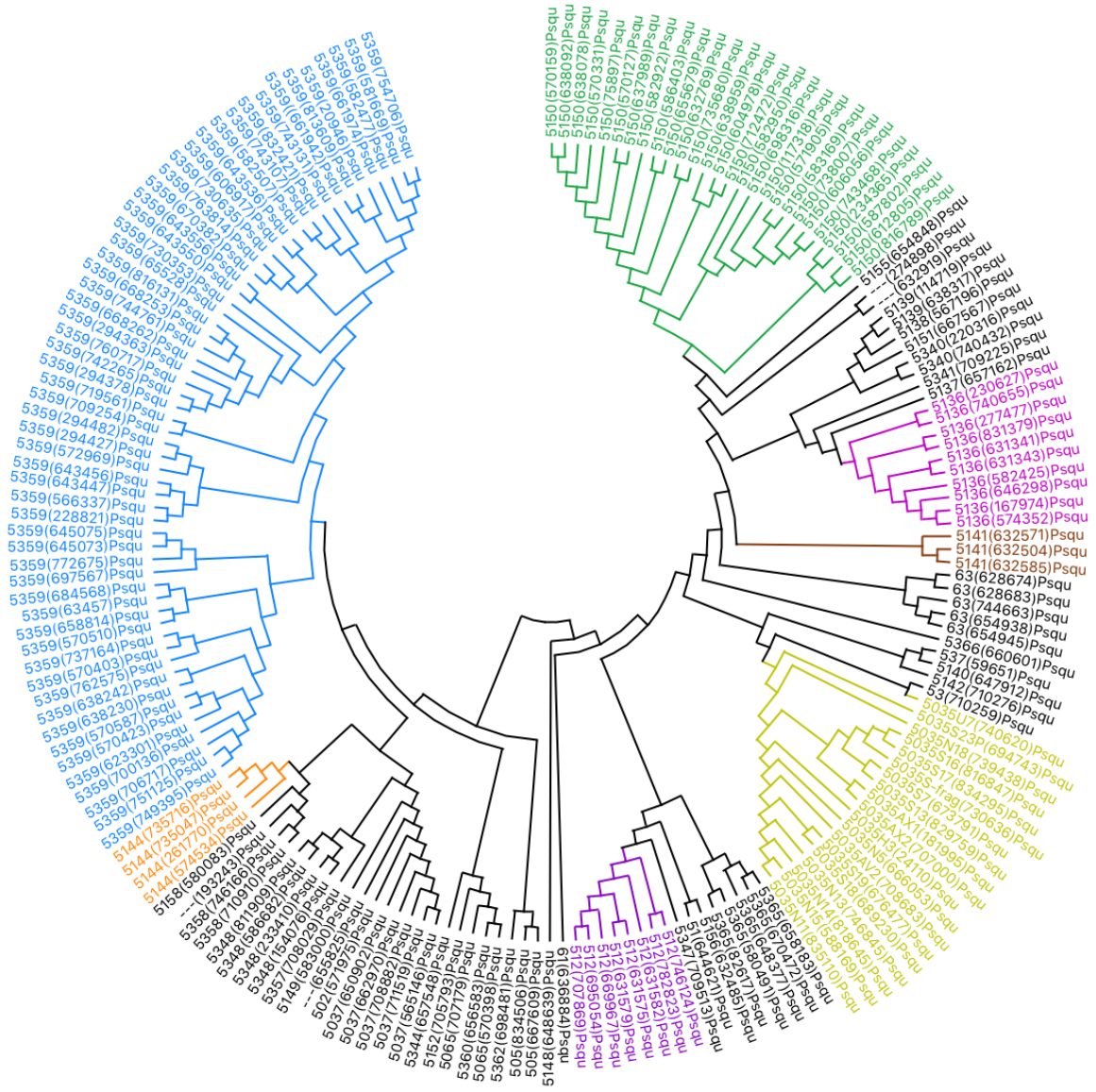

Fig. S10: A minimum evolution tree of the P450ome of *P. squamosus* involving 184 amino acid sequences. CYP512 (purple), CYP5035 (dark yellow), CYP5136 (violet), CYP5141 (brown), CYP5144 (orange), CYP5150 (green) and CYP5359 (blue) have been coloured. The P450 nomenclature of the CYP5035 selected and expressed for a functional screening is shown in red. The tree was constructed using the close-neighbour-interchange algorithm in MEGA X.

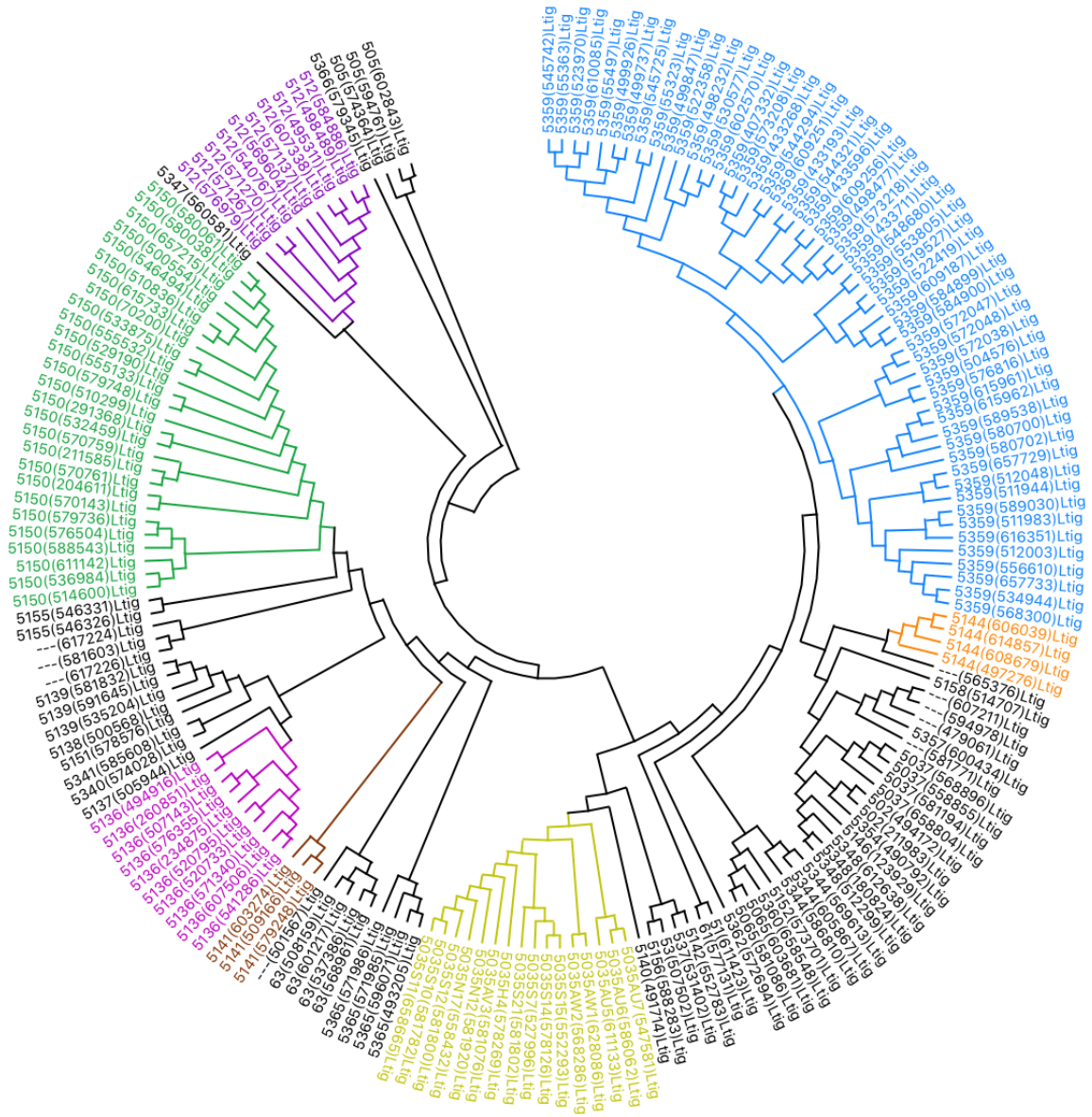

Fig. S11: A minimum evolution tree of the P450ome of *L. tigrinus* involving 184 amino acid sequences. CYP512 (purple), CYP5035 (dark yellow), CYP5136 (violet), CYP5141 (brown), CYP5144 (orange), CYP5150 (green) and CYP5359 (blue) have been coloured. The P450 nomenclature of the CYP5035 selected and expressed for a functional screening is shown in red. The tree was constructed using the close-neighbour-interchange algorithm in MEGA X.

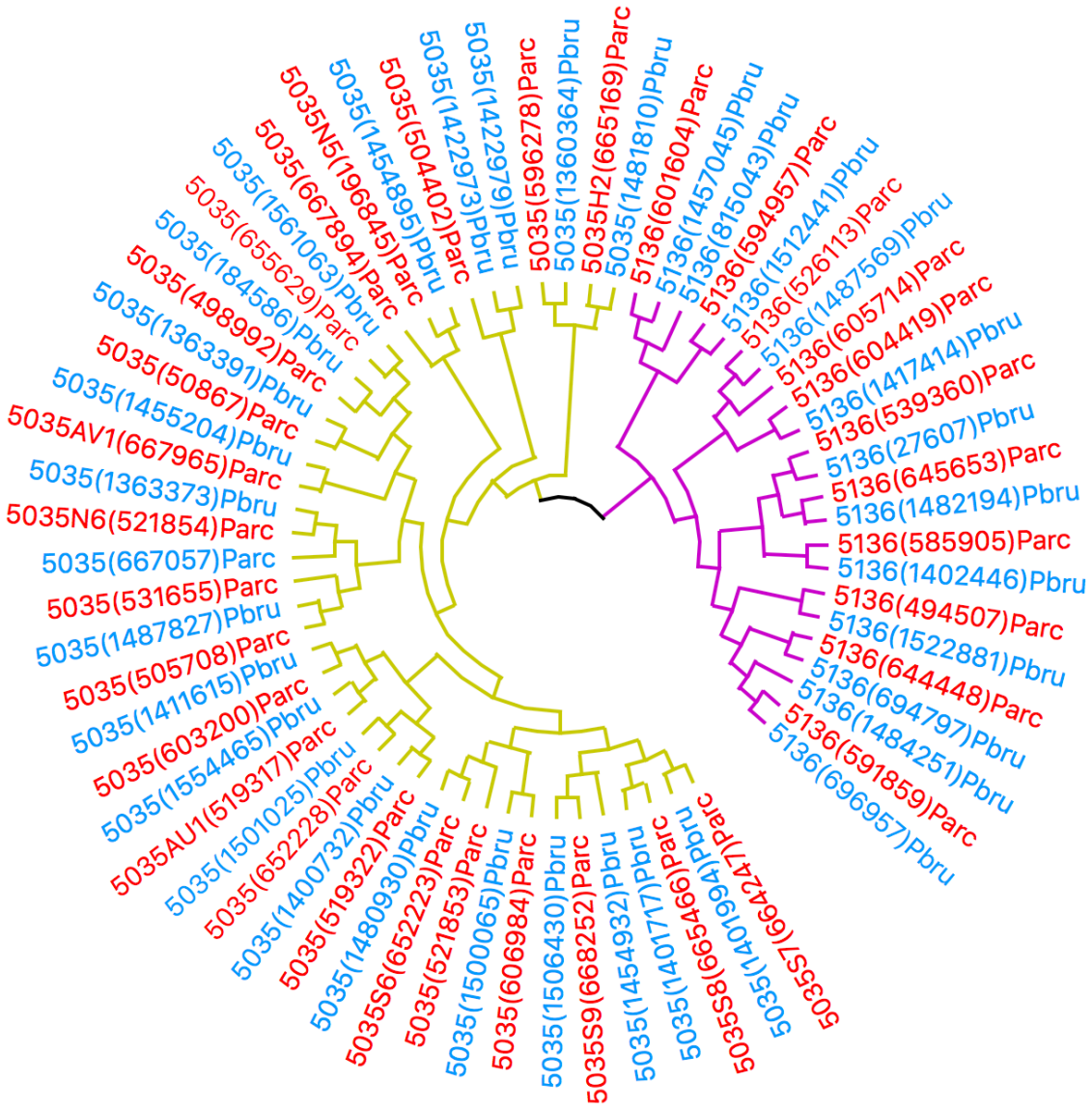

Fig. S12: Displayed is a minimum evolution tree of the CYP5035 and CYP5136 families of *P. arcularius* (Parc; red) and *P. brumalis* (Pbru; blue). Evidence for their close phylogeny is an alternating pattern of red and blue sequences almost throughout the tree. This analysis involved 67 amino acid sequences. The tree was constructed using the close-neighbour-interchange algorithm in MEGA X.

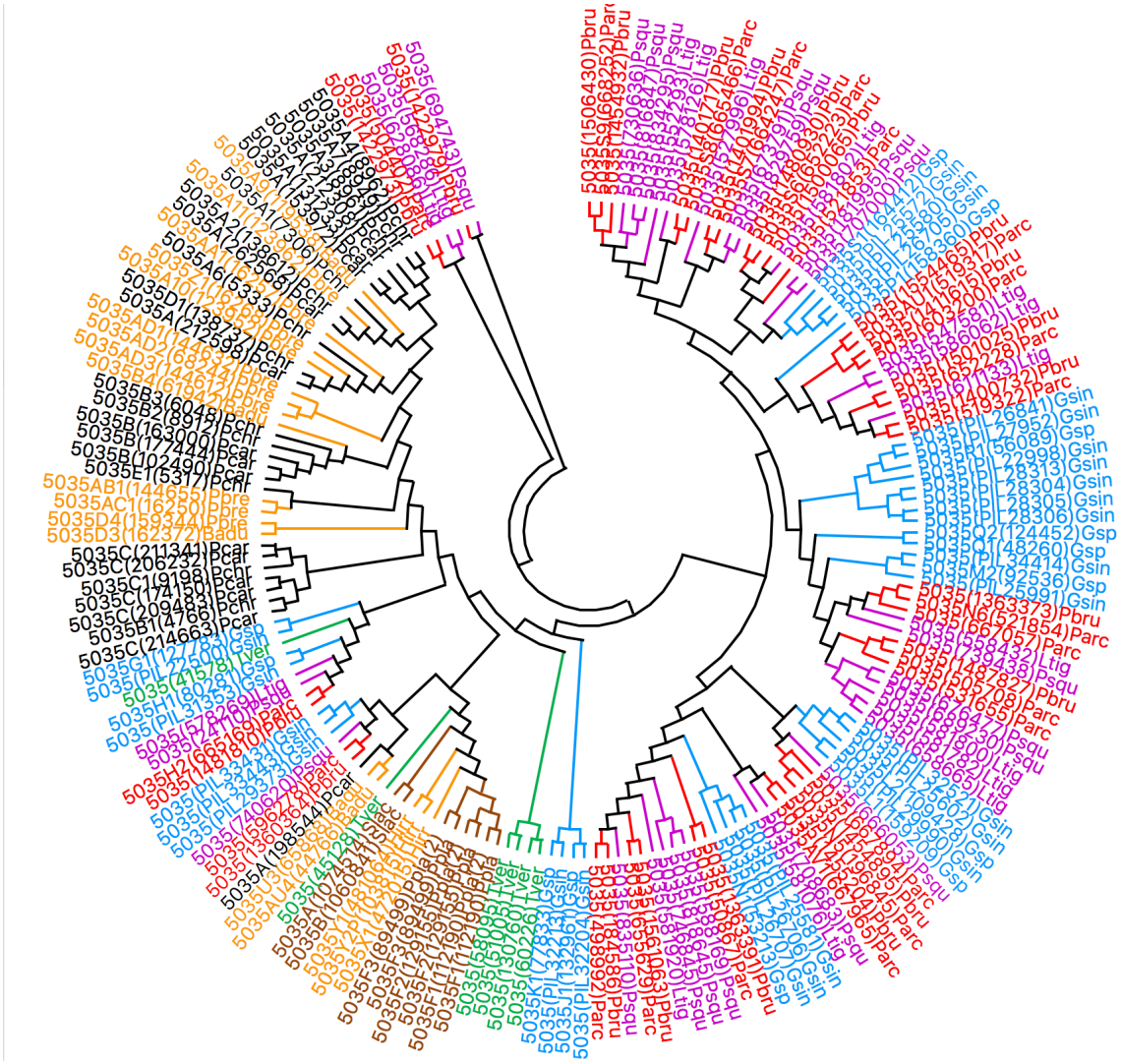

Fig. S13: Displayed is a minimum evolution tree of the CYP5035 family involving 174 amino acid sequences. Phylogeny of CYP5035 enzymes of the fungus *P. arcularius* and *P. brumalis* (Parc and Pbru; red) compared to related species *L. tigrinus* and *P. squamosus* (Ltig and Psqu; violet), and the other model white-rot fungi *Ganoderma* sp. and G. sinense (Gsp and Gsin; blue), *T. versicolor* (Tver; green), *P. chrysosporium* and *P. carnosa* (Pchr and Pcar; black), *B. adusta* and *P. brevispora* and *Heterobasidion irregulare* (Badu and Pbre and Hirr; orange) as well as brown-rot fungi *P. placenta* and *Serpula lacrymans* (Ppla and Slac; brown) in order to get an insight into the evolution of this P450 family. The tree was constructed using the close-neighbour-interchange algorithm in MEGA X.

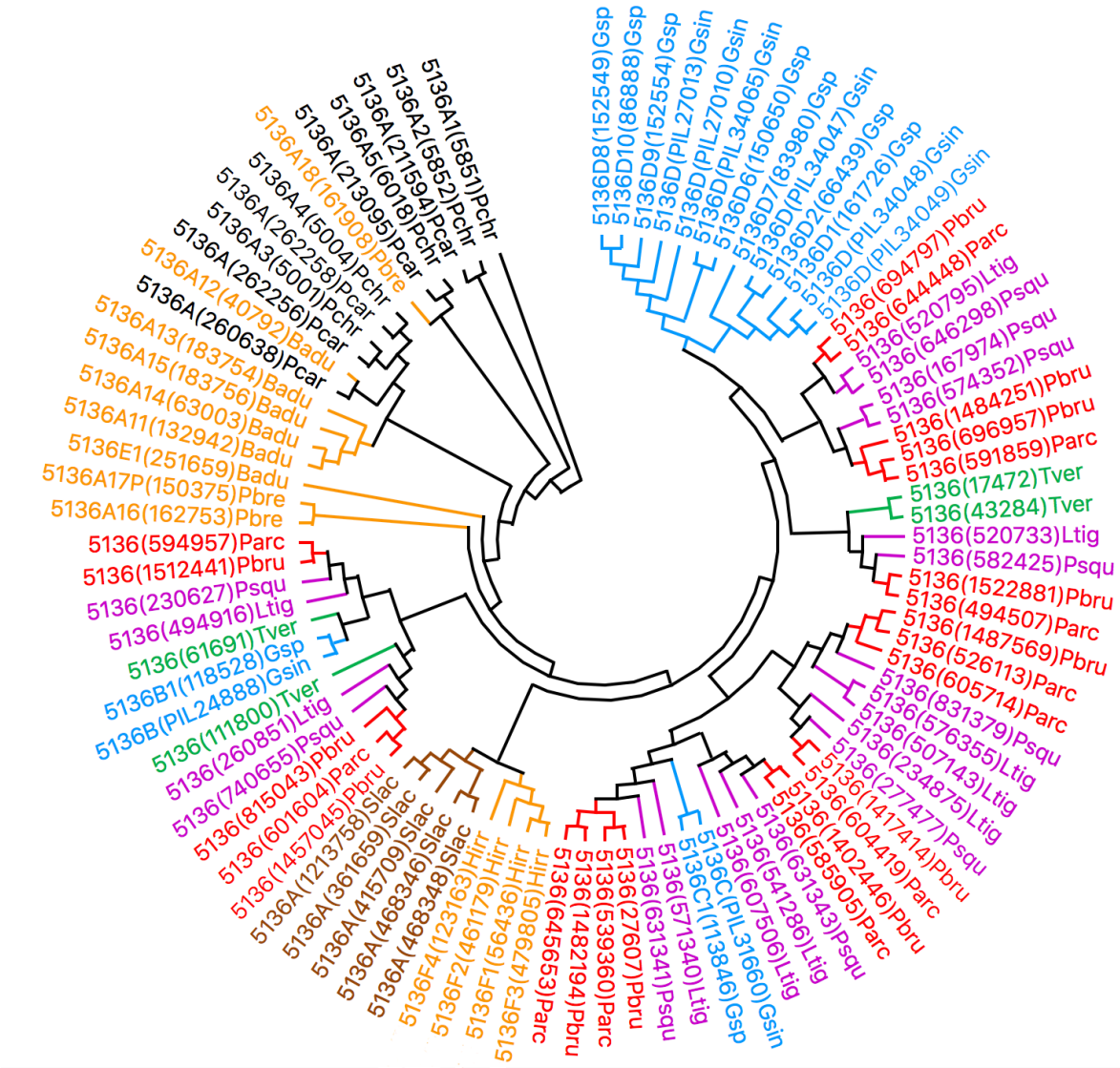

Fig. S14: Displayed is a minimum evolution tree of the CYP5136 family involving 92 amino acid sequences. Phylogeny of CYP5136 enzymes of the fungus *P. arcularius* and *P. brumalis* (Parc and Pbru; red) compared to related species *L. tigrinus* and *P. squamosus* (Ltig and Psqu; violet), and the other model white-rot fungi *Ganoderma* sp. and G. sinense (Gsp and Gsin; blue), *T. versicolor* (Tver; green), *P. chrysosporium* and *P. carnosa* (Pchr and Pcar; black), *B. adusta* and *P. brevispora* and *H. irregulare* (Badu and Pbre and Hirr; orange) as well as brown-rot fungus *Serpula lacrymans* (Slac; brown) in order to get an insight into the evolution of this P450 family. The tree was constructed using the close-neighbour-interchange algorithm in MEGA X.

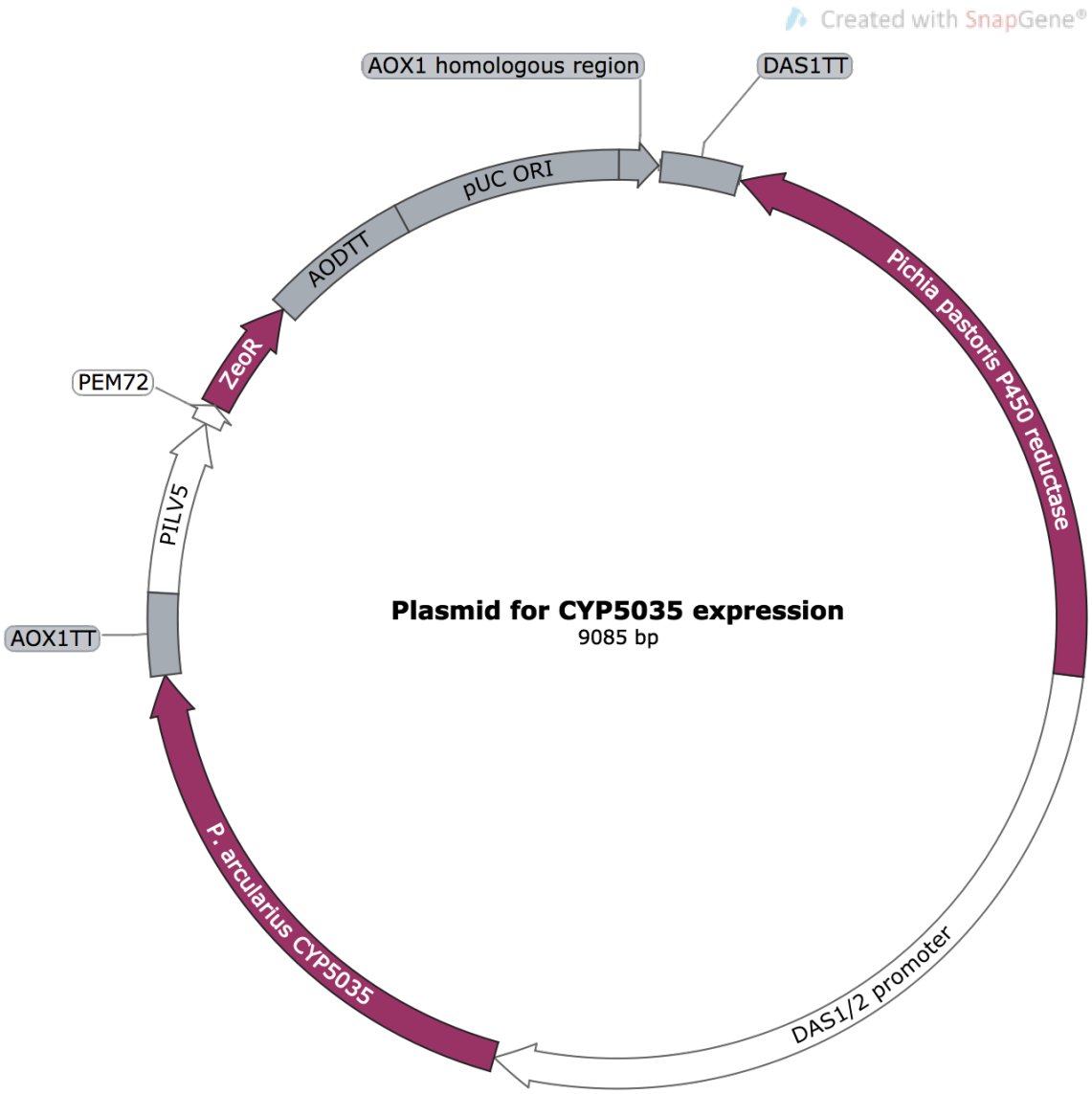

Fig. S15: Plasmid used for the coexpression of the CYP5035 enzymes and *P. pastoris*' native P450 reductase enzyme in the yeast.

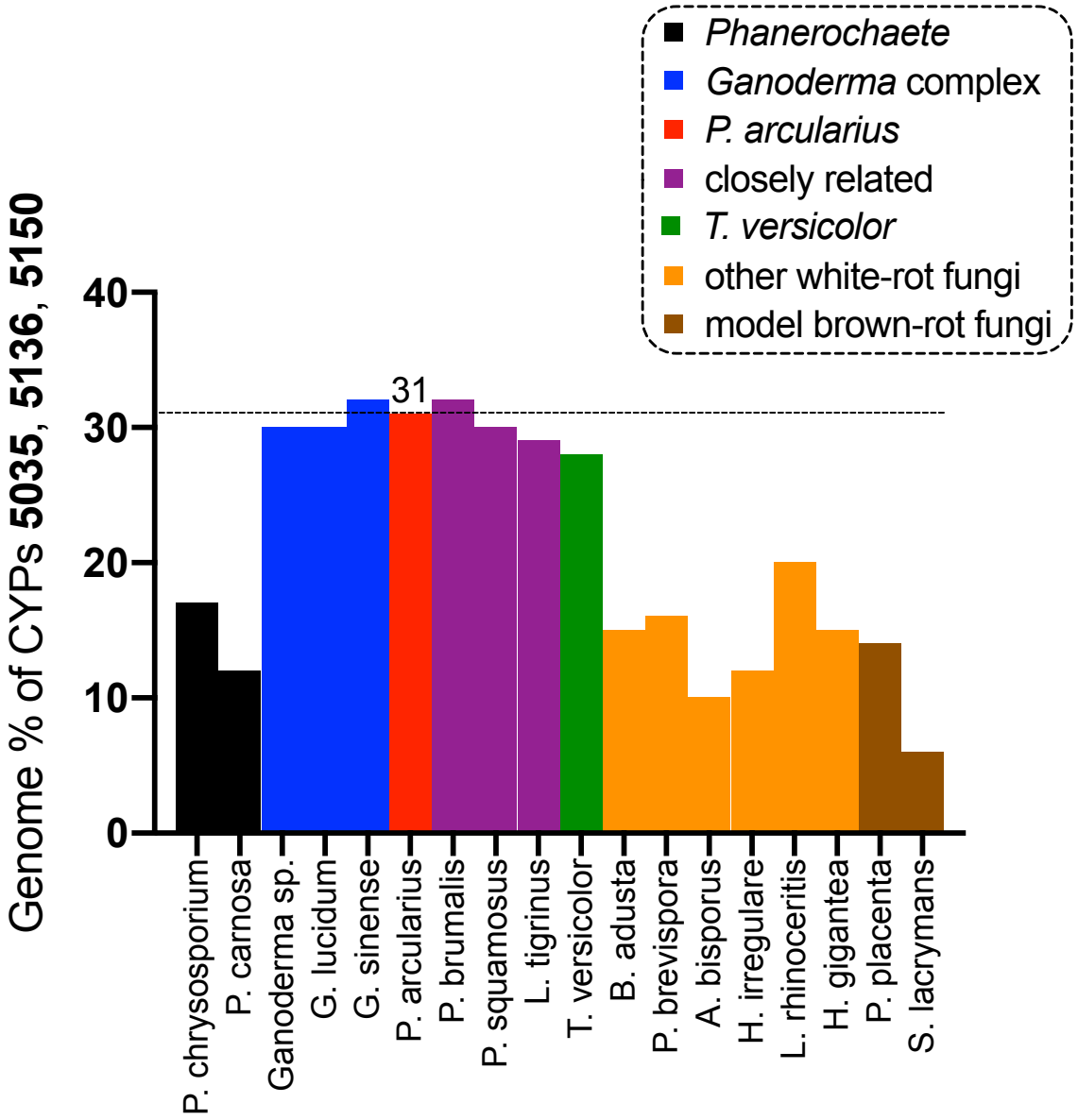

Fig. S16: Comparison of the percentage of P450 families 5035, 5136 and 5150 in the genome of *P. arcularius* versus a variety of white- and brown-rot fungi.

Binder M, Justo A, Riley R, Salamov A, Lopez-Giraldez F, Sjökvist E, Copeland A, Foster B, Sun H, Larsson E, Larsson K-H, Townsend J, Grigoriev I V., Hibbett DS (2013) Phylogenetic and phylogenomic overview of the Polyporales. Mycologia 105:1350–1373 . https://doi.org/10.3852/13-003

Floudas D, Binder M, Riley R, Barry K, Blanchette RA, Henrissat B, Martínez AT, Otillar R, Spatafora JW, Yadav JS, Aerts A, Benoit I, Boyd A, Carlson A, Copeland A, Coutinho PM, de Vries RP, Ferreira P, Findley K, Foster B, Gaskell J, Glotzer D, Górecki P, Heitman J, Hesse C, Hori C, Igarashi K, Jurgens JA, Kallen N, Kersten P, Kohler A, Kües U, Kumar TKA, Kuo A, LaButti K, Larrondo LF, Lindquist E, Ling A, Lombard V, Lucas S, Lundell T, Martin R, McLaughlin DJ, Morgenstern I, Morin E, Murat C, Nagy LG, Nolan M, Ohm RA, Patyshakuliyeva A, Rokas A, Ruiz-Dueñas FJ, Sabat G, Salamov A, Samejima M, Schmutz J, Slot JC, St. John F, Stenlid J, Sun H, Sun S, Syed K, Tsang A, Wiebenga A, Young D, Pisabarro A, Eastwood DC, Martin F, Cullen D, Grigoriev I V.,

Hibbett DS (2012) The Paleozoic Origin of Enzymatic Lignin Decomposition Reconstructed from 31 Fungal Genomes. Science (80-) 336:1715–1719 . https://doi.org/10.1126/science.1221748

Justo A, Hibbett DS (2011) Phylogenetic classification of Trametes (Basidiomycota, Polyporales) based on a five-marker dataset. Taxon 60:1567–1583 . https://doi.org/10.1002/tax.606003

Online Resources 1: P450ome comparison of white- and brown-rot fungi

DOI	10.1371/journal.pone.0086683					.1016/j.phytochem.2014.11.01	1038/srep110	
P450 family (CYP)	P. chrysosporium	P. carnosa	A. bisporus	P. placenta	S. lacrymans	Ganoderma sp.	G. lucidum	G. sinense
51	1	2	1	1	1	1	2	1
53	1	7	2	7	1	1	1	1
61	1	1	1	1	2	1	1	1
63	7	9	6	5	7	5	6	7
66								
502	1	1	1	4	2	1	1	1
504					1			
505	7	4		2		3	4	3
509								
512	14	27	12	14	11	19	22	31
526					1			
530			1					
537				2		1	1	2
548					1			
553					1			
613					3			
620		1	2		4			
634					1			
642						1	1	1
645					1			
661					4			
5025		1			1			
5027				9				
5032			3		1			

5035	13	14		3	3	13	16	25
5036	5	8			1			
5037	5	8	5	13	18	5	6	6
5046								
5065			3		2	1	1	1
5068			1					
5070								
5082					1			
5093								
5136	5	8			5	9	7	9
5137	2	4	1	6	6	1	1	1
5138	1	2		1	1	1	1	1
5139	1	11	3	8	1	4	7	8
5140	1	1	1	1	1	1	1	2
5141	7	9	7	4	5	2	2	2
5142	7	8	1		2			
5143	2	2			2			
5144	34	71	43	3	29	4	3	4
5145	3	2	1		1			
5146	6	15			2			
5147	6	7						
5148	2	7	2	1	1	3	2	4
5149	1	3		1				
5150	7	10	12	23	2	33	36	39
5151	1	2	1	1	3	1	1	1
5152	2	4		2	12	1	1	1
5153		1	1					
5154	1	4			5			
5155	1	1						

5156	2	1	1	1	5	1	1	1
5157	1	1			1			
5158	1	5		2		1	1	1
5323								
5339				2				
5340				1		3	2	1
5341				3		2	2	1
5342				1				
5343				1				
5344				3				
5346				1				
5347				2		1	1	1
5348				34		4	3	3
5349				2		1	1	1
5350				11				
5351				1		1	1	1
5352				1				
5353				1				
5354				2				
5355				1				
5356				1				
5357						2	2	2
5358						2	1	2
5359						40	47	53
5360						1	1	1
5361						1	1	1
5362						1	1	1
5363							1	
5364						4	3	2

5365						1	1	1
5366						1	1	1
5374								
5416								
5424								
5427								
5428								
5429								
5430								
5431								
5432								
5433								
5434								
5445				1				
6001		4						
6004								
6005						2	2	2
NA			3		7			
???								
P450 count	**149**	**266**	**115**	**184**	**159**	**181**	**197**	**228**
% of 512	9	10	10	8	7	10	11	14
% of 5035	9	5	0	2	2	7	8	11
% of 5136	3	3	0	0	3	5	4	4
% of 5141	5	3	6	2	3	1	1	1
% of 5144	23	27	37	2	18	2	2	2
% of 5150	5	4	10	13	1	18	18	17
% of 5144	0	0	0	0	0	22	24	23
% of 5035,5136,5150	17	12	10	14	6	30	30	32
% of 5035,5136,5150,5141,512	31	26	27	24	16	42	42	46

This work				10.3852/13-002		/j.funbio.201	86/1471-2164-1	This work using data from 10.1371/journal.pone.0095616
P. brumalis	P. arcularius	L. tigrinus	P. squamosus	B. adusta	P. brevispora	H. irregulare	L. rhinoceritis	T. vesicolor
1	1	1	1	1	1	1	1	1
1	1	1	1	8	1	1	1	2
1	1	1	1	1	1	1	1	1
4	4	4	5	5	7	4	5	5
							2	
2	2	2	1	3	1	5	1	5
							6	
2	2	3	2		3	1	5	3
							1	
13	15	10	8	18	6	3	6	7
							1	
1	1	1	1				1	3
							3	1
								2
					7			

21	23	16	19	6	10	3	6	6
				3	5			
5	4	4	5	5	10	7	14	16
							2	
2	2	2	2		4	5	5	1
							1	
12	11	10	10	6	3	4	3	4
1	1	1	1	1	1		1	1
1	1	1	1	1	1	1	1	2
2	2	3	2	3	4	4	4	14
1	2	1	1	2	1	1	1	
3	3	3	3	8	5	1		3
2	2	1	1	5	7		1	
				1		2		6
4	4	4	4	67	12	49	35	48
1	1	1		7	3		1	1
					2		1	1
1	1		1	2	2	1		1
			1		1			
27	26	27	27	18	20	10	20	43
1	1	1	1	1	2	1	2	1
1	1	1	1	3	2	2	1	2
				1	1	1		
				2	2			
1	1	2	1	1			1	1

1	1	1	1	1	1	1	1	1
				1			1	1
1	2	1	1	3	1		1	
					1			
1	1	1	2			5		1
1	2	1	1	1		2		1
1	2	3	1		43	10		
1	1	1	1					
3	3	3	4			1		
	1							
					1			
					4			
				1		3		
		1						
3	3	1	1		1			
2	2		2		1	1		
47	47	54	58					
1	1	1	1					
1	1	1	1					
					2			
2	3			1				

3	3	4	5	1				
1	1	1	1					
				1				
						1	1	
				3	2			
				3				
				1				
				1		1	1	
						1	1	
						1	1	
						1	1	
					1			
					23			
							1	
							1	
				2	3	2	2	
								1
6	6	9	4					
186	**193**	**184**	**185**	**199**	**209**	**138**	**146**	**186**
7	8	5	4	9	3	2	4	4
11	12	9	10	3	5	2	4	3
6	6	5	5	3	1	3	2	2
2	2	2	2	4	2	1	0	2
2	2	2	2	34	6	36	24	26
15	13	15	15	9	10	7	14	23
25	24	29	31	0	0	0	0	0
32	31	29	30	15	16	12	20	28
41	40	36	36	28	21	15	24	34

Online Resource 2: P450ome of Polyporus arcularius

	Sequence ID	Hit type	PSSM-ID	From	To	E-Value	Bitscore	Shortname	FCPD family assignment	Chosen CYP5035s
Q#1	536006	superfam	386267	42	488	5,34E-20	107.359	p450	5366	
Q#2	593528	superfam	386267	40	522	3,13E-61	222.148	p450	5150	
	579848	superfam	386267	17	93	4,09E-01	430.303	p450		
Q#3	560790	superfam	386267	80	521	2,02E-56	205.97	p450	5140	
Q#4	477387	superfam	386267	56	547	2,31E-52	198.266	p450	51	
Q#5	561511	superfam	386267	99	536	7,48E-72	250.653	p450	63	
Q#6	658545	superfam	386267	30	497	6,49E-64	227.926	p450	502	
Q#7	580991	superfam	386267	37	514	2,74E-62	224.459	p450	5150	
Q#8	478773	superfam	386267	37	513	1,94E-58	211.748	p450	5150	
Q#9	658552	superfam	386267	37	513	2,67E-61	222.148	p450	5150	
Q#10	538088	superfam	386267	28	492	1,71E-65	232.163	p450	502	
Q#11	129741	superfam	386267	38	521	9,94E-69	241.408	p450	5150	
Q#12	594622	superfam	386267	129	447	1,04E-47	184.013	p450	5365	
Q#13	479337	superfam	386267	49	475	4,17E-71	246.416	p450	5152	
Q#14	581329	superfam	386267	105	479	3,31E-48	186.325	p450	61	
Q#15	594805	superfam	386267	37	484	2,35E-59	215.6	p450	5037	
Q#16	658901	superfam	386267	42	487	2,29E-62	223.689	p450	5037	
Q#17	594952	superfam	386267	34	432	3,30E-26	124.693	p450	512	
Q#18	581595	superfam	386267	61	471	8,23E-32	141.256	p450	512	
Q#19	581596	superfam	386267	7	430	9,09E-35	148.19	p450	512	
Q#20	594957	superfam	386267	33	518	7,61E-71	246.801	p450	5136	
Q#21	539360	superfam	386267	34	527	2,55E-72	248.342	p450	5136	
Q#22	659192	superfam	386267	41	484	3,70E-67	234.86	p450	5359	
Q#23	595132	superfam	386267	51	493	1,06E-61	222.919	p450	5359	
Q#24	217978	superfam	386267	51	490	1,69E-72	251.038	p450	5359	

Q#25	595134	superfam	386267	47	475	1,62E-62	224.845	p450	5359
Q#26	624427	superfam	386267	49	485	4,01E-58	212.903	p450	5359
Q#27	581800	superfam	386267	48	484	4,24E-53	199.807	p450	5359
Q#28	218197	superfam	386267	94	547	3,07E-68	238.326	p450	5359
Q#29	581809	superfam	386267	40	486	1,24E-65	232.549	p450	5359
Q#30	539654	superfam	386267	35	513	1,69E-55	206.74	p450	5150
Q#31	227973	superfam	386267	48	445	1,03E-51	193.643	p450	5359
Q#32	659256	superfam	386267	51	447	2,18E-62	222.148	p450	5359
Q#33	643322	superfam	386267	42	467	4,48E-60	217.526	p450	5359
Q#34	562530	superfam	386267	40	469	2,53E-55	205.199	p450	5359
Q#35	481770	superfam	386267	35	505	3,00E-59	216.37	p450	5150
Q#36	278097	superfam	386267	34	508	2,83E-63	227.156	p450	5150
Q#37	595715	superfam	386267	36	497	4,24E-31	139.33	p450	512
Q#38	540845	superfam	386267	61	492	5,96E-29	133.167	p450	512
Q#39	482521	superfam	386267	96	500	1,60E-37	157.82	p450	5364
Q#40	322895	superfam	386267	30	468	2,45E-69	241.793	p450	5357
Q#41	651118	superfam	386267	102	527	1,45E-42	172.072	p450	5364
Q#42	542019	superfam	386267	111	509	1,53E-40	166.294	p450	5364
Q#43	596278	superfam	386267	93	508	1,53E-53	201.347	p450	5035
Q#44	583037	superfam	386267	116	514	2,68E-54	203.273	p450	5150
Q#45	651168	superfam	386267	46	513	9,48E-56	207.511	p450	5150
Q#46	483272	superfam	386267	121	526	7,39E-45	177.85	p450	5150
Q#47	483404	superfam	386267	194	482	1,69E-19	105.818	p450	5347
Q#48	596366	superfam	386267	28	481	1,38E-70	245.26	p450	5360
Q#49	483652	superfam	386267	40	534	5,68E-60	216.37	p450	5151
Q#50	660397	superfam	386267	13	302	9,56E-09	740.021	p450	505
Q#51	484469	superfam	386267	60	498	8,08E-54	201.733	p450	5359
Q#52	516981	superfam	386267	10	433	2,95E-68	237.941	p450	5359
Q#53	596855	superfam	386267	4	400	2,34E-51	193.258	p450	5359

Q#54	484614	superfam	386267	43	485	1,51E-56	209.051	p450	5359	
Q#55	596871	superfam	386267	43	497	3,38E-76	258.357	p450	5359	
Q#56	644448	superfam	386267	33	517	4,42E-57	210.592	p450	5136	
Q#57	583821	superfam	386267	99	549	6,05E-62	225.23	p450	63	
Q#58	583913	superfam	386267	31	525	9,34E-73	251.808	p450	5137	
Q#59	597164	superfam	386267	40	496	2,70E-68	236.786	p450	???	
Q#60	584056	superfam	386267	35	488	9,87E-37	149.345	p450	512	
Q#61	485429	superfam	386267	35	488	1,84E-34	148.575	p450	512	
Q#62	413458	superfam	386267	32	505	6,92E-67	236.4	p450	5150	
Q#63	518012	superfam	386267	44	467	3,30E-55	205.199	p450	5144	
	486090	superfam	386267	2	95	0.00663934	353.263	p450		
Q#64	518528	superfam	386267	42	511	5,35E-63	226	p450	5359	
Q#65	584392	superfam	386267	37	475	2,28E-68	239.482	p450	5359	
Q#66	486432	superfam	386267	1	408	2,20E-70	242.564	p450	5359	
Q#67	609542	superfam	386267	50	492	2,13E-69	242.564	p450	5359	
Q#68	564198	superfam	386267	57	493	2,56E-67	237.171	p450	5359	
Q#69	545400	superfam	386267	39	507	3,11E-65	232.163	p450	5139	
Q#70	564210	superfam	386267	48	476	1,08E-67	237.171	p450	5359	
Q#71	645008	superfam	386267	44	464	1,14E-60	216.37	p450	5359	
Q#72	597885	superfam	386267	48	495	6,74E-54	202.118	p450	5359	
Q#73	487219	superfam	386267	3	436	1,93E-53	199.421	p450	5357	
Q#74	652223	superfam	386267	110	544	1,09E-46	180.932	p450	5035	**CYP5035S6**
Q#75	519317	superfam	386267	174	558	1,61E-36	155.509	p450	5035	**CYP5035AU1**
Q#76	519322	superfam	386267	193	534	2,93E-34	148.96	p450	5035	
	584822	superfam	386267	1	98	1,25E-08	657.571	p450		
Q#77	652228	superfam	386267	183	384	1,44E-07	682.241	p450	5035	
Q#78	598120	superfam	386267	83	513	1,05E-17	100.81	p450	5156	
Q#79	585007	superfam	386267	92	481	1,05E-64	230.237	p450	5141	
Q#80	598232	superfam	386267	202	494	4,77E-33	142.027	p450	512	

Q#81	585120	superfam	386267	64	486	2,67E-29	131.241	p450	512	
Q#82	598234	superfam	386267	60	491	1,46E-35	151.657	p450	512	
Q#83	52385	superfam	386267	35	470	5,08E-38	158.205	p450	512	
Q#84	585508	superfam	386267	1	595	1,11E-46	184.399	p450	5138	
	488976	superfam	386267	610	988	0.000275006	443.418	p450		
Q#85	598718	superfam	386267	6	424	7,91E-68	236.4	p450	5065	
Q#86	613998	superfam	386267	53	509	8,32E-73	251.808	p450	5344	
Q#87	489225	superfam	386267	35	514	3,98E-62	224.074	p450	5150	
Q#88	585702	superfam	386267	52	457	1,25E-59	213.674	p450	5144	
Q#89	78860	superfam	386267	41	472	6,54E-59	214.444	p450	5357	
Q#90	489477	superfam	386267	56	487	8,86E-58	211.748	p450	5359	
Q#91	598902	superfam	386267	41	501	1,04E-71	248.727	p450	5348	
Q#92	645653	superfam	386267	33	526	8,39E-68	239.097	p450	5136	
Q#93	585905	superfam	386267	32	507	5,58E-74	255.275	p450	5136	
	575626	superfam	386267	6	423	4,26E-49	187.095	p450		
Q#94	521853	superfam	386267	121	568	7,11E-41	167.835	p450	5035	
Q#95	521854	superfam	386267	85	511	4,08E-42	170.531	p450	5035	**CYP5035N6**
Q#96	548323	superfam	386267	36	509	1,58E-51	195.955	p450	5150	
Q#97	616801	superfam	386267	63	453	4,65E-71	246.801	p450	5146	
Q#98	565622	superfam	386267	56	487	2,32E-58	213.289	p450	5359	
Q#99	523239	superfam	386267	121	443	2,99E-55	204.044	p450	5365	
Q#100	576254	superfam	386267	30	474	1,26E-39	162.827	p450	5142	
Q#101	663628	superfam	386267	44	495	1,04E-57	209.051	p450	5359	
Q#102	550216	superfam	386267	35	516	5,24E-64	229.467	p450	5150	
Q#103	646392	superfam	386267	30	469	4,36E-74	254.505	p450	5358	
Q#104	587429	superfam	386267	36	507	5,59E-58	213.289	p450	5150	
Q#105	600528	superfam	386267	33	510	3,18E-58	210.977	p450	5150	
Q#106	663938	superfam	386267	35	512	1,87E-59	217.141	p450	5150	
Q#107	493524	superfam	386267	28	476	1,92E-56	207.896	p450	---	

Q#108	551231	superfam	386267	27	449	5,18E-39	160.901	p450		537	
Q#109	587771	superfam	386267	44	522	5,89E-56	207.511	p450		5340	
Q#110	664247	superfam	386267	91	537	5,71E-47	184.013	p450		5035	**CYP5035S7**
Q#111	525426	superfam	386267	34	507	1,09E-57	212.133	p450		5150	
Q#112	551670	superfam	386267	95	566	3,51E-57	212.518	p450		5150	
Q#113	601004	superfam	386267	1030	1102	0.00212994	417.321	p450		???	
Q#114	654155	superfam	386267	18	243	1,34E-36	147.419	p450		5359	
Q#115	664361	superfam	386267	58	482	1,38E-44	176.695	p450		5359	
Q#116	494347	superfam	386267	46	480	1,88E-66	234.86	p450		5359	
Q#117	182864	superfam	386267	38	473	8,06E-75	256.431	p450		5359	
Q#118	664364	superfam	386267	55	492	1,07E-72	251.423	p450		5359	
Q#119	494507	superfam	386267	61	536	1,71E-47	185.169	p450		5136	
Q#120	196845	superfam	386267	114	537	2,30E-49	190.562	p450		5035	**CYP5035N5**
Q#121	526113	superfam	386267	81	546	7,30E-59	216.37	p450		5136	
Q#122	552430	superfam	386267	46	476	1,21E-38	160.516	p450		5142	
Q#123	495226	superfam	386267	44	498	1,39E-57	211.363	p450		5359	
Q#124	601604	superfam	386267	33	529	7,75E-73	252.194	p450		5136	
Q#125	601725	superfam	386267	64	496	4,26E-53	200.577	p450		5140	
Q#126	588674	superfam	386267	40	455	3,15E-64	229.082	p450		5348	
Q#127	215171	superfam	386267	45	533	5,45E-63	224.074	p450		5139	
Q#128	496471	superfam	386267	41	456	1,43E-67	237.941	p450		5348	
Q#129	665169	superfam	386267	105	547	1,29E-50	193.643	p450		5035	**CYP5035H2**
Q#130	588982	superfam	386267	32	497	2,25E-62	219.067	p450		5150	
Q#131	229680	superfam	386267	34	497	2,43E-72	250.268	p450		5144	
Q#132	528046	superfam	386267	23	479	5,82E-78	264.52	p450		5359	
Q#133	665466	superfam	386267	92	558	3,31E-45	179.391	p450		5035	**CYP5035S8**
Q#134	497709	superfam	386267	35	482	4,71E-69	241.408	p450		5037	
Q#135	258059	superfam	386267	50	487	1,13E-73	253.734	p450		5359	
Q#136	498253	superfam	386267	32	475	3,63E-67	236.786	p450		5359	

Q#137	655167	superfam	386267	6	423	3,01E-69	240.638	p450	5359
Q#138	665759	superfam	386267	40	483	1,14E-72	251.038	p450	5359
	665760	superfam	386267	51	212	4,84E-45	170.146	p450	
Q#139	498617	superfam	386267	31	493	6,69E-88	290.328	p450	5148
Q#140	589813	superfam	386267	37	463	1,91E-65	229.467	p450	5358
Q#141	498992	superfam	386267	118	529	3,74E-45	179.006	p450	5035
	603107	superfam	386267	118	398	2,94E-13	865.579	p450	
Q#142	603124	superfam	386267	36	517	4,26E-61	226	p450	5150
Q#143	499122	superfam	386267	36	544	6,57E-60	219.452	p450	5155
Q#144	603200	superfam	386267	117	531	1,06E-41	169.761	p450	5035
Q#145	555704	superfam	386267	35	514	6,61E-54	202.118	p450	5150
Q#146	281328	superfam	386267	72	497	6,55E-63	220.607	p450	5341
Q#147	666211	superfam	386267	34	510	5,10E-61	220.993	p450	5150
Q#148	655629	superfam	386267	118	529	6,19E-41	167.835	p450	5035
Q#149	530146	superfam	386267	6	450	1,52E-75	270.298	p450	505
	603539	superfam	386267	35	455	9,12E-40	163.213	p450	
Q#150	500016	superfam	386267	59	517	8,41E-59	215.6	p450	5150
Q#151	603545	superfam	386267	35	528	4,60E-64	229.467	p450	5150
Q#152	603959	superfam	386267	84	476	1,29E-58	214.059	p450	5141
Q#153	314587	superfam	386267	58	488	2,09E-63	226.771	p450	5141
Q#154	557072	superfam	386267	138	570	1,59E-62	226.771	p450	63
Q#155	590818	superfam	386267	122	565	1,91E-70	247.571	p450	63
Q#156	604006	superfam	386267	34	479	6,68E-75	253.734	p450	5158
Q#157	648176	superfam	386267	3	302	1,26E-53	194.414	p450	5359
Q#158	590870	superfam	386267	43	482	1,10E-68	240.252	p450	5359
Q#159	317566	superfam	386267	6	437	7,29E-67	234.475	p450	5359
	462549	superfam	386267	1	79	1,48E-07	611.347	p450	
Q#160	501493	superfam	386267	33	518	1,34E-60	219.837	p450	5150
Q#161	604316	superfam	386267	35	511	7,38E-66	231.393	p450	5150

Q#162	667057	superfam	386267	78	526	1,67E-37	157.82	p450	5035	
Q#163	531655	superfam	386267	93	548	2,27E-44	177.465	p450	5035	
Q#164	604419	superfam	386267	35	524	3,47E-63	226.771	p450	5136	
	604423	superfam	386267	1	39	4,94E-01	418.747	p450		
Q#165	633973	superfam	386267	32	493	2,56E-80	268.372	p450	5144	
Q#166	578626	superfam	386267	54	535	7,45E-79	267.602	p450	53	
Q#167	591428	superfam	386267	28	440	1,07E-48	187.095	p450	5362	
	502978	superfam	386267	46	492	4,65E-44	175.539	p450		
Q#168	503598	superfam	386267	11	427	1,53E-69	241.793	p450	5344	
Q#169	667629	superfam	386267	66	511	1,79E-52	198.266	p450	5150	
Q#170	503897	superfam	386267	32	478	6,67E-66	232.934	p450	5158	
Q#171	591859	superfam	386267	32	519	3,09E-69	242.564	p450	5136	
Q#172	504015	superfam	386267	6	386	1,00E-36	149.731	p450	5359	
	569821	superfam	386267	89	255	1,00E-03	553.567	p450		
Q#173	504402	superfam	386267	1	230	2,39E-39	153.968	p450	5035	
Q#174	605621	superfam	386267	44	482	4,21E-59	215.215	p450	5359	
Q#175	605622	superfam	386267	49	483	9,05E-58	210.977	p450	5359	
Q#176	605714	superfam	386267	40	505	1,68E-61	221.763	p450	5136	
Q#177	667894	superfam	386267	97	535	2,71E-52	198.266	p450	5035	
Q#178	605842	superfam	386267	190	493	2,92E-38	159.361	p450	512	
Q#179	667965	superfam	386267	111	536	5,80E-48	186.71	p450	5035	**CYP5035AV1**
Q#180	415721	superfam	386267	143	491	1,15E-36	154.738	p450	512	
Q#181	505427	superfam	386267	37	492	2,25E-56	208.281	p450	5341A	
Q#182	505424	superfam	386267	37	489	3,94E-36	147.805	p450	512	
Q#183	505708	superfam	386267	69	527	1,54E-42	172.072	p450	5035	
Q#184	579223	superfam	386267	38	500	4,60E-31	139.33	p450	512	
Q#185	579255	superfam	386267	230	325	5,07E-14	873.283	p450	5037	
Q#186	506201	superfam	386267	12	424	7,92E-44	172.072	p450	5349	
Q#187	668252	superfam	386267	108	554	1,03E-51	196.725	p450	5035	**CYP5035S9**

Q#188	50867	superfam	386267	165	578	1,04E-43	176.309	p450	5035
Q#189	612527	superfam	386267	44	492	5,89E-67	236.015	p450	5359
Q#190	592701	superfam	386267	12	449	7,44E-86	284.55	p450	5065
Q#191	506971	superfam	386267	1	208	1,85E-46	173.228	p450	5359
Q#192	606984	superfam	386267	10	131	1,04E-11	757.723	p450	5035
	607385	superfam	386267	1	39	4,94E-01	418.747	p450	
Q#193	668557	superfam	386267	117	468	9,99E-49	186.71	p450	5365
	668586	superfam	386267	1	176	1,05E-16	911.803	p450	

P450ome of Polyporus brumalis

	Hit	type	PSSM-ID	From	To	E-Value	Bitscore	Shortname	FCPD family assignment
Q#1	34973	superfamily	386267	89	570	1,88E-56	207.125	p450	51
Q#2	27607	superfamily	386267	34	527	1,81E-69	243.334	p450	5136
Q#3	1396656	superfamily	386267	36	368	1,64E-48	184.399	p450	61
Q#4	1478525	superfamily	386267	44	466	9,87E-60	214.444	p450	5359
Q#5	1397405	superfamily	386267	99	534	1,05E-72	252.964	p450	63
Q#6	962776	superfamily	386267	28	461	3,07E-66	231.393	p450	502
Q#7	962848	superfamily	386267	37	513	3,51E-61	221.763	p450	5150
Q#8	1340785	superfamily	386267	37	513	3,02E-58	211.363	p450	5150
Q#9	1415279	superfamily	386267	37	514	1,45E-60	220.222	p450	5150
Q#10	963629	superfamily	386267	30	497	1,10E-63	227.541	p450	502
Q#11	1398119	superfamily	386267	38	488	2,85E-62	223.304	p450	---
Q#12	1398198	superfamily	386267	54	535	7,01E-79	265.29	p450	53
Q#13	1398222	superfamily	386267	42	486	3,09E-41	167.45	p450	5142
Q#14	1398228	superfamily	386267	46	476	4,72E-39	161.672	p450	5142
Q#15	729817	superfamily	386267	116	419	1,12E-39	161.287	p450	512
Q#16	734651	superfamily	386267	80	521	6,11E-55	204.814	p450	5140
Q#17	1539061	superfamily	386267	42	467	4,99E-61	220.222	p450	5359
Q#18	1479188	superfamily	386267	3	427	1,80E-66	232.549	p450	5359
Q#19	1066776	superfamily	386267	48	481	9,11E-64	222.533	p450	5359
Q#20	1453282	superfamily	386267	43	499	1,82E-57	210.977	p450	5359
Q#21	1398535	superfamily	386267	191	542	1,65E-49	190.562	p450	5365
Q#22	1398536	superfamily	386267	121	443	1,04E-54	202.888	p450	5365
Q#23	1398762	superfamily	386267	138	565	9,98E-65	232.549	p450	63
Q#24	1479457	superfamily	386267	122	562	3,42E-68	241.793	p450	63
Q#25	1344264	superfamily	386267	42	487	1,91E-61	221.378	p450	5037
Q#26	82622	superfamily	386267	37	484	5,45E-55	204.429	p450	5037

Q#27	1343438	superfamily	386267	43	475	4,01E-75	254.505	p450		5152
Q#28	1223734	superfamily	386267	1	400	5,35E-50	189.406	p450		5359
Q#29	1343449	superfamily	386267	43	486	8,87E-61	220.222	p450		5359
Q#30	1453844	superfamily	386267	8	395	9,07E-53	196.725	p450		5359
Q#31	1225203	superfamily	386267	52	511	2,41E-63	227.541	p450		5359
Q#32	1453857	superfamily	386267	34	492	1,42E-68	240.252	p450		5359
Q#33	1453858	superfamily	386267	1	408	3,18E-58	210.977	p450		5359
Q#34	1228724	superfamily	386267	192	511	2,42E-28	131.626	p450		512
Q#35	1399478	superfamily	386267	195	497	2,95E-27	128.545	p450		512
Q#36	1553630	superfamily	386267	43	480	1,13E-59	216.755	p450		5359
	1230244	superfamily	386267	20	114	1,17E-03	513.621	p450		
	1230216	superfamily	386267	65	335	7,11E-42	164.368	p450		
Q#37	1399488	superfamily	386267	35	482	7,27E-74	254.12	p450		5359
Q#38	1416167	superfamily	386267	6	407	9,08E-48	185.554	p450		5359
	1454199	superfamily	386267	6	427	8,69E-50	189.021	p450		
Q#39	1344287	superfamily	386267	35	514	3,34E-62	224.459	p450		5150
Q#40	1433703	superfamily	386267	53	508	6,07E-76	259.898	p450		5344
Q#41	1400720	superfamily	386267	34	469	5,66E-58	209.437	p450		5357
Q#42	1480930	superfamily	386267	109	544	9,21E-45	178.235	p450		5035
Q#43	1554465	superfamily	386267	174	558	5,17E-38	159.361	p450		5035
Q#44	1400732	superfamily	386267	193	534	4,15E-34	148.575	p450		5035
Q#45	1501025	superfamily	386267	118	537	1,19E-35	153.197	p450		5035
	1481154	superfamily	386267	49	98	0.000583054	372.523	p450		
Q#46	243688	superfamily	386267	7	367	4,67E-68	229.852	p450		5359
Q#47	1417036	superfamily	386267	52	479	8,67E-66	232.934	p450		5359
Q#48	1346472	superfamily	386267	35	513	5,29E-54	202.888	p450		5150
Q#49	1401994	superfamily	386267	91	537	9,27E-46	180.932	p450		5035
Q#50	1455204	superfamily	386267	111	533	1,44E-46	182.858	p450		5035
Q#51	1402266	superfamily	386267	54	516	6,29E-85	283.395	p450		5148

Q#52	1454895	superfamily	386267	112	536	2,95E-48	187.48	p450	5035
Q#53	1347121	superfamily	386267	40	471	3,96E-67	236.4	p450	5358
Q#54	1454924	superfamily	386267	49	485	2,99E-72	250.268	p450	5359
Q#55	1454932	superfamily	386267	53	411	3,90E-22	112.366	p450	5035
Q#56	1506430	superfamily	386267	129	583	5,89E-50	190.177	p450	5035
Q#57	1401717	superfamily	386267	92	558	3,13E-47	184.784	p450	5035
Q#58	1417414	superfamily	386267	35	524	3,63E-63	226.771	p450	5136
Q#59	1401775	superfamily	386267	42	488	7,85E-21	109.67	p450	5366
Q#60	1481810	superfamily	386267	90	547	3,90E-49	189.791	p450	5035
Q#61	1482194	superfamily	386267	33	526	2,87E-69	237.556	p450	5136
Q#62	1402446	superfamily	386267	51	526	6,59E-74	255.66	p450	5136
Q#63	1348623	superfamily	386267	34	470	4,49E-37	155.894	p450	512
Q#64	1349082	superfamily	386267	54	492	2,90E-29	134.708	p450	512
Q#65	1482265	superfamily	386267	37	467	1,40E-30	137.789	p450	512
Q#66	1512441	superfamily	386267	33	518	1,44E-70	246.03	p450	5136
Q#67	1348894	superfamily	386267	194	482	9,52E-19	103.507	p450	5347
Q#68	1555694	superfamily	386267	95	548	9,24E-72	250.268	p450	5360
Q#69	1482505	superfamily	386267	1	433	5,35E-62	221.763	p450	5359
Q#70	1482506	superfamily	386267	31	474	2,12E-66	234.475	p450	5359
Q#71	1349193	superfamily	386267	44	488	6,05E-78	264.905	p450	5359
Q#72	475029	superfamily	386267	1	404	1,08E-63	225.23	p450	5359
Q#73	1349155	superfamily	386267	7	353	1,15E-51	191.717	p450	5359
Q#74	474968	superfamily	386267	74	514	6,25E-71	249.497	p450	5359
Q#75	474995	superfamily	386267	40	498	5,82E-74	254.505	p450	5359
Q#76	1437903	superfamily	386267	41	496	4,49E-54	202.118	p450	5359
Q#77	1404374	superfamily	386267	35	455	3,63E-36	153.197	p450	537
Q#78	1404396	superfamily	386267	40	534	4,26E-58	214.059	p450	5151
Q#79	1483639	superfamily	386267	13	425	3,63E-67	247.186	p450	505
Q#80	1404557	superfamily	386267	31	525	6,47E-73	252.194	p450	5137

Q#81	1403300	superfamily	386267	41	468	2,82E-58	212.903	p450	5357	
Q#82	1403310	superfamily	386267	56	456	4,96E-59	214.829	p450	5144	
Q#83	615091	superfamily	386267	41	456	5,50E-67	236.4	p450	5348	
Q#84	617221	superfamily	386267	143	491	3,81E-35	150.501	p450	512	
Q#85	1483511	superfamily	386267	41	501	5,06E-72	249.497	p450	5348	
Q#86	1519860	superfamily	386267	35	482	5,49E-69	241.408	p450	5037	
Q#87	1440502	superfamily	386267	34	497	1,98E-72	250.268	p450	5144	
Q#88	1483829	superfamily	386267	36	463	9,62E-67	235.245	p450	5358	
Q#89	694797	superfamily	386267	33	501	1,42E-52	197.881	p450	5136	
Q#90	1484251	superfamily	386267	32	507	2,93E-72	250.653	p450	5136	
Q#91	696957	superfamily	386267	32	519	2,40E-66	232.549	p450	5136	
Q#92	1522881	superfamily	386267	61	528	3,94E-52	197.495	p450	5136	
	676168	superfamily	386267	610	988	0.00143138	420.306	p450		
Q#93	518838	superfamily	386267	32	493	1,88E-78	266.061	p450	5144	
Q#94	1484657	superfamily	386267	40	496	6,99E-67	236.015	p450	---	
Q#95	1484803	superfamily	386267	43	467	3,58E-56	207.896	p450	5144	
Q#96	1354439	superfamily	386267	32	505	1,21E-66	236.015	p450	5150	
Q#97	1354661	superfamily	386267	32	497	6,53E-60	217.526	p450	5150	
Q#98	1484863	superfamily	386267	87	488	2,58E-63	224.074	p450		5141
Q#99	786385	superfamily	386267	84	476	4,73E-68	236.4	p450		5141
Q#100	1354575	superfamily	386267	110	482	1,05E-65	232.934	p450		5141
Q#101	1419739	superfamily	386267	84	514	5,82E-17	984.991	p450		5156
Q#102	1354652	superfamily	386267	40	640	1,32E-45	182.473	p450		5138
Q#103	1465036	superfamily	386267	34	508	1,06E-64	230.623	p450	5150	
Q#104	774929	superfamily	386267	66	511	1,25E-52	199.036	p450	5150	
Q#105	1354288	superfamily	386267	35	528	1,83E-63	227.926	p450	5150	
Q#106	775522	superfamily	386267	48	531	1,49E-61	223.304	p450	5150	
Q#107	775515	superfamily	386267	65	508	1,73E-55	206.355	p450	5150	
Q#108	1484419	superfamily	386267	2	427	2,29E-77	262.209	p450	5344	

Q#109	815043	superfamily	386267	34	546	1,85E-68	241.023	p450	5136
Q#110	1457045	superfamily	386267	37	520	1,93E-70	245.645	p450	5136
Q#111	1485266	superfamily	386267	39	492	8,30E-36	152.427	p450	512
Q#112	1355519	superfamily	386267	35	488	4,87E-35	150.116	p450	512
Q#113	1386986	superfamily	386267	46	519	1,54E-69	243.334	p450	5037
Q#114	1407595	superfamily	386267	40	486	3,10E-68	239.482	p450	5359
Q#115	924881	superfamily	386267	50	482	2,00E-69	240.252	p450	5359
Q#116	923943	superfamily	386267	48	484	1,93E-55	205.97	p450	5359
Q#117	1532319	superfamily	386267	48	472	7,51E-62	222.919	p450	5359
Q#118	1485980	superfamily	386267	3	127	4,06E-15	865.579	p450	5359
Q#119	1485981	superfamily	386267	47	497	3,14E-61	221.378	p450	5359
Q#120	1357020	superfamily	386267	51	486	9,25E-69	241.023	p450	5359
Q#121	925480	superfamily	386267	41	483	5,88E-63	226.385	p450	5359
Q#122	907593	superfamily	386267	36	517	4,70E-60	223.304	p450	5150
Q#123	938853	superfamily	386267	45	523	2,50E-64	229.852	p450	5139
Q#124	1486149	superfamily	386267	40	489	5,23E-66	233.704	p450	5348
Q#125	1457631	superfamily	386267	172	447	2,19E-47	183.243	p450	5365
Q#126	1536834	superfamily	386267	36	546	5,04E-58	214.444	p450	5155
Q#127	1017154	superfamily	386267	72	497	1,07E-61	219.837	p450	5341
Q#128	1356013	superfamily	386267	16	486	2,05E-61	221.378	p450	5150
Q#129	841225	superfamily	386267	34	508	7,09E-63	226	p450	5150
Q#130	1407700	superfamily	386267	40	522	7,03E-60	218.296	p450	5150
Q#131	1358486	superfamily	386267	35	510	3,54E-61	221.763	p450	5150
Q#132	1537019	superfamily	386267	35	512	4,85E-61	221.378	p450	5150
Q#133	1408386	superfamily	386267	33	510	2,08E-58	211.748	p450	5150
Q#134	1486573	superfamily	386267	35	507	1,91E-59	217.141	p450	5150
Q#135	1457700	superfamily	386267	16	364	4,59E-23	115.063	p450	5359
Q#136	1009070	superfamily	386267	28	436	2,39E-47	180.932	p450	5362
	1009564	superfamily	386267	25	109	1,21E-12	776.983	p450	

Q#137	1486980	superfamily	386267	44	182	1,36E-33	138.56	p450	5359
Q#138	1540158	superfamily	386267	60	271	2,48E-46	175.539	p450	5359
Q#139	1474355	superfamily	386267	48	488	4,88E-52	196.34	p450	5359
Q#140	1559629	superfamily	386267	82	550	1,41E-64	231.778	p450	5139
Q#141	1457975	superfamily	386267	57	493	8,11E-68	238.326	p450	5359
Q#142	1359462	superfamily	386267	48	478	1,92E-54	197.881	p450	5359
Q#143	1487024	superfamily	386267	55	492	1,77E-71	248.342	p450	5359
Q#144	1092243	superfamily	386267	38	473	1,31E-75	258.357	p450	5359
Q#145	1359512	superfamily	386267	43	477	6,42E-72	249.112	p450	5359
Q#146	1487028	superfamily	386267	46	483	3,58E-41	167.45	p450	5359
Q#147	1092514	superfamily	386267	100	289	1,07E-35	147.419	p450	5359
	1359434	superfamily	386267	36	98	0.00521977	347.173	p450	
Q#148	1409124	superfamily	386267	6	450	3,18E-76	272.224	p450	505
	1359306	superfamily	386267	46	480	7,17E-44	174.769	p450	
Q#149	1486878	superfamily	386267	44	522	5,60E-56	207.896	p450	5340
Q#150	1487569	superfamily	386267	40	536	5,46E-54	202.888	p450	5136
Q#151	1409550	superfamily	386267	102	527	8,28E-44	172.843	p450	5364
Q#152	1360364	superfamily	386267	39	464	3,92E-52	196.34	p450	5035
Q#153	1176709	superfamily	386267	30	468	9,27E-70	242.949	p450	5357
Q#154	1114440	superfamily	386267	99	549	3,15E-62	223.304	p450	63
Q#155	1239160	superfamily	386267	38	520	3,14E-68	237.556	p450	5150
Q#156	1487827	superfamily	386267	84	532	1,23E-46	183.628	p450	5035
Q#157	1466636	superfamily	386267	46	463	5,37E-72	248.727	p450	5065
Q#158	1410592	superfamily	386267	35	470	5,01E-41	163.983	p450	512
Q#159	1410594	superfamily	386267	60	491	1,52E-31	140.486	p450	512
Q#160	1249799	superfamily	386267	62	472	7,18E-26	124.307	p450	512
Q#161	1361826	superfamily	386267	62	494	2,54E-32	142.797	p450	512
Q#162	1410767	superfamily	386267	56	487	4,16E-59	215.215	p450	5359
Q#163	1362123	superfamily	386267	56	487	1,70E-57	210.977	p450	5359

Q#164	1362959	superfamily	386267	96	518	4,01E-38	159.361	p450	5364
Q#165	1363166	superfamily	386267	60	465	1,08E-55	204.044	p450	5359
Q#166	1411667	superfamily	386267	36	506	8,41E-55	204.429	p450	5150
Q#167	1363702	superfamily	386267	39	510	1,40E-56	209.437	p450	5150
Q#168	1363727	superfamily	386267	34	507	1,72E-58	211.748	p450	5150
Q#169	1497793	superfamily	386267	121	526	7,76E-45	177.85	p450	---
Q#170	1488894	superfamily	386267	44	505	1,16E-55	206.355	p450	---
Q#171	1363258	superfamily	386267	116	514	2,32E-53	200.962	p450	---
Q#172	1498436	superfamily	386267	34	479	6,28E-73	251.038	p450	5158
Q#173	1362353	superfamily	386267	44	456	9,11E-76	259.127	p450	5146
Q#174	151883	superfamily	386267	43	524	8,74E-56	207.511	p450	5150
Q#175	1411615	superfamily	386267	122	531	1,35E-41	169.376	p450	5035
Q#176	1363391	superfamily	386267	103	522	4,40E-45	178.621	p450	5035
Q#177	1363373	superfamily	386267	99	525	6,02E-41	167.45	p450	5035
Q#178	184586	superfamily	386267	118	529	2,32E-46	182.473	p450	5035
Q#179	1500065	superfamily	386267	118	558	4,22E-44	176.695	p450	5035
Q#180	1422973	superfamily	386267	76	549	1,20E-49	190.947	p450	5035
Q#181	1422979	superfamily	386267	8	208	1,54E-23	110.825	p450	5035
Q#182	1364780	superfamily	386267	34	510	1,72E-62	225.23	p450	5150
Q#183	1561063	superfamily	386267	118	529	3,35E-42	171.302	p450	5035
Q#184	1412649	superfamily	386267	49	491	9,54E-85	283.01	p450	5065
Q#185	304414	superfamily	386267	68	481	2,53E-57	210.207	p450	---
Q#186	1490679	superfamily	386267	35	511	3,07E-64	229.467	p450	5150

P450ome of Lentinus tigrinus

	Hit	type	PSSM-ID	From	To	E-Value	Bitscore	Accession	Short	FCPD family assignment
Q#1	568961	superfamily	386267	123	562	1,52E-69	245.26	cl12078	p450	63
Q#2	537386	superfamily	386267	83	542	1,17E-59	219.067	cl12078	p450	63
Q#3	568896	superfamily	386267	61	484	9,83E-54	200.962	cl12078	p450	5037
Q#4	558855	superfamily	386267	42	491	2,14E-61	221.378	cl12078	p450	5037
Q#5	491714	superfamily	386267	85	505	1,55E-52	198.651	cl12078	p450	5140
Q#6	569604	superfamily	386267	198	493	6,68E-33	144.338	cl12078	p450	512
Q#7	569613	superfamily	386267	86	521	6,38E-66	234.089	cl12078	p450	5344
Q#8	605867	superfamily	386267	50	476	1,21E-74	256.816	cl12078	p450	5344
Q#9	490792	superfamily	386267	61	483	1,07E-50	192.873	cl12078	p450	5354
Q#10	493205	superfamily	386267	29	448	1,14E-45	174.924	cl12078	p450	5365
Q#11	123929	superfamily	386267	66	456	2,68E-75	255.275	cl12078	p450	5146
Q#12	606039	superfamily	386267	34	517	3,28E-63	226.771	cl12078	p450	5144
Q#13	570143	superfamily	386267	34	509	1,62E-52	198.651	cl12078	p450	5150
Q#14	204611	superfamily	386267	35	506	1,58E-66	235.63	cl12078	p450	5150
Q#15	494172	superfamily	386267	28	463	9,06E-64	224.845	cl12078	p450	502
Q#16	570759	superfamily	386267	37	513	5,37E-62	223.689	cl12078	p450	5150
Q#17	570761	superfamily	386267	37	547	1,04E-59	217.911	cl12078	p450	5150
Q#18	211585	superfamily	386267	82	558	2,24E-62	226	cl12078	p450	5150
Q#19	211983	superfamily	386267	30	481	3,24E-63	226.385	cl12078	p450	502
Q#20	479061	superfamily	386267	1	451	5,66E-63	224.074	cl12078	p450	---
Q#21	607211	superfamily	386267	2	371	2,10E-45	175.539	cl12078	p450	---
Q#22	260851	superfamily	386267	37	533	1,40E-77	262.209	cl12078	p450	5136
Q#23	540767	superfamily	386267	35	489	2,86E-33	145.108	cl12078	p450	512
Q#24	571137	superfamily	386267	220	486	6,18E-29	130.471	cl12078	p450	512
Q#25	607338	superfamily	386267	61	493	1,76E-33	145.879	cl12078	p450	512
Q#26	495311	superfamily	386267	35	487	6,93E-44	174.383	cl12078	p450	512

Q#27	560581	superfamily	386267	312	510	6,32E-19	104.277	cl12078	p450	5347
Q#28	494916	superfamily	386267	33	520	2,49E-77	263.75	cl12078	p450	5136
Q#29	571267	superfamily	386267	34	467	1,52E-23	117.759	cl12078	p450	512
Q#30	571270	superfamily	386267	39	471	1,32E-30	137.789	cl12078	p450	512
Q#31	541286	superfamily	386267	32	521	5,43E-70	242.178	cl12078	p450	5136
Q#32	607506	superfamily	386267	32	527	5,52E-68	239.482	cl12078	p450	5136
Q#33	571340	superfamily	386267	33	526	7,27E-68	239.097	cl12078	p450	5136
Q#34	519527	superfamily	386267	49	488	5,58E-66	233.704	cl12078	p450	5359
	571722	superfamily	386267	660	995	3,25E-02	539.717	cl12078	p450	
Q#35	571985	superfamily	386267	121	443	1,28E-52	197.11	cl12078	p450	5365
Q#36	571986	superfamily	386267	117	468	7,41E-49	187.095	cl12078	p450	5365
Q#37	572038	superfamily	386267	41	452	9,55E-68	237.556	cl12078	p450	5359
Q#38	572047	superfamily	386267	35	478	1,59E-78	266.061	cl12078	p450	5359
Q#39	572048	superfamily	386267	50	470	3,16E-69	242.178	cl12078	p450	5359
Q#40	520733	superfamily	386267	38	503	1,98E-62	224.845	cl12078	p450	5136
Q#41	520795	superfamily	386267	33	521	1,46E-58	214.444	cl12078	p450	5136
Q#42	591645	superfamily	386267	39	526	2,85E-70	245.645	cl12078	p450	5139
Q#43	608679	superfamily	386267	55	485	3,27E-60	217.911	cl12078	p450	5144
Q#44	497276	superfamily	386267	32	491	4,92E-75	257.201	cl12078	p450	5144
Q#45	572694	superfamily	386267	28	446	3,37E-47	183.243	cl12078	p450	5362
Q#46	407332	superfamily	386267	2	433	2,75E-65	230.237	cl12078	p450	5359
Q#47	522358	superfamily	386267	7	478	7,42E-69	240.638	cl12078	p450	5359
Q#48	609187	superfamily	386267	36	470	3,15E-57	210.592	cl12078	p450	5359
Q#49	498232	superfamily	386267	58	481	1,75E-70	245.645	cl12078	p450	5359
Q#50	522419	superfamily	386267	36	474	8,68E-75	256.431	cl12078	p450	5359
Q#51	498489	superfamily	386267	63	494	1,77E-29	134.708	cl12078	p450	512
Q#52	584886	superfamily	386267	63	496	5,44E-38	158.205	cl12078	p450	512
Q#53	584899	superfamily	386267	41	466	3,53E-59	215.6	cl12078	p450	5359
Q#54	584900	superfamily	386267	46	434	1,58E-40	164.368	cl12078	p450	5359

Q#55	433193	superfamily	386267	42	488	5,93E-71	246.801	cl12078	p450	5359
Q#56	544294	superfamily	386267	42	498	1,24E-69	243.334	cl12078	p450	5359
Q#57	609251	superfamily	386267	2	435	4,68E-74	250.653	cl12078	p450	5359
Q#58	433268	superfamily	386267	47	483	2,12E-64	229.467	cl12078	p450	5359
Q#59	573208	superfamily	386267	39	485	1,85E-72	250.653	cl12078	p450	5359
Q#60	433596	superfamily	386267	37	478	5,14E-71	246.416	cl12078	p450	5359
Q#61	609256	superfamily	386267	45	489	9,75E-70	243.334	cl12078	p450	5359
Q#62	498477	superfamily	386267	32	473	7,43E-73	251.423	cl12078	p450	5359
Q#63	573218	superfamily	386267	32	488	9,19E-73	251.423	cl12078	p450	5359
Q#64	433711	superfamily	386267	40	495	2,78E-67	237.171	cl12078	p450	5359
Q#65	544321	superfamily	386267	47	487	6,59E-68	238.712	cl12078	p450	5359
Q#66	573701	superfamily	386267	46	461	4,47E-73	249.112	cl12078	p450	5152
Q#67	574028	superfamily	386267	44	522	2,30E-58	214.059	cl12078	p450	5340
Q#68	545725	superfamily	386267	49	484	3,65E-64	229.082	cl12078	p450	5359
Q#69	499847	superfamily	386267	5	432	6,54E-64	226.385	cl12078	p450	5359
Q#70	545742	superfamily	386267	42	482	4,76E-62	223.304	cl12078	p450	5359
Q#71	523970	superfamily	386267	38	480	7,26E-67	236.015	cl12078	p450	5359
Q#72	55323	superfamily	386267	34	464	1,51E-63	227.156	cl12078	p450	5359
Q#73	610085	superfamily	386267	38	477	1,35E-65	232.163	cl12078	p450	5359
Q#74	55363	superfamily	386267	45	406	2,39E-54	200.962	cl12078	p450	5359
	55340	superfamily	386267	51	494	1,24E-68	241.023	cl12078	p450	
	55550	superfamily	386267	2	62	0.00151195	359.812	cl12078	p450	
Q#75	55497	superfamily	386267	38	294	1,55E-47	179.776	cl12078	p450	5359
Q#76	499926	superfamily	386267	43	489	1,09E-62	225.615	cl12078	p450	5359
Q#77	499737	superfamily	386267	54	472	2,72E-53	200.577	cl12078	p450	5359
	610280	superfamily	386267	49	117	2,32E-08	696.091	cl12078	p450	
Q#78	500568	superfamily	386267	40	655	6,66E-45	180.932	cl12078	p450	5138
Q#79	574364	superfamily	386267	6	450	2,10E-71	259.127	cl12078	p450	505
Q#80	585608	superfamily	386267	45	497	1,94E-61	221.763	cl12078	p450	5341

Q#81	546326	superfamily	386267	49	550	1,09E-54	205.585	cl12078	p450	5155
Q#82	546331	superfamily	386267	34	538	3,40E-54	204.044	cl12078	p450	5155
Q#83	70200	superfamily	386267	38	524	2,69E-66	235.245	cl12078	p450	5150
Q#84	500554	superfamily	386267	35	509	3,30E-59	216.37	cl12078	p450	5150
Q#85	546494	superfamily	386267	35	524	1,25E-58	215.215	cl12078	p450	5150
Q#86	600434	superfamily	386267	30	463	1,01E-69	242.949	cl12078	p450	5357
Q#87	547581	superfamily	386267	114	530	2,20E-34	149.345	cl12078	p450	5035
Q#88	611133	superfamily	386267	122	556	4,30E-31	140.101	cl12078	p450	5035
Q#89	586062	superfamily	386267	109	527	4,14E-32	143.182	cl12078	p450	5035
Q#90	501567	superfamily	386267	42	458	2,15E-34	149.345	cl12078	p450	---
Q#91	611142	superfamily	386267	1	239	1,07E-40	158.59	cl12078	p450	5150
	611143	superfamily	386267	66	245	4,05E-04	565.123	cl12078	p450	
Q#92	611423	superfamily	386267	56	533	1,69E-57	211.748	cl12078	p450	51
Q#93	601217	superfamily	386267	109	540	6,23E-65	229.852	cl12078	p450	63
Q#94	548680	superfamily	386267	43	494	4,90E-58	212.518	cl12078	p450	5359
Q#95	628086	superfamily	386267	73	522	4,63E-33	146.264	cl12078	p450	5035
Q#96	576355	superfamily	386267	42	525	7,10E-65	231.393	cl12078	p450	5136
Q#97	576504	superfamily	386267	35	514	9,33E-66	233.704	cl12078	p450	5150
Q#98	586810	superfamily	386267	2	442	1,76E-70	244.104	cl12078	p450	5344
Q#99	527996	superfamily	386267	91	532	6,24E-49	189.406	cl12078	p450	5035
Q#100	504576	superfamily	386267	46	488	1,24E-59	216.755	cl12078	p450	5359
Q#101	576816	superfamily	386267	47	488	1,16E-57	211.363	cl12078	p450	5359
Q#102	612638	superfamily	386267	43	503	1,88E-73	253.349	cl12078	p450	5348
Q#103	180824	superfamily	386267	41	499	6,43E-70	244.104	cl12078	p450	5348
Q#104	576979	superfamily	386267	204	489	1,32E-35	151.657	cl12078	p450	512
Q#105	577131	superfamily	386267	36	368	1,36E-43	171.302	cl12078	p450	61
Q#106	529190	superfamily	386267	39	521	4,65E-64	226.771	cl12078	p450	5150
	587244	superfamily	386267	46	487	1,07E-40	165.909	cl12078	p450	
Q#107	505944	superfamily	386267	32	526	1,16E-75	259.512	cl12078	p450	5137

Q#108	565376	superfamily	386267	40	496	3,85E-67	236.4	cl12078	p450		---
Q#109	594761	superfamily	386267	6	450	1,52E-68	251.038	cl12078	p450		505
Q#110	530577	superfamily	386267	37	493	1,55E-79	269.142	cl12078	p450		5359
Q#111	602570	superfamily	386267	43	491	1,25E-75	256.046	cl12078	p450		5359
Q#112	552293	superfamily	386267	93	531	9,58E-50	191.332	cl12078	p450		5035
Q#113	578126	superfamily	386267	92	532	5,58E-52	195.184	cl12078	p450		5035
Q#114	507143	superfamily	386267	42	525	1,64E-66	235.63	cl12078	p450		5136
Q#115	234875	superfamily	386267	37	517	8,52E-64	228.697	cl12078	p450		5136
Q#116	578269	superfamily	386267	90	521	1,08E-48	188.636	cl12078	p450		5035
Q#117	552783	superfamily	386267	38	489	5,72E-40	163.983	cl12078	p450		5142
Q#118	507502	superfamily	386267	54	536	1,94E-72	251.038	cl12078	p450		53
Q#119	594978	superfamily	386267	29	479	1,13E-57	210.977	cl12078	p450		---
Q#120	602843	superfamily	386267	6	450	2,31E-69	253.349	cl12078	p450		505
Q#121	578576	superfamily	386267	40	534	8,98E-61	220.993	cl12078	p450		5151
Q#122	531402	superfamily	386267	27	451	4,93E-38	158.205	cl12078	p450		537
Q#123	508159	superfamily	386267	107	545	6,32E-61	222.533	cl12078	p450		63
Q#124	553805	superfamily	386267	44	470	1,10E-59	216.755	cl12078	p450		5359
Q#125	614857	superfamily	386267	40	467	1,10E-65	232.934	cl12078	p450		5144
Q#126	532459	superfamily	386267	32	504	1,12E-66	236.015	cl12078	p450		5150
Q#127	291368	superfamily	386267	32	500	1,09E-61	222.533	cl12078	p450		5150
Q#128	579248	superfamily	386267	143	575	1,33E-67	240.252	cl12078	p450		5141
Q#129	603274	superfamily	386267	117	498	6,06E-56	207.511	cl12078	p450		5141
Q#130	509166	superfamily	386267	74	446	8,27E-64	226.771	cl12078	p450		5141
Q#131	588283	superfamily	386267	144	543	9,64E-14	890.019	cl12078	p450		5156
Q#132	579345	superfamily	386267	44	490	1,15E-17	100.425	cl12078	p450		5366
	603414	superfamily	386267	36	136	5,62E-03	515.047	cl12078	p450		
Q#133	579736	superfamily	386267	38	518	2,66E-68	240.638	cl12078	p450		5150
Q#134	579748	superfamily	386267	34	507	1,47E-61	222.533	cl12078	p450		5150
Q#135	588543	superfamily	386267	33	513	2,23E-54	203.659	cl12078	p450		5150

Q#136	510299	superfamily	386267	39	508	5,62E-55	205.199	cl12078	p450	5150
Q#137	555133	superfamily	386267	36	514	4,10E-49	189.406	cl12078	p450	5150
Q#138	603681	superfamily	386267	31	485	2,06E-76	260.668	cl12078	p450	5065
Q#139	657215	superfamily	386267	20	498	1,59E-61	222.148	cl12078	p450	5150
	595751	superfamily	386267	36	524	5,42E-50	192.103	cl12078	p450	
Q#140	615733	superfamily	386267	53	532	1,06E-61	224.074	cl12078	p450	5150
Q#141	580038	superfamily	386267	35	504	4,90E-60	218.681	cl12078	p450	5150
Q#142	555532	superfamily	386267	35	514	2,08E-58	214.444	cl12078	p450	5150
Q#143	580061	superfamily	386267	35	514	4,39E-67	234.86	cl12078	p450	5150
Q#144	510836	superfamily	386267	36	513	1,42E-58	212.133	cl12078	p450	5150
Q#145	533875	superfamily	386267	35	508	2,40E-65	232.549	cl12078	p450	5150
Q#146	615961	superfamily	386267	46	500	8,42E-53	198.266	cl12078	p450	5359
Q#147	615962	superfamily	386267	58	469	3,82E-47	182.858	cl12078	p450	5359
Q#148	657729	superfamily	386267	46	484	3,53E-44	175.539	cl12078	p450	5359
Q#149	580700	superfamily	386267	44	492	6,19E-69	241.408	cl12078	p450	5359
Q#150	580702	superfamily	386267	105	514	6,93E-53	199.807	cl12078	p450	???
Q#151	512003	superfamily	386267	16	450	5,31E-42	168.991	cl12078	p450	5359
Q#152	657733	superfamily	386267	49	483	9,72E-63	225.23	cl12078	p450	5359
Q#153	534944	superfamily	386267	8	427	9,26E-54	199.807	cl12078	p450	5359
Q#154	556610	superfamily	386267	7	406	1,08E-49	188.251	cl12078	p450	5359
Q#155	616351	superfamily	386267	55	474	2,40E-68	239.867	cl12078	p450	5359
Q#156	589030	superfamily	386267	38	494	7,33E-72	246.03	cl12078	p450	5359
Q#157	511983	superfamily	386267	44	512	1,27E-61	222.533	cl12078	p450	5359
Q#158	596071	superfamily	386267	172	449	2,41E-50	191.332	cl12078	p450	5365
	604200	superfamily	386267	35	443	2,58E-52	196.34	cl12078	p450	
Q#159	512048	superfamily	386267	40	489	2,27E-52	197.495	cl12078	p450	5359
Q#160	511944	superfamily	386267	38	473	1,36E-48	187.48	cl12078	p450	5359
Q#161	535204	superfamily	386267	46	518	5,15E-58	213.289	cl12078	p450	5139
Q#162	512299	superfamily	386267	40	500	6,37E-68	238.712	cl12078	p450	5348

Q#163	581076	superfamily	386267	98	550	6,51E-53	200.577	cl12078	p450	5035
Q#164	581086	superfamily	386267	49	490	6,73E-88	291.484	cl12078	p450	5065
Q#165	581194	superfamily	386267	35	474	2,21E-67	237.171	cl12078	p450	5037
Q#166	617224	superfamily	386267	121	529	1,70E-40	165.909	cl12078	p450	---
Q#167	617226	superfamily	386267	38	531	4,80E-54	202.888	cl12078	p450	---
Q#168	581603	superfamily	386267	116	514	5,26E-50	191.717	cl12078	p450	---
Q#169	581771	superfamily	386267	29	475	1,87E-60	218.681	cl12078	p450	---
Q#170	658548	superfamily	386267	28	481	6,51E-67	235.63	cl12078	p450	5360
Q#171	581782	superfamily	386267	88	559	2,15E-37	158.205	cl12078	p450	5035
Q#172	581800	superfamily	386267	76	565	1,68E-40	164.368	cl12078	p450	5035
Q#173	568286	superfamily	386267	21	414	3,10E-44	173.228	cl12078	p450	5035
Q#174	581802	superfamily	386267	105	544	3,75E-43	173.998	cl12078	p450	5035
Q#175	568300	superfamily	386267	50	464	4,14E-57	210.207	cl12078	p450	5359
Q#176	589538	superfamily	386267	37	451	3,18E-66	230.237	cl12078	p450	5359
Q#177	581832	superfamily	386267	39	526	1,06E-68	241.408	cl12078	p450	5139
Q#178	581920	superfamily	386267	117	528	4,34E-46	181.702	cl12078	p450	5035
Q#179	558432	superfamily	386267	75	515	1,72E-39	163.213	cl12078	p450	5035
Q#180	658665	superfamily	386267	117	585	1,49E-41	170.146	cl12078	p450	5035
Q#181	514600	superfamily	386267	19	500	2,12E-56	208.666	cl12078	p450	5150
Q#182	536984	superfamily	386267	35	517	2,06E-52	198.651	cl12078	p450	5150
Q#183	514707	superfamily	386267	34	478	5,20E-79	266.831	cl12078	p450	5158
Q#184	658804	superfamily	386267	37	319	1,33E-54	198.266	cl12078	p450	5037

P450ome of Polyporus squamosus

	Hit	type	PSSM-ID	From	To	E-Value	Bitscore	Accession	Short	FCPD family assignment
Q#1	114719	superfamily	386267	45	525	1,08E-68	241.408	cl12078	p450	5139
Q#2	117318	superfamily	386267	37	513	1,01E-58	215.215	cl12078	p450	5150
Q#3	154076	superfamily	386267	41	501	3,04E-74	255.275	cl12078	p450	5348
Q#4	167974	superfamily	386267	33	506	7,27E-68	239.097	cl12078	p450	5136
Q#5	181995	superfamily	386267	105	563	1,09E-41	170.146	cl12078	p450	5035
Q#6	193243	superfamily	386267	40	496	7,43E-68	238.326	cl12078	p450	---
Q#7	20946	superfamily	386267	50	492	8,88E-75	256.816	cl12078	p450	5359
Q#8	220316	superfamily	386267	44	522	4,35E-60	218.681	cl12078	p450	5340
Q#9	228821	superfamily	386267	1	403	6,66E-62	217.911	cl12078	p450	5359
Q#10	230627	superfamily	386267	33	521	2,89E-73	250.653	cl12078	p450	5136
Q#11	233410	superfamily	386267	41	501	2,01E-74	255,66	cl12078	p450	5348
Q#12	234365	superfamily	386267	76	556	7,32E-61	226.385	cl12078	p450	5150
Q#13	24110	superfamily	386267	90	521	4,87E-50	192.103	cl12078	p450	5035
Q#14	261770	superfamily	386267	54	455	3,24E-60	217.911	cl12078	p450	5144
Q#15	274898	superfamily	386267	121	525	9,61E-44	174.769	cl12078	p450	---
Q#16	277477	superfamily	386267	36	524	2,30E-63	227.156	cl12078	p450	5136
Q#17	294363	superfamily	386267	44	486	3,73E-73	252.579	cl12078	p450	5359
Q#18	294378	superfamily	386267	42	498	1,40E-72	250.653	cl12078	p450	5359
Q#19	294427	superfamily	386267	100	537	2,26E-70	246.416	cl12078	p450	5359
Q#20	294482	superfamily	386267	124	297	5,39E-49	182.858	cl12078	p450	5359
Q#21	565146	superfamily	386267	42	487	2,48E-58	210.592	cl12078	p450	5037
Q#22	566337	superfamily	386267	49	484	1,93E-69	239.867	cl12078	p450	5359
Q#23	567196	superfamily	386267	43	659	6,52E-46	180.932	cl12078	p450	5138
Q#24	570127	superfamily	386267	35	518	3,19E-57	211.363	cl12078	p450	5150
Q#25	570159	superfamily	386267	35	512	1,06E-51	194.029	cl12078	p450	5150
Q#26	570331	superfamily	386267	35	518	2,61E-58	214.059	cl12078	p450	5150

Q#27	570398	superfamily	386267	49	515	5,35E-83	278.772	cl12078	p450	5065
Q#28	570403	superfamily	386267	50	481	1,64E-64	229.852	cl12078	p450	5359
Q#29	570423	superfamily	386267	49	478	1,90E-64	229.467	cl12078	p450	5359
Q#30	570510	superfamily	386267	45	471	4,34E-57	209.051	cl12078	p450	5359
Q#31	570587	superfamily	386267	43	484	8,86E-65	231.393	cl12078	p450	5359
Q#32	571905	superfamily	386267	37	513	1,36E-57	212.133	cl12078	p450	5150
Q#33	571975	superfamily	386267	28	475	6,96E-64	227.926	cl12078	p450	502
Q#34	572969	superfamily	386267	30	462	1,03E-51	195.569	cl12078	p450	5359
Q#35	574352	superfamily	386267	33	519	5,89E-56	207.511	cl12078	p450	5136
Q#36	574534	superfamily	386267	32	493	8,63E-80	269.528	cl12078	p450	5144
Q#37	580083	superfamily	386267	35	480	2,06E-70	244,49	cl12078	p450	5158
Q#38	580491	superfamily	386267	117	461	1,40E-51	194.029	cl12078	p450	5365
Q#39	581669	superfamily	386267	41	487	8,22E-66	233.704	cl12078	p450	5359
Q#40	582425	superfamily	386267	60	527	1,10E-67	236.015	cl12078	p450	5136
Q#41	582477	superfamily	386267	43	476	5,68E-58	212.518	cl12078	p450	5359
Q#42	582507	superfamily	386267	49	486	4,43E-69	242.178	cl12078	p450	5359
Q#43	582922	superfamily	386267	34	514	9,74E-64	228.311	cl12078	p450	5150
Q#44	582950	superfamily	386267	36	514	2,83E-58	210.977	cl12078	p450	5150
Q#45	583000	superfamily	386267	1	422	7,17E-59	213.674	cl12078	p450	5149
Q#46	583169	superfamily	386267	123	513	9,59E-60	217.911	cl12078	p450	5150
Q#47	586403	superfamily	386267	41	527	2,99E-61	222.148	cl12078	p450	5150
Q#48	586682	superfamily	386267	40	491	7,96E-60	217.526	cl12078	p450	5348
Q#49	587802	superfamily	386267	65	518	3,77E-55	205.585	cl12078	p450	5150
Q#50	588169	superfamily	386267	95	508	2,44E-46	179.391	cl12078	p450	5035
Q#51	59651	superfamily	386267	27	434	5,73E-34	146.649	cl12078	p450	537
	597486	superfamily	386267	5	87	8,44E-14	800.095	cl12078	p450	
Q#52	604978	superfamily	386267	34	506	2,16E-60	219.452	cl12078	p450	5150
Q#53	606056	superfamily	386267	37	513	1,27E-60	220.222	cl12078	p450	5150
Q#54	606917	superfamily	386267	2	419	1,33E-63	225.615	cl12078	p450	5359

Q#55	612805	superfamily	386267	35	513	2,07E-62	224.845	cl12078	p450	5150
Q#56	623301	superfamily	386267	15	437	8,14E-40	162.442	cl12078	p450	5359
Q#57	628674	superfamily	386267	83	562	5,86E-63	227.541	cl12078	p450	63
Q#58	628683	superfamily	386267	122	557	1,49E-67	239.867	cl12078	p450	63
Q#59	631341	superfamily	386267	33	526	4,42E-75	255.275	cl12078	p450	5136
Q#60	631343	superfamily	386267	32	522	3,73E-72	250.268	cl12078	p450	5136
Q#61	631575	superfamily	386267	195	448	9,43E-27	127.004	cl12078	p450	512
Q#62	631579	superfamily	386267	246	477	2,45E-33	145.493	cl12078	p450	512
Q#63	631582	superfamily	386267	199	452	1,22E-23	117.759	cl12078	p450	512
Q#64	632485	superfamily	386267	83	500	2,15E-17	100,04	cl12078	p450	5156
Q#65	632504	superfamily	386267	92	481	1,79E-65	229.467	cl12078	p450	5141
Q#66	632571	superfamily	386267	162	542	3,07E-45	179.776	cl12078	p450	5141
Q#67	632585	superfamily	386267	53	380	1,67E-22	113.137	cl12078	p450	5141
Q#68	632769	superfamily	386267	32	505	2,59E-64	229.852	cl12078	p450	5150
Q#69	632919	superfamily	386267	116	529	8,04E-58	212.518	cl12078	p450	---
Q#70	63457	superfamily	386267	53	475	5,64E-57	209.437	cl12078	p450	5359
Q#71	636884	superfamily	386267	105	479	1,27E-47	184.784	cl12078	p450	61
Q#72	637989	superfamily	386267	35	511	3,46E-63	224.074	cl12078	p450	5150
Q#73	638078	superfamily	386267	35	479	4,46E-48	185.939	cl12078	p450	5150
Q#74	638092	superfamily	386267	35	507	2,40E-56	208.666	cl12078	p450	5150
Q#75	638210	superfamily	386267	2	82	3,56E-09	665.275	cl12078	p450	5359
Q#76	638230	superfamily	386267	47	483	2,27E-41	167.835	cl12078	p450	5359
Q#77	638242	superfamily	386267	38	487	9,33E-53	198.651	cl12078	p450	5359
Q#78	638317	superfamily	386267	39	526	1,47E-70	246.416	cl12078	p450	5139
Q#79	638959	superfamily	386267	35	506	1,70E-64	230.237	cl12078	p450	5150
	641477	superfamily	386267	30	464	3,01E-51	194.414	cl12078	p450	
Q#80	643447	superfamily	386267	117	546	5,01E-68	240.638	cl12078	p450	5359
Q#81	643456	superfamily	386267	44	472	2,79E-66	234.089	cl12078	p450	5359
Q#82	643536	superfamily	386267	52	465	1,79E-59	216,37	cl12078	p450	5359

Q#83	643550	superfamily	386267	43	478	1,34E-73	253.349	cl12078	p450	5359
Q#84	643556	superfamily	386267	43	489	3,41E-56	207.896	cl12078	p450	5359
Q#85	644621	superfamily	386267	49	505	2,52E-54	201.888	cl12078	p450	51
Q#86	645073	superfamily	386267	34	475	1,97E-75	257.972	cl12078	p450	5359
Q#87	645075	superfamily	386267	46	479	1,53E-70	244,49	cl12078	p450	5359
	645743	superfamily	386267	62	425	4,60E-04	580.531	cl12078	p450	
Q#88	646298	superfamily	386267	33	542	1,69E-57	209.437	cl12078	p450	5136
Q#89	647912	superfamily	386267	80	521	3,51E-54	202.888	cl12078	p450	5140
Q#90	648377	superfamily	386267	199	474	6,86E-48	185.169	cl12078	p450	5365
Q#91	648639	superfamily	386267	38	478	3,66E-81	272.994	cl12078	p450	5148
Q#92	650902	superfamily	386267	40	511	7,76E-67	236.015	cl12078	p450	5037
Q#93	654848	superfamily	386267	60	535	9,30E-54	202.888	cl12078	p450	5155
Q#94	654938	superfamily	386267	98	532	4,05E-68	240.638	cl12078	p450	63
Q#95	654945	superfamily	386267	111	547	3,47E-77	264.905	cl12078	p450	63
Q#96	65528	superfamily	386267	48	482	3,28E-71	247.186	cl12078	p450	5359
Q#97	655679	superfamily	386267	56	542	4,70E-61	222.148	cl12078	p450	5150
Q#98	655825	superfamily	386267	35	477	2,65E-56	207.511	cl12078	p450	---
Q#99	656583	superfamily	386267	28	483	3,41E-50	191.717	cl12078	p450	5360
Q#100	657162	superfamily	386267	32	526	1,26E-75	259.512	cl12078	p450	5137
Q#101	657548	superfamily	386267	30	485	9,84E-79	266.446	cl12078	p450	5344
Q#102	658183	superfamily	386267	121	446	7,30E-54	200.577	cl12078	p450	5365
	658599	superfamily	386267	58	467	2,50E-23	113.907	cl12078	p450	
	658670	superfamily	386267	171	446	1,90E-21	111.211	cl12078	p450	
Q#103	658814	superfamily	386267	1	392	8,46E-55	201.733	cl12078	p450	5359
Q#104	660601	superfamily	386267	48	495	1,54E-20	103.121	cl12078	p450	5366
	661254	superfamily	386267	1	415	1,32E-35	150.116	cl12078	p450	
Q#105	661942	superfamily	386267	5	417	8,54E-59	210.207	cl12078	p450	5359
Q#106	661974	superfamily	386267	51	494	8,15E-70	243.334	cl12078	p450	5359
Q#107	662970	superfamily	386267	63	507	3,80E-57	207.896	cl12078	p450	5037

Q#108	666053	superfamily	386267	162	305	8,51E-19	101.195	cl12078	p450	5035
Q#109	667567	superfamily	386267	40	534	1,03E-58	215,6	cl12078	p450	5151
Q#110	667609	superfamily	386267	13	450	9,65E-62	231.778	cl12078	p450	505
Q#111	668253	superfamily	386267	41	474	2,68E-78	265.676	cl12078	p450	5359
Q#112	668262	superfamily	386267	42	495	1,32E-65	230.237	cl12078	p450	5359
	668294	superfamily	386267	17	245	1,18E-45	166.679	cl12078	p450	
Q#113	669967	superfamily	386267	198	493	7,49E-37	155.123	cl12078	p450	512
Q#114	670382	superfamily	386267	35	468	8,21E-78	264.135	cl12078	p450	5359
Q#115	670472	superfamily	386267	121	446	7,85E-54	200.577	cl12078	p450	5365
	671111	superfamily	386267	38	216	1,54E-02	522.751	cl12078	p450	
Q#116	673791	superfamily	386267	46	370	1,89E-45	170.531	cl12078	p450	5035
Q#117	676477	superfamily	386267	87	526	1,44E-47	185.554	cl12078	p450	5035
	676537	superfamily	386267	10	45	1,88E+00	391.783	cl12078	p450	
Q#118	684568	superfamily	386267	39	439	1,57E-52	196.725	cl12078	p450	5359
Q#119	689230	superfamily	386267	91	523	9,48E-43	172.457	cl12078	p450	5035
Q#120	694743	superfamily	386267	452	621	3,42E-02	530.455	cl12078	p450	5035
Q#121	695054	superfamily	386267	35	474	3,98E-33	144.723	cl12078	p450	512
Q#122	697567	superfamily	386267	47	485	1,88E-57	210.977	cl12078	p450	5359
Q#123	698316	superfamily	386267	157	499	2,03E-32	143.182	cl12078	p450	5150
Q#124	698481	superfamily	386267	28	439	1,00E-34	149.345	cl12078	p450	5362
Q#125	700136	superfamily	386267	39	477	1,27E-75	253.349	cl12078	p450	5359
Q#126	705793	superfamily	386267	43	427	3,66E-61	219.452	cl12078	p450	5152
Q#127	706717	superfamily	386267	32	479	1,44E-59	216,37	cl12078	p450	5359
Q#128	707000	superfamily	386267	16	378	6,85E-15	911.803	cl12078	p450	5035
Q#129	707179	superfamily	386267	31	431	4,79E-65	229.082	cl12078	p450	5065
Q#130	707869	superfamily	386267	85	492	1,57E-33	146.264	cl12078	p450	512
Q#131	708029	superfamily	386267	30	438	1,60E-51	194.414	cl12078	p450	5357
Q#132	708683	superfamily	386267	193	534	1,86E-35	152.427	cl12078	p450	5035
Q#133	708882	superfamily	386267	35	465	1,50E-64	229.467	cl12078	p450	5037

Q#134	709225	superfamily	386267	72	497	4,98E-58	212.903	cl12078	p450	5341
Q#135	709254	superfamily	386267	41	495	5,50E-58	209.437	cl12078	p450	5359
Q#136	709513	superfamily	386267	246	482	3,75E-20	107.744	cl12078	p450	5347
Q#137	710259	superfamily	386267	54	535	1,48E-77	264,52	cl12078	p450	53
Q#138	710276	superfamily	386267	136	488	1,70E-35	148,96	cl12078	p450	5142
Q#139	710910	superfamily	386267	30	486	2,88E-65	231.393	cl12078	p450	5358
Q#140	711519	superfamily	386267	37	464	6,25E-43	171.302	cl12078	p450	5037
Q#141	712472	superfamily	386267	34	490	1,90E-54	203.273	cl12078	p450	5150
Q#142	719561	superfamily	386267	46	468	2,77E-49	188.251	cl12078	p450	5359
	720495	superfamily	386267	47	487	8,09E-59	214.829	cl12078	p450	
Q#143	730353	superfamily	386267	37	230	5,59E-52	188.251	cl12078	p450	5359
Q#144	730635	superfamily	386267	79	178	1,66E-10	738.463	cl12078	p450	5359
Q#145	730636	superfamily	386267	167	215	7,73E-01	457.267	cl12078	p450	5035
Q#146	735047	superfamily	386267	22	420	2,96E-63	225.615	cl12078	p450	5144
Q#147	735680	superfamily	386267	31	500	5,99E-65	226	cl12078	p450	5150
Q#148	735716	superfamily	386267	44	467	6,39E-61	220.222	cl12078	p450	5144
Q#149	737164	superfamily	386267	38	473	1,30E-74	255,66	cl12078	p450	5359
Q#150	738007	superfamily	386267	20	439	6,53E-52	195.184	cl12078	p450	5150
	739085	superfamily	386267	59	281	3,49E-19	981.139	cl12078	p450	
Q#151	739438	superfamily	386267	73	283	4,56E-33	140.101	cl12078	p450	5035
Q#152	740432	superfamily	386267	125	415	5,42E-28	130.471	cl12078	p450	5340
Q#153	740620	superfamily	386267	93	454	1,49E-24	117.374	cl12078	p450	5035
Q#154	740655	superfamily	386267	33	529	2,74E-77	263,75	cl12078	p450	5136
Q#155	742265	superfamily	386267	35	234	6,68E-09	707.647	cl12078	p450	5359
Q#156	743107	superfamily	386267	13	437	1,09E-56	206,74	cl12078	p450	5359
Q#157	743131	superfamily	386267	42	485	8,32E-57	209.437	cl12078	p450	5359
	743138	superfamily	386267	26	297	3,57E-23	112.366	cl12078	p450	
	743336	superfamily	386267	40	497	1,13E-46	182.473	cl12078	p450	
Q#158	743468	superfamily	386267	30	390	2,13E-49	184.399	cl12078	p450	5150

	744034	superfamily	386267	656	988	0,00017068	451.122	cl12078	p450	
Q#159	744663	superfamily	386267	119	526	8,03E-58	213.674	cl12078	p450	63
Q#160	744761	superfamily	386267	32	488	1,08E-73	253.734	cl12078	p450	5359
Q#161	746124	superfamily	386267	191	491	3,56E-35	150.501	cl12078	p450	512
Q#162	746166	superfamily	386267	40	493	1,25E-65	232.549	cl12078	p450	5358
Q#163	746845	superfamily	386267	70	481	7,77E-42	168.991	cl12078	p450	5035
	746847	superfamily	386267	38	182	1,73E-02	499.639	cl12078	p450	
Q#164	749395	superfamily	386267	51	473	2,24E-52	196,34	cl12078	p450	5359
Q#165	751125	superfamily	386267	1	170	2,91E-22	114.677	cl12078	p450	5359
Q#166	754706	superfamily	386267	41	468	2,10E-51	195.184	cl12078	p450	5359
Q#167	75897	superfamily	386267	38	526	2,54E-69	243.334	cl12078	p450	5150
	760431	superfamily	386267	49	329	2,00E-03	553.567	cl12078	p450	
Q#168	760717	superfamily	386267	59	459	1,15E-57	210.977	cl12078	p450	5359
Q#169	762575	superfamily	386267	55	474	2,99E-71	248.727	cl12078	p450	5359
Q#170	763814	superfamily	386267	47	489	1,50E-66	232.934	cl12078	p450	5359
Q#171	772675	superfamily	386267	37	454	2,24E-70	244,49	cl12078	p450	5359
	781146	superfamily	386267	64	483	3,58E-75	256.816	cl12078	p450	
Q#172	782823	superfamily	386267	205	367	2,55E-16	946.471	cl12078	p450	512
Q#173	811909	superfamily	386267	41	501	1,22E-68	240.638	cl12078	p450	5348
Q#174	813609	superfamily	386267	5	452	2,11E-55	204.429	cl12078	p450	5359
Q#175	816131	superfamily	386267	46	499	2,54E-64	230.237	cl12078	p450	5359
Q#176	816789	superfamily	386267	34	510	1,01E-65	233.704	cl12078	p450	5150
Q#177	816847	superfamily	386267	78	530	1,78E-48	187.865	cl12078	p450	5035
Q#178	818645	superfamily	386267	118	528	2,79E-39	163.213	cl12078	p450	5035
Q#179	82617	superfamily	386267	117	461	5,20E-51	192.873	cl12078	p450	5365
Q#180	829759	superfamily	386267	91	537	1,90E-46	182.858	cl12078	p450	5035
Q#181	831379	superfamily	386267	40	518	6,31E-61	220.993	cl12078	p450	5136
Q#182	832421	superfamily	386267	102	568	1,64E-63	228.311	cl12078	p450	5359
Q#183	834295	superfamily	386267	92	536	6,87E-45	177,85	cl12078	p450	5035

Q#184	834506	superfamily	386267	6	450	1,08E-72	262.594	cl12078	p450		505
Q#185	835110	superfamily	386267	118	515	3,79E-30	137.404	cl12078	p450		5035

Online Resources 3: BLAST results for CYP5035S7-similar CYP5035 sequences

BLASTP 2.2.19

Query= (565 letters)

Database: CYP5035.314seqs.txt
313 sequences; 176,209 total letters

Searching.....done

Sequences producing significant alignments

Sequences Nr.	Score (bits)	E Value
189	1154	0.0
188	1059	0.0
153	985	0.0
187	941	0.0
186	941	0.0
185	941	0.0
184	941	0.0
<80% -> no orthologue of 5035S7		
155	811	0.0
154	811	0.0
158	784	0.0
157	784	0.0

Sequences Nr.	**seq ID**
1	jgi|Phaca1|153972|estExt_Genewise1Plus.C_13_t10148
2	jgi|Phaca1|131233|estExt_Genewise1.C_13_t10190
3	jgi|Clibor1|119449|CE119448_2934
4	jgi|Irplac1|743245|CE743244_3999
5	jgi|Irplac1|1640241|MIX38339_784_26
6	jgi|Abobie1|721434|e_gw1.24.75.1
7	jgi|Panru1|1112951|CE1112950_7139
8	jgi|Panru1|1251950|CE1251949_2310
9	jgi|Cytmel1|1423468|gm1.13794_g
10	jgi|Suibr2|843826|Suibr1.fgenesh1_pm.7_#_53
11	jgi|Obbri1|890182|estExt_Genemark1.C_1790010
12	jgi|Spalat1|479667|CE479666_4080
13	jgi|Spalat1|746579|fgenesh1_pg.6_#_56

156	784	0.0	14	jgi|Trace1|1049863|CE1049862_12876
193	783	0.0	15	jgi|Trace1|1342868|fgenesh1_pg.4_#_46
159	774	0.0	16	jgi|Trace1|1354516|fgenesh1_kg.6_#_129_#_Locus4841v6rpkm0.47_PR
190	773	0.0	17	jgi|Abobie1|826912|MIX14629_1887_37
192	769	0.0	18	jgi|Cytmel1|1418953|gm1.9279_g
191	755	0.0	19	jgi|Trace1|1409937|fgenesh1_pm.40_#_10
160	746	0.0	20	jgi|Dicsqu18370_1|806887|gm1.5849_g
173	621	e-180	21	jgi|Dicsqu464_1|919019|fgenesh1_kg.11_#_191_#_Locus4750v1rpkm4(
			22	jgi|Dicsqu463_1|988899|fgenesh1_pm.58_#_29
<55% -> no subfamily S			23	jgi|Dicsq1|179419|estExt_Genemark1.C_70316
174	615	e-178	24	jgi|Earsca1|733523|fgenesh1_kg.9_#_519_#_TRINITY_DN8112_c3_g3_i1
166	613	e-177	25	jgi|Dicsq1|151582|estExt_fgenesh1_pm.C_1_t20343
165	613	e-177	26	jgi|Dicsqu18370_1|660324|e_gw1.25.174.1
164	613	e-177	27	jgi|Dicsqu463_1|993380|fgenesh1_pm.294_#_6
181	608	e-176	28	jgi|Dicsqu464_1|918682|fgenesh1_kg.10_#_364_#_Locus6722v1rpkm23
167	607	e-175	29	jgi|Polbr1|1481810|gm1.5391_g
169	605	e-175	30	jgi|Polar1|665169|estExt_Genemark1.C_3560004
180	597	e-172	31	jgi|Earsca1|728492|fgenesh1_kg.7_#_1669_#_TRINITY_DN8962_c3_g1_
240	593	e-171	32	jgi|Fomfom1|424094|CE424093_631
183	592	e-171	33	jgi|Polsqu1|24110|CE24109_7285
179	590	e-170	34	jgi|Hexnit1|1215331|fgenesh1_pm.1_#_175
241	588	e-170	35	jgi|Lenti6_1|578269|fgenesh1_kg.34_#_55_#_Locus13854v1rpkm1.21
136	580	e-167	36	jgi|Lenti7_1|564891|gm1.695_g
135	580	e-167	37	jgi|Sisbr1|574375|fgenesh1_kg.2_#_756_#_Locus5232v1rpkm24.84
134	580	e-167	38	jgi|Trave1|41578|gm1.462_g
133	580	e-167	39	jgi|Trapol1|105914|CE105913_5115
271	578	e-167	40	jgi|Traci1|1521520|gm1.6319_g
177	577	e-166	41	jgi|Tralj1|428191|CE428190_1838
176	577	e-166	42	jgi|Pycsa1|1577749|e_gw1.7180000650838.306.1

242	577	e-166	43	jgi|Pycco1|1370331|e_gw1.30.134.1
168	575	e-166	44	jgi|Artele1122_1|466036|e_gw1.2.699.1
145	574	e-166	45	jgi|Pycpun1|308909|CE308908_3418
146	574	e-166	46	jgi|Artel1|850992|fgenesh1_pm.18_#_46
243	573	e-165	47	jgi|Tramax1|1068035|fgenesh1_pm.5_#_366
178	573	e-165	48	jgi|Pycco1662_1|876088|gm1.4639_g
147	571	e-165	49	jgi|Tramey1|997533|fgenesh1_pm.1_#_949
151	571	e-165	50	jgi|Leisp1|1318962|fgenesh1_kg.12_#_150_#_Locus5637v1rpkm21.26
175	570	e-164	51	jgi|Tramen1|1047947|fgenesh1_pm.42_#_35
163	569	e-164	52	jgi|Tralac1|370287|CE370286_1031
171	569	e-164	53	jgi|Paxin1|88877|e_gw1.305.4.1
162	568	e-164	54	jgi|Pycci1|9212|scf185013.g82
161	567	e-163	55	jgi|Dicsqu18370_1|765132|fgenesh1_kg.80_#_126_#_Locus8784v1rpkm
152	566	e-163	56	jgi|Dicsqu18370_1|779171|fgenesh1_pm.51_#_9
144	566	e-163	57	jgi|Dicsq1|161810|estExt_fgenesh1_pg.C_170002
138	564	e-163	58	jgi|Dicsqu463_1|995233|fgenesh1_pm.605_#_1
117	563	e-162	59	jgi|Dicsqu464_1|953386|fgenesh1_pm.286_#_1
141	562	e-162	60	jgi|Sisbr1|623797|gm1.4470_g
118	562	e-162	61	jgi|Polsqu1|835110|estExt_Genemark1.C_2790009
150	561	e-162	62	jgi|Lenti6_1|581920|fgenesh1_kg.91_#_6_#_Locus2506v1rpkm67.23
140	560	e-161	63	jgi|Lenti7_1|538117|fgenesh1_kg.30_#_15_#_Locus2021v2rpkm35.61
139	560	e-161	64	jgi|Sisbr1|585391|fgenesh1_kg.48_#_39_#_Locus9062v1rpkm5.09
143	554	e-159	65	jgi|Pyccin1|1050305|gm1.4848_g
64	553	e-159	66	jgi|Polsqu1|746845|gm1.13007_g
63	553	e-159	67	jgi|Polsqu1|818645|estExt_Genewise1Plus.C_2790008
62	553	e-159	68	jgi|Polsqu1|588169|e_gw1.213.21.1
142	553	e-159	69	jgi|Polar1|667057|estExt_Genemark1.C_6280002
72	552	e-159	70	jgi|Lenti6_1|558432|estExt_Genewise1Plus.C_910024
71	552	e-159	71	jgi|Lenti7_1|468757|e_gw1.30.223.1

70	552	e-159	72	jgi|Sisbr1|570632|estExt_Genewise1Plus.C_480102
268	552	e-159	73	jgi|Trave1|60226|estExt_fgenesh1_pm.C_100063
115	551	e-159	74	jgi|Trapol1|1067680|e_gw1.19.24.1
114	547	e-157	75	jgi|Tramey1|1003669|fgenesh1_pm.18_#_22
253	546	e-157	76	jgi|Tramax1|1055064|fgenesh1_kg.21_#_1051_#_TRINITY_DN2932_c0_
116	546	e-157	77	jgi|Leisp1|1345114|fgenesh1_pm.29_#_11
252	545	e-157	78	jgi|Tramen1|1064764|MIX4850_687_91
251	545	e-157	79	jgi|Tramey1|1032777|MIX17440_258_22
67	542	e-156	80	jgi|Tramax1|1024787|fgenesh1_kg.7_#_529_#_TRINITY_DN3128_c0_g1
123	541	e-156	81	jgi|Pycpun1|540139|gm1.7844_g
127	541	e-156	82	jgi|Dicsq1|72385|e_gw1.93.13.1
122	540	e-155	83	jgi|Dicsqu18370_1|665075|e_gw1.45.36.1
170	540	e-155	84	jgi|Dicsqu463_1|1021296|gm1.7704_g
83	540	e-155	85	jgi|Dicsqu464_1|935554|fgenesh1_kg.102_#_58_#_Locus7221v1rpkm19
254	538	e-155	86	jgi|Dicsqu18370_1|843352|MIX30610_11074_94
120	537	e-155	87	jgi|Dicsqu463_1|967109|fgenesh1_kg.258_#_53_#_Locus5792v1rpkm30
119	536	e-154	88	jgi|Dicsqu464_1|935562|fgenesh1_kg.102_#_66_#_Locus7221v1rpkm19
247	533	e-153	89	jgi|Dicsq1|94181|estExt_Genewise1.C_930024
246	533	e-153	90	jgi|Trave1|130760|e_gw1.10.841.1
148	532	e-153	91	jgi|Trave1|45128|gm1.4012_g
244	532	e-153	92	jgi|Tralac1|205625|CE205624_1029
245	531	e-153	93	jgi|Leisp1|1371152|gm1.5594_g
107	531	e-152	94	jgi|Traci1|1402223|e_gw1.15.531.1
269	530	e-152	95	jgi|Tragib1|1412667|fgenesh1_pm.40_#_57
89	529	e-152	96	jgi|Trabet1|826979|fgenesh1_kg.21_#_762_#_TRINITY_DN4756_c0_g1_
126	528	e-152	97	jgi|Tralj1|1037740|fgenesh1_pm.46_#_21
60	528	e-152	98	jgi|Pycco1|1468281|gm1.5790_g
149	527	e-151	99	jgi|Pycpun1|508212|fgenesh1_pg.13_#_60
172	527	e-151	100	jgi|Tramey1|914922|e_gw1.11.457.1

78	527	e-151	101	jgi|Pyccin1|1043044|fgenesh1_pm.32_#_65
261	526	e-151	102	jgi|Tramax1|1073440|gm1.413_g
69	525	e-151	103	jgi|Pycco1662_1|60791|CE60790_3985
248	525	e-151	104	jgi|Artel1|806710|fgenesh1_kg.13_#_28_#_Locus2015v1rpkm83.20
270	524	e-151	105	jgi|Artele1122_1|650705|MIX32502_84_36
131	524	e-150	106	jgi|Rhives1|3443|genemark-NODE_21236_length_42204_cov_51%252E1
85	523	e-150	107	jgi|Polbr1|1454895|fgenesh1_pm.17_#_33
84	523	e-150	108	jgi|Polbr1|1501025|MIX9741_377_27
108	522	e-150	109	jgi|Hexnit1|1217413|fgenesh1_pm.3_#_379
289	520	e-149	110	jgi|Earsca1|801067|gm1.12137_g
77	520	e-149	111	jgi|Fomfom1|1363762|gm1.1556_g
82	520	e-149	112	jgi|Polar1|521854|estExt_Genewise1.C_1740023
287	519	e-149	113	jgi|Polbr1|1363373|e_gw1.115.31.1
76	517	e-148	114	jgi|Polar1|498992|e_gw1.455.14.1
113	516	e-148	115	jgi|Polbr1|184586|CE184585_735
90	514	e-148	116	jgi|Hexnit1|1266762|gm1.2639_g
55	514	e-148	117	jgi|Fomfom1|1363757|gm1.1551_g
88	514	e-148	118	jgi|Earsca1|801019|gm1.12089_g
87	514	e-148	119	jgi|Earsca1|799697|gm1.10767_g
256	513	e-147	120	jgi|Earsca1|770306|fgenesh1_pm.13_#_369
112	512	e-147	121	jgi|Earsca1|626821|e_gw1.14.577.1
61	512	e-147	122	jgi|Polar1|655629|estExt_fgenesh1_pg.C_5030002
274	511	e-147	123	jgi|Polbr1|1561063|estExt_Genemark1.C_1100031
299	511	e-146	124	jgi|Earsca1|161568|CE161567_965
280	509	e-146	125	jgi|Fomfom1|1343990|estExt_Genewise1Plus.C_1_t60416
110	509	e-146	126	jgi|Polar1|50867|CE50866_1041
260	508	e-146	127	jgi|Polbr1|1363391|e_gw1.115.20.1
258	508	e-146	128	jgi|Dicsqu464_1|827640|e_gw1.102.67.1
257	508	e-146	129	jgi|Dicsqu463_1|992959|fgenesh1_pm.258_#_5

275	508	e-146	130	jgi|Dicsqu464_1|951341|fgenesh1_pm.102_#_14
73	507	e-145	131	jgi|Dicsqu18370_1|373931|CE373930_7707
74	507	e-145	132	jgi|Dicsq1|147086|fgenesh1_pm.13_#_95
124	506	e-145	133	jgi|Dicsq1|172004|gm1.7773_g
285	505	e-145	134	jgi|Dicsqu18370_1|706065|estExt_Genewise1.C_1720009
137	505	e-145	135	jgi|Dicsqu463_1|974740|fgenesh1_kg.631_#_1_#_Locus3772v1rpkm55.
132	504	e-145	136	jgi|Dicsqu464_1|938285|fgenesh1_kg.134_#_59_#_Locus5823v1rpkm29
86	504	e-144	137	jgi|Earsca1|801066|gm1.12136_g
259	503	e-144	138	jgi|Dicsqu18370_1|373775|CE373774_947
283	503	e-144	139	jgi|Dicsq1|72391|e_gw1.93.9.1
80	503	e-144	140	jgi|Dicsqu463_1|1045640|MIX20831_915_32
68	503	e-144	141	jgi|Dicsq1|94627|estExt_Genewise1.C_1180011
109	502	e-144	142	jgi|Lenti6_1|581782|fgenesh1_kg.85_#_2_#_Locus7014v1rpkm12.86
282	502	e-144	143	jgi|Lenti7_1|540886|fgenesh1_kg.70_#_5_#_Locus10473v1rpkm2.88
304	501	e-144	144	jgi|Sisbr1|586078|fgenesh1_kg.66_#_6_#_Locus5591v1rpkm22.10
250	501	e-144	145	jgi|Lenti6_1|658665|estExt_Genemark1.C_910014
249	501	e-144	146	jgi|Lenti7_1|538108|fgenesh1_kg.30_#_6_#_Locus7399v1rpkm10.51
277	501	e-144	147	jgi|Sisbr1|585400|fgenesh1_kg.48_#_48_#_Locus5591v1rpkm22.10
75	501	e-143	148	jgi|Hexnit1|1160509|fgenesh1_kg.5_#_112_#_TRINITY_DN3552_c1_g1_
262	499	e-143	149	jgi|Earsca1|162544|CE162543_209
295	499	e-143	150	jgi|Lenti6_1|581800|fgenesh1_kg.85_#_20_#_Locus7488v1rpkm10.32
94	499	e-143	151	jgi|Lenti7_1|540902|fgenesh1_kg.70_#_21_#_Locus7399v1rpkm10.51
306	499	e-143	152	jgi|Sisbr1|586093|fgenesh1_kg.66_#_21_#_Locus5591v1rpkm22.10
121	498	e-143	153	jgi|Polsqu1|829759|estExt_Genemark1.C_480067
279	497	e-142	154	jgi|Lenti7_1|572566|gm1.8370_g
290	497	e-142	155	jgi|Sisbr1|627566|gm1.8239_g
301	497	e-142	156	jgi|Lenti7_1|489422|estExt_Genewise1.C_190148
96	496	e-142	157	jgi|Polbr1|1506430|MIX15146_586_20
305	496	e-142	158	jgi|Sisbr1|544206|estExt_Genewise1.C_170201

302	496	e-142	159	jgi|Polsqu1|834295|estExt_Genemark1.C_1970014
307	496	e-142	160	jgi|Lenti6_1|578126|fgenesh1_kg.33_#_59_#_Locus7286v1rpkm11.29
296	495	e-142	161	jgi|Polsqu1|689230|fgenesh1_kg.927_#_2_#_TRINITY_DN13709_c0_g3_
303	495	e-142	162	jgi|Fomfom1|1363759|gm1.1553_g
255	495	e-142	163	jgi|Polsqu1|676477|fgenesh1_kg.308_#_4_#_TRINITY_DN13709_c0_g3_
97	494	e-142	164	jgi|Lenti6_1|581802|fgenesh1_kg.85_#_22_#_Locus4085v1rpkm37.01
128	493	e-141	165	jgi|Lenti7_1|540912|fgenesh1_kg.70_#_31_#_Locus4424v1rpkm31.63
130	491	e-141	166	jgi|Sisbr1|586099|fgenesh1_kg.66_#_27_#_Locus7819v1rpkm9.02
129	491	e-141	167	jgi|Polbr1|1500065|MIX8781_4600_46
81	491	e-140	168	jgi|Hexnit1|1146372|fgenesh1_kg.3_#_1593_#_TRINITY_DN1931_c0_g1
284	490	e-140	169	jgi|Earsca1|639881|estExt_Genewise1.C_1_t70018
66	489	e-140	170	jgi|Polar1|505708|e_gw1.1106.2.1
182	489	e-140	171	jgi|Polbr1|1487827|gm1.11408_g
286	488	e-140	172	jgi|Polar1|531655|estExt_Genewise1.C_6280007
288	486	e-139	173	jgi|Polar1|521853|estExt_Genewise1.C_1740022
298	486	e-139	174	jgi|Earsca1|162226|CE162225_1265
292	483	e-138	175	jgi|Dicsqu18370_1|696349|estExt_Genewise1.C_450102
300	483	e-138	176	jgi|Dicsqu463_1|967115|fgenesh1_kg.258_#_59_#_Locus10482v1rpkm6
79	481	e-138	177	jgi|Dicsqu464_1|935569|fgenesh1_kg.102_#_73_#_Locus3504v1rpkm59
311	479	e-137	178	jgi|Dicsq1|164054|estExt_fgenesh1_pg.C_930009
310	479	e-137	179	jgi|Earsca1|683000|estExt_Genewise1Plus.C_17_t20107
291	478	e-137	180	jgi|Polbr1|1480930|gm1.4511_g
276	475	e-136	181	jgi|Fomfom1|1233304|fgenesh1_kg.1_#_10316_#_TRINITY_DN5777_c0_
264	475	e-136	182	jgi|Earsca1|262364|CE262363_3037
309	474	e-135	183	jgi|Polar1|652223|estExt_fgenesh1_pg.C_1210011
273	473	e-135	184	jgi|Lenti6_1|527996|estExt_Genewise1.C_230015
312	472	e-135	185	jgi|Lenti7_1|510889|estExt_Genewise1Plus.C_180357
263	471	e-135	186	jgi|Polsqu1|816847|estExt_Genewise1Plus.C_1840030
265	471	e-134	187	jgi|Sisbr1|582002|fgenesh1_kg.19_#_12_#_Locus8995v1rpkm5.22

308	471	e-134	188	jgi|Polbr1|1401994|fgenesh1_kg.19_#_14_#_Locus7266v1rpkm14.58
95	470	e-134	189	jgi|Polar1|664247|estExt_Genemark1.C_2700006
313	470	e-134	190	jgi|Polbr1|1401717|fgenesh1_kg.17_#_218_#_Locus8255v1rpkm9.99
267	470	e-134	191	jgi|Polar1|665466|estExt_Genemark1.C_3880010
65	464	e-133	192	jgi|Lenti6_1|552293|estExt_Genewise1Plus.C_330049
47	464	e-133	193	jgi|Polar1|668252|estExt_Genemark1.C_12380002
281	464	e-132	194	jgi|Armosto1|262563|mRNA_AROS_05965_AROS_05965
34	464	e-132	195	jgi|Clapy1|1913257|gm1.3000_g
49	463	e-132	196	jgi|Lacqui1|1804036|gm1.10497_g
293	463	e-132	197	jgi|Scysp1_1|1357562|fgenesh1_kg.10_#_75_#_Locus16315v3rpkm2.64
266	461	e-132	198	jgi|Phlcen1|8958|scaffold_2756.3
46	461	e-132	199	jgi|Clibor1|1197786|fgenesh1_kg.12_#_558_#_TRINITY_DN6225_c0_g4_
44	461	e-132	200	jgi|Cytmel1|1284143|e_gw1.178.7.1
42	458	e-131	201	jgi|Hydfim1|986302|fgenesh1_pm.21_#_30
212	457	e-130	202	jgi|Irplac1|1595468|gm1.9138_g
21	457	e-130	203	jgi|Cytmel1|1406248|fgenesh1_pm.68_#_6
43	457	e-130	204	jgi|Irplac1|1595456|gm1.9126_g
45	456	e-130	205	jgi|Panru1|1664624|fgenesh1_kg.84_#_44_#_Locus2489v1rpkm66.46
30	456	e-130	206	jgi|Phlcen1|13562|scaffold_967.15
39	456	e-130	207	jgi|Phlcen1|13559|scaffold_967.12
48	456	e-130	208	jgi|Xerba1|1485051|gm1.5292_g
125	455	e-130	209	jgi|Boled1|909694|estExt_Genewise1Plus.C_4_t20194
32	455	e-130	210	jgi|Leumo1|1005994|e_gw1.00033.92.1
104	455	e-130	211	jgi|Conol1|919316|fgenesh1_pm.38_#_30
209	454	e-130	212	jgi|Pyccin1|1039701|fgenesh1_pm.7_#_185
24	454	e-130	213	jgi|Paxam1|966266|fgenesh1_kg.28_#_55_#_Locus9771v1rpkm13.15
230	454	e-129	214	jgi|Gyrli1|796093|fgenesh1_pm.14_#_124
53	454	e-129	215	jgi|Fibsp1|889927|fgenesh1_pg.56_#_70
29	454	e-129	216	jgi|Fibsp1|743454|e_gw1.82.162.1

35	452	e-129	217	jgi|Fibsp1|923026|estExt_fgenesh1_pm.C_3120003
37	452	e-129	218	jgi|Fibsp1|779072|estExt_Genewise1.C_220025
36	452	e-129	219	jgi|Fibsp1|1051510|estExt_Genemark1.C_2070036
106	450	e-128	220	jgi|Thega1|3184669|gm1.2733_g
5	449	e-128	221	jgi|Paxru2|31013|Paxru1.fgenesh1_pm.62_#_8
33	449	e-128	222	jgi|Suilu3|24266|Suilu1.fgenesh1_pm.129_#_13
51	448	e-128	223	jgi|Cersu1|119768|estExt_fgenesh1_kg.C_290013
294	448	e-128	224	jgi|Suitom1|746520|fgenesh1_pm.11_#_71
31	447	e-127	225	jgi|Suigr1|580326|CE580325_2365
200	447	e-127	226	jgi|Suidec1|1093418|fgenesh1_kg.15_#_127_#_Locus9003v1rpkm11.04
278	447	e-127	227	jgi|Denbi1|815498|fgenesh1_pm.4_#_20
297	447	e-127	228	jgi|Suipic1|1478630|gm1.2487_g
213	446	e-127	229	jgi|Hexnit1|1268939|gm1.4816_g
15	446	e-127	230	jgi|Rhisa1|731579|e_gw1.86.88.1
210	444	e-127	231	jgi|Rhivi1|681821|e_gw1.22.70.1
38	444	e-127	232	jgi|Pisti1|991388|fgenesh1_kg.1_#_205_#_Locus3709v1rpkm55.36
232	444	e-126	233	jgi|Pismi1|551133|CE426681_14791
221	444	e-126	234	jgi|Sclci1|1219887|fgenesh1_kg.105_#_5_#_Locus4318v1rpkm35.56
105	444	e-126	235	jgi|Plicr1|432908|CE251633_8389
100	443	e-126	236	jgi|Anobom1|1218668|e_gw1.230.7.1
208	443	e-126	237	jgi|Gyman1|804697|e_gw1.2.217.1
23	443	e-126	238	jgi|Suiame1|1052513|MIX32399_696_33
18	442	e-126	239	jgi|Plicr1|52981|fgenesh1_pm.6_#_209
22	442	e-126	240	jgi|Polbr1|1554465|estExt_Genemark1.C_130187
20	442	e-126	241	jgi|Polar1|519317|estExt_Genewise1.C_1210033
201	442	e-126	242	jgi|Polar1|603200|gm1.10163_g
99	441	e-126	243	jgi|Polbr1|1411615|fgenesh1_kg.118_#_36_#_Locus7271v1rpkm14.54
40	441	e-125	244	jgi|Polar1|519322|estExt_Genewise1.C_1210038
50	441	e-125	245	jgi|Polbr1|1400732|fgenesh1_kg.13_#_277_#_Locus4005v1rpkm39.25

52	440	e-125	246	jgi|Lenti6_1|611133|gm1.6018_g
229	440	e-125	247	jgi|Lenti7_1|390492|CE390491_458
14	439	e-125	248	jgi|Polar1|196845|CE196844_3694
231	438	e-125	249	jgi|Lenti6_1|586062|fgenesh1_pm.16_#_60
92	437	e-124	250	jgi|Lenti7_1|545110|fgenesh1_pm.9_#_56
203	436	e-124	251	jgi|Lenti6_1|547581|estExt_Genewise1Plus.C_160214
17	436	e-124	252	jgi|Lenti7_1|533921|fgenesh1_kg.9_#_130_#_Locus5292v1rpkm23.53
198	436	e-124	253	jgi|Sisbr1|577407|fgenesh1_kg.6_#_311_#_Locus8114v1rpkm7.82
199	436	e-124	254	jgi|Polar1|667894|estExt_Genemark1.C_9200003
41	435	e-124	255	jgi|Polbr1|1455204|fgenesh1_pm.20_#_1
9	434	e-124	256	jgi|Dicsqu18370_1|762016|fgenesh1_kg.57_#_118_#_Locus11179v1rpk
233	434	e-124	257	jgi|Dicsqu463_1|903800|estExt_Genewise1.C_4460006
236	434	e-123	258	jgi|Dicsqu464_1|887949|estExt_Genewise1Plus.C_1340006
214	434	e-123	259	jgi|Artele1122_1|246774|CE246773_339
28	434	e-123	260	jgi|Fomfom1|130388|CE130387_124
27	434	e-123	261	jgi|Earsca1|184441|CE184440_1205
26	434	e-123	262	jgi|Dicsq1|156277|estExt_fgenesh1_pm.C_280013
25	434	e-123	263	jgi|Polsqu1|708683|fgenesh1_pm.56_#_8
6	432	e-123	264	jgi|Lenti6_1|581076|fgenesh1_kg.66_#_42_#_Locus8502v1rpkm6.30
217	432	e-123	265	jgi|Lenti7_1|548440|fgenesh1_pm.57_#_9
98	431	e-123	266	jgi|Sisbr1|640151|MIX7816_141_38
202	431	e-122	267	jgi|Trapol1|1218738|fgenesh1_pm.9_#_230
234	431	e-122	268	jgi|Sisbr1|571658|estExt_Genewise1Plus.C_660043
93	430	e-122	269	jgi|Polsqu1|834477|estExt_Genemark1.C_2130002
204	429	e-122	270	jgi|Polbr1|1422973|fgenesh1_pg.126_#_11
12	427	e-121	271	jgi|Polsqu1|181995|CE181994_2271
216	427	e-121	272	jgi|Polsqu1|707000|fgenesh1_pm.22_#_3
215	427	e-121	273	jgi|Trave1|51005|gm1.9889_g
111	427	e-121	274	jgi|Traci1|116365|CE116364_5445

102	427	e-121	275	jgi|Tralj1|559700|CE559699_1981
4	425	e-121	276	jgi|Trabet1|922101|MIX14000_10_17
11	424	e-120	277	jgi|Traci1|268679|CE268678_1423
3	423	e-120	278	jgi|Trapol1|352087|CE352086_1039
56	422	e-120	279	jgi|Tramax1|1065145|fgenesh1_pm.1_#_36
10	421	e-119	280	jgi|Leisp1|1369699|gm1.4141_g
57	421	e-119	281	jgi|Tragib1|1392952|fgenesh1_kg.40_#_670_#_TRINITY_DN4393_c4_g2
59	418	e-119	282	jgi|Pyccin1|1041334|fgenesh1_pm.17_#_35
58	418	e-119	283	jgi|Polar1|667965|estExt_Genemark1.C_9660001
103	418	e-119	284	jgi|Pycsa1|1595909|fgenesh1_kg.sc_7180000650843_#_64_#_Locus943
223	417	e-118	285	jgi|Pycco1662_1|864896|estExt_fgenesh1_pg.C_40068
7	417	e-118	286	jgi|Tralac1|748415|fgenesh1_pm.18_#_114
222	417	e-118	287	jgi|Artele1122_1|495741|fgenesh1_pg.45_#_14
219	417	e-118	288	jgi|Tramen1|1044824|fgenesh1_pm.12_#_77
226	416	e-118	289	jgi|Artel1|812991|fgenesh1_kg.54_#_104_#_Locus4343v1rpkm35.12
218	416	e-118	290	jgi|Pycsa1|1754665|estExt_Genemark1.C_sc_71800006507350015
91	416	e-118	291	jgi|Pycci1|2784|scf184791.g34
101	415	e-118	292	jgi|Pycci1|4037|scf184844.g119
19	414	e-117	293	jgi|Pycco1|1362943|e_gw1.9.574.1
8	413	e-117	294	jgi|Pycco1662_1|872263|gm1.814_g
235	412	e-117	295	jgi|Trave1|58095|estExt_fgenesh1_pm.C_5_t10054
16	412	e-117	296	jgi|Tragib1|694241|CE694240_16222
2	411	e-116	297	jgi|Trabet1|477754|CE477753_479
1	409	e-116	298	jgi|Lenti6_1|628086|MIX9889_14_24
211	408	e-115	299	jgi|Tramey1|1003781|fgenesh1_pm.18_#_134
13	406	e-115	300	jgi|Pycco1662_1|432733|CE432732_1267
220	406	e-115	301	jgi|Pycpun1|540945|gm1.8650_g
207	405	e-115	302	jgi|Pycsa1|1754664|estExt_Genemark1.C_sc_71800006507350014
224	404	e-114	303	jgi|Pycco1662_1|816086|estExt_Genewise1.C_650085

228	403	e-114	304	jgi|Pycco1|1461855|estExt_fgenesh1_pg.C_640034
225	402	e-114	305	jgi|Pyccin1|168386|CE168385_664
205	400	e-113	306	jgi|Pycco1|1450696|estExt_fgenesh1_pm.C_90107
237	400	e-113	307	jgi|Pyccin1|1049319|gm1.3862_g
239	392	e-111	308	jgi|Earsca1|604737|e_gw1.1.2281.1
227	387	e-109	309	jgi|Pycci1|4039|scf184844.g121
206	382	e-108	310	jgi|Pycci1|4038|scf184844.g120
195	372	e-105	311	jgi|Pycsa1|1672486|gm1.2126_g
238	372	e-105	312	jgi|Pycco1|1292875|CE1292874_4946
196	370	e-104	313	jgi|Pyccin1|1050304|gm1.4847_g
272	348	6,00E-98		
194	342	7,00E-96		
54	335	1,00E-93		
197	329	4,00E-92		

CYP5035S7-similar CYP5035 sequences sorted by subfamilies

	seq ID	species	best hit	%ID	aln length
1	jgi|Phaca1|153972|estExt_Genewise1P	Phanerochaete carnosa HHB-10118-Sp v1.0	CYP5035A_Phanerochaete_carnosa	100	524
2	jgi|Phaca1|131233|estExt_Genewise1.(	Phanerochaete carnosa HHB-10118-Sp v1.0	CYP5035A_Phanerochaete_carnosa	44,51	519
3	jgi|Clibor1|119449|CE119448_2934	Climacocystis borealis CliBor001 v1.0	CYP5035A10 Phlebia brevispora	57,82	486
4	jgi|Irplac1|743245|CE743244_3999	Irpex lacteus CCBAS Fr. 238 617/93 v1.0	CYP5035A10 Phlebia brevispora	53,61	485
5	jgi|Irplac1|1640241|MIX38339_784_26	Irpex lacteus CCBAS Fr. 238 617/93 v1.0	CYP5035A11 Phlebia brevispora	54,84	547
6	jgi|Abobie1|721434|e_gw1.24.75.1	Abortiporus biennis CIRM-BRFM1778 v1	CYP5035A11 Phlebia brevispora	54,1	549
7	jgi|Panru1|1112951|CE1112950_7139	Panus rudis PR-1116 ss-1 v1.0	CYP5035A11 Phlebia brevispora	51,47	544
8	jgi|Panru1|1251950|CE1251949_2310	Panus rudis PR-1116 ss-1 v1.0	CYP5035A11 Phlebia brevispora	50,83	545
9	jgi|Cytmel1|1423468|gm1.13794_g	Cytidiella melzeri FP 102339 v1.0	CYP5035A11 Phlebia brevispora	49,91	553
10	jgi|Suibr2|843826|Suibr1.fgenesh1_pm	Suillus brevipes Sb2 v2.0	CYP5035B	100	561
11	jgi|Obbri1|890182|estExt_Genemark1.(	Obba rivulosa 3A-2 v1.0	CYP5035B	85,41	555
12	jgi|Spalat1|479667|CE479666_4080	Sparassis latifolia CCMJ1100 v1.0	CYP5035B	55,07	552
13	jgi|Spalat1|746579|fgenesh1_pg.6_#_5	Sparassis latifolia CCMJ1100 v1.0	CYP5035B	53,99	552
14	jgi|Trace1|1049863|CE1049862_12876	Trametopsis cervina CIRM-BRFM 1824 v1.0	CYP5035D2 Phlebiopsis	58,78	541
15	jgi|Trace1|1342868|fgenesh1_pg.4_#_4	Trametopsis cervina CIRM-BRFM 1824 v1.0	CYP5035D2 Phlebiopsis	58,7	540
16	jgi|Trace1|1354516|fgenesh1_kg.6_#_1	Trametopsis cervina CIRM-BRFM 1824 v1.0	CYP5035D2 Phlebiopsis	58,12	554
17	jgi|Abobie1|826912|MIX14629_1887_3	Abortiporus biennis CIRM-BRFM1778 v1	CYP5035D3 Bjerkandera adusta	62,09	517
18	jgi|Cytmel1|1418953|gm1.9279_g	Cytidiella melzeri FP 102339 v1.0	CYP5035D3 Bjerkandera adusta	61,85	540
19	jgi|Trace1|1409937|fgenesh1_pm.40_#	Trametopsis cervina CIRM-BRFM 1824 v1.0	CYP5035D3 Bjerkandera adusta	57,01	542
20	jgi|Dicsqu18370_1|806887|gm1.5849_	Dichomitus squalens OM18370.1 v1.0	CYP5035G1 Ganoderma lucidum	78	622
21	jgi|Dicsqu464_1|919019|fgenesh1_kg.1	Dichomitus squalens CBS464.89 v1.0	CYP5035G1 Ganoderma lucidum GL(	81	598
22	jgi|Dicsqu463_1|988899|fgenesh1_pm.	Dichomitus squalens CBS463.89 v1.0	CYP5035G1 Ganoderma lucidum GL(	77	622
23	jgi|Dicsq1|179419|estExt_Genemark1.(	Dichomitus squalens LYAD-421 SS1 v1.0	CYP5035G1 Ganoderma lucidum GL(	77	622
24	jgi|Earsca1|733523|fgenesh1_kg.9_#_5	Earliella scabrosa CIRM-BRFM 1817 v1.0	CYP5035G1_Ganoderma_sinense	73	563
25	jgi|Dicsq1|151582|estExt_fgenesh1_pm	Dichomitus squalens LYAD-421 SS1 v1.0	CYP5035H1_Ganoderma_sinense	80,55	550
26	jgi|Dicsqu18370_1|660324|e_gw1.25.1	Dichomitus squalens OM18370.1 v1.0	CYP5035H1_Ganoderma_sinense	80,55	550
27	jgi|Dicsqu463_1|993380|fgenesh1_pm.	Dichomitus squalens CBS463.89 v1.0	CYP5035H1_Ganoderma_sinense	80,55	550
28	jgi|Dicsqu464_1|918682|fgenesh1_kg.1	Dichomitus squalens CBS464.89 v1.0	CYP5035H1_Ganoderma_sinense	80,55	550

29	jgi|Polbr1|1481810|gm1.5391_g	Polyporus brumalis BRFM 1820 v1.0	CYP5035H2_Polyporus brumalis	100	556
30	jgi|Polar1|665169|estExt_Genemark1.C	Polyporus arcularius v1.0	CYP5035H2_Polyporus_arcularius	100	556
31	jgi|Earsca1|728492|fgenesh1_kg.7_#_1	Earliella scabrosa CIRM-BRFM 1817 v1.0	CYP5035H2_Polyporus_arcularius	83,3	545
32	jgi|Fomfom1|424094|CE424093_631	Fomes fomentarius CIRM-BRFM 1821 v1.0	CYP5035H2_Polyporus_arcularius	81,97	549
33	jgi|Polsqu1|24110|CE24109_7285	Polyporus squamosus CCBS 676 v1.0	CYP5035H3_Polyporus squamosus	100	556
34	jgi|Hexnit1|1215331|fgenesh1_pm.1_#	Hexagonia nitida CIRM-BRFM 1802 v1.0	CYP5035H3_Polyporus squamosus	82	550
35	jgi|Lenti6_1|578269|fgenesh1_kg.34_#	Lentinus tigrinus ALCF2SS1-6 v1.0	CYP5035H4_Lentinus tigrinus	100	558
36	jgi|Lenti7_1|564891|gm1.695_g	Lentinus tigrinus ALCF2SS1-7 v1.0	CYP5035H4_Lentinus tigrinus	99,64	558
37	jgi|Sisbr1|574375|fgenesh1_kg.2_#_75	Lentinus tigrinus v1.0	CYP5035H4_Lentinus tigrinus	99,64	558
38	jgi|Trave1|41578|gm1.462_g	Trametes versicolor v1.0	CYP5035H5_Trametes_versicolor	100	554
39	jgi|Trapol1|105914|CE105913_5115	Trametes polyzona CIRM-BRFM 1798 v1.0	CYP5035H5_Trametes_versicolor	87,18	554
40	jgi|Traci1|1521520|gm1.6319_g	Trametopsis cervina CIRM-BRFM 1824 v1.0	CYP5035H5_Trametes_versicolor	84,78	552
41	jgi|Tralj1|428191|CE428190_1838	Trametes ljubarskyi CIRM1659 v1.0	CYP5035H5_Trametes_versicolor	82,97	552
42	jgi|Pycsa1|1577749|e_gw1.718000065(	Pycnoporus sanguineus BRFM 1264 v1.0	CYP5035H5_Trametes_versicolor	81,74	553
43	jgi|Pycco1|1370331|e_gw1.30.134.1	Pycnoporus coccineus BRFM 310 v1.0	CYP5035H5_Trametes_versicolor	81,56	553
44	jgi|Artele1122_1|466036|e_gw1.2.699.	Artolenzites elegans CIRM-BRFM 1663 v1.	CYP5035H5_Trametes_versicolor	80,51	554
45	jgi|Pycpun1|308909|CE308908_3418	Pycnoporus puniceus CIRM-BRFM 1868 v1.0	CYP5035H5_Trametes_versicolor	80,25	552
46	jgi|Artel1|850992|fgenesh1_pm.18_#_4	Artolenzites elegans CIRM-BRFM 1663 v1.	CYP5035H5_Trametes_versicolor	80,14	554
47	jgi|Tramax1|1068035|fgenesh1_pm.5_3	Trametes maxima CIRM-BRFM 1813 v1.0	CYP5035H5_Trametes_versicolor	80,14	554
48	jgi|Pycco1662_1|876088|gm1.4639_g	Pycnoporus coccineus CIRM1662	CYP5035H5_Trametes_versicolor	79,78	554
49	jgi|Tramey1|997533|fgenesh1_pm.1_#	Trametes meyenii CIRM-BRFM 1810 v1.0	CYP5035H5_Trametes_versicolor	79,71	552
50	jgi|Leisp1|1318962|fgenesh1_kg.12_#_	Leiotrametes sp BRFM 1775 v1.0	CYP5035H5_Trametes_versicolor	79,68	556
51	jgi|Tramen1|1047947|fgenesh1_pm.42	Leiotrametes menziesii CIRM-BRFM 1781 v1.0	CYP5035H5_Trametes_versicolor	79,53	552
52	jgi|Tralac1|370287|CE370286_1031	Leiotrametes lactinea CIRM-BRFM 1664 v1.0	CYP5035H5_Trametes_versicolor	79,3	546
53	jgi|Paxin1|88877|e_gw1.305.4.1	Paxillus involutus ATCC 200175 v1.0	CYP5035H5_Trametes_versicolor	79,17	552
54	jgi|Pycci1|9212|scf185013.g82	Pycnoporus cinnabarinus BRFM 137	CYP5035H5_Trametes_versicolor	74,78	452
55	jgi|Dicsqu18370_1|765132|fgenesh1_k	Dichomitus squalens OM18370.1 v1.0	CYP5035J1_Ganoderma_sp._10597	72,74	565
56	jgi|Dicsqu18370_1|779171|fgenesh1_p	Dichomitus squalens OM18370.1 v1.0	CYP5035L1 Ganoderma lucidum GLC	61	481
57	jgi|Dicsq1|161810|estExt_fgenesh1_pg	Dichomitus squalens LYAD-421 SS1 v1.0	CYP5035L1 Ganoderma lucidum GLC	60	482
58	jgi|Dicsqu463_1|995233|fgenesh1_pm.	Dichomitus squalens CBS463.89 v1.0	CYP5035L1 Ganoderma lucidum GLC	60	481
59	jgi|Dicsqu464_1|953386|fgenesh1_pm.	Dichomitus squalens CBS464.89 v1.0	CYP5035L1 Ganoderma lucidum GLC	60	481
60	jgi|Sisbr1|623797|gm1.4470_g	Lentinus tigrinus v1.0	CYP5035N10_Polyporus	100	560

61	jgi|Polsqu1|835110|estExt_Genemark1	Polyporus squamosus CCBS 676 v1.0	CYP5035N11_Polyporus	100	550
62	jgi|Lenti6_1|581920|fgenesh1_kg.91_#	Lentinus tigrinus ALCF2SS1-6 v1.0	CYP5035N12_Lentinus	100	563
63	jgi|Lenti7_1|538117|fgenesh1_kg.30_#	Lentinus tigrinus ALCF2SS1-7 v1.0	CYP5035N12_Lentinus	100	563
64	jgi|Sisbr1|585391|fgenesh1_kg.48_#_3	Lentinus tigrinus v1.0	CYP5035N12_Lentinus	100	563
65	jgi|Pyccin1|1050305|gm1.4848_g	Pycnoporus cinnabarinus CIRM-BRFM 50 v1.0	CYP5035N12_Lentinus	51,75	570
66	jgi|Polsqu1|746845|gm1.13007_g	Polyporus squamosus CCBS 676 v1.0	CYP5035N13_Polyporus	100	517
67	jgi|Polsqu1|818645|estExt_Genewise1F	Polyporus squamosus CCBS 676 v1.0	CYP5035N14_Polyporus	100	564
68	jgi|Polsqu1|588169|e_gw1.213.21.1	Polyporus squamosus CCBS 676 v1.0	CYP5035N15_Polyporus	100	544
69	jgi|Polar1|667057|estExt_Genemark1.C	Polyporus arcularius v1.0	CYP5035N16_Polyporus	100	550
70	jgi|Lenti6_1|558432|estExt_Genewise1	Lentinus tigrinus ALCF2SS1-6 v1.0	CYP5035N17_Lentinus	100	544
71	jgi|Lenti7_1|468757|e_gw1.30.223.1	Lentinus tigrinus ALCF2SS1-7 v1.0	CYP5035N17_Lentinus	100	544
72	jgi|Sisbr1|570632|estExt_Genewise1Plu	Lentinus tigrinus v1.0	CYP5035N17_Lentinus	100	544
73	jgi|Trave1|60226|estExt_fgenesh1_pm.	Trametes versicolor v1.0	CYP5035N19_Trametes_versicolor	100	553
74	jgi|Trapol1|1067680|e_gw1.19.24.1	Trametes polyzona CIRM-BRFM 1798 v1.0	CYP5035N19_Trametes_versicolor	70,47	552
75	jgi|Tramey1|1003669|fgenesh1_pm.18	Trametes meyenii CIRM-BRFM 1810 v1.0	CYP5035N19_Trametes_versicolor	66,54	541
76	jgi|Tramax1|1055064|fgenesh1_kg.21_	Trametes maxima CIRM-BRFM 1813 v1.0	CYP5035N19_Trametes_versicolor	65,93	546
77	jgi|Leisp1|1345114|fgenesh1_pm.29_#	Leiotrametes sp BRFM 1775 v1.0	CYP5035N19_Trametes_versicolor	62,41	540
78	jgi|Tramen1|1064764|MIX4850_687_9	Leiotrametes menziesii CIRM-BRFM 1781 v1.0	CYP5035N19_Trametes_versicolor	62,39	553
79	jgi|Tramey1|1032777|MIX17440_258_	Trametes meyenii CIRM-BRFM 1810 v1.0	CYP5035N19_Trametes_versicolor	61,21	531
80	jgi|Tramax1|1024787|fgenesh1_kg.7_#	Trametes maxima CIRM-BRFM 1813 v1.0	CYP5035N19_Trametes_versicolor	60,18	550
81	jgi|Pycpun1|540139|gm1.7844_g	Pycnoporus puniceus CIRM-BRFM 1868 v1.0	CYP5035N19_Trametes_versicolor	59,2	549
82	jgi|Dicsq1|72385|e_gw1.93.13.1	Dichomitus squalens LYAD-421 SS1 v1.0	CYP5035N2_Ganoderma_sinense	73,33	540
83	jgi|Dicsqu18370_1|665075|e_gw1.45.3	Dichomitus squalens OM18370.1 v1.0	CYP5035N2_Ganoderma_sinense	73,1	554
84	jgi|Dicsqu463_1|1021296|gm1.7704_g	Dichomitus squalens CBS463.89 v1.0	CYP5035N2_Ganoderma_sinense	73,1	554
85	jgi|Dicsqu464_1|935554|fgenesh1_kg.1	Dichomitus squalens CBS464.89 v1.0	CYP5035N2_Ganoderma_sinense	73,1	554
86	jgi|Dicsqu18370_1|843352|MIX30610_	Dichomitus squalens OM18370.1 v1.0	CYP5035N2_Ganoderma_sinense	70,38	557
87	jgi|Dicsqu463_1|967109|fgenesh1_kg.2	Dichomitus squalens CBS463.89 v1.0	CYP5035N2_Ganoderma_sinense	70,02	557
88	jgi|Dicsqu464_1|935562|fgenesh1_kg.1	Dichomitus squalens CBS464.89 v1.0	CYP5035N2_Ganoderma_sinense	70,02	557
89	jgi|Dicsq1|94181|estExt_Genewise1.C_	Dichomitus squalens LYAD-421 SS1 v1.0	CYP5035N2_Ganoderma_sinense	69,84	557
90	jgi|Trave1|130760|e_gw1.10.841.1	Trametes versicolor v1.0	CYP5035N20_Trametes_versicolor	100	581
91	jgi|Trave1|45128|gm1.4012_g	Trametes versicolor v1.0	CYP5035N20_Trametes_versicolor	100	542
92	jgi|Tralac1|205625|CE205624_1029	Leiotrametes lactinea CIRM-BRFM 1664 v1.0	CYP5035N20_Trametes_versicolor	71,51	551

93	jgi|Leisp1|1371152|gm1.5594_g	Leiotrametes sp BRFM 1775 v1.0	CYP5035N20_Trametes_versicolor	71,14	551
94	jgi|Traci1|1402223|e_gw1.15.531.1	Trametopsis cervina CIRM-BRFM 1824 v1.0	CYP5035N20_Trametes_versicolor	70,56	540
95	jgi|Tragib1|1412667|fgenesh1_pm.40_	Trametes gibbosa CIRM-BRFM 1770 v1.0	CYP5035N20_Trametes_versicolor	70,43	531
96	jgi|Trabet1|826979|fgenesh1_kg.21_#_	Trametes betulina CIRM-BRFM 1801 v1.0	CYP5035N20_Trametes_versicolor	70,38	530
97	jgi|Tralj1|1037740|fgenesh1_pm.46_#_	Trametes ljubarskyi CIRM1659 v1.0	CYP5035N20_Trametes_versicolor	69,56	542
98	jgi|Pycco1|1468281|gm1.5790_g	Pycnoporus coccineus BRFM 310 v1.0	CYP5035N20_Trametes_versicolor	69,38	552
99	jgi|Pycpun1|508212|fgenesh1_pg.13_#	Pycnoporus puniceus CIRM-BRFM 1868 v1.0	CYP5035N20_Trametes_versicolor	69,23	546
100	jgi|Tramey1|914922|e_gw1.11.457.1	Trametes meyenii CIRM-BRFM 1810 v1.0	CYP5035N20_Trametes_versicolor	68,81	529
101	jgi|Pyccin1|1043044|fgenesh1_pm.32_	Pycnoporus cinnabarinus CIRM-BRFM 50 v1.0	CYP5035N20_Trametes_versicolor	68,39	560
102	jgi|Tramax1|1073440|gm1.413_g	Trametes maxima CIRM-BRFM 1813 v1.0	CYP5035N20_Trametes_versicolor	67,47	541
103	jgi|Pycco1662_1|60791|CE60790_3985	Pycnoporus coccineus CIRM1662	CYP5035N20_Trametes_versicolor	66,03	577
104	jgi|Artel1|806710|fgenesh1_kg.13_#_2	Artolenzites elegans CIRM-BRFM 1663 v1.	CYP5035N20_Trametes_versicolor	64,8	537
105	jgi|Artele1122_1|650705|MIX32502_8	Artolenzites elegans CIRM-BRFM 1663 v1.	CYP5035N20_Trametes_versicolor	63,25	536
106	jgi|Rhives1|3443|genemark-NODE_212	Rhizopogon vesiculosus Smith	CYP5035N20_Trametes_versicolor	60,79	556
107	jgi|Polbr1|1454895|fgenesh1_pm.17_#	Polyporus brumalis BRFM 1820 v1.0	CYP5035N5_Polyporus	100	565
108	jgi|Polbr1|1501025|MIX9741_377_27	Polyporus brumalis BRFM 1820 v1.0	CYP5035N5_Polyporus_arcularius	100	566
109	jgi|Hexnit1|1217413|fgenesh1_pm.3_#	Hexagonia nitida CIRM-BRFM 1802 v1.0	CYP5035N5_Polyporus_arcularius	64,75	556
110	jgi|Earsca1|801067|gm1.12137_g	Earliella scabrosa CIRM-BRFM 1817 v1.0	CYP5035N5_Polyporus_arcularius	64,23	562
111	jgi|Fomfom1|1363762|gm1.1556_g	Fomes fomentarius CIRM-BRFM 1821 v1.0	CYP5035N5_Polyporus_arcularius	59,18	561
112	jgi|Polar1|521854|estExt_Genewise1.C	Polyporus arcularius v1.0	CYP5035N6_Polyporus_arcularius	100	538
113	jgi|Polbr1|1363373|e_gw1.115.31.1	Polyporus brumalis BRFM 1820 v1.0	CYP5035N6v2_Polyporus	100	552
114	jgi|Polar1|498992|e_gw1.455.14.1	Polyporus arcularius v1.0	CYP5035N7_Polyporus	100	564
115	jgi|Polbr1|184586|CE184585_735	Polyporus brumalis BRFM 1820 v1.0	CYP5035N7_Polyporus	97,7	564
116	jgi|Hexnit1|1266762|gm1.2639_g	Hexagonia nitida CIRM-BRFM 1802 v1.0	CYP5035N7_Polyporus	70,97	558
117	jgi|Fomfom1|1363757|gm1.1551_g	Fomes fomentarius CIRM-BRFM 1821 v1.0	CYP5035N7_Polyporus	69,82	560
118	jgi|Earsca1|801019|gm1.12089_g	Earliella scabrosa CIRM-BRFM 1817 v1.0	CYP5035N7_Polyporus	66,9	565
119	jgi|Earsca1|799697|gm1.10767_g	Earliella scabrosa CIRM-BRFM 1817 v1.0	CYP5035N7_Polyporus	59,82	555
120	jgi|Earsca1|770306|fgenesh1_pm.13_#	Earliella scabrosa CIRM-BRFM 1817 v1.0	CYP5035N7_Polyporus arcularius	49	573
121	jgi|Earsca1|626821|e_gw1.14.577.1	Earliella scabrosa CIRM-BRFM 1817 v1.0	CYP5035N7_Polyporus arcularius	47	569
122	jgi|Polar1|655629|estExt_fgenesh1_pg.	Polyporus arcularius v1.0	CYP5035N8_Polyporus	100	564
123	jgi|Polbr1|1561063|estExt_Genemark1	Polyporus brumalis BRFM 1820 v1.0	CYP5035N8_Polyporus	99,47	564
124	jgi|Earsca1|161568|CE161567_965	Earliella scabrosa CIRM-BRFM 1817 v1.0	CYP5035N8_Polyporus	54,8	562

125	jgi|Fomfom1|1343990|estExt_Genewis	Fomes fomentarius CIRM-BRFM 1821 v1.0	CYP5035N8_Polyporus	51,83	573
126	jgi|Polar1|50867|CE50866_1041	Polyporus arcularius v1.0	CYP5035N9_Polyporus	100	613
127	jgi|Polbr1|1363391|e_gw1.115.20.1	Polyporus brumalis BRFM 1820 v1.0	CYP5035N9_Polyporus arcularius	94	543
128	jgi|Dicsqu464_1|827640|e_gw1.102.67	Dichomitus squalens CBS464.89 v1.0	CYP5035P1 Ganoderma	62,01	487
129	jgi|Dicsqu463_1|992959|fgenesh1_pm.	Dichomitus squalens CBS463.89 v1.0	CYP5035P1 Ganoderma	61,04	498
130	jgi|Dicsqu464_1|951341|fgenesh1_pm.	Dichomitus squalens CBS464.89 v1.0	CYP5035P1 Ganoderma	61,04	498
131	jgi|Dicsqu18370_1|373931|CE373930_	Dichomitus squalens OM18370.1 v1.0	CYP5035P1 Ganoderma	58	551
132	jgi|Dicsq1|147086|fgenesh1_pm.13_#_	Dichomitus squalens LYAD-421 SS1 v1.0	CYP5035Q1 Ganoderma	64,73	550
133	jgi|Dicsq1|172004|gm1.7773_g	Dichomitus squalens LYAD-421 SS1 v1.0	CYP5035Q1 Ganoderma	55,58	556
134	jgi|Dicsqu18370_1|706065|estExt_Gen	Dichomitus squalens OM18370.1 v1.0	CYP5035Q1 Ganoderma	55,58	556
135	jgi|Dicsqu463_1|974740|fgenesh1_kg.(	Dichomitus squalens CBS463.89 v1.0	CYP5035Q1 Ganoderma	55,58	556
136	jgi|Dicsqu464_1|938285|fgenesh1_kg.1	Dichomitus squalens CBS464.89 v1.0	CYP5035Q1 Ganoderma	55,58	556
137	jgi|Earsca1|801066|gm1.12136_g	Earliella scabrosa CIRM-BRFM 1817 v1.0	CYP5035Q1 Ganoderma lucidum GL(	47	578
138	jgi|Dicsqu18370_1|373775|CE373774_(	Dichomitus squalens OM18370.1 v1.0	CYP5035R1 Ganoderma	54,24	601
139	jgi|Dicsq1|72391|e_gw1.93.9.1	Dichomitus squalens LYAD-421 SS1 v1.0	CYP5035R1 Ganoderma	54,08	601
140	jgi|Dicsqu463_1|1045640|MIX20831_9	Dichomitus squalens CBS463.89 v1.0	CYP5035R1 Ganoderma	54,08	601
141	jgi|Dicsq1|94627|estExt_Genewise1.C_	Dichomitus squalens LYAD-421 SS1 v1.0	CYP5035R1 Ganoderma	53,91	601
142	jgi|Lenti6_1|581782|fgenesh1_kg.85_#	Lentinus tigrinus ALCF2SS1-6 v1.0	CYP5035S10_Lentinus	100	592
143	jgi|Lenti7_1|540886|fgenesh1_kg.70_#	Lentinus tigrinus ALCF2SS1-7 v1.0	CYP5035S10_Lentinus	99,83	590
144	jgi|Sisbr1|586078|fgenesh1_kg.66_#_6	Lentinus tigrinus v1.0	CYP5035S10_Lentinus	98,61	577
145	jgi|Lenti6_1|658665|estExt_Genemark:	Lentinus tigrinus ALCF2SS1-6 v1.0	CYP5035S11_Lentinus	100	614
146	jgi|Lenti7_1|538108|fgenesh1_kg.30_#	Lentinus tigrinus ALCF2SS1-7 v1.0	CYP5035S11_Lentinus	100	585
147	jgi|Sisbr1|585400|fgenesh1_kg.48_#_4	Lentinus tigrinus v1.0	CYP5035S11_Lentinus	99,66	585
148	jgi|Hexnit1|1160509|fgenesh1_kg.5_#_	Hexagonia nitida CIRM-BRFM 1802 v1.0	CYP5035S11_Lentinus	58,23	589
149	jgi|Earsca1|162544|CE162543_209	Earliella scabrosa CIRM-BRFM 1817 v1.0	CYP5035S11_Lentinus tigrinus	48	576
150	jgi|Lenti6_1|581800|fgenesh1_kg.85_#	Lentinus tigrinus ALCF2SS1-6 v1.0	CYP5035S12_Lentinus	100	594
151	jgi|Lenti7_1|540902|fgenesh1_kg.70_#	Lentinus tigrinus ALCF2SS1-7 v1.0	CYP5035S12_Lentinus	96,79	592
152	jgi|Sisbr1|586093|fgenesh1_kg.66_#_2	Lentinus tigrinus v1.0	CYP5035S12_Lentinus	95,61	592
153	jgi|Polsqu1|829759|estExt_Genemark1	Polyporus squamosus CCBS 676 v1.0	CYP5035S13_Polyporus	100	563
154	jgi|Lenti7_1|572566|gm1.8370_g	Lentinus tigrinus ALCF2SS1-7 v1.0	CYP5035S14_Lentinus	100	560
155	jgi|Sisbr1|627566|gm1.8239_g	Lentinus tigrinus v1.0	CYP5035S14_Lentinus	100	560
156	jgi|Lenti7_1|489422|estExt_Genewise1	Lentinus tigrinus ALCF2SS1-7 v1.0	CYP5035S15_Lentinus	100	560

157	jgi|Polbr1|1506430|MIX15146_586_20	Polyporus brumalis BRFM 1820 v1.0	CYP5035S15_Lentinus	100	560
158	jgi|Sisbr1|544206|estExt_Genewise1.C_	Lentinus tigrinus v1.0	CYP5035S15_Lentinus	100	560
159	jgi|Polsqu1|834295|estExt_Genemark1	Polyporus squamosus CCBS 676 v1.0	CYP5035S16_Polyporus	100	550
160	jgi|Lenti6_1|578126|fgenesh1_kg.33_#	Lentinus tigrinus ALCF2SS1-6 v1.0	CYP5035S17_Polyporus	100	538
161	jgi|Polsqu1|689230|fgenesh1_kg.927_#	Polyporus squamosus CCBS 676 v1.0	CYP5035S18_Polyporus	100	564
162	jgi|Fomfom1|1363759|gm1.1553_g	Fomes fomentarius CIRM-BRFM 1821 v1.0	CYP5035S18_Polyporus	65,26	567
163	jgi|Polsqu1|676477|fgenesh1_kg.308_#	Polyporus squamosus CCBS 676 v1.0	CYP5035S19_Polyporus	100	558
164	jgi|Lenti6_1|581802|fgenesh1_kg.85_#	Lentinus tigrinus ALCF2SS1-6 v1.0	CYP5035S21_Lentinus	100	573
165	jgi|Lenti7_1|540912|fgenesh1_kg.70_#	Lentinus tigrinus ALCF2SS1-7 v1.0	CYP5035S21_Lentinus	100	573
166	jgi|Sisbr1|586099|fgenesh1_kg.66_#_2	Lentinus tigrinus v1.0	CYP5035S21_Lentinus	99,65	573
167	jgi|Polbr1|1500065|MIX8781_4600_46	Polyporus brumalis BRFM 1820 v1.0	CYP5035S22_Polyporus	100	587
168	jgi|Hexnit1|1146372|fgenesh1_kg.3_#_	Hexagonia nitida CIRM-BRFM 1802 v1.0	CYP5035S22_Polyporus	57,27	578
169	jgi|Earsca1|639881|estExt_Genewise1.(	Earliella scabrosa CIRM-BRFM 1817 v1.0	CYP5035S22_Polyporus	55,67	582
170	jgi|Polar1|505708|e_gw1.1106.2.1	Polyporus arcularius v1.0	CYP5035S24_Polyporus	100	561
171	jgi|Polbr1|1487827|gm1.11408_g	Polyporus brumalis BRFM 1820 v1.0	CYP5035S24_Polyporus arcularius	89	556
172	jgi|Polar1|531655|estExt_Genewise1.C	Polyporus arcularius v1.0	CYP5035S25_Polyporus	100	580
173	jgi|Polar1|521853|estExt_Genewise1.C	Polyporus arcularius v1.0	CYP5035S26_Polyporus	100	560
174	jgi|Earsca1|162226|CE162225_1265	Earliella scabrosa CIRM-BRFM 1817 v1.0	CYP5035S26_Polyporus	58,73	550
175	jgi|Dicsqu18370_1|696349|estExt_Gen	Dichomitus squalens OM18370.1 v1.0	CYP5035S3_Ganoderma_sinense GS	74	554
176	jgi|Dicsqu463_1|967115|fgenesh1_kg.2	Dichomitus squalens CBS463.89 v1.0	CYP5035S3_Ganoderma_sinense GS	74	554
177	jgi|Dicsqu464_1|935569|fgenesh1_kg.1	Dichomitus squalens CBS464.89 v1.0	CYP5035S3_Ganoderma_sinense GS	74	554
178	jgi|Dicsq1|164054|estExt_fgenesh1_pg	Dichomitus squalens LYAD-421 SS1 v1.0	CYP5035S3_Ganoderma_sinense GS	73	554
179	jgi|Earsca1|683000|estExt_Genewise1F	Earliella scabrosa CIRM-BRFM 1817 v1.0	CYP5035S3_Ganoderma_sinense GS	56	587
180	jgi|Polbr1|1480930|gm1.4511_g	Polyporus brumalis BRFM 1820 v1.0	CYP5035S6_Polyporus	100	569
181	jgi|Fomfom1|1233304|fgenesh1_kg.1_	Fomes fomentarius CIRM-BRFM 1821 v1.0	CYP5035S6_Polyporus	57,8	564
182	jgi|Earsca1|262364|CE262363_3037	Earliella scabrosa CIRM-BRFM 1817 v1.0	CYP5035S6_Polyporus	46,55	580
183	jgi|Polar1|652223|estExt_fgenesh1_pg.	Polyporus arcularius v1.0	CYP5035S6_Polyporus_arcularius	100	569
184	jgi|Lenti6_1|527996|estExt_Genewise1	Lentinus tigrinus ALCF2SS1-6 v1.0	CYP5035S7_Lentinus	100	558
185	jgi|Lenti7_1|510889|estExt_Genewise1	Lentinus tigrinus ALCF2SS1-7 v1.0	CYP5035S7_Lentinus	100	558
186	jgi|Polsqu1|816847|estExt_Genewise1F	Polyporus squamosus CCBS 676 v1.0	CYP5035S7_Lentinus	100	558
187	jgi|Sisbr1|582002|fgenesh1_kg.19_#_1	Lentinus tigrinus v1.0	CYP5035S7_Lentinus	100	558
188	jgi|Polbr1|1401994|fgenesh1_kg.19_#_	Polyporus brumalis BRFM 1820 v1.0	CYP5035S7_Polyporus	100	562

189	jgi|Polar1|664247|estExt_Genemark1.C	Polyporus arcularius v1.0	CYP5035S7_Polyporus_arcularius	100	565
190	jgi|Polbr1|1401717|fgenesh1_kg.17_#_	Polyporus brumalis BRFM 1820 v1.0	CYP5035S8_Polyporus	100	568
191	jgi|Polar1|665466|estExt_Genemark1.C	Polyporus arcularius v1.0	CYP5035S8_Polyporus_arcularius	100	568
192	jgi|Lenti6_1|552293|estExt_Genewise1	Lentinus tigrinus ALCF2SS1-6 v1.0	CYP5035S9_Polyporus	100	590
193	jgi|Polar1|668252|estExt_Genemark1.C	Polyporus arcularius v1.0	CYP5035S9_Polyporus_arcularius	100	564
194	jgi|Armosto1|262563|mRNA_AROS_05	Armillaria ostoyae C18/9	CYP5035U4 Bjerkandera adusta	49,79	480
195	jgi|Clapy1|1913257|gm1.3000_g	Clavicorona pyxidata HHB10654 v1.0	CYP5035X1 Heterobasidion annosun	56,05	562
196	jgi|Lacqui1|1804036|gm1.10497_g	Lactarius quietus S23C v1.0	CYP5035X1 Heterobasidion annosun	53,02	530
197	jgi|Scysp1_1|1357562|fgenesh1_kg.10_	Scytinostroma sp. KUC9335 v1.0	CYP5035X1 Heterobasidion annosun	48,52	573
198	jgi|Phlcen1|8958|scaffold_2756.3	Phlebia centrifuga FBCC195	CYP5035Z1 Phlebia brevispora	61,51	530
199	jgi|Clibor1|1197786|fgenesh1_kg.12_#_	Climacocystis borealis CliBor001 v1.0	CYP5035Z1 Phlebia brevispora	56,25	544
200	jgi|Cytmel1|1284143|e_gw1.178.7.1	Cytidiella melzeri FP 102339 v1.0	CYP5035Z1 Phlebia brevispora	55,33	544
201	jgi|Hydfim1|986302|fgenesh1_pm.21_#	Hydnopolyporus fimbriatus CBS384.51 v1.0	CYP5035Z1 Phlebia brevispora	53,64	550
202	jgi|Irplac1|1595468|gm1.9138_g	Irpex lacteus CCBAS Fr. 238 617/93 v1.0	CYP5035Z1 Phlebia brevispora	53,64	550
203	jgi|Cytmel1|1406248|fgenesh1_pm.68_	Cytidiella melzeri FP 102339 v1.0	CYP5035Z1 Phlebia brevispora	53,28	548
204	jgi|Irplac1|1595456|gm1.9126_g	Irpex lacteus CCBAS Fr. 238 617/93 v1.0	CYP5035Z1 Phlebia brevispora	52,73	550
205	jgi|Panru1|1664624|fgenesh1_kg.84_#_	Panus rudis PR-1116 ss-1 v1.0	CYP5035Z1 Phlebia brevispora	51,92	547
206	jgi|Phlcen1|13562|scaffold_967.15	Phlebia centrifuga FBCC195	CYP5035AD1 Phlebia brevispora	60,53	451
207	jgi|Phlcen1|13559|scaffold_967.12	Phlebia centrifuga FBCC195	CYP5035AD1 Phlebia brevispora	59,71	489
208	jgi|Xerba1|1485051|gm1.5292_g	Xerocomus badius 84.06 v1.0	CYP5035AF1_Hydnomerulius_pinast	79,29	589
209	jgi|Boled1|909694|estExt_Genewise1Pl	Boletus edulis BED1 v4.0	CYP5035AF1_Hydnomerulius_pinast	77,97	581
210	jgi|Leumo1|1005994|e_gw1.00033.92.:	Leucogyrophana mollusca KUC20120723A-06 v1	CYP5035AF1_Hydnomerulius_pinast	71,6	581
211	jgi|Conol1|919316|fgenesh1_pm.38_#_	Coniophora olivacea MUCL 20566 v1.0	CYP5035AF1_Hydnomerulius_pinast	59,72	581
212	jgi|Pyccin1|1039701|fgenesh1_pm.7_#_	Pycnoporus cinnabarinus CIRM-BRFM 50 v1.0	CYP5035AF2_Paxillus_involutus_ATC	100	579
213	jgi|Paxam1|966266|fgenesh1_kg.28_#_	Paxillus ammoniavirescens Pou09.2 v1.0	CYP5035AF2_Paxillus_involutus_ATC	95,86	580
214	jgi|Gyrli1|796093|fgenesh1_pm.14_#_1	Gyrodon lividus BX v1.0	CYP5035AF2_Paxillus_involutus_ATC	86,2	558
215	jgi|Fibsp1|889927|fgenesh1_pg.56_#_7	Fibulorhizoctonia sp. CBS 109695 v1.0	CYP5035AF2_Paxillus_involutus_ATC	55,32	555
216	jgi|Fibsp1|743454|e_gw1.82.162.1	Fibulorhizoctonia sp. CBS 109695 v1.0	CYP5035AF2_Paxillus_involutus_ATC	54,95	555
217	jgi|Fibsp1|923026|estExt_fgenesh1_pm	Fibulorhizoctonia sp. CBS 109695 v1.0	CYP5035AF2_Paxillus_involutus_ATC	54,95	555
218	jgi|Fibsp1|779072|estExt_Genewise1.C	Fibulorhizoctonia sp. CBS 109695 v1.0	CYP5035AF2_Paxillus_involutus_ATC	54,61	542
219	jgi|Fibsp1|1051510|estExt_Genemark1	Fibulorhizoctonia sp. CBS 109695 v1.0	CYP5035AF2_Paxillus_involutus_ATC	54,48	558
220	jgi|Thega1|3184669|gm1.2733_g	Thelephora ganbajun P2 v1.0	CYP5035AF2_Paxillus_involutus_ATC	48,63	547

221	jgi|Paxru2|31013|Paxru1.fgenesh1_pm	Paxillus rubicundulus Ve08.2h10 v2.0	CYP5035AF3_Paxillus_rubicundulus_	100	580
222	jgi|Suilu3|24266|Suilu1.fgenesh1_pm.1	Suillus luteus UH-Slu-Lm8-n1 v3	CYP5035AF4_Suillus_luteus_UH-Slu-	100	559
223	jgi|Cersu1|119768|estExt_fgenesh1_kg	Ceriporiopsis (Gelatoporia) subvermispora B	CYP5035AF4_Suillus_luteus_UH-Slu-	96,96	559
224	jgi|Suitom1|746520|fgenesh1_pm.11_#	Suillus tomentosus FC115 v1.0	CYP5035AF4_Suillus_luteus_UH-Slu-	91,67	552
225	jgi|Suigr1|580326|CE580325_2365	Suillus granulatus EM37 v1.0	CYP5035AF4_Suillus_luteus_UH-Slu-	91,07	560
226	jgi|Suidec1|1093418|fgenesh1_kg.15_#	Suillus decipiens EM49 v1.0	CYP5035AF4_Suillus_luteus_UH-Slu-	90,36	560
227	jgi|Denbi1|815498|fgenesh1_pm.4_#_2	Dendrothele bispora CBS 962.96 v1.0	CYP5035AF4_Suillus_luteus_UH-Slu-	89,54	564
228	jgi|Suipic1|1478630|gm1.2487_g	Suillus pictus EM44 v1.0	CYP5035AF4_Suillus_luteus_UH-Slu-	87,99	566
229	jgi|Hexnit1|1268939|gm1.4816_g	Hexagonia nitida CIRM-BRFM 1802 v1.0	CYP5035AF4_Suillus_luteus_UH-Slu-	78,55	564
230	jgi|Rhisa1|731579|e_gw1.86.88.1	Rhizopogon salebrosus TDB-379 v1.0	CYP5035AF4_Suillus_luteus_UH-Slu-	78,05	565
231	jgi|Rhivi1|681821|e_gw1.22.70.1	Rhizopogon vinicolor AM-OR11-026 v1.0	CYP5035AF4_Suillus_luteus_UH-Slu-	77,27	572
232	jgi|Pisti1|991388|fgenesh1_kg.1_#_205	Pisolithus tinctorius Marx 270 v1.0	CYP5035AF5_Pisolithus_tinctorius_M	100	594
233	jgi|Pismi1|551133|CE426681_14791	Pisolithus microcarpus 441 v1.0	CYP5035AF6_Pisolithus_microcarpu	100	589
234	jgi|Sclci1|1219887|fgenesh1_kg.105_#_	Scleroderma citrinum Foug A v1.0	CYP5035AF7_Scleroderma_citrinum	100	585
235	jgi|Plicr1|432908|CE251633_8389	Plicaturopsis crispa v1.0	CYP5035AG1_Plicaturopsis_crispa_v	100	571
236	jgi|Anobom1|1218668|e_gw1.230.7.1	Anomoporia bombycina ATCC 64506 v1.0	CYP5035AG1_Plicaturopsis_crispa_v	62,39	561
237	jgi|Gyman1|804697|e_gw1.2.217.1	Gymnopus androsaceus JB14 v1.0	CYP5035AG2_Hebeloma_cylindrosp	47,39	536
238	jgi|Suiame1|1052513|MIX32399_696_3	Suillus americanus EM31 v1.0	CYP5035AG2_Hebeloma_cylindrosp	45,97	546
239	jgi|Plicr1|52981|fgenesh1_pm.6_#_209	Plicaturopsis crispa v1.0	CYP5035AG3_Plicaturopsis_crispa_v	100	662
240	jgi|Polbr1|1554465|estExt_Genemark1	Polyporus brumalis BRFM 1820 v1.0	CYP5035AU1_Polyporus	100	560
241	jgi|Polar1|519317|estExt_Genewise1.C	Polyporus arcularius v1.0	CYP5035AU1_Polyporus_arcularius	100	560
242	jgi|Polar1|603200|gm1.10163_g	Polyporus arcularius v1.0	CYP5035AU2_Polyporus	100	560
243	jgi|Polbr1|1411615|fgenesh1_kg.118_#	Polyporus brumalis BRFM 1820 v1.0	CYP5035AU2_Polyporus	95,54	560
244	jgi|Polar1|519322|estExt_Genewise1.C	Polyporus arcularius v1.0	CYP5035AU3_Polyporus	100	559
245	jgi|Polbr1|1400732|fgenesh1_kg.13_#_	Polyporus brumalis BRFM 1820 v1.0	CYP5035AU3_Polyporus	99,64	559
246	jgi|Lenti6_1|611133|gm1.6018_g	Lentinus tigrinus ALCF2SS1-6 v1.0	CYP5035AU5_Lentinus	100	559
247	jgi|Lenti7_1|390492|CE390491_458	Lentinus tigrinus ALCF2SS1-7 v1.0	CYP5035AU5_Lentinus	100	559
248	jgi|Polar1|196845|CE196844_3694	Polyporus arcularius v1.0	CYP5035AU5_Lentinus tigrinus	66	562
249	jgi|Lenti6_1|586062|fgenesh1_pm.16_#	Lentinus tigrinus ALCF2SS1-6 v1.0	CYP5035AU6_Lentinus	100	556
250	jgi|Lenti7_1|545110|fgenesh1_pm.9_#_	Lentinus tigrinus ALCF2SS1-7 v1.0	CYP5035AU6_Lentinus	100	556
251	jgi|Lenti6_1|547581|estExt_Genewise1	Lentinus tigrinus ALCF2SS1-6 v1.0	CYP5035AU7_Lentinus	100	559
252	jgi|Lenti7_1|533921|fgenesh1_kg.9_#_	Lentinus tigrinus ALCF2SS1-7 v1.0	CYP5035AU7_Lentinus	100	559

253	jgi|Sisbr1|577407|fgenesh1_kg.6_#_31	Lentinus tigrinus v1.0	CYP5035AU7_Lentinus	85,69	559
254	jgi|Polar1|667894|estExt_Genemark1.C	Polyporus arcularius v1.0	CYP5035AU7_Lentinus	84,62	559
255	jgi|Polbr1|1455204|fgenesh1_pm.20_#	Polyporus brumalis BRFM 1820 v1.0	CYP5035AV1_Polyporus	100	563
256	jgi|Dicsqu18370_1|762016|fgenesh1_k	Dichomitus squalens OM18370.1 v1.0	CYP5035AV1_Polyporus	64,53	561
257	jgi|Dicsqu463_1|903800|estExt_Genew	Dichomitus squalens CBS463.89 v1.0	CYP5035AV1_Polyporus	64,41	562
258	jgi|Dicsqu464_1|887949|estExt_Genew	Dichomitus squalens CBS464.89 v1.0	CYP5035AV1_Polyporus	64,41	562
259	jgi|Artele1122_1|246774|CE246773_33	Artolenzites elegans CIRM-BRFM 1663 v1.	CYP5035AV1_Polyporus_arcularius	100	566
260	jgi|Fomfom1|130388|CE130387_124	Fomes fomentarius CIRM-BRFM 1821 v1.0	CYP5035AV1_Polyporus_arcularius	67,25	571
261	jgi|Earsca1|184441|CE184440_1205	Earliella scabrosa CIRM-BRFM 1817 v1.0	CYP5035AV1_Polyporus_arcularius	64,36	592
262	jgi|Dicsq1|156277|estExt_fgenesh1_pm	Dichomitus squalens LYAD-421 SS1 v1.0	CYP5035AV1_Polyporus_arcularius	64,3	563
263	jgi|Polsqu1|708683|fgenesh1_pm.56_#	Polyporus squamosus CCBS 676 v1.0	CYP5035AV2_Polyporus	100	564
264	jgi|Lenti6_1|581076|fgenesh1_kg.66_#	Lentinus tigrinus ALCF2SS1-6 v1.0	CYP5035AV3_Lentinus	100	580
265	jgi|Lenti7_1|548440|fgenesh1_pm.57_	Lentinus tigrinus ALCF2SS1-7 v1.0	CYP5035AV3_Lentinus	99,31	580
266	jgi|Sisbr1|640151|MIX7816_141_38	Lentinus tigrinus v1.0	CYP5035AV3_Lentinus	96,81	565
267	jgi|Trapol1|1218738|fgenesh1_pm.9_#	Trametes polyzona CIRM-BRFM 1798 v1.0	CYP5035AW1_Lentinus	100	605
268	jgi|Sisbr1|571658|estExt_Genewise1Plu	Lentinus tigrinus v1.0	CYP5035AW1_Lentinus	73,58	564
269	jgi|Polsqu1|834477|estExt_Genemark1	Polyporus squamosus CCBS 676 v1.0	CYP5035AW1_Lentinus tigrinus	62	571
270	jgi|Polbr1|1422973|fgenesh1_pg.126_#	Polyporus brumalis BRFM 1820 v1.0	CYP5035AW1_Lentinus tigrinus	61	549
271	jgi|Polsqu1|181995|CE181994_2271	Polyporus squamosus CCBS 676 v1.0	CYP5035AX1_Polyporus	100	588
272	jgi|Polsqu1|707000|fgenesh1_pm.22_#	Polyporus squamosus CCBS 676 v1.0	CYP5035AX2_Polyporus	100	407
273	jgi|Trave1|51005|gm1.9889_g	Trametes versicolor v1.0	CYP5035AZ1_Trametes_versicolor	100	558
274	jgi|Traci1|116365|CE116364_5445	Trametopsis cervina CIRM-BRFM 1824 v1.0	CYP5035AZ1_Trametes_versicolor	68,86	546
275	jgi|Tralj1|559700|CE559699_1981	Trametes ljubarskyi CIRM1659 v1.0	CYP5035AZ1_Trametes_versicolor	68,53	556
276	jgi|Trabet1|922101|MIX14000_10_17	Trametes betulina CIRM-BRFM 1801 v1.0	CYP5035AZ1_Trametes_versicolor	65,34	551
277	jgi|Traci1|268679|CE268678_1423	Trametopsis cervina CIRM-BRFM 1824 v1.0	CYP5035AZ1_Trametes_versicolor	65,3	559
278	jgi|Trapol1|352087|CE352086_1039	Trametes polyzona CIRM-BRFM 1798 v1.0	CYP5035AZ1_Trametes_versicolor	65,25	564
279	jgi|Tramax1|1065145|fgenesh1_pm.1_	Trametes maxima CIRM-BRFM 1813 v1.0	CYP5035AZ1_Trametes_versicolor	65,04	552
280	jgi|Leisp1|1369699|gm1.4141_g	Leiotrametes sp BRFM 1775 v1.0	CYP5035AZ1_Trametes_versicolor	64,26	554
281	jgi|Tragib1|1392952|fgenesh1_kg.40_#	Trametes gibbosa CIRM-BRFM 1770 v1.0	CYP5035AZ1_Trametes_versicolor	63,99	547
282	jgi|Pyccin1|1041334|fgenesh1_pm.17_	Pycnoporus cinnabarinus CIRM-BRFM 50 v1.0	CYP5035AZ1_Trametes_versicolor	63,86	559
283	jgi|Polar1|667965|estExt_Genemark1.C	Polyporus arcularius v1.0	CYP5035AZ1_Trametes_versicolor	63,59	563
284	jgi|Pycsa1|1595909|fgenesh1_kg.sc_71	Pycnoporus sanguineus BRFM 1264 v1.0	CYP5035AZ1_Trametes_versicolor	63,2	557

285	jgi|Pycco1662_1|864896|estExt_fgenes	Pycnoporus coccineus CIRM1662	CYP5035AZ1_Trametes_versicolor	62,66	557
286	jgi|Tralac1|748415|fgenesh1_pm.18_#	Leiotrametes lactinea CIRM-BRFM 1664 v1.0	CYP5035AZ1_Trametes_versicolor	62,57	561
287	jgi|Artele1122_1|495741|fgenesh1_pg.	Artolenzites elegans CIRM-BRFM 1663 v1.	CYP5035AZ1_Trametes_versicolor	62,46	562
288	jgi|Tramen1|1044824|fgenesh1_pm.12	Leiotrametes menziesii CIRM-BRFM 1781 v1.0	CYP5035AZ1_Trametes_versicolor	62,32	552
289	jgi|Artel1|812991|fgenesh1_kg.54_#_1	Artolenzites elegans CIRM-BRFM 1663 v1.	CYP5035AZ1_Trametes_versicolor	62,28	562
290	jgi|Pycsa1|1754665|estExt_Genemark1	Pycnoporus sanguineus BRFM 1264 v1.0	CYP5035AZ1_Trametes_versicolor	61,73	567
291	jgi|Pycci1|2784|scf184791.g34	Pycnoporus cinnabarinus BRFM 137	CYP5035AZ1_Trametes_versicolor	60,36	507
292	jgi|Pycci1|4037|scf184844.g119	Pycnoporus cinnabarinus BRFM 137	CYP5035AZ1_Trametes_versicolor	60,21	563
293	jgi|Pycco1|1362943|e_gw1.9.574.1	Pycnoporus coccineus BRFM 310 v1.0	CYP5035AZ1_Trametes_versicolor	58,61	546
294	jgi|Pycco1662_1|872263|gm1.814_g	Pycnoporus coccineus CIRM1662	CYP5035AZ1_Trametes_versicolor	56,26	503
295	jgi|Trave1|58095|estExt_fgenesh1_pm.	Trametes versicolor v1.0	CYP5035AZ2_Trametes_versicolor	100	576
296	jgi|Tragib1|694241|CE694240_16222	Trametes gibbosa CIRM-BRFM 1770 v1.0	CYP5035AZ2_Trametes_versicolor	76,63	582
297	jgi|Trabet1|477754|CE477753_479	Trametes betulina CIRM-BRFM 1801 v1.0	CYP5035AZ2_Trametes_versicolor	75,82	517
298	jgi|Lenti6_1|628086|MIX9889_14_24	Lentinus tigrinus ALCF2SS1-6 v1.0	CYP5035AZ2_Trametes_versicolor	74,26	575
299	jgi|Tramey1|1003781|fgenesh1_pm.18	Trametes meyenii CIRM-BRFM 1810 v1.0	CYP5035AZ2_Trametes_versicolor	59,15	585
300	jgi|Pycco1662_1|432733|CE432732_12	Pycnoporus coccineus CIRM1662	CYP5035AZ2_Trametes_versicolor	58,76	565
301	jgi|Pycpun1|540945|gm1.8650_g	Pycnoporus puniceus CIRM-BRFM 1868 v1.0	CYP5035AZ2_Trametes_versicolor	57,75	587
302	jgi|Pycsa1|1754664|estExt_Genemark1	Pycnoporus sanguineus BRFM 1264 v1.0	CYP5035AZ2_Trametes_versicolor	57,39	582
303	jgi|Pycco1662_1|816086|estExt_Genew	Pycnoporus coccineus CIRM1662	CYP5035AZ2_Trametes_versicolor	57,24	573
304	jgi|Pycco1|1461855|estExt_fgenesh1_p	Pycnoporus coccineus BRFM 310 v1.0	CYP5035AZ2_Trametes_versicolor	56,94	576
305	jgi|Pyccin1|168386|CE168385_664	Pycnoporus cinnabarinus CIRM-BRFM 50 v1.0	CYP5035AZ2_Trametes_versicolor	56,78	583
306	jgi|Pycco1|1450696|estExt_fgenesh1_p	Pycnoporus coccineus BRFM 310 v1.0	CYP5035AZ2_Trametes_versicolor	56,54	573
307	jgi|Pyccin1|1049319|gm1.3862_g	Pycnoporus cinnabarinus CIRM-BRFM 50 v1.0	CYP5035AZ2_Trametes_versicolor	56,17	575
308	jgi|Earsca1|604737|e_gw1.1.2281.1	Earliella scabrosa CIRM-BRFM 1817 v1.0	CYP5035AZ2_Trametes_versicolor	55,76	590
309	jgi|Pycci1|4039|scf184844.g121	Pycnoporus cinnabarinus BRFM 137	CYP5035AZ2_Trametes_versicolor	55,52	589
310	jgi|Pycci1|4038|scf184844.g120	Pycnoporus cinnabarinus BRFM 137	CYP5035AZ2_Trametes_versicolor	54,59	599
311	jgi|Pycsa1|1672486|gm1.2126_g	Pycnoporus sanguineus BRFM 1264 v1.0	CYP5035AZ2_Trametes_versicolor	54,51	587
312	jgi|Pycco1|1292875|CE1292874_4946	Pycnoporus coccineus BRFM 310 v1.0	CYP5035AZ2_Trametes_versicolor	53,55	577
313	jgi|Pyccin1|1050304|gm1.4847_g	Pycnoporus cinnabarinus CIRM-BRFM 50 v1.0	CYP5035AZ2_Trametes_versicolor	52,15	581

CYP5035S7-similar CYP5035 sequences sorted by %ID

seq ID	species	best hit	%ID	aln length
jgi|Phaca1|153972|estExt_Genewise1Plus.C_	Phanerochaete carnosa HHB-10118-Sp v1.0	CYP5035A_Phanerochaete_carnosa	100	524
jgi|Suibr2|843826|Suibr1.fgenesh1_pm.7_#_	Suillus brevipes Sb2 v2.0	CYP5035B	100	561
jgi|Polbr1|1481810|gm1.5391_g	Polyporus brumalis BRFM 1820 v1.0	CYP5035H2_Polyporus	100	556
jgi|Polar1|665169|estExt_Genemark1.C_356	Polyporus arcularius v1.0	CYP5035H2_Polyporus_arcularius	100	556
jgi|Polsqu1|24110|CE24109_7285	Polyporus squamosus CCBS 676 v1.0	CYP5035H3_Polyporus	100	556
jgi|Lenti6_1|578269|fgenesh1_kg.34_#_55_#	Lentinus tigrinus ALCF2SS1-6 v1.0	CYP5035H4_Lentinus	100	558
jgi|Trave1|41578|gm1.462_g	Trametes versicolor v1.0	CYP5035H5_Trametes_versicolor	100	554
jgi|Sisbr1|623797|gm1.4470_g	Lentinus tigrinus v1.0	CYP5035N10_Polyporus	100	560
jgi|Polsqu1|835110|estExt_Genemark1.C_27	Polyporus squamosus CCBS 676 v1.0	CYP5035N11_Polyporus	100	550
jgi|Lenti6_1|581920|fgenesh1_kg.91_#_6_#_	Lentinus tigrinus ALCF2SS1-6 v1.0	CYP5035N12_Lentinus	100	563
jgi|Lenti7_1|538117|fgenesh1_kg.30_#_15_#	Lentinus tigrinus ALCF2SS1-7 v1.0	CYP5035N12_Lentinus	100	563
jgi|Sisbr1|585391|fgenesh1_kg.48_#_39_#_1	Lentinus tigrinus v1.0	CYP5035N12_Lentinus	100	563
jgi|Polsqu1|746845|gm1.13007_g	Polyporus squamosus CCBS 676 v1.0	CYP5035N13_Polyporus	100	517
jgi|Polsqu1|818645|estExt_Genewise1Plus.C	Polyporus squamosus CCBS 676 v1.0	CYP5035N14_Polyporus	100	564
jgi|Polsqu1|588169|e_gw1.213.21.1	Polyporus squamosus CCBS 676 v1.0	CYP5035N15_Polyporus	100	544
jgi|Polar1|667057|estExt_Genemark1.C_628	Polyporus arcularius v1.0	CYP5035N16_Polyporus	100	550
jgi|Lenti6_1|558432|estExt_Genewise1Plus.C	Lentinus tigrinus ALCF2SS1-6 v1.0	CYP5035N17_Lentinus	100	544
jgi|Lenti7_1|468757|e_gw1.30.223.1	Lentinus tigrinus ALCF2SS1-7 v1.0	CYP5035N17_Lentinus	100	544
jgi|Sisbr1|570632|estExt_Genewise1Plus.C_4	Lentinus tigrinus v1.0	CYP5035N17_Lentinus	100	544
jgi|Trave1|60226|estExt_fgenesh1_pm.C_10	Trametes versicolor v1.0	CYP5035N19_Trametes_versicolor	100	553
jgi|Trave1|130760|e_gw1.10.841.1	Trametes versicolor v1.0	CYP5035N20_Trametes_versicolor	100	581
jgi|Trave1|45128|gm1.4012_g	Trametes versicolor v1.0	CYP5035N20_Trametes_versicolor	100	542
jgi|Polbr1|1454895|fgenesh1_pm.17_#_33	Polyporus brumalis BRFM 1820 v1.0	CYP5035N5_Polyporus	100	565
jgi|Polbr1|1501025|MIX9741_377_27	Polyporus brumalis BRFM 1820 v1.0	CYP5035N5_Polyporus_arcularius	100	566
jgi|Polar1|521854|estExt_Genewise1.C_174	Polyporus arcularius v1.0	CYP5035N6_Polyporus_arcularius	100	538
jgi|Polbr1|1363373|e_gw1.115.31.1	Polyporus brumalis BRFM 1820 v1.0	CYP5035N6v2_Polyporus	100	552
jgi|Polar1|498992|e_gw1.455.14.1	Polyporus arcularius v1.0	CYP5035N7_Polyporus	100	564
jgi|Polar1|655629|estExt_fgenesh1_pg.C_50	Polyporus arcularius v1.0	CYP5035N8_Polyporus	100	564

jgi|Polar1|50867|CE50866_1041	Polyporus arcularius v1.0	CYP5035N9_Polyporus	100	613
jgi|Lenti6_1|581782|fgenesh1_kg.85_#_2_#_	Lentinus tigrinus ALCF2SS1-6 v1.0	CYP5035S10_Lentinus	100	592
jgi|Lenti6_1|658665|estExt_Genemark1.C_9	Lentinus tigrinus ALCF2SS1-6 v1.0	CYP5035S11_Lentinus	100	614
jgi|Lenti7_1|538108|fgenesh1_kg.30_#_6_#_	Lentinus tigrinus ALCF2SS1-7 v1.0	CYP5035S11_Lentinus	100	585
jgi|Lenti6_1|581800|fgenesh1_kg.85_#_20_#	Lentinus tigrinus ALCF2SS1-6 v1.0	CYP5035S12_Lentinus	100	594
jgi|Polsqu1|829759|estExt_Genemark1.C_48	Polyporus squamosus CCBS 676 v1.0	CYP5035S13_Polyporus	100	563
jgi|Lenti7_1|572566|gm1.8370_g	Lentinus tigrinus ALCF2SS1-7 v1.0	CYP5035S14_Lentinus	100	560
jgi|Sisbr1|627566|gm1.8239_g	Lentinus tigrinus v1.0	CYP5035S14_Lentinus	100	560
jgi|Lenti7_1|489422|estExt_Genewise1.C_19	Lentinus tigrinus ALCF2SS1-7 v1.0	CYP5035S15_Lentinus	100	560
jgi|Polbr1|1506430|MIX15146_586_20	Polyporus brumalis BRFM 1820 v1.0	CYP5035S15_Lentinus	100	560
jgi|Sisbr1|544206|estExt_Genewise1.C_1702	Lentinus tigrinus v1.0	CYP5035S15_Lentinus	100	560
jgi|Polsqu1|834295|estExt_Genemark1.C_19	Polyporus squamosus CCBS 676 v1.0	CYP5035S16_Polyporus	100	550
jgi|Lenti6_1|578126|fgenesh1_kg.33_#_59_#	Lentinus tigrinus ALCF2SS1-6 v1.0	CYP5035S17_Polyporus	100	538
jgi|Polsqu1|689230|fgenesh1_kg.927_#_2_#_	Polyporus squamosus CCBS 676 v1.0	CYP5035S18_Polyporus	100	564
jgi|Polsqu1|676477|fgenesh1_kg.308_#_4_#_	Polyporus squamosus CCBS 676 v1.0	CYP5035S19_Polyporus	100	558
jgi|Lenti6_1|581802|fgenesh1_kg.85_#_22_#	Lentinus tigrinus ALCF2SS1-6 v1.0	CYP5035S21_Lentinus	100	573
jgi|Lenti7_1|540912|fgenesh1_kg.70_#_31_#	Lentinus tigrinus ALCF2SS1-7 v1.0	CYP5035S21_Lentinus	100	573
jgi|Polbr1|1500065|MIX8781_4600_46	Polyporus brumalis BRFM 1820 v1.0	CYP5035S22_Polyporus	100	587
jgi|Polar1|505708|e_gw1.1106.2.1	Polyporus arcularius v1.0	CYP5035S24_Polyporus	100	561
jgi|Polar1|531655|estExt_Genewise1.C_628(	Polyporus arcularius v1.0	CYP5035S25_Polyporus	100	580
jgi|Polar1|521853|estExt_Genewise1.C_174(	Polyporus arcularius v1.0	CYP5035S26_Polyporus	100	560
jgi|Polbr1|1480930|gm1.4511_g	Polyporus brumalis BRFM 1820 v1.0	CYP5035S6_Polyporus	100	569
jgi|Polar1|652223|estExt_fgenesh1_pg.C_12	Polyporus arcularius v1.0	CYP5035S6_Polyporus_arcularius	100	569
jgi|Lenti6_1|527996|estExt_Genewise1.C_23	Lentinus tigrinus ALCF2SS1-6 v1.0	CYP5035S7_Lentinus	100	558
jgi|Lenti7_1|510889|estExt_Genewise1Plus.(	Lentinus tigrinus ALCF2SS1-7 v1.0	CYP5035S7_Lentinus	100	558
jgi|Polsqu1|816847|estExt_Genewise1Plus.C	Polyporus squamosus CCBS 676 v1.0	CYP5035S7_Lentinus	100	558
jgi|Sisbr1|582002|fgenesh1_kg.19_#_12_#_L	Lentinus tigrinus v1.0	CYP5035S7_Lentinus	100	558
jgi|Polbr1|1401994|fgenesh1_kg.19_#_14_#_	Polyporus brumalis BRFM 1820 v1.0	CYP5035S7_Polyporus	100	562
jgi|Polar1|664247|estExt_Genemark1.C_270	Polyporus arcularius v1.0	CYP5035S7_Polyporus_arcularius	100	565
jgi|Polbr1|1401717|fgenesh1_kg.17_#_218_	Polyporus brumalis BRFM 1820 v1.0	CYP5035S8_Polyporus	100	568
jgi|Polar1|665466|estExt_Genemark1.C_388	Polyporus arcularius v1.0	CYP5035S8_Polyporus_arcularius	100	568
jgi|Lenti6_1|552293|estExt_Genewise1Plus.(	Lentinus tigrinus ALCF2SS1-6 v1.0	CYP5035S9_Polyporus	100	590

jgi|Polar1|668252|estExt_Genemark1.C_123	Polyporus arcularius v1.0	CYP5035S9_Polyporus_arcularius	100	564
jgi|Pyccin1|1039701|fgenesh1_pm.7_#_185	Pycnoporus cinnabarinus CIRM-BRFM 50 v1.0	CYP5035AF2_Paxillus_involutus_AT	100	579
jgi|Paxru2|31013|Paxru1.fgenesh1_pm.62_#	Paxillus rubicundulus Ve08.2h10 v2.0	CYP5035AF3_Paxillus_rubicundulus	100	580
jgi|Suilu3|24266|Suilu1.fgenesh1_pm.129_#	Suillus luteus UH-Slu-Lm8-n1 v3	CYP5035AF4_Suillus_luteus_UH-Slu	100	559
jgi|Pisti1|991388|fgenesh1_kg.1_#_205_#_L	Pisolithus tinctorius Marx 270 v1.0	CYP5035AF5_Pisolithus_tinctorius_	100	594
jgi|Pismi1|551133|CE426681_14791	Pisolithus microcarpus 441 v1.0	CYP5035AF6_Pisolithus_microcarpu	100	589
jgi|Sclci1|1219887|fgenesh1_kg.105_#_5_#	Scleroderma citrinum Foug A v1.0	CYP5035AF7_Scleroderma_citrinum	100	585
jgi|Plicr1|432908|CE251633_8389	Plicaturopsis crispa v1.0	CYP5035AG1_Plicaturopsis_crispa_	100	571
jgi|Plicr1|52981|fgenesh1_pm.6_#_209	Plicaturopsis crispa v1.0	CYP5035AG3_Plicaturopsis_crispa_	100	662
jgi|Polbr1|1554465|estExt_Genemark1.C_13	Polyporus brumalis BRFM 1820 v1.0	CYP5035AU1_Polyporus	100	560
jgi|Polar1|519317|estExt_Genewise1.C_121(	Polyporus arcularius v1.0	CYP5035AU1_Polyporus_arcularius	100	560
jgi|Polar1|603200|gm1.10163_g	Polyporus arcularius v1.0	CYP5035AU2_Polyporus	100	560
jgi|Polar1|519322|estExt_Genewise1.C_121(	Polyporus arcularius v1.0	CYP5035AU3_Polyporus	100	559
jgi|Lenti6_1|611133|gm1.6018_g	Lentinus tigrinus ALCF2SS1-6 v1.0	CYP5035AU5_Lentinus	100	559
jgi|Lenti7_1|390492|CE390491_458	Lentinus tigrinus ALCF2SS1-7 v1.0	CYP5035AU5_Lentinus	100	559
jgi|Lenti6_1|586062|fgenesh1_pm.16_#_60	Lentinus tigrinus ALCF2SS1-6 v1.0	CYP5035AU6_Lentinus	100	556
jgi|Lenti7_1|545110|fgenesh1_pm.9_#_56	Lentinus tigrinus ALCF2SS1-7 v1.0	CYP5035AU6_Lentinus	100	556
jgi|Lenti6_1|547581|estExt_Genewise1Plus.(	Lentinus tigrinus ALCF2SS1-6 v1.0	CYP5035AU7_Lentinus	100	559
jgi|Lenti7_1|533921|fgenesh1_kg.9_#_130_#	Lentinus tigrinus ALCF2SS1-7 v1.0	CYP5035AU7_Lentinus	100	559
jgi|Polbr1|1455204|fgenesh1_pm.20_#_1	Polyporus brumalis BRFM 1820 v1.0	CYP5035AV1_Polyporus	100	563
jgi|Artele1122_1|246774|CE246773_339	Artolenzites elegans CIRM-BRFM 1663 v1.	CYP5035AV1_Polyporus_arcularius	100	566
jgi|Polsqu1|708683|fgenesh1_pm.56_#_8	Polyporus squamosus CCBS 676 v1.0	CYP5035AV2_Polyporus	100	564
jgi|Lenti6_1|581076|fgenesh1_kg.66_#_42_#	Lentinus tigrinus ALCF2SS1-6 v1.0	CYP5035AV3_Lentinus	100	580
jgi|Trapol1|1218738|fgenesh1_pm.9_#_230	Trametes polyzona CIRM-BRFM 1798 v1.0	CYP5035AW1_Lentinus	100	605
jgi|Polsqu1|181995|CE181994_2271	Polyporus squamosus CCBS 676 v1.0	CYP5035AX1_Polyporus	100	588
jgi|Polsqu1|707000|fgenesh1_pm.22_#_3	Polyporus squamosus CCBS 676 v1.0	CYP5035AX2_Polyporus	100	407
jgi|Trave1|51005|gm1.9889_g	Trametes versicolor v1.0	CYP5035AZ1_Trametes_versicolor	100	558
jgi|Trave1|58095|estExt_fgenesh1_pm.C_5_	Trametes versicolor v1.0	CYP5035AZ2_Trametes_versicolor	100	576
jgi|Lenti7_1|540886|fgenesh1_kg.70_#_5_#	Lentinus tigrinus ALCF2SS1-7 v1.0	CYP5035S10_Lentinus	99,83	590
jgi|Sisbr1|585400|fgenesh1_kg.48_#_48_#_L	Lentinus tigrinus v1.0	CYP5035S11_Lentinus	99,66	585
jgi|Sisbr1|586099|fgenesh1_kg.66_#_27_#_L	Lentinus tigrinus v1.0	CYP5035S21_Lentinus	99,65	573
jgi|Lenti7_1|564891|gm1.695_g	Lentinus tigrinus ALCF2SS1-7 v1.0	CYP5035H4_Lentinus	99,64	558

jgi|Sisbr1|574375|fgenesh1_kg.2_#_756_#_L	Lentinus tigrinus v1.0	CYP5035H4_Lentinus	99,64	558
jgi|Polbr1|1400732|fgenesh1_kg.13_#_277_	Polyporus brumalis BRFM 1820 v1.0	CYP5035AU3_Polyporus	99,64	559
jgi|Polbr1|1561063|estExt_Genemark1.C_11	Polyporus brumalis BRFM 1820 v1.0	CYP5035N8_Polyporus	99,47	564
jgi|Lenti7_1|548440|fgenesh1_pm.57_#_9	Lentinus tigrinus ALCF2SS1-7 v1.0	CYP5035AV3_Lentinus	99,31	580
jgi|Sisbr1|586078|fgenesh1_kg.66_#_6_#_Lc	Lentinus tigrinus v1.0	CYP5035S10_Lentinus	98,61	577
jgi|Polbr1|184586|CE184585_735	Polyporus brumalis BRFM 1820 v1.0	CYP5035N7_Polyporus	97,7	564
jgi|Cersu1|119768|estExt_fgenesh1_kg.C_29	Ceriporiopsis (Gelatoporia) subvermispora B	CYP5035AF4_Suillus_luteus_UH-Slu	96,96	559
jgi|Sisbr1|640151|MIX7816_141_38	Lentinus tigrinus v1.0	CYP5035AV3_Lentinus	96,81	565
jgi|Lenti7_1|540902|fgenesh1_kg.70_#_21_#	Lentinus tigrinus ALCF2SS1-7 v1.0	CYP5035S12_Lentinus	96,79	592
jgi|Paxam1|966266|fgenesh1_kg.28_#_55_#	Paxillus ammoniavirescens Pou09.2 v1.0	CYP5035AF2_Paxillus_involutus_AT	95,86	580
jgi|Sisbr1|586093|fgenesh1_kg.66_#_21_#_L	Lentinus tigrinus v1.0	CYP5035S12_Lentinus	95,61	592
jgi|Polbr1|1411615|fgenesh1_kg.118_#_36_	Polyporus brumalis BRFM 1820 v1.0	CYP5035AU2_Polyporus	95,54	560
jgi|Polbr1|1363391|e_gw1.115.20.1	Polyporus brumalis BRFM 1820 v1.0	CYP5035N9_Polyporus arcularius	94	543
jgi|Suitom1|746520|fgenesh1_pm.11_#_71	Suillus tomentosus FC115 v1.0	CYP5035AF4_Suillus_luteus_UH-Slu	91,67	552
jgi|Suigr1|580326|CE580325_2365	Suillus granulatus EM37 v1.0	CYP5035AF4_Suillus_luteus_UH-Slu	91,07	560
jgi|Suidec1|1093418|fgenesh1_kg.15_#_127	Suillus decipiens EM49 v1.0	CYP5035AF4_Suillus_luteus_UH-Slu	90,36	560
jgi|Denbi1|815498|fgenesh1_pm.4_#_20	Dendrothele bispora CBS 962.96 v1.0	CYP5035AF4_Suillus_luteus_UH-Slu	89,54	564
jgi|Polbr1|1487827|gm1.11408_g	Polyporus brumalis BRFM 1820 v1.0	CYP5035S24_Polyporus arcularius	89	556
jgi|Suipic1|1478630|gm1.2487_g	Suillus pictus EM44 v1.0	CYP5035AF4_Suillus_luteus_UH-Slu	87,99	566
jgi|Trapol1|105914|CE105913_5115	Trametes polyzona CIRM-BRFM 1798 v1.0	CYP5035H5_Trametes_versicolor	87,18	554
jgi|Gyrli1|796093|fgenesh1_pm.14_#_124	Gyrodon lividus BX v1.0	CYP5035AF2_Paxillus_involutus_AT	86,2	558
jgi|Sisbr1|577407|fgenesh1_kg.6_#_311_#_L	Lentinus tigrinus v1.0	CYP5035AU7_Lentinus	85,69	559
jgi|Obbri1|890182|estExt_Genemark1.C_179	Obba rivulosa 3A-2 v1.0	CYP5035B	85,41	555
jgi|Traci1|1521520|gm1.6319_g	Trametopsis cervina CIRM-BRFM 1824 v1.0	CYP5035H5_Trametes_versicolor	84,78	552
jgi|Polar1|667894|estExt_Genemark1.C_920	Polyporus arcularius v1.0	CYP5035AU7_Lentinus	84,62	559
jgi|Earsca1|728492|fgenesh1_kg.7_#_1669_#	Earliella scabrosa CIRM-BRFM 1817 v1.0	CYP5035H2_Polyporus_arcularius	83,3	545
jgi|Tralj1|428191|CE428190_1838	Trametes ljubarskyi CIRM1659 v1.0	CYP5035H5_Trametes_versicolor	82,97	552
jgi|Hexnit1|1215331|fgenesh1_pm.1_#_175	Hexagonia nitida CIRM-BRFM 1802 v1.0	CYP5035H3_Polyporus	82	550
jgi|Fomfom1|424094|CE424093_631	Fomes fomentarius CIRM-BRFM 1821 v1.0	CYP5035H2_Polyporus_arcularius	81,97	549
jgi|Pycsa1|1577749|e_gw1.7180000650838.1	Pycnoporus sanguineus BRFM 1264 v1.0	CYP5035H5_Trametes_versicolor	81,74	553
jgi|Pycco1|1370331|e_gw1.30.134.1	Pycnoporus coccineus BRFM 310 v1.0	CYP5035H5_Trametes_versicolor	81,56	553
jgi|Dicsqu464_1|919019|fgenesh1_kg.11_#_	Dichomitus squalens CBS464.89 v1.0	CYP5035G1 Ganoderma lucidum GL	81	598

jgi|Dicsq1|151582|estExt_fgenesh1_pm.C_1_	Dichomitus squalens LYAD-421 SS1 v1.0	CYP5035H1_Ganoderma_sinense	80,55	550
jgi|Dicsqu18370_1|660324|e_gw1.25.174.1	Dichomitus squalens OM18370.1 v1.0	CYP5035H1_Ganoderma_sinense	80,55	550
jgi|Dicsqu463_1|993380|fgenesh1_pm.294_	Dichomitus squalens CBS463.89 v1.0	CYP5035H1_Ganoderma_sinense	80,55	550
jgi|Dicsqu464_1|918682|fgenesh1_kg.10_#_	Dichomitus squalens CBS464.89 v1.0	CYP5035H1_Ganoderma_sinense	80,55	550
jgi|Artele1122_1|466036|e_gw1.2.699.1	Artolenzites elegans CIRM-BRFM 1663 v1.	CYP5035H5_Trametes_versicolor	80,51	554
jgi|Pycpun1|308909|CE308908_3418	Pycnoporus puniceus CIRM-BRFM 1868 v1.0	CYP5035H5_Trametes_versicolor	80,25	552
jgi|Artel1|850992|fgenesh1_pm.18_#_46	Artolenzites elegans CIRM-BRFM 1663 v1.	CYP5035H5_Trametes_versicolor	80,14	554
jgi|Tramax1|1068035|fgenesh1_pm.5_#_366	Trametes maxima CIRM-BRFM 1813 v1.0	CYP5035H5_Trametes_versicolor	80,14	554
jgi|Pycco1662_1|876088|gm1.4639_g	Pycnoporus coccineus CIRM1662	CYP5035H5_Trametes_versicolor	79,78	554
jgi|Tramey1|997533|fgenesh1_pm.1_#_949	Trametes meyenii CIRM-BRFM 1810 v1.0	CYP5035H5_Trametes_versicolor	79,71	552
jgi|Leisp1|1318962|fgenesh1_kg.12_#_150_#	Leiotrametes sp BRFM 1775 v1.0	CYP5035H5_Trametes_versicolor	79,68	556
jgi|Tramen1|1047947|fgenesh1_pm.42_#_35	Leiotrametes menziesii CIRM-BRFM 1781 v1.0	CYP5035H5_Trametes_versicolor	79,53	552
jgi|Tralac1|370287|CE370286_1031	Leiotrametes lactinea CIRM-BRFM 1664 v1.0	CYP5035H5_Trametes_versicolor	79,3	546
jgi|Xerba1|1485051|gm1.5292_g	Xerocomus badius 84.06 v1.0	CYP5035AF1_Hydnomerulius_pinas	79,29	589
jgi|Paxin1|88877|e_gw1.305.4.1	Paxillus involutus ATCC 200175 v1.0	CYP5035H5_Trametes_versicolor	79,17	552
jgi|Hexnit1|1268939|gm1.4816_g	Hexagonia nitida CIRM-BRFM 1802 v1.0	CYP5035AF4_Suillus_luteus_UH-Slu	78,55	564
jgi|Rhisa1|731579|e_gw1.86.88.1	Rhizopogon salebrosus TDB-379 v1.0	CYP5035AF4_Suillus_luteus_UH-Slu	78,05	565
jgi|Dicsqu18370_1|806887|gm1.5849_g	Dichomitus squalens OM18370.1 v1.0	CYP5035G1 Ganoderma lucidum	78	622
jgi|Boled1|909694|estExt_Genewise1Plus.C_	Boletus edulis BED1 v4.0	CYP5035AF1_Hydnomerulius_pinas	77,97	581
jgi|Rhivi1|681821|e_gw1.22.70.1	Rhizopogon vinicolor AM-OR11-026 v1.0	CYP5035AF4_Suillus_luteus_UH-Slu	77,27	572
jgi|Dicsqu463_1|988899|fgenesh1_pm.58_#_	Dichomitus squalens CBS463.89 v1.0	CYP5035G1 Ganoderma lucidum GL	77	622
jgi|Dicsq1|179419|estExt_Genemark1.C_703	Dichomitus squalens LYAD-421 SS1 v1.0	CYP5035G1 Ganoderma lucidum GL	77	622
jgi|Tragib1|694241|CE694240_16222	Trametes gibbosa CIRM-BRFM 1770 v1.0	CYP5035AZ2_Trametes_versicolor	76,63	582
jgi|Trabet1|477754|CE477753_479	Trametes betulina CIRM-BRFM 1801 v1.0	CYP5035AZ2_Trametes_versicolor	75,82	517
jgi|Pycci1|9212|scf185013.g82	Pycnoporus cinnabarinus BRFM 137	CYP5035H5_Trametes_versicolor	74,78	452
jgi|Lenti6_1|628086|MIX9889_14_24	Lentinus tigrinus ALCF2SS1-6 v1.0	CYP5035AZ2_Trametes_versicolor	74,26	575
jgi|Dicsqu18370_1|696349|estExt_Genewise	Dichomitus squalens OM18370.1 v1.0	CYP5035S3_Ganoderma_sinense GS	74	554
jgi|Dicsqu463_1|967115|fgenesh1_kg.258_#	Dichomitus squalens CBS463.89 v1.0	CYP5035S3_Ganoderma_sinense GS	74	554
jgi|Dicsqu464_1|935569|fgenesh1_kg.102_#	Dichomitus squalens CBS464.89 v1.0	CYP5035S3_Ganoderma_sinense GS	74	554
jgi|Sisbr1|571658|estExt_Genewise1Plus.C_6	Lentinus tigrinus v1.0	CYP5035AW1_Lentinus	73,58	564
jgi|Dicsq1|72385|e_gw1.93.13.1	Dichomitus squalens LYAD-421 SS1 v1.0	CYP5035N2_Ganoderma_sinense	73,33	540
jgi|Dicsqu18370_1|665075|e_gw1.45.36.1	Dichomitus squalens OM18370.1 v1.0	CYP5035N2_Ganoderma_sinense	73,1	554

jgi|Dicsqu463_1|1021296|gm1.7704_g	Dichomitus squalens CBS463.89 v1.0	CYP5035N2_Ganoderma_sinense	73,1	554
jgi|Dicsqu464_1|935554|fgenesh1_kg.102_#	Dichomitus squalens CBS464.89 v1.0	CYP5035N2_Ganoderma_sinense	73,1	554
jgi|Earsca1|733523|fgenesh1_kg.9_#_519_#	Earliella scabrosa CIRM-BRFM 1817 v1.0	CYP5035G1_Ganoderma_sinense	73	563
jgi|Dicsq1|164054|estExt_fgenesh1_pg.C_93	Dichomitus squalens LYAD-421 SS1 v1.0	CYP5035S3_Ganoderma_sinense GS	73	554
jgi|Dicsqu18370_1|765132|fgenesh1_kg.80_	Dichomitus squalens OM18370.1 v1.0	CYP5035J1_Ganoderma_sp._10597	72,74	565
jgi|Leumo1|1005994|e_gw1.00033.92.1	Leucogyrophana mollusca KUC20120723A-06	CYP5035AF1_Hydnomerulius_pinas	71,6	581
jgi|Tralac1|205625|CE205624_1029	Leiotrametes lactinea CIRM-BRFM 1664 v1.0	CYP5035N20_Trametes_versicolor	71,51	551
jgi|Leisp1|1371152|gm1.5594_g	Leiotrametes sp BRFM 1775 v1.0	CYP5035N20_Trametes_versicolor	71,14	551
jgi|Hexnit1|1266762|gm1.2639_g	Hexagonia nitida CIRM-BRFM 1802 v1.0	CYP5035N7_Polyporus	70,97	558
jgi|Traci1|1402223|e_gw1.15.531.1	Trametopsis cervina CIRM-BRFM 1824 v1.0	CYP5035N20_Trametes_versicolor	70,56	540
jgi|Trapol1|1067680|e_gw1.19.24.1	Trametes polyzona CIRM-BRFM 1798 v1.0	CYP5035N19_Trametes_versicolor	70,47	552
jgi|Tragib1|1412667|fgenesh1_pm.40_#_57	Trametes gibbosa CIRM-BRFM 1770 v1.0	CYP5035N20_Trametes_versicolor	70,43	531
jgi|Dicsqu18370_1|843352|MIX30610_11074	Dichomitus squalens OM18370.1 v1.0	CYP5035N2_Ganoderma_sinense	70,38	557
jgi|Trabet1|826979|fgenesh1_kg.21_#_762_	Trametes betulina CIRM-BRFM 1801 v1.0	CYP5035N20_Trametes_versicolor	70,38	530
jgi|Dicsqu463_1|967109|fgenesh1_kg.258_#	Dichomitus squalens CBS463.89 v1.0	CYP5035N2_Ganoderma_sinense	70,02	557
jgi|Dicsqu464_1|935562|fgenesh1_kg.102_#	Dichomitus squalens CBS464.89 v1.0	CYP5035N2_Ganoderma_sinense	70,02	557
jgi|Dicsq1|94181|estExt_Genewise1.C_93002	Dichomitus squalens LYAD-421 SS1 v1.0	CYP5035N2_Ganoderma_sinense	69,84	557
jgi|Fomfom1|1363757|gm1.1551_g	Fomes fomentarius CIRM-BRFM 1821 v1.0	CYP5035N7_Polyporus	69,82	560
jgi|Tralj1|1037740|fgenesh1_pm.46_#_21	Trametes ljubarskyi CIRM1659 v1.0	CYP5035N20_Trametes_versicolor	69,56	542
jgi|Pycco1|1468281|gm1.5790_g	Pycnoporus coccineus BRFM 310 v1.0	CYP5035N20_Trametes_versicolor	69,38	552
jgi|Pycpun1|508212|fgenesh1_pg.13_#_60	Pycnoporus puniceus CIRM-BRFM 1868 v1.0	CYP5035N20_Trametes_versicolor	69,23	546
jgi|Traci1|116365|CE116364_5445	Trametopsis cervina CIRM-BRFM 1824 v1.0	CYP5035AZ1_Trametes_versicolor	68,86	546
jgi|Tramey1|914922|e_gw1.11.457.1	Trametes meyenii CIRM-BRFM 1810 v1.0	CYP5035N20_Trametes_versicolor	68,81	529
jgi|Tralj1|559700|CE559699_1981	Trametes ljubarskyi CIRM1659 v1.0	CYP5035AZ1_Trametes_versicolor	68,53	556
jgi|Pyccin1|1043044|fgenesh1_pm.32_#_65	Pycnoporus cinnabarinus CIRM-BRFM 50 v1.0	CYP5035N20_Trametes_versicolor	68,39	560
jgi|Tramax1|1073440|gm1.413_g	Trametes maxima CIRM-BRFM 1813 v1.0	CYP5035N20_Trametes_versicolor	67,47	541
jgi|Fomfom1|130388|CE130387_124	Fomes fomentarius CIRM-BRFM 1821 v1.0	CYP5035AV1_Polyporus_arcularius	67,25	571
jgi|Earsca1|801019|gm1.12089_g	Earliella scabrosa CIRM-BRFM 1817 v1.0	CYP5035N7_Polyporus	66,9	565
jgi|Tramey1|1003669|fgenesh1_pm.18_#_22	Trametes meyenii CIRM-BRFM 1810 v1.0	CYP5035N19_Trametes_versicolor	66,54	541
jgi|Pycco1662_1|60791|CE60790_3985	Pycnoporus coccineus CIRM1662	CYP5035N20_Trametes_versicolor	66,03	577
jgi|Polar1|196845|CE196844_3694	Polyporus arcularius v1.0	CYP5035AU5_Lentinus tigrinus	66	562
jgi|Tramax1|1055064|fgenesh1_kg.21_#_105	Trametes maxima CIRM-BRFM 1813 v1.0	CYP5035N19_Trametes_versicolor	65,93	546

jgi|Trabet1|922101|MIX14000_10_17	Trametes betulina CIRM-BRFM 1801 v1.0	CYP5035AZ1_Trametes_versicolor	65,34	551
jgi|Traci1|268679|CE268678_1423	Trametopsis cervina CIRM-BRFM 1824 v1.0	CYP5035AZ1_Trametes_versicolor	65,3	559
jgi|Fomfom1|1363759|gm1.1553_g	Fomes fomentarius CIRM-BRFM 1821 v1.0	CYP5035S18_Polyporus	65,26	567
jgi|Trapol1|352087|CE352086_1039	Trametes polyzona CIRM-BRFM 1798 v1.0	CYP5035AZ1_Trametes_versicolor	65,25	564
jgi|Tramax1|1065145|fgenesh1_pm.1_#_36	Trametes maxima CIRM-BRFM 1813 v1.0	CYP5035AZ1_Trametes_versicolor	65,04	552
jgi|Artel1|806710|fgenesh1_kg.13_#_28_#_I	Artolenzites elegans CIRM-BRFM 1663 v1.	CYP5035N20_Trametes_versicolor	64,8	537
jgi|Hexnit1|1217413|fgenesh1_pm.3_#_379	Hexagonia nitida CIRM-BRFM 1802 v1.0	CYP5035N5_Polyporus_arcularius	64,75	556
jgi|Dicsq1|147086|fgenesh1_pm.13_#_95	Dichomitus squalens LYAD-421 SS1 v1.0	CYP5035Q1	64,73	550
jgi|Dicsqu18370_1|762016|fgenesh1_kg.57_	Dichomitus squalens OM18370.1 v1.0	CYP5035AV1_Polyporus	64,53	561
jgi|Dicsqu463_1|903800|estExt_Genewise1.(	Dichomitus squalens CBS463.89 v1.0	CYP5035AV1_Polyporus	64,41	562
jgi|Dicsqu464_1|887949|estExt_Genewise1P	Dichomitus squalens CBS464.89 v1.0	CYP5035AV1_Polyporus	64,41	562
jgi|Earsca1|184441|CE184440_1205	Earliella scabrosa CIRM-BRFM 1817 v1.0	CYP5035AV1_Polyporus_arcularius	64,36	592
jgi|Dicsq1|156277|estExt_fgenesh1_pm.C_2(	Dichomitus squalens LYAD-421 SS1 v1.0	CYP5035AV1_Polyporus_arcularius	64,3	563
jgi|Leisp1|1369699|gm1.4141_g	Leiotrametes sp BRFM 1775 v1.0	CYP5035AZ1_Trametes_versicolor	64,26	554
jgi|Earsca1|801067|gm1.12137_g	Earliella scabrosa CIRM-BRFM 1817 v1.0	CYP5035N5_Polyporus_arcularius	64,23	562
jgi|Tragib1|1392952|fgenesh1_kg.40_#_670_	Trametes gibbosa CIRM-BRFM 1770 v1.0	CYP5035AZ1_Trametes_versicolor	63,99	547
jgi|Pyccin1|1041334|fgenesh1_pm.17_#_35	Pycnoporus cinnabarinus CIRM-BRFM 50 v1.0	CYP5035AZ1_Trametes_versicolor	63,86	559
jgi|Polar1|667965|estExt_Genemark1.C_966	Polyporus arcularius v1.0	CYP5035AZ1_Trametes_versicolor	63,59	563
jgi|Artele1122_1|650705|MIX32502_84_36	Artolenzites elegans CIRM-BRFM 1663 v1.	CYP5035N20_Trametes_versicolor	63,25	536
jgi|Pycsa1|1595909|fgenesh1_kg.sc_718000(	Pycnoporus sanguineus BRFM 1264 v1.0	CYP5035AZ1_Trametes_versicolor	63,2	557
jgi|Pycco1662_1|864896|estExt_fgenesh1_p	Pycnoporus coccineus CIRM1662	CYP5035AZ1_Trametes_versicolor	62,66	557
jgi|Tralac1|748415|fgenesh1_pm.18_#_114	Leiotrametes lactinea CIRM-BRFM 1664 v1.0	CYP5035AZ1_Trametes_versicolor	62,57	561
jgi|Artele1122_1|495741|fgenesh1_pg.45_#_	Artolenzites elegans CIRM-BRFM 1663 v1.	CYP5035AZ1_Trametes_versicolor	62,46	562
jgi|Leisp1|1345114|fgenesh1_pm.29_#_11	Leiotrametes sp BRFM 1775 v1.0	CYP5035N19_Trametes_versicolor	62,41	540
jgi|Tramen1|1064764|MIX4850_687_91	Leiotrametes menziesii CIRM-BRFM 1781 v1.0	CYP5035N19_Trametes_versicolor	62,39	553
jgi|Anobom1|1218668|e_gw1.230.7.1	Anomoporia bombycina ATCC 64506 v1.0	CYP5035AG1_Plicaturopsis_crispa_	62,39	561
jgi|Tramen1|1044824|fgenesh1_pm.12_#_7	Leiotrametes menziesii CIRM-BRFM 1781 v1.0	CYP5035AZ1_Trametes_versicolor	62,32	552
jgi|Artel1|812991|fgenesh1_kg.54_#_104_#_	Artolenzites elegans CIRM-BRFM 1663 v1.	CYP5035AZ1_Trametes_versicolor	62,28	562
jgi|Abobie1|826912|MIX14629_1887_37	Abortiporus biennis CIRM-BRFM1778 v1	CYP5035D3	62,09	517
jgi|Dicsqu464_1|827640|e_gw1.102.67.1	Dichomitus squalens CBS464.89 v1.0	CYP5035P1	62,01	487
jgi|Polsqu1|834477|estExt_Genemark1.C_21	Polyporus squamosus CCBS 676 v1.0	CYP5035AW1_Lentinus tigrinus	62	571
jgi|Cytmel1|1418953|gm1.9279_g	Cytidiella melzeri FP 102339 v1.0	CYP5035D3	61,85	540

jgi|Pycsa1|1754665|estExt_Genemark1.C_sc	Pycnoporus sanguineus BRFM 1264 v1.0	CYP5035AZ1_Trametes_versicolor	61,73	567
jgi|Phlcen1|8958|scaffold_2756.3	Phlebia centrifuga FBCC195	CYP5035Z1	61,51	530
jgi|Tramey1|1032777|MIX17440_258_22	Trametes meyenii CIRM-BRFM 1810 v1.0	CYP5035N19_Trametes_versicolor	61,21	531
jgi|Dicsqu463_1|992959|fgenesh1_pm.258_	Dichomitus squalens CBS463.89 v1.0	CYP5035P1	61,04	498
jgi|Dicsqu464_1|951341|fgenesh1_pm.102_	Dichomitus squalens CBS464.89 v1.0	CYP5035P1	61,04	498
jgi|Dicsqu18370_1|779171|fgenesh1_pm.51_	Dichomitus squalens OM18370.1 v1.0	CYP5035L1 Ganoderma lucidum GL(	61	481
jgi|Polbr1|1422973|fgenesh1_pg.126_#_11	Polyporus brumalis BRFM 1820 v1.0	CYP5035AW1_Lentinus tigrinus	61	549
jgi|Rhives1|3443|genemark-NODE_21236_le	Rhizopogon vesiculosus Smith	CYP5035N20_Trametes_versicolor	60,79	556
jgi|Phlcen1|13562|scaffold_967.15	Phlebia centrifuga FBCC195	CYP5035AD1	60,53	451
jgi|Pycci1|2784|scf184791.g34	Pycnoporus cinnabarinus BRFM 137	CYP5035AZ1_Trametes_versicolor	60,36	507
jgi|Pycci1|4037|scf184844.g119	Pycnoporus cinnabarinus BRFM 137	CYP5035AZ1_Trametes_versicolor	60,21	563
jgi|Tramax1|1024787|fgenesh1_kg.7_#_529_	Trametes maxima CIRM-BRFM 1813 v1.0	CYP5035N19_Trametes_versicolor	60,18	550
jgi|Dicsq1|161810|estExt_fgenesh1_pg.C_17	Dichomitus squalens LYAD-421 SS1 v1.0	CYP5035L1 Ganoderma lucidum GL(	60	482
jgi|Dicsqu463_1|995233|fgenesh1_pm.605_	Dichomitus squalens CBS463.89 v1.0	CYP5035L1 Ganoderma lucidum GL(	60	481
jgi|Dicsqu464_1|953386|fgenesh1_pm.286_	Dichomitus squalens CBS464.89 v1.0	CYP5035L1 Ganoderma lucidum GL(	60	481
jgi|Earsca1|799697|gm1.10767_g	Earliella scabrosa CIRM-BRFM 1817 v1.0	CYP5035N7_Polyporus	59,82	555
jgi|Conol1|919316|fgenesh1_pm.38_#_30	Coniophora olivacea MUCL 20566 v1.0	CYP5035AF1_Hydnomerulius_pinas	59,72	581
jgi|Phlcen1|13559|scaffold_967.12	Phlebia centrifuga FBCC195	CYP5035AD1	59,71	489
jgi|Pycpun1|540139|gm1.7844_g	Pycnoporus puniceus CIRM-BRFM 1868 v1.0	CYP5035N19_Trametes_versicolor	59,2	549
jgi|Fomfom1|1363762|gm1.1556_g	Fomes fomentarius CIRM-BRFM 1821 v1.0	CYP5035N5_Polyporus_arcularius	59,18	561
jgi|Tramey1|1003781|fgenesh1_pm.18_#_13	Trametes meyenii CIRM-BRFM 1810 v1.0	CYP5035AZ2_Trametes_versicolor	59,15	585
jgi|Trace1|1049863|CE1049862_12876	Trametopsis cervina CIRM-BRFM 1824 v1.0	CYP5035D2	58,78	541
jgi|Pycco1662_1|432733|CE432732_1267	Pycnoporus coccineus CIRM1662	CYP5035AZ2_Trametes_versicolor	58,76	565
jgi|Earsca1|162226|CE162225_1265	Earliella scabrosa CIRM-BRFM 1817 v1.0	CYP5035S26_Polyporus	58,73	550
jgi|Trace1|1342868|fgenesh1_pg.4_#_46	Trametopsis cervina CIRM-BRFM 1824 v1.0	CYP5035D2	58,7	540
jgi|Pycco1|1362943|e_gw1.9.574.1	Pycnoporus coccineus BRFM 310 v1.0	CYP5035AZ1_Trametes_versicolor	58,61	546
jgi|Hexnit1|1160509|fgenesh1_kg.5_#_112_	Hexagonia nitida CIRM-BRFM 1802 v1.0	CYP5035S11_Lentinus	58,23	589
jgi|Trace1|1354516|fgenesh1_kg.6_#_129_#	Trametopsis cervina CIRM-BRFM 1824 v1.0	CYP5035D2	58,12	554
jgi|Dicsqu18370_1|373931|CE373930_7707	Dichomitus squalens OM18370.1 v1.0	CYP5035P1	58	551
jgi|Clibor1|119449|CE119448_2934	Climacocystis borealis CliBor001 v1.0	CYP5035A10	57,82	486
jgi|Fomfom1|1233304|fgenesh1_kg.1_#_103	Fomes fomentarius CIRM-BRFM 1821 v1.0	CYP5035S6_Polyporus	57,8	564
jgi|Pycpun1|540945|gm1.8650_g	Pycnoporus puniceus CIRM-BRFM 1868 v1.0	CYP5035AZ2_Trametes_versicolor	57,75	587

jgi|Pycsa1|1754664|estExt_Genemark1.C_sc	Pycnoporus sanguineus BRFM 1264 v1.0	CYP5035AZ2_Trametes_versicolor	57,39	582
jgi|Hexnit1|1146372|fgenesh1_kg.3_#_1593	Hexagonia nitida CIRM-BRFM 1802 v1.0	CYP5035S22_Polyporus	57,27	578
jgi|Pycco1662_1|816086|estExt_Genewise1.	Pycnoporus coccineus CIRM1662	CYP5035AZ2_Trametes_versicolor	57,24	573
jgi|Trace1|1409937|fgenesh1_pm.40_#_10	Trametopsis cervina CIRM-BRFM 1824 v1.0	CYP5035D3	57,01	542
jgi|Pycco1|1461855|estExt_fgenesh1_pg.C_6	Pycnoporus coccineus BRFM 310 v1.0	CYP5035AZ2_Trametes_versicolor	56,94	576
jgi|Pyccin1|168386|CE168385_664	Pycnoporus cinnabarinus CIRM-BRFM 50 v1.0	CYP5035AZ2_Trametes_versicolor	56,78	583
jgi|Pycco1|1450696|estExt_fgenesh1_pm.C_	Pycnoporus coccineus BRFM 310 v1.0	CYP5035AZ2_Trametes_versicolor	56,54	573
jgi|Pycco1662_1|872263|gm1.814_g	Pycnoporus coccineus CIRM1662	CYP5035AZ1_Trametes_versicolor	56,26	503
jgi|Clibor1|1197786|fgenesh1_kg.12_#_558_	Climacocystis borealis CliBor001 v1.0	CYP5035Z1	56,25	544
jgi|Pyccin1|1049319|gm1.3862_g	Pycnoporus cinnabarinus CIRM-BRFM 50 v1.0	CYP5035AZ2_Trametes_versicolor	56,17	575
jgi|Clapy1|1913257|gm1.3000_g	Clavicorona pyxidata HHB10654 v1.0	CYP5035X1	56,05	562
jgi|Earsca1|683000|estExt_Genewise1Plus.C_	Earliella scabrosa CIRM-BRFM 1817 v1.0	CYP5035S3_Ganoderma_sinense GS	56	587
jgi|Earsca1|604737|e_gw1.1.2281.1	Earliella scabrosa CIRM-BRFM 1817 v1.0	CYP5035AZ2_Trametes_versicolor	55,76	590
jgi|Earsca1|639881|estExt_Genewise1.C_1_t	Earliella scabrosa CIRM-BRFM 1817 v1.0	CYP5035S22_Polyporus	55,67	582
jgi|Dicsq1|172004|gm1.7773_g	Dichomitus squalens LYAD-421 SS1 v1.0	CYP5035Q1	55,58	556
jgi|Dicsqu18370_1|706065|estExt_Genewise	Dichomitus squalens OM18370.1 v1.0	CYP5035Q1	55,58	556
jgi|Dicsqu463_1|974740|fgenesh1_kg.631_#	Dichomitus squalens CBS463.89 v1.0	CYP5035Q1	55,58	556
jgi|Dicsqu464_1|938285|fgenesh1_kg.134_#	Dichomitus squalens CBS464.89 v1.0	CYP5035Q1	55,58	556
jgi|Pycci1|4039|scf184844.g121	Pycnoporus cinnabarinus BRFM 137	CYP5035AZ2_Trametes_versicolor	55,52	589
jgi|Cytmel1|1284143|e_gw1.178.7.1	Cytidiella melzeri FP 102339 v1.0	CYP5035Z1	55,33	544
jgi|Fibsp1|889927|fgenesh1_pg.56_#_70	Fibulorhizoctonia sp. CBS 109695 v1.0	CYP5035AF2_Paxillus_involutus_AT	55,32	555
jgi|Spalat1|479667|CE479666_4080	Sparassis latifolia CCMJ1100 v1.0	CYP5035B	55,07	552
jgi|Fibsp1|743454|e_gw1.82.162.1	Fibulorhizoctonia sp. CBS 109695 v1.0	CYP5035AF2_Paxillus_involutus_AT	54,95	555
jgi|Fibsp1|923026|estExt_fgenesh1_pm.C_3	Fibulorhizoctonia sp. CBS 109695 v1.0	CYP5035AF2_Paxillus_involutus_AT	54,95	555
jgi|Irplac1|1640241|MIX38339_784_26	Irpex lacteus CCBAS Fr. 238 617/93 v1.0	CYP5035A11	54,84	547
jgi|Earsca1|161568|CE161567_965	Earliella scabrosa CIRM-BRFM 1817 v1.0	CYP5035N8_Polyporus	54,8	562
jgi|Fibsp1|779072|estExt_Genewise1.C_220	Fibulorhizoctonia sp. CBS 109695 v1.0	CYP5035AF2_Paxillus_involutus_AT	54,61	542
jgi|Pycci1|4038|scf184844.g120	Pycnoporus cinnabarinus BRFM 137	CYP5035AZ2_Trametes_versicolor	54,59	599
jgi|Pycsa1|1672486|gm1.2126_g	Pycnoporus sanguineus BRFM 1264 v1.0	CYP5035AZ2_Trametes_versicolor	54,51	587
jgi|Fibsp1|1051510|estExt_Genemark1.C_20	Fibulorhizoctonia sp. CBS 109695 v1.0	CYP5035AF2_Paxillus_involutus_AT	54,48	558
jgi|Dicsqu18370_1|373775|CE373774_947	Dichomitus squalens OM18370.1 v1.0	CYP5035R1	54,24	601
jgi|Abobie1|721434|e_gw1.24.75.1	Abortiporus biennis CIRM-BRFM1778 v1	CYP5035A11	54,1	549

jgi|Dicsq1|72391|e_gw1.93.9.1	Dichomitus squalens LYAD-421 SS1 v1.0	CYP5035R1	54,08	601
jgi|Dicsqu463_1|1045640|MIX20831_915_3	Dichomitus squalens CBS463.89 v1.0	CYP5035R1	54,08	601
jgi|Spalat1|746579|fgenesh1_pg.6_#_56	Sparassis latifolia CCMJ1100 v1.0	CYP5035B	53,99	552
jgi|Dicsq1|94627|estExt_Genewise1.C_1180	Dichomitus squalens LYAD-421 SS1 v1.0	CYP5035R1	53,91	601
jgi|Hydfim1|986302|fgenesh1_pm.21_#_30	Hydnopolyporus fimbriatus CBS384.51 v1.0	CYP5035Z1	53,64	550
jgi|Irplac1|1595468|gm1.9138_g	Irpex lacteus CCBAS Fr. 238 617/93 v1.0	CYP5035Z1	53,64	550
jgi|Irplac1|743245|CE743244_3999	Irpex lacteus CCBAS Fr. 238 617/93 v1.0	CYP5035A10	53,61	485
jgi|Pycco1|1292875|CE1292874_4946	Pycnoporus coccineus BRFM 310 v1.0	CYP5035AZ2_Trametes_versicolor	53,55	577
jgi|Cytmel1|1406248|fgenesh1_pm.68_#_6	Cytidiella melzeri FP 102339 v1.0	CYP5035Z1	53,28	548
jgi|Lacqui1|1804036|gm1.10497_g	Lactarius quietus S23C v1.0	CYP5035X1	53,02	530
jgi|Irplac1|1595456|gm1.9126_g	Irpex lacteus CCBAS Fr. 238 617/93 v1.0	CYP5035Z1	52,73	550
jgi|Pyccin1|1050304|gm1.4847_g	Pycnoporus cinnabarinus CIRM-BRFM 50 v1.0	CYP5035AZ2_Trametes_versicolor	52,15	581
jgi|Panru1|1664624|fgenesh1_kg.84_#_44_#	Panus rudis PR-1116 ss-1 v1.0	CYP5035Z1	51,92	547
jgi|Fomfom1|1343990|estExt_Genewise1Plu	Fomes fomentarius CIRM-BRFM 1821 v1.0	CYP5035N8_Polyporus	51,83	573
jgi|Pyccin1|1050305|gm1.4848_g	Pycnoporus cinnabarinus CIRM-BRFM 50 v1.0	CYP5035N12_Lentinus	51,75	570
jgi|Panru1|1112951|CE1112950_7139	Panus rudis PR-1116 ss-1 v1.0	CYP5035A11	51,47	544
jgi|Panru1|1251950|CE1251949_2310	Panus rudis PR-1116 ss-1 v1.0	CYP5035A11	50,83	545
jgi|Cytmel1|1423468|gm1.13794_g	Cytidiella melzeri FP 102339 v1.0	CYP5035A11	49,91	553
jgi|Armosto1|262563|mRNA_AROS_05965_A	Armillaria ostoyae C18/9	CYP5035U4	49,79	480
jgi|Earsca1|770306|fgenesh1_pm.13_#_369	Earliella scabrosa CIRM-BRFM 1817 v1.0	CYP5035N7_Polyporus arcularius	49	573
jgi|Thega1|3184669|gm1.2733_g	Thelephora ganbajun P2 v1.0	CYP5035AF2_Paxillus_involutus_AT	48,63	547
jgi|Scysp1_1|1357562|fgenesh1_kg.10_#_75	Scytinostroma sp. KUC9335 v1.0	CYP5035X1	48,52	573
jgi|Earsca1|162544|CE162543_209	Earliella scabrosa CIRM-BRFM 1817 v1.0	CYP5035S11_Lentinus tigrinus	48	576
jgi|Gyman1|804697|e_gw1.2.217.1	Gymnopus androsaceus JB14 v1.0	CYP5035AG2_Hebeloma_cylindrosp	47,39	536
jgi|Earsca1|626821|e_gw1.14.577.1	Earliella scabrosa CIRM-BRFM 1817 v1.0	CYP5035N7_Polyporus arcularius	47	569
jgi|Earsca1|801066|gm1.12136_g	Earliella scabrosa CIRM-BRFM 1817 v1.0	CYP5035Q1 Ganoderma lucidum GL	47	578
jgi|Earsca1|262364|CE262363_3037	Earliella scabrosa CIRM-BRFM 1817 v1.0	CYP5035S6_Polyporus	46,55	580
jgi|Suiame1|1052513|MIX32399_696_33	Suillus americanus EM31 v1.0	CYP5035AG2_Hebeloma_cylindrosp	45,97	546
jgi|Phaca1|131233|estExt_Genewise1.C_13_	Phanerochaete carnosa HHB-10118-Sp v1.0	CYP5035A_Phanerochaete_carnosa	44,51	519

CYP5035S7-similar CYP5035 sequences sorted by fungal species

seq ID	species	best hit	%ID	aln length
jgi|Abobie1|826912|MIX14629_1887_37	Abortiporus biennis CIRM-BRFM1778 v1	CYP5035D3	62,09	517
jgi|Abobie1|721434|e_gw1.24.75.1	Abortiporus biennis CIRM-BRFM1778 v1	CYP5035A11	54,1	549
jgi|Anobom1|1218668|e_gw1.230.7.1	Anomoporia bombycina ATCC 64506 v1.0	CYP5035AG1_Plicaturopsis_c	62,39	561
jgi|Armosto1|262563|mRNA_AROS_059	Armillaria ostoyae C18/9	CYP5035U4	49,79	480
jgi|Artele1122_1|246774|CE246773_339	Artolenzites elegans CIRM-BRFM 1663 v1.	CYP5035AV1_Polyporus_arcu	100	566
jgi|Artele1122_1|466036|e_gw1.2.699.1	Artolenzites elegans CIRM-BRFM 1663 v1.	CYP5035H5_Trametes_versic	80,51	554
jgi|Artel1|850992|fgenesh1_pm.18_#_4	Artolenzites elegans CIRM-BRFM 1663 v1.	CYP5035H5_Trametes_versic	80,14	554
jgi|Artel1|806710|fgenesh1_kg.13_#_28	Artolenzites elegans CIRM-BRFM 1663 v1.	CYP5035N20_Trametes_versi	64,8	537
jgi|Artele1122_1|650705|MIX32502_84_	Artolenzites elegans CIRM-BRFM 1663 v1.	CYP5035N20_Trametes_versi	63,25	536
jgi|Artele1122_1|495741|fgenesh1_pg.4	Artolenzites elegans CIRM-BRFM 1663 v1.	CYP5035AZ1_Trametes_versi	62,46	562
jgi|Artel1|812991|fgenesh1_kg.54_#_10	Artolenzites elegans CIRM-BRFM 1663 v1.	CYP5035AZ1_Trametes_versi	62,28	562
jgi|Boled1|909694|estExt_Genewise1Plu	Boletus edulis BED1 v4.0	CYP5035AF1_Hydnomerulius	77,97	581
jgi|Cersu1|119768|estExt_fgenesh1_kg.(	Ceriporiopsis (Gelatoporia) subvermispora B	CYP5035AF4_Suillus_luteus_l	96,96	559
jgi|Clapy1|1913257|gm1.3000_g	Clavicorona pyxidata HHB10654 v1.0	CYP5035X1	56,05	562
jgi|Clibor1|119449|CE119448_2934	Climacocystis borealis CliBor001 v1.0	CYP5035A10	57,82	486
jgi|Clibor1|1197786|fgenesh1_kg.12_#_	Climacocystis borealis CliBor001 v1.0	CYP5035Z1	56,25	544
jgi|Conol1|919316|fgenesh1_pm.38_#_3	Coniophora olivacea MUCL 20566 v1.0	CYP5035AF1_Hydnomerulius	59,72	581
jgi|Cytmel1|1418953|gm1.9279_g	Cytidiella melzeri FP 102339 v1.0	CYP5035D3	61,85	540
jgi|Cytmel1|1284143|e_gw1.178.7.1	Cytidiella melzeri FP 102339 v1.0	CYP5035Z1	55,33	544
jgi|Cytmel1|1406248|fgenesh1_pm.68_#	Cytidiella melzeri FP 102339 v1.0	CYP5035Z1	53,28	548
jgi|Cytmel1|1423468|gm1.13794_g	Cytidiella melzeri FP 102339 v1.0	CYP5035A11	49,91	553
jgi|Denbi1|815498|fgenesh1_pm.4_#_2(	Dendrothele bispora CBS 962.96 v1.0	CYP5035AF4_Suillus_luteus_l	89,54	564
jgi|Dicsqu463_1|993380|fgenesh1_pm.2	Dichomitus squalens CBS463.89 v1.0	CYP5035H1_Ganoderma_sine	80,55	550
jgi|Dicsqu463_1|988899|fgenesh1_pm.5	Dichomitus squalens CBS463.89 v1.0	CYP5035G1 Ganoderma lucid	77	622
jgi|Dicsqu463_1|967115|fgenesh1_kg.25	Dichomitus squalens CBS463.89 v1.0	CYP5035S3_Ganoderma_sine	74	554
jgi|Dicsqu463_1|1021296|gm1.7704_g	Dichomitus squalens CBS463.89 v1.0	CYP5035N2_Ganoderma_sine	73,1	554
jgi|Dicsqu463_1|967109|fgenesh1_kg.25	Dichomitus squalens CBS463.89 v1.0	CYP5035N2_Ganoderma_sine	70,02	557
jgi|Dicsqu463_1|903800|estExt_Genewi	Dichomitus squalens CBS463.89 v1.0	CYP5035AV1_Polyporus	64,41	562

jgi|Dicsqu463_1|992959|fgenesh1_pm.2	Dichomitus squalens CBS463.89 v1.0	CYP5035P1	61,04	498
jgi|Dicsqu463_1|995233|fgenesh1_pm.6	Dichomitus squalens CBS463.89 v1.0	CYP5035L1 Ganoderma lucidu	60	481
jgi|Dicsqu463_1|974740|fgenesh1_kg.63	Dichomitus squalens CBS463.89 v1.0	CYP5035Q1	55,58	556
jgi|Dicsqu463_1|1045640|MIX20831_91	Dichomitus squalens CBS463.89 v1.0	CYP5035R1	54,08	601
jgi|Dicsqu464_1|919019|fgenesh1_kg.11	Dichomitus squalens CBS464.89 v1.0	CYP5035G1 Ganoderma lucid	81	598
jgi|Dicsqu464_1|918682|fgenesh1_kg.10	Dichomitus squalens CBS464.89 v1.0	CYP5035H1_Ganoderma_sine	80,55	550
jgi|Dicsqu464_1|935569|fgenesh1_kg.10	Dichomitus squalens CBS464.89 v1.0	CYP5035S3_Ganoderma_sine	74	554
jgi|Dicsqu464_1|935554|fgenesh1_kg.10	Dichomitus squalens CBS464.89 v1.0	CYP5035N2_Ganoderma_sine	73,1	554
jgi|Dicsqu464_1|935562|fgenesh1_kg.10	Dichomitus squalens CBS464.89 v1.0	CYP5035N2_Ganoderma_sine	70,02	557
jgi|Dicsqu464_1|887949|estExt_Genewi	Dichomitus squalens CBS464.89 v1.0	CYP5035AV1_Polyporus	64,41	562
jgi|Dicsqu464_1|827640|e_gw1.102.67.1	Dichomitus squalens CBS464.89 v1.0	CYP5035P1	62,01	487
jgi|Dicsqu464_1|951341|fgenesh1_pm.1	Dichomitus squalens CBS464.89 v1.0	CYP5035P1	61,04	498
jgi|Dicsqu464_1|953386|fgenesh1_pm.2	Dichomitus squalens CBS464.89 v1.0	CYP5035L1 Ganoderma lucidu	60	481
jgi|Dicsqu464_1|938285|fgenesh1_kg.13	Dichomitus squalens CBS464.89 v1.0	CYP5035Q1	55,58	556
jgi|Dicsq1|151582|estExt_fgenesh1_pm.	Dichomitus squalens LYAD-421 SS1 v1.0	CYP5035H1_Ganoderma_sine	80,55	550
jgi|Dicsq1|179419|estExt_Genemark1.C_	Dichomitus squalens LYAD-421 SS1 v1.0	CYP5035G1 Ganoderma lucid	77	622
jgi|Dicsq1|72385|e_gw1.93.13.1	Dichomitus squalens LYAD-421 SS1 v1.0	CYP5035N2_Ganoderma_sine	73,33	540
jgi|Dicsq1|164054|estExt_fgenesh1_pg.C	Dichomitus squalens LYAD-421 SS1 v1.0	CYP5035S3_Ganoderma_sine	73	554
jgi|Dicsq1|94181|estExt_Genewise1.C_9	Dichomitus squalens LYAD-421 SS1 v1.0	CYP5035N2_Ganoderma_sine	69,84	557
jgi|Dicsq1|147086|fgenesh1_pm.13_#_9	Dichomitus squalens LYAD-421 SS1 v1.0	CYP5035Q1	64,73	550
jgi|Dicsq1|156277|estExt_fgenesh1_pm.	Dichomitus squalens LYAD-421 SS1 v1.0	CYP5035AV1_Polyporus_arcu	64,3	563
jgi|Dicsq1|161810|estExt_fgenesh1_pg.C	Dichomitus squalens LYAD-421 SS1 v1.0	CYP5035L1 Ganoderma lucidu	60	482
jgi|Dicsq1|172004|gm1.7773_g	Dichomitus squalens LYAD-421 SS1 v1.0	CYP5035Q1	55,58	556
jgi|Dicsq1|72391|e_gw1.93.9.1	Dichomitus squalens LYAD-421 SS1 v1.0	CYP5035R1	54,08	601
jgi|Dicsq1|94627|estExt_Genewise1.C_1	Dichomitus squalens LYAD-421 SS1 v1.0	CYP5035R1	53,91	601
jgi|Dicsqu18370_1|660324|e_gw1.25.17	Dichomitus squalens OM18370.1 v1.0	CYP5035H1_Ganoderma_sine	80,55	550
jgi|Dicsqu18370_1|806887|gm1.5849_g	Dichomitus squalens OM18370.1 v1.0	CYP5035G1 Ganoderma lucid	78	622
jgi|Dicsqu18370_1|696349|estExt_Gene	Dichomitus squalens OM18370.1 v1.0	CYP5035S3_Ganoderma_sine	74	554
jgi|Dicsqu18370_1|665075|e_gw1.45.36	Dichomitus squalens OM18370.1 v1.0	CYP5035N2_Ganoderma_sine	73,1	554
jgi|Dicsqu18370_1|765132|fgenesh1_kg	Dichomitus squalens OM18370.1 v1.0	CYP5035J1_Ganoderma_sp._	72,74	565
jgi|Dicsqu18370_1|843352|MIX30610_1	Dichomitus squalens OM18370.1 v1.0	CYP5035N2_Ganoderma_sine	70,38	557
jgi|Dicsqu18370_1|762016|fgenesh1_kg	Dichomitus squalens OM18370.1 v1.0	CYP5035AV1_Polyporus	64,53	561

jgi|Dicsqu18370_1|779171|fgenesh1_pm	Dichomitus squalens OM18370.1 v1.0	CYP5035L1 Ganoderma lucidu	61	481
jgi|Dicsqu18370_1|373931|CE373930_7	Dichomitus squalens OM18370.1 v1.0	CYP5035P1	58	551
jgi|Dicsqu18370_1|706065|estExt_Gene	Dichomitus squalens OM18370.1 v1.0	CYP5035Q1	55,58	556
jgi|Dicsqu18370_1|373775|CE373774_9	Dichomitus squalens OM18370.1 v1.0	CYP5035R1	54,24	601
jgi|Earsca1|728492|fgenesh1_kg.7_#_16	Earliella scabrosa CIRM-BRFM 1817 v1.0	CYP5035H2_Polyporus_arcula	83,3	545
jgi|Earsca1|733523|fgenesh1_kg.9_#_51	Earliella scabrosa CIRM-BRFM 1817 v1.0	CYP5035G1_Ganoderma_sine	73	563
jgi|Earsca1|801019|gm1.12089_g	Earliella scabrosa CIRM-BRFM 1817 v1.0	CYP5035N7_Polyporus	66,9	565
jgi|Earsca1|184441|CE184440_1205	Earliella scabrosa CIRM-BRFM 1817 v1.0	CYP5035AV1_Polyporus_arcu	64,36	592
jgi|Earsca1|801067|gm1.12137_g	Earliella scabrosa CIRM-BRFM 1817 v1.0	CYP5035N5_Polyporus_arcula	64,23	562
jgi|Earsca1|799697|gm1.10767_g	Earliella scabrosa CIRM-BRFM 1817 v1.0	CYP5035N7_Polyporus	59,82	555
jgi|Earsca1|162226|CE162225_1265	Earliella scabrosa CIRM-BRFM 1817 v1.0	CYP5035S26_Polyporus	58,73	550
jgi|Earsca1|683000|estExt_Genewise1Pl	Earliella scabrosa CIRM-BRFM 1817 v1.0	CYP5035S3_Ganoderma_sine	56	587
jgi|Earsca1|604737|e_gw1.1.2281.1	Earliella scabrosa CIRM-BRFM 1817 v1.0	CYP5035AZ2_Trametes_versi	55,76	590
jgi|Earsca1|639881|estExt_Genewise1.C	Earliella scabrosa CIRM-BRFM 1817 v1.0	CYP5035S22_Polyporus	55,67	582
jgi|Earsca1|161568|CE161567_965	Earliella scabrosa CIRM-BRFM 1817 v1.0	CYP5035N8_Polyporus	54,8	562
jgi|Earsca1|770306|fgenesh1_pm.13_#_	Earliella scabrosa CIRM-BRFM 1817 v1.0	CYP5035N7_Polyporus arcula	49	573
jgi|Earsca1|162544|CE162543_209	Earliella scabrosa CIRM-BRFM 1817 v1.0	CYP5035S11_Lentinus tigrinu	48	576
jgi|Earsca1|626821|e_gw1.14.577.1	Earliella scabrosa CIRM-BRFM 1817 v1.0	CYP5035N7_Polyporus arcula	47	569
jgi|Earsca1|801066|gm1.12136_g	Earliella scabrosa CIRM-BRFM 1817 v1.0	CYP5035Q1 Ganoderma lucid	47	578
jgi|Earsca1|262364|CE262363_3037	Earliella scabrosa CIRM-BRFM 1817 v1.0	CYP5035S6_Polyporus	46,55	580
jgi|Fibsp1|889927|fgenesh1_pg.56_#_7(	Fibulorhizoctonia sp. CBS 109695 v1.0	CYP5035AF2_Paxillus_involut	55,32	555
jgi|Fibsp1|743454|e_gw1.82.162.1	Fibulorhizoctonia sp. CBS 109695 v1.0	CYP5035AF2_Paxillus_involut	54,95	555
jgi|Fibsp1|923026|estExt_fgenesh1_pm.	Fibulorhizoctonia sp. CBS 109695 v1.0	CYP5035AF2_Paxillus_involut	54,95	555
jgi|Fibsp1|779072|estExt_Genewise1.C_	Fibulorhizoctonia sp. CBS 109695 v1.0	CYP5035AF2_Paxillus_involut	54,61	542
jgi|Fibsp1|1051510|estExt_Genemark1.(	Fibulorhizoctonia sp. CBS 109695 v1.0	CYP5035AF2_Paxillus_involut	54,48	558
jgi|Fomfom1|424094|CE424093_631	Fomes fomentarius CIRM-BRFM 1821 v1.0	CYP5035H2_Polyporus_arcula	81,97	549
jgi|Fomfom1|1363757|gm1.1551_g	Fomes fomentarius CIRM-BRFM 1821 v1.0	CYP5035N7_Polyporus	69,82	560
jgi|Fomfom1|130388|CE130387_124	Fomes fomentarius CIRM-BRFM 1821 v1.0	CYP5035AV1_Polyporus_arcu	67,25	571
jgi|Fomfom1|1363759|gm1.1553_g	Fomes fomentarius CIRM-BRFM 1821 v1.0	CYP5035S18_Polyporus	65,26	567
jgi|Fomfom1|1363762|gm1.1556_g	Fomes fomentarius CIRM-BRFM 1821 v1.0	CYP5035N5_Polyporus_arcula	59,18	561
jgi|Fomfom1|1233304|fgenesh1_kg.1_#	Fomes fomentarius CIRM-BRFM 1821 v1.0	CYP5035S6_Polyporus	57,8	564
jgi|Fomfom1|1343990|estExt_Genewise	Fomes fomentarius CIRM-BRFM 1821 v1.0	CYP5035N8_Polyporus	51,83	573

jgi|Gyman1|804697|e_gw1.2.217.1	Gymnopus androsaceus JB14 v1.0	CYP5035AG2_Hebeloma_cyli	47,39	536
jgi|Gyrli1|796093|fgenesh1_pm.14_#_1	Gyrodon lividus BX v1.0	CYP5035AF2_Paxillus_involut	86,2	558
jgi|Hexnit1|1215331|fgenesh1_pm.1_#_	Hexagonia nitida CIRM-BRFM 1802 v1.0	CYP5035H3_Polyporus	82	550
jgi|Hexnit1|1268939|gm1.4816_g	Hexagonia nitida CIRM-BRFM 1802 v1.0	CYP5035AF4_Suillus_luteus_l	78,55	564
jgi|Hexnit1|1266762|gm1.2639_g	Hexagonia nitida CIRM-BRFM 1802 v1.0	CYP5035N7_Polyporus	70,97	558
jgi|Hexnit1|1217413|fgenesh1_pm.3_#_	Hexagonia nitida CIRM-BRFM 1802 v1.0	CYP5035N5_Polyporus_arcul	64,75	556
jgi|Hexnit1|1160509|fgenesh1_kg.5_#_1	Hexagonia nitida CIRM-BRFM 1802 v1.0	CYP5035S11_Lentinus	58,23	589
jgi|Hexnit1|1146372|fgenesh1_kg.3_#_1	Hexagonia nitida CIRM-BRFM 1802 v1.0	CYP5035S22_Polyporus	57,27	578
jgi|Hydfim1|986302|fgenesh1_pm.21_#_	Hydnopolyporus fimbriatus CBS384.51 v1.0	CYP5035Z1	53,64	550
jgi|Irplac1|1640241|MIX38339_784_26	Irpex lacteus CCBAS Fr. 238 617/93 v1.0	CYP5035A11	54,84	547
jgi|Irplac1|1595468|gm1.9138_g	Irpex lacteus CCBAS Fr. 238 617/93 v1.0	CYP5035Z1	53,64	550
jgi|Irplac1|743245|CE743244_3999	Irpex lacteus CCBAS Fr. 238 617/93 v1.0	CYP5035A10	53,61	485
jgi|Irplac1|1595456|gm1.9126_g	Irpex lacteus CCBAS Fr. 238 617/93 v1.0	CYP5035Z1	52,73	550
jgi|Lacqui1|1804036|gm1.10497_g	Lactarius quietus S23C v1.0	CYP5035X1	53,02	530
jgi|Tralac1|370287|CE370286_1031	Leiotrametes lactinea CIRM-BRFM 1664 v1.0	CYP5035H5_Trametes_versic	79,3	546
jgi|Tralac1|205625|CE205624_1029	Leiotrametes lactinea CIRM-BRFM 1664 v1.0	CYP5035N20_Trametes_versi	71,51	551
jgi|Tralac1|748415|fgenesh1_pm.18_#_	Leiotrametes lactinea CIRM-BRFM 1664 v1.0	CYP5035AZ1_Trametes_versi	62,57	561
jgi|Tramen1|1047947|fgenesh1_pm.42_	Leiotrametes menziesii CIRM-BRFM 1781 v1.0	CYP5035H5_Trametes_versic	79,53	552
jgi|Tramen1|1064764|MIX4850_687_91	Leiotrametes menziesii CIRM-BRFM 1781 v1.0	CYP5035N19_Trametes_versi	62,39	553
jgi|Tramen1|1044824|fgenesh1_pm.12_	Leiotrametes menziesii CIRM-BRFM 1781 v1.0	CYP5035AZ1_Trametes_versi	62,32	552
jgi|Leisp1|1318962|fgenesh1_kg.12_#_1	Leiotrametes sp BRFM 1775 v1.0	CYP5035H5_Trametes_versic	79,68	556
jgi|Leisp1|1371152|gm1.5594_g	Leiotrametes sp BRFM 1775 v1.0	CYP5035N20_Trametes_versi	71,14	551
jgi|Leisp1|1369699|gm1.4141_g	Leiotrametes sp BRFM 1775 v1.0	CYP5035AZ1_Trametes_versi	64,26	554
jgi|Leisp1|1345114|fgenesh1_pm.29_#_	Leiotrametes sp BRFM 1775 v1.0	CYP5035N19_Trametes_versi	62,41	540
jgi|Lenti6_1|578269|fgenesh1_kg.34_#_	Lentinus tigrinus ALCF2SS1-6 v1.0	CYP5035H4_Lentinus	100	558
jgi|Lenti6_1|581920|fgenesh1_kg.91_#_	Lentinus tigrinus ALCF2SS1-6 v1.0	CYP5035N12_Lentinus	100	563
jgi|Lenti6_1|558432|estExt_Genewise1P	Lentinus tigrinus ALCF2SS1-6 v1.0	CYP5035N17_Lentinus	100	544
jgi|Lenti6_1|581782|fgenesh1_kg.85_#_	Lentinus tigrinus ALCF2SS1-6 v1.0	CYP5035S10_Lentinus	100	592
jgi|Lenti6_1|658665|estExt_Genemark1.	Lentinus tigrinus ALCF2SS1-6 v1.0	CYP5035S11_Lentinus	100	614
jgi|Lenti6_1|581800|fgenesh1_kg.85_#_	Lentinus tigrinus ALCF2SS1-6 v1.0	CYP5035S12_Lentinus	100	594
jgi|Lenti6_1|578126|fgenesh1_kg.33_#_	Lentinus tigrinus ALCF2SS1-6 v1.0	CYP5035S17_Polyporus	100	538
jgi|Lenti6_1|581802|fgenesh1_kg.85_#_	Lentinus tigrinus ALCF2SS1-6 v1.0	CYP5035S21_Lentinus	100	573

jgi|Lenti6_1|527996|estExt_Genewise1.(	Lentinus tigrinus ALCF2SS1-6 v1.0	CYP5035S7_Lentinus	100	558
jgi|Lenti6_1|552293|estExt_Genewise1P	Lentinus tigrinus ALCF2SS1-6 v1.0	CYP5035S9_Polyporus	100	590
jgi|Lenti6_1|611133|gm1.6018_g	Lentinus tigrinus ALCF2SS1-6 v1.0	CYP5035AU5_Lentinus	100	559
jgi|Lenti6_1|586062|fgenesh1_pm.16_#	Lentinus tigrinus ALCF2SS1-6 v1.0	CYP5035AU6_Lentinus	100	556
jgi|Lenti6_1|547581|estExt_Genewise1P	Lentinus tigrinus ALCF2SS1-6 v1.0	CYP5035AU7_Lentinus	100	559
jgi|Lenti6_1|581076|fgenesh1_kg.66_#_	Lentinus tigrinus ALCF2SS1-6 v1.0	CYP5035AV3_Lentinus	100	580
jgi|Lenti6_1|628086|MIX9889_14_24	Lentinus tigrinus ALCF2SS1-6 v1.0	CYP5035AZ2_Trametes_versi	74,26	575
jgi|Lenti7_1|538117|fgenesh1_kg.30_#_	Lentinus tigrinus ALCF2SS1-7 v1.0	CYP5035N12_Lentinus	100	563
jgi|Lenti7_1|468757|e_gw1.30.223.1	Lentinus tigrinus ALCF2SS1-7 v1.0	CYP5035N17_Lentinus	100	544
jgi|Lenti7_1|538108|fgenesh1_kg.30_#_	Lentinus tigrinus ALCF2SS1-7 v1.0	CYP5035S11_Lentinus	100	585
jgi|Lenti7_1|572566|gm1.8370_g	Lentinus tigrinus ALCF2SS1-7 v1.0	CYP5035S14_Lentinus	100	560
jgi|Lenti7_1|489422|estExt_Genewise1.(	Lentinus tigrinus ALCF2SS1-7 v1.0	CYP5035S15_Lentinus	100	560
jgi|Lenti7_1|540912|fgenesh1_kg.70_#_	Lentinus tigrinus ALCF2SS1-7 v1.0	CYP5035S21_Lentinus	100	573
jgi|Lenti7_1|510889|estExt_Genewise1P	Lentinus tigrinus ALCF2SS1-7 v1.0	CYP5035S7_Lentinus	100	558
jgi|Lenti7_1|390492|CE390491_458	Lentinus tigrinus ALCF2SS1-7 v1.0	CYP5035AU5_Lentinus	100	559
jgi|Lenti7_1|545110|fgenesh1_pm.9_#_	Lentinus tigrinus ALCF2SS1-7 v1.0	CYP5035AU6_Lentinus	100	556
jgi|Lenti7_1|533921|fgenesh1_kg.9_#_1	Lentinus tigrinus ALCF2SS1-7 v1.0	CYP5035AU7_Lentinus	100	559
jgi|Lenti7_1|540886|fgenesh1_kg.70_#_	Lentinus tigrinus ALCF2SS1-7 v1.0	CYP5035S10_Lentinus	99,83	590
jgi|Lenti7_1|564891|gm1.695_g	Lentinus tigrinus ALCF2SS1-7 v1.0	CYP5035H4_Lentinus	99,64	558
jgi|Lenti7_1|548440|fgenesh1_pm.57_#	Lentinus tigrinus ALCF2SS1-7 v1.0	CYP5035AV3_Lentinus	99,31	580
jgi|Lenti7_1|540902|fgenesh1_kg.70_#_	Lentinus tigrinus ALCF2SS1-7 v1.0	CYP5035S12_Lentinus	96,79	592
jgi|Sisbr1|623797|gm1.4470_g	Lentinus tigrinus v1.0	CYP5035N10_Polyporus	100	560
jgi|Sisbr1|585391|fgenesh1_kg.48_#_39	Lentinus tigrinus v1.0	CYP5035N12_Lentinus	100	563
jgi|Sisbr1|570632|estExt_Genewise1Plus	Lentinus tigrinus v1.0	CYP5035N17_Lentinus	100	544
jgi|Sisbr1|627566|gm1.8239_g	Lentinus tigrinus v1.0	CYP5035S14_Lentinus	100	560
jgi|Sisbr1|544206|estExt_Genewise1.C_	Lentinus tigrinus v1.0	CYP5035S15_Lentinus	100	560
jgi|Sisbr1|582002|fgenesh1_kg.19_#_12	Lentinus tigrinus v1.0	CYP5035S7_Lentinus	100	558
jgi|Sisbr1|585400|fgenesh1_kg.48_#_48	Lentinus tigrinus v1.0	CYP5035S11_Lentinus	99,66	585
jgi|Sisbr1|586099|fgenesh1_kg.66_#_27	Lentinus tigrinus v1.0	CYP5035S21_Lentinus	99,65	573
jgi|Sisbr1|574375|fgenesh1_kg.2_#_756	Lentinus tigrinus v1.0	CYP5035H4_Lentinus	99,64	558
jgi|Sisbr1|586078|fgenesh1_kg.66_#_6_	Lentinus tigrinus v1.0	CYP5035S10_Lentinus	98,61	577
jgi|Sisbr1|640151|MIX7816_141_38	Lentinus tigrinus v1.0	CYP5035AV3_Lentinus	96,81	565

jgi|Sisbr1|586093|fgenesh1_kg.66_#_21	Lentinus tigrinus v1.0	CYP5035S12_Lentinus	95,61	592
jgi|Sisbr1|577407|fgenesh1_kg.6_#_311	Lentinus tigrinus v1.0	CYP5035AU7_Lentinus	85,69	559
jgi|Sisbr1|571658|estExt_Genewise1Plus	Lentinus tigrinus v1.0	CYP5035AW1_Lentinus	73,58	564
jgi|Leumo1|1005994|e_gw1.00033.92.1	Leucogyrophana mollusca KUC20120723A-06 v1.0	CYP5035AF1_Hydnomerulius	71,6	581
jgi|Obbri1|890182|estExt_Genemark1.C	Obba rivulosa 3A-2 v1.0	CYP5035B	85,41	555
jgi|Panru1|1664624|fgenesh1_kg.84_#_	Panus rudis PR-1116 ss-1 v1.0	CYP5035Z1	51,92	547
jgi|Panru1|1112951|CE1112950_7139	Panus rudis PR-1116 ss-1 v1.0	CYP5035A11	51,47	544
jgi|Panru1|1251950|CE1251949_2310	Panus rudis PR-1116 ss-1 v1.0	CYP5035A11	50,83	545
jgi|Paxam1|966266|fgenesh1_kg.28_#_5	Paxillus ammoniavirescens Pou09.2 v1.0	CYP5035AF2_Paxillus_involut	95,86	580
jgi|Paxin1|88877|e_gw1.305.4.1	Paxillus involutus ATCC 200175 v1.0	CYP5035H5_Trametes_versic	79,17	552
jgi|Paxru2|31013|Paxru1.fgenesh1_pm.6	Paxillus rubicundulus Ve08.2h10 v2.0	CYP5035AF3_Paxillus_rubicu	100	580
jgi|Phaca1|153972|estExt_Genewise1Plu	Phanerochaete carnosa HHB-10118-Sp v1.0	CYP5035A_Phanerochaete_ca	100	524
jgi|Phaca1|131233|estExt_Genewise1.C_	Phanerochaete carnosa HHB-10118-Sp v1.0	CYP5035A_Phanerochaete_ca	44,51	519
jgi|Phlcen1|8958|scaffold_2756.3	Phlebia centrifuga FBCC195	CYP5035Z1	61,51	530
jgi|Phlcen1|13562|scaffold_967.15	Phlebia centrifuga FBCC195	CYP5035AD1	60,53	451
jgi|Phlcen1|13559|scaffold_967.12	Phlebia centrifuga FBCC195	CYP5035AD1	59,71	489
jgi|Pismi1|551133|CE426681_14791	Pisolithus microcarpus 441 v1.0	CYP5035AF6_Pisolithus_micr	100	589
jgi|Pisti1|991388|fgenesh1_kg.1_#_205_	Pisolithus tinctorius Marx 270 v1.0	CYP5035AF5_Pisolithus_tinct	100	594
jgi|Plicr1|432908|CE251633_8389	Plicaturopsis crispa v1.0	CYP5035AG1_Plicaturopsis_c	100	571
jgi|Plicr1|52981|fgenesh1_pm.6_#_209	Plicaturopsis crispa v1.0	CYP5035AG3_Plicaturopsis_c	100	662
jgi|Polar1|665169|estExt_Genemark1.C_	Polyporus arcularius v1.0	CYP5035H2_Polyporus_arcula	100	556
jgi|Polar1|667057|estExt_Genemark1.C_	Polyporus arcularius v1.0	CYP5035N16_Polyporus	100	550
jgi|Polar1|521854|estExt_Genewise1.C_	Polyporus arcularius v1.0	CYP5035N6_Polyporus_arcula	100	538
jgi|Polar1|498992|e_gw1.455.14.1	Polyporus arcularius v1.0	CYP5035N7_Polyporus	100	564
jgi|Polar1|655629|estExt_fgenesh1_pg.C	Polyporus arcularius v1.0	CYP5035N8_Polyporus	100	564
jgi|Polar1|50867|CE50866_1041	Polyporus arcularius v1.0	CYP5035N9_Polyporus	100	613
jgi|Polar1|505708|e_gw1.1106.2.1	Polyporus arcularius v1.0	CYP5035S24_Polyporus	100	561
jgi|Polar1|531655|estExt_Genewise1.C_	Polyporus arcularius v1.0	CYP5035S25_Polyporus	100	580
jgi|Polar1|521853|estExt_Genewise1.C_	Polyporus arcularius v1.0	CYP5035S26_Polyporus	100	560
jgi|Polar1|652223|estExt_fgenesh1_pg.C	Polyporus arcularius v1.0	CYP5035S6_Polyporus_arcula	100	569
jgi|Polar1|664247|estExt_Genemark1.C_	Polyporus arcularius v1.0	CYP5035S7_Polyporus_arcula	100	565
jgi|Polar1|665466|estExt_Genemark1.C_	Polyporus arcularius v1.0	CYP5035S8_Polyporus_arcula	100	568

jgi|Polar1|668252|estExt_Genemark1.C_	Polyporus arcularius v1.0	CYP5035S9_Polyporus_arcula	100	564
jgi|Polar1|519317|estExt_Genewise1.C_	Polyporus arcularius v1.0	CYP5035AU1_Polyporus_arcu	100	560
jgi|Polar1|603200|gm1.10163_g	Polyporus arcularius v1.0	CYP5035AU2_Polyporus	100	560
jgi|Polar1|519322|estExt_Genewise1.C_	Polyporus arcularius v1.0	CYP5035AU3_Polyporus	100	559
jgi|Polar1|667894|estExt_Genemark1.C_	Polyporus arcularius v1.0	CYP5035AU7_Lentinus	84,62	559
jgi|Polar1|196845|CE196844_3694	Polyporus arcularius v1.0	CYP5035AU5_Lentinus tigrinu	66	562
jgi|Polar1|667965|estExt_Genemark1.C_	Polyporus arcularius v1.0	CYP5035AZ1_Trametes_versi	63,59	563
jgi|Polbr1|1481810|gm1.5391_g	Polyporus brumalis BRFM 1820 v1.0	CYP5035H2_Polyporus	100	556
jgi|Polbr1|1454895|fgenesh1_pm.17_#_	Polyporus brumalis BRFM 1820 v1.0	CYP5035N5_Polyporus	100	565
jgi|Polbr1|1501025|MIX9741_377_27	Polyporus brumalis BRFM 1820 v1.0	CYP5035N5_Polyporus_arcula	100	566
jgi|Polbr1|1363373|e_gw1.115.31.1	Polyporus brumalis BRFM 1820 v1.0	CYP5035N6v2_Polyporus	100	552
jgi|Polbr1|1506430|MIX15146_586_20	Polyporus brumalis BRFM 1820 v1.0	CYP5035S15_Lentinus	100	560
jgi|Polbr1|1500065|MIX8781_4600_46	Polyporus brumalis BRFM 1820 v1.0	CYP5035S22_Polyporus	100	587
jgi|Polbr1|1480930|gm1.4511_g	Polyporus brumalis BRFM 1820 v1.0	CYP5035S6_Polyporus	100	569
jgi|Polbr1|1401994|fgenesh1_kg.19_#_1	Polyporus brumalis BRFM 1820 v1.0	CYP5035S7_Polyporus	100	562
jgi|Polbr1|1401717|fgenesh1_kg.17_#_2	Polyporus brumalis BRFM 1820 v1.0	CYP5035S8_Polyporus	100	568
jgi|Polbr1|1554465|estExt_Genemark1.(	Polyporus brumalis BRFM 1820 v1.0	CYP5035AU1_Polyporus	100	560
jgi|Polbr1|1455204|fgenesh1_pm.20_#_	Polyporus brumalis BRFM 1820 v1.0	CYP5035AV1_Polyporus	100	563
jgi|Polbr1|1400732|fgenesh1_kg.13_#_2	Polyporus brumalis BRFM 1820 v1.0	CYP5035AU3_Polyporus	99,64	559
jgi|Polbr1|1561063|estExt_Genemark1.(	Polyporus brumalis BRFM 1820 v1.0	CYP5035N8_Polyporus	99,47	564
jgi|Polbr1|184586|CE184585_735	Polyporus brumalis BRFM 1820 v1.0	CYP5035N7_Polyporus	97,7	564
jgi|Polbr1|1411615|fgenesh1_kg.118_#_	Polyporus brumalis BRFM 1820 v1.0	CYP5035AU2_Polyporus	95,54	560
jgi|Polbr1|1363391|e_gw1.115.20.1	Polyporus brumalis BRFM 1820 v1.0	CYP5035N9_Polyporus arcula	94	543
jgi|Polbr1|1487827|gm1.11408_g	Polyporus brumalis BRFM 1820 v1.0	CYP5035S24_Polyporus arcul	89	556
jgi|Polbr1|1422973|fgenesh1_pg.126_#_	Polyporus brumalis BRFM 1820 v1.0	CYP5035AW1_Lentinus tigrin	61	549
jgi|Polsqu1|24110|CE24109_7285	Polyporus squamosus CCBS 676 v1.0	CYP5035H3_Polyporus	100	556
jgi|Polsqu1|835110|estExt_Genemark1.(	Polyporus squamosus CCBS 676 v1.0	CYP5035N11_Polyporus	100	550
jgi|Polsqu1|746845|gm1.13007_g	Polyporus squamosus CCBS 676 v1.0	CYP5035N13_Polyporus	100	517
jgi|Polsqu1|818645|estExt_Genewise1Pl	Polyporus squamosus CCBS 676 v1.0	CYP5035N14_Polyporus	100	564
jgi|Polsqu1|588169|e_gw1.213.21.1	Polyporus squamosus CCBS 676 v1.0	CYP5035N15_Polyporus	100	544
jgi|Polsqu1|829759|estExt_Genemark1.(	Polyporus squamosus CCBS 676 v1.0	CYP5035S13_Polyporus	100	563
jgi|Polsqu1|834295|estExt_Genemark1.(	Polyporus squamosus CCBS 676 v1.0	CYP5035S16_Polyporus	100	550

jgi|Polsqu1|689230|fgenesh1_kg.927_#	Polyporus squamosus CCBS 676 v1.0	CYP5035S18_Polyporus	100	564
jgi|Polsqu1|676477|fgenesh1_kg.308_#	Polyporus squamosus CCBS 676 v1.0	CYP5035S19_Polyporus	100	558
jgi|Polsqu1|816847|estExt_Genewise1Pl	Polyporus squamosus CCBS 676 v1.0	CYP5035S7_Lentinus	100	558
jgi|Polsqu1|708683|fgenesh1_pm.56_#	Polyporus squamosus CCBS 676 v1.0	CYP5035AV2_Polyporus	100	564
jgi|Polsqu1|181995|CE181994_2271	Polyporus squamosus CCBS 676 v1.0	CYP5035AX1_Polyporus	100	588
jgi|Polsqu1|707000|fgenesh1_pm.22_#	Polyporus squamosus CCBS 676 v1.0	CYP5035AX2_Polyporus	100	407
jgi|Polsqu1|834477|estExt_Genemark1.(	Polyporus squamosus CCBS 676 v1.0	CYP5035AW1_Lentinus tigrin	62	571
jgi|Pycci1|9212|scf185013.g82	Pycnoporus cinnabarinus BRFM 137	CYP5035H5_Trametes_versic	74,78	452
jgi|Pycci1|2784|scf184791.g34	Pycnoporus cinnabarinus BRFM 137	CYP5035AZ1_Trametes_versi	60,36	507
jgi|Pycci1|4037|scf184844.g119	Pycnoporus cinnabarinus BRFM 137	CYP5035AZ1_Trametes_versi	60,21	563
jgi|Pycci1|4039|scf184844.g121	Pycnoporus cinnabarinus BRFM 137	CYP5035AZ2_Trametes_versi	55,52	589
jgi|Pycci1|4038|scf184844.g120	Pycnoporus cinnabarinus BRFM 137	CYP5035AZ2_Trametes_versi	54,59	599
jgi|Pyccin1|1039701|fgenesh1_pm.7_#_	Pycnoporus cinnabarinus CIRM-BRFM 50 v1.0	CYP5035AF2_Paxillus_involut	100	579
jgi|Pyccin1|1043044|fgenesh1_pm.32_#	Pycnoporus cinnabarinus CIRM-BRFM 50 v1.0	CYP5035N20_Trametes_versi	68,39	560
jgi|Pyccin1|1041334|fgenesh1_pm.17_#	Pycnoporus cinnabarinus CIRM-BRFM 50 v1.0	CYP5035AZ1_Trametes_versi	63,86	559
jgi|Pyccin1|168386|CE168385_664	Pycnoporus cinnabarinus CIRM-BRFM 50 v1.0	CYP5035AZ2_Trametes_versi	56,78	583
jgi|Pyccin1|1049319|gm1.3862_g	Pycnoporus cinnabarinus CIRM-BRFM 50 v1.0	CYP5035AZ2_Trametes_versi	56,17	575
jgi|Pyccin1|1050304|gm1.4847_g	Pycnoporus cinnabarinus CIRM-BRFM 50 v1.0	CYP5035AZ2_Trametes_versi	52,15	581
jgi|Pyccin1|1050305|gm1.4848_g	Pycnoporus cinnabarinus CIRM-BRFM 50 v1.0	CYP5035N12_Lentinus	51,75	570
jgi|Pycco1|1370331|e_gw1.30.134.1	Pycnoporus coccineus BRFM 310 v1.0	CYP5035H5_Trametes_versic	81,56	553
jgi|Pycco1|1468281|gm1.5790_g	Pycnoporus coccineus BRFM 310 v1.0	CYP5035N20_Trametes_versi	69,38	552
jgi|Pycco1|1362943|e_gw1.9.574.1	Pycnoporus coccineus BRFM 310 v1.0	CYP5035AZ1_Trametes_versi	58,61	546
jgi|Pycco1|1461855|estExt_fgenesh1_pg	Pycnoporus coccineus BRFM 310 v1.0	CYP5035AZ2_Trametes_versi	56,94	576
jgi|Pycco1|1450696|estExt_fgenesh1_pr	Pycnoporus coccineus BRFM 310 v1.0	CYP5035AZ2_Trametes_versi	56,54	573
jgi|Pycco1|1292875|CE1292874_4946	Pycnoporus coccineus BRFM 310 v1.0	CYP5035AZ2_Trametes_versi	53,55	577
jgi|Pycco1662_1|876088|gm1.4639_g	Pycnoporus coccineus CIRM1662	CYP5035H5_Trametes_versic	79,78	554
jgi|Pycco1662_1|60791|CE60790_3985	Pycnoporus coccineus CIRM1662	CYP5035N20_Trametes_versi	66,03	577
jgi|Pycco1662_1|864896|estExt_fgenesh	Pycnoporus coccineus CIRM1662	CYP5035AZ1_Trametes_versi	62,66	557
jgi|Pycco1662_1|432733|CE432732_126	Pycnoporus coccineus CIRM1662	CYP5035AZ2_Trametes_versi	58,76	565
jgi|Pycco1662_1|816086|estExt_Genewi	Pycnoporus coccineus CIRM1662	CYP5035AZ2_Trametes_versi	57,24	573
jgi|Pycco1662_1|872263|gm1.814_g	Pycnoporus coccineus CIRM1662	CYP5035AZ1_Trametes_versi	56,26	503
jgi|Pycpun1|308909|CE308908_3418	Pycnoporus puniceus CIRM-BRFM 1868 v1.0	CYP5035H5_Trametes_versic	80,25	552

jgi|Pycpun1|508212|fgenesh1_pg.13_#_	Pycnoporus puniceus CIRM-BRFM 1868 v1.0	CYP5035N20_Trametes_versi	69,23	546
jgi|Pycpun1|540139|gm1.7844_g	Pycnoporus puniceus CIRM-BRFM 1868 v1.0	CYP5035N19_Trametes_versi	59,2	549
jgi|Pycpun1|540945|gm1.8650_g	Pycnoporus puniceus CIRM-BRFM 1868 v1.0	CYP5035AZ2_Trametes_versi	57,75	587
jgi|Pycsa1|1577749|e_gw1.7180000650	Pycnoporus sanguineus BRFM 1264 v1.0	CYP5035H5_Trametes_versic	81,74	553
jgi|Pycsa1|1595909|fgenesh1_kg.sc_718	Pycnoporus sanguineus BRFM 1264 v1.0	CYP5035AZ1_Trametes_versi	63,2	557
jgi|Pycsa1|1754665|estExt_Genemark1.(	Pycnoporus sanguineus BRFM 1264 v1.0	CYP5035AZ1_Trametes_versi	61,73	567
jgi|Pycsa1|1754664|estExt_Genemark1.(	Pycnoporus sanguineus BRFM 1264 v1.0	CYP5035AZ2_Trametes_versi	57,39	582
jgi|Pycsa1|1672486|gm1.2126_g	Pycnoporus sanguineus BRFM 1264 v1.0	CYP5035AZ2_Trametes_versi	54,51	587
jgi|Rhisa1|731579|e_gw1.86.88.1	Rhizopogon salebrosus TDB-379 v1.0	CYP5035AF4_Suillus_luteus_U	78,05	565
jgi|Rhives1|3443|genemark-NODE_2123	Rhizopogon vesiculosus Smith	CYP5035N20_Trametes_versi	60,79	556
jgi|Rhivi1|681821|e_gw1.22.70.1	Rhizopogon vinicolor AM-OR11-026 v1.0	CYP5035AF4_Suillus_luteus_U	77,27	572
jgi|Sclci1|1219887|fgenesh1_kg.105_#_5	Scleroderma citrinum Foug A v1.0	CYP5035AF7_Scleroderma_ci	100	585
jgi|Scysp1_1|1357562|fgenesh1_kg.10_#	Scytinostroma sp. KUC9335 v1.0	CYP5035X1	48,52	573
jgi|Spalat1|479667|CE479666_4080	Sparassis latifolia CCMJ1100 v1.0	CYP5035B	55,07	552
jgi|Spalat1|746579|fgenesh1_pg.6_#_56	Sparassis latifolia CCMJ1100 v1.0	CYP5035B	53,99	552
jgi|Suiame1|1052513|MIX32399_696_3	Suillus americanus EM31 v1.0	CYP5035AG2_Hebeloma_cyli	45,97	546
jgi|Suibr2|843826|Suibr1.fgenesh1_pm.1	Suillus brevipes Sb2 v2.0	CYP5035B	100	561
jgi|Suidec1|1093418|fgenesh1_kg.15_#_	Suillus decipiens EM49 v1.0	CYP5035AF4_Suillus_luteus_U	90,36	560
jgi|Suigr1|580326|CE580325_2365	Suillus granulatus EM37 v1.0	CYP5035AF4_Suillus_luteus_U	91,07	560
jgi|Suilu3|24266|Suilu1.fgenesh1_pm.12	Suillus luteus UH-Slu-Lm8-n1 v3	CYP5035AF4_Suillus_luteus_U	100	559
jgi|Suipic1|1478630|gm1.2487_g	Suillus pictus EM44 v1.0	CYP5035AF4_Suillus_luteus_U	87,99	566
jgi|Suitom1|746520|fgenesh1_pm.11_#_	Suillus tomentosus FC115 v1.0	CYP5035AF4_Suillus_luteus_U	91,67	552
jgi|Thega1|3184669|gm1.2733_g	Thelephora ganbajun P2 v1.0	CYP5035AF2_Paxillus_involut	48,63	547
jgi|Trabet1|477754|CE477753_479	Trametes betulina CIRM-BRFM 1801 v1.0	CYP5035AZ2_Trametes_versi	75,82	517
jgi|Trabet1|826979|fgenesh1_kg.21_#_7	Trametes betulina CIRM-BRFM 1801 v1.0	CYP5035N20_Trametes_versi	70,38	530
jgi|Trabet1|922101|MIX14000_10_17	Trametes betulina CIRM-BRFM 1801 v1.0	CYP5035AZ1_Trametes_versi	65,34	551
jgi|Tragib1|694241|CE694240_16222	Trametes gibbosa CIRM-BRFM 1770 v1.0	CYP5035AZ2_Trametes_versi	76,63	582
jgi|Tragib1|1412667|fgenesh1_pm.40_#	Trametes gibbosa CIRM-BRFM 1770 v1.0	CYP5035N20_Trametes_versi	70,43	531
jgi|Tragib1|1392952|fgenesh1_kg.40_#_	Trametes gibbosa CIRM-BRFM 1770 v1.0	CYP5035AZ1_Trametes_versi	63,99	547
jgi|Tralj1|428191|CE428190_1838	Trametes ljubarskyi CIRM1659 v1.0	CYP5035H5_Trametes_versic	82,97	552
jgi|Tralj1|1037740|fgenesh1_pm.46_#_2	Trametes ljubarskyi CIRM1659 v1.0	CYP5035N20_Trametes_versi	69,56	542
jgi|Tralj1|559700|CE559699_1981	Trametes ljubarskyi CIRM1659 v1.0	CYP5035AZ1_Trametes_versi	68,53	556

jgi|Tramax1|1068035|fgenesh1_pm.5_#	Trametes maxima CIRM-BRFM 1813 v1.0	CYP5035H5_Trametes_versic	80,14	554
jgi|Tramax1|1073440|gm1.413_g	Trametes maxima CIRM-BRFM 1813 v1.0	CYP5035N20_Trametes_versi	67,47	541
jgi|Tramax1|1055064|fgenesh1_kg.21_#	Trametes maxima CIRM-BRFM 1813 v1.0	CYP5035N19_Trametes_versi	65,93	546
jgi|Tramax1|1065145|fgenesh1_pm.1_#	Trametes maxima CIRM-BRFM 1813 v1.0	CYP5035AZ1_Trametes_versi	65,04	552
jgi|Tramax1|1024787|fgenesh1_kg.7_#_	Trametes maxima CIRM-BRFM 1813 v1.0	CYP5035N19_Trametes_versi	60,18	550
jgi|Tramey1|997533|fgenesh1_pm.1_#_	Trametes meyenii CIRM-BRFM 1810 v1.0	CYP5035H5_Trametes_versic	79,71	552
jgi|Tramey1|914922|e_gw1.11.457.1	Trametes meyenii CIRM-BRFM 1810 v1.0	CYP5035N20_Trametes_versi	68,81	529
jgi|Tramey1|1003669|fgenesh1_pm.18_	Trametes meyenii CIRM-BRFM 1810 v1.0	CYP5035N19_Trametes_versi	66,54	541
jgi|Tramey1|1032777|MIX17440_258_2	Trametes meyenii CIRM-BRFM 1810 v1.0	CYP5035N19_Trametes_versi	61,21	531
jgi|Tramey1|1003781|fgenesh1_pm.18_	Trametes meyenii CIRM-BRFM 1810 v1.0	CYP5035AZ2_Trametes_versi	59,15	585
jgi|Trapol1|1218738|fgenesh1_pm.9_#_	Trametes polyzona CIRM-BRFM 1798 v1.0	CYP5035AW1_Lentinus	100	605
jgi|Trapol1|105914|CE105913_5115	Trametes polyzona CIRM-BRFM 1798 v1.0	CYP5035H5_Trametes_versic	87,18	554
jgi|Trapol1|1067680|e_gw1.19.24.1	Trametes polyzona CIRM-BRFM 1798 v1.0	CYP5035N19_Trametes_versi	70,47	552
jgi|Trapol1|352087|CE352086_1039	Trametes polyzona CIRM-BRFM 1798 v1.0	CYP5035AZ1_Trametes_versi	65,25	564
jgi|Trave1|41578|gm1.462_g	Trametes versicolor v1.0	CYP5035H5_Trametes_versic	100	554
jgi|Trave1|60226|estExt_fgenesh1_pm.C	Trametes versicolor v1.0	CYP5035N19_Trametes_versi	100	553
jgi|Trave1|130760|e_gw1.10.841.1	Trametes versicolor v1.0	CYP5035N20_Trametes_versi	100	581
jgi|Trave1|45128|gm1.4012_g	Trametes versicolor v1.0	CYP5035N20_Trametes_versi	100	542
jgi|Trave1|51005|gm1.9889_g	Trametes versicolor v1.0	CYP5035AZ1_Trametes_versi	100	558
jgi|Trave1|58095|estExt_fgenesh1_pm.C	Trametes versicolor v1.0	CYP5035AZ2_Trametes_versi	100	576
jgi|Traci1|1521520|gm1.6319_g	Trametopsis cervina CIRM-BRFM 1824 v1.0	CYP5035H5_Trametes_versic	84,78	552
jgi|Traci1|1402223|e_gw1.15.531.1	Trametopsis cervina CIRM-BRFM 1824 v1.0	CYP5035N20_Trametes_versi	70,56	540
jgi|Traci1|116365|CE116364_5445	Trametopsis cervina CIRM-BRFM 1824 v1.0	CYP5035AZ1_Trametes_versi	68,86	546
jgi|Traci1|268679|CE268678_1423	Trametopsis cervina CIRM-BRFM 1824 v1.0	CYP5035AZ1_Trametes_versi	65,3	559
jgi|Trace1|1049863|CE1049862_12876	Trametopsis cervina CIRM-BRFM 1824 v1.0	CYP5035D2	58,78	541
jgi|Trace1|1342868|fgenesh1_pg.4_#_4(	Trametopsis cervina CIRM-BRFM 1824 v1.0	CYP5035D2	58,7	540
jgi|Trace1|1354516|fgenesh1_kg.6_#_1	Trametopsis cervina CIRM-BRFM 1824 v1.0	CYP5035D2	58,12	554
jgi|Trace1|1409937|fgenesh1_pm.40_#_	Trametopsis cervina CIRM-BRFM 1824 v1.0	CYP5035D3	57,01	542
jgi|Xerba1|1485051|gm1.5292_g	Xerocomus badius 84.06 v1.0	CYP5035AF1_Hydnomerulius	79,29	589

Conclusion

Increasing health threats to human health like the growing microbial resistance to antibiotics[1] or the increasing frequency of cancer occurrence[2] in combination with the pharmaceutical industry's lack of success in expensive clinical trials of synthetic lead compounds derived from high-throughput screening (HTS) campaigns demanded urgent actions.[3–6] Therefore, natural products are once again receiving more and more attention by the pharmaceutical industry, although they often do not meet desired attributes like the physiochemical properties summarised in the Lipinski's Rule of Five,[3,7,8] suitability for industrial HTS[9] or easy access to sufficient quantities.[7,10,11] However, having been submitted to and passed the screening platform of the natural environment, natural products possess excellent pharmacological profiles. Since their extraordinary diversity and inherent complexity still results in stable discovery rates of structurally unique natural product scaffolds,[12] they are rightfully acknowledged as the hope and best chance to tackle pharmaceutical challenges such as the antibiotic crisis[7,13–16] and even cancer.[17–19]

Ultimately, versatile tools for facile natural product diversification are necessary and remain highly desired in order to improve their drug properties or to explore their mode of action. By showcasing the potential of P450s for this purpose, **Chapter 1** of this thesis extended the synthetic toolbox for lead diversification.[20] It could be concluded that the late-stage functionalisation ability of P450 *via* C–H bond activation indeed works beautifully for generating analogues of such complex scaffolds. Subsequently published articles already picked up this concept and added different perspectives to it.[21,22]

One of the main reasons for the hesitant implementation of such P450-catalysed syntheses in industry are the poor biocatalyst stability and low expression levels, which in turn impact the scale-up of processes targeted in synthetic chemistry.[23,24] In nature, biochemical life happens under conditions of high dilution and at very small-scales, and inhibition of P450 catalysts by higher substrate concentrations is a common problem. Thus, the successful bioreactor application of *P. pastoris*-expressed P450s demonstrated in **Chapter 2** was an important piece of evidence for several technical issues:

[1] competence of *P. pastoris* as excellent protein production host for (human) P450s at high expression levels
[2] profound enhancement of P450 catalyst stability upon application of *P. pastoris* whole-cell biocatalysts
[3] high biomass and connected whole-cell biocatalyst productivity of *P. pastoris* in preparative-scale bioreactor experiment under industrially relevant conditions
[4] possibility for executing P450-catalysed diversifications of natural products like testosterone in a preparative-scale bioreactor experiment
[5] potential for further up-scaling
[6] feasibility of downstream purification and product isolation processes *via* standard chemical procedures
[7] successful storage and subsequent usefulness of eukaryotic P450 whole-cell biocatalysts,

which symbolises a critical step forward towards industrial or synthetic implementation of this novel biocatalytic tool. At the same time, the unexpected diversity of testosterone metabolites generated by the principal human drug detoxification enzyme in the liver adds to the many interesting properties of the multifaceted P450 3A4, which are still not completely understood.[25] P450 3A4 certainly holds a lot of still hidden potential and also the newly generated metabolites await further research.

Not only since the 2018 Nobel Prize in Chemistry for the directed evolution of enzymes is this technique inevitably entangled to the topic of biocatalysis.[26] Astonishing engineering successes were achieved with P450 enzymes alone[21,27–33] such as the evolution of BM3 to catalyse unnatural reactions.[34–42] Also the engineering strategies were continuously refined or reshaped in order to save time, resources and costs for mutagenesis and screening until high quality enzyme candidates are identified. Nevertheless, in view of the Green Chemistry principles biocatalytic superiority to modern synthetic chemistry methods can hardly been justified when facing tedious efforts in the hope for prosperous screening.
Perhaps human-made enzyme engineering is not all that necessary, if there are already enzymes with the desired activity or selectivity?
Continuous natural enzyme evolution has forged P450s into the efficient machinery that they are in order to enable life as cost-effective as possible. Many P450 families of WR fungi have a large substrate scope because they are employed by the fungal defence against life-threatening xenobiotics, usually of plant origin.[43] These so-called phytochemicals are natural products that include terpenoids and steroids, or polyphenols such as flavonoids and stilbenoids, all of which comprise members with anti-oxidative, -inflammatory, -microbial, -cancer properties with health benefits for humans.[44] Hence, the P450's natural function makes them the ideal candidates for the late-stage diversification of such natural product scaffolds to enable the chemoenzymatic synthesis of novel, potentially bioactive derivatives for the pharmaceutical, or fragrance and flavour industry. Indeed, **Chapter 3** was a fantastic demonstration that there are plenty of P450s —many of them multifunctional— out there that are perfectly fit for the described task.
Yet, the relatively few number of studies available to date on the bioprospecting for such P450s of wood-degrading fungi *via* functional profiling[43,45,54–60,46–53] mirrors nicely how immensely understudied the enzymatic repertoire of fungi of the Basidiomycota as a whole really is.[61] Perhaps the fact that successful expression of such P450s even in fungal yeasts like *S. cerevisiae* or *P. pastoris* is usually based on trial and error[61] as also observed in **Chapter 3** scares researchers off. In addition, their selectivity is often restricted to a narrow range of substrates and products. However, this should not discourage as shown by a functional survey of the P450ome of the model WR fungi *Phanerochaete chrysosporium*, which demonstrated that a good percentage of P450s present could be successfully over-expressed.
Considering the natural habitats of the host organisms can provide hints for possible substrates and selectivities as was demonstrated by the discovery and catalytic characterisation of a new recombinant P450: CYP5035S7 (**Chapter 3**). In addition, the alignment of this enzyme to thousands of putative P450 sequences of dozens other fungal species provides the basis for further bioprospecting. Information about the activities of only three CYP5035 subfamilies were uncovered to date, although already >50 different CYP5035 subfamilies were categorised. Hence, this demonstrates what large functional gap and an unhidden catalytic potential remains for CYP5035, and eukaryotic P450 families.

In conclusion, the late-stage diversification of natural products catalysed by P450 enzymes is a highly versatile synthetic strategy that has already been implemented into the synthetic and pharmaceutical toolbox (**Chapter 1**).
In combination with efficient expression levels, whole-cell biocatalytic stabilities and *P. pastoris* production host characteristics this strategy can be used for the preparative-

scale synthesis of natural product analogues and may be implemented into industrial-scale processes *via* bioreactor up-scaling (**Chapter 2**).
Bioprospecting for novel and innovative P450s will further catch momentum in the future as more studies reveal the true potential of the enzymatic repertoire of WR fungi (**Chapter 3**).

[1] C. L. Ventola, *P T* **2015**, *40*, 277–83.
[2] C. P. Wild, *Nat. Rev. Cancer* **2019**, *19*, 123–124.
[3] I. B. Campbell, S. J. F. Macdonald, P. A. Procopiou, *Drug Discov. Today* **2018**, *23*, 219–234.
[4] T. Rodrigues, D. Reker, P. Schneider, G. Schneider, *Nat. Chem.* **2016**, *8*, 531–541.
[5] A. L. Harvey, R. Edrada-Ebel, R. J. Quinn, *Nat. Rev. Drug Discov.* **2015**, *14*, 111–129.
[6] M. Hay, D. W. Thomas, J. L. Craighead, C. Economides, J. Rosenthal, *Nat Biotech* **2014**, *32*, 40–51.
[7] D. J. Newman, G. M. Cragg, *J. Nat. Prod.* **2020**, *83*, 770–803.
[8] F. E. Koehn, *Med. Chem. Commun.* **2012**, *3*, 854–865.
[9] G. M. Rishton, *Am. J. Cardiol.* **2008**, *101*, 43–49.
[10] D. J. Newman, *Pharmacol. Ther.* **2016**, *162*, 1–9.
[11] B. David, J.-L. Wolfender, D. A. Dias, *Phytochem. Rev.* **2015**, *14*, 299–315.
[12] C. R. Pye, M. J. Bertin, R. S. Lokey, W. H. Gerwick, R. G. Linington, *Proc. Natl. Acad. Sci.* **2017**, *114*, 5601–5606.
[13] K. Lewis, *Cell* **2020**, *181*, 29–45.
[14] M. I. Hutchings, A. W. Truman, B. Wilkinson, *Curr. Opin. Microbiol.* **2019**, *51*, 72–80.
[15] M. Tyers, G. D. Wright, *Nat. Rev. Microbiol.* **2019**, *17*, 141–155.
[16] G. D. Wright, *Nat. Prod. Rep.* **2017**, *34*, 694–701.
[17] Q. Wu, J. P. C. Wong, H. F. Kwok, *Cells* **2020**, *9*, 1213.
[18] T. Efferth, M. E. M. Saeed, O. Kadioglu, E.-J. Seo, S. Shirooie, A. T. Mbaveng, S. M. Nabavi, V. Kuete, *Biotechnol. Adv.* **2020**, *38*, 107342.
[19] S. Dutta, S. Mahalanobish, S. Saha, S. Ghosh, P. C. Sil, *Food Chem. Toxicol.* **2019**, *128*, 240–255.
[20] N. D. Fessner, *ChemCatChem* **2019**, *11*, 2226–2242.
[21] V. B. Urlacher, M. Girhard, *Trends Biotechnol.* **2019**, *37*, 882–897.
[22] G. Di Nardo, G. Gilardi, *Trends Biochem. Sci.* **2020**, *45*, 511–525.
[23] J. Chapman, A. Ismail, C. Dinu, *Catalysts* **2018**, *8*, 238.
[24] M. T. Lundemo, J. M. Woodley, *Appl. Microbiol. Biotechnol.* **2015**, *99*, 2465–2483.
[25] F. P. Guengerich, *Chem. Res. Toxicol.* **2017**, *30*, 2–12.
[26] "The Nobel Prize in Chemistry 2018. NobelPrize.org. Nobel Media AB 2018. Sat. 10 Nov 2018," can be found under https://www.nobelprize.org/prizes/chemistry/2018/summary/, **2018**.
[27] Y. Wei, E. L. Ang, H. Zhao, *Curr. Opin. Chem. Biol.* **2018**, *43*, 1–7.
[28] R. A. Sheldon, D. Brady, *Chem. Commun.* **2018**, *54*, 6088–6104.
[29] Y. Gumulya, J.-M. Baek, S.-J. Wun, R. E. S. Thomson, K. L. Harris, D. J. B. Hunter, J. B. Y. H. Behrendorff, J. Kulig, S. Zheng, X. Wu, et al., *Nat. Catal.* **2018**, *1*, 878–888.
[30] D. Petrović, A. Bokel, M. Allan, V. B. Urlacher, B. Strodel, *J. Chem. Inf. Model.* **2018**, *58*, 848–858.
[31] J. B. Y. H. Behrendorff, W. Huang, E. M. J. Gillam, *Biochem. J.* **2015**, *467*, 1–15.
[32] S. Hoebenreich, F. E. Zilly, C. G. Acevedo-Rocha, M. Zilly, M. T. Reetz, *ACS Synth. Biol.* **2015**, *4*, 317–331.
[33] J. A. McIntosh, C. C. Farwell, F. H. Arnold, *Curr. Opin. Chem. Biol.* **2014**, *19*, 126–134.
[34] N. P. Dunham, F. H. Arnold, *ACS Catal.* **2020**, *10*, 12239–12255.

[35] K. Chen, F. H. Arnold, *Nat. Catal.* **2020**, *3*, 203–213.
[36] C. Empel, S. Jana, R. M. Koenigs, *Molecules* **2020**, *25*, 880.
[37] R. B. Leveson-Gower, C. Mayer, G. Roelfes, *Nat. Rev. Chem.* **2019**, *3*, 687–705.
[38] C. Perez-Rizquez, A. Rodriguez-Otero, J. M. Palomo, *Org. Biomol. Chem.* **2019**, *17*, 7114–7123.
[39] Y. Gu, S. N. Natoli, Z. Liu, D. S. Clark, J. F. Hartwig, *Angew. Chemie - Int. Ed.* **2019**, *58*, 13954–13960.
[40] F. H. Arnold, *Angew. Chemie - Int. Ed.* **2018**, *57*, 4143–4148.
[41] S. C. Hammer, A. M. Knight, F. H. Arnold, *Curr. Opin. Green Sustain. Chem.* **2017**, *7*, 23–30.
[42] O. F. Brandenberg, R. Fasan, F. H. Arnold, *Curr. Opin. Biotechnol.* **2017**, *47*, 102–111.
[43] K. Syed, K. Shale, N. S. Pagadala, J. Tuszynski, *PLoS One* **2014**, *9*, e86683.
[44] L. S. Oliveira, A. L. B. D. Santana, C. A. Maranhão, R. D. C. M. de Miranda, V. L. A. Galvão de Lima, S. I. da Silva, M. S. Nascimento, L. Bieber, *Int. Biodeterior. Biodegradation* **2010**, *64*, 711–715.
[45] J. Wang, H. Ohno, Y. Ide, H. Ichinose, T. Mori, H. Kawagishi, H. Hirai, *J. Hazard. Mater.* **2019**, *371*, 494–498.
[46] H. Ichinose, T. Kitaoka, *Microb. Biotechnol.* **2018**, *11*, 952–965.
[47] K. Sakai, F. Matsuzaki, L. Wise, Y. Sakai, S. Jindou, H. Ichinose, N. Takaya, M. Kato, H. Wariishi, M. Shimizu, *Appl. Environ. Microbiol.* **2018**, *84*, 1–15.
[48] C. Yang, W. Li, C. Li, Z. Zhou, Y. Xiao, X. Yan, *Phytochemistry* **2018**, *155*, 83–92.
[49] M. Hatakeyama, T. Kitaoka, H. Ichinose, *Enzyme Microb. Technol.* **2016**, *89*, 7–14.
[50] K. Syed, A. Porollo, Y. W. Lam, P. E. Grimmett, J. S. Yadav, *Appl. Environ. Microbiol.* **2013**, *79*, 2692–2702.
[51] K. Syed, A. Porollo, D. Miller, J. S. Yadav, *Protein Eng. Des. Sel.* **2013**, *26*, 553–557.
[52] M. Ide, H. Ichinose, H. Wariishi, *Arch. Microbiol.* **2012**, *194*, 243–253.
[53] H. Ichinose, H. Wariishi, *Arch. Biochem. Biophys.* **2012**, *518*, 8–15.
[54] S. Hirosue, M. Tazaki, N. Hiratsuka, S. Yanai, H. Kabumoto, R. Shinkyo, A. Arisawa, T. Sakaki, H. Tsunekawa, O. Johdo, et al., *Biochem. Biophys. Res. Commun.* **2011**, *407*, 118–123.
[55] K. Syed, A. Porollo, Y. W. Lam, J. S. Yadav, *PLoS One* **2011**, *6*, e28286.
[56] K. Syed, H. Doddapaneni, V. Subramanian, Y. W. Lam, J. S. Yadav, *Biochem. Biophys. Res. Commun.* **2010**, *399*, 492–497.
[57] N. Kasai, S. Ikushiro, S. Hirosue, A. Arisawa, H. Ichinose, Y. Uchida, H. Wariishi, M. Ohta, T. Sakaki, *J. Biochem.* **2010**, *147*, 117–125.
[58] N. Kasai, S. Ikushiro, R. Shinkyo, K. Yasuda, S. Hirosue, A. Arisawa, H. Ichinose, H. Wariishi, T. Sakaki, *Appl. Microbiol. Biotechnol.* **2010**, *86*, 773–780.
[59] N. L. Chigu, S. Hirosue, C. Nakamura, H. Teramoto, H. Ichinose, H. Wariishi, *Appl. Microbiol. Biotechnol.* **2010**, *87*, 1907–1916.
[60] N. Kasai, S. Ikushiro, S. Hirosue, A. Arisawa, H. Ichinose, H. Wariishi, M. Ohta, T. Sakaki, *Biochem. Biophys. Res. Commun.* **2009**, *387*, 103–108.
[61] C. Schmidt-Dannert, *Curr. Opin. Chem. Biol.* **2016**, *31*, 40–49.

Appendix

Protein sequences

1. CYP5035N5 of *P. arcularius* (JGI: 196845; NCBI accession number: TFK85288.1)

MELDGHIYVWSPERLTATYAAVLGLLTHQVFRRHETYCISAHLTLLLAPPLLIALTVSDSWQCIPKTRLLVSYAAYLSTLVLSLVSY
RLSPLHPLARYPGPLGCRVSKLWMASLSRAGYQHVYYRDLHKRYGSVVRIGPNELSIREPSAVMALVGPSGLPKGPHVTGRLLTD
KDLPMIGIEDLSTHMTRRRAWNRGFSSAAIAEYEELVGRRAMQLVQRLEEHQGKQVDIERWFDYFSYDAMCDMTFGGGSELLR
DGDENNVWSVLSAGMTAMTFFGHVPWLGVYFGYLPAATRPIKSLLAACKGLVEQRMQQGSRTRDLFHYLNHEDQMEQSPPPM
RQLVDDGILAIVGGADTVSGALTSVIFCLLTHPETYDKLQVEVDKYYPPGEDVSSTRWHRDMKYLEAVINETLRVYSPGLGGSQR
KVPADGPGVTVGSLYIPPGTALWVHAFSLHRDPSNFFPFPDDFWPERWLLAPHSPDLLSPEAADAKPTNFVHNEEAYMPFSHG
PMNCVGKNFALMEMRIVICALVQRFRFRLREDYDRADYDRNFKDYLIASRPNLPVIIELRE

2. CYP5035AU1 of *P. arcularius* (JGI: 519317; NCBI accession number: TFK89225.1)

MLKRAYSSPGAVSVALALITHQVFRRYETYSWFIHGCLLFGPPTLVATFVSDTADTTRSLLQGFFRALPIHLITLSISVILYRLSPLH
PLAGYPGPLSRKVSMLVPAYLSLSGRKCQYSQALHKQYGDVVRTGPNELSIIDTAAMQHLWNLPRGPMNVGISLSDKLVPLMGIQ
DPAEHARRRRPWNRGMSQAAVKEYEHVFADRVHLLVRRLEEQPGKADLAKWIEYLTYDFMCDMAFGGGSELLREGDKESVFS
VMEHGLMVAGALMLVPWLGVYMGYIPGAAKALATLHQTGTRFVLERLERGSTTRDLFHYLNNEDLPDTPPPPRQHLVDDGILA
VVAGSDTVSSTATSLIYCLITHPDAYADLKVEVDKYYHPGDDPCNPRHYQDMHYLNAVINETLRIFHPAAAGGQRRVPWDSEPV
VAGPYVIPPGTIIMMPQYTIHRDARYFSYPDDFWPERWLIASGDLRLEDARMPPGKPQLARGEFVHNDAAFIPFGHGPIHCVGKA
LGVLEMRMLTCALVHKFHFQAPQGWDAGTYPEQIKEYVTVTRPPLPVVIKPRW

3. CYP5035N6 of *P. arcularius* (JGI: 521854;NCBI accession number: TFK87858.1)

MFRRHETYSIAIHALLLFGAPLLLTVGTASTLTFGVLLSACWTYLVTLILSILLYRLSHLHPLSKYPGPICCRASKLWHACVVLKGR
QHEYLQALHERYGDVVRIGPNDLSIRDASLIPAILGASGVPKGPNFHGSMLTATNPPMVGIQDTRLHLARRRPWARGLALSALKE
YHRLVGKRTNQLVHLLENRHGTVVVLGEMFDYFSYDLMCDMAFGGGAELMEEGDPKQVWCLLTEGLEAGASFHQMDWLGVY
FGHIPAVVKPLQTFLTHGKTLALERMQRGSTRRDLFHYLNEEDLPERTSPPLQQLVDDGILAIVGGSDTTSSCLTSVFFALLTHPE
TYVKLQAEVDKYYPAGENPCATKQHRDMTYLHAVINEALRLFPPVMTLSTRKVPARAPGVHIRSLYIPPGTSISIPPYALQRDPR
NFSFPSAFWPERWLIASGQIKLEDAPPPAAASSRTFEFVHNEVAFMAFSHGPMNCVGKGFALQEIRTVVCALLQRFSFRLGEGW
DPREYEATVRDYIVSSRPALPVILERRTSS

4. CYP5035S6 of *P. arcularius* (JGI: 652223; NCBI accession number: TFK89222.1)

MRVVGQSAVPTIILALIAHQIFRRHETYYISVHASLLFGVPAGVVLALCWGSHPANALHIGLEVFKTYLITLGISVAVYRVSPWHPL
ARFPGPYLRRISHFVSACIYIPGNRSRHFAALHRQYGDVVRTGPNELCIVDPSMIPHILGVPGVPKGPIWVGGSLSYKTLPLVGIAD
TEEHMLRRRAWNRGLAPPALREYEVVTASRAKQLVQRLQEQVGEMNLGDWMNRFTYDFMSDMAFGGGSELLNDGDKDNM
WTTISDAMKIAMFLGHVPWLGVYLGYIPPAVSQLKRLLSRGEELAAQRLARGSTTRDLFHYLNNEDLPDKEPAPRRQLIDDGVL
AVVAGSDTTSIVLTSTFYCVLTNPDAYEELQAEIDRHFPQGDDPYITQHHRNMPYLQAVINEALRLFPPVPGGTERRVPQHGEPV
IAGSLRIPPGTSIFMPPWVLHRDARNFTFPTSFWPERWLIASGQLSLEKARLPSSIRSPWAQAGDQGAIHPVDFVHNESAYIPFSY
GPMNCPGKGLALMELRMVVTAVFQRFKIRLREGWDPSEYDSGFKDYFNATRPELPVTLERR

5. CYP5035S7 of *P. arcularius* (JGI: 664247; NCBI accession number: TFK85799.1)

MSLREVSPLTIPLAIATHQVFRRYEIYSVSVHACLFLVPPALVAAHISSQSYSPSSIPATFVIALVSYVAAIAASVIVYRLSPLHPLARY
PGPVWRKVSMIGPAILATTGNRAWAFADMHRKYGDIVRSGPNELSIIDPSFIGPLLGASGLPKGPYHVGASVTPEHVSMAGLQDI
PYHLQRRRPWNRGLNPSALKDYQPLIVERLQLLVRRLHEQSGIIDLGLWLKYFAYDFMSDMAFGGGSELLKDGDKNNIWSIIEEG
MVFATILHTLPWLGAYLFKIPGSVKPLLAMQQTTARLAEERFKRGSKTRDLYYYLSNEDLPDKPPPPLRELADDGVLAVVAGSD
TASLTMTSVFYLLLTHPEAYTKLQEEIDTSYHPGEPNAGTKRHREMPYLHAVINEALRLFPPVPLGTQRQVPHDASPVVFGSVVI
PPGTSVYLPTLALHRDPRNFTCADDFWPERWLIASGQLRYKEARRPPSLSSLKAADLPDFVHNDVAFTPFSVGPMNCPGKGLA
MLEMRMVIVELVKNFVFKLWDGWDPATYEKEFKDYFTAARPGLPVVLEPRQQL

6. CYP5035S8 of *P. arcularius* (JGI: 665466; NCBI accession number: TFK83982.1)

MSLREVSLLTIPFAILAHQVLRRYETYRIYVHACLLLGPPILAAARLTSFRPTPALPPILFNSLVSYLAALVTSVIAYRLSPFHPLAQY
PGPLWRRISMFGPAAMATTGNRHRAFASLHQKYGDVVRTGPNELSIADASFVGPLLGASGLPKGPNHVGASMSDTKMSMVGIQ
DIPHHLQRRRPWNRGLSQQALKGYEPLMAERAQLLVQRLTQQSGPVDLGLWLKYFAYDFMSDVAFGDGSDLLREGDKANIWSI
IEDGMVVCTIAHSLPWLGIYLSMIPSAAGPMLAFQENGRRLARERLERGSKTRDLYHYLCNEDLSDNPPPTLDELADDGTLAIVA
GSDTVSVALTSVFYCLLTDTEAHRNVQQEIDRLYPVGEPFSETKHHREMHYLQAVINEAMRLFPPIPLGSQRQVPHDAASVVVGS
VVIPPGTAIYLPPWVLQRDPRNFTFPDAFWPERWLIASGQLHYGDARLPSSAKRGHERPDFVHHEATFIPFSAGPMNCPGKGLA
MMEMRSVVIALMKNFGMKLRDGWNPATFDQEFKDYFTAARPELPVVLEPRLHVETKAYE

7. CYP5035AV1 of *P. arcularius* (JGI: 667965; NCBI accession number: TFK79795.1)

MSTMWYSLAVSALIAHESFKRYETYSIRAHTALLLGPPSLALGFLGSTGSSSRSVLHTLPLAYAAYVGALTVYTILYRISPFHPLAQ
YPGPLGCKVSQWWMACKSWSGYEHLYISELHRKYGDVVRIGPNELSIRDASAISPIMSIAKGPQYVGRMLSDGIHLPIIGIQDPAE
HLRRRRPWNRAFTVPALRGYEETIARRARQLVDALERHNGGQEEVILGKWFNDFAYDFMCDMAFGGGSELLQERDDSNVWRV
LDEGMKVGTLLAHVPWLGVYLSHVPLATGALDVLISHCRMLTTQRVQRGATQKDLFHYLNDEDLANSSEKPRAQPPLRQLTDD
GCLIVVAGADTTSSALTSLFYCLLTNPETYRRLQDEVDKFYPRGEDACDTRYHREMRWLNAVICETLRLFPPVPGGSQRQVPHNS
AIGVMAGDAFIPPGTSVWAHTWSIHRDPRNFSRPDAFWPDRWLLASTTLRSSPSSASSSVEADGVRDFVHNEDAWIPFAQGQM
NCVGKNLALLEIRMVVCALMQRFEMRLSEGWDAREYERKFRAYLVATRPEMPVRLRVRCT

8. CYP5035S9 of *P. arcularius* (JGI: 668252; NCBI accession number: TFK79033.1)

MSLREVSPLTLPLALIAHQVFRRHETYRVAVHLSLLLAPPALVAAYVARSQPYSAFLTAFVNALLSYLAALVTSVVVYRLSSFHPL
ASYPGPVWRRVSMIGPAAATVSGNRHRTFADMHKQYGDIVRTGPNELSIVDPTFVEPLLGTGGLPKGPNHIGGNMSEETNLVGI
VDIPYHLQRRRPWNRGLKQSALKEYEPLLAERAQLLVQRLGDQSGSADLGLWLKYFGYDFMCDMAFGGGSELLRNGDKNNVW
AIIEEGMVVCTVLHTLPWLGIYLGKIPSVVKPMLLLQENGRQMAKKRLERGSKTRDLYHYLCNEDLSDRSPPAIAELADDGILTV
VAGSDTASMTMTNVFYCLLTHPEAYAKLQAEIDKFYPAGEPASETKHHRDMHYLHAVINEALRLYPPVPLGSQRRVPHSGAPVV
VGSTVLPPGTVVYLPPWILHRDPRNFSFPDAFWPERWLITSGQLRHEDAQPPSSAKDATKMDISGLVHNEAAFTPFSIGPMNCP
GKGLAMLEMRTVIVSLMKNFSFKLRDGWDPAKFEEELKDYFLVARPELPVTIERRRIVT

9. CYP57A2 / PDA6-1 of *Nectria haematococca* (NCBI accession number: P38364.1)

MLVDTGLGLISELRARLGWAALLQIVPVTVVAYNLLWFIYTSFFSSLRKIPGPFLARISRVWEIKKAATGNIHEIVMDLHRCHGPIV
RIGPNRYDFDTMEALKIIYRIGNALPKADYYIPFGLPSSPNLFDVQNPARHSAMKKQVASLYTMTALLSYEAGVDGQTIILKEQLQ
RFCDQKQVIDLPQFLQYYAFDVIGVITVGKSMGMMETNSDTNGACGALDAMWHYSSMMAFIPHMHAWWLRLSSLLPIDVPIKG
LTEYVEQRIIQYRLKAAEFGDDDALKGENNFLAKLILMERQGTVTSTETQQAVGLNIGAGSDTTANALSSILYFLYTNPRTLRRLR
EELDTHVKEDPIRFQQSQSMPYLQAVIKEALRLHPGVGTQLTRVVPKGGLVIEGQFFPEGAEVGVNGWALYHNKAIFGNDASVF
RPERWLETKGNLNIGGSFAFGAGSRSCIGKNISILEMSKAIPQIVRNFDIEINHGDMTWKNECWWFVKPEYKAMIKPRAA

10. CYP5035H2 of *P. arcularius* (JGI: 665169; NCBI accession number: TFK84406.1)

MVFQLPAHHALFTVVGSAFIVHLIFKRYEPHRVAVHALLLLAVPSFLSVLLLDRMPAIKALSASFLTFWTALVSSVALYRLSPWHP
LARYPGPVSLRLSKLSMAWISRGGRRHLYTQELHRRYGDIVRVGPNEVSVSNAAAIHPLMGTSGLHKGPQWEARTATQSVLPLI
AIGDPKEHLRRRKPWNRALNVASLKDFEPFVTHRAEQLVSRLASQKETTNLARWFGWFTYDLMSDMAFGGGSEMMLNGDDG
SVWPLLEIGLLNSDTYGHLPWMADYIRAVPSLGTNMKQMRSFCIQRTEERIKLGNTSRKDLFYYLNNEDGAEPTPPVPEVTADG
TLAIVAGSDTTSSVLSNVFYCLLTHPEAYARLRAEVDSYYPPGEDALNTKHHADMPYLNAVINETMRLFPPVTDGSQRIVPTGSG
GRIIGDSYLPEGTITTVHMYSIQRDARNFAPLPDSFWPERWLHAAEGARSVIGMKLVHNPTAFFPFSYGPGNCAGKGLALQEMR
MVVSAMMQKLELSLAEGFDAVAYENEMHDYLILSRPPLPVVVKQRKVCTAEA

11. P450 reductase of *P. pastoris* (NCBI accession number: XP_002494255.1)

MDTLDLSVLIAIALALIAYFSKGSLWGKEDDNSVHGVAGGFQTRDLVEILNSTNKKALVLYGSQTGTSEDYAHKYARELQSKFSIP
TLCGDLSEFDFDNLNDIPEQVEGFTFITFFMATYGEGEPTDNAVEFIEFLKNDAEDLSNLKYTVFGLGNSTYEFYNQMGKTTNKR
FSELGAQLVGTFGEGDDGQATMDEDFLAWKDSLFDTIKKDLHLEEHEVVYQPGLKVKENTALTTSSPNVSVGEPNKAYVLREDE
NLLQYGPFDHTHPYIAPISSSRELCSETSERNCIHLEFDLSNTNLRYSTGDHLAVWPSNANEHVESFLKVFNLTDKRSSVFDIEFL
DPTVTVHFPFPTTYEAVVRHHLEISGPISRQTLKQFIPYAPDQSTKQEVIRLSESKDVFHNEVTAKYYNLADLLFKVSKETPWNVP
FNFLIETMPNLQHRYYSISSSSLSEKQTIHITAMIEAFTPTGSDHIVTGVTTNLLWNIQLNQDKSTVKAPVSYDLNGPRNLFSPYKL
PVHIRRSTFKLPSNPALPVIMIGPGTGVAPFRGFIRERCQQVDNGTPNIGQSILYYGCRNSEQDFLYRDEWPTYSKKLGDKFKMYT
AFSRENSHKVYVQHRLLENSREFIELMDQGAFIYVCGDAGKMAKDVNKAIVEILIKEKGLSEEDATESIREFKTSNRYQEDVW

Plasmids and strains

Table 1: Plasmids and strains produced and used during this thesis.

Glycerol stocks	CC number	Strain designation	Plasmid name	Plates	Organism	Host strain
NF1		plasmid 1.6	pBSY-stuffer-pDAS1/DAS2-AtCPRwt	LB-Zeo	E.coli	
NF2		plasmid 2.2 (*A. thaliana* reductase - stuffer)	pBSY-stuffer-pDAS1/DAS2-AtCPRopt	LB-Zeo	E.coli	
NF3		Pichia P450 reductase knock-out strain 5		YPD	Pichia	Δku70
NF4		Pichia P450 reductase knock-out strain 8		YPD	Pichia	Δku70
NF5		knock-out cassette (ΔNCPI; + ZeoR) in Pichia	NCP1-FLP_Zeo cassette	YPD-Zeo	Pichia	Δku70
NF6		gBlock Erg 3.2	CRISPR plasmid + gBlock3.2	LB-Zeo	E.coli	
NF7		gBlock Erg 5.3	CRISPR plasmid + gBlock5.3	LB-Zeo	E.coli	
NF8		gBlock Erg 3.1	CRISPR plasmid + gBlock3.1	LB-Zeo	E.coli	
NF9		gBlock potential 1	CRISPR plasmid + gBlockpot1	LB-Zeo	E.coli	
NF10		gBlock Erg 11.2	CRISPR plasmid + gBlock11.2	LB-Zeo	E.coli	
NF11		gBlock potential 3	CRISPR plasmid + gBlockpot3	LB-Zeo	E.coli	
NF12		gBlock Erg 5.1	CRISPR plasmid + gBlock5.1	LB-Zeo	E.coli	
NF13		gBlock potential 2	CRISPR plasmid + gBlockpot2	LB-Zeo	E.coli	
NF14		gBlock Erg11.1	CRISPR plasmid + gBlock11.1	LB-Zeo	E.coli	
NF15		gBlock Erg11.3	CRISPR plasmid + gBlock11.3	LB-Zeo	E.coli	
NF16		gBlock Erg 5.2	CRISPR plasmid + gBlock5.2	LB-Zeo	E.coli	
NF17		potential P450 crispred		YPD	Pichia	BSYBG11
NF18		Erg 5 crispred		YPD	Pichia	BSYBG11
NF19		Erg 3 crispred		YPD	Pichia	BSYBG11
NF20		Erg 3 + pot double crispred		YPD	Pichia	BSYBG11
NF21		Erg 5 + pot double crispred		YPD	Pichia	BSYBG11
NF22		P450 reductase + Erg 5		YPD	Pichia	Δku70
NF23		Potential P450 overexpression	pBSY-PotP450-pDAS1/DAS2-PpCPR.clc	YPD-Zeo	Pichia	BSYBG11
NF24		Erg 11 overexpression	pBSY-Erg11-pDAS1/DAS2-PpCPR.clc	YPD-Zeo	Pichia	BSYBG11

NF25		Erg 5 overexpression	pBSY-Erg5-pDAS1/DAS2-PpCPR.clc	YPD-Zeo	Pichia	BSYBG11
NF26	**8197**	Red-stuffer in 2.2 (Pichia red. overexpression)	pBSY-stuffer-pDAS1/DAS2-PpCPR	YPD-Zeo	Pichia	BSYBG11
NF27		Pichia red.-2.2 plasmid	pBSY-stuffer-pDAS1/DAS2-PpCPR	LB-Zeo	E.coli	
NF28		Erg 3 in plasmid	pBSY-Erg3-pDAS1/DAS2-PpCPR.clc	LB-Zeo	E.coli	
NF29		Erg 25 in plasmid	pBSY-Erg25-pDAS1/DAS2-PpCPR.clc	LB-Zeo	E.coli	
NF30		Erg 26 in plasmid	pBSY-Erg26-pDAS1/DAS2-PpCPR.clc	LB-Zeo	E.coli	
NF31		stuffer-stuffer in 2.2	pBSY-stuffer-pDAS1/DAS2-stuffer	LB-Zeo	E.coli	
NF32		Erg 3 overexpression	pBSY-Erg3-pDAS1/DAS2-PpCPR.clc	YPD-Zeo	Pichia	BSYBG11
NF33		Erg 25 overexpression	pBSY-Erg25-pDAS1/DAS2-PpCPR.clc	YPD-Zeo	Pichia	BSYBG11
NF34		Erg 26 overexpression	pBSY-Erg26-pDAS1/DAS2-PpCPR.clc	YPD-Zeo	Pichia	BSYBG11
NF35		stuffer-stuffer in 2.2 (empty vector)	pBSY-stuffer-pDAS1/DAS2-stuffer	YPD-Zeo	Pichia	BSYBG11
NF36		stuffer-CYP1A2 overexpression	pBSY-CYP1A2-pDAS1/DAS2-stuffer	YPD-Zeo	Pichia	BSYBG11
NF37		reductase-1A2 overexpression	pBSY-CYP1A2-pDAS1/DAS2-PpCPR	YPD-Zeo	Pichia	BSYBG11
NF38		P. arcularius gBlock 1 (196845)	pBSY-CYP5035N5-pDAS1/DAS2-PpCPR	LB-Zeo	E. coli	
NF39		P. arcularius gBlock 2 (519317)	pBSY-CYP5035AU1-pDAS1/DAS2-PpCPR	LB-Zeo	E. coli	
NF40		P. arcularius gBlock 3 (521854)	pBSY-CYP5035N6-pDAS1/DAS2-PpCPR	LB-Zeo	E. coli	
NF41		P. arcularius gBlock 4 (652223)	pBSY-CYP5035S6-pDAS1/DAS2-PpCPR	LB-Zeo	E. coli	
NF42		P. arcularius gBlock 5 (664247)	pBSY-CYP5035S7-pDAS1/DAS2-PpCPR	LB-Zeo	E. coli	
NF43		P. arcularius gBlock 6 (665466)	pBSY-CYP5035S8-pDAS1/DAS2-PpCPR	LB-Zeo	E. coli	
NF44		P. arcularius gBlock 7 (667965)	pBSY-CYP5035AV1-pDAS1/DAS2-PpCPR	LB-Zeo	E. coli	
NF45		P. arcularius gBlock 8 (668252)	pBSY-CYP5035S9-pDAS1/DAS2-PpCPR	LB-Zeo	E. coli	
NF46		N. haematococca 9 (PDA6-1)	pBSY-PDA6-1-Nhaematococca-pDAS1/DAS2-PpCPR	LB-Zeo	E. coli	
NF47		P. arcularius gBlock 10 (665169)	pBSY-CYP5035H2-pDAS1/DAS2-PpCPR	LB-Zeo	E. coli	
NF48	**8191**	P. arcularius 5 (664247)	pBSY-CYP5035S7-pDAS1/DAS2-PpCPR	YPD-Zeo	Pichia	BSYBG11
NF49	**8195**	N. haematococca 9 (PDA6-1)	pBSY-PDA6-1-Nhaematococca-pDAS1/DAS2-PpCPR	YPD-Zeo	Pichia	BSYBG11
NF50		A9 CYP3A4 wildtype of Matic		YPD-Zeo	Pichia	
NF51	**8187**	P. arcularius 1 (196845)	pBSY-CYP5035N5-pDAS1/DAS2-PpCPR	YPD-Zeo	Pichia	BSYBG11
NF52	**8188**	P. arcularius 2 (519317)	pBSY-CYP5035AU1-pDAS1/DAS2-PpCPR	YPD-Zeo	Pichia	BSYBG11
NF53	**8189**	P. arcularius 3 (521854)	pBSY-CYP5035N6-pDAS1/DAS2-PpCPR	YPD-Zeo	Pichia	BSYBG11
NF54	**8190**	P. arcularius 4 (652223)	pBSY-CYP5035S6-pDAS1/DAS2-PpCPR	YPD-Zeo	Pichia	BSYBG11

NF55	**8192**	P. arcularius 6 (665466)	pBSY-CYP5035S8-pDAS1/DAS2-PpCPR	YPD-Zeo	Pichia	BSYBG11
NF56	**8193**	P. arcularius 7 (667965)	pBSY-CYP5035AV1-pDAS1/DAS2-PpCPR	YPD-Zeo	Pichia	BSYBG11
NF57	**8194**	P. arcularius 8 (668252)	pBSY-CYP5035S9-pDAS1/DAS2-PpCPR	YPD-Zeo	Pichia	BSYBG11
NF58	**8196**	P. arcularius 10 (665169)	pBSY-CYP5035H2-pDAS1/DAS2-PpCPR	YPD-Zeo	Pichia	BSYBG11